ENGINEERING PROPERTIES OF SULPHATE-BEARING CLAY SOILS STABILISED WITH LIME-ACTIVATED GROUND GRANULATED BLAST FURNACE SLAG (GGBS)

Gabriele Helene Veith

A submission presented in partial fulfilment of the requirements of the University of Glamorgan/Prifysgol Morgannwg for the degree of Doctor of Philosophy
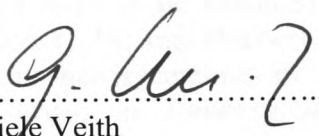
May 2000

CERTIFICATE OF RESEARCH

This is to certify that, except where specific reference is made, the work described in this thesis is the result of the candidate. Neither this thesis, nor any part of it, has been presented, or is currently submitted, in candidature for any degree at any other university.

....
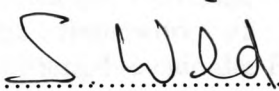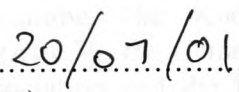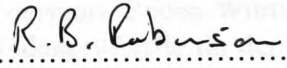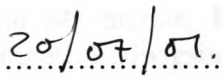
Gabriele Veith   18-07-01
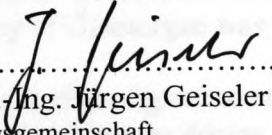
(Candidate)   (date)

....
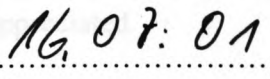
Prof Stan Wild   20/07/01

University of Glamorgan, (Director of Studies)   (date)

....

Dr Roderick B Robinson   20/07/01

University of Glamorgan, (Supervisor)   (date)

....

Prof. Dr. Ing. Jürgen Geiseler   16 07: 01

Forschungsgemeinschaft   (date)

Eisenhüttenschlacken e.V., (Supervisor)

ACKNOWLEDGEMENTS

ABSTRACT

This research studied the effects of the addition of ground granulated blast furnace slag (ggbs), activated by 2% calcium hydroxide (Ca(OH)$_2$, on the strength, permeability and porosity development of a laboratory prepared clay mix (kaolinite with and without 6% gypsum) and a natural sulphide-bearing clay soil, Lower Oxford Clay. Based on shear, compressive and indirect tensile strength testing, it was found that an increase in the stabiliser slag/lime ratio results in substantial strength increase even after short curing periods (up to 12 weeks). This increase in strength is more pronounced if curing is at elevated temperatures (30 °C). The presence of sulphates (6% gypsum=2.73% SO$_3$) resulted in an accelerated increase in the strength development for stabilised kaolinite, which was comparable to that of stabilised Lower Oxford Clay. In the absence of sulphates, large ggbs additions were only activated effectively at higher curing temperatures (20 and 30 °C) after curing periods of 24 weeks and beyond, although it is suggested that 2% lime creates a sufficiently alkaline environment for activation. The degree of slag activation and thus the subsequent cementation process was reflected by an increase in the percentage of the pore volume occupied by pores with a radius ≤0.05μm, which is usually associated with the pore fraction characteristic of cementitious gels. The increase in slag addition, for kaolinite mixes, was accompanied by a reduction in total porosity. Specimens made from Lower Oxford Clay exhibited a significant increase in pore volume at higher slag additions. This is interpreted as being due to the creation of pore space resulting from restrained shrinkage of gels by inert particles during drying in this coarser, natural clay. No significant trend in the effect of curing temperature on the pore size distribution could be identified from the data.

The development of permeability, however, showed some sensitivity to curing temperature. Results from specimens cured at 20 and 30 °C showed an accelerated reduction in their k-values in comparison to samples which had been cured at 10 °C. However, little correlation between measured permeability and exhibited pore size distribution could be established which is believed to be due to the strong influence of shrinkage during drying prior to mercury intrusion porosimetry in the dimensionally semi-stable soil system.

The volume stability of stabilised specimens during frost action was assessed in a series of 12 freeze-thaw cycles, which were carried out in accordance to the German proposal for a European Pre-Standard. Generally an increase in the curing period prior to frost action and higher overall sample porosity resulted in relatively better performance during frost action.

The influence of the slag/lime and slag/gypsum ratio on the swelling potential upon soaking was assessed in long-term soaking tests and the underlying causes were identified by findings from microstructural investigations including SEM and TG analysis. These results contributed to a better understanding of the slag activation process. In an alkaline environment slag hydration appears to be triggered earlier by sulphate, due to the more intensive disturbance of a thin protective layer of cementitious products on the slag grains. Disruption of this layer, for example by ettringite formation, exposes more unreacted slag grain surface, which will subsequently start to hydrate.

Findings were complemented by two case studies, one which investigated the cause of substantial heave on a German highway on a microscale and the other which assessed the technical performance and the economic implications of a full-scale trial utilising the stabilisation technique with lime and ggbs for a temporary diversion. The overall findings from the projects indicate that soil stabilisation with lime and ggbs is, particularly for soils with significant sulphate/sulphide content, a feasible and environmentally friendly alternative to the classic soil stabilisation methods.

LIST OF ABBREVIATIONS AND SYMBOLS

General

AAS(C)   alkali-activated slag (cement)

amu   atomic mass unit

BOS   basic oxygen steelmaking slag

EAF   electric arc furnace slag

GDS   Geotechnical Digital System

GGBS   ground granulated blast furnace slag

ICL   Initial consumption of lime

IT   indirect tensile

MDD   maximum dry density

MIP   Mercury intrusion porosimetry

OMC   optimum moisture content

Op   Outer product (in slag hydration)

(O)PC   (ordinary) Portland cement

PFA   pulverised fuel-ash

SEM   scanning electron microscopy

SP   segregation potential

TGA   thermogravimetric analysis

TSA   thaumasite form of sulphate attack

UCS   unconfined compressive strength

XRD   X-ray (powder) diffraction

Chemistry

A Al_2O_3

AFm   a metastable phase (mainly monosulphate) in a hydrating system

AFt   a metastable phase (mainly ettringite) in a hydrating system

C CaO

H H_2O

$\bar{S}$ SO_3

S SiO_2

Symbols

a	'cohesion' intercept obtained from modified failure envelope
A	activity (of clay soils)
α	'angle of internal friction' obtained from modified failure envelope
B	pore pressure coefficient
B/A	ratio of basic to acidic compounds in slag
c_u	apparent cohesion in terms of total stress
ϕ_u	undrained, unconsolidated angle of internal friction
v_u	water intake flux
θ	contact angle of intrusion liquid in MIP investigations
k	coefficient of permeability of soil
q	flow rate of water
R_f	fines factor
S	degree of saturation
σ_n	(normal) stress on slip surface
σ_1	axial stress
σ_3	(cell) confining pressure
τ_f	shear strength at failure
τ_u	undrained shear strength
T_f	temperature at freezing front
u	pore pressure
w/c	water to cement ratio

TABLE OF CONTENTS

LIST OF FIGURES

Chapter 7

LIST OF TABLES

Chapter 1 - Introduction

1.1 General

The year 1999, during which large parts of this thesis were compiled, will go down in history as the year in which the world population increased beyond the "magic" figure of 6 billion with the birth of a child in Sarajewo/Yugoslavia. From an environmental point of view, 1999 will also be remembered as the year of the World Climate Summit in Bonn/Germany, where the nations of the world met to discuss the greenhouse effect, the subsequent heat retention and the resultant induced climate change within the earth's atmosphere. After earlier summits in Rio de Janeiro/Brazil and Kyoto/Japan, the negotiated results of which have unfortunately not yet been ratified by most of the participating nations, this summit was called to mainly discuss and outline a series of regulations which will be established to allow the introduction of a trading scheme of nation–specified emission quotas. With a contribution of 19 t/year of CO_2 emissions per inhabitant deriving from the combustion of fossil fuels (in comparison: Germany 11 t/year, China 2t/year and India 1 t/year), the United States of America is amongst the largest producers of green-house gases. The fact that it might soon be able to buy further emission allowances, for example from countries like Russia or China, - like trading in stocks and shares - throws new light on a quote from the Greenpeace Annual Report 1998:

"'Environment' can no longer be meaningfully separated from health, quality of life, democracy, education, economy or trade."

Although CO_2 is not the only gas which absorbs thermal radiation emitted by the earth's crust (and thus has a blanketing effect on the atmosphere), it does contribute substantially (by approximately 70%) to the so called 'anthropogenic' green house effect. It is mainly generated as a result of combustion of fossil fuels (i.e. by power stations, industry and traffic) and by deforestation [Houghton, 1997]. It remains for approximately 6-10 years in the troposphere. Closely linked to the production of green house gases is the issue of depletion of resources. This is perceived (together with population growth and associated demands for food, energy and work to generate the means of livelihood particularly in developing countries and increasing poverty and disparity in wealth between the developed and the developing world) to be one of the most important issues in combating global warming. Within the framework of a 'Global Marshall Plan' Al Gore, the Vice President of the United States has recommended as one of the five salient strategic goals *"the rapid creation and development of environmentally appropriate technologies"*, also emphasising that *"resources for the plan would need to come from the world's major wealthy countries"* [1992].

In addition to the moral imperatives, economic considerations are the prime motivation in increasing the pressure to use raw materials economically, reduce energy consumption and thus minimise the impact of production processes on the environment. Due to the fact that large amounts of natural resources are required in the construction industry, it was amongst the first branches to be forced to look into possible uses of recycled or waste material. This has led to a wide range of materials being introduced over the last decade for various purposes, for example by replacing cement in concrete and thus reducing the CO_2 emission per tonne of concrete utilised (the production of one tonne of cement results in one tonne of CO_2 emissions). Successfully utilised replacement materials are, for example, pulverised fuel-ash, condensed silica fume or even exotic agricultural residues such as rice-husk ash. With regard to geotechnical applications, particularly soil stabilisation techniques, the introduction of the landfill tax on 1st October 1996 was an additional incentive provided by the British government for the promotion of sustainable waste management and has – due to increasing tax rates – given an impetus to civil engineers to devise more imaginative schemes incorporating 'waste' in tax-exempt uses [Craighill and Powell, 1998]. Another, most promising method of policy intervention, suggested in a report on the occurrence and utilisation of waste materials by Whitbread et al. [1991], would be to introduce a tax on the use of primary aggregates and thus further encourage greater use of alternative materials. A

less controversial approach would be to impose a general requirement that a given proportion of the materials used in a construction project should be either waste or recycled material [Sherwood, 1995]. Although the Germans and the Dutch have already opted for such an approach, there is currently little indication that a similar regulation will be introduced in Britain in the near future. However, the introduction of the controversial landfill tax has led to the fact that soils with inferior engineering properties are now more often considered for stabilisation techniques in order to ensure that they can be utilised during the construction process and less material has to be discarded. The classic soil stabilisation technique implies usually the incorporation of lime and/or cement, the production of both of which results in large quantities of CO_2 being released. In the case of cement, large amounts of energy are required to win the raw materials, prepare the feedstock (ground and blended limestone or chalk with clay or shale), fire the kiln in order to produce the cement clinker and finally grind the clinker to required fineness. During the production of lime, limestone has to be calcined to calcium oxide, in the process of which large quantities of CO_2 are not only released as a result of the chemical reaction but also from the combustion of the fuel [Haynes and Cornell, 1996]. Not to counteract the environmental benefit which is gained from the utilisation of soils at site by stabilisation, the introduction of an environmentally-friendly stabilising agent, preferably a waste or by-product with no or little additional energy requirement during its production phase, would be a preferable solution. For example old shredded car and/or truck tyres have been shown to have some potential in improving the engineering properties of weak soils for specific applications [Al-Tabbaa, 1998]. Particularly with regard to its utilisation as a landfill liner, shredded tyre was found to be useful, because it has a tendency to absorb a variety of organic compounds which would potentially leach from the landfill into the groundwater. There is also some indication that waste paper sludge, a by-product of the paper-making industry, could be utilised for stabilisation purposes. Within the scope of this thesis, however, the suitability for soil stabilisation of a by-product of the iron-making industry will be investigated. It is a material, on the medical properties of which the scientist and philosopher Aristotle commented as early as 350 BC *"...if iron is purified by fire, there forms a stone, known as iron slag. It is wonderfully effective in drying out wounds and results in other benefits... "* [Geiseler, 1996]: Ground granulated blast furnace slag (ggbs).

1.2 Slag production and history

Slag is a by-product from the iron-making industry with a large range of possible uses not only in the areas of civil and agricultural engineering. The earliest recorded use of ggbs in the construction industry dates back to 1774, when it was added to a mortar based on slaked lime. The hydraulic properties of water-cooled blast furnace slag were discovered in 1862 by Emil Langen from Troisdorf, Germany: *"...feuerflüssige Hochofenschlacke erhält nach dem Einleiten in Wasser wertvolle hydraulische Eigenschaften...(if subjected to cold water treatment, liquid blast furnace slag is given valuable hydraulic properties..)"* [Geiseler, 1992]. It was also in Germany where the first commercial use of slag-lime cements started in 1865. Over the decades a Portland clinker-slag-calcium sulphate cement was mainly used for concrete exposed to harsh conditions, for example for a North Sea Canal lock near Ijmuiden in the Netherlands. Finally, in 1917 after investigations carried out by the Material Testing Institute (Materialprüfungsamt) in Berlin, slag cement was allocated the same standing as Portland cement within the cement range in Germany [Bijen, 1996].

The general term 'slag' is transferred from the German expression 'schlagen', meaning 'to beat' and refers to the separation of the non-metallurgical compounds from the molten steel itself, which was achieved in the 18th century by beating the liquid material [Geiseler, 1992]. In practice, however, various types of slag deriving from the steel production process can be distinguished. During steel production, blast furnace slag, steel slag and slag from secondary metallurgical processes are generated at different stages. Whereas blast furnace slag separates naturally from the molten iron at the bottom of the furnace and is tapped off separately, steel slag is a by-product generated during the conversion process of pig iron into steel. Depending on the type of conversion method utilised, two main types, basic oxygen steelmaking slag (BOS) and electric arc furnace slag (EAF) can be distinguished [Geiseler, 1996]. Finally, slag from secondary metallurgical processes is separated when steel is further purified during additional treatment resulting in a lower sulphur content. Figure 1.1 shows a schematic overview of the steel production and the generation of the different slag types at the various stages.

The world production of iron blast furnace slag is approximately 100 million tonnes/year (UK: approximately 3.8 million tonnes/year). However in some countries

such as the United States, Canada and Australia, only limited use is made of the cementitious properties of the slag due to the fact that only 8-10 % of the slag yield is granulated. In contrast, Germany and Japan make extensive use of the cementitious properties of quenched slag. [Malhotra and Mehta, 1996, Hanafusa and Watanabe, 1991]. In Great Britain approximately 40% of the total yield of blast furnace slag of around 3.8 million tonnes/year are granulated, still leaving substantial potential for utilisation of this comparably cheap, latent-hydraulic material unused.
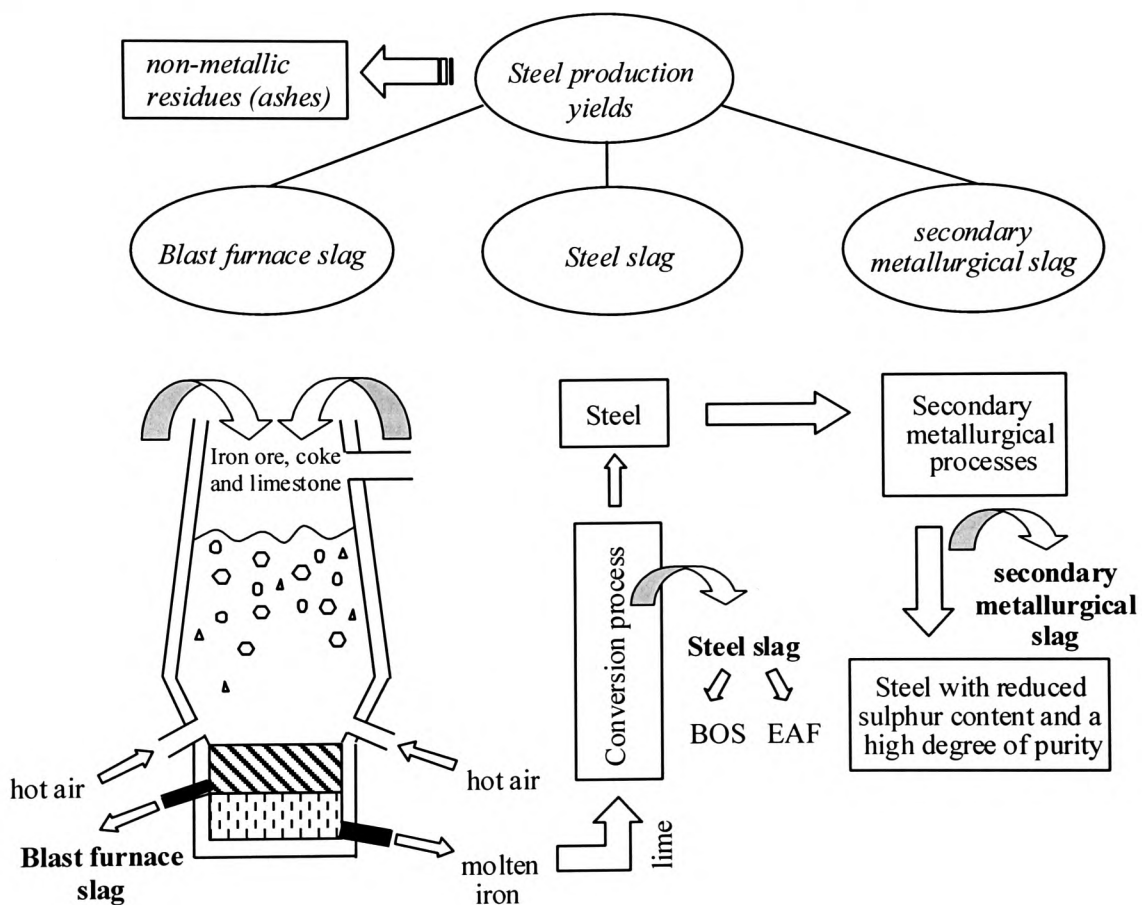
Figure 1.1 Schematic view of steel production

1.3 Structure of the thesis and experimental range involved

This introduction is followed by two general chapters giving an overview of clay mineralogy and classic stabilisation methods. The reactions between the additives and the soil compounds are explained and the reader is familiarised with reaction changes particularly in the presence of sulphates in the ground. Subsequently a critical review summarises the way in which slag is used in concrete technology or – mostly as the sole stabiliser – in soil stabilisation. In addition, mechanisms, which have been suggested to explain the reactions occurring when slag in used in cement, are assessed. A separate section places particular emphasis on the effects of frost on stabilised soils. No previous research work could be identified, which had studied the behaviour of lime-slag stabilised ground during frost action. Subsequent chapters give an overview of the materials utilised in this project and identify and describe the test procedures adopted to obtain reliable and repeatable research results. The presentation and analysis of results is followed by a chapter summarising the case studies carried out appropriate to the scope of this project. The thesis is concluded with the discussion and synthesis of the results and recommendations for future work.

The main emphasis in the current work was put on observations with regard to changes in the engineering properties of sulphate-bearing clay soils stabilised with lime-activated ggbs. However, it soon became apparent that it would be helpful to introduce some microstructural techniques (scanning electron microscopy (SEM), thermogravimetric analysis (TGA) and X-ray powder diffraction (XRD)) in order to characterise and identify involved mechanisms. In the current work these techniques were used to investigate the mechanisms by which delayed swelling occurs when kaolinite is stabilised by ggbs only. If kaolinite is mixed with ggbs, moist cured and then soaked, there is a small initial expansion on soaking followed by no expansion for a prolonged period and then a sudden renewed period of expansion (see section 7.3). This phenomenon was first reported by Kinuthia [1997]. Some of these techniques were also used to characterise the expansive phases present in a soil sample from a case study of a German construction project (brought to the attention of the author by the Ministry of Environment and Transport Baden-Württemberg in Stuttgart/Germany), where heave had occurred (section 8.1). Finally XRD investigations were utilised to identify the minerals present in some of the clays employed (chapter 5).

The progress of this research was regularly presented to a steering group of industrial partners, (Cementitious Slag Makers Association, Buxton Lime Industries, RMS Industrial Materials Ltd and Singleton Birch Ltd) to ensure the relevance of the work for practical application. Results were documented in a series of progress reports [Wild et al., 1997, 1998a+b, 1999a+b]. External supervision provided by representatives of the Forschungsgemeinschaft Eisenhüttenschlacken e.V. (Research Association Iron Slags) in Duisburg/Germany completed the supervision team and ensured a critical assessment of the work from both, a practice-related and scientific standpoint.

1.4. Research objectives and contribution to knowledge

Although a wide range of research projects into the utilisation of ggbs in concrete technology has been carried out already, only few researchers have looked at the possible use of slag in combination of lime-stabilised ground, assessed its performance in extreme climates (frost action) and investigated the microstructural changes which result in modified engineering properties of the treated soils. The role of sulphates in the soil-lime-slag system has yet to be fully established. Thus the salient aims of the current research project are

☐ to carry out investigations into the strength development of soils stabilised with lime-activated ggbs and to assess the influence of sulphates

☐ to assess how the engineering properties (strength, permeability and frost resistance) of the stabilised soils are modified by the lime-activated slag

☐ to relate changes in microstructural characteristics (porosity and pore size distribution), initiated by lime-activated ggbs, to the observed changes in the engineering properties of the soils

☐ to gain knowledge on slag hydration in clays in the absence of lime as an activator and

☐ to identify the microstructural parameters which control the durability of soils stabilised by lime-activated ggbs and to asses how these parameters are modified by the addition of sulphates

The research project will allow an overall assessment of the feasibility of utilising lime-activated ggbs as a stabilising agent in sulphate-bearing clay soils. Investigations into the structure of stabilised samples will allow identification of underlying mechanisms and extend the knowledge on slag activation, slag hydration and its subsequent effects on the durability of stabilised soils.

Chapter 2 – Clay soil mineralogy and engineering properties

This chapter introduces the reader to the basic clay mineral structure types and gives an overview of clay classification and composition. A brief section outlines technical methods for clay identification and the reader is familiarised with the effects of moisture on clay particles. The influence of clay mineral composition on some relevant engineering properties is explained and the section concludes with a detailed outline of the mechanisms involved in frost action on soils. The chapter is finalised with an overview of the occurrence of sulphates in clay soils, an aspect which will be of particular importance for the next chapter, which introduces soil stabilisation methods.

2.1 Clays in engineering geology

A basic understanding of bonding, crystal structure and surface characteristics of clay soils is important when interactions between clay soils, chemically active additives and water have to be assessed. Water absorption, for example, is determined by the type of bonding between the layers of clay minerals and in turn absorption processes have an influence on the chemical reactions occurring between the soil and additive. Interactions of this kind affect the flow of water through porous soil media and changes in surface forces owing to changes in the chemical environment may alter the performance of a soil when tested for a wide range of engineering properties.

Although every geotechnical engineer is aware of the fact that water wets clays and is adsorbed on particle surfaces, it might not be general knowledge that clays are nevertheless classified as lyophobis (liquid hating) or hydrophobis (water hating) colloids [Mitchell, 1993]. Generally, a clay mineral (argillaceous mineral) is identified by a particle diameter of less than 2 μm[1] and a sheet-like crystallographic habit, allocating it to the larger group of phyllosilicates [Brown, 1984]. When over 35 % of a soil deposit consists of particles with a diameter of 0.002 mm and smaller, resulting in a cohesive material, the soil is termed clay. In addition to clay minerals the solid phase of a soil may contain various amounts of crystalline and non-crystalline minerals, organic matter and precipitated salts. The most abundant minerals in soils are quartz, feldspar and mica (together with amphibole, pyroxene and olivine called 'primary minerals'). The totality of organic substances comprises plant parts, microorganisms and humus,

---

[1] It should be noted that a "size-basis" -although widely found in literature- is not technically correct [Vitton and Harris, 1996]. Clay minerals can occur in particles with a diameter larger than 2 μm (Dennen and Moore [1986] consider the size limit to be 4 μm), thus clay mineral identification should be based on mineralogy, not on size.

the latter of which controls largely soil acidity [Sposito, 1989]. The type and concentration of natural salts in the ground is primarily a result of the climate and geology of the strata in question. Most commonly encountered are chlorides (for example NaCl), sulphates and carbonates of alkalies (for example Na_2CO_3), with chlorides mainly deriving from seawater (salt migration), whereas sulphates are usually associated with being the result of a weathering process [Obika and Freer-Hewish, 1990, Mitchell, 1993]. With regard to the current project sulphates as salt in the clay soil are of some significance and are discussed in more detail in section 2.7

2.2 Clay identification

X-ray powder diffraction is by far the most powerful tool with regard to day-to-day soil mineralogy identification. However, some soil components, such as poorly crystallised iron oxides, particularly when they occur in low abundance and very small grain sizes, are difficult to detect [Velde, 1992]. Clay particle identification can also involve the utilisation of a scanning electron microscope, which allows detection of the characteristic shapes of kaolinite (hexagonal plates), halloysite (elongated tubular crystals) or montmorillonite (thin bent plates of irregular shape) [Gillott, 1987]. Finally thermogravimetric analysis often supplements the information obtained by X-ray diffraction. Although the retention of surface water on particles is similar for all clay minerals, it varies as a function of the surface area of the crystal, and smaller crystallites will hold more water per unit mass [Velde, 1992]. The three basic "types" of water associated with clays are surface water, interlayer water and crystalline water and are released from the clay structure at temperature ranges of 100-110 °C, approximately 300 °C and 400-800 °C, respectively. Table 2.1 shows the typical temperature ranges and amounts of water loss for common clay minerals. However, impurities in the soil sample can mask clay peaks and thus lead to difficulties in interpretation of TGA results.

Table 2.1   *Weight loss [%] for some clay minerals during TG analysis [after Velde, 1992]*

Clay mineral	Weight loss [%]			
	0-110 $^\circ$C	200-300 $^\circ$C	500-600 $^\circ$C	>600 $^\circ$C
Kaolinite	1	-	14	-
Montmorillonite	12	3	4	-
Illite	1	2	5	-
Halloysite	7	-	13	-

2.3 Clay composition and clay structure

Generally, clay minerals are aluminosilicates, with a sandwich structure consisting of tetrahedral and octahedral sheets[2]. These sheets are formed from two fundamental building blocks which can be seen in Figures 2.1 and 2.2, and form the basic clay mineral structure. The silicon tetrahedron consists basically of a silicon atom "encapsulated" by four oxygen atoms. Bonding of the tetrahedron, to form a silica sheet of basic units (Figure 2.3) is through the basal oxygen atoms, which are shared by neighbouring tetrahedra. The positive valence of four, deriving from the silicon, is counter balanced by four surrounding oxygen atoms with a total negative charge of eight. However, due to the fact that every basal oxygen is connected to two silicon atoms, only one negative valance charge of the basal oxygen is left to be counterbalanced.
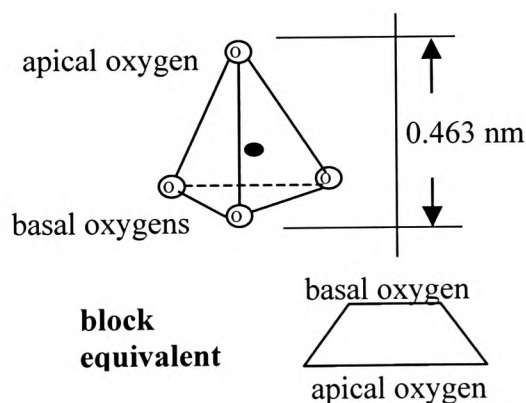
Figure 2.1 *Simplified diagram of the silica tetrahedron*

---

[2] Based on recommendations of the Clay Minerals Society, the nomenclatura as summarised by Bailey et al. [1971] is adopted as follows: atoms are arranged in a *plane*, basic structural units form a *sheet* and a *layer* of unit cells is composed of a number of sheets.

The other basic building block comprises cations (in most cases Al or Mg, rarely Fe, Ti, Ni, Cr or Li), which are surrounded by six oxygens or hydroxyl units, resulting in an octahedron. Isomorphous substitution of the tetrahedron (aluminium in place of silicon) and the octahedron (brucite (Mg) or gibbsite (Al)) may develop during the initial formation or subsequent alteration of the mineral [Mitchell, 1993].

**block
equivalent**

B=brucite (Mg)   G=gibbsite (Al)
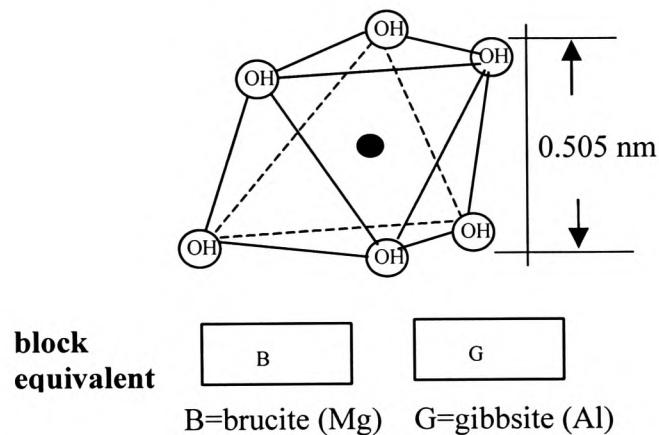
Figure 2.2 *Simplified diagram of the octahedron*
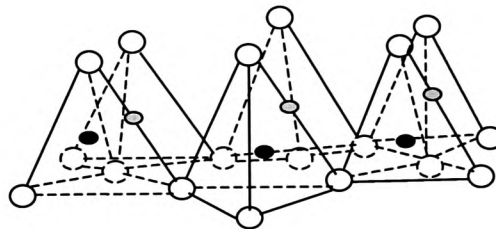
Figure 2.3 *Tetrahedral units forming silica sheet [after Grim, 1962]*

Clays are generally classified in layer types, depending on how the tetrahedral and octahedral sheets are stacked to form layers, and into clay groups, which are determined by the elements found in the different coordination layers. Differences among minerals within the clay mineral groups arise primarily from differences in the type and amount of isomorphous substitution within the structure (for example Al^{3+} instead of Si^{4+} in the centre of a tetrahedral unit). This presence of an 'unusual' cation, found in a space of a tretrahedral or octahedral unit, results (for replacement of a cation of higher charge with one of lower charge, for example Al^{3+} for Si^{4+} or Mg^{2+} for Al^{3+}) in a net negative charge. Ionic substitution appears to be the result of an effort to relieve stress deriving from the fact that slight differences in the size of octahedral and tetrahedral sheets lead

to a small misfit when stacked in layers [Gillott, 1987]. Electrical neutrality is obtained by the attraction of cations, which are either held between the layers or on the surfaces and edges of the particles. A large number of these attached cations are referred to as *exchangeable cations*, because they can easily be replaced by cations of another type, resulting in the cation exchange capacity of the clay minerals (unit: miliequivalents (meq^3) per 100 grams of dry clay). It should be noted, that the rate of cation exchange depends on various environmental factors, such as temperature, pressure, pH of the surrounding solution, thus clay minerals are allocated ranges of exchange capacity, a brief compilation of which is given in Table 2.2.

Table 2.2 *Cation exchange capacity of selected clay minerals [after Grim, 1962]*

	Cation exchange capacity [meq^3 per 100 gram of dry clay]			
	0	50	100	150
Kaolinite	▬ 3-15			
Montmorillonite			80-150 ▬▬▬▬▬▬▬▬	
Illite		▬▬▬▬ 10-40		
Chlorite		▬▬▬▬ 10-40		

The ease of displacement of cations depends mainly on valence, size and abundance of the various ions. As a general rule trivalent ions are held more tightly than monovalent ions and large cations are more readily replaced than small ones. Based on this, Mitchell [1993] gives a typical replacement series as

$$Na^+ < Li^+ < K^+ < Rb^+ < Cs^+ < Mg^{2+} < Ca^{2+} < Ba^{2+} < Cu^{2+} < Al^{3+} < Fe^{3+} < Th^{4+}$$
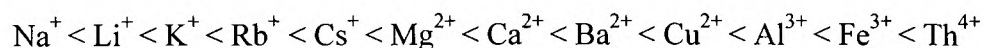
2.4 Layer types and interlayer bonding

A stack comprising one octahedral sheet and one tetrahedral sheet is referred to as a 1:1 layer. If the octahedral layer is brucite, a mineral of the serpentine subgroup ($Mg_6Si_4O_{10}(OH)_8$) results, whereas a combination of gibbsite and a silica sheet forms a mineral of the kaolinite subgroup ($(OH)_8Si_4Al_4O_{10}$). A similar linkage can occur on the other side of the octahedral sheet, where the "exposed" surface consists of OH groups. The resulting mineral montmorillonite belongs to the dioctahedral 2:1 layer group and has two surfaces formed by the hexagonal mesh of the basal oxygen atoms (Figure 2.4). The layer type 2:1+1, with a brucite sheet replacing the hydrated cation interlayer in, for example, a montmorillonitic clay mineral, results in minerals of the chlorite group.

It should be noted that there exist clay minerals in which the 1:1 or 2:1 layers are not electrically neutral. Charge balance in such minerals is achieved by an interlayer material, which may be individual cations as in the mica group (the interlayer ion is almost uniquely potassium [Velde, 1992]), hydrated cations as in smectites (Figure 2.4a) or octahedrally coordinated hydroxide groups or linked sheets of the latter, as in chlorite minerals [Brown, 1984]. If the *high* charge imbalance on the basic 2:1 structure of a mineral from the mica group is compensated by an interlayer ion, the latter is held *firmly* between the adjacent layers, bonding them together. In contrast, a *low* net charge
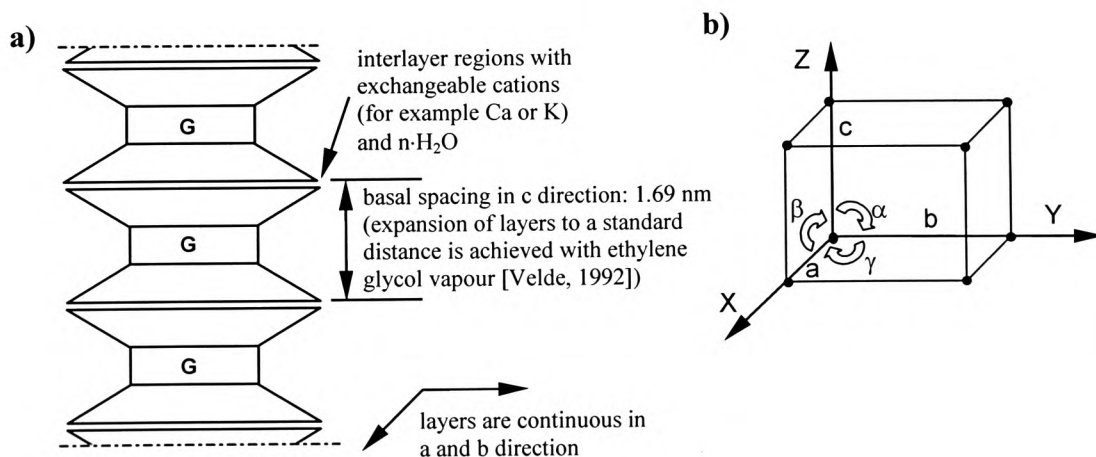
Figure 2.4 *Schematic diagram of (a) the structure of montmorillonite with repeat distances (a-b-c) based on (b) nomenclatura introduced by the unit cell of crystallography*

imbalance, as exhibited by smectites, is compensated by *loosely* held ions in the interlayer position. These ions can be easily exchanged in aqueous solutions and affect the swelling properties of the clay mineral. A smectite basal spacing of 1 nm in an anhydrous environment can increase to 1.5 nm in humid conditions and to 1.7 nm in wet conditions by acceptance of further polar molecules between the layers [Velde, 1992].

Bonds, holding layers together may be of several types with varying degrees of stability. Some of these bond types are susceptible to changes in environmental conditions, for example, when cations, needed for electrical neutrality, are located in positions controlling interlayer bonding. The introduction of sea water as a large cation source might then radically change the strength of the interlayer bonding and subsequently the expansive behaviour of the soil [Marshall, 1964, Grim, 1962]. Bonding between sheets of basic units is of primary valence type and very strong. However, the range of possible interlayer bonding forces is wide and the strength varies considerably. Marshall [1964] summarised the basic types:

i) van der Waals forces, holding neutral layers weakly together

ii) Opposing layers of oxygen and hydroxyls or hydroxyls and hydroxyl forming hydrogen and van der Waals bonding (for example in kaolinite), the former remaining stable in the presence of water

iii) Cations needed for electrical neutrality might just fit in the holes created by the arrangement of basic units in the plane and thus lead to strong bonding (for example in mica)

2.5 Swelling and related clay water interaction

Volume change in clay soils due to alternating phases of desiccation and soil suction can occur in depths of up to 8m and thus substantially affect not only shallow foundations but also underpinning or deep foundations [Chandler et al., 1992]. Krohn et al. [1980] calculated damage due to expansive soils in the USA at $7 billion in 1980 alone, whereas a cost estimation carried out by Holtz [1983] yielded about $6 billion in 1982.

It has been established that the effects of water on the behaviour of clay soils are largely determined by the clay mineralogy and structure. Mitchell [1973] summarises his studies into the influence of mineralogy and pore chemistry of clays by allocating the key role in swelling to the type and amount of clay mineral present, but also emphasises that they in return determine particle sizes and shapes, surface charge and interlayer bonding. However, as outlined by Terzaghi and Peck [1967], *all* clays have a tendency to swell when the confining pressure is reduced, particularly when the material is remoulded. During remoulding, clay particles are realigned into a more parallel orientation and attractive bonds, that may have existed between particles, are destroyed [Ladd, 1959, Grim, 1962, Gillott, 1987]. In addition, entrapped air results in air pressure built up within the sample and produces tension in the soil skeleton leading to subsequent slaking when immersed in water [Day, 1992].

With regard to swelling as a result of clay-water interaction, Mielenz and King [1955] have proposed two mechanisms. Swelling can either be caused by enlargement of capillary films, surrounding clay particles or it can be initiated by water imbibition of minerals with expanding structures (for example montmorillonite).

2.5.1 Interlayer swelling

Generally, three basic components form a clay mineral: a silica sheet, an octahedral sheet and a water layer. Previous sections introduced the first two parts. The third component is a structural water layer, which can be contaminated with various foreign ions. The rigidity of this water layer, the thickness of which can vary, is reduced with increasing thickness and it provides both, an interparticle bond and an interparticle lubricant. If its thickness increases, interlayer (=intracrystalline/interlameller/ intramicellar) swelling can be observed.

First suggested by Brindley and MacEwan [1953], it has been recognised for some years that structural charge imbalances have a profound effect on the swelling properties of clay minerals. As stated in section 2.4, low charge imbalances in clay minerals result in loosely held interlayer cations. Under conditions of some humidity and at temperatures below 100 °C, these cations can hydrate. Depending on the charge to diameter ratio of the ion, it will be hydrated with either three or six water molecules, the latter resulting in a two-layer interlayer water structure. As a general rule, the higher the temperature and the lower the relative humidity, the less water will be held on the cation in the interlayer [Velde, 1992].

Mitchell [1973] discusses the reduced swelling when cation-hydroxyl interlayers (for example Fe-OH or Al-OH) form in clay minerals, resulting in reduced cation exchange capacity and changed basal spacings. These interlayer materials appear to bind adjacent layers more strongly together. Research carried out by Foster [1953 and 1955] showed, however, that swelling is mainly influenced by octahedral substitution in dioctahedral structures and that there is no consistent relationship with cation exchange capacity.

2.5.2 Clay mineral surface/water interaction

In addition to interlayer swelling, a second mechanism, resulting from clay mineral surface-water interaction, has to be discussed. The associated clay-water interactions result, over a certain range of moisture contents, in the appearance of the clay as a liquid slurry, a plastic material and eventually a brittle solid. On moisture uptake there is generally a volume increase, whereas moisture loss is accompanied by shrinkage. Clay particles, as previously discussed, develop electric charge and – when in contact with water- form a 'diffuse electrical double layer' (Figure 2.5). Oriented water, directly adsorbed on the surfaces of the clay minerals, has a thickness of approximately 5 to 10 molecules [Grim, 1962]. In the case of kaolinite, a monolayer of water molecules is weakly adsorbed. Amongst both the water molecules themselves, and between them and the atoms in the basal plane, stability is gained by hydrogen bonds [Sposito, 1989]. The high adsorption values exhibited by, for example, montmorillonites are a consequence of their ability to disperse into extremely small particles, resulting in a large adsorbing surface. The adsorption potential is further influenced by the type of cation (resulting from isomorphous substitution) balancing negative charges on the clay surfaces and the

density of electric charge. Mitchell [1973] speculates that substitution might result in less cation dissociation and thus a thinner diffuse double layer. He subsequently expects less swelling.
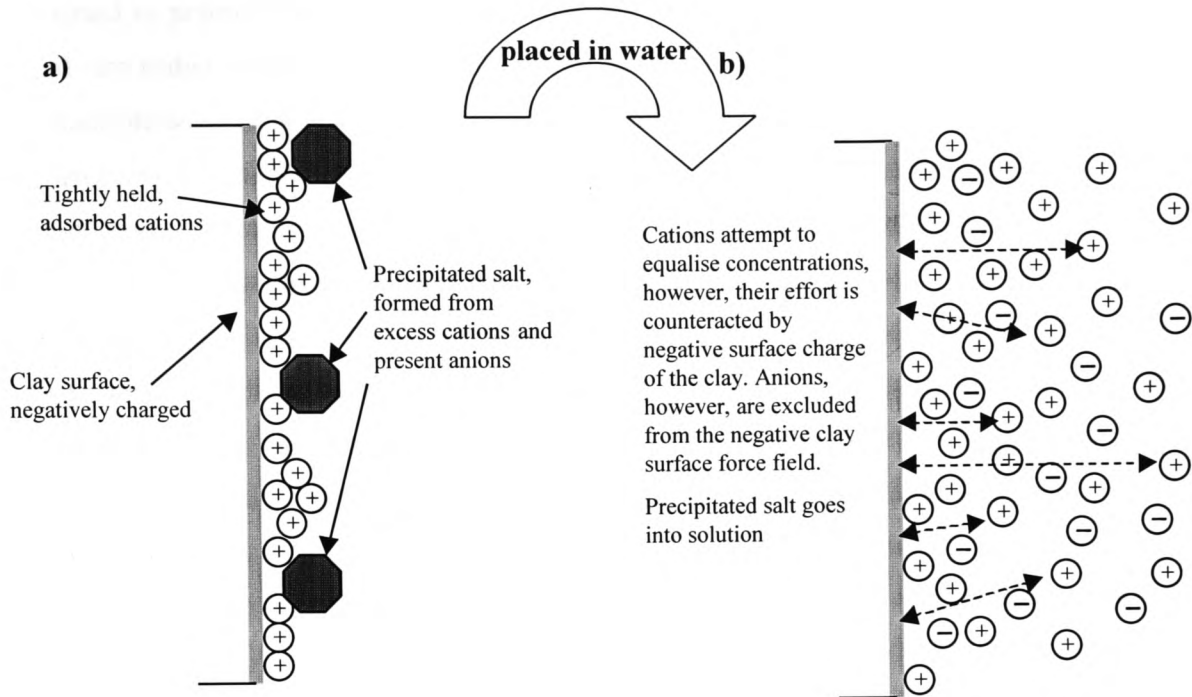
Figure 2.5 *Changes to the clay microstructure when placed in water*

  a) dry clay   *b) formation of diffuse double layer*

2.6 Engineering properties and performance of clays

It has been established that engineering properties directly related to water access, such as permeability and reaction to frost action of soils, do vary with clay fraction and clay mineral type in the material. In addition to the clay mineral composition, however, the performance of clays is also a function of factors such as the presence of organic matter, particle size distribution, non clay mineral composition and entrapped pore solutions and air. The arrangement of clay particles with respect to each other (for example parallel or random arrangement of clay minerals) and the stress history of a clay material is directly reflected by the performance of specimens when subjected to compressive or shear strength testing. Thus knowledge of soil composition provides indications of the probable performance of a soil with regard to its engineering properties and their variability and sensitivity to changes in environmental conditions.

2.6.1 Strength development

The strength determination of the pure clay minerals is generally of little use with regard to practical applications because strength varies considerably when sand/and or silt are added. Milenz and King [1955] replaced up to 50% of a sand with clay minerals (kaolinte/and or sodium-montmorillonite) and obtained a clayey mix with higher compressive strength than that of sand or pure clay alone. However, no clear trends, i.e. continuous strength increase with increase in replacement level could be established.

It is generally accepted that the total shear strength parameters (cohesion and angle of internal friction) of a clay soil, depend mainly on its degree of saturation, mineralogy and test conditions. However, the effective cohesion c', for saturated clay mineral samples, as reflected by the cohesion intercept on the y-axis of the effective failure envelopes (Figure 2.6), is either zero or very small [Lambe and Whitman, 1979, Mitchell, 1993].

Mitchell [1993] emphasises that a significant true cohesion, when defined as strength in the absence of any loading pressure, does not exist in the absence of chemical bonding, i.e. added stabilising agents.
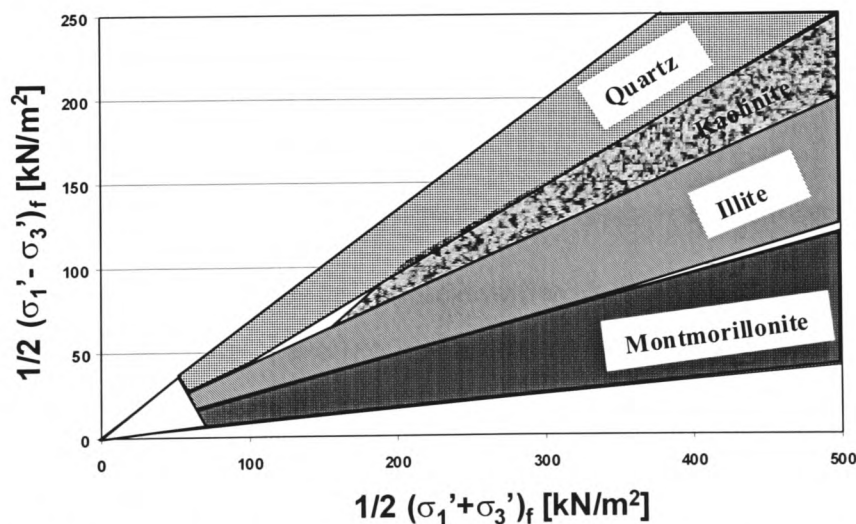
Figure 2.6 *Ranges of effective stress failure envelopes for pure clay minerals and quartz [after Olson, 1974]*

In effective strength terms, i.e. when the created pore water pressure is allowed to dissipate during shearing, the basic factor responsible for soil strength, depending on its mineralogy, is thus the friction angle, resulting from inter-particle friction,

rearrangement and crushing of particles under normal stress (see Figure 2.6). Chattopadhyay [1972] found good agreement between the interlayer bond strength of pure clay minerals and the observed angle of friction. However, Mitchell [1993] also emphasises the importance of factors such as surface roughness and thus size of solid contact area, electrical forces of repulsion and attraction and contamination of "clean" clay particle surfaces with adsorbed contaminants. All these factors result in difficulties when direct measurements of the friction of clay minerals are attempted.

Total shear strength parameters showed increasing cohesion and reduced friction as a result of an increase in both plasticity index (reflecting type and amount of clay minerals in a soil) and activity (equ. 2.1) [Mitchell, 1993].

$$\text{activity} = \frac{\text{plasticity index}}{\text{fraction} \leq 2 \ \mu m \text{ expressed as \% of dry weight}} \qquad \textbf{(equ 2.1)}$$

Clay activity, introduced by Skempton in 1953, varies with type of exchangeable cations in the clay minerals. Typically it may range, for example, from 0.5 to 7 for montmorillonites, from 0.01 to 0.41 for kaolinites and from 0.23 to 0.58 for illites. The high values for montmorillonites are interpreted as a consequence of their ability to disperse into extremely small particles resulting in a large adsorbing surface area. This leads to a high plasticity index and subsequently high activity. Thus, active clays (activity≥1.25) would generally be expected to have a comparably high water-holding capacity, high cation exchange capacity and thus exhibit a high degree of variation with regard to their engineering properties [Grim, 1962].

2.6.2 Permeability

Due to their characteristic size, clay minerals have a tendency to block the pores within the grain skeleton of silt, sands and gravel and result overall in a reduction of permeability. However, in addition to the filling of voids and thus the reduction of water flow in a mechanical way, clay particles affect permeability depending on their mineral composition, exchangeable cation composition and their degree of saturation.

Samules [1950], investigated the influence of various exchangeable cations on the permeability of kaolintie and montmorillonite under pressure and was thus able to modify and monitor the influence of the void ratio in the samples. In addition to an

increased coefficient of permeability with increased void ratio, he found that the increase is relatively small when sodium is the exchangeable ion. However, exchange with ions of higher valance, such as Al^{3+} or Th^{4+}, results in more significant changes to the measured values. Grim [1962] suggests that in addition to the dispersing effect of the cations, their effect on permeability originates mainly from their influence on the nature and thickness of water adsorbed on the clay mineral surface, i.e. the diffuse double layer. This might result in changes to flow through the clay because of modifications to the dimensions of pore space and also due to interference of the movement of the liquid against an adsorbed outer molecular layer of water, surrounding the clay grain.

2.6.3 Frost action

2.6.3.1 General

The effects of frost action and subsequent thawing periods can be visible on a scale ranging from dimensions of fractions of a millimetre up to several metres, manifesting themselves in translocation mechanisms, soil heave, consolidating processes, fine and coarse particles and microscopic disturbances [Van Vliet-Lanoë, 1985]. These phenomena were first investigated on a laboratory scale when electric refrigerators became commercially available in the 1930s. Earlier findings by Buoyoucos [1920], suggesting that water in soils does not all freeze at one temperature, had been reported using data from natural trials, in which specimens had to be kept outside on cold winter nights when the temperatures were sufficiently low. Taber [1929] was amongst the first researchers to investigate the mechanisms by which soil heaves during frost action. Until he published his results it was generally assumed that heaving was the result of approximately 9.1% volumetric expansion of existing moisture in the soil during freezing. This change in volume was first recorded as early as 1765 by E O Runeberg who stated that "*it is no wonder then, that a clay layer can displace a load that rests on it, when the water freezes*" after he had determined the water content of a frozen piece of clay. Taber, however, replaced water with liquids which actually solidify during freezing with a decrease in volume (nitrobenzene and benzene) and still observed heave in clay samples. Thus he concluded that other mechanisms must be responsible for heave due to frost action in addition to the volume change on freezing. After having published much of his experimental work in 1929, he subsequently [1930] suggested a

more detailed plausible theory for the mechanisms behind heave relating to the formation of ice lenses, which was later greatly extended by Beskow [1935].

2.6.3.2 Mechanism of frost heave in soils

If a soil is subjected to subzero temperatures, all phases comprising the soil system (soil particle network, pore water and pore air) are affected and respond to the reduced ambient temperature. Most changes, however, happen in the area where the heat loss leads to the formation of ice-liquid interfaces. Water has a tendency to move from warm to cold areas, due to changes in the chemical potential of water at different temperatures (thermo osmosis) [Marion, 1995]. The pressure of the growing ice lens is exerted in the direction of growth of the ice lens, which is parallel to the direction of the heat flow rate. At the freezing front, the ice tends to form as a pure phase, leaving impurities behind and thus increasing the concentration in the remaining liquid in contact with the ice. The resulting capillary osmosis, endeavouring to achieve a solute equilibrium near the ice-liquid interface, creates an even stronger sink for liquid water close to the freezing front. The original model, often referred to as the "primary heaving model" outlines that the thin water film between the ice lens and the soil particles, on which the ice lens grows, retains its integrity until the liquid source is exhausted. Figure 2.7 illustrates the ice-water transition zone. Water migrates to this region due to the osmotic effects described above and as the water molecules 'link' onto the solid ice the soluble atoms are rejected, thus increasing the solute atom concentration of the water at the interface. This will result in more water being drawn to this area. As the ice front moves downward from the 'cold' surface to the 'warm' interior, the upward forces crated by the rising water cause the frozen layer to rise. If the liquid supply is finally exhausted, the growth of the ice lens will stop. This theory, which assumes a planar ice-liquid interface, does not explain the formation of new lenses ahead in the distance. Therefore Miller [1977], introduced a "secondary heave model", which incorporates a "frozen fringe" in order to provide a plausible explanation of the mechanisms involved. Figure 2.8 illustrates schematically the difference between the original primary heave model (in continental Europe also known as the "Everett model") and the secondary model, introducing the frozen fringe.
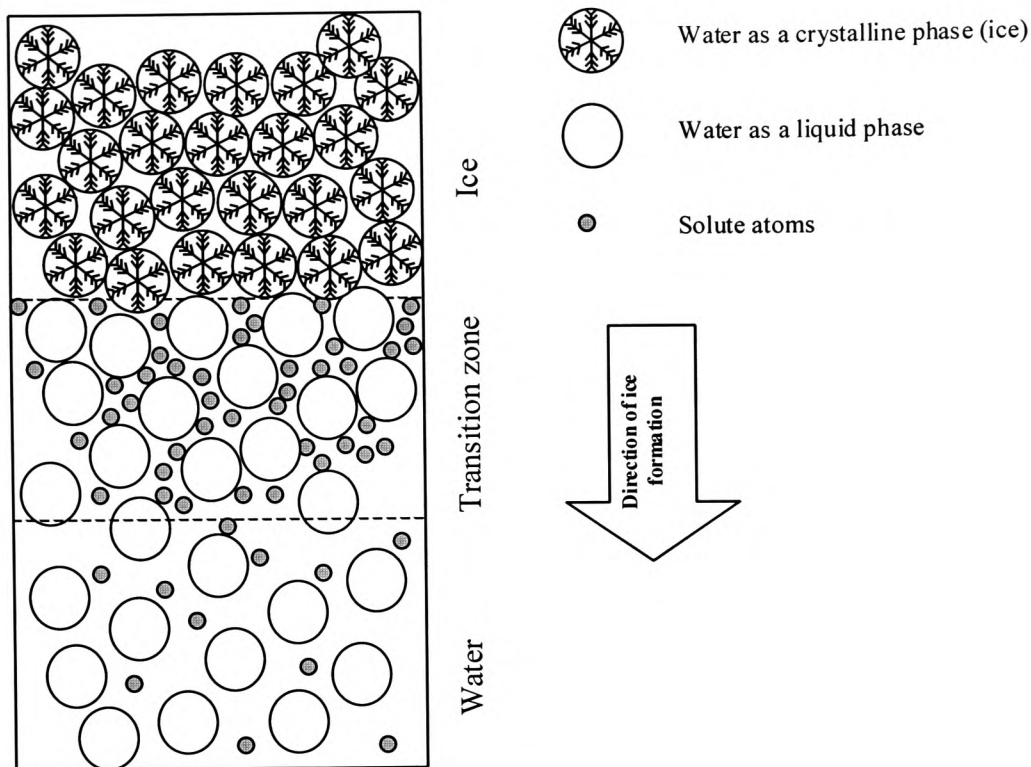
Figure 2.7 *Ice-water transition zone*

In order to obtain a comprehensive engineering frost theory for incompressible fine-grained soils, Konrad and Morgenstern [1980] modelled a freezing soil and characterised it by two parameters, the segregation freezing temperature T_s, which develops independent of variation in the cold side temperature to which a soil is exposed, and the overall permeability of the frozen fringe k_f. They assumed that the permeability of the frozen fringe is comparably low and thus reduces the amount of water which is attracted by the forming ice lens. A value for k_f lies in the region of 0.8 x 10^{-9} cm/s. The frozen fringe tends to thicken with time, resulting in a further decrease in its permeability. Water has more and more difficulty getting to the ice lens and supplying the molecules necessary for further growth. Finally water migration will stop completely below the growing ice lens and a new ice lens will be initiated there just behind the frozen fringe. In 1981 Konrad and Morgenstern introduced the segregation potential (SP), an input parameter to the model which reflects the physics of the frozen
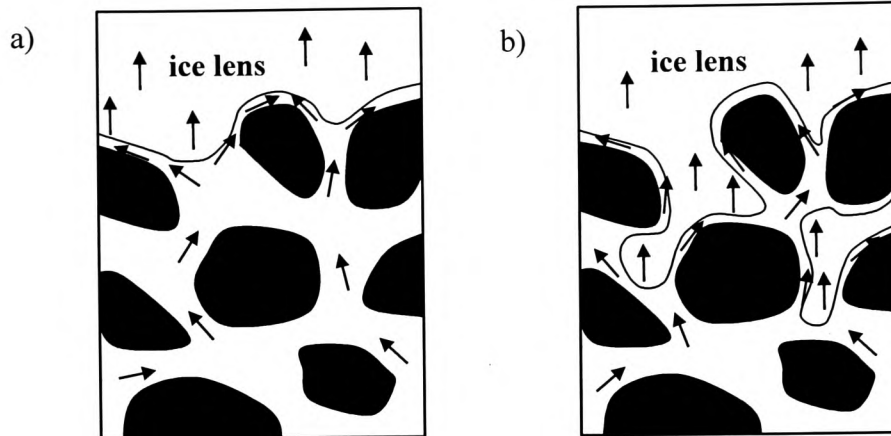
Figure 2.8   *a) Primary heaving in the mode visualised by Taber and Beskow*

            b) secondary heaving [after Miller, 1980]

fringe and allows the calculation of the moisture migration rate v_u (=water intake flux) (equ. 2.2) as a function of the average temperature gradient across the frozen front T_f:

$$v_u = SP \times grad \ T_f \qquad \textbf{(equ. 2.2)}$$

Values for SP range, for example, for Saint Alban clay between 450 to 600 x 10^{-5} $mm^2/(s \cdot °C)$ and higher values are associated with a higher degree of frost susceptibility. They do, however, vary with geological factors such as soil porosity, structure, mineralogy, specific surface and solute type and concentration in the pore fluid.

2.6.3.3 Factors influencing the effects of frost action

There is mutual agreement about the general factors influencing ice lens growth and thus frost heave in soils. These include pore size distribution, solute concentration, water availability, freezing rate and external pressure. The pore size distribution is of particular interest because not all water in the soil structure freezes at a temperature below 0 °C. Depending on the diameter of the pore in which freezing takes place and the concentration of the pore liquid, the eutectic point at which ice nucleation will start,

can be as low as –40 to –50 °C [Miller, 1980]. The highest point (below a temperature of 0 °C) at which ice could form and exist in a soil mass is called the freezing point depression. For an ice nucleus to be stable at –1 °C its radius must be larger than 59 nm, based on an equation derived by Lindmark [1999]. This requires that 26 million molecules adopt the appropriate structure simultaneously. If the temperature, however, is reduced to –30 °C, only 290 molecules are required to form the initial ice core. This phenomenon, which makes the formation of ice far more likely in the latter case is called super-cooling.

The pore size distribution controls capillary rise, soil suction and hydraulic conductivity, all of which have influence on the rate of movement of water through the soil to the freezing front. In addition, the pore size distribution and the porosity depend on the particle size distribution within a given soil mass. Thus, the effect of fines content (d<75 μm) on the frost heave of crushed limestone was investigated by researchers at the US Army Cold Regions Research and Engineering Laboratory [Tester and Gaskin, 1996]. They found that there exists a linear relationship between an increase in the fines content of the material and the rate of frost heave observed. A threshold percentage of fines content beyond which the heave would all of a sudden increase, could not be identified. It should be noted, however, that frost susceptibility criteria based on grain size distribution measurements, are only of limited significance in comparison to those, involving pore size parameters. The advantage of the latter is that the variation of compaction variables such as density and moisture content are also taken into account, because they directly affect the pore size distribution but not the grain size distribution of the soil in question [Reed at al., 1979].

Water availability is obviously of significance during frost action in any material. Depending on whether the access of water during a freeze test in the laboratory is inhibited or not, the terms 'closed' and 'open system' are used. Burns [1977] showed that the water migration and thus the resulting frost heave is greatly reduced, when the water table in a soil is lowered, thus emphasising the importance of good drainage conditions for applications in practice.

Generally, the movement of water and its redistribution within a given soil mass is described by the potential energy of the water. By definition, water tends to move from a higher to a lower potential [Anderson et al., 1978]. The total potential within a soil matrix is the sum of the matric, gravitational, pressure (=submergence), temperature and osmotic potential. The matric potential, which is negative above the water table, arises

mainly from capillary suction and is a characteristic of the soil in question. The other potentials depend on the influence of external factors such as the presence of solutes (osmotic potential), overburden weights (pressure potential), different temperatures or differences in height (gravitational potential). Although movement in the gas phase is insignificant in saturated soils, water can move either as vapour or in the liquid state. Even in the frozen zone of the soil, water transport is of significance and is mainly temperature induced. Mageau and Morgenstern [1980] suggested that the migration rate is mainly controlled by the apparent permeability of the frozen soil. The permeability is reduced by an increased tortuosity of the pore structure deriving from the pore blocking effect of ice crystals forming in the structure of the soil during freezing. In addition to transport through the existing soil-ice-pore structure, water transport on an even more microscopic scale along a liquid film separating ice from the mineral grains in the frozen soil will take place even at temperatures around –15 °C. Harlan and Nixon [1978] outline that, depending on the water migration rate to the freezing front, the speed with which the freezing front progresses varies. Based on the fact that the amount of liberated heat during freezing is greater in the case of a fully saturated soil in comparison to a partially saturated one, they concluded that the more extensive heat transfer in the former case results in a slower advance of the freezing front.

2.6.3.4 Effect of frost action on clays and their engineering properties

Freezing of frost susceptible soils such as clays in open systems (i.e. with water available in abundance), results in ice segregation, frost heave and also affects the engineering properties of the material. Clay soils generally consolidate during freeze-thaw action and their density increases due to particle rearrangement [Chamberlain, 1989]. Although one would then expect the permeability to decrease as well, Chamberlain and Gow [1979], who conducted a comprehensive study on the effects of freeze-thaw cycling on four fine-grained soils, observed an increase in the coefficient of permeability of up to three orders of magnitude. They attributed this to the formation of shrinkage cracks, which were created during the frost phase and further widened by flow of melting water during thawing in clays with plasticity indexes ranging from 0 to 20. White and Williams [1994] also observed a pattern of overall increase in permeability for three silty clays investigated in their study, however, Moley clay from France with high plasticity exhibited a slightly reduced coefficient of permeability after

10 freeze-thaw cycles. Yong et al. [1985] compared the behaviour of sensitive Matagami Clay, originating from Quebec/Canada, after freeze-thaw cycling to the results obtained from investigations carried out on laboratory-prepared soils (kaolinite and bentontite). A significant decrease in the liquid limit of the natural clay was observed, which was attributed to the aggregation of soil particles due to freezing. The laboratory clays, however, showed little change, the reasons for which could lie in the absence of initial bonding of the remoulded material, the mono-mineralic nature (no organic compounds or amorphous materials) or an already initially dispersed fabric of the 'artificial' soils. In addition a reduction in the cation exchange capacity and specific surface area was observed, accompanied by a significant decrease in the undrained shear strength. Czurda and Schaeberle [1988] could not confirm any changes in the cation exchange capacity of a quaternary clay after frost action, however, Na-bentonite exhibited a small surface area reduction. The significance of specific surface was also pointed out by Rieke et al. [1983], emphasising early findings by Beskow [1935] with regard to its influence on the adsorbed water layer on the surface of soil particles. Based on their observations of the behaviour of sand-kaolinite-montmorillonite mixes, the introduction of a fines factor R_f (equ. 2.3) is an attempt to relate the liquid limit and its correlation to specific surface of the fines fraction, to frost heave susceptibility of the sand-clay mixes.

$$R_f = \frac{\text{Fines fraction in soil [\%]} \times \text{Clay sizes in fines fraction}^3 \text{ [\%]}}{\text{Liquid Limit of the fines fraction [-]}} \qquad \textbf{(equ.2.3)}$$

However, it should be noted that the equation for R_f was derived based on a modified definition of the activity of a soil sample, in which the liquid limit is employed in the numerator instead of the plasticity index. Also the activity is associated with the fines fraction only, rather than the whole soil sample. These modifications appear somewhat arbitrary, however, a reasonable correlation between an increase in R_f and an increase in the segregation potential of the investigated soils, as an indication of their increased frost susceptibility, could be shown.

A number of researchers [Czurda and Schaeberle, 1988, Chuvilin and Yazynin, 1988, Chamberlain, 1989] emphasise the influence of the mineralogical composition of the clays on aggregation and water mobility during frost action. A more prominent

aggregation in the presence of monovalent ions (Na^+) in comparison to bivalent ions (Ca^{2+} and Mg^{2+}) made Chuvilin and Yazynin [1988] conclude that dehydration during formation of ice lenses leads to a higher availability of fine grained material capable of aggregation. The increase in microaggregates for a montmorillonitic clay was found to be only around 12 %, whereas kaolinite showed an increase in microaggregation of around 200%. The reason for this could be the fact that monovalent ions have generally a bigger mobility than bivalent ions in the pore fluid, which seems to be due to a smaller need of hydration energy [Czurda and Schaeberle, 1988]. Yong et al. [1985] agree that the pore fluid chemistry might be a governing factor for inducing particle aggregation which they observed during the freezing of natural Matagami clay. The current author feels that an increase in solute concentration might compress the diffuse double layer and thus allow the particles to move together more closely, forming floccs. However, Yong et al. [1985] outline that natural bonds between fabric units will be broken by pressure exerted by growing ice lenses and new bonds due to compression of the soil structure will form subsequently and result in aggregation. These bonds are suggested to be rather weak in nature and thus relatively unstable.

2.7 Occurrence of sulphates in clay soils

In Great Britain sulphates occur widely in the major Mesozoic and Tertiary clay formations, particularly as sulphates of calcium, magnesium and the alkali metals in various quantities [Bessey and Lea, 1953]. Design recommendations for concrete structures, published by the Building Research Establishment [1991] identify strata of London Clay, Lower Lias, Wealden Clay, Oxford Clay, Kimmeridge Clay and Mercia Mudstone (Keuper Marl) to be the most likely clay types to contain larger amounts of sulphates , although other authors [Bessey and Lea, 1953, Department of Environment, Transport and the Regions, 1999] point out that some of these clays are frequently covered with superficial, substantially sulphate-free deposits. Salt damage to cement or lime-stabilised soils or concrete structures, buried in the ground, has been reported by a large number of researchers and has led to increased awareness amongst engineers with regard to possible interference when sulphates are present in clay soils.

---

[3] Fines fraction is here defined as particles with a diameter ≤ 74 µm

The concentration of sulphates varies considerably with depth and as a general rule, the amount of sulphates encountered increases with depth. This is mainly due to sulphates being re-deposited at the bottom of the weathering zone after the leaching action of rainfall over the past millenia [Sherwood, 1992, Sposito, 1989]. The intensity of this "downward" movement due to leaching action and subsequent precipitation is governed by the solubility of the minerals and conditions on the earth's surface. Typically some potassium sulphates or even hemihydrate ($CaSO_4 \cdot 0.5H_2O$), a form of calcium sulphate, are found at the top of soil profiles as they dry through evaporation [Sposito, 1989, Doner and Warren, 1977].

The most commonly encountered sulphates are *calcium sulphate* in the form of gypsum ($CaSO_4 \cdot H_2O$) or selenite, *sodium sulphate* (Na_2SO_4) as mirabelite ($Na_2SO_4 \cdot 10H_2O$) and *magnesium sulphate* ($MgSO_4$) as, for example, epsomite ($MgSO_4 \cdot 7H_2O$). It should be noted that the stability of sulphate salts varies with temperature and that they exhibit various values of solubility. The solubility of gypsum of approximately 1.4 g SO_3 per litre can be considered almost negligible in comparison to solubility values of beyond 225 g SO_3 per litre for magnesium and sodium sulphates and thus emphasises the importance of clear sulphate identification to assess the possible impact on buried structures.

It is now generally accepted that many geological strata may in addition to sulphates contain sulphides, which can decompose due to oxidation and subsequently contribute to the formation of sulphates. Sulphides are the result of a chemical reduction phase in acid sulphate soils, for example initiated by intensive leaching by fresh water [Sposito, 1989]. Because of its sulphate requirement during formation, in addition to sources of iron and sulphate reducing bacteria, sulphide accumulation can mainly be found alongside coastal margins or in basins of river deltas [Doner and Warren, 1977]. Sulphides are commonly encountered in the form of iron sulphides as either pyrite, marcasite (FeS_2) or pyrrhotite (FeS), with pyrite being the most abundant [Deer et al., 1992].

The oxidation of pyrites is overall a comparably slow reaction with optimum conditions being with a temperature range of 25 to 45 °C and a pH range of between 1.0 to 2.5. However, the reaction can be catalysed by the bacterium Thiobacillus ferrooxidans, which is commonly found in acid sulphate soils (pH range 1.5-5.0) and soil exposure to the atmosphere, ensuring an ample supply of oxygen and carbon dioxide (the latter

being the sole source of carbon for the micro organism, controlling its growth rate) [Jackson and Cripps, 1997].

The oxidation of pyrites (FeS_2) occurs on reaction with air and/or ground water and results in the formation of ferrous sulphate and sulphuric acid (Fasiska et al., 1974):

$$2FeS_2 + 2H_2O + 7\ O_2 \rightarrow 2FeSO_4 + 2H_2SO_4 \qquad \textbf{(equ. 2.4)}$$
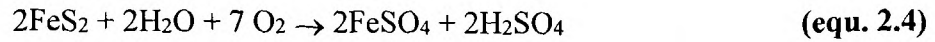
A possible second step could either lead to the oxidation of ferrous sulphate to ferric sulphate (equ. 2.5) [Thomas et al., 1989],

$$(4FeSO_4 + O_2 + 2H_2SO_4 \rightarrow 2Fe(SO_4)_3 + 2H_2O \qquad \textbf{(equ. 2.5)}$$
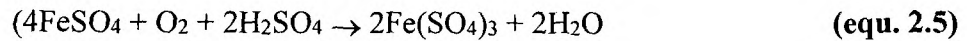
or – in the presence of calcium carbonate – to the crystallisation of gypsum (accompanied by a volume increase) [Doner and Warren, 1977, Gillott et al., 1974]. In a noncalcareous environment Gillott et al. [1974] reported the formation of jarosite.

Various factors affect the distribution of sulphates and oxidised sulphides in the ground (Figure 2.9), resulting in randomly distributed concentrations over different depths.
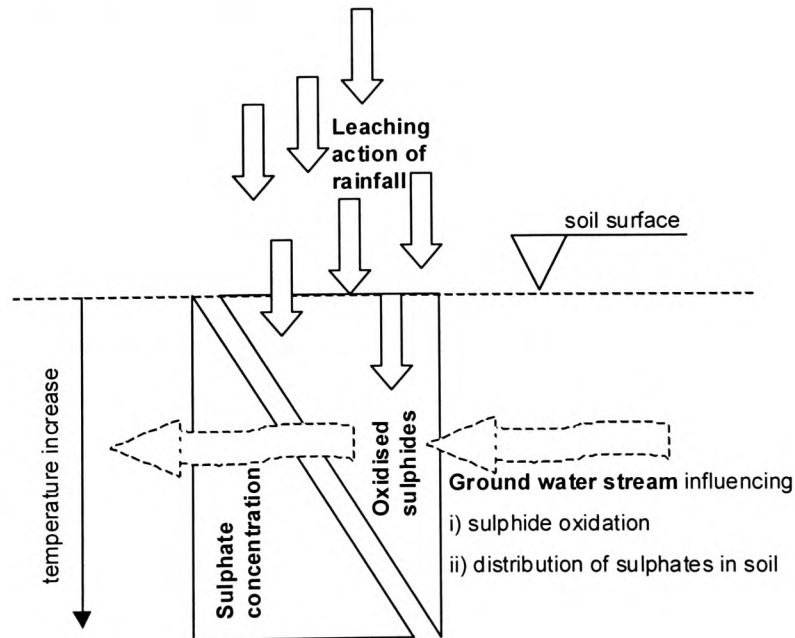
Figure 2.9 *Factors influencing the distribution of sulphates/oxidised sulphides in the ground*

Thus, detailed ground investigations are highly advisable in order to obtain complete information about the distribution of sulphates and sulphides within the soil profile. With regard to the engineering properties of soils, sulphates particularly influence the behaviour during frost action. Sulphate salts, when present in the pore fluid, lower the freezing point of water and lead to a freezing point depression. Depending on the solute type and the solute concentration, a solution will remain liquid, when the temperature drops below 0 °C. When ice starts to precipitate, it excludes the solute from the crystal. Precipitation will continue until the solution is cooled to a point at which the residual solution (now at a much higher concentration) solidifies [Marion, 1995]. This temperature is known as the eutectic temperature of a solution. Water will travel from regions of low solute concentration to high-solute regions and thus the high solute concentration prevailing at the ice-liquid interface of a soil tends to act as a sink for further pore liquid from the surrounding area. Nevertheless, Sheeran and Yong [1975] stated that due to desiccating mechanisms of the soil ahead of the ice-liquid interface, initiated by the "high suction region" (due to high solute concentrations), the water transport to the ice lens could be reduced. This could be the explanation for an observation made by Beskow [1935]. He noted that the addition of a sulphite leachate to a clayey silt resulted in heave reduction with increasing concentration of the solution and subsequently suggested this as a remedy for frost susceptible soil.

Chapter 3 - Soil stabilisation – methods, mechanisms and deficiencies

In this chapter the reader is introduced to the classic soil stabilisation methods with lime and/or cement and their effects on the relevant engineering properties. The interactions between sulphates and stabilised ground are outlined and a separate section is dedicated to modified freezing mechanisms when soil is stabilised and thus partially cemented.

3.1 The need for soil stabilisation

In an attempt to utilise the most abundant and least expensive construction material available, man's creativity has developed over the millenia and led to a wide range of soil improvement techniques. By *wetting, drying, heating, freezing, pounding on, vibrating, pushing and driving things into, squeezing water out of and mixing in* of sometimes exotic additives such as horsehair or shredded tyres, man has modified soil properties in such a way that it has allowed him to utilise the improved material for use in and for support of his structures [Mitchell, 1982]. Lack of suitable raw material has always been and still is the primary reason to add stabilising agents. The Assyrians, for example, added lotus to a water-clay mixture in order to obtain a suitable raw material for bricks (3000 BC). In a very early effort to recycle waste in the stabilisation of ground, which is more symptomatic for the last decades of our century, the Aryans added broken pottery to the sub-base of roads (800 BC).

Currently considerations with regard to sustainability, the limited availability of primary resources, such as imported crushed rock, the speed of construction progress and the reduction of off-site construction traffic have led to more economic and environmental awareness. This has changed the way in which stabilisation techniques are perceived and an appropriate technique is chosen. However, not only has the motivation for soil stabilisation changed but also more recently the range of methods has been greatly extended. Whereas classic soil stabilisation techniques, involving the addition of lime and/or cement are still widely used, researchers have also identified other suitable materials, such as shredded tyres or power station wastes (pulverised fuel-ash and

furnace bottom ash), as possible stabilising agents. More rarely encountered are stabilisation methods utilising thermal treatment or the addition of bitumen or acids.

3.2 'Classic' soil stabilisation methods

Records published by the UK stabilisation contractors show a general increase in the use of cement and lime for soil stabilisation from 1982 onwards, which Slavin [1999] attributes to government action such as the introduction of new road building programmes and the expansion of airports. The sales figures have, however, soared since 1996, with the introduction of the landfill tax (Figure 3.1). Early estimates for 1999 lie in the region of 2 million m^3 of soil improved by the addition of lime and/or cement [Greaves, 1999].
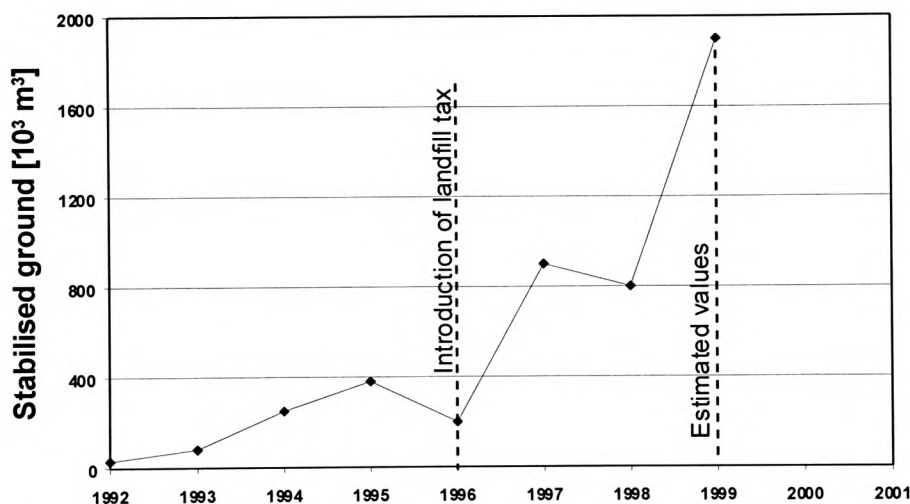
Figure 3.1 *Development of the UK market for soil stabilisation*

Figure 3.2 [after Vosteen, 1993] gives an overview of the suitability of the classic soil stabilisation techniques depending on the grain size distribution of the soil in question (the grain size distribution of kaolinite, used for the current project, is added for information). However, in practice other suitability criteria such as clay/soil mineralogy, organic matter and the presence of sulphates or sulphides have to be taken into account in order to choose the adequate stabilising agent for a given case. It should be noted that there is a wider range of stabilisation methods available, including exotic techniques such as thermal treatment (with heat or cold) or stabilisation with various chemical

additives. For the scope of the current project only the mechanisms induced by lime and/or cement stabilisation are of importance and thus discussed in more detail.
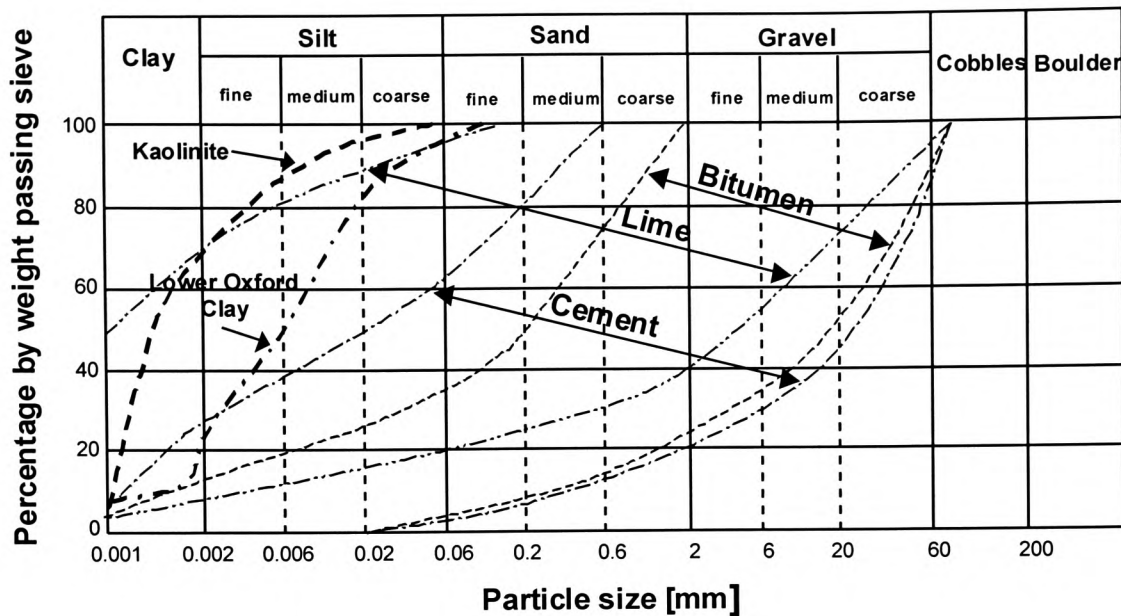
Figure 3.2 *Grain size distribution ranges for lime, cement and bitumen stabilisation*

3.2.1 Lime stabilisation

Early evidence for the use of lime in the stabilisation of soils with poor engineering properties dates back more than 5 millenia, when the pyramids of Shensi on the Tibetian-Mongolian Plateau were built using a compacted mixture of clay and lime, with the added lime resulting in improved strength and workability of the soil used for the building blocks [Mitchell, 1982]. This double effect of lime addition, resulting in an immediate soil modification and a more long-term stabilisation effect has been investigated by a large number of researchers. Lime can be added either in the form of calcium oxide (CaO='quicklime') or calcium hydroxide (Ca(OH)$_2$='slaked lime'), the former of which has the additional advantage of resulting in a 'drying out' effect due to chemical removal of water and the the exothermic nature of the chemical reaction. The CaO reacts with water in the soil and is transformed to calcium hydroxide (equ. 3.1).

$$CaO + H_2O \rightarrow Ca(OH)_2 + heat\uparrow \qquad \textbf{(equ. 3.1)}$$
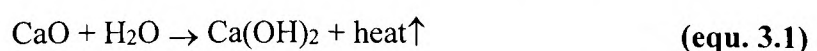
Rarely encountered for soil stabilisation purposes in Great Britain are dolomitic limes, some of the calcium in which is substituted by magnesium [Sherwood, 1992, Transport Research Board, 1976].

The amount of lime needed to obtain long-term strength changes is usually determined from observations of the pH development of a soil slurry after the addition of various percentages of lime. It is referred to as 'the initial consumption of lime (ICL)' according to BS 1924: 1990: Part 2 (Stabilised materials for civil engineering purposes) and is explained in more detail in section 6.1. It should be noted, however, that results of this test have been described as both 'inconsistent and excessively conservative' by Rogers et al. [1997]. With the results of the ICL test depending on the clay mineralogy, some clays even respond in such a way that a pH equivalent to that of the saturated lime, i.e. 12.4, is not achieved. Nevertheless, substantial stabilisation success was reported when lime was added to such clays, amongst which Rogers et al. identified English China clay. This is the clay which is utilised for large parts of the current project. The current author generally agrees with the criticism of the ICL test and considers that it often fails to identify the most economic approach with regard to the required quantity of lime to be added to the soil. Figure 3.3 [after Rogers et al., 1997] outlines an improved and less conservative interpretation of the full pH vs lime addition curve.
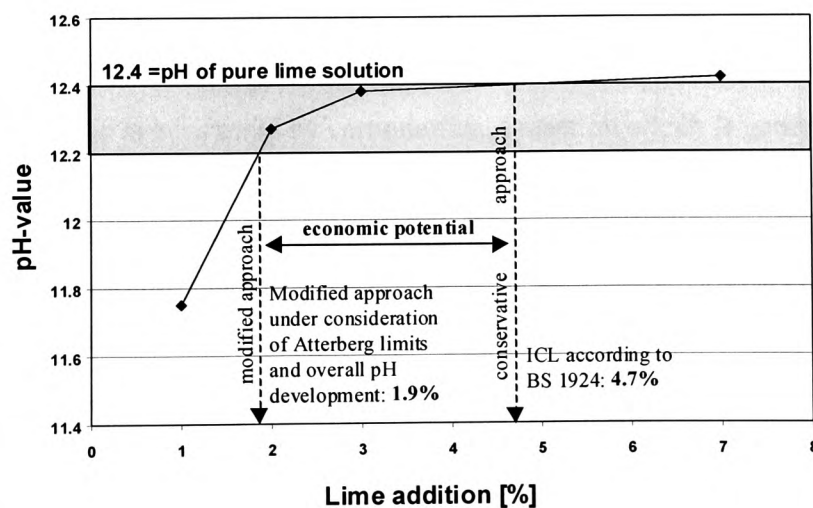
Figure 3.3 *Classic ICL test interpretation and modified approach*

The gradient of the pH curve reduces with the gradual addition of small quantities of lime and the curve rapidly achieves pH values within a comparably narrow pH bandwidth (12.2 to 12.4) of the desired pH value of 12.4. Beyond that point, any further

small increase in pH towards the 'target' of 12.4 requires relatively large changes in lime content, resulting in expensive lime requirements at site. The BS ICL interpretation in comparison to the new modified, asymptotic interpretation, without consideration of parallel changes in Atterberg limits (which are – depending on the clay mineralogy-already established after the addition of very small lime addition) is thus no longer suitable for practical work.

3.2.1.1 Mechanisms in lime-stabilised ground

The addition of lime results in immediate *modification* to the consistency of the treated material due to cation exchange and flocculation and subsequently results in long term *stabilisation* due to pozzolanic reaction, thus upgrading the treated clay as a foundation material. Both mechanisms are affected by the mineralogy of the treated clay, its moisture content and the presence of organic matter, and have been extensively investigated by a large number of researchers [for example Bell and Coulthard, 1990, Arabi and Wild, 1989, Sherwood, 1992, Brandl, 1981]. Organic matter has generally a tendency to absorb calcium ions and thus clays containing large amounts of organic matter, for example plant parts or microorganisms, respond either very little or not at all to lime treatment. Sherwood [1992], however, points out, that not only the total amount but also the type of organic matter should be considered, when the possibility of lime treatment of a soil is being assessed. In addition to modification and stabilisation mechanisms, lime is consumed by carbonation, a reaction which is generally considered undesirable because it results in the consumption of lime reacting with carbon dioxide from the air to form pore blocking calcium carbonate (equ. 3.2), making only a minor contribution to strength [Bell and Coulthard, 1990, Bell, 1988, Sherwood, 1992].

$$Ca(OH)_2 + CO_2 \rightarrow CaCO_3 + H_2O \qquad \textbf{(equ. 3.2)}$$
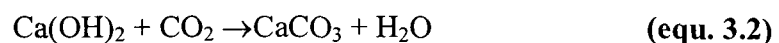
Bagonza et al. [1987] reported on the effect of carbonation on changes in the consistency limits of lime-stabilised clayey sand and found that the reduced plasticity index as a result of lime-clay interaction is partially reversed by carbonation. However, it should be noted that the samples were exposed to pure carbon dioxide, so that there is little likelihood of such an effect occurring in normal, practical work (there is only 0.03% CO_2 in the atmosphere).

The presence of sulphates in lime-treated clays has little effect at the modification stage but affects substantially the pozzolanic reaction and thus the stabilisation stage. These reactions and the involved mechanisms are described in section 3.3.

3.2.1.1.1 Soil modification process- cation exchange and flocculation

It is generally recognised that lime, when added to a heavy clay soil, transforms the originally lumpy material into a friable soil with good compaction properties. Upon lime addition, a soft dispersive clay, characterised by a high percentage of dissolved sodium cations in its pore water, is immediately transformed into a stronger, water-resistant material [Bell and Tyrer, 1987 and McElroy, 1987]. These initial changes are due to cation exchange processes involving Ca^{2+} ions and cations on the clay mineral surfaces according to a replacement series introduced in section 2.3. Cobbe [1988] emphasises that the replacement of cations on the clay mineral surface affects both, the zeta potential and the van der Waal's forces, which are responsible for the relative state of the clay particles with regard to being in a dispersed or flocculated state. The zeta potential, which is a measure of the particles negative charges (causing repulsion between particles), is reduced as monovalent ions are replaced by divalent calcium ions. Van der Waal's forces, which cause attraction between matter, overcome the weaker repulsion deriving from reduced zeta potential and clay particles eventually accumulate in floccs. This means that upon lime addition not only does the actual cation exchange capacity of the soil influence the changes in the consistency, but also the type of cation originally held by the clay particles. In addition the thickness of the hydrous double layer surrounding the clay mineral is reduced by exchanged cations (for example sodium replaced by calcium) and further contributes to closer appproach and easier attraction between the single particles and also reduced moisture absorption [Eades and Grim, 1960, Hilt and Davidson, 1960].

Brandl [1981] challenges the view that it is mainly Ca^{2+}, which is responsible for the structural changes in lime-stabilised soils and thus puts more emphasis on the importance of modifications to the hydrous double layer. He bases this on the fact that when calcium is added in the form of $CaCl_2$, no improvement in the consistency limits could be observed. Petry and Armstrong [1989], supported by Locat et al. [1996], raise suspicion that the pH resulting from $CaCl_2$ addition is not sufficient to adequately promote cation exchange, which again shows good agreement with the suggestion of

Brandl [1981] that the OH⁻ concentration of the pore solution has a large influence not only on consistency changes but also on subsequent reactions.

As a general rule, the liquid limit decreases and the plastic limit increases, resulting in a decrease in the plasticity index of lime treated clay soils [Cobbe, 1988, Arabi and Wild, 1989, Brandl, 1981, Buxton Lime Industries, 1990, Rogers et al., 1997, Clare and Cruchley, 1957]. However, depending on the predominant clay mineral in the clay soil and its associated activity Arabi and Wild [1989] observed an increase in liquid limit for illitic soils and Abdi [1992] reported similar findings for kaolinitic soils upon lime addition. Brandl [1981] emphasises the importance of activity of a soil with regard to the magnitude of changes in consistency when lime is added and reports that a more pronounced decrease in liquid limit is observed for active soils (A>1.25) and an increase in the plasticity index is observed for inactive soils (A<0.75).

It is of economic significance, particularly with regard to the current project, that quite small additions of lime initiate changes in consistency. Bell and Tyrer [1987] showed that as little as 2 % lime resulted in a 50 % reduction of the plasticity index of a montmorillonitic clay. Sherwood [1993] illustrates the immediate and striking effects of the addition of 2 % lime on London Clay, with a plastic limit of 25% and a natural water content of 35%. The plastic limit increases to 40% after lime is mixed in and the clay, even at a water content of 35%, is then readily compactable. Mateos [1964] emphasises that the optimum lime addition required for maximum modification lies usually in the range of 1-3 wt.%, which is also suggested by Ingles and Metcalf [1972] even for the modification of very heavy clay. However, Eades and Grim [1960] and Hilt and Davidson [1960] have shown that, depending on the cations originally held by the clay minerals and thus by the type of clay mineral, different lime additions are required to initiate the desired consistency changes. Locat et al. [1996] raise concern that 2% of lime added to a marine clay might not be enough to allow the formation of detectable secondary cementitious materials, although this percentage of lime addition is considered sufficient to ensure flocculation.

3.2.1.1.2 Soil stabilisation process – pozzolanic reaction

The pozzolanic reaction, which is the driving force behind the strength development of lime stabilised ground, occurs (in comparison to immediate cation exchange and subsequent flocculation) at a very slow rate. The speed of this reaction, during which

poorly crystalline calcium silicate and calcium aluminate hydrates form, is highly temperature dependent and it is generally accepted that it slows down substantially at low temperatures and can even be dormant over periods of time until temperature rises again [Bell and Coulthard, 1990, Sherwood, 1992]. Thus the Department of Transport recommends that *"lime stabilisation work is only undertaken during the months of March to September and when the shade temperature is not below 7 °C (series 600, clause 615-8)"* [Department of Transport, 1993, also Highways Agency, 1995]. Cobbe [1988] points out, however, that significant pozzolanic reaction occurs only at temperatures of beyond 16 °C.

Two explanations for the formation of the cementitious products as a result of the pozzolanic reaction are still being discussed. The first interpretation, which is strongly supported by, for example Arabi and Wild [1989] and Kawamura and Diamond [1975], involves an increases of the pH of the soil pore solution by the addition of lime, which allows the silica and alumina from the clay mineral lattice to go into solution. This *'precipitation from solution mechanism'* leads to the formation of various cementitious products at critical concentrations of the solution. The second theory, originally suggested by Eades and Grim [1960] and further promoted by Bell and Coulthard [1990], is known as *the 'solid state reaction mechanism'*. Depending on the type of clay mineral, the reactions between lime and clay occur either first around the edges of the clay mineral (for example in kaolinitc soils [Arabi and Wild, 1986]) or new phases form from in between the sheets of the clay minerals (for example in the case of montmorillonite).

The products of the pozzolanic reaction are mainly poorly crystalline C-S-H and C-A-H phases, although the formation of more crystalline C-A-S-H phases have been observed when pure kaolinite reacts with lime in solution [Sloan, 1965, Arabi and Wild, 1989]. Arabi and Wild [1986], however, point out, that the identification of various compounds based on a limited number of X-ray patterns is sometimes difficult due to the fact that prominent reflections are often part of the X-ray patterns of a wide range of related compounds. They backed up their X-ray results with thermogravimetric analysis and scanning electron microscopy and found a slow but consistent growth of an interlocking network of plate-like particles, with an increased density after longer curing periods. Although complete identification was not possible due to the poor crystallinity of the observed phases, resemblance to C-S-H and C-A-H phase in Portland cement (similar

weight loss band in the temperature region of 100 to 250 °C and good relation between increase in compressive strength and weight percent of consumed lime) was observed. Investigations into a comparable system (Al_2O_3-SiO_2-$Ca(OH)_2$) based on lime-activated metakaolin were carried out by De Silva and Glasser [1992]. They found C-S-H and C_4AH_{13} to be amongst the initial hydration products followed by gehlenite hydrate and hydrogarnet ($C_3AS_3H_{2x}$ where x=0 to 3). However, they also observed that C_4AH_{13} and gehlenite hydrate are not stable and have a tendency to be converted in hydrogarnet with increasing curing periods.

3.2.1.2 Changes in engineering properties of lime-stabilised ground

During the current project lime was mainly added to make use of the effects of cation exchange and flocculation and thus modify the soil consistency. In addition, the alkaline environment provided by the lime could be utilised to activate the ggbs efficiently. Little or no effects with regard to engineering properties, such as strength or permeability, were expected from the lime-clay raction. However, it is possible that some of the lime was utilised for the pozzolanic reaction (in addition to slag hydration and cation exchange), thus it is useful to outline the effects of the normal lime-clay reaction on the investigated engineering properties.

3.2.1.2.1 Strength development in lime-stabilised clays

The amount of strength increase in clay soils, and in fact the degree to which all engineering properties are affected by the addition of lime, depend on a wide range of factors, such as predominant clay mineral type, amount of lime added, water content, curing temperature and time elapsed between mixing and compaction [Mitchell and Hooper, 1961]. According to Bell and Tyrer [1987] expansive clays, for example montmorillonite, respond more quickly with respect to strength increase, although the final strength achieved is greater for kaolintic soils. The highest compressive strength for montmorillonite was achieved after a lime addition of only 2%, with larger stabiliser additions resulting in strength loss for all curing periods. Excessive lime appears to dilute the natural cohesion and friction forces of the clay and in itself imparts negligible strength deriving from these parameters . Observations made by Thompson and Harty [1973] and confirmed by experiments carried out by Bell and Tyrer [1987] suggest that

only a small amount of clay is needed in a soil in order to achieve significant strength gain upon lime addition. Thus small amounts of silica and alumina would generally be sufficient to sustain pozzolanic reaction in a soil.

Thompson [1966] subjected Illinois clay samples (predominant clay mineral illite) after curing at comparably high temperatures (> 48 °C) to unconsolidated, undrained shear tests and found a substantial increase in cohesion after lime addition. Elevated curing temperatures (in comparison to curing at room temperature) and prolonged curing periods resulted in reduced failure strains due to higher cementation and an overall increase in shear strength.

3.2.1.2.2 Permeability of lime-stabilised clays

Various researchers [Brandl, 1981, Arabi and Wild, 1989, Kertscher, 1988, McCallister et al., 1992] agree that the addition of lime to clayey soils, which exhibit usually rather low coefficients of permeability, results in an initial increase in k-values due to cation exchange and associated flocculation. This increase in permeability depends on the actual water content of the treated material and is more pronounced when the material is compacted slightly wet of optimum [Sabry and Parcher, 1979, El-Rawi and Awad, 1981]. Kertscher [1988] also emphasises the influence of the initial water content of lime-stabilised cohesive soils on the measured hydraulic conductivity and points out that lime addition is particularly helpful in the case of wet soils in order to improve their compactability. Clay soils, if compacted dry of optimum, have generally a more open and flocculated structure which undergoes little change when lime is added. Lack of moisture might also result in not all of the lime being able to go into solution and thus low availability of Ca ions. This would limit changes in consistency and the reaction with the clay minerals during the pozzolanic reaction. Locat et al. [1996], who investigated the hydraulic conductivity of a clayey sediment, found that the permeability is highly related to the amount of lime added. However, any effects of curing time on permeability could not be identified. It should be noted that Locat et al. worked with very high water contents and thus the resulting pore ratio (often in the region of between 1.0 to 3.5) might have masked the comparably small effect of lime addition on the microstructure and subsequently the hydraulic conductivity of the stabilised material.

Although some authors suggest that the permeability of cured compacted clay-lime specimens tends to decrease with an increase in curing period [Brandl, 1981] due to the pore blocking effect of developed cementitious gels and precipitated calcium carbonate, Wild et al. [1987] emphasise that this might be an oversimplification. A comprehensive study, assessing the relation between pore size distribution, permeability development and cementitious gel formation in cured Devonian Red Marl-lime specimens, revealed that curing temperature in particular significantly affects the pore size distribution and thus the k-value of cured specimens.

Investigations by Kertscher [1988] into the permeability of a lime-stabilised silty clay revealed that after an initial increase in hydraulic conductivity due to lime addition (larger lime additions were found to result in a more pronounced increase), a small reduction in permeability – initiated after curing periods of between 120 and 200 days – could be observed. During the rest of the observation period (up to two years), little further changes in permeability occurred. Kertscher could not identify any clear correlation between resulting porosity and hydraulic conductivity, however, consideration of pore size distribution revealed a strong influence of lime addition. He reported an increase in the percentage of pores with a diameter of $10\mu m \geq d \geq 6\mu m$ and a significant reduction in pores with a diameter between 6 and 1.5 μm with increasing lime addition. According to Kertscher, the former pore diameter group is the main contributor to the flow of water in porous media and responsible for the increase in permeability. Although a large number of researchers [Hughes, 1985, Nyame and Illston, 1980, Mehta and Manmohan, 1980, Goto and Roy, 1981] shares this view with regard to the fact that permeability is principally determined by the volume of pores beyond a certain diameter, it should also be noted that other factors such as pore conductance, tortuosity and isotropy have to be taken into consideration. Kertscher [1988] concludes that his observations are mainly the result of a reduction in the thickness of the water layer surrounding the clay mineral particles, although the current author feels that modification of the water layer is virtually an instantaneous action, which should not affect the permeability of samples cured for longer periods.

The significant influence of pore structure and pore size distribution on the flow through porous media of cementitious systems (stabilised soils or concrete with various additions) is discussed in detail in chapter 4 (section 4.5.2.1).

3.2.1.2.3 Frost resistance

In addition to the basic frost heave mechanism in pure soils described in the previous chapter, the modified reactions occurring in lime-stabilised and thus cemented soils are similar to those occurring in concrete. In some ways hardened cement paste with its pores, holding water that freezes upon cooling, could be considered to be analogous to the soil structure. The difference is, however, that pure unstabilised soil is made up of discrete particles that contact each other at single points, whereas cemented material can be seen more as a continuum in which there are pores of various sizes. Schulson [1998] suggests that hardened cement or indeed, lime-stabilised ground, is more suitably perceived as a solid skeleton traversed by a more or less interconnected network of pores. Therefore, the volumetric expansion of water forms the basis for the simplest mechanism in frost attack on cemented soils or concrete, which is usually referred to as the "closed container mechanism" [Fagerlund, 1997]. During freezing the cement paste surrounding the aggregate grains, or the cementitious gel formed as a result of the pozzolanic reaction, is subjected to a gradual freezing process. The volumetric expansion of water during freezing results in the development of a large hydraulic pressure on the walls of a closed, impermeable container, which could for example represent a pore in the cement paste. Due to the lower density of ice of only 916.4 kg/m^3 at 0 °C in comparison to water (density of 999.84 kg/m^3) [Fletcher, 1970], the specific volume of ice is larger than that of the corresponding amount of liquid water. If the effective degree of saturation within the container is below a critical value of 91.7 %, however, no tensile stress as a result of hydraulic pressure will occur on the walls of the container.

Powers introduced the "hydraulic pressure hypothesis" in 1945. He had noted that although concrete specimens contain a sufficient amount of entrained air, they are not frost resistant. He suggested that hydraulic pressure, generated when water is expelled from a pore during the ice formation stage, can build up to such an extent that the concrete will be damaged. This is particularly the case, when surrounding pores are too small to allow water comparably quick access. He further extended his theory by calculating the critical distance below which escaping water can travel (to the next pore large enough to accommodate that water) while still maintaining protection from frost damage. Powers [1954] stated a value of 250 μm, which has since been referred to as the "Powers spacing factor", although nowadays a maximum distance of 200 μm is

usually recommended [Neville, 1995]. If the spacing factor exceeds this value the material is susceptible to frost damage.

Observations in 1953 by Powers and Helmuth, however, forced them to suggest a further theory. Specimens made of air-entrained cement paste were found to contract by greater amounts than the expansion coefficient allowed during cooling to sub-zero temperatures, whereas samples of non air-entrained pastes expanded. The mechanism proposed to account for this observation is known as the "osmotic micro ice body growth theory". Ice crystals will initially form in larger voids (and also in artificially induced air voids if some water is present in them). The increased concentration of dissolved salts will, due to the osmotic effect, attract water from smaller pores or capillaries into which it was expelled in the initial stages of the freezing process. Ice in large and partially water-filled air voids can grow without any confinement by the pore walls. However, due to surface effects ice growth is severely inhibited in the finer capillaries. Although Powers and Helmuth [1953] claim that the expansion observed in non air-entrained paste is due to the generation of hydraulic pressure, which cannot be relieved by capillary flow into air spaces, Lindmark [1999] suggests that a more likely explanation is either the static ice pressure resulting from local over saturation or osmotic ice lens growth according to the mechanism outlined by Taber [1930].

Brandl [1981], who carried out frost heave tests on lime-stabilised, highly plastic clays, found that the frost heave increased with the addition of 1 % lime but decreased with higher lime additions and longer curing periods. He concluded that due to the flocculation after the lime addition, a bigger void ratio would be produced within the soil structure and hence a lower thermal conductivity. He suggested that in comparison to cement stabilised soils, the speed with which frost could penetrate the material would be reduced when lime is used as a stabilising agent. Arabi and Wild [1989] found that Devonian marl stabilised with only 2 % lime exhibited at various curing temperatures substantial heave, which was almost twice the amount that developed for the untreated soil. With large lime additions, however, a significant reduction in heave could be achieved. The authors concluded that increased permeability due to the flocculated structure and little interparticle bonding was responsible for the large heave when only small amounts of lime are added. With larger lime additions, however, the mechanical properties of the soil were improved and the developed strength restricts ice segregation and reduces heave.

3.2.2 Cement stabilisation

In comparison to the two twofold mechanism (immediate modification and subsequent stabilisation) when lime is used as a stabilising agent, cement has little immediate effect on the consistency of the treated soils. Thus, the cement stabilisation of heavy clay soils involves usually an additional modification step by pre-treatment with 1-3% lime to render the soils more workable [Ingles and Metcalf, 1972, Chaddock and Atkinson, 1997]. It is generally recognised that, similar to lime stabilisation, organic matter and excess salt content can substantially retard or even prevent the stabilising process (in this case cement hydration) in stabilised ground.

Portland cement (PC), a mixture of calcium silicates and aluminates, which hydrate in the presence of water, is most frequently used for soil stabilisation in Great Britain. In comparison to lime, which literally 'attacks' the clay minerals in order to recombine the reactive alumina and silica components in cementitious gels, the hydration products of cement, as outlined in Figure 3.4, develop over a comparably short period in time and form a strong, interlocking network, in which the soil grains are embedded.
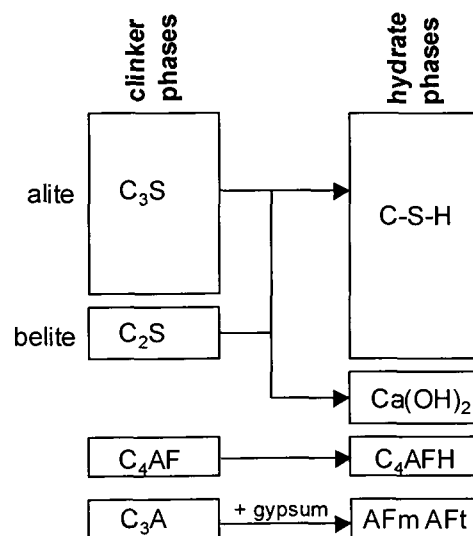
Figure 3.4 *Hydration of Portland cement*

The strength gain of cement stabilised material is generally more rapid and less temperature sensitive than the strength improvement as a result of the pozzolanic lime-clay reaction (Figure 3.5).
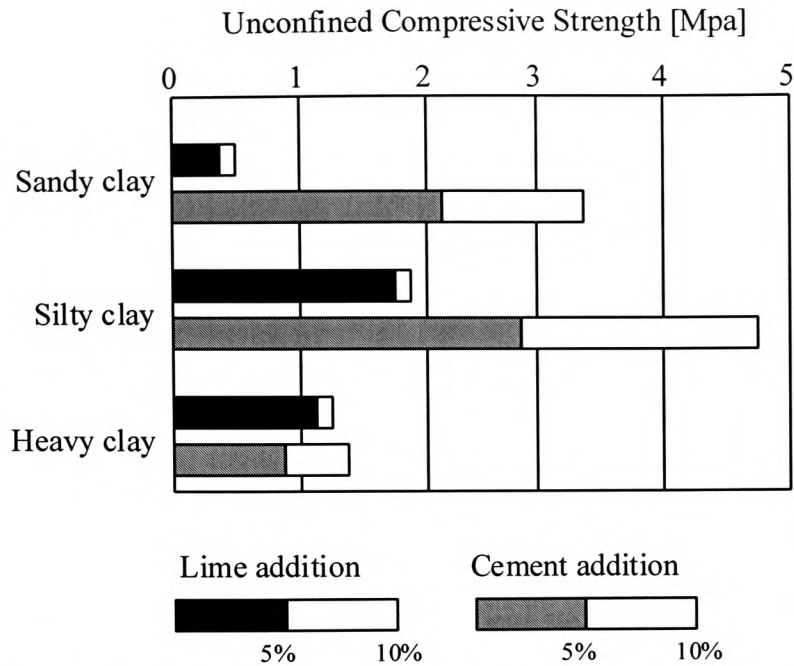
Figure 3.5 *Effect on 7-day unconfined compressive strength of clay type and lime or cement content [after Dumbleton, 1962]*

However, Sherwood [1992] reports that the strength gain exhibited by a highly plastic clay, was far more pronounced on stabilisation with 8% lime than when 8% cement was used as the stabilising agent.

Improvements in the frost resistance of clayey sub-base material, particularly for road foundations, have been achieved by the introduction of cement. Croney and Jacobs [1967] achieved very encouraging results by adding small percentages of cement to slightly frost-susceptible granular material. Balduzzi [1973] also obtained drastically reduced heave after a silty gravel was stabilised with 3 % Portland cement. He noted that the resultant heave was less, when the initial curing period prior to frost action was increased.

3.3 Interference with sulphates

Sulphate attack is a feared phenomenon which in concrete manifests itself in different forms including expansion, cracking, spalling and loss of strength, resulting finally in the destruction of the cement structure. Sulphate attack in soils is mostly accompanied by strength loss and large volume changes, resulting in substantial heave in stabilised earthworks.

3.3.1 Sulphate attack in practice

A large number of researchers have reported examples of the detrimental effects of sulphates, either naturally present in the ground or artificially added, when soils are modified/stabilised with lime and/or cement. One of the earliest reports was given by Sherwood [1962], who found that samples of cement-stabilised clay exhibited a strength loss of more than 50% (100%=strength exhibited by control specimen immersed in water) when immersed in magnesium sulphate solution (0.2% SO_3). In 1988 Hunter reported that expansive reactions resulted in substantial heave of a sulphate-bearing clay soil forming the sub-base of a road in Las Vegas after 4.5% quicklime had been added to condition the material. First evidence of distress appeared within six months of construction and Hunter found good correlation with an increase in the rate of distress with increase in the percentage of clay and colloidal sized particles. Snedker and Temporal [1990] outlined the disastrous results of lime stabilisation during the construction of the M40 motorway near Banbury, where the presence of 0.4% sulphates resulted in 60% heave of the stabilised capping layer. Observations of substantial heave of a lime-stabilised sub-base in Las Vegas/Nevada made by Mitchell [1986] showed that the affected areas were associated with lower density and higher moisture content and these areas also contained high percentages of sodium and calcium sulphates.

If Portland cement with a low C_3A content is used for soil stabilisation purposes, there is less likelihood of sulphate attack leading to damage, because the quantity of expansive sulpho-aluminate phases which are able to form is much reduced. If PC is mixed with high proportions of ggbs, its reaction products result in a denser hardened cement paste, which can (if high quality curing is carried out) less easily be penetrated by sulphate ions [Locher, 1998]. Regourd [1986] points out, that if cement with more

than 65 % slag as a PC replacement is used, concrete becomes basically impermeable to aggressive ions. In stabilised soils, it is almost impossible to create a fully impermeable structure, although unstabilised clay does itself have very low permeability. In order to avoid contact with sulphates in, for example aggressive ground water, artificial barriers incorporating plastic foils or other waterproof membranes have to be utilised.

3.3.2 Formation of expansive products

The basic chemical reactions resulting in the formation of expansive and/or damaging phases, such as ettringite or thaumasite, are best described based on knowledge deriving from cement technology. This is well illustrated by the reports of a number of researchers [for example Odler and Jawed, 1991, Mehta, 1992]. In order to prevent the "flash setting" phenomenon in cement, which is intitated by a reaction between C_3A[1] and portlandite (a 'by-product' during the hydration of C_2S and C_3S), gypsum is added. Tricalcium aluminate will react preferably with gypsum to form ettringite (equ 3.3a+b), a calcium sulphoaluminate hydrate which was discovered more than 100 years ago [Michaelis, 1892] and is in fact part of a series of structurally and chemically similar compounds, known as AFt phases

$$3 \, CaO \cdot Al_2O_3 + 3 \, CaSO_4 + 32 \, H_2O \rightarrow 3 \, CaO \cdot Al_2O_3 \cdot 3 \, CaSO_4 \cdot 32 \, H_2O \quad \textbf{(equ 3.3a)}$$
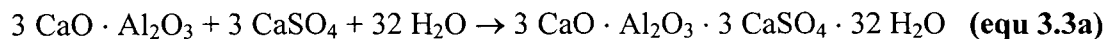
or in commonly used cement notation:

$$C_3A \quad + \quad 3C\overline{S} \quad + \quad 32 \, H \quad \rightarrow \quad C_3A \cdot 3C\overline{S} \cdot 32H \qquad \textbf{(equ.3.3b)}$$

The general formulation of AFt phase is $C_3X \cdot 3CY \cdot 32H$, where C_3X is a tricalcium aluminate (C_3A) or ferrite (C_3F) and CY a calcium salt.

If enough gypsum is added (commercially available PC contains around 5 %, depending on composition of the clinker and the grinding fineness of the cement), all reactive alumina is converted from C_3A to ettringite, being the stable sulfoaluminate phase in a sulphate environment [Mehta, 1992]. In the presence of larger C_3A contents (most commercially available PCs contain more than 5 % C_3A, so not all reactive alumina can be converted by the added gypsum), however, monosulphate hydrate, an AFm phase ($C_3A \cdot C\overline{S} \cdot 12H$) , equ. 3.4, and calcium aluminate hydrate will form. The latter can

form additional ettringite in the presence of $Ca(OH)_2$, deriving from the hydration of alite and belite, if sulphates gain access.

$$C_3A \cdot 3C\overline{S} \cdot 32H + 2C_3A + 4H \rightarrow 3C_3A \cdot C\overline{S} \cdot 12H \qquad \text{(equ. 3.4)}$$
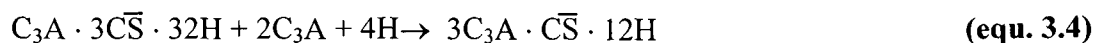
If additional sulphates gain access, the AFm phase can react to produce the Aft phase, the most important of which is ettringite.

$$C_3A \cdot C\overline{S} \cdot 12H + 2C\overline{S}H_2 + 16H \rightarrow C_3A \cdot 3C\overline{S} \cdot 32H \qquad \text{(equ. 3.5)}$$
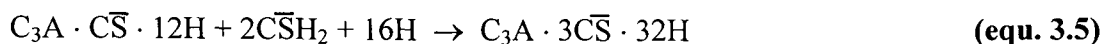
There appears to be a strong relation between ettringite formation and cement/concrete expansion when sulphates gain access, however, there are plenty of cases where ettringite forms without resulting in any harmful volume changes, for example in supersulphated cement [Odler and Jawed, 1991] (see also chapter 4). The formation of ettringite, until depletion of the sulphate source, is usually complete before the setting of the cement and Odler and Jawed [1991] point out that formation of this phase is often accompanied by a moderate contraction of the cement paste. In fact, Mehta [1973a] showed that the reaction of C_3A with gypsum and water to form ettringite gives an overall volume reduction of 7-8%. However, he also points out [1973b] that this colloidal ettringite product, if in contact with an outside source of water during formation, is capable of developing large expansion.

The primary reason for sulphate expansion is still being controversially discussed based on two main theories. The first hypothesis, the *'crystal growth theory'* supported by Xie and Beaudoin [1992], considers primarily the crystallisation pressure, created during the formation of the needle-shaped ettringite crystals, to be responsible for the expansion. The actual formation process is characterised as a 'topochemical mode', during which an in-situ conversion of alumina-bearing solid in contact with solution occurs, in comparison to an explanation based on a 'precipitation through solution' mechanism in the 'swelling theory'. Mehta [1983, 1992], main supporter of the second theory, suggests that the expansion is the result of the increase in volume deriving from the water absorption of ettringite, which initially develops in a colloidal form. In his earlier work [1973b] he gave some evidence that the shape and size of ettringite particles depends on the presence of lime in solution (pH around 12.4). He observed colloidal ettringite particles, about 1 μm long, which possess a high specific surface with a

---

[1] $C=CaO$, $S=SiO_2$, $A=Al_2O_3$, $H=H_2O$, $\overline{S}=SO_3$

negative net charge, attracting a large number of water molecules. Chartschenko et al. [1993] made investigations into changes of the habit of ettringite depending on the pH-value of the pore solution. They considered that the control of the Ca ion concentration can somehow influence the habit of the crystals and also outlined the importance of the OH^- concentration. In experiments with artificially produced ettringite, they observed the colloidal ('microcrystalline') form at a pH of around 13.0, created by NaOH solution. Stark et al. [1998] generally reviewed the contribution of ettringite formation to damage in concretes and suggest that microcracks, already existing in concretes, possibly as a result of poor compaction, favour the crystallisation of ettringite which subsequently promotes further physical damage, for example during freeze-thaw attack. They conclude that "*the occurrence of large ettringite crystals in concrete cracks is, as a rule, only a consequence and rarely the cause of the cracks*". In a critical review of sulphate attack on concrete [1992] Mehta comes to similar conclusions. He points out that sulphate attack is rarely encountered as the sole phenomenon responsible for the deterioration of concrete structures but that microcracks and the permeability of concrete determine its durability when sulphates gain access.

It should also be noted that Mehta et al. [1979] showed that the crystallisation of gypsum, formed as a result of sulphate attack on C_3S paste (and on the portlandite), resulted in substantial expansion (equ. 3.6).

$$M_2SO_4 + Ca(OH)_2 + 2\ H_2O \rightarrow CaSO_4 \cdot 2H_2O + 2\ MOH \qquad \textbf{(equ. 3.6)}$$
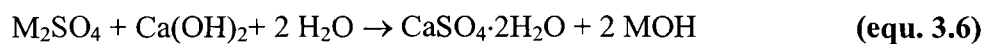
where M is an alkali metal ion.

Small amounts of sulphate ions, however, incorporated in the hydrated C_3S have been shown to have a positive effect on the strength, whereas strength loss has been observed if larger amounts are added. According to Mehta [1983] sulphate ions, adsorbed on the C-S-H surface result in a reduction of its 'adhesive ability' and thus promote expansion initiated by subsequently formed ettringite. Odler and Jawed [1991] outline that the formation of gypsum often precedes the formation of ettringite, which is then initiated when an aluminate phase is also present.

Sulphate attack due to magnesium sulphate is generally considered more severe than attack initiated by alkali sulphates or calcium sulphate. This is due to the fact that

magnesium hydroxide, formed as a precipitate according to equ. 3.6, remains insoluble in the pore solution and reduces the pH. This initiates the decomposition of the C-S-H gel in a 'decalcification reaction' and results in substantial strength loss, accompanied by the 'classic' sulphate expansion, although the levels of expansion are often less than those produced with other sulphates.

3.3.3 Thaumasite formation

A recently discussed form of sulphate attack, observed in a number of buried bridge abutments in Gloucestershire [Department of the Environment, 1999], involves the formation of large amounts of thaumasite ($CaSiO_3 \cdot CaSO_4 \cdot CaCO_3 \cdot 15\ H_2O$), which resembles a "carbonated ettringite" [Bensted, 1999]. In this particular case of the 'thaumasite form of sulphate attack (TSA)', the external sulphate source was found to be oxidised pyrite from the surrounding backfill, which was also found to be the 'culprit' in a case of thaumasite attack on a tunnel lining in the upper Formazza valley/Northern Italy [Berra and Baronio, 1989]. Various researchers have reported that structures were damaged by thaumasite attack [Bickley et al., 1994, Collepardi, 1999, Department of the Environment, 1999, Gaze, 1997] and the following ingredients/conditions could be identified as prerequisites for the TSA:

❑   a source of calcium silicate

❑   sulphate ions

❑   carbonate ions

❑   a sufficiently moist and cold environment

In particular the part played by temperature is still widely debated. The thaumasite expert group [Department of the Environment, 1999] considers that environments below 15 °C facilitate the formation process, whereas other researchers insist the temperatures should be certainly below 10 °C, preferably at 0-5°C [Bensted, 1988, Gaze, 1997]. Van Aardt and Visser [1975] suggest that the reaction takes place more readily at lower temperatures due to a higher solubility of calcium salts at lower temperatures. However, Bensted and Varma [1976] point out that the solubility at lower temperatures is only increased in the case of calcium hydroxide and suggest that an explanation for enhanced formation of thaumasite at lower temperatures arises from the 'co-ordination temperature rule'. According to this rule, a reduction in temperature results in an

increase in the co-ordination number of a molecule (*'the number of ions having a charge opposite to that of a given central ion, which are equal (or nearly equal) distances from it, is known as the co-ordination number*' [Kleber, 1970]). A higher co-ordination number thus facilitates formation of $Si(OH)_6$ groups (due to an expansion in the co-ordination sphere of silicon at lower temperatures), which are an important part of the thaumasite structure. Lower temperatures also promote the stability of the modified co-ordination shells and are thus a requirement for thaumasite formation. It should be noted, however, that there is evidence that thaumasite, as observed in the walls of historic buildings in South Italy, can form at temperatures of beyond 20 °C [Collepardi, 1999].

Thaumasite appears to form comparably slowly, typically over 6 to 12 months [Hartshorn et al., 1999, Varma and Bensted, 1973]. This is due to the fact that thaumasite formation utilises the hydration reaction products, i.e. C-S-H gel from the cement or from pozzolanic reaction and calcium hydroxide which interact with the sulphate ions. The main reason for the deleterious effect of TSA on cement or stabilised soil is the fact that during its formation the strength-creating C-S-H gels are attacked [Crammond and Halliwell, 1995]. According to suggestions by Hartshorn et al. [1999] both C-S-H gel and portlandite are consumed in the process, resulting in a reduced pH of the pore solution, which further increases the vulnerability of C-S-H to sulphate attack. The authors refer to the reaction as 'delayed' thaumasite reaction.

Thaumasite is of particular interest in the current project, because of the utilisation of Lower Oxford Clay, which is a source of calcite and sulphides (pyrites)/sulphates. Cured at low temperatures (10 °C), lime-stabilised Lower Oxford Clay specimens are expected to promote particularly the formation of thaumasite crystals.

3.3.4 Prevention of sulphate attack

To prevent sulphate attack, there are basically two possibilities available. Firstly, the formation of expansive phases can be prevented. Ferris et al. [1991] obtained good results by treatment of sulphate bearing ground with barium compounds (barium hydroxide or barium chloride) prior to lime stabilisation. Barium sulphates 'fix' the sulphate ions as they exhibit very low solubility. Thus sulphates are no longer available to react with added lime. However, the researchers admit that they have not carried out

any investigations yet to identify the impact of the newly formed compounds on the environment, particularly the ground water. In a second approach, efforts can be made to control the formation of expansive phases in such a way that no detrimental effects are induced. There is some indication that potentially expansive phases which form in the absence of excess moisture have no detrimental effect on the volume stability of lime/cement stabilised ground [Mehta, 1973b]. In addition it is well known that ettringite forms, for example, in supersulphated cements in large quantities without resulting in expansion but in good strength and improved resistance to sulphate attack.

Based on findings from the cement technology, the introduction of ground granulated blast furnace slag has been shown to increase the durability of concrete and its resistance to sulphate attack. The next chapter outlines these findings and introduces the associated mechanisms by which ggbs modifies the performance of cement pastes.

Chapter 4 - The utilisation of activated ground granulated blast furnace slag (ggbs)

The properties of ggbs are explained and its structure is outlined. The slag hydration process, mainly based on findings deriving from cement technology, is outlined and aspects of specimen durability such as permeability, porosity or pore size distribution are discussed in more detail. Changes in relevant engineering properties resulting from reactions of the latent-hydraulic slag, activated by an alkaline environment, are summarised.

4.1 General

Ground granulated blast furnace slag derives from the process of iron production as outlined in Chapter 1. Depending on the iron content of the utilised iron ore, the yield of blast furnace slag is approximately 250 to 350 kg slag per ton of produced raw iron [Asim, 1992]. The main chemical compounds are CaO, SiO_2, Al_2O_3 and MgO. In contrast to steel slag, blast furnace slag never develops significant levels of free oxides, such as free FeO or CaO, which can affect the volume stability of the slag [Geiseler, 1996, Smolzcyk, 1980]. However, Hiersche and Wörner [1990] emphasise that the introduction of sufficient periods of stockpiling prior to utilisation in, for example, road sub-bases, results in good performance of air-cooled steel slags. Tüfekci et al. [1997] utilised steel slag as a cement additive and found that the compressive strength of Portland cement is only marginally reduced if up to 10 % of steel slag is added.

It is generally accepted that the density, porosity and reactivity of blast furnace slag are mainly determined by the cooling regime. In the liquid state, blast furnace slag has a high (approximately 406 kcal/kg) thermal energy content [Smolczyk, 1980]. If small droplets of the broken, molten blast furnace slag are cooled very quickly, for example in water jets (wet granulation) or in an air current (dry granulation), there is no time for the atoms to arrange themselves in a crystalline order and the structure of the cold slag granules is amorphous and glassy. Depending on the original temperature of the slag melt (usually around 1350-1550°C) and the efficiency and speed with which cooling is carried out, glass contents of beyond 95 % can be achieved [Asim, 1992]. This slag glass, rich in energy, has latent-hydraulic properties. The residual energy is utilised when hydration products are formed in an exothermic reaction after the activation of the slag grains in an alkaline or acidic environment. If, however, cooling is slow and the

inherent energy of the slag melt dissipates fully, stable crystalline slag compounds, comparable to those of an igneous rock, form. This type of slag ('air-cooled') has only negligible hydraulic or latent-hydraulic properties and has proven quite popular as aggregate in concrete or a granular sub-base material in road construction [Asim, 1992, Motz and Geiseler, 1987].

Further sections will concentrate on the vitreous form of blast furnace slag, which was used in the course of the current project.

4.2 Slag reactivity

In contrast to steel slag, which cannot be granulated due to the presence of steel pellets [Sharma and Ahluwalia, 1995] and the fact that at a prevailing basicity of around 2.0 the formation of a glassy substance is very hard to achieve [Geiseler, 1992], quenched blast furnace slag is a carrier of latent-hydraulic properties. The inherent reactivity depends on the chemical composition, the glass content and the grinding fineness, all of which are discussed in the following sections.

4.2.1. Chemical compounds

The chemical composition of blast furnace slag is heavily influenced by the type of ore, coal and flux agent utilised during production of the pig iron. However, emphasis lies usually on four main components, when quick-cooled blast furnace slag is characterised chemically. These components are SiO_2 (28-38%), CaO (30-50 %), MgO (1-18 %) and Al_2O_3 (8-24%) [Moranville-Regourd, 1998]. In addition, negligible percentages of minor components such as TiO_2, MnO, FeO, S, Na_2O and K_2O can be detected. The chemical composition determines the basicity and the structure of the glass. Various chemical moduli have been suggested to describe the reactivity of quenched slag based on the acid-base relationship of some of its components [Smolzyk, 1980, Moranville-Regourd, 1998]. The ratio of basic to acidic compounds (B/A index), for example defined by the relationships CaO/SiO_2 or the even more popular $(CaO+MgO+Al_2O_3)/SiO_2$, (index of hydraulicity) is used as an indicator for the reacitvity of the slag. If the former value is below 1.0, the slag is termed "acidic slag". Daugherty et al. [1983] utilised a B/A index defined as $(CaO+MgO)/(SiO_2+Al_2O_3)$ in their investigations into the hydraulic activicity of various synthetically produced slags

and found that higher B/A ratios would result in improved activity, particularly when the material is highly amorphous. It should be noted, however, that granulation – the process determining the glass content - of the molten slag becomes increasingly difficult, when the CaO content, and thus the basicity, increases.

Bijen [1996] summarises some general trends with regard to hydraulicity when chemical compositions change and reports that there are negative effects produced with an increase in the SiO_2 content, whereas an increase in CaO is beneficial. An increase of the MgO content is recommended up to 18 % and a higher Al_2O_3 content promotes the development of early strength in blast furnace cement. However, Talling and Brandstetr [1989] suggest that the Al_2O_3 content should not exceed 15 %. Pèra et al. [1999] investigated the effect of high manganese contents in blast furnace slag and found that high percentages (5.4 -21 %) have a negative effect on the initial reactivity, although long term activation is not hindered.

4.2.2 Glass content

There is general agreement in literature that the glass content in slag is the governing factor with regard to its reactivity during hydration. The proportion and composition of the glass phase depends heavily on the cooling regime, defined by the temperature at which cooling is initiated and the speed of cooling. However, Frearson and Uren [1986] found that the reactivity of the slag glass can be increased by the incorporation of crystals, for example merwinitic crystallites. They based their work on observations made by Demoulian et al. [1980], who found that during the crystallisation of merwinite lime, magnesia and silica are removed from the melt, leaving an alumina-enriched and thus more reactive slag glass behind.

Figure 4.1 shows the schematic structural arrangement within the slag glass. The overall structure is based on a network of SiO_4 tetrahedra, with silica being a "network former". However, glassy slag does not consist of an ordered repetitive pattern, as the network is modified by broken Si-O bonds. Neutralisation is achieved by metal cations (network modifiers), the position of which is indicated by the arrows in Figure 4.1. Alumina and magnesia can occur either as network modifiers or can replace silica as network formers [Smolzcyk, 1980, Uchikawa, 1986]. Considerations of some atomic ratios within ggbs,

however, made Taylor [1997] suggest that a structure resembling branched or straight chains of the network forming atoms is more likely than a continuous network.

O   oxygen

·   silica

⇨   place for network
     modifier, (e.g. Ca^{++})
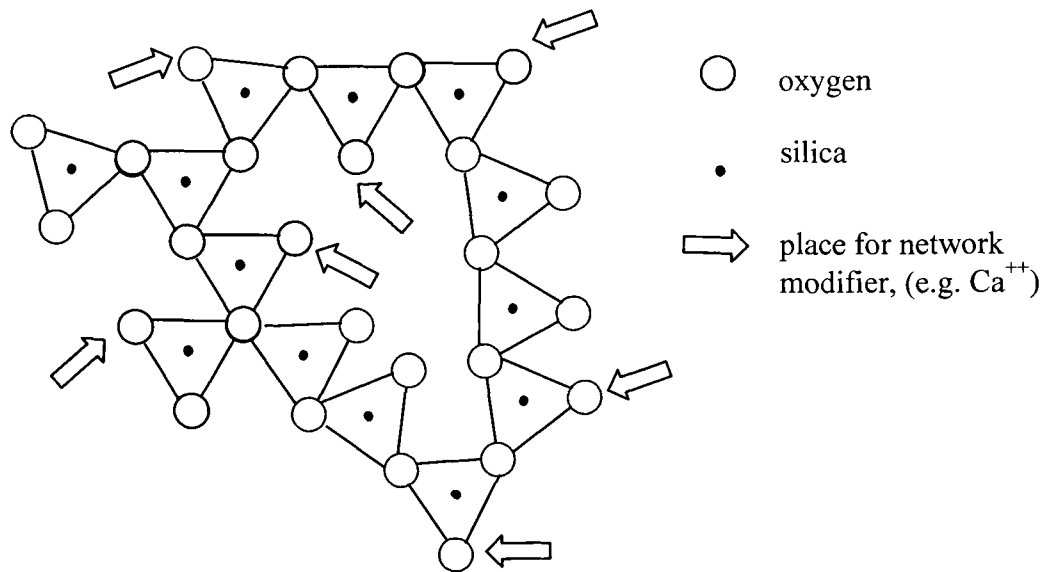
Figure 4.1 *Glass structure of slag [after Regourd, 1986]*

It should be noted, however, that Smoltzyk [1980] and Daimon [1980] raise concern that neither the hydraulic moduli nor the glass content of super-cooled slag allows for conclusions to be drawn with regard to its reactivity. Bijen [1996] also concludes that slag quality is best determined by direct measurement of engineering properties, such as strength development, when slag is incorporated in blended cements.

4.2.3 Grinding fineness

The reactivity of slag is improved if ground to a high fineness, resulting in a larger specific surface and thus a larger area available on which reaction can occur. Particularly since the introduction of very energy-efficient and better-quality roller mills in comparison to the older ball mills, ground slag shows a tendency to a narrower band of grain size distribution and thus lower packing capacity, resulting in a high quality-persistant milling product [Osbaeck, 1989]. Moranville-Regourd [1998] reports that substantial improvements in the compressive strength of Portland blast furnace cements can be achieved when the specific surface area of the added slag is increased by almost 100 % from 3095 cm^2/g to 6140 cm^2/g, particularly for curing periods of 28 days and

beyond. Gjorv [1989] observed significant improvement in an alkaline activated slag cement, even after only 24 hours of curing at temperatures of 20 and 60 °C, when the grinding fineness is increased from 4200 cm^2/g to 6400 cm^2/g. A similar increase in grinding fineness from 4500 to 6000 cm^2/g was also found [Hogan and Meusel, 1981] to produce an increase in the compressive strength of mortars at replacement levels of PC by slag of 40%. These increases were less pronounced for higher replacement levels and at shorter curing periods of 1 and 3 days. Uchikawa [1986] and Daugherty et al. [1983] found that the hydraulic activity of slag is improved, when it is ground to a particle size of 43 µm in diameter or less. These results show good agreement with investigations into the strength development of Portland cement-slag blends carried out by Wada and Igawa [1966], who found that slag particles beyond 40 µm in diameter show only negligible activity and thus contribute only little to the bending and compressive strength at an early age. If ground more finely, however, slag particles with a diameter smaller than 10 µm were found to result in early strength development (up to 28 days). Particles with a diameter in the range of 10-40 µm hydrate more slowly and thus result in higher strength at an older age. Cook et al. [1988] suggest that an increase in slag fineness and thus reactive surface is generally advantageous for further dissolution of slag through the barrier resulting from hydration products which accumulate on the slag grain surface. Thus higher grinding fineness is a more effective approach with regard to best harnessing the potential slag reactivity.

4.3 Slag hydration process

The hydration reaction of slag varies considerably depending on the type of activator, the physical and chemical characteristics of the slag and the reaction environment, and is not yet fully understood. Knowledge of the chemical reactions initiating the hydration of slag derives mainly from the use of ggbs in concrete and only little work has been carried out with regard to slag hydration when incorporated within a soil structure.

4.3.1 Slag activators

In general, slag can be activated thermally, chemically or mechanically. *Mechanical activation* is achieved by grinding the slag to a desired particle size or specific surface to provide the degree of activation needed, within the existing economic limitations. It should be noted, that the ground slag loses its activity within a month if stored in a moist environment [Uchikawa, 1986]. Autoclaving at approximately 180 °C and at elevated pressure is utilised *to activate slag thermally* [Regourd, 1986]. The most important activation method, however, is *activation with chemical substances*. Slag hydrates efficiently only in the presence of chemical activators. In their absence, after exposure to water a highly impermeable coating of aluminosilicate hydrates forms rapidly on the surface of the slag grains (within a few minutes) and subsequent reaction is strongly inhibited [Mehta, 1989]. Shi and Day [1995] describe the reaction in more detail and suggest that the polarisation effect of OH⁻ results in the breakage of Al-O, Si-O, Mg-O and Ca-O bonds on the slag surface. However, the weaker Mg-O and Ca-O bonds are more easily attacked and result in Ca and Mg entering the pore water, whereas Al and Si form the protective layer on the slag grain surface. The hydrate component of the layer might derive from the absorption of H^+ ions from the water, simultaneously leading to an increase in pH. But even at this increased pH-value not enough Al and Si can be dissolved to form cementitious gels, which would finally result in a cemented slag structure.

Slag activators can either be alkaline or sulphate activators [Häkkinen, 1993, Daimon, 1980, Regourd, 1980]. In slag cement, the alkaline activator is predominately $Ca(OH)_2$ (portlandite), deriving from the hydration of alite and belite. Sulphate activation, reported by Regourd [1980] and Daimon [1980], utilising for example gypsum or anhydrite, appears to be less effective and thus slower than alkaline activation. Daimon [1980] however, based on investigations into the amount of reacted slag in the presence of $CaSO_4 \cdot 2H_2O$, insists that gypsum is not only an 'exciter' but also an 'important reactant' in this system. Teoreanu [1991] also confirms the possibility of sulphate activation of ggbs and suggests that in the pre-induction period of activation of ggbs-PC mixes, gypsum is the main hydration activator. Yuan et al. [1988] however, consider that slag activation by sulphates is not possible at all. In their opinion, the concentration of OH⁻ of a gypsum solution at a pH of 10.6 is not high enough to initiate sufficient solubilisation of silica from the slag and thus no cementitious phases can be produced.

Song and Jennings [1999] also emphasise that a pH of at least 11.5 is required to activate ggbs effectively due to reduced solubility of silica at lower pH-values. There is, however, general agreement that sulphates have an accelerating effect when added to an alkaline activator solution and enhance the strength development of the slag paste [Taylor, 1997, Yuan et al., 1988]. This appears to be due to the fact that in the presence of gypsum ettringite can precipitate, for the formation of which Ca^{2+} and $Al(OH)_4^-$ released from the slag are utilised [Taylor, 1997].

Slag self activation is possible to a certain degree. The process, however, is slow and limited [Cook et al., 1988]. Malhotra [1989] found that concrete, in which PC was completely replaced by ggbs, showed some strength but concluded that the rate of strength gain and the values obtained after 28 and 90 days of curing were too low to be of any practical significance. Motz and Geiseler [1987] describe the utilisation of ggbs in self-hardening capping layers during a full-scale trial in Germany and conclude that long-term leaching of $Ca(OH)_2$ from the slag results in a self-activation process. Song and Jennings [1999] observed that ggbs paste mixed with de-ionised water exhibited an increase in pH from 10.3 to 12.0 after 56 days, which could be taken as an indication of the release of calcium and thus support Motz and Geiseler's observations. Veith et al. [1999] also observed a substantial increase in the pH of soaking water in which sulphate bearing kaolinite specimens, stabilised with 6% ggbs were kept while the linear expansion was monitored. The increase in pH was observed prior to the start of expansion, indicating the formation of expansive phases in the specimen. Wilson [1978] even observed the formation of thaumasite in stockpiled weathered furnace slag and suggested that the weathering process must have resulted in considerable amounts of sulphates being leached out, which were combined with calcium and aluminium, also deriving from the slag material. However, the slag had been exposed to the atmosphere for more than 150 years, confirming that the processes involved occur at a very slow rate.

With regard to the current project, slag activation by an alkaline environment (lime) is of most interest. The amount of lime required to sufficiently activate slag was found to be very small. Daimon [1980] identified a lime addition of between 0.3% and 0.5% to be most beneficial for quick activation in the presence of 10% sulphates in a supersulphated cement. Coale et al. [1973] also report that slag hydrates sufficiently in the presence of 2% lime and results in good strength development, particularly in the long term.

4.3.2 The slag activation process

After Zhou et al. [1993] the chemical slag activation process can be sub-divided into 5 stages, namely initial reaction (pre-induction period), induction, acceleration of reaction, deceleration and final. During the initial stage, the activation of slag is initiated in an alkaline environment at a pH of at least 11.5, in which the water-impermeable layer, coating the slag grain, breaks down in the presence of the activator [Mehta, 1989, Song and Jennings, 1999]. OH⁻ is capable of breaking down the "pseudomorphic" coating, attacking the chain structure of SiO_4 and Al_2O_6, and leaving a negative surface charge behind. Neutrality is gained by absorption from Ca^{2+} ions from the surrounding solution. The pH rises and further silica and alumina is dissolved in the liquid phase [Takemoto and Uchikawa, 1980]. Subsequently Ca, Si and Al ions migrate to the outer boundaries of the slag grain and leave a core, rich in magnesium behind.

Depending on the type and thus pH and chemical composition of the activator used, the disruption and initial hydration of the slag grains starts intensively after only a few minutes in the case of activation with waterglass (sodium ($NaSiO_3$) or potassium ($KSiO_3$) silicate) [Zhou et al., 1993] or occurs over a long period with less intensity when $Ca(OH)_2$ is chosen as activator [Fernandez-Jimenez et al., 1996]. Both the initial slag dissolution and the precipitation of reaction products are exothermic reactions, thus the intensity can either be detected primarily by conduction calorimetry or secondary conclusions can be drawn by measuring the effect of the reaction on resulting engineering properties, such as compressive strength. Observations on the compressive strength development of slag pastes made by Wu et al. [1990] also show that slag activated with $Ca(OH)_2$ has, in comparison to activators such as NaOH or alum, the slowest and most inferior compressive strength development which is in good agreement with the calorimetric investigations carried out by Fernandez-Jimenez et al. [1996].

During the induction stage, a protecting surface film of poorly crystalline C-S-H gel forms on the slag grain as Ca^{2+} from either the activator or the slag itself reacts with silica and alumina dissolved from the slag in the presence of an increased concentration of OH⁻ ions. Up to this dormant period, the duration of which depends on the type of activator solution [Zhou et al., 1993, Fernandez-Jimenez et al., 1996], the degree of hydration of the slag is only around 2 % [Uchikawa, 1986]. At the end of the dormant

period aluminate ($Al_2O_3{}^{6-}$) and silicate ion groups ($SiO_4{}^{4-}$), dissolved from the slag, react with metal ions provided by the activator solution (e.g. Na^+, Ca^{2+} or Mg^{2+}) to precipitate as low-solubility secondary C-S-H, C-A-H, M-A-H or other hydrates. This initiates the acceleration period, which is characterised by exothermic hydration reactions, which are assumed to be most effective at a pH of around 12.0 [Wu et al., 1990]. Eventually during deceleration and the final phase, the free water in the microstructure is consumed and hydration products precipitate in thick layers on the slag grains. The hydration process then slows down.

4.3.3 Hydration products

The activator used has a large influence on the reaction products which result from the hydration of slag [Fernandez-Jimenez et al., 1996, Cook et al., 1988]. Regourd [1980] reports that ettringite is amongst the first reaction products, when sulphates are used as an activator, with its morphology depending on the slag content of the blend. At high slag additions, its habit is characterised by comparably short needles, which appear to play the 'role of a binder'. Similar observations were made by Smolczyk [1961], who found that ettringite crystals formed in cement pastes with high slag contents are very tiny (about 5 µm in length) and thus not likely to cause any disruption to the system.

C-S-H gel appears to be the main hydration product regardless of the activator type, although its structure and Ca/Si ratio vary with the type of activator used. Talling and Brandstetr [1989] and Song and Jennings [1999] report that completely amorphous C-S-H gel is the principal hydration product of alkali-activated slag, which contradicts Taylor [1997], who emphasises that activation with NaOH results in C-S-H (I) which possesses a higher degree of crystallinity. Regourd [1980] found that C-S-H gel as a product of the slag hydration is usually not very well crystallised, although, generally it is denser than C-S-H gel formed during PC hydration. This was partially confirmed by Richardson and Groves [1992], who examined the hardened cement paste of OPC-ggbs mixes and described the hydrated slag grain. Figure 4.2 shows a systematic sketch of a hydrated slag grain, based on their observations. The inner product (Ip) consists mainly of C-S-H gel, into which Mg-Al containing platelets can be incorporated (also observed by Regourd [1980]). Richardson [1999] showed that the amount of Al increased linearly

with the amount of silica and depends on the percentage slag content in the cement blend. The outer product (Op) consists of fibrillar C-S-H gel, the habit of which changes with increasing PC replacement to a completely foil-like structure, plus AFm and AFt phases. Richardson and Groves [1992] suggest that the foil-like C-S-H gel pores are less well interconnected in comparison to the fibrillar habit of C-S-H gel in pure PC pastes and thus result in the overall reduced diffusion rates of ggbs-PC blends. The unhydrated remains of the slag grain in the unreacted cores, exhibit, particularly in the case of smaller grains, substantial porosity [Richardson,1999].
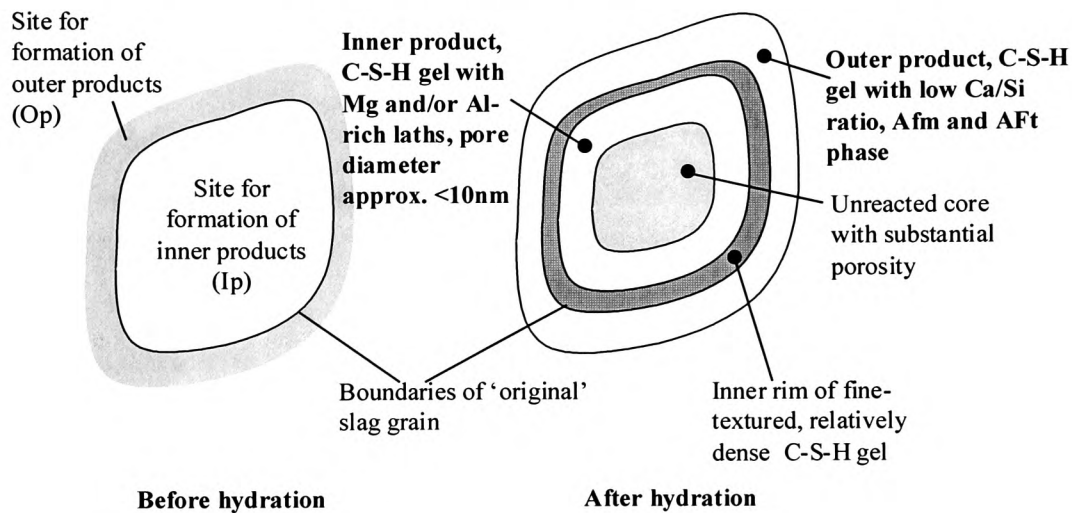
Figure 4.2 *Slag grain before and after hydration*

In addition to C-S-H, C_4AH_{13} and C_2ASH_8 were formed when ggbs was activated by NaOH, however, if $Ca(OH)_2$ is chosen as an activator Regourd [1980] found that C_2ASH_8 did not form because it is unstable in the presence of $Ca(OH)_2$.

Although Richardson and Groves [1992] observed AFm phase, Wang and Scrivener [1995] pointed out that depending on the type of activator, the formation of AFm phase can be avoided. In supersulphated cements, however, the main hydration products are C-S-H gel and ettringite [Taylor, 1997], the latter of which contributes significantly to the developed strength due to its habit of up to 100 μm long and several micrometers thick lath-like crystals [Mehta, 1992]. Due to a sufficiently large source of sulphates and a limited number of Ca^{2+} ions, all ettringite forms during the early stages of hydration, when the cement paste has not yet set. It thus contributes to strength without any detrimental effect on the structure of the cement stone.

4.4 Use of slag as a cement admixture in concrete

Cement pastes and concretes with blast furnace slag additions have been studied by a large number of researchers [Totani et al., 1980, Wang et al., 1995, Talling and Brandstetr, 1989, Malhotra and Mehta, 1996]. There are basically two ways in which slag can be utilised in concrete technology. Firstly, as a partial replacement for ordinary Portland cement (slag cements), where the slag is activated by portlandite $(CaOH)_2$ liberated during the hydration of the clinker phases C_2S and C_3S and gypsum, which is added to cement to prevent "flash setting". Super-sulphated cement (SSC), consisting of ggbs (70-85 %), a small percentage of clinker (up to 5 %) and sulphates (usually 10-25 % gypsum or anhydrite), is a special case of slag cement in which slag is the main cementing agent [Neville, 1995, Dutta and Borthakur, 1990]. Secondly, slag can be used in alkali-activated slag cements (AASC), which are a mixture of ground granulated slag and an alkaline activator. The slag is activated by the alkaline additive, which can be alkali hydroxide (ROH), non-silicic salts of the $R_2O\cdot(n)SiO_2$ type, with R being an alkali metal ion such as Na, K or Li [Wang et al., 1995]. With regard to slag cements, there is general agreement about the initially lower speed of hydration in comparison to PC alone, however, the ultimate strength of blast furnace slag cement, although it is equal to the compressive strength of pure Portland cement at 28 days, is higher. The lower hydration heat development is particularly useful in mass concrete, where cooling, especially after high initial temperatures originating from the hydration, can result in cracks and thus reduce the durability of the concrete. Improvements in the durability of slag cements are mainly attributed to the comparably finer pore structures of these cements in comparison to PC. Uchikawa [1986] reports that the pores size distribution of hardened blast furnace slag cement at early ages is similar to that of PC paste, however in the long term, the percentage of pores with radii of between 3-5 nm becomes larger in slag cements as the hydration proceeds.

In comparison to slag cements, AASC have very rapid strength development. However, the variation in strength can be high and the alkaline activator has to be selected carefully with respect to the composition of the slag utilised [Wang et al., 1995]. Generally, the hydration heat of AASC is even lower than the heat generated during the hydration of slag-PC mixes, which makes AASC cements also very suitable for large concrete constructions. However, Shi and Day [1995] emphasise that in the case of some sodium based activators, the total heat generation during hydration can surpass the

heat generated during the hydration of PC. Some other drawbacks in the utilisation of AASC include the occurrence of efflorescence (white deposits on the concrete surface due to leaching of free alkali) and high shrinkage values if waterglass solution ($NaSiO_3$) is used as activator [Wang et al., 1995, Häkkinen, 1993]. However, Xuequan et al. [1991] report that when AASC, activated with waterglass, was utilised as an immobilisation matrix for radioactive waste, high compressive strength, high resistance to heat and chemical corrosion and low porosity, was achieved.

The incorporation of slag in cement or soils results initially in a bluish-green colour when the interior of a specimen is exposed to the atmosphere. This phenomenon, deriving from the formation of iron (FeS) and manganese sulphides (MnS) during the dissolution of the slag, disappears when the sulphides subsequently oxidise to sulphates ($FeSO_4$ and $MnSO_4$) [Malhotra and Mehta, 1996, Malhotra, 1989, Bijen, 1996]. Bijen [1996] even suggests that the colour in the centre of a concrete construction and the speed with which the change in colour on the surface occurs, can be taken as a simple indication of the concrete quality.

4.5 Effects of ggbs on engineering properties in concrete and soil

The engineering properties of cement and soil are influenced significantly by the incorporation of activated ggbs. Changes in the investigated engineering properties, i.e. strength, porosity, permeability and frost resistance, are related and discussed in the following sections.

4.5.1 Strength development and influence of temperature

Various researchers [Malhotra, 1989, Bijen, 1996] have reported higher long term strength if cement is blended with ggbs, although the strength development at short curing periods is usually inferior to pure PC. Tan and Pu [1998] showed, that the initially inferior strength development of concrete, in which some of the PC is replaced by ggbs, could be compensated for by additions of ground fly-ash. Hooton [1986] found that the compressive strength of cement pastes in which 65% of Portland cement had been replaced by ggbs was particularly inferior to the control specimens (pure PC) at higher water/binder ratios after curing periods of only 7 days. After curing for 28 days and beyond, however, the blended pastes exhibited strength values similar to those of pure cement.

Roy and Idorn [1985] investigated the influence of curing temperature (27 to 250 °C) on the compressive strength development of mortar in which around 38% of the cement was replaced by ggbs. All specimens exhibited greater strength than the control specimens (cement as the sole binder) and an increase in strength could be observed with increase in curing temperature up to 175 °C. At a curing temperature of 250 °C, however, strength loss occurred in comparison to curing at 175 °C. The measured values were nevertheless considerably higher than those exhibited by specimens cured at only 90 °C. In parallel with this a systematic decrease in porosity with increase in curing temperature and curing period could be established. Earlier results published by Roy and Parker [1983] on investigations into cement paste cured at elevated temperatures in which 60% of the cement was replaced by slag, showed that the critical pore radius increases when curing is at temperatures beyond 60 °C. The subsequently reduced degree of pore refinement is even more pronounced at water /binder ratios

beyond 0.3. The authors attributed this to the fact that the cement paste was comparably open and contained C-S-H gel of the type I structure, which is more ordered than the poorly crystalline C-S-H gel formed at normal temperatures during cement hydration. Taylor [1997], however, points out that C-S-H (I) is usually only encountered as a hydrothermal reaction product at temperatures beyond 180 °C, for example during autoclave treatment. Uomoto and Kobayashi [1989] made investigations into the strength development of cement-slag concretes cured at 10 to 40 °C for up to 26 weeks and found that the strength was greatly reduced at lower curing temperatures and at high slag additions in comparison to the values exhibited by ordinary concrete. Similar findings were presented by Hogan and Meusel [1981] as a result of investigations into cement-slag mortars cured at 4.4 °C (40 °F) for up to 7 days. Wimpenny et al. [1989], however, observed that the strength of slag-PC concretes was generally higher after curing beyond 28 days at temperatures of 5, 10, 20 and 40 °C than the corresponding strength of PC concrete. The highest strength values were exhibited by all specimens for a curing temperature of 20 °C, and a depression in strength could be observed when the curing temperature was raised to 40 °C. The drop in compressive strength, however, was more pronounced for pure PC mixes than for the specimens in which 30 or 70% of the PC were replaced with slag.

Hasaba et al. [1982] were amongst the first to utilise lime-gypsum-slag mixes to stabilise cohesive soils. They found that larger gypsum additions result in higher compressive strength at early ages and attributed this mainly to the formation of ettringite, the habit of which was observed to vary with the lime/gypsum ratio. Gupta and Seehra [1989] also found that the compressive strength of sand stabilised with lime and ggbs was greatly improved by the addition of gypsum. It should be noted, however, that they utilised binder additions of around 30%, which are not feasible for practical purposes. With regard to the use of lime-activated ggbs Kennedy [1996] reported a full-scale trial where a clayey sand was stabilised with 8% ggbs and 2% lime to form the sub-base for the lorry-loading area of a distribution warehouse. He found that the 7-day cube strengths were in the region of 2/3 of the strength obtained for the cubes in which the clayey sand had been stabilised with 9% cement. However, after longer curing periods of 28 and 90 days the compressive strength of the lime-ggbs mix outperformed the strength of the specimens which had been stabilised with cement. Wild et al. [1996] stabilised sulphate-bearing kaolinite (4% gypsum = 1.86 SO_3) with a total binder

content of 10%, consisting of lime and ggbs with slag/lime ratios of 4/6, 6/4 and 8/2. The compressive strength development showed non-systematic variation. In the absence of gypsum, however, an increase in the slag/lime ratio produced a consistent increase in strength. More recent work by Wild et al. [1998] utilising a total binder content of 6% and a wider 'lime by slag replacement range', established that a binder combination of 5% slag and 1% lime results, both in the presence and absence of sulphates (3% SO_3), in the highest 7-day compressive strength for the stabilised kaolinite. Further increase in strength was obtained with increase in the curing period (28 days in comparison to 7 days). Higher gypsum additions were also found to be particularly advantageous for high slag/low lime combinations, if curing periods are prolonged, whereas they resulted in reduced strength development if curing is only for 7 days.

No published research work on the effect of curing temperature on ggbs-stabilised ground could be identified.

4.5.2 Durability aspects

The main durability criteria with regard to soil are usually low permeability, high frost resistance, negligible carbonation and resistance to sulphate attack and swelling. In concrete technology, the durability criteria also include acid resistance, good performance in marine environments and resistance to alkali-silica reaction. An underlying factor in most of those criteria is the porosity and pore size distribution of the soil and its influence on permeability. The role of these crucial factors with regard to durability was further emphasised by a comment made by Mehta [1992], who stated that for the prevention of chemical attack in concrete "*the control of permeability is more important than control of the chemistry of cement*". The issue of sulphate attack and its dangers were introduced in the previous chapter. Because carbonation could be a concern with regard to its influence on permeability measurements, a brief overview is dedicated to this problem.

4.5.2.1 Porosity, pore size distribution and permeability

4.5.2.1.1 General

It has been established that permeability is perceived as key to the durability of concrete or stabilised ground. Its role in sulphate attack has been addressed by a number of researchers [Khatri and Sirivatnanon, 1997, Mehta, 1992] and attempts to determine the coefficients of permeability of materials by secondary measurements and thus draw conclusions with regard to their resistance to chemical attack started as early as 1899. The American Scientist C. S. Slichter made an attempt to correlate the water permeability of a porous system consisting of spherical grains of uniform size to the volume of an ideal capillary tube with constant cross section and thus to the porosity within the system. Earlier in the 20th century (1927), a group of scientists headed by Kozeny suggested a relationship between the permeability and the hydraulic radius and surface area of the solid particles, in what is known as the 'Carman-Kozeny model' [Marshall, 1958]. Both methods are based on the particle size distribution of a sample and fail to predict the permeability of a material precisely, when the variety in particle size is large. However, as outlined in a critical review by Brown et al. [1991], these models do not make any assumptions with regard to the shape of the pores as more recent ones do and thus neglect a large source of error.

With new technical developments, allowing the measurement of the distribution of pores within a material structure, a new dimension in the predictability of flow through porous media opened up. Childs and Collis-George [1950] were amongst the first researchers to develop a permeability equation, which took account of the variety in pore diameter when pores are randomly arranged in a porous system. Marshall [1958] went a step further and suggested an equation based on the assumption *"that the rate of flow is controlled by the cross-sectional area connecting the pores"*. He achieved good agreement between calculated and measured coefficients of permeability of sand and sandstone.

More recent attempts by researchers to correlate permeability and pore structure of cement paste have yielded interesting results and suggest that the pore size distribution of a cement paste is the governing factor with regard to permeability [Manmohan and Mehta, 1981]. A pore radius above approximately 50 nm was found sufficient to contribute significantly to permeability [Goto and Roy, 1981 and Mehta and

Manmohan, 1980]. Marsh [1984], who worked on OPC-pulverised fuel-ash (PFA) pastes, also confirmed the existence of a relationship between permeability and volume of pores of radius greater than 50 nm. He also identified that high permeability OPC/PFA pastes exhibit a clearly defined threshold radius (or primary continuous pore radius), suggesting *"the existence of a channel of pore space containing a large volume within a small range of pore sizes (i.e. the channel is of reasonably consistent dimension)"*. However, no general relationship between pore radius and permeability could be established for pure cement paste. Nyame and Illston [1980] defined a maximum continuous pore radius ($\delta v/\delta p$ has a maximum value during mercury intrusion porosimetry (MIP)) for hardened cement paste, which was closely related to the measured permeability at different stages of hydration and for a variety of w/c ratios. During further investigations on the same material, they found that neither porosity, hydraulic radius nor surface area are uniquely related to measured permeability. However, it should be outlined that pore characteristics such as tortuosity (relation between effective pore length and direct distance between inlet and outlet), pore conductance and accessibility are of great importance in determining the flow through a material [Wild et al., 1987, Hughes, 1985]. Hughes [1985] developed a mathematical model which introduced a tortuosity factor and allowed the calculation of the total flow rate of cement paste under consideration of the total pore volume and pore size distribution. The model is based on the assumption that all pores are interconnected and pores with a radius below 7.5 nm are not taken into account. Wild et al. [1987] utilised Hughes' model to identify the relationship between the percentage of pores with a radius greater than 40 nm and the coefficients of permeability of cured soil-lime systems, and found a strong correlation.

In this context it should be noted, that conventionally employed pore investigation techniques, such as MIP, can only measure pores from a continuum down to the size of small mesopores (pore range 2-50 nm). Only sorption techniques allow investigations into finer pores [Rahmann, 1984]. However, Nyame and Illston [1981] claim that pores with a radius below the minimum pores size detectable by MIP techniques (in the current project 0.0037 μm=3.7 nm) are very unlikely to contribute to the flow of water and thus can be neglected. Bàgel and Zivica [1997] made investigations to identify the 'relevant porosity' (introduced by Meng [1994] to characterise the voids available for water transport) of mortar specimens and found micropores with a radius of up to 7500

nm to constitute the 'relevant pore range' with regard to measured k-values. Young [1988] emphasises that there are several assumptions inherent in the calculations of pore sizes from porosimetry data and that no absolute values are measured. Hooton [1986] agreed and concluded from investigations into blended cement pastes that there "appears to be no accurate way of predicting permeability from porosity or pore size parameters obtained by mercury intrusion".

4.5.2.1.2 Effect of ggbs on microstructure

Chemical reactions initiated by the addition of ggbs as partial replacement in cement, or lime and ggbs as a stabilising agent in soil are bound to change the microstructure and thus the way in which water can flow through the porous media. Ggbs is generally known to result in pore refinement when added as a cement replacement [Uchikawa, 1980, Roy and Idorn, 1985], although the pore size distribution of hardened cement paste with ggbs is almost the same as that of OPC paste at an early age. However, as the slag hydration reaction proceeds, the percentage of pores in the range of 3 to 5 nm becomes larger. Manmohan and Mehta [1981] found that large additions of ggbs increase the total pore volume of cement paste, however, the pore size distribution was shifted towards finer pores, thus the permeability of the paste was reduced. Smolzcyk [1980] states that the capillary porosity is reduced by 30 % in comparison to pure PC, when 65 % of the PC in the cement is replaced by ggbs. In such blended cements, the hydration products form between the PC clinker and the slag grains and thus fill the pore space [Regourd, 1986]. This was confirmed in an attempt by Feng et al. [1989] to relate chemical migration within cement slag blends during hydration with reduced permeability. They found that chemical transport from the slag grains to the hydrates resulted in the redistribution of pore space and left behind a residual slag glass with higher porosity [confirmed by Richardson, 1999]. The pores of the hydrates were distributed evenly in the densified paste and this re-allocation of pore space resulted in lower permeability.

4.5.2.2 Sulphate attack

The cause of sulphate attack, manifested in expansion and subsequent deterioration of the cement structure, is generally accepted to derive from the formation of calcium sulphoaluminate hydrates (ettringite), as outlined in chapter 3. Hydrated cement paste can be the source of calcium (Ca^{2+}) and aluminium (Al^{3+}) ions, deriving from the hydration of the clinker phases, which can be combined with sulphate to give ettringite when external sulphates gain access. It is generally accepted that the incorporation of ggbs increases the sulphate resistance of cement [Frearson, 1986, Hogan and Meusel, 1981] due to modifications of physical and chemical aspects during sulphate attack. The former is manifested in the fact that ggbs produces, on hydration, a very dense hardened cement paste, into which sulphates are virtually unable to penetrate [Locher, 1998, Gutierrez et al., 1998, Roy and Parker, 1983] and thus reduces the permeability. Khatri and Sirivatnanon [1997] claimed, that lower permeability values resulted in reduced expansion when concrete specimens were immersed in 5% $NaSO_4$ solution. However, samples in which slag was incorporated exhibited even less expansion, although their observed coefficients of permeability were greater than the values observed for the control mixes. This highlights the importance of the second modification initiated by the addition of slag, i.e. chemical modifications. The chemical modifications initiated by added ggbs during slag hydration involve the consumption of portlandite (resulting from the hydration of alite and belite) and thus eliminate calcium ions as potential and essential components for the formation of ettringite (see chapter 3). However, studies undertaken by Rasheeduzzafar et al. [1990] to assess the resistance of PC-ggbs (40:60) blends to magnesium and sodium sulphate attack revealed interesting results. After two years of exposure to the hostile environment, the samples prepared with blended cement showed severe signs of deterioration, characterised by scaling and softening, in comparison to the control specimens (pure PC). Microstructural investigations revealed the presence of significant amounts of gypsum and M-S-H gel and it was clear that substantial decomposition of C-S-H had taken place. The authors concluded that the lack of CH, which provided the Ca^{2+} ions to form gypsum, depressed the pH and promoted the attack on C-S-H gel. However, as outlined in chapter 3, the formation of gypsum can also result in significant expansion and would have led to severe disruption of the structure of the specimens.

Another approach is chosen when 'sulphate resisting Portland cement' is used. In order to starve the reaction leading to expansive ettringite, the C_3A content and thus the availability of Al^{3+} is strictly reduced by utilisation of PC with a low C_3A content or replacement of PC by ggbs with low alumina levels. Osborne [1999] showed that combinations of PC with low alumina slag (<14% Al_2O_3) exhibit high resistance to sodium sulphate solution. However, slag cements appear to have increased sensitivity to magnesium sulphate solution. Cao et al. [1997] point out that the effects of reduced alumina content are far more distinguishable after long-term exposure (> 1 year) to a sulphate source, and thus suggest that performance assessment of cement admixtures should be based on long term observations. The need for long term observations is also emphasised by the fact that in some cases, where a PC-slag blend was utilised to increase the sulphate resistance of concrete, anomalous expansion was only observed after prolonged exposure to sulphate solution. Cao et al. [1997] report that accelerating expansion of PC-slag blends (40 and 60% PC replacement by slag) exposed to 5% $NaSO_4$ solution occurs after between 30 and 40 weeks, whereas initially only negligible expansion occurs. Frearson [1986] also observed sudden expansion of cement-slag blends after the specimens had been immersed in sulphate solution for more than 2 years. Kinuthia [1997] encountered a similar phenomenon during his investigations into the linear expansion of slag-stabilised sulphate-bearing kaolinite. Specimens to which only slag and gypsum (as an artificial sulphate source) had been added, showed only negligible expansion upon soaking, however, after a dormant period of around 40 days, sudden expansion could be observed. It is interesting to see that all affected specimens were stabilised with comparably small amounts of ggbs, whereas larger ggbs additions appear to counteract the described observations. Based on suggestions by Richardson and Groves [1992], who carried out a comprehensive analysis of the hydration products of cement pastes involving ggbs, the key to the observed behaviour could lie in the fact that substantial amounts of $Ca(OH)_2$ (in excess of what is expected from the OPC content alone) are produced in the initial stages of the hydration of the cement-ggbs blends. They suggest that this is due to an accelerating effect of ggbs on the hydration of PC and found that the slag hydration subsequently utilises the alkaline activator and thus reduces the amount of portlandite in the system. However, depending on the amount of ggbs in the cement blend (Richardson and Groves point out that in the long term only negligible amounts of $Ca(OH)_2$ can be expected in blends of ggbs/PC with proportions in excess of 3:1), substantial amounts of $Ca(OH)_2$ can remain present for

long time periods. Together with external sulphates and alumina compounds from the hydration products, excess calcium availability at extended exposure periods could result in the delayed formation of ettringite and thus be the reason for the observed anomalous expansion after long exposure periods, particularly in the presence of smaller ggbs additions.

4.5.2.3 Effect of ggbs on carbonation

Although air contains only about 0.03% CO_2 it has the capability of reacting with $Ca(OH)_2$ within stabilised soil or concrete, forming $CaCO_3$. This diffusion controlled process, which can in fact involve all alkaline compounds of hydration products, results in the formation of carbonates and oxides and is known as carbonation (equ. 4.1).

$$Ca(OH)_2 + CO_2 \rightarrow CaCO_3 + H_2O \qquad \textbf{(equ. 4.1)}$$
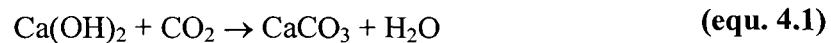
(accompanied by a drop in pH from 12.4 to 7-8)

In concrete the production of $CaCO_3$, which can basically occur in three modifications (calcite, vaterite and aragonite) [Knöfel and Wang, 1993], results in a dramatic decrease in the pH value of the pore water, exposing the embedded steel, which was previously in a higher pH environment and protected by passivation, to corrosion [Neville, 1995]. Due to the reduced $Ca(OH)_2$ content of OPC-slag cements (ggbs reacts with portlandite to from C-S-H), less CO_2 is necessary to remove all the calcium hydroxide, resulting in a faster reduction in the pH-value of the pore solution. This is in agreement with the findings of Li et al. [1998] who reported that OPC-slag cements with high ggbs additions show a larger degree of carbonation in comparison to pure OPC. However, if the grinding fineness of the ggbs is increased beyond 1800 m^2/kg, significantly less carbonation occurs. Similar findings are reported by Nakamoto and Togawa [1995].

CO_2 can also react with C-S-H or C-A-H gels, which form during slag hydration. The carbonation of the former results in the formation of a porous silica gel, which due to its larger pores allows even further carbonation to occur [Bier et al., 1989]. Alumina gel, which is formed during the carbonation of C-A-H, has a lower strength than the original hydrate, affecting the strength of the cement paste.

The rate of carbonation depends heavily on temperature, moisture conditions, pore size distribution within the material structure and the availability of alkaline compounds. Smolczyk [1980] claims that the carbonation of slag cements is not greater than that of PC, if the concrete is compact and stored in a sufficiently humid atmosphere. Carbonation affects particularly those durability aspects which are governed by the permeability. The developing $CaCO_3$ blocks pore space by occupying a greater volume than the $Ca(OH)_2$ from which it is formed and thus reduces the overall porosity and the rate at which solutions or gases can migrate into the soil or concrete structure. However, if C-S-H gel is attacked by CO_2 during carbonation the resulting silica gel exhibits pores with radii of around 300 nm, which are arranged in a continuous interconnected pore system. Subsequently Bier et al. [1989] observed an increase in the permeability of the carbonated PC-slag cement paste of up to two orders of magnitude. Ngala and Page [1997] confirmed earlier findings by Bier at al. [1989] and observed higher gas diffusion coefficients for carbonated PC-ggbs pastes in comparison to uncarbonated mixes and attributed this increase to the larger capillary porosity (diameter > 30 nm) present in carbonated specimens. Due to curing at high relative humidity, the likelihood of carbonation occurring and influencing results obtained in the course of the current project was ruled out to a very high degree. In addition, a CO_2 absorbing agent ("Carbosorb") was employed to reduce the CO_2 content of the air during the drying regime.

4.5.3 Frost resistance

Some investigations have already been carried out on the influence of ggbs on the freeze-thaw characteristics of concrete. The Concrete Society [1992] warned in a technical report that concrete containing high additions of ggbs (>60 %) may be more susceptible to frost damage without air entrainment, particularly at an early age. Stark and Ludwig [1997] pointed out that concrete rich in ggbs performed generally well during frost action [also shown by Fukodome et al., 1992]. However, in the presence of deicing salts it exhibited very poor frost resistance. They concluded that a high degree of carbonation on the surface of test specimens led to a coarser, thus more vulnerable structure, resulting in significant surface scaling under freeze-de-icing salt attack.

Although Stark and Ludwig [1995] emphasise that chemical transformation processes are generally of far less significance with respect to the freeze-thaw durability of concrete than are the physical effects, they should not be neglected completely. They found that ettringite behaved in a stable manner in specimens made of a synthesised C_3A-gypsum mixture after 28 freeze-thaw cycles (+20 °C/-20 °C), whereas monosulphate (AFm) was transformed to ettringite (AFt) during freezing. This was also found by Auberg and Setzer [1997], who looked in detail at the water uptake of cement pastes during freeze-thaw cycles. Both authors point out that the volume increase as a result of the latter reaction would significantly influence the freeze-thaw resistance of concrete. Stark and Ludwig [1995] also observed that more AFm was converted to AFt when the C_3A content of the cement was low. The authors outline also the importance of the carbonation process for the resistance of concrete to frost. Hydrate phases are converted to calcium carbonate (calcite), which provides high resistance to freeze-thaw attack of concrete. Whereas $CaCO_3$ was the only carbonation product found in carbonated cement paste made from Portland cement, blast furnace cements with a slag content of > 60 %, produced calcite modifications, such as aragonite, vaterite and amorphous $CaCO_3$. This seems, however, only of importance when thawing is induced by de-icing salts, because the solubility of aragonite and especially of vaterite increases sharply in the presence of chlorides. SEM investigations carried out by Stark and Ludwig [1995] showed that frost attack and subsequent "normal" thawing conditions did not change the appearance of the well-crystallised needles of the $CaCO_3$ modifications.

Investigations into underwater concrete, carried out by Fukudome et al. [1992], revealed that cement containing ggbs exhibited improved freeze-thaw resistance. They found that in particular the percentage of coarser pores (i.e. with a radius of 10 to 10^3 nm) decreases when ggbs with a high specific surface is added, and experienced an overall increase in smaller pores. Based on the fact that water in smaller pores requires lower temperatures to freeze, the authors suggested that the higher resistance of concrete containing ggbs to frost action is due to the fact that the amount of water that freezes at a given temperature is generally reduced. In a more recent publication Stark and Ludwig [1997] emphasise that there exists a linear relationship between the degree of hydration of blast furnace cement and hence the amount of gel pores (pore radius < 0.01 μm) or capillary pores (pore radius 0.01<r<10 μm) formed, and the frost resistance of the

cement paste. In comparison to Portland cement (PC), blast furnace slag cement forms a denser structure at a lower degree of hydration and thus compensates for the fact that its hydration rate is significantly slower compared to PC. Results obtained by Malhotra [1989] from conducting freeze-thaw cycles on concrete prisms made with slag blended cement, confirmed the aforementioned findings. Although the compressive strengths of the concretes incorporating slag were considerably less when specimens after 14 days of curing were subjected to frost action, they were found to perform equally well to the prisms prepared with 100 % cement.

To the author's knowledge no research work has been published yet on the resistance to frost action of soils stabilised with lime-activated ggbs.

Chapter 5 - Materials

5.1. Soils

The range of soils on which experimental investigations have been carried out during this project comprises three natural clays (Kimmeridge Clay, Lower Oxford Clay and Tingewick Boulder Clay) and two artificially constituted soil mixtures (pure kaolinite and kaolinite with the addition of 6 % gypsum). Natural soils with their individual geological history and their chemical and mineralogical composition are not always homogenous and thus their properties can vary from one batch to another. Thus, it was ensured that the natural clays involved in the study derived from only one field sample (Kimmeridge and Tingewick Boulder Clay) or delivery (Lower Oxford Clay). On arrival the clay lumps were dried at room temperature, then crushed in a Pascall jaw crusher and subsequently ground to powder fineness with a Pascall disc grinder. Finally the powder was homogenised by mixing it in a pan mixer with a capacity of 0.06 m^3 for several minutes.

For comparison purposes and in order to obtain results from a soil with known geochemical properties, standardised kaolinite was introduced into the project. In related experimental studies undertaken by Abdi [1992] and Kinuthia [1997], kaolinite had proven to be a suitable material with consistent properties on its own or with the addition of metal sulphates as an artificial sulphate source. It should be noted that Rossato et al. [1992] emphasised that kaolinite is a monomineralic clay with a very narrow grading curve and thus its properties are not really typical of natural clays. During their studies into the properties of some kaolin-based model clays, however, they concluded that the inherent advantages, such as commercial availability, relatively high permeability and high suitability for microfabric studies, suggest that it is generally well considered for laboratory research.

5.1.1 Kaolinite

The kaolinite used is commercially available under the trade name "Standard Porcelain" and was provided by ECC International Ltd, St Austell, Cornwall, UK. It consists of 93% kaolinite, 4% mica, 1% feldspar and 2% other minerals [ECC International, 1987].

The results of a chemical analysis and a particle size distribution are given in Tables 5.1 and 5.2, respectively and the basic engineering properties are summarised in Table 5.3.

Table 5.1 *Chemical analysis of Standard Porcelain [after ECC International, 1987]*

Chemical analysis	weight %
SiO_2	48
Al_2O_3	37
Fe_2O_3	0.65
TiO_2	0.02
CaO	0.07
MgO	0.30
K_2O	1.60
Na_2O	0.10
Loss on ignition (L.O.I.)	12.5

Table 5.2 *Particle size distribution of Standard Porcelain [after ECC International, 1987]*

Particle size	%
> 75 μm	0
> 53 μm	0.03
> 10 μm	4
< 2 μm	70

Table 5.3 *Engineering properties of Standard Porcelain*

Test	value
Liquid limit	60
Plastic limit	29
Plasticity index	31
pH	5.2
Dry density	1.493 Mg/m^3
Optimum moisture content	25.7 %

5.1.2 Kimmeridge Clay

The Kimmeridge Clay originated from Blackbird Leys near Oxford and was obtained with the kind support of Oxford City Design. The results of chemical and mineral analyses of the Kimmeridge Clay were carried out by Frodingham Cement Company Ltd and are shown in Table 5.4. The basic engineering properties are summarised in Table 5.5. The Kimmeridge Clay was excavated from a depth of approximately 2.5 to 3 metres with an in-situ moisture content of 27.8%.

Table 5.4 *Mineral phases in Kimmeridge Clay*

Mineral	Chemical Formula
Quartz	SiO_2
Calcite	$CaCO_3$
Ankerite	$Ca,(Fe,Mg)(CO_3)_2$
Dolomite	$CaMg(CO_3)_2$
Gypsum (Selenite crystals)	$CaSO_4.2H_2O$
Muscovite (Mica)	$(K,Na)(Al,Mg,Fe)_2(Si_{3.1}Al_{0.9})O_{10}(OH)_2$
Illite (Mica)	$(K,H_3O)Al_2Si_3AlO_{10}(OH)_2$
Dickite (Kaolin)	$Al_2Si_2O_5(OH)_4$
Anatase	+ probable trace amount TiO_2

Frodingham Cement Company Ltd

Table 5.5 *Engineering properties of Kimmeridge Clay*

Test	value
Liquid Limit	65
Plastic Limit	33
Plasticity Index	32
Initial consumption of lime	3.5%
Optimum moisture content	23.70%
Maximum dry density	1.550 [Mg/m^3]

Although initially utilised for the test programme, its total sulphate content determined by Frodingham Cement Company Ltd and confirmed by Bodycote Materials Testing, was only 0.13 %SO_3. This value was considered too low for the purpose of the research,

so additional tests with this clay were discontinued. However, results obtained from the utilisation of Kimmeridge Clay in the early stages of the testing programme can be found in some of the publications in the appendix of this thesis.

5.1.3 Lower Oxford Clay

Due to the fact that the Kimmeridge Clay obtained did not contain the expected high sulphate levels, Lower Oxford Clay was introduced into the test programme. Its main engineerinmg properties can be found in Table 5.6 and the particle size distribution is plotted in Figure 3.2.

Table 5.6 *Engineering properties of Lower Oxford Clay*

Test	value
Liquid Limit	64
Plastic Limit	32
Plasticity Index	32
Optimum moisture content	22.60%
Maximum dry density	1.490 Mg/m^3

Chemical analysis, kindly provided by Hanson Brick Ltd, Ripley, Derby, suggested a sulphate content of approximately 6.24 %SO_4 (=5.2 % SO_3). This would have been equivalent to a gypsum content of 11.18% and was considered to be very high. Approximately 500 kg of crushed clay were supplied. The clay was dried at room temperature and then ground to produce a fine powder. Analysis for acid soluble sulphates, however, carried out by Bodycote Materials Testing Ltd, Bridgewater and Frodingham Cement Company Ltd, Lincolnshire on the material supplied, gave values of only 0.62% and 0.22% SO_3, respectively. Results obtained from external laboratories was generally found to be very reliable. In addition, the total sulphur content of the clay was determined by the author according to BS 1047:1983: Methods for the chemical analysis of blast furnace slag. This gave a sulphur level of 2.5%, which is equivalent to 6.25%SO_3, if all the sulphur was fully oxidised.

A technique utilised in order to determine the pyrite content of the clay (based on a method developed at the Department of Earth Sciences at the University of Sheffield)

was carried out by the University of Sheffield. A pyrite content of 1.2% was obtained, which corresponds to a sulphur content of 0.64% or 1.6 %SO_3 [Wild et al., 1998]. It should be noted, however, that this value takes only iron sulphides into account. Organic sulphur, for example, which is known to be present in the sample, would not be determined using this analytical method. Previous data reported by Wild et al. [1996a] on the mineralogical composition of the Lower Oxford Clay used by Hanson Brick showed a pyrites content of 3.25% (Table 5.7). Although there is likely to be variation in the compositions observed, due to both sample variation and analytical method, there is clearly a significant level of sulphide in the Lower Oxford Clay being used. Therefore it was decided to use the Lower Oxford Clay as a typical material with a high sulphide content and substantial heave potential (depending on the oxidation rate of the sulphur pyrites) when stabilised with lime alone.

Table 5.7 *Mineralogical analysis of Lower Oxford Clay [after Wild et al., 1996a]*

Mineral	wt%
Chlorite	6.47
Illite	22.02
Gypsum	1.30
Kaolinite	7.62
Quartz	28.50
K-feldspar	2.37
Plagioclase	4.15
Calcite	10.44
Siderite	1.14
Anatase	0.82
Pyrite	3.25
Apatite	0.41

A comparison between the results of the chemical analysis of a range of Lower Oxford Clay samples given in literature supplied by London Brick Company Ltd and that carried out at the University of Sheffield on the Lower Oxford Clay utilised for the project is given in Table 5.8. The analysis did not include measurement of sulphur as sulphide or carbon as carbonate. However, x-ray analysis indicates that much of the

CaO present is as carbonate. Carbonate needs to be present in a soil in addition to sulphate in order to initiate the formation of thaumasite [Collepardi, 1999]. Thus Lower Oxford Clay is an ideal clay to employ in order to investigate expansion due to ettringite/thaumasite formation. It was therefore decided to use Lower Oxford Clay together with kaolinite for the main part of the project, which involves low temperature curing over a period of up to one year.

Table 5.8 *Chemical analysis of Lower Oxford Clay*

Oxide	University of Sheffield [wt%]	London Brick Company [wt%] [Wild, 1996b]
SiO_2	43.8	55.42
TiO_2	0.75	0.86
Al_2O_3	15.97	19.88
Fe_2O_3	4.94	6.21
FeO	-	0.68
Mn_2O	-	0.07
CaO	8.55	8.56
MgO	1.53	1.83
K_2O	2.42	3.22
SO_3	0.15	-
P_2O_5	0.60	-
Na_2O_3	0.68	0.68

5.1.4 Tingewick Boulder Clay

Tingwick Boulder Clay was introduced with respect to a case study of slag-lime-stabilised road subbase for a temporary diversion in Tingewick, Buckinghamshire. Its engineering properties are summarised in Table 5.9. The sulphate content was determined prior to stabilisation and can be seen in Table 5.10. Tests were mainly carried out on the stabilised material and detailed results can be found in Chapter 8 (case studies).

Table 5.9 *Engineering properties of Tingewick Boulder Clay*

Test	value
Liquid limit	41
Plastic limit	19
Plasticity index	22
Maximum dry density	1.650 Mg/m^3
Optimum moisture content	21.8%

Table 5.10 *Sulphate contents of Tingewick Boulder Clay (CL Associates, Wokingham)*

Trial pit	water soluble sulphates*[g/l]	total sulphates* [%]	total sulphur [%]	potential total sulphates* [%]
510A	0.0033(=0.033%)	0.10	0.59	$\xrightarrow{\times 2.5**}$ 1.47
513A	0.0019(=0.019%)	0.06	0.86	$\xrightarrow{\times 2.5**}$ 2.15

* expressed as SO_3
** sulphur (S) = 32 amu and SO_3 = 80 amu

5.2 Additives

5.2.1 Lime

Hydrated lime ($Ca(OH)_2$) used for testing, was produced and supplied by Buxton Lime Industries Ltd, Buxton, Derbyshire, UK and is known under the trade name "Limbux". The physical properties and the chemical composition of a typical sample used for the current study are shown in Tables 5.11 and 5.12 respectively.

Table 5.11 *Physical properties of hydrated lime (Buxton Lime Industries Ltd.)*

Properties	Description
☐ chemical name	Hydrated lime calcium hydroxide
☐ physical form	dry white powder
☐ melting/decomposition	580 °C
☐ bulk density	480 kg/m^3
☐ specific gravity	2.3
☐ specific surface	300-1500 m^2/kg
☐ solubility in water	1.76 g/l sat. sol. at 10 °C
☐ pH value	12.4

Table 5.12 *Chemical composition of lime (Buxton Lime Industries Ltd.)*

Compound	Chemical Formula	Composition [%]
☐ Hydrated Lime	$Ca(OH)_2$	96.76
☐ Calcia (Calcium Carbonate)	$CaCO_3$	1.36
☐ Anhydrite (Calcium Sulphate)	$CaSO_4$	0.06
☐ Magnesia	MgO	0.83
☐ Ferric Oxide	Fe_2O_3	0.06
☐ Alumina	Al_2O_3	0.10
☐ Silica	SiO_2	0.46
☐ Excess moisture	H_2O	0.34

5.2.2 Sulphate

The sulphate used to produce laboratory simulated sulphate bearing clay was produced by Riedel-de-Haën AG, Seelze, Germany, as calcium sulphate-2-hydrate R.G. ($CaSO_4 \cdot 2H_2O$, M = 172.17 g/mol).

Table 5.13 shows its chemical composition provided by Riedel-de-Haën AG.

Table 5.13 *Chemical composition of calcium sulphate-2-hydrate (Riedel-de-Häen AG)*

Assay	min. 99 %
Insoluble in HCI	max. 0.02 %
Free acid (as H_2SO_4)	max. 0.01 %
Cu	max. 0.0005 %
Fe	max. 0.0005 %
K	max. 0.002 %
Mg	max. 0.002 %
Na	max. 0.02 %
Pb	max. 0.0002 %
Zn	max. 0.0005 %
Carbonate	max. 0.005 %
Chloride (Cl)	max. 0.02 %
Nitrate (NO_3)	max. 0.005 %

5.2.3 Ground granulated blast furnace slag

Ground granulated blastfurnace slag was supplied by Civil and Marine Slag Cement Ltd., Llanwern, Newport, UK. Its chemical composition and physical properties are shown in Tables 5.14 and 5.15 respectively.

Table 5.16 shows the composition of ggbs in direct comparison with Portland cement.

Table 5.14 *Chemical composition of ggbs (Civil & Marine Slag Cement Ltd., UK)*

Oxide	Composition [%]
CaO	41.99
SiO_2	35.34
Al_2O_3	11.59
MgO	8.04
Fe_2O_3	1.18
MnO	0.45
S_2	1.18
SO_3	0.23

Table 5.15 *Physical properties of ggbs (Civil & Marine Slag Cement Ltd., UK)*

Insoluble Residue	0.3 %
Relative density	2.9 t/m^3
Bulk density	1.2 t/m^3
Colour	off-white
Glass content	$\approx$ 90 %

Table 5.16 *Chemical composition and physical properties of ggbs and Portland cement (Civil & Marine Slag Cement Ltd., UK)*

Oxide	Composition [%]	
	GGBS	Portland Cement
CaO	41	63
SiO_2	35	20
Al_2O_3	11	6
Fe_2O_3	1	3
Insoluble Residue	0.3	0.5
Relative Density	2.9	3.15
Bulk Density [kg/m^3]	1200	1400
Colour	Off-white	Grey

Chapter 6 – Experimental procedure

This chapter discusses the mix compositions used in the current work, outlines the sample preparation and describes the experimental equipment and procedures used to determine material properties and performance. Due to the partly cementitious nature of the samples, the chosen tests reflect both concrete and soil testing methodology.

6.1 Soil mix range

Previous results obtained by Wild et al. [1996] have established that best results with respect to strength and linear expansion of lime/slag stabilised sulphate-bearing clays are obtained when small additions of lime are utilised to activate larger percentages of slag. In order to determine the necessary lime addition at which sufficient alkalinity would be provided to activate the added slag, tests for the determination of the initial consumption of lime (ICL) according to BS1924: part 2: 1990 were carried out. The ICL is usually determined before soils are subjected to lime stabilisation in order to obtain an indication of the minimum amount of lime required to achieve a significant change in the properties of the soil. The test is based on the pH development of a soil slurry (20 g soil + 100 ml of distilled water) with increasing lime addition. The minimum amount of lime required to give a pH of 12.4 (= pH value of pure lime solution) is called the ICL. For kaolinite the ICL was reached with the addition of 6.5% lime, whereas the slurry made of Lower Oxford Clay and distilled water exhibited a pH value of 12.4 after only 2.5% of lime had been added (the detailed results of the ICL tests can be found in Appendix 1). It should be noted, however, that in both cases the pH of the slurry increases rapidly for small lime additions and at values of 1 or 2 percent of added lime values close to the desired 12.4 are obtained. Based on these observations and the fact that Wild et al. [1996] had obtained a high degree of slag activation with additions of only 1% lime for a kaolinitic soil, 2% lime was chosen as the basic activator for the ggbs.

In order to asses the effects of various slag additions, mixes with 2 % lime only and 0, 2, 4, 6 and 8 % ggbs were prepared. Figure 6.1 gives a schematic overview of the overall scope of the project.

Kaolinite + 6 % gypsum

pure Kaolinite

Lower Oxford Clay

Mix compositions

2L0S 2L2S 2L4S 2L6S 2L8S

Sample
h=100 mm
d=50 mm

Scope of test programme

Sample
h= 76 mm
d=38 mm

UCS*

Curing for
1 week
4 weeks
12 weeks

IT⁺

Curing for
1 week
4 weeks
12 weeks

Expansion and frost resistance

Curing for
1 week
4 weeks
12 weeks
24 weeks

Curing temperature 30 °C

Curing temperature 10, 20 and 30 °C

Shear strength

Curing for
1 week
4 weeks
12 weeks
24 weeks
1 year

Permeability

Curing for
1 week
4 weeks
12 weeks
24 weeks
1 year

Porosity

Curing for
1 week
4 weeks
12 weeks
24 weeks
1 year

*Unconfined Compressive Strength, ⁺ Indirect Tensile Strength

Figure 6.1 *Schematic overview of the experimental programme*

Two basic sample sizes with·a height:diameter ratio of 2:1 were prepared. Cylinders with a diameter of 50 mm and a height of 100 mm were prepared for testing with regard to compressive strength, indirect tensile strength and frost resistance. Smaller cylindrical samples with a diameter of 38 mm and a height of 76 mm were produced to obtain results for permeability and shear strength. The smaller size of the latter specimens was dictated by the experimental set-up employed. Porosity measurements were carried out on fractions of broken and dried samples after testing.

6.2 Sample preparation

6.2.1 Mixing and compaction

Depending on the amount and type of additive, the maximum dry denity (MDD) and the related optimum moisture content (OMC) of a given soil vary. Initial compaction trials revealed that a single moisture content/dry density combination for all slag/lime ratios, would not always lead to well-compacted samples. Typically samples with high slag content exhibited comparably large air-filled pores when compacted to an average density established from a series of standard Proctor compaction tests (2.5 kg rammer method in accordance with BS 1377:part 4: 1990) on mixes with various slag/lime ratios. Thus it was decided to utilise the 'mix-specific' MDD and OMC values for the different mix compositions. These values are listed in Appendix 2.

To avoid moisture loss during mixing, enough material to produce only one cylindrical sample at a time was mixed in a Kenwood Chef Excell mixer for 2 minutes before slowly adding the calculated amount of water. Automatic mixing was followed by a manual mixing phase with palette knives until a homogenous soil mix was achieved. The material was then contained in a steel split mould and compacted in one layer in a hydraulic jack (Figure 6.2). The sample was left to consolidate for a minute and then the mould was taken out of the compaction frame. Subsequently the specimen was extruded with a plunger and cleaned of releasing oil. Based on pre-calculated material weights and the known mould volume, the compacted sample exhibited the anticipated density at a given moisture content and was not over-compressed. Based on the final weight of the sample and the determined moisture content, the ultimate values for the OMC and MDD were compared with the anticipated values and good agreement was found.

Finally the specimen was labelled, prior to being wrapped in several layers of cling film.

> Compaction in one layer with hydraulic jack

soil sample

soil mix in bulk
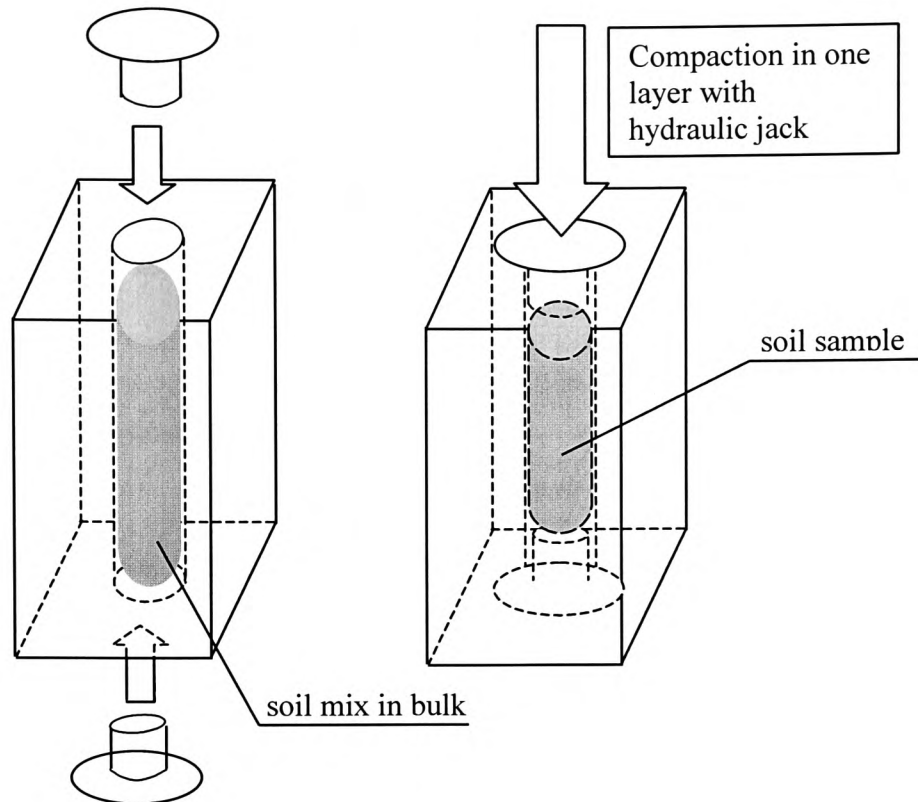
Figure 6.2 *Systematic sample compaction*

6.2.2 Curing conditions

To allow an assessment of the rate of cementation within the specimens for various environments, curing temperatures were chosen to be 10, 20 and 30 °C. To ensure a high relative humidity and thus only negligible moisture loss during curing, the samples were stored over water in a closed container as outlined in Figure 6.3.

sealed container

wrapped soil specimens

tray

water level
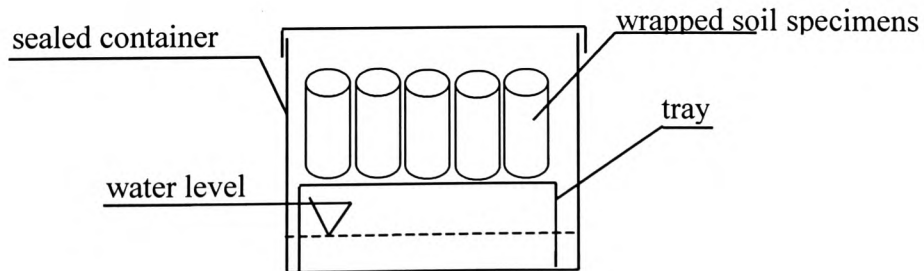
Figure 6.3 *Schematic view of soil storage container*

Confirmation of only minor moisture loss (up to 1%) was gained by comparing the weights of the samples before and after curing. The weight loss was found to be independent of time and curing temperature and was considered to be insignificant.

Curing at 30 °C was done utilising an industrial oven, whereas samples were kept at 10 °C in a an ordinary household refrigerator. A constant temperature room provided the environment for curing at 20 °C. Permanent temperature checks ensured that the temperatures were kept within a range of ± 2 °C.

6.3 Engineering properties

6.3.1 Strength assessment

There is no precise definition of the "strength of a material" as the strength obtained is influenced by the way in which it is measured. Although the term tends to refer to the compressive strength of a specimen, strength has to be specified. Stress as a result of a force exerted on a certain area of a material can - depending on its nature - result in either no harm to the material tested, partly damage its structure or make it collapse. Concrete, for example, which is generally considered a building material with high "strength", performs very well in the presence of a compressive force. Under tensile stress, however, failure occurs at much lower values of stress. Modern building materials have to withstand different types of forces. The stabilised subbase layer of road has to be able to bear the weight of flowing traffic resulting in a general compressive force and also resist tensile forces which may arise from, for example, ice lens formation during frost action. Finally a compressive force in the presence of edge confinement, usually imposed by surrounding material, can result development of shear forces and subsequently the formation of a failure plane. Thus, the stabilised soils were subjected to various tests in order to assess their performance under tensile stress, compressive stress and shear stress.

6.3.1.1 Unconfined compressive strength (UCS)

Testing for unconfined compressive strength was carried out utilising a JJ30 MK compression testing machine, applying load at a rate of 1 mm/min. Prior to aligning the samples centrally between the upper and lower platten, a self-levelling device was

placed between the tops of the samples and the upper platten in order to achieve uniaxial stress. Load was applied until failure was recorded. To establish consistency, two samples were prepared per mix and if the results of these differed by more than 20 %, a third specimen was prepared and tested in order to determine the true trend.

6.3.1.2 Undrained, unconsolidated shear strength

6.3.1.2.1 Theoretical background

Knowledge of the shear strength of soils is of significance for construction purposes since the correct assessment of stress distribution and deformation leads to a solution of the bearing capacity problem, resulting in an optimised design of foundation or subbase constructions.

The shear strength of a soil is defined as the maximum – or limiting – value of shear stress that may be induced within its mass before the soil yields [Whitlow, 1990]. Usually a shear slip surface will form, which is comparable to the failure of land in practice, for example landslip, rotational slip and excavation failures. Evaluation of the parameters of shear strength is a necessary part of analytical and design procedures in connection with foundations, retaining walls and earth slopes. Generally the formation of shear strength within a soil mass is due to the development of particle interlocking, meshing of irregularities on particle surfaces, adhesion, cohesion and cementation. Clay minerals in a soil are of fundamental importance in establishing the shear resistance of a soil: At low water content, restricted water films subject the mass to compressive stresses of considerable magnitude and thus increase shear resistance. However, an increasing degree of saturation decreases the effective compressive stress due to the development of water films around the clay minerals. Therefore, an unsaturated soil is considered to be a three-phase system consisting of the phases solid (mineral particles), gas (air) and liquid (water). The introduction of the air-water interface, commonly referred to as the "contractile skin", takes the phase approach a step further and converts the unsaturated system into a four-phase system [Fredlund and Rahardjo, 1993].

A simple equation and theory relating the shear strength of soil to the applied normal (=vertical) stress was first suggested by Coulomb in 1776. The cohesive resistance to shearing is assumed to be constant for a given soil and independent of the applied stress,

whereas the frictional resistance varies directly with the magnitude of the normal stress developed on the failure surface.

A straight line equation for the limiting shear stress τ_f is given by equation 6.1:

$$\tau_f = c + \sigma_n \tan\phi \qquad\qquad \textbf{(equ.6.1)}$$

where: c = cohesion

σ_n = normal stress on slip surface

ϕ = angle of internal friction
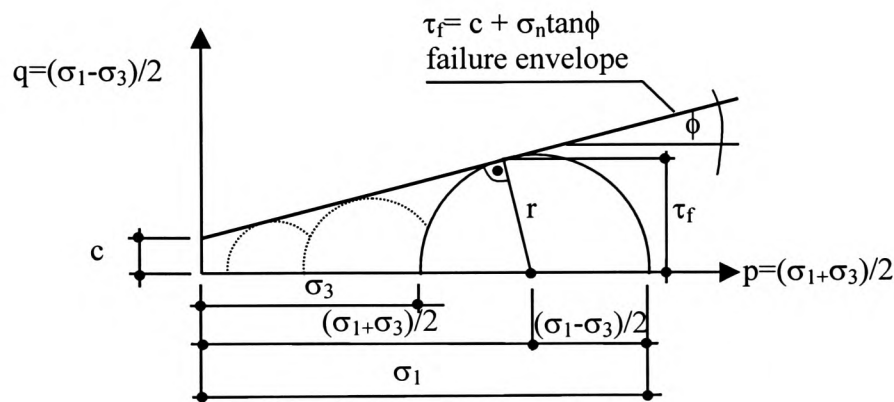
Figure 6.4 *Shear strength theory*

As Figure 6.4 indicates, the value of the cohesion is the intercept on the shear stress axis and the slope of the line is $\tan\phi$.

It should be noted that the values for effective stress are obtained by reducing the measured (= total) values by the value of the pore pressure (u) in a saturated sample. Lade and De Boer [1997] gave a useful definition of the effective stress in a soil by describing it as "the stress that controls the stress-strain, volume change and strength behaviour of a given porous medium, independent of the pore pressure". This emphasises the importance of a correct pore pressure measurement. The soil samples in the project, however, showed only saturation values of around 80 %, thus no effective stress was calculated, which was considered to be outside the scope of the current project. Hence the undrained, unconsolidated triaxial test was selected as an effective means of evaluating the shear strength development.

Another important factor, influencing the performance of a sample during shearing is the water content of the material relative to the optimum moisture content, which influences the development of flocculated and dispersed structures in a clay. The generally accepted theory behind this is the fact that water in a sample, compacted on the wet side of the optimum moisture content, ensures the full development of the 'electrical' double layer, thus preventing a close approach resulting in parallel arranged clay particles. If material is compacted on the dry side of the OMC, shrinkage of the double layer of the clay particles leads to a closer approach and the particles approach close enough for face to edge contact, leading to a higher resistance to shear [Barden, 1971]. To prevent the influence of this phenomenon, all samples were compacted at OMC.

It should be noted that the kaolinite used in the current project, is characteristic of clay soils with a narrow grading curve and little or no fractions of sand and/or silt, and will thus have a tendency to develop quickly a polished failure plane during the shearing process. Rossato et al. [1992] stated that this is due to orientation of the fine particles adjacent to the failure surface. Soils with a wider grain size distribution create interlocking bonds due to the frictional and interlocking effects between coarse and fine particles. Within the framework of the current project, however, use of kaolinite provides information on how slag/lime mixes would influence the shear behaviour of a soil which has limited variation in grain size.

6.2.1.2.2 Test procedure

For this research it was decided to investigate the shear strength development of the cured clay plus stabiliser specimens in the framework of an undrained unconsolidated triaxial test. To determine the shear strength of the samples a computer controlled hydraulic triaxial testing system (Geotechnical Digital System - GDS) was used (Figure 6.5). Prior to mounting the samples onto a porous disc covering the base piston of the lower chamber, the GDS was de-aired by injecting deionised water with a syringe. Utilising a vacuum membrane stretcher, the sample was covered with a rubber membrane to prevent the access of water from the surrounding perspex cell. Then the cell was flooded and the hydraulic controller, responsible for the application of the normal pressure was zeroed. Cell pressures of 200, 350 or 700 kPa were applied via a second hydraulic controller. The reaction rod on top of the cell was then "docked". The

strain rate was chosen as 90 mm/min in order to ensure a failure within the period suggested for the undrained unconsolidated triaxial test of between 5 to 15 minutes according to BS 1377: 1990: part 7. It should be noted that for some of the tested samples, especially those with a high content of ggbs cured at higher temperatures, the GDS was not capable of obtaining the failure condition at a cell pressure of 700 kPa. This was mainly due to the fact that the pressure transducers of the hydraulic controllers are only capable of measuring pressures up to 2000 kPa. In these cases in order to achieve shear failure the test was repeated at a lower confining pressure. During the test the GDS logs all pressures at each increment of increasing strain and computes automatically values for the principle stresses and finally prints the results. After termination of the test, the sample was dismantled, its moisture content determined, a short sketch of the failure plane drawn and a small sample taken for the microstructural investigations.
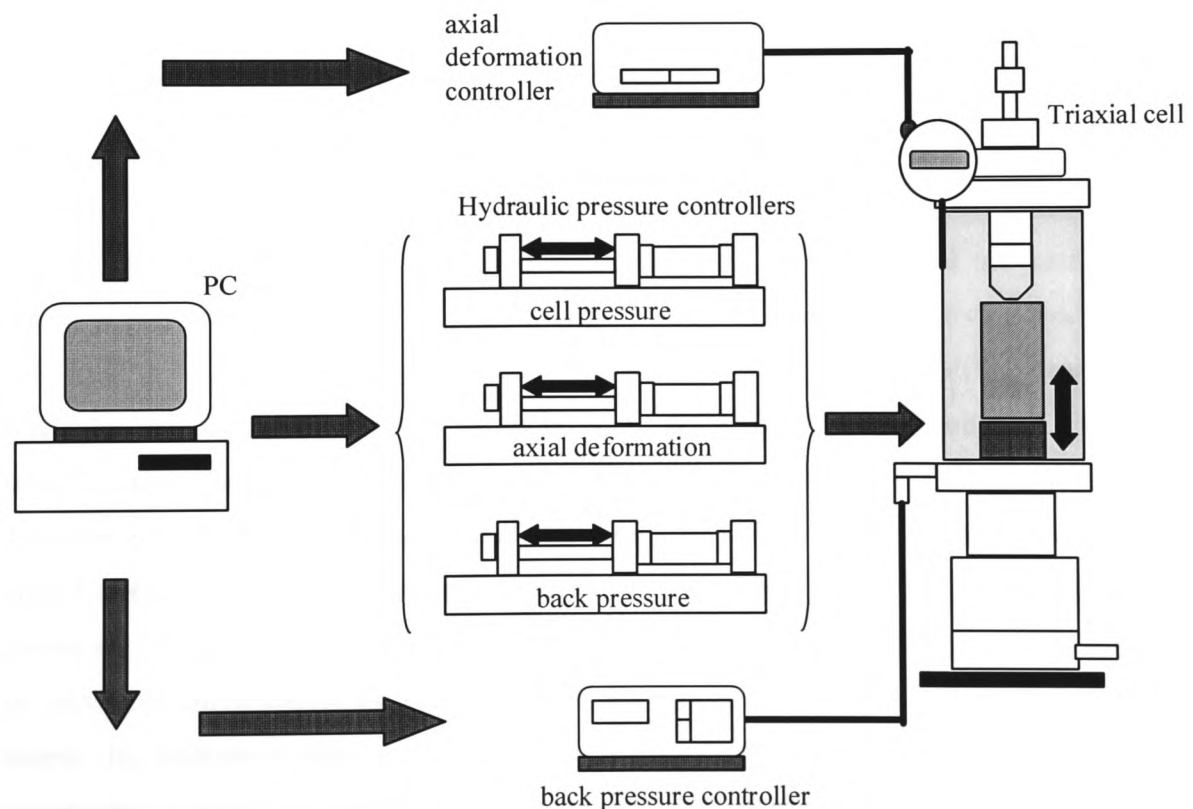
Figure 6.5 *Diagrammatic layout of the GDS equipment [after Menzies, 1988]*

The GDS records stress paths up to the maximum values at failure and beyond that point until a pre-set percentage of strain is achieved. If the stress combinations at failure

for different confining pressures are joined by a line, the modified failure envelope is created (Figure 6.6). To obtain the classic Mohr circle failure envelope, designated by the tangential points of the circles, a simple trigonometrical conversion is necessary.
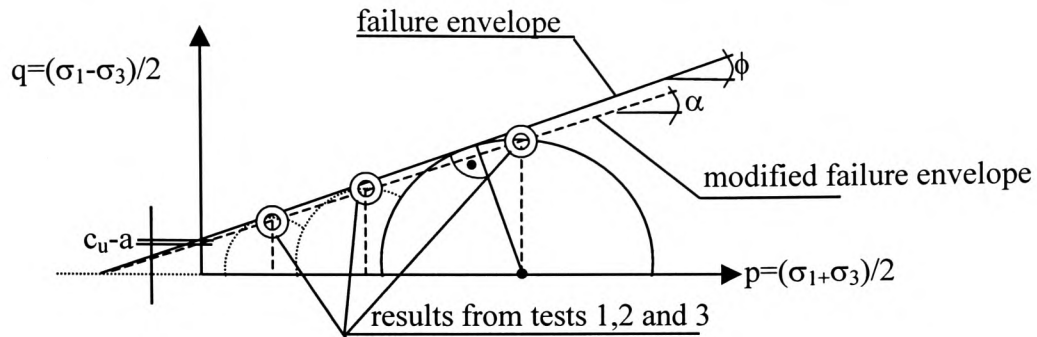
Figure 6.6 *Failure envelope and modified failure envelope*

6.3.1.3 Indirect Tensile Strength

6.3.1.3.1 Theoretical background

Strength investigations of the stabilised soil have in the past referred mainly to strength exhibited by stabilised material under compression. Tensile stress, however, cannot be avoided. It can be associated with shear and is generated by differential movements, which occur, when the stabilised material (for example the capping layer of a road) is subjected to traffic loading. Another cause of differential movement causing tension might be shrinkage, which could result in cracking or other deformation and which would seriously impair the durability of the material. Thus, determination of the tensile strength of stabilised material in addition to compressive strength is of practical significance. The tensile strength of a material can be measured by three different tests, which are outlined in Figure 6.7 [after Neville, 1995].

In pavement construction, direct tensile tests are currently used in France in order to assess the necessary thickness of subbase layers. These tests, however, are quite complicated to carry out and difficulties are frequently experienced with the satisfactory gripping of the test specimen in order to avoid premature failure near the end attachment during testing. Other European countries – and even France itself – tend to apply indirect tensile tests instead [Neville, 1995, Geiseler, 1997].
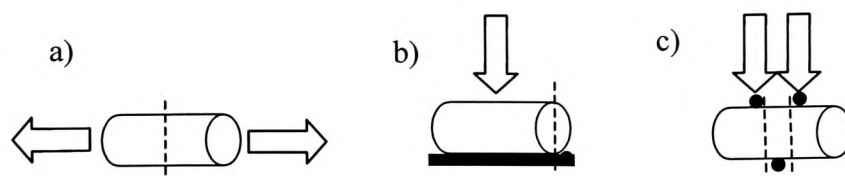
Figure 6.7 *Different types of tests tests for tensile strength (dotted lines indicate the failure planes): a) direct tensile test, b) indirect tensile test (splitting tension test) and c) flexural strength test*

The value obtained from the indirect tensile test is generally slightly higher than that produced from the direct tensile test. This is due to the fact that the indirect test method involves non-uniform stress distributions, which might be beneficial for parts of the specimen, where weak bonding would (when subjected to equal stresses all through the sample) lead to lower ultimate strength on failure. Also the direct tensile test is susceptible to the development of high stress concentrations in the regions of the specimen adjacent to the grip. Bearing this in mind, pilot trials with a loading rig according to the draft of the European Standard, were carried out, utilising packing strips of various materials in order to achieve the best stress distribution. Finally, strips made of balsa wood were chosen, as these were able to deform more effectively and distribute the load more evenly than those made of polystyrene or hardboard.

6.3.1.3.2 Test procedure

Based on the draft of a European Pre-Standard "Mixtures bound with hydraulic binder – Test method for indirect tensile strength – January 1997", cylindrical samples with a diameter of 50 mm and a height of 100 mm were placed in the testing rig, which had been manufactured according to European pre-standard specifications, and loaded uniformly at a rate of 4.8 kN/min. A test value consisted of an average failure value from three test specimens. If one test result was more or less than 20 % of the average of the two others, this value was discarded and the average of the two last values was taken as the load at failure. In general, however, variations in the failure load of less than 5% were observed. The indirect tensile strength of the specimens was calculated from the force at failure F by the equation (6.2):

$$R_{it} = 2 \times F / \pi HD$$ (equ.6.2)

where F = force at failure [N]

H = length of the specimen [mm]

D = diameter of the specimen [mm]

R_{it} = indirect tensile strength of the mixture [N/mm^2]

6.3.2 Permeability

The capacity for fluid flow through any porous medium is an engineering property termed permeability, the value of which – usually expressed as the permeability coefficient k [m/h] – is significant in calculations regarding seepage, settlement or stability problems. Permeability is, however, also of critical importance with regard to microstructural types of distress, namely sulphate attack and frost resistance [Young, 1988].

Whereas in concrete technology the permeability can be expressed either as the permeability to air, water vapour, gases (for example O_2 or N_2) or to liquids (liquid water or even oil) [Hooton, 1989], the permeability of soils is generally understood to relate to the permeability to water. Of particular interest in connection with permeability measurements is the initial saturation of the samples. Bjerrum and Huder [1975] report that the experimental determination of the permeability of compacted soils is in general complicated by the fact that the samples are initially not fully saturated. The errors incurred in conventional permeability tests on partially saturated samples are, in the first place, due to incorrect measurements of the flow of water, resulting from the change in volume of the entrapped air. In the second place the gas bubbles have a tendency to accumulate in the sample where the water emerges, which inhibits flow and results in erroneous permeability values. Kertscher [1988] and Hooton et al. [1988], also refer to the insufficient saturation of the samples as the major source of misleading results. Kertscher [1988] obtained – depending on the grade of saturation – permeability results within a huge bandwidth. He found that the coefficient of permeability k for a silty clay increased from a value of 1.0×10^{-8} cm/s to 1.0×10^{-6} cm/s when the moisture content is

reduced from 23 % to 12 %. Arabi [1987] immersed specimens initially for 48 hours in de-ionised water in order to ensure complete saturation before permeability tests started, employing a triaxial cell and a constant head. However, pilot tests carried out by the author did not lead to satisfactory results when the material was just immersed in water. In comparison, high grades of saturation were obtained employing a method introduced by Bjerrum and Huder [1975], which is a refinement of procedures adopted by Lowe and Johnson in 1960. Saturation is achieved by an increase in the pressure in the pore fluid, forcing air in the pores to go into solution, utilising a triaxial cell with the possibility of back pressure adjustments. The theory behind this is mainly based on Henry's law, referring to the fact that the mass of a gas dissolved by a fixed amount of liquid is directly proportional to the gas pressure at a constant temperature [Buttle et al., 1981]. The original three-phase-system comprising soil particle network, pore water and pore air is thereby converted into a two-phase system by replacing the pore air by water [Bjerrum and Huder, 1975 and Kertscher, 1988]. A more modern approach looks at the unsaturated soil as a four-phase-system, adding the air-water interface, the "contractile skin", as the fourth phase [Black and Lee, 1973]. Generally two factors influence the saturation of a sample via the application of a back pressure [Head, 1986]:

i)   the pressure applied

ii)   the length of time required

Various authors [Kertscher, 1988, Bjerrum and Huder, 1975, Black and Lee, 1973, Head, 1986] state guidelines for time and pressure requirements in order to achieve satisfactory saturation, which is taken as the point at which a B-value of at least 0.97 is displayed. A B-value is a geotechnical parameter, expressing the change in pore pressure after an increment in cell pressure was applied [Skempton, 1954, Bishop, 1954]. However, the fact that stabilised soils exhibit a different saturation behaviour due to the formation of cementitious gels in the pores is usually neglected. Therefore a division of soils into specific categories is necessary. Black and Lee [1973] have summarised their results of a study into the saturation behaviour of different types of soils in Table 6.1.

Table 6.1 *Values of B for typical soils at and near full saturation [after Black and Lee, 1973]*

Soil category	Saturation = 100%	Saturation = 99.5 %	Saturation = 99 %
soft	0.9998	0.992	0.986
medium	0.9988	0.963	0.930
stiff	0.9877	0.69	0.510
very stiff (including soils with a cementing agent)	0.913	0.20	0.10

Based on their results it is clear that effort could be wasted on the soils dealt with in this research, since it appears impossible to achieve a pore pressure coefficient B of 0.97 even at 100 % saturation for soils containing a cementitious agent. Pilot trials revealed that depending on the type and amount of cementitious agents added and the curing time allowed before saturation commenced, B-values of between 0.45 and 1.00 were achieved. Based on equation 6.3 [Head, 1986] and on an original degree of saturation of 80 %, the back pressure theoretically necessary to increase the degree of saturation up to 99 % was calculated.

$$u_b = 4965 \ (1-S_0) \ [kPa] \hspace{3cm} \textbf{(equ. 6.3)}$$

u_b is therein defined as the theoretical additional back pressure required to increase the degree of saturation from an initial value S_0 to a final value S. In this case S was assumed to be 99 % (near full saturation), which delivers a back pressure of 943 kPa. It was decided to increase the back pressure up to 950 kPa, a value which also correlated well with a back pressure determined from a graph introduced by Kertscher [1988]. Simultanuously the confining pressure was increase up to 1000 kPa to ensure that the sample would not collapse.

Based on calculations by Black and Lee [1973], a saturation period of approximately 4 days would be required. However, Kertscher [1988] subjected lime-stabilised clay samples to a back pressure up to 850 kPa and found that even a comparably short saturation period of 50 minutes leads to satisfactory B-values. Trials involving the stabilised samples revealed that saturation ramps over 8 hours delivered B-values reflecting basically full saturation (≥ 0.99). The chosen saturation ramp is illustrated in Figure 6.8. Once the saturation ramp is completely applied over the chosen period of 8

hours, the permeability test is carried out by applying a hydraulic gradient to the sample. In the current work, the test was carried out using equipment produced by Geotechnical Digital Systems (GDS), with a numerically controlled triaxial cell, capable of working within a cell pressure range of zero up to 1700 kPa. The set up is further explained in a publication by the founder of the GDS company [Menzies, 1988] and consists basically of a computer controlled cell, with the computer monitoring sets of readings at a frequency of typically less than once a second and therefore providing continuous control.
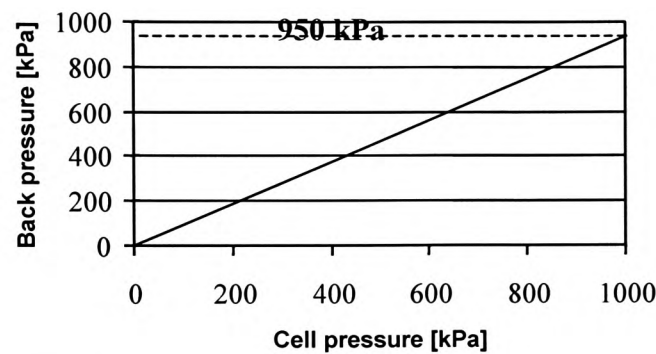
Figure 6.8 *Saturation ramp with a final back pressure of 950 kPa and a simultaneously increased cell pressure up to 1000 kPA*

The cell pressure was kept constant throughout the test in order to maintain the achieved degree of saturation. A flow was then initiated from the bottom to the top of the sample by a uniform increase of pore pressure through the bottom filter plate. The flow rate, which needed to be roughly calculated prior to the start of the test from an expected permeability of the test soil, was finally achieved by adjusting the pore pressure. Once a laminar and constant flow was achieved, which could be detected by no further changes in the pore pressure over a period in time, the test was terminated. The GDS recorded all pressures and the corresponding flow rates to a high degree of precision. To determine the permeability and therefore achieve a constant flow, recordings over a period of 24 to 36 hours have proved satisfactory. From the results the permeability can be calculated using Darcy' s law (6.4):

$$k = \frac{q \times l}{A \times h} \ [m/h]$$

(equ. 6.4)

where   q = flow rate [m/h]

l = height of the sample [m]

A = cross-sectional area of the sample [m^2]

h = differential head [m]

Figures 6.9 illustrates the development of the flow until the permeability stabilises.
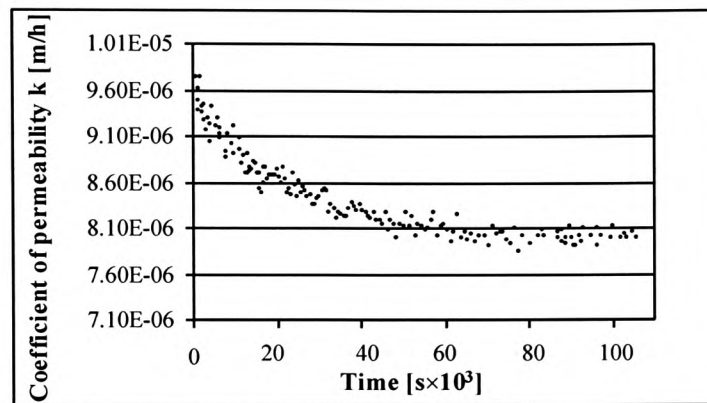
Figure 6.9 *Development of the flow measurements during a test over a period of 28 hours*

From this example the permeability would have a k-value of 7.9 x 10^{-6} m/h, since a pre-chosen flow rate could be obtained with a constant back pressure of 1200 kPa (automatically targeted and adjusted by the system) at a confining pressure of 1500 kPa.

6.3.3 Mercury intrusion porosimetry and pore size distribution

6.3.3.1 Theoretical background

For cementitious materials, it is well recognised that both total porosity and the pore size distribution determine not only permeability, durability (e.g. the rate at which aggressive agents enter a mass and cause disruption) and the resistance to frost action but also strength development. Various methods employed in investigations into the porosity of cement bound materials can be found in the literature, the most popular of which appears to be mercury intrusion porosimetry (MIP).

Prior to the application of this technique on a wide range of samples, it was necessary to establish that at the highest pressures applied (about 2000 kPa) the intrusion curve (which shows the relationship between intruded pore size and amount of mercury intruded) flattened out. A flattened curve at the end of the experiment indicates that no further intrusion is recorded. Depending on the material's internal stability high pressures could cause the crushing of sealed pores, leading to erroneous results [Winslow, 1989, Feldman, 1984]. A mercury intrusion curve, still increasing in the presence of the highest pressures towards the end of an intrusion run would suggest that there are still empty pores which have not yet been reached by the mercury (Figure 6.10). Pilot tests, however, confirmed that the pressure range available was appropriate for the stabilised soil samples.
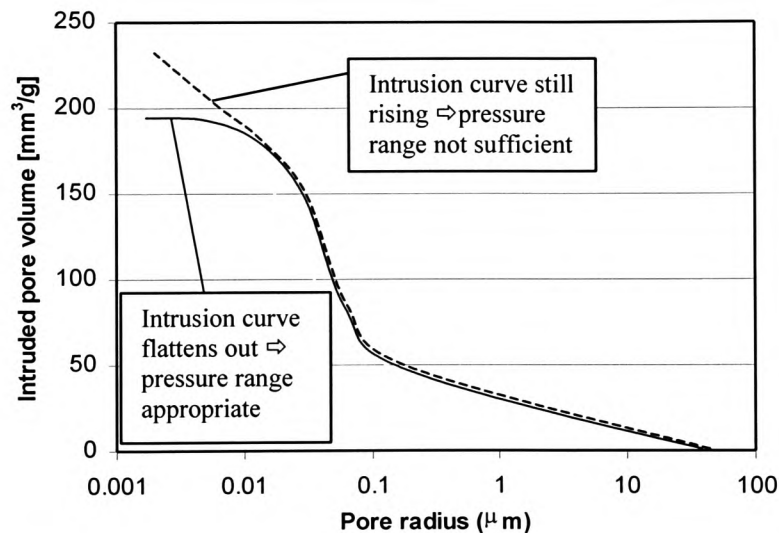
Figure 6.10 *Applicability of pressure range within MIP*

It is a necessary condition for mercury intrusion porosimetry that the specimens are dry, i.e. free of all evaporable water. To achieve that, various techniques can be employed. Most commonly encountered are:

i) direct oven drying

ii) solvent replacement drying

iii) freeze drying

iv) critical region drying

With regard to the employment of drying technique i), it should be noted that some studies [Winslow and Diamond, 1970, Konecny and Naqvi, 1993] indicate that the proportion of pores with a diameter <100 nm tends to decrease in comparison to less rigorous drying regimes. Winslow and Lovell [1981] and Diamond [1970] also advise against this technique because of the related large shrinkage rates, due to tension forces on pore wall surfaces when the air-water meniscus radius becomes smaller during water evaporation. This can lead to the collapse of weaker pore structures, for example in the case of clay soils with high initial moisture contents.

Solvent replacement drying (ii) involves the storage of samples in propanol until weight consistency is achieved prior to drying. It is advantageous with respect to preserving the pores in the fine pore size region in cementitious materials [Konecny and Naqvi, 1993]. Little information could be found with regard to how soil specimens would react to an initial soaking period in propanol.

Prior to vacuum drying the specimens are quickly frozen during a freeze-drying process (iii) to achieve water removal by sublimation (solid converts directly into a gas). Thus, the shrinkage effect, which causes specimens to shrink when liquid water evaporates during oven drying is eliminated. Both, quick freezing and the vacuum drying process are critical for the success of the technique. If the freezing rate is not high enough, ice crystal formation could be initiated, resulting in the expansion of pores. During the vacuum drying process the samples need to be heated up in such a way that no liquid water phase forms in the sample. This requires a strict control of temperature and pressure in the vacuum chamber. If, however, liquid water forms, the same mechanism which leads to shrinkage in oven dried specimens will result in shrinkage of the freeze-dried specimens.

The complex procedure of dehydration during critical region drying (iv) implies the application of temperature and pressure until the liquid and the gas phase of water can coexist in a single phase ("critical region"). Winslow and Lovell [1981] state that there is some indication that critical region drying can alter the mineralogical composition of soils.If, however, the other techniques are not suitable for a material in question, critical region drying can be the only alternative available.

This list of drying techniques is not comprehensive. For example Winslow and Diamond [1970] employed evacuation over a dry ice trap and equilibration over magnesium perchlorate hydrates to dry samples of Portland cement. Based on this assessment, a "gentle" drying regime at approximately 30 °C over silica gel and

carbosorb in a vacuum desiccator was adopted in the current work. The silica gel and carbosorb was changed regularly and the specimens remained in the vacuum desiccators until weight consistency was achieved.

Based on Winslow's original model, it is assumed that all intruded pores are cylindrically shaped and thus the entry diameter and the pore diameter would be equal. There are, however, pore shape anomalies, which have to be considered. Figure 6.11 shows schematically ink-bottle pores and isolated pores in comparison to a normal cylindrical pore, on which Washburn's model is based.
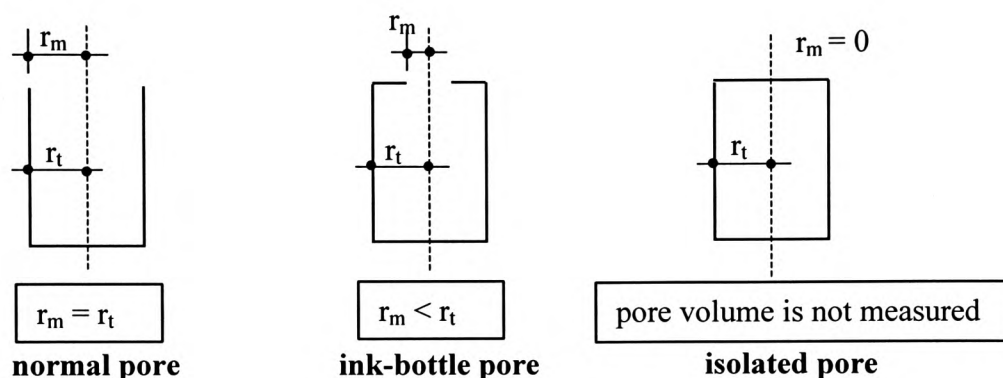
Figure 6.11 *Types of pores and their radii* (r_m = *measured radius,* r_t = *true radius*)

An isolated pore has either no access to surrounding capillary systems or an entry size smaller than the minimum intrudable channel. Thus, the volume of such a pore will not be represented in the total pore volume measurements or pore size distribution curves. The volume of ink bottle-shaped pores, however, is measured, but the total volume will be attributed to the pore group with the radius r_m, instead of the correct pore size group with the true radius r_t.

It is difficult to assess the effect of ink bottle and isolated pores exactly, but the possibility of their presence should be borne in mind when interpreting results.

6.3.3.2 Test procedure

The porosimeter used was a Fisons Macropore Unit 120 and a Fisons Porosimeter 2000W (pressure generation up to 2000 kPa and pore size measurements down to a

diameter of 0.0037 µm), which is software-operated (software "Milestone 2000" by Carlo-Erba Instruments) from a dedicated PC.

Prior to filling a dilatometer (containing a sample of approximately 1.0 g and prysmatic in shape) with mercury under vacuum conditions, the dilotometer was evacuated utilising the Macropore unit. Subsequently the pressure was increased incrementally by means of a bleeder valve up to atmospheric pressure and the intruded volume of mercury was noted at each stage. The macropore pore size distribution data are subsequently input manually into the "Milestone 200" software, which processes the data and allows for further calculations to be carried out on the subsequently and separately captured micropore measurement data. The micropore pore size distribution data are obtained using the porosimeter 2000 W unit by relating measurements of the volume of mercury that penetrates pores of the sample to the hydraulic pressure exerted at different stages.

Washburn's equation [1921] (6.5), given below,

$$ r = \frac{2\sigma\cos\theta}{P} \qquad \text{(equ. 6.5)} $$

is used to calculate pore sizes from intrusion pressures. P is the pressure required to intrude a pore with a radius r. The results depend also on the surface tension σ and the contact angle θ of the intrusion liquid. It is a requirement for pressure-induced intrusion that the liquid has to display a contact angle of at least 90°, resulting in failure to "wet" the surface of the specimens. The contact angle depends on the nature of the sample and can vary considerably. Winslow and Lovell [1981] and Diamond [1970] give values of 147 °for both kaolinitic and illitic clays and average values of 139° for montmorillonitic clays. It was, however, decided to work with a contact angle of 141°, as recommended by the manufacturers of the porosimeter (Fisons Instruments, Italy). The equation requires also knowledge of the surface tension σ of mercury, which varies with temperature. Based on recommendations by Fisons Instruments and confirmed by literature reports [Diamond, 1970], a value of 480 N/m (=dyne/cm) was adopted.

In addition to the overall pore size distribution within the tested specimen, the derivation of the threshold radius from the MIP data is useful (Figure 6.12). This radius, sometimes also referred to as 'continuous pore size radius', is a measure of pore connectivity and also assists in assessing the obtained degree of pore refinement.

Intrusion curves usually exhibit at a certain pressure (on which the threshold radius determination will be based) a significant increase in intruded pore volume, which is believed to reflect the presence of a large number of well connected pores of a certain size. The threshold radius is thus the entry radius of this pore fraction and a reduction in the threshold radius is generally associated with a more refined pore structure.
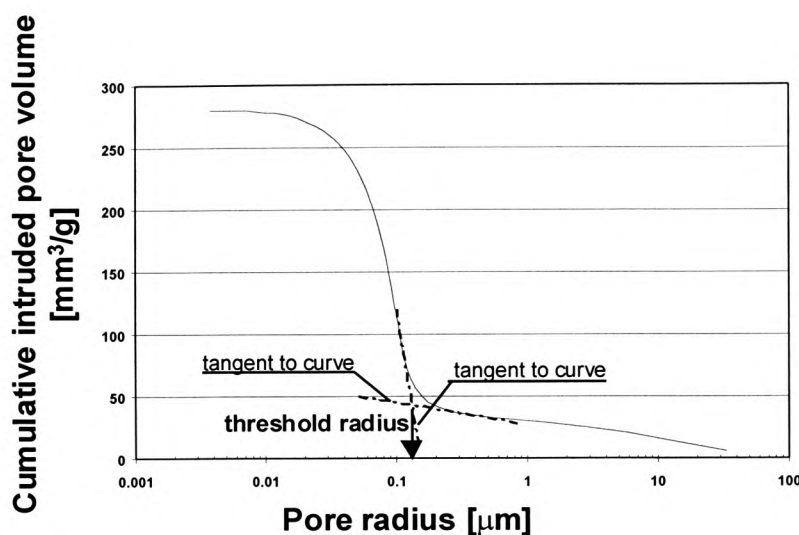
Figure 6.12 *Determination of threshold pore radius*

6.3.4 Frost resistance

6.3.4.1 Theoretical background

Laboratory freezing tests are necessary to characterise the frost susceptibility potential of sub-base material. Initial tests developed, for example a frost heave test introduced by the US Army Corps of Engineers and referred to as the CRREL (Cold Regions Research & Engineering Laboratory) standard freezing test, had several limitations. The test was long, it did not include the effects of freeze-thaw cycling and, due to a required constant frost penetration rate, was comparably difficult to carry out. Chamberlain [1987] suggested large modifications to the test, which involved for example the assessment of the bearing strength after test termination and an overall reduction in test duration from 12 days to 5 days. Based on his suggestions the "Standard test methods for frost heave and thaw weakening susceptibility of soils – ASTM D5918-96" [American Society for Testing and Materials, 1996] was released. In 1967 the British

Road Research Laboratory at the Ministry of Transport described a frost test to investigate the frost susceptibility of soils and road materials [Croney and Jacobs, 1967]. This test, commonly referred to as the "LR 90 frost heave test", was extended in 1977 by interim specifications for use with granular material [Transport and Road Research Laboratory].

Based on the latest developments with regard to the European Standardisation process, however, the "German proposal for a test method on freeze-thaw resistance of hydraulically bound bases", CEN/TC 227/WG 4 N187E [Deutsches Institut für Normung, 1996] was utilised in the current work. Due to the nature of the samples, however, some modifications to the original test procedures with regard to sample preparation and generation of results had to be made.

6.3.4.2 Test procedure

At the end of the prescribed moist curing periods of 7, 28, 90 and 180 days at 30 °C, cylindrical samples with a height of 100 mm and a diameter of 50 mm – prepared as described in section 6.2 - were removed from the curing chamber and unwrapped.

Utilising a vacuum membrane stretcher, a natural rubber membrane was folded over each sample and the ends confined with saturated porous discs (d= 50 mm and h = 2 mm) (Figure 6.13). Then the height of the samples (including the porous discs) was measured to an accuracy of 0.1 mm with a dial gauge fixed in position on a dial gauge holder (Figure 6.14). The specimens were then weighed and the diameters measured at the top, the bottom and in the middle of the sample. The average value was used as the original diameter, based on which the volume changes of the samples were determined. Prior to being placed in an airtight container, which was filled with water up to the height of the porous disc to allow permanent water access, the samples were mounted on small supports to avoid direct contact with the bottom of the container. Finally the container was placed in a programmable Prior Clave LCH/600/25 environmental chamber where it was initially kept for 4 hours at 20 °C to condition the samples and allow water absorption. Then the freeze-thaw regime was started. The samples were subjected to 12 freeze-thaw cycles, each lasting for 24 hours. Figure 6.15 outlines the temperature regime during the cycle. During the thawing period at 20 °C a relative humidity of 95 % prevailed. After every freeze-thaw cycle, the length change and change in diameter and weight were determined and the samples were inverted when

replaced onto the sample supports. The changes in dimensions were expressed as a percentage of the original measurements taken prior to the specimens being brought in contact with the water.
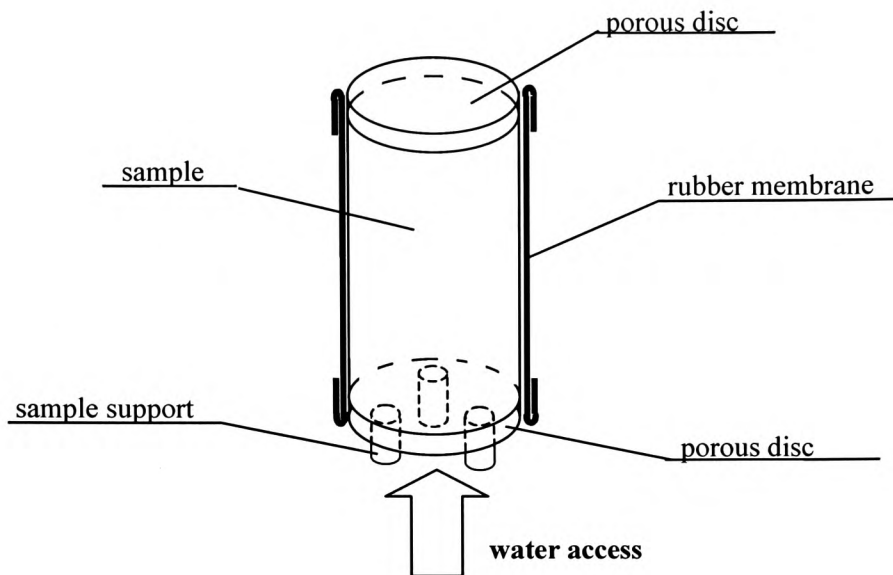
Figure 6.13 *Schematic view of sample set-up*
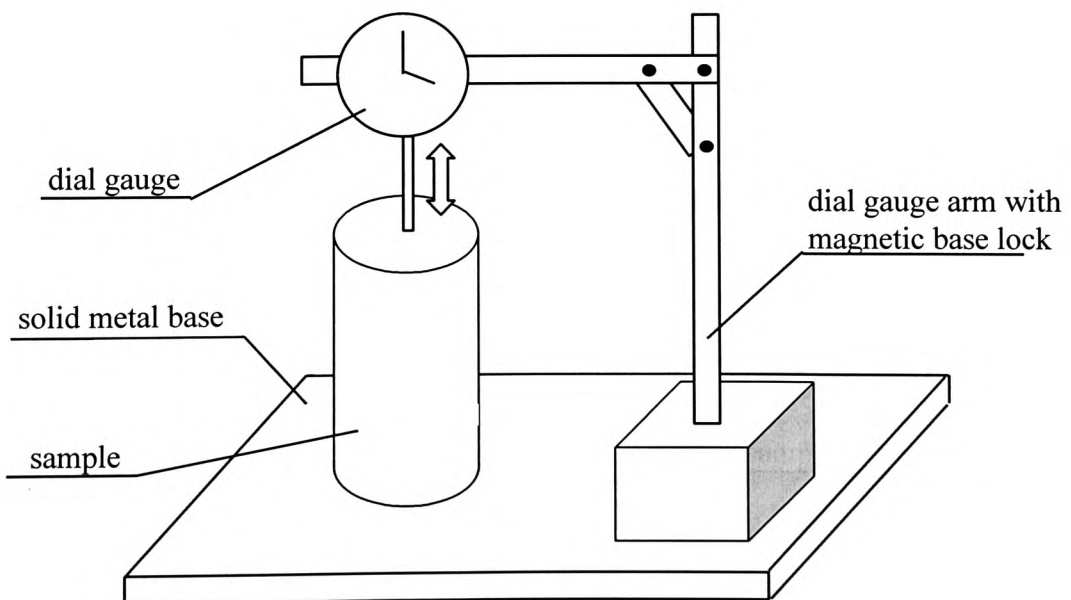
Figure 6.14 *Set-up for determination of length change*
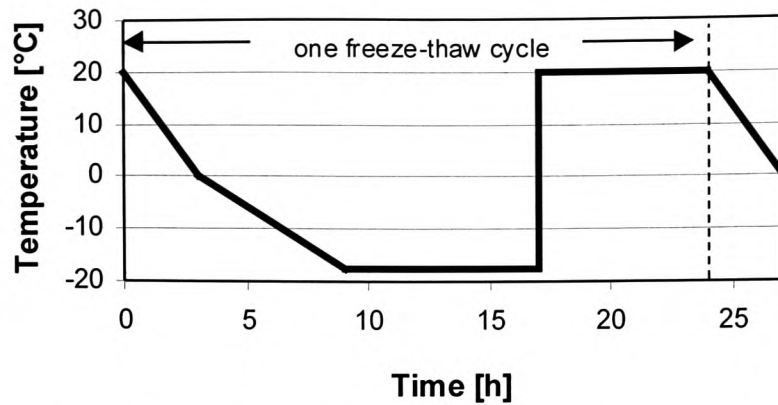
Figure 6.15 *Temperature regime during the freeze-thaw cycle*

6.3.5 Swelling

In order to assess the linear expansion of samples due to chemical reactions and water absorption, an experimental set-up as introduced by Kinuthia (1997), was utilised. However, whereas Kinuthia had used only one tank in which a complete series of samples had been accommodated during the observations, in the current project each sample was allocated its own specific container. Thus, no cross-contamination between specimens could take place, which eliminates the possibility of chemical interaction between different samples. A typical sample unit is shown in Figure 6.16. The samples were tested unrestrained except for a thin layer of cling film around the sides. Each sample was placed onto a porous disc, thus allowing unhindered access of water, and mounted on a perspex tray in a glass jar, fitted with a dial gauge on top. After 7 days of moist curing at 30 °C, samples were soaked in de-ionised water and the linear expansion was monitored on a daily basis.
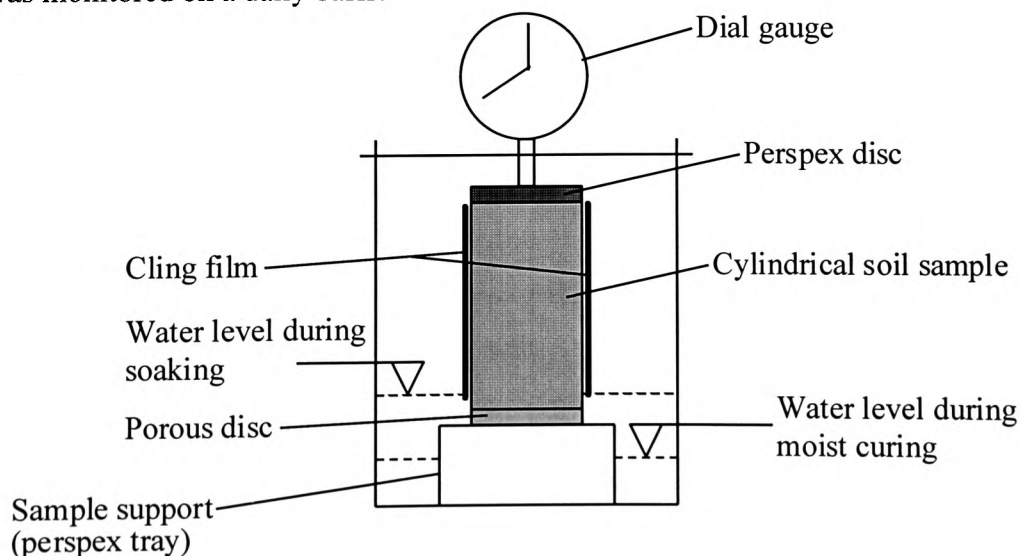
Figure 6.16 *Experimental set-up to investigate linear expansion*

6.4 Microanalytical techniques

For specimens where slag was added as the sole stabiliser (see section 7.3), scanning electron microscopy (SEM) and thermogravimetric analysis (TGA) were employed. In combination with X-ray powder diffraction (XRD), TGA and SEM form a set of powerful tools which are frequently utilised in the identification, characterisation and systematic study of clay minerals.

6.4.1 Scanning electron microscopy (SEM)

SEM was used to identify the presence of crystalline substances and to get a general idea of the morphology and texture of the treated material. The SE microscope processes the flux of secondary and backscattered electrons from the material under investigation, which has been probed by a scanning electron beam. The electron beam is generated by heating up a tungsten filament to such a high temperature that the electrons in the tungsten become sufficiently excited to escape (thermionic emission). Accelerated by the anode disc, the diameter of the electron beam is controlled by the condensers. When it finally bombardes the specimen, many different interactions occur between the sample and the electrons, not all of which are of use for the SEM analysis. If the electrons have sufficient energy, they will simply pass through the specimen (unscattered electrons). This can happen when the specimen is extremely thin (< 1 μm). Of more use are elastically scattered electrons, which change their direction due to charge differences when the electron passes close to a positively charged nucleus of the specimen. In addition, loosely bound conduction electrons might be knocked out of the sample and escape as "secondary " electrons, contributing to the SEM image. The beam impact can also produce Auger electrons and X-rays, which can be picked up by the installation of suitable detectors. In order to obtain an image of the specimen, a large number of points over an area have to be probed. Thus, scan coils, which are effectively electromagnets, control the scan and ensure that an area is systematically sampled in a raster scan, known as a 'frame'. The definition or resolution of the resulting three-dimensional image is of the order of approximately 0.01 μm. Figure 6.17 gives a schematic overview of a scanning electron microscope.

Electron gun

Anode disc 2-25 kV)

Condenser lens

Scan coils

objective lens

Specimen on
specimen holder

Unscattered,
transmitted
electrons

Electron beam

Magnification control

Detector

Vacuum connection

Waveform
generator

Signal amplifier

Display screen
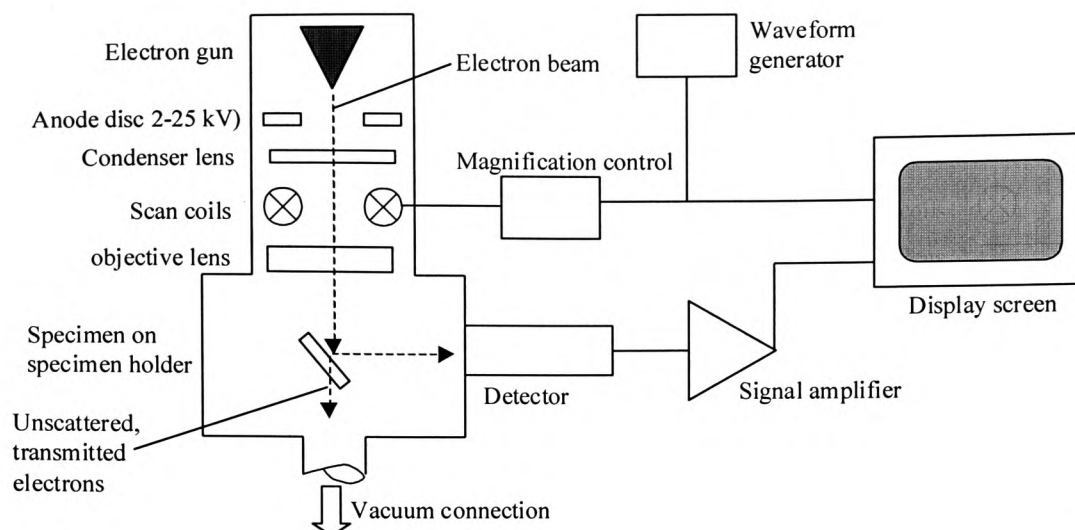
Figure 6.17 *Schematic overview of scanning electron microscope [after Lawes, 1987]*

It should be noted that non-conductive specimens collect a surplus of electrons on their surface, once subjected to 'electron bombardment'. Lawes [1987] points out that specimens which have pointed projections (for example needled-shaped crystals) are particularly susceptible because the charge accumulates at these points. This built-up of charge affects the image quality, results in immense contrast and can even deflect the electron beam. Thus specimens are made conductive with a thin uniform coating, which also conducts beam-induced heat away from the specimen. Most commonly employed are coatings of gold, gold/palladium alloy or carbon, which are either applied in a vacuum evaporator or during a sputter coating process.

The current work was conducted in the Department of Civil Engineering at the University of Wales in Cardiff on a stereoscan microscope S570 produced by Hitachi. A small piece of a specimen with a freshly broken surface was glued onto a specimen holder with a conductive liquid adhesive. Then the samples were vacuum-dried and coated with a thin layer of gold as a conductor in a vacuum evaporator, prior to being investigated under the microscope.

6.4.2. Thermogravimetric analysis

Thermogravimetric analysis (TGA) is a thermal analysis technique for measuring the amount and rate of change in sample mass as a function of temperature and time. It can be used to characterise basically any material that exhibits weight change as a result of crystallisation, phase change (some crystal structures change from one form to another, for example quartz, which changes from the α to the β form at 573 °C), dehydration (loss of absorbed water), dehydroxylation (loss of OH ions) and oxidation (for example combustion of organic matter). Results are influenced by various factors, for example, sample size, heating rate or packing density. Standardisation is thus necessary to ensure that reliable and repeatable results can be obtained.

Heating of clay results in a pattern of weight loss, which is characterised by the force with which water is retained within or on the clay structure at different temperatures. The major thermogravimetric effects on clay soils can be observed at temperature ranges of between 50 and 300 °C (loss of absorbed water and water of hydration) and between 450 and 1000 °C (dehydroxilation). At temperatures of beyond 900 °C most clay minerals undergo an exothermic recrystallisation phase and new crystals form from amorphous materials or from old crystals destroyed at lower temperatures [Mitchell, 1993]. It should be noted, however, that the thermal behaviour of clay soils can differ considerable from that of pure clay minerals, due to the presence of various organic additions or carbonates, which decompose on heating.

For the current work, TGA was carried out at TA Instruments Ltd, Leatherhead, Surrey, employing a thermogravimetric analyser Hi-Res [TM] TGA 2950 with a TA5000 Thermal Analyst Controller and dedicated software. The heating rate was chosen as 10°C per minute within a temperature range of 25 to 1000 °C. The sample was heated in nitrogen in a sealed aluminium pan with a 70 μm laser drilled hole in the lid. Weight loss and temperature increase are logged during the test and the resulting graph supplies the TGA weight loss curve [%] and the derivative weight loss curve (DTG) [%/°C]. The former plots the total weight loss in percent over the temperature range to which the sample was subjected, whereas the latter shows the derivative of the weight loss (d/d) with increase in temperature, resulting in a graph with pronounced peaks, which allows conclusions to be drawn as to the identity and quantity of particular compounds or phases present. A sharper weight loss resolution curve was obtained by opting for the

'HighResolution (HiRes)' mode, which means that the heating rate slows down when weight losses occur. Thus the definition of the weight loss curve is improved.

The accuracy of the TGA system was estimated using analytical gypsum ($CaSO_4 \cdot 2H_2O$) as a standard control (Figure 6.18a). This had the added advantage that many of the clays investigated contained gypsum. The theoretical weight loss of the bound water is based on a molecular weight for gypsum of 172.14 atomic mass units (amu), i.e.

$$CaSO_4 \qquad\qquad 2\ H_2O$$
$$(40.08 + 32.06 + 4 \times 16) \quad + \quad [2 \times (2 \times 1 + 16)]$$
$$136.14 \qquad\qquad + \qquad 36$$
$$= 172.14\ amu$$

The loss of water (36 amu) is therefore 20.91% relative to the gypsum molecule. The observed weight loss during the TGA run was found to be 20.05%, showing good agreement to the calculated result. Figure 6.18a shows the total and derivative weight loss of the used gypsum during TGA and also confirms that the dehydration of gypsum occurs as a two-stage process [Dunn et al., 1987].

It should be noted, however, that during the course of the project two different thermogravimetric analysers had to be used. Comparison of the results in a later stage of the project (the initial TG analysis was done externally) revealed similar weight loss patterns for, for example analytical gypsum, but the weight loss occurred over a shifted temperature range. This was mainly attributed to differences in calibration of the equipment used. To prove this point, analytical gypsum was analysed on the same TGA before and after calibration, i.e. readjustment of the height of the thermocouples within the furnace. Whereas the characteristic double peak (①+②) of gypsum could initially be found at approximately 160 and 210 °C, recalibration resulted in a shift of these peaks to 130 and 165 °C (Figure 6.18 a+b).

Although attempts were undertaken to rerun critical samples of specimens after recalibration to ensure consistency and good comparability of the results, some of them were found to have decomposed or carbonated during storage. Thus, the shift in temperature had to be taken into consideration when those results were interpreted. The reader is made aware of the situation with regard to calibration when the TGA results are presented in detail in chapter 7.
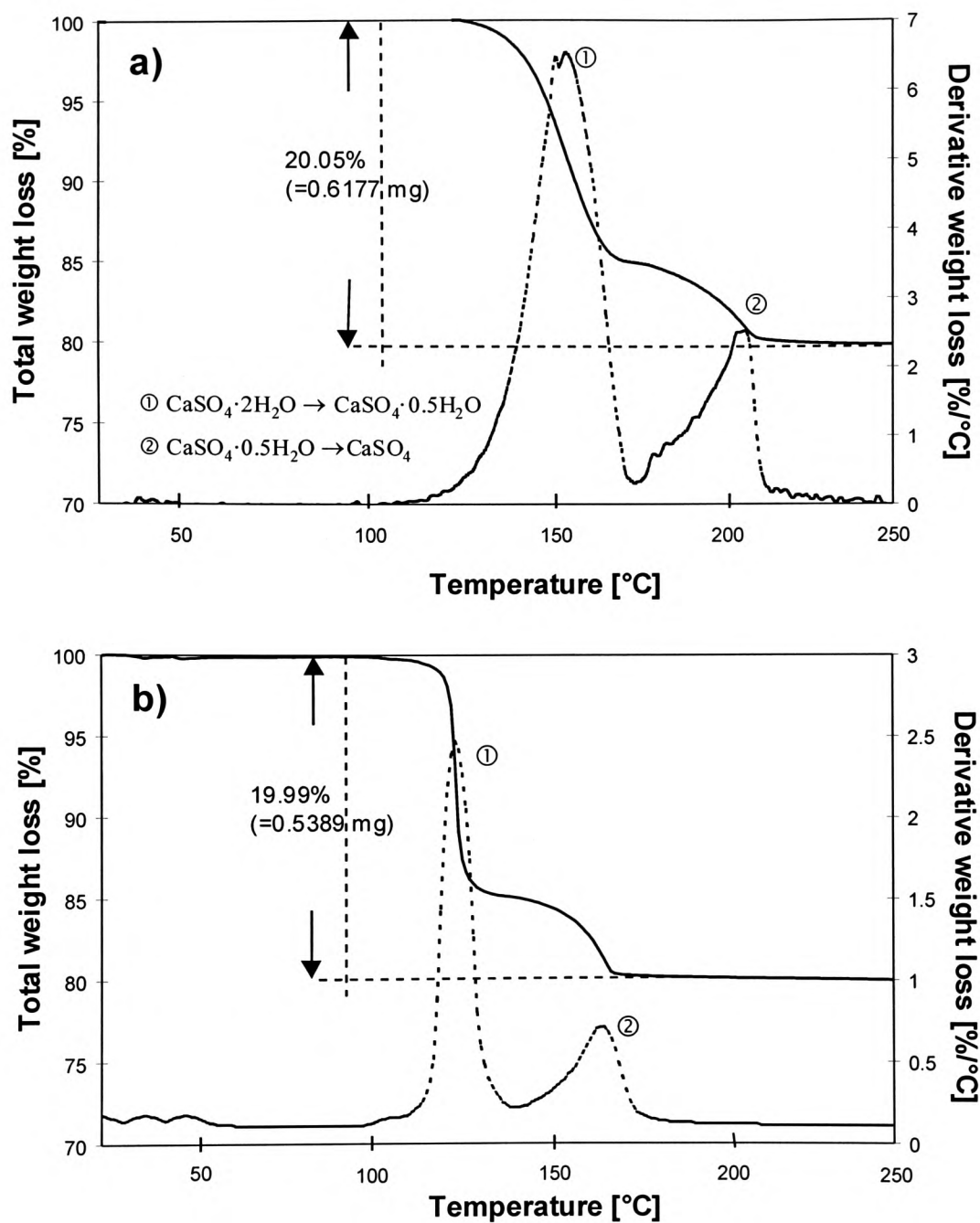
Figure 6.18 *TG analysis of analytical gypsum before (a) and after (b) recalibration of the equipment*

Chapter 7 – Engineering properties of soils stabilised with lime-activated ggbs

In this chapter the results from experiments carried out on the "main soils" of the project, kaolinite and Lower Oxford Clay, are presented. Due to the different nature of the soils, the chapter is sub-divided into two main sections dealing with results obtained from tests with stabilised kaolinite (with and without gypsum addition) and results from experiments carried out on stabilised Lower Oxford Clay. Within the kaolinite part, a separate section summarises all results obtained from experiments investigating swelling and strength properties of kaolinite samples with various gypsum additions, to which slag had been added as the only stabiliser. In addition investigations into the development of compressive strength (soaked and unsoaked) and linear expansion of these specimens stabilised with high slag/lime ratios (5 and 11) were carried out. This section also describes results of microstructural investigations (TGA and SEM) which were utilised to further understand and clarify the observations made on those mix compositions. All results are discussed in detail in Chapter 9.

7.1 Kaolinite stabilised with 2% lime and various slag additions in the presence and absence of sulphates (6% gypsum)

In order to assess the effects of sulphates on the relevant engineering properties, various percentages of gypsum (2, 4 and 6%) were added to the kaolinite prior to the addition of the stabilising additives lime and ggbs. Control mixes without gypsum addition were prepared to allow direct comparison to be made and conclusions to be drawn with regard to the effect of the presence of calcium sulphate on the stabilising process.

Throughout this chapter, sample composition is abbreviated using the following notation: 'L' indicates the lime addition, 'S' the slag and 'G' the addition of gypsum, all as percentages of the dry weight of the soil. Thus a kaolinite sample abbreviated '2L6S4G' is composed of the clay plus 2% lime, 6% slag and 4% gypsum. No gypsum was added to samples made from Lower Oxford Clay to allow an assessment of the effects of the natural sulphate/sulphide content of the material on the relevant engineering properties.

The term "high slag/lime ratios" in this section is used to describe mixes, in which slag was utilised as the main stabiliser, whereas the added lime played only a minor role as activator and soil modifying agent. However, in order to compare the development in engineering properties of samples stabilised with only 2% lime to those in which ggbs was the predominant stabiliser, the results are presented in parallel.

7.1.1 Strength development

7.1.1.1 Shear strength development

A series of unconsolidated, undrained shear strength triaxial tests were carried out on kaolinite stabilised with 2% lime and various slag additions and 6% gypsum (=2.79%SO_3). Samples were cured for 1, 4, 12, 24 and 52 weeks at 10, 20 and 30 °C prior to testing and values for τ_u were calculated from the measured undrained shear strength parameters.

Figure 7.1 illustrates a typical set of modified failure envelopes derived from experimental results obtained from a test series on Kimmeridge Clay. A trigonometrical conversion of the values obtained from the modified failure envelope (Figure 6.6) results in the final values for c_u and ϕ_u given in Table 7.1.
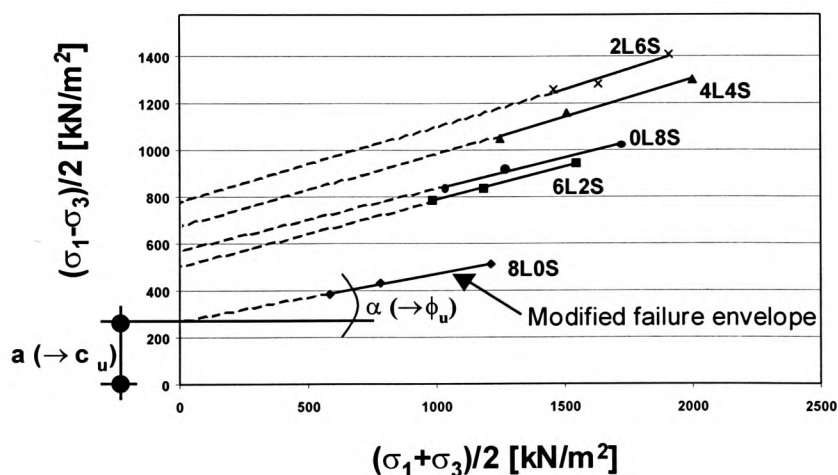
Figure 7.1 *Derivation of shear strength parameters cohesion (c_u) and angle of internal friction (ϕ_u) from the modified failure envelope of an undrained, unconsolidated triaxial test (here: Kimmeridge Clay stabilised with various slag/lime ratios and cured for 12 weeks at 20 °C prior to shear testing)*

To compare the development of the undrained shear strength parameters from all the experimental data, it was decided to take a normal stress level of σ_n=1000 kN/m^2 and establish 'typical' τ_u-values for the various design mixes.

Table 7.1 Apparent shear strength parameters cohesion c_u [kN/m²] and angle of internal friction ϕ_u [°] of kaolinite stabilised with 2% lime and 0, 2, 4 6 and 8% ggbs in the presence of 6% gypsum (=2.79% SO_3) after curing periods of 1, 4, 12, 24 weeks and 1 year at 10, 20 and 30 °C

Curing time	Sample composition	Curing temperature 10 °C		Curing temperature 20 °C		Curing temperature 30 °C	
		c_u [kN/m²]	ϕ_u [°]	c_u [kN/m²]	ϕ_u [°]	c_u [kN/m²]	ϕ_u [°]
1 week	2L0S6G	122	9.1	211	6.0	222	8.1
	2L2S6G	138	11.2	256	12.3	246	12.3
	2L4S6G	163	11.2	287	16.7	412	19.0
	2L6S6G	164	12.3	305	17.8	476	19.0
	2L8S6G	184	12.3	436	17.8	645	19.0
4 weeks	2L0S6G	176	7.1	242	7.1	254	10.2
	2L2S6G	277	13.3	338	12.3	379	12.3
	2L4S6G	330	14.4	351	14.4	458	20.1
	2L6S6G	423	14.4	429	21.3	472	21.3
	2L8S6G	431	17.8	586	20.1	295	38.7
12 weeks	2L0S6G	366	5.0	343	7.1	209	16.7
	2L2S6G	395	9.1	449	11.2	415	20.1
	2L4S6G	344	16.7	381	19.0	623	21.3
	2L6S6G	350	27.8	472	32.1	644	40.5
	2L8S6G	229	29.2	437	32.1	513	40.5
24 weeks	2L0S6G	316	11.2	235	12.3	306	11.2
	2L2S6G	296	19.0	303	22.6	449	16.7
	2L4S6G	389	17.8	444	22.6	564	16.7
	2L6S6G	578	17.8	740	19.0	758	22.6
	2L8S6G	536	26.4	732	23.8	626	36.9
1 year	2L0S6G	407	5.0	182	9.1	202	8.1
	2L2S6G	413	14.4	418	11.2	354	8.1
	2L4S6G	407	16.7	322	21.3	360	19.0
	2L6S6G	650	19.0	442	25.1	736	22.6
	2L8S6G	429	21.3	630	29.2	651	30.6

Figure 7.2 indicates that the addition of ggbs results in a substantial increase in the shear strength τ_u of the specimens and is more pronounced for higher ggbs additions. This rate of strength gain, as a function of ggbs content, increases with both increase in curing temperature and increase in curing period. However, specimens to which only lime had been added (2L0S) showed little strength increase with both increase in curing time and temperature. Particularly if curing is at only 10 °C, shorter curing periods, i.e. 1 to 4 weeks, result in little strength gain. However, if curing is for 12 weeks or beyond, τ_u-values similar to those for specimens cured at elevated temperatures are obtained. Specimens stabilised with large slag additions show marked sensitivity to curing temperature if curing is for only 1 week, however, if curing is for longer periods, the strength developed is less affected by temperature. Table 7.2 gives the approximate increase in shear strength for specimens of the mix composition 2L8S after various curing periods if the curing temperature is raised from 10 to 30 °C. This table further confirms that longer curing can compensate to some degree for lower temperature in the curing environment.

Table 7.2 *Shear strength gain [%] for kaolinite stabilised with 2% lime and 8% ggbs (2L8S) after various curing periods when the curing temperature is increased from 10 to 30 °C*

Curing period	1 week	4 weeks	12 weeks	24 weeks	1 year
Strength gain [%]	250	163	174	135	155

The higher shear strength of specimens containing larger amounts of ggbs is almost certainly due to the higher degree of cementation in these specimens and is also reflected in the development of cumulative strain at shear failure (Figure 7.3). Smaller strain at failure is associated with a higher degree of brittleness, which is found in well-cemented samples. In contrast, large percentages of strain are associated with soft, deformable and plastic samples. Independent of curing temperature and sample composition, the lowest percentages of strain are exhibited by specimens which have been cured for 1 year prior to testing (Figure 7.3). Larger ggbs additions result in a reduction of strain at failure, which is particularly pronounced for specimens which have been cured at higher temperatures. If curing is at 30 °C, the addition of 8% ggbs
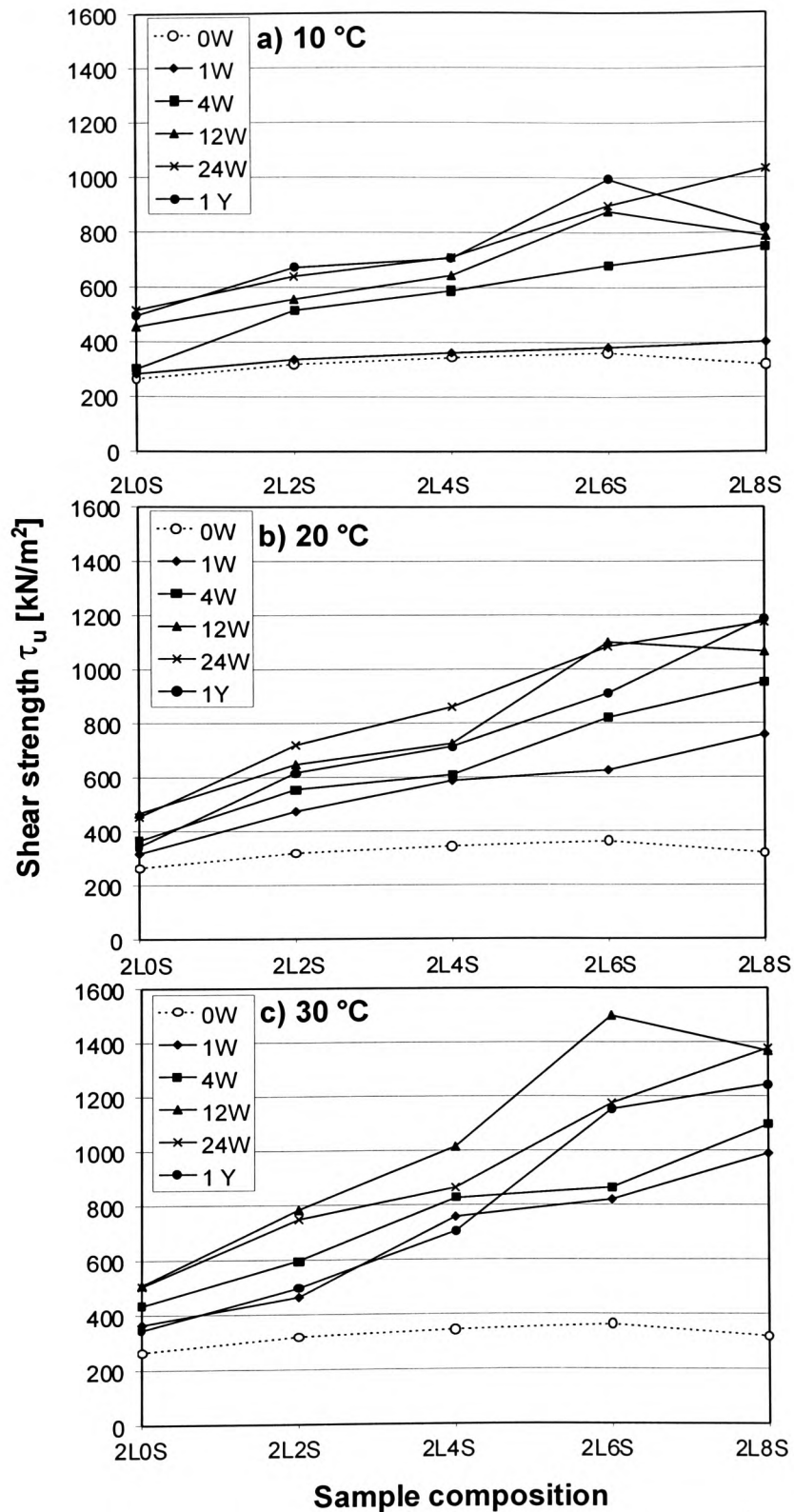
Figure 7.2 *Shear strength τ_u development (normal stress σ_n=1000 kN/m²) of kaolinite stabilised with 2% lime and 0, 2, 4 6 and 8% ggbs in the presence of 6% gypsum (=2.79% SO₃) after curing periods of 1, 4, 12, 24 weeks and 1 year at a) 10 °C, b) 20 °C and c) 30 °C*

results in a reduction in strain at failure of 68% after a curing period of 1 week. However, curing at 10 °C reduces the failure strain by only 5% and curing at 20 °C results in a reduction in percentage of strain of 45% after 1 week when 8% of ggbs is added to specimens modified with 2% lime.

Figure 7.4 gives an overview of the development of the apparent undrained shear strength parameters c_u and ϕ_u depending on curing temperature and curing period (1 week and 1 year). The values for the angle of internal friction (Figure 7.4a) remain constant for curing periods of 1 week at all three curing temperatures for slag additions of 4% and above. This could be indicative of a limiting degree of cementation resulting from a specified amount of hydration product after this comparably short curing period and the uniform degree of saturation of the soil samples. Further hydration will affect the densification and thus result in modified ϕ_u-values. Potential for higher degrees of hydration and thus higher apparent internal friction angles are indicated by the ϕ_u-values exhibited by specimens cured for 1 year. It would be expected that the influence of this mechanism would be more evident in the effective stress parameters, however, this is outside the scope of this dissertation.

The magnitude of c_u is affected principally by the accumulation of hydration products surrounding slag grains, which reduce pore space, and the increasing cementation of the soil. This results in higher cohesion. Figure 7.4b shows that there is a general increase of c_u with increase in curing period and curing temperature. As would be expected the lowest c_u values are exhibited for specimens cured for 1 week at 10 °C. Although in this case a relative increase in apparent cohesion of almost 60% can be achieved if 8% ggbs is added to the mix 2L0S, the absolute c_u value is still rather low when compared to those obtained from specimens which have been subjected to longer curing periods and elevated curing temperatures.
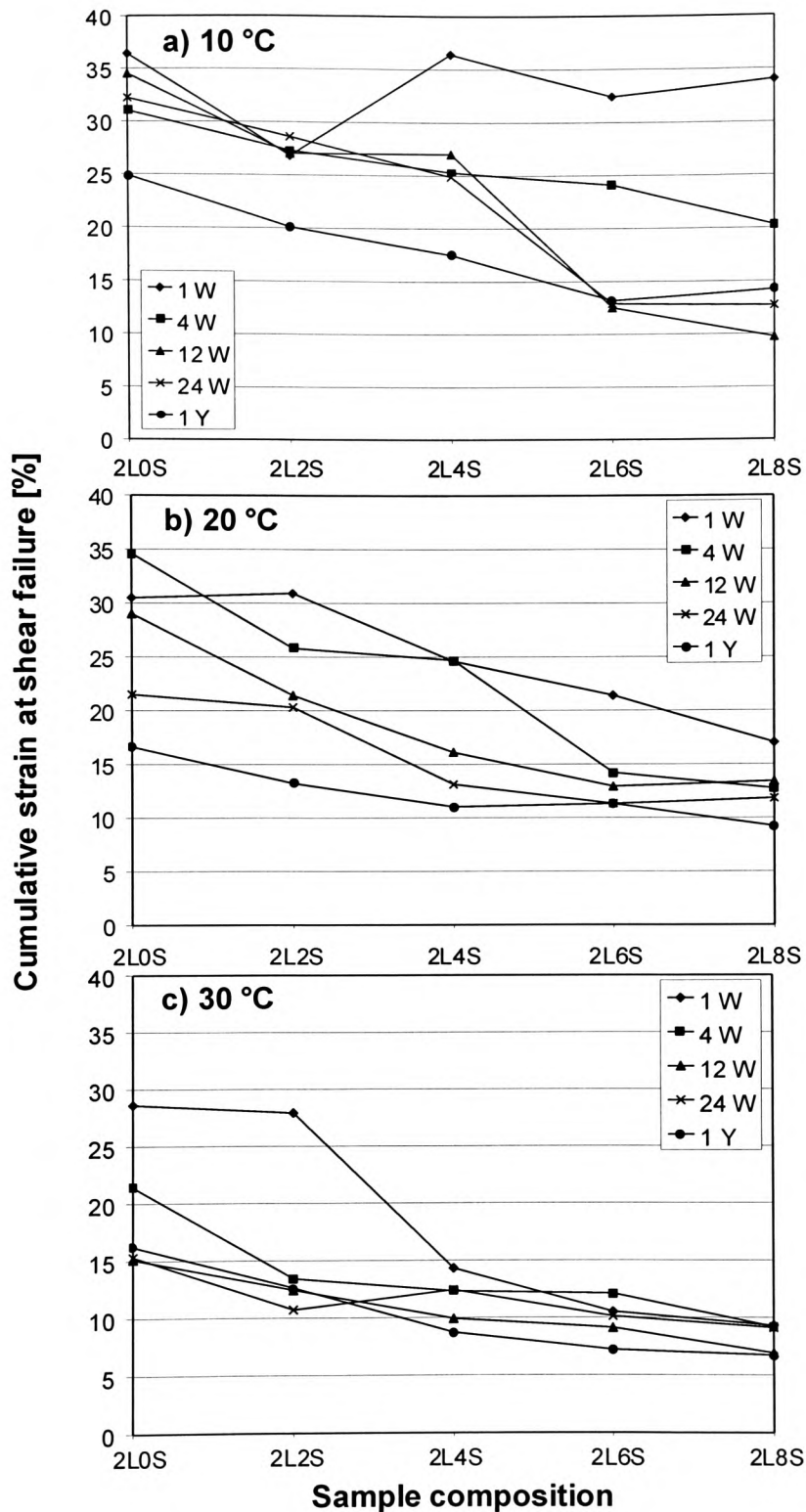
Figure 7.3 *Cumulative strain at shear failure of kaolinite stabilised with 2% lime and 0, 2, 4, 6 and 8% ggbs in the presence of 6% gypsum (=2.79% SO₃) after curing periods of 1, 4, 12, 24 weeks and 1 year at a) 10 °C, b) 20 °C and c) 30 °C*
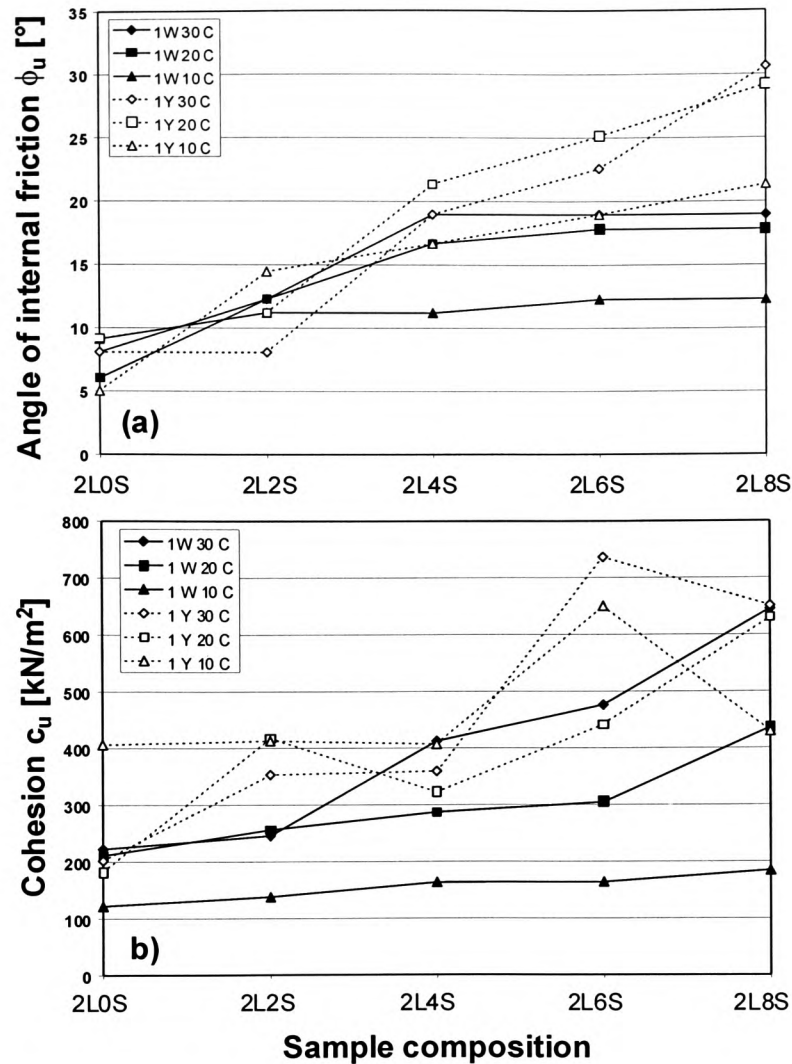
Figure 7.4 *Influence of curing time and temperature on the development of the apparent shear strength parameters ϕ_u (a) and c_u (b) of slag/lime stabilised kaolinite in the presence of 6% gypsum*

The shear strength τ_u development for lime-ggbs-stabilised kaolinite specimens in the absence of gypsum is given in Figure 7.5. Little effect of sample composition on the unconsolidated, undrained shear strength can be observed when testing is after curing periods of up to 12 weeks. Exhibited values for τ_u are comparably low and lie in the region observed for the weak mix 2L0S in the presence of gypsum. However, if curing is prolonged to 24 weeks and beyond, an increase in slag addition results in significantly enhanced shear strength values. This is particularly pronounced if curing is at elevated

temperatures. The shear strength of 1 year old specimens stabilised with 2% lime and 8% ggbs (cured at 20 and 30 °C) outperforms the strength development of equivalent samples containing gypsum. Curing temperature and time, however, hardly affect the specimens which were stabilised with lime only (2L0S).

Changes in the shear strength parameters c_u and ϕ_u with curing temperature and time are illustrated in Table 7.3. In contrast to the variations in c_u exhibited by specimens stabilised in the presence of sulphate, the changes with curing time and sample compositions are (up to a sample age of 12 weeks) almost negligible. An overall increase in ϕ_u can, however, be observed for higher ggbs additions cured at 20 and 30 °C for curing periods of 24 weeks. The c_u values encountered are the highest values experienced in the course of the project.

In order to identify the strength enhancing agents within specimens, which have been cured for longer periods at 30 °C in the presence of high ggbs addtions, TG analysis was carried out on dried, pulverised samples of the mix composition 2L8S0G.The results obtained from specimens cured for 1 year were compared to those which were obtained from samples cured for only 1 week. The results of the TG analysis are given in Figure 7.6. Curing after 1 year results in a well-defined peak at around 120 °C (together with the standard kaolinite dehydroxylation peak at 580 °C), which is characteristic of cementitious gel (C-S-H) and would explain the substantial strength obtained from this specimen whereas only the kaolinite dehydroxylation peak ② is displayed by the TGA trace of the specimen cured for only 1 week. No lime could be identified on the derivative weight loss trace of Figure 7.6b. The reason for this could either be the fact that the small addition of only 2% $Ca(OH)_2$ would be rather difficult to detect, particularly in the presence of the large kaolinite peak or it could be due to the fact that the small amount of lime available was already bound to the surfaces of the kaolinite particles [Abdi, 1992].
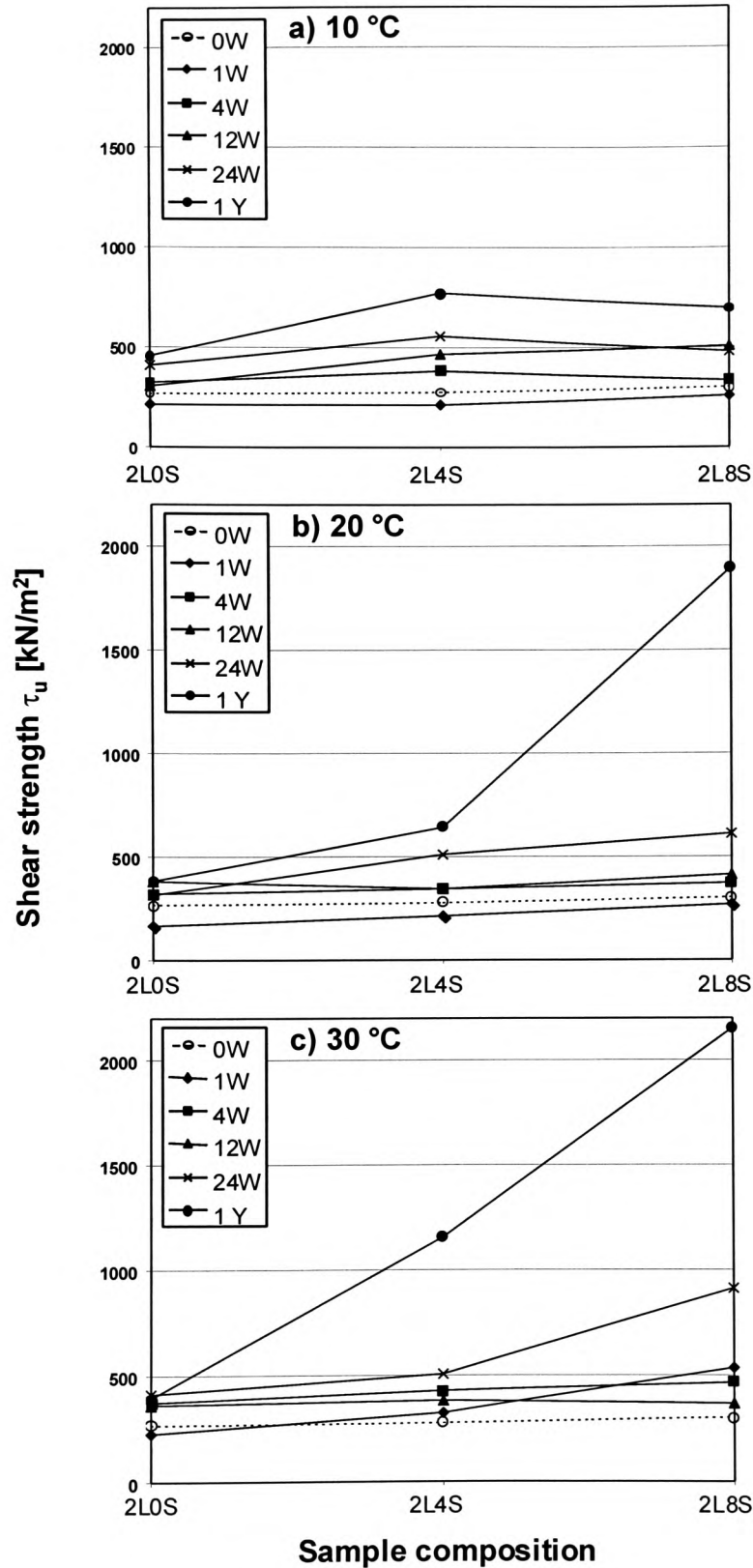
Figure 7.5 *Shear strength τ_u development (normal stress $\sigma_n = 1000$ kN/m²) of kaolinite stabilised with 2% lime and 0, 2, 4 6 and 8% ggbs curing periods of 1, 4, 12, 24 weeks and 1 year at a) 10 °C, b) 20 °C and c) 30 °C*

Table 7.3 *Shear strength parameters c_u [kN/m²] and ϕ_u [°] of kaolinite stabilised with 2% lime and 0, 4 and 8% ggbs after curing periods of 1, 4, 12, 24 weeks and 1 year at 10, 20 and 30 °C*

Curing time	Sample composition	Curing temperature 10 °C		Curing temperature 20 °C		Curing temperature 30 °C	
		c_u [kN/m²]	ϕ_u [°]	c_u [kN/m²]	ϕ_u [°]	c_u [kN/m²]	ϕ_u [°]
1 week	2L0S6G	160	3.0	130	2.0	121	6.0
	2L4S6G	160	3.0	160	3.0	182	8.1
	2L8S6G	171	5.0	181	5.0	317	12.3
4 weeks	2L0S6G	216	6.0	102	12.3	73	16.7
	2L4S6G	203	10.2	202	8.1	85	19.0
	2L8S6G	77	14.4	173	11.2	75	21.3
12 weeks	2L0S6G	87	12.3	144	13.3	123	13.3
	2L4S6G	167	16.7	202	8.1	184	11.2
	2L8S6G	164	19.0	194	12.3	188	10.2
24 weeks	2L0S6G	229	10.2	117	11.2	155	14.4
	2L4S6G	299	14.4	189	17.8	248	14.4
	2L8S6G	202	15.5	195	22.6	283	32.1
1 year	2L0S6G	313	8.1	164	12.3	114	15.5
	2L4S6G	405	20.1	320	17.8	596	29.2
	2L8S6G	170	27.8	1425	25.1	1401	36.9
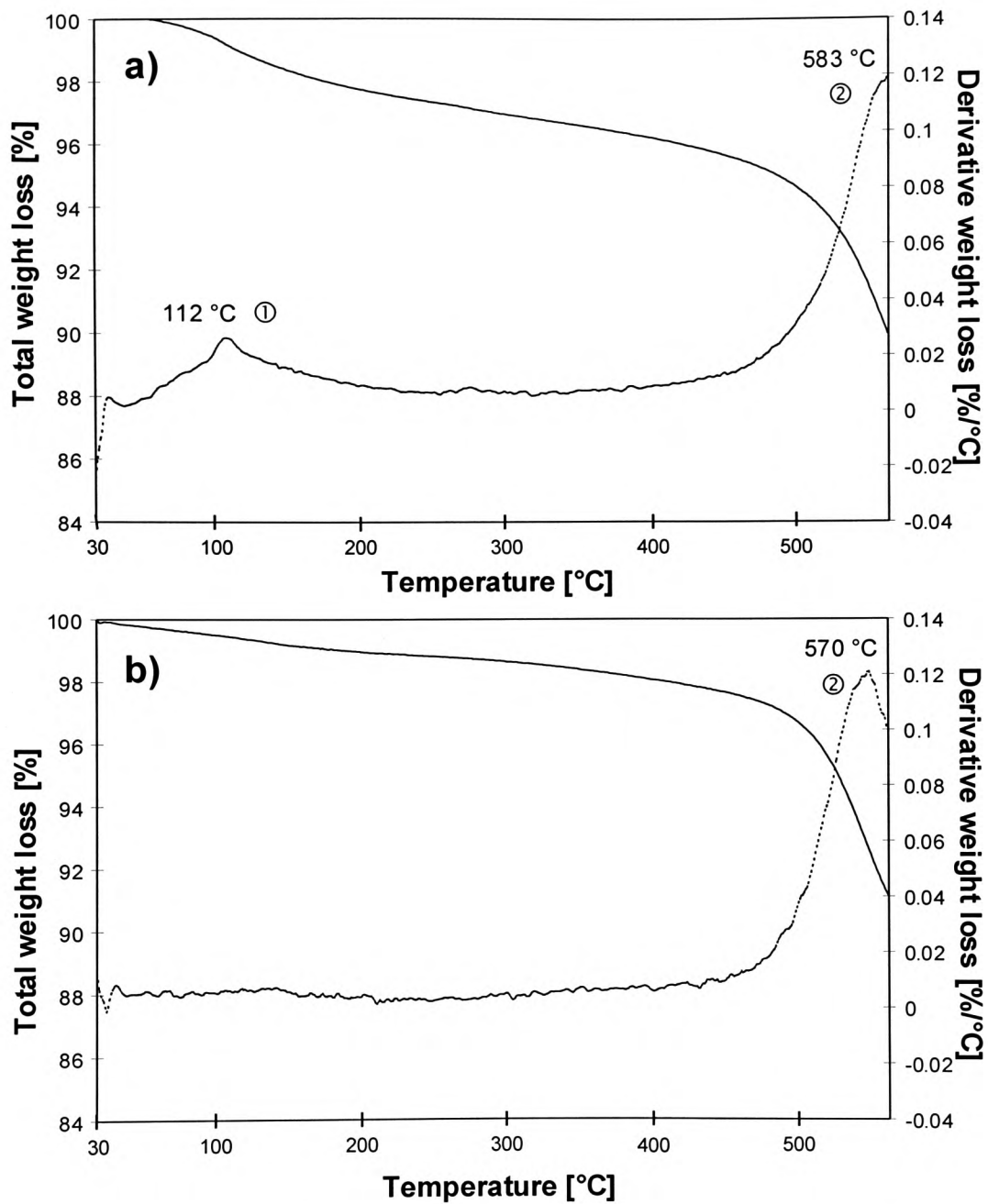
Figure 7.6 *Thermogravimetrical analysis for the sample 2L8S0G after curing periods of a) 1 year and b) 1 week at 30 °C*

7.1.1.2. Unconfined compressive strength

The effect of the addition of various amounts of gypsum on the unconfined compressive strength (UCS) development of stabilised kaolinite specimens cured for 1, 4 and 12 weeks can be seen in Figure 7.7. In the presence of gypsum (Figure 7.7b-d) higher slag additions result in an increase in UCS-values. In particular specimens with higher slag-lime ratios (2L4S and beyond) were found to 'profit' by the addition of sulphates and exhibit significant strength gain over all curing periods. The advantage of higher gypsum additions is reflected by steeper strength gradients with increase in slag/lime ratios. Curing period and slag addition have only negligible effect on compressive strength in the absence of gypsum and even in the presence of 2 and 4% gypsum, a marked increase in strength is observed only for specimens with slag additions of 4% and beyond. If 6% gypsum is added, however, even for specimens with only 2% ggbs there is a substantial strength improvement. It is interesting to see that in the absence of gypsum (Figure 7.7a) the addition of ggbs results in a reduction in compressive strength for curing periods of 1 and 4 weeks. Samples with larger ggbs additions are generally compacted at a slightly higher density and one would thus expect them – even at a very low hydration rate - to exhibit a marginally higher strength than specimens to which only lime was added. However, as indicated by the dotted lines in Figure 7.7a+d (for gypsum additions of 0 and 6%) for specimens which have been tested immediately after compaction, the effect of small variation in compaction density due to sample composition on measured strength is negligible. If no gypsum is added, curing for 12 weeks results in small absolute strength improvement when ggbs is added. It is likely that this strength enhancement is due to the first stages of slag activation and subsequent hydration, the intensity of which appears to be inferior to that observed in the presence of sulphates.

Based on work by Thompson [1966], who investigated the correlation between the shear strength parameters c_u and ϕ_u and the related compressive strength of lime-stabilised Bryce Clay, an attempt was made to combine the results obtained from triaxial testing and compressive strength testing in the current project (Figure 7.8). Thompson [1966] found that an increase in compressive strength is well reflected in an increase in cohesion but not angle of internal friction, whereas Figure 7.8 shows
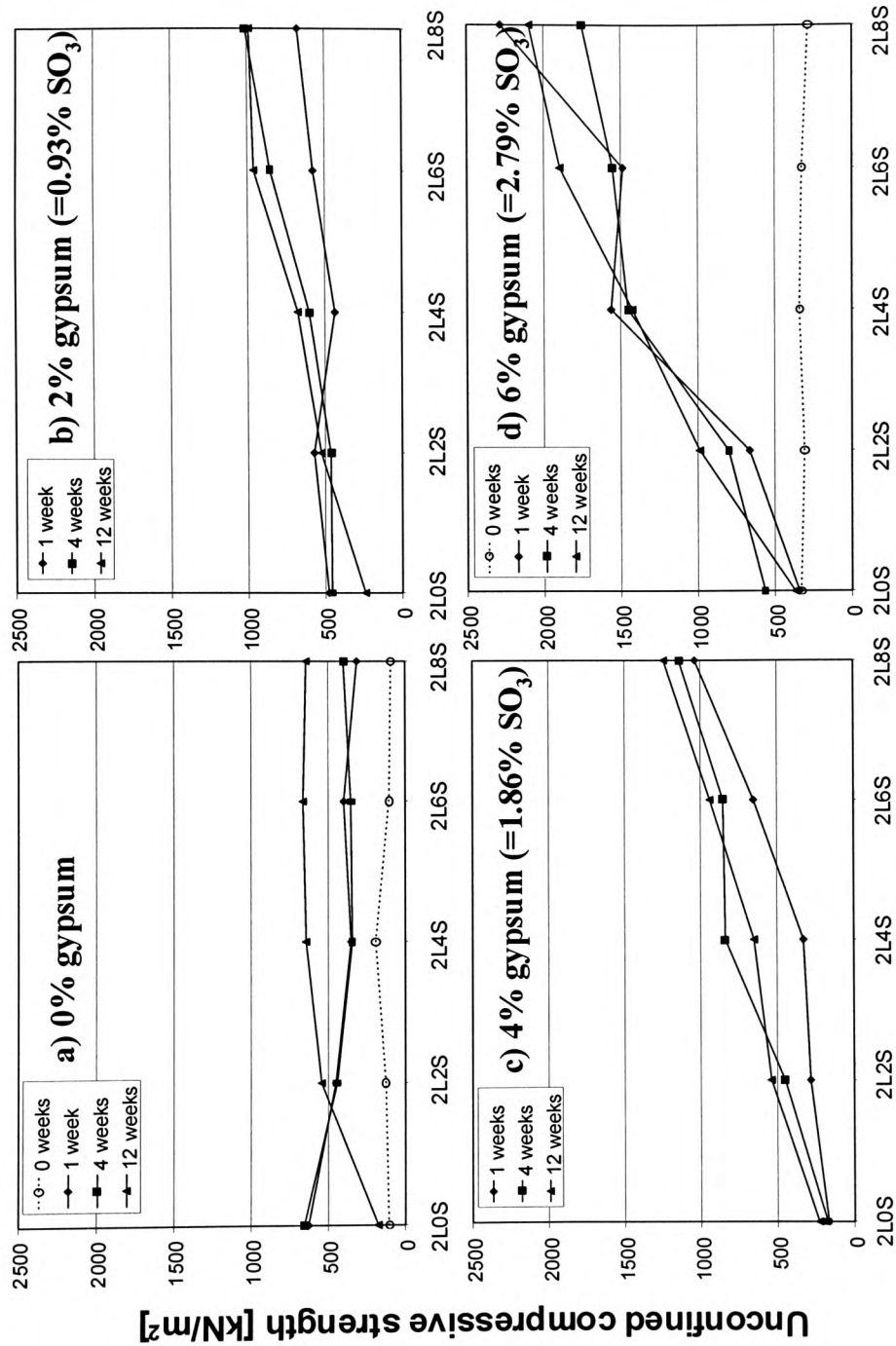
Figure 7.7 *Unconfined compressive strength [kN/m²] of kaolinite stabilised with 2% lime and 0, 2, 4, 6 and 8% ggbs in the presence of 0, 2, 4 and 6% gypsum after curing periods of 1, 4 and 12 weeks at 30 °C*

Gabriele Veith
University of Glamorgan

reasonable correlation between increase in compressive strength and both the increase in cohesion and in the angle of internal friction. It should be noted, however, that Thompson only assessed specimens cured for up to 7 days and utilised rather small confining pressures (up to 240 kPa).
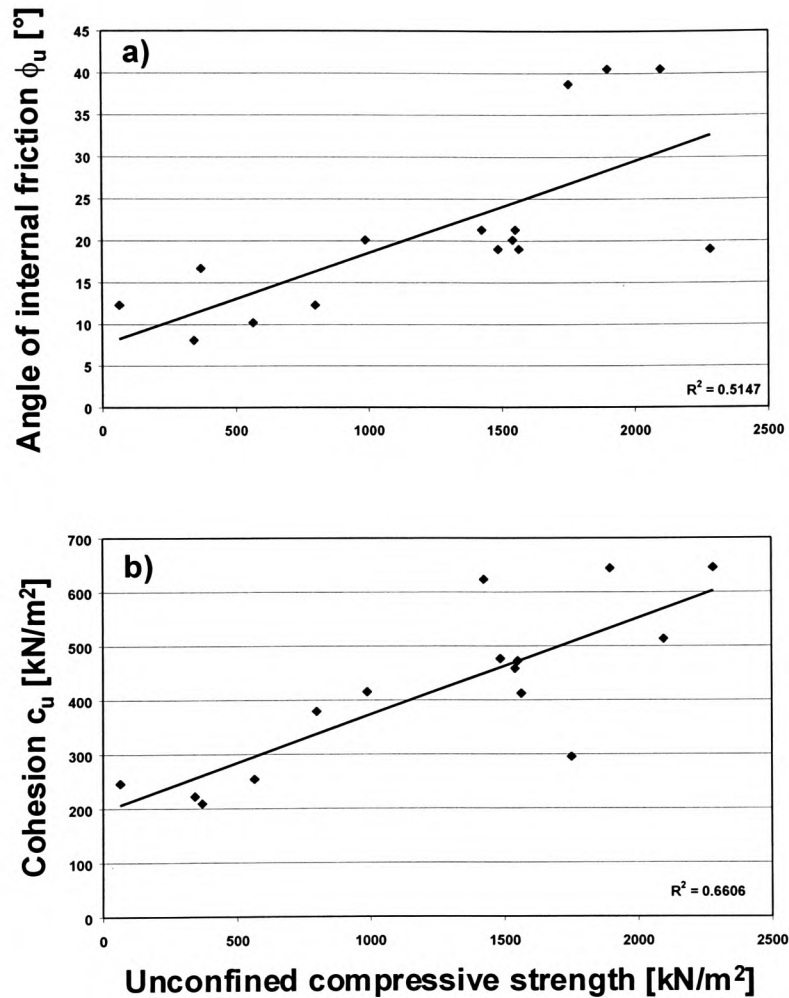
Figure 7.8 *Angle of internal friction (a) and cohesion (b) versus unconfined compressive strength of lime-slag stabilised kaolinite specimens cured for up to 12 weeks at 30 °C*

7.1.1.3 Indirect tensile strength

Figure 7.9 reflects the development of indirect tensile strength and presents a similar pattern to that which was portrayed for compressive and shear strength (Figures 7.7 and 7.2) when ggbs is introduced as stabiliser. Generally, higher slag additions result in higher R_{it}-values. This trend is further enhanced by an increase in the curing period and the presence of higher gypsum additions. Strength development for specimens to which 2 and 4% gypsum have been added is very similar for all curing periods. Considering the UCS development illustrated in Figure 7.7 b+c with 2 and 4% gypsum for the various curing periods, the small difference in behaviour for the 2% and 4% gypsum compositions is also reflected in the indirect tensile strength data. Specimens which were compacted in the absence of sulphates showed basically no indirect tensile strength improvement with increase in ggbs addition or curing period. It is not clear if an extension of the curing period beyond 12 weeks would have resulted in delayed strength development, as observed for specimens compacted in the absence of lime (see section 7.3). However, with regard to practical considerations, early strength development is important. Hence, no strength gain after curing for up to 12 weeks would not be acceptable for application in practice.

Figure 7.10 shows that there is generally good correlation between the increase in UCS and IT values for specimens cured for up to 90 days. This is not necessarily the case in all systems. It has been shown for concrete that the type of mechanical interlocking can adversely affect strength in tension and improve strength under compression and vice versa [Neville, 1994]. In concrete, the ultimate failure under compression is usually initiated by a tensile failure of the cement grains [Neville, 1994]. Thus, the significance of the tensile strength should not be underestimated. The good correlation in Figure 7.10 is indicative of a binding force within the specimens, which is effective under both tensile and compressive stress.
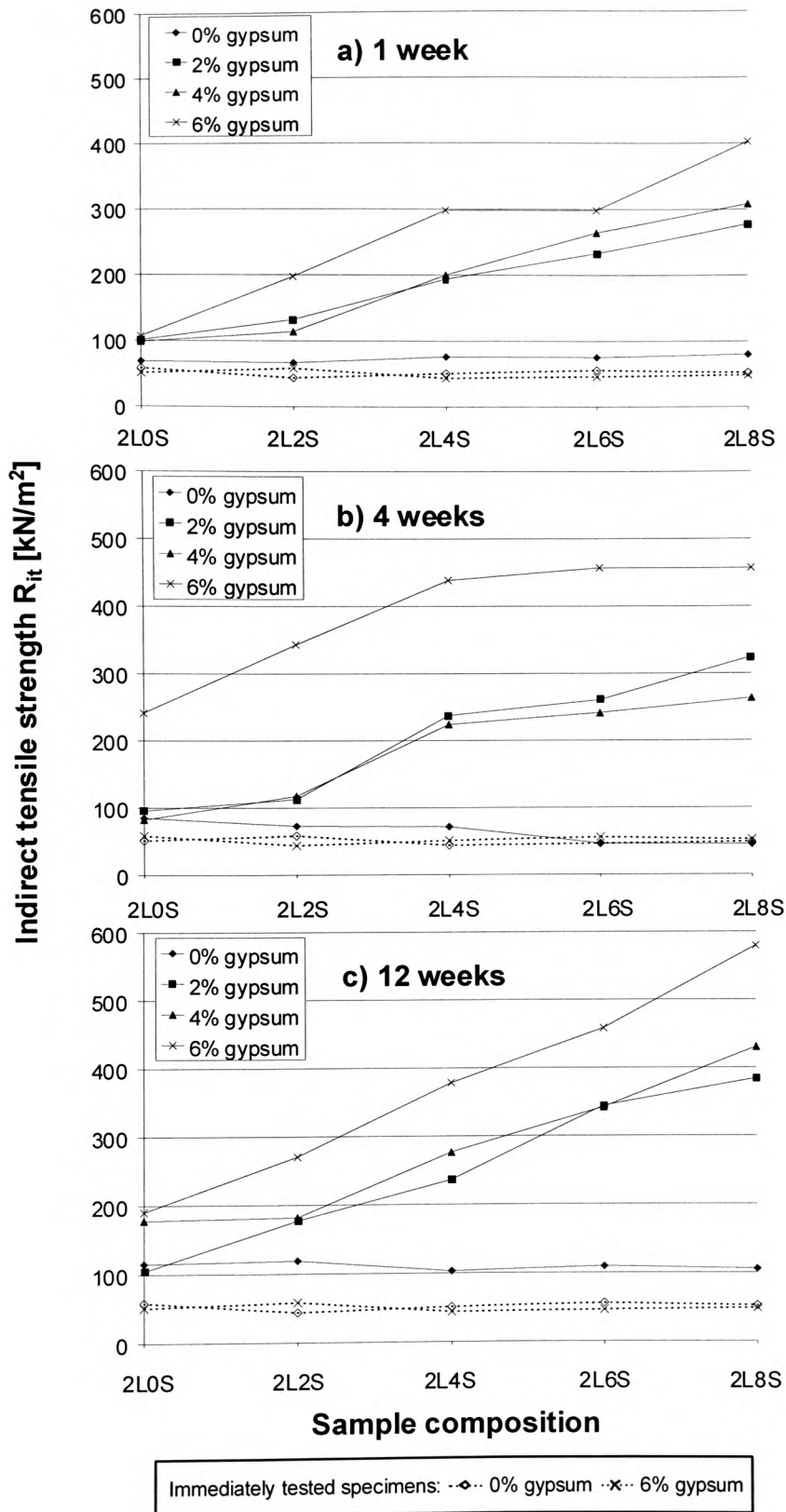
Figure 7.9 *Indirect tensile strength R_{it} for kaolinite (+0, 2, 4 and 6% gypsum), stabilised with lime and ggbs after curing periods of 1, 4 and 12 weeks at 30 °C (dotted lines indicate results obtained from immediately tested specimens (only in the absence and presence of 6% gypsum)*
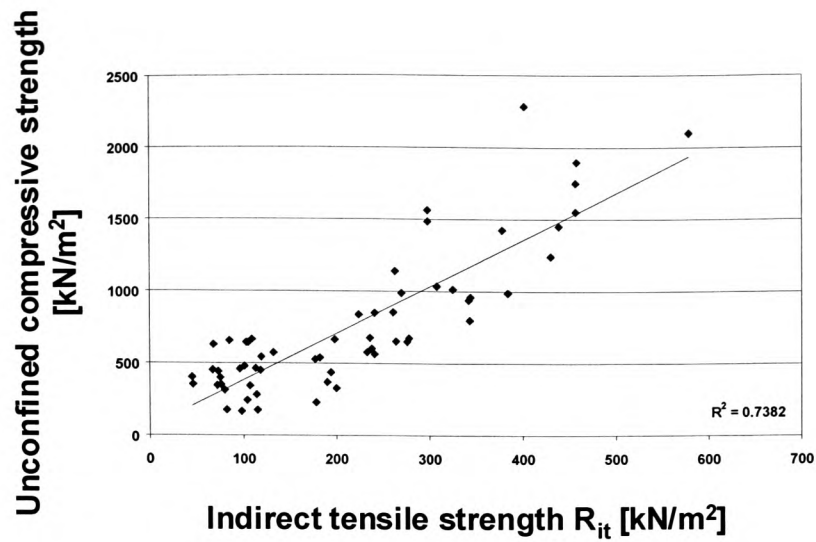
Figure 7.10 *Indirect tensile versus unconfined compressive strength of kaolinite specimens stabilised with 2% lime and various ggbs additions after curing at 30 ℃ for up to 12 weeks*

7.1.2 Porosity and pore size distribution of kaolinite stabilised with lime-activated ggbs

Mercury intrusion porosimetry (MIP) was carried out on a wide range of dried lime-slag-specimens which had been subjected to different curing regimes and curing periods prior to testing. Although the results reveal some interesting trends it should be noted that drying of specimens – even if it is performed in a very gentle manner as in the current study – will affect the specimen structure to some degree. In addition the correlation of MIP results obtained from dried samples with, for example, coefficients of permeability or strength values measured on specimens in their 'natural' and moist state has to be assessed carefully. However, mercury intrusion is a useful instrument for assessing the influence of microstructural changes on internal structure and its results can contribute significantly to the understanding of pore structure development of partially cemented, stabilised soils.

7.1.2.1 Preliminary considerations

In order to assess how sample size would affect the microstructural development of the specimens, MIP investgations were carried out on samples deriving from specimens with a diameter of 38 mm and a height of 76 mm and also on samples, deriving from specimens with a diameter of 50 mm and a height of 100 mm. The results for both specimens, cured for 4 weeks at 30 °C prior to MIP testing can be seen in Figure 7.11. Variation with regard to pore fineness (characterised by the percentage of pores with radius < 0.05 μm) was found to be within ±1% (Fig 7.11a), which was considered acceptable. The total pore volume developed (Figure 7.11b) varied up to ±5% and was also acceptable in terms of what would be expected with respect to specimen variability. Another initial concern was how the slightly different dry density values and optimum moisture contents to which the various mixes had been compacted would affect the MIP results. Comparison of the development of certain pore distribution parameters would have been more difficult, if the initial 'starting values' of uncured specimens were substantially different for mixes of different mix compositions. MIP testing on uncured specimens revealed that there was an overall reduction in total pore volume with increase in slag addition (see, for example, dotted lines in Figure 7.15). This was
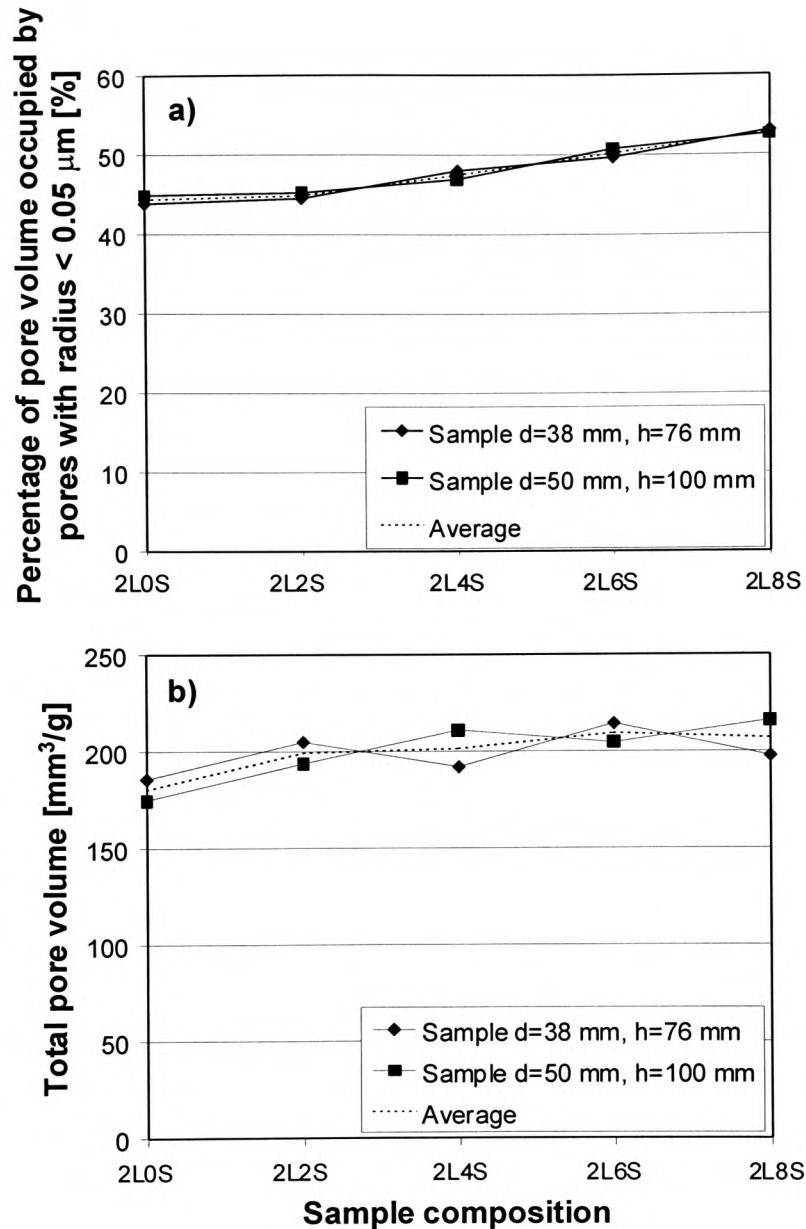
Figure 7.11 *Influence of sample dimensions on mercury intrusion results (percentage of pore volume occupied by pores with radius ≤0.05 μm (a) and total intruded pore volume(b)) obtained from Lower Oxford Clay stabilised with 2% lime and 0, 2, 4, 6 and 8% ggbs after curing for 4 weeks at 30 °C*

expected due to an increase in compaction density, based on results from a series of Proctor compaction tests (see Appendix 2). Comparison of the pore size distribution of the various mixes revealed, that this was mainly caused by a reduction of the percentage of pores with a radius < 0.1 μm (see dotted lines in Figure 7.17) which suggests that it is the coarser pores which are being removed by the slag. Smaller pore ranges were less

affected. However, in order to allow thorough comparison of pore size distribution changes, experimental results of cured specimens are always given together with results obtained from equivalent uncured specimens. It is appreciated that the type of stabilised soil with its specific grain size distribution and thus pore size distribution will affect the pore structure parameters. Figure 7.12 gives an overview over the general intrusion curves for the soils investigated in the course of the project. Specimens were prepared from Lower Oxford Clay and kaolinite with and without 6% gypsum and compacted with 2% lime and 8% ggbs. The mercury intrusion curves of samples tested immediately after compaction are given in Figure 7.12. It can be seen that hardly any differences in pore size distribution can be observed for a pore size with radius r≥0.1μm. However, below this pore radius, the development of the curves representing Lower Oxford Clay and kaolinite (with and without the addition of 6% gypsum), is different. The natural Lower Oxford Clay exhibits the lowest total pore volume and a less defined threshold radius (for determination of threshold pore radius see Figure 6.12), the latter being probably due to its rather wide grain size distribution. Kaolinite (in the presence of gypsum) has a far better defined intrusion curve turning point and an overall higher intruded pore volume. The highest pore volume, however, was recorded for kaolinite if the addition of gypsum is omitted. The definition of the threshold radius is very clear and pore size ranges are well defined.
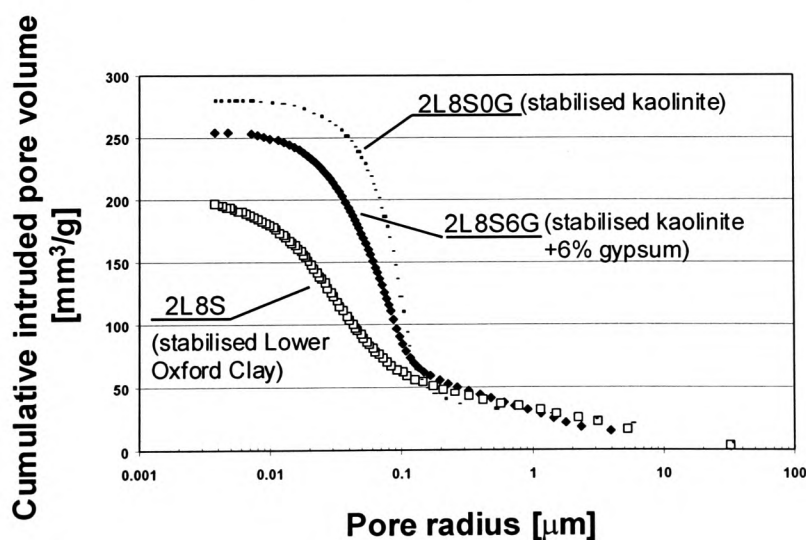
Figure 7.12 *Typical intrusion curves for kaolinite with and without 6% gypsum (2L8S6G and 2L8S0G respectively) and Lower Oxford Clay (2L8S) specimens tested immediately after compaction*

Figure 7.13 outlines how the addition of gypsum affects the intruded pore volume of kaolinite cured for 4 weeks prior to MIP testing for the investigated range of gypsum
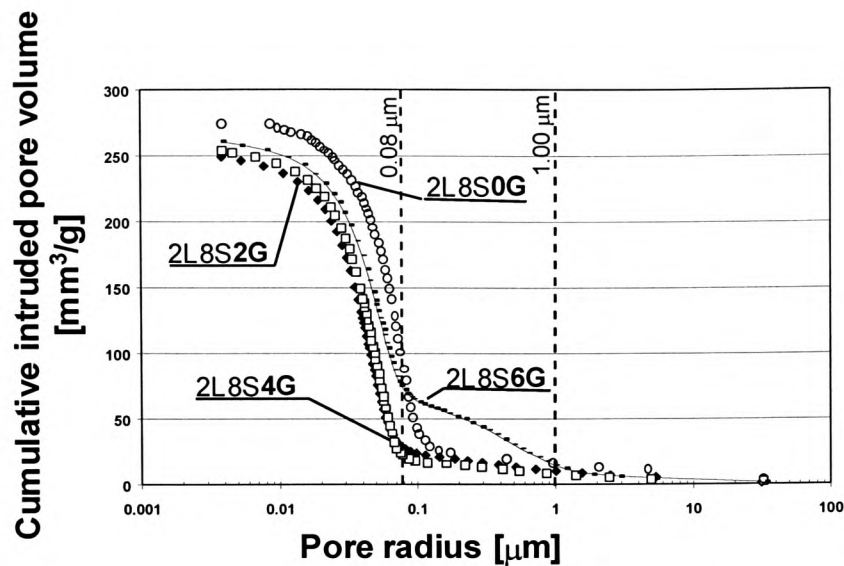
Figure 7.13 *Mercury intrusion curves for kaolinite stabilised with 2% lime and 8% ggbs in the presence of 0, 2, 4 and 6% gypsum after curing for 4 weeks at 30 °C*

additions (0, 2, 4 and 6%). The lowest total pore volume is exhibited by the specimen to which only 2% gypsum had been added, and the volume gradually increases with higher gypsum additions. The highest porosity was found for kaolinite without sulphate addition. The mercury intrusion curve also showed that the gypsum content affected significantly the development of the pore range with a radius $0.1\mu m<r<1\mu m$. The highest percentage of the pore volume occupied by pores in this radius range was identified for the specimen with a gypsum content of 6%. Thus further MIP analysis was undertaken to assess the percentage of pores of this pore size range and how it was affected by gypsum content and curing time.

7.1.2.2 Total intruded pore volume of stabilised kaolinite

It has been established that the total pore volume of a stabilised specimen varies with mix composition, compaction density, curing age and curing environment and the type of soil utilised. An overall assessment of sample performance cannot solely be based on the porosity, it also has to take into consideration how the pore volume is distributed in the specimen. However, it does give a first indication of the microstructural developments initiated by various additives.

The development of the total pore volume for specimens made of lime-slag-stabilised kaolinite in the presence and absence of 6% gypsum after various curing periods at 10, 20 and 30 °C is shown in Figure 7.14 and 7.15 respectively. In all cases porosity should be considered relative to the dotted curves which represent the porosity immediately after compaction. In general, for the 6% gypsum containing samples (Figures 7.14), both immediately after compaction and at the various curing periods, porosity decreases with increasing slag content. Although no well-defined systematic changes with regard to the influence of curing period could be identified, there is a clear tendency for longer curing periods (24 weeks and 1 year) to produce higher pore volumes in comparison to shorter curing durations. This is particularly so when curing at 10 °C, where the pore volume range is greater than at higher curing temperatures. It should also be noted that 1 week cured specimens consistently show a smaller pore volume than compacted specimens prior to curing. Whereas specimens containing gypsum exhibit a general trend of decreasing pore volume with increasing slag content (Figure 7.14), this trend is less apparent or absent for specimens without gypsum (Figure 7.15). Thus for specimens with high slag content, intruded pore volumes are significantly smaller for gypsum containing specimens than for gypsum free samples, particularly at higher curing temperatures. Overall, gypsum-free specimens exhibited a reduction in total intruded porosity with increase in curing period and increase in slag addition. No other systematic trends could be identified.
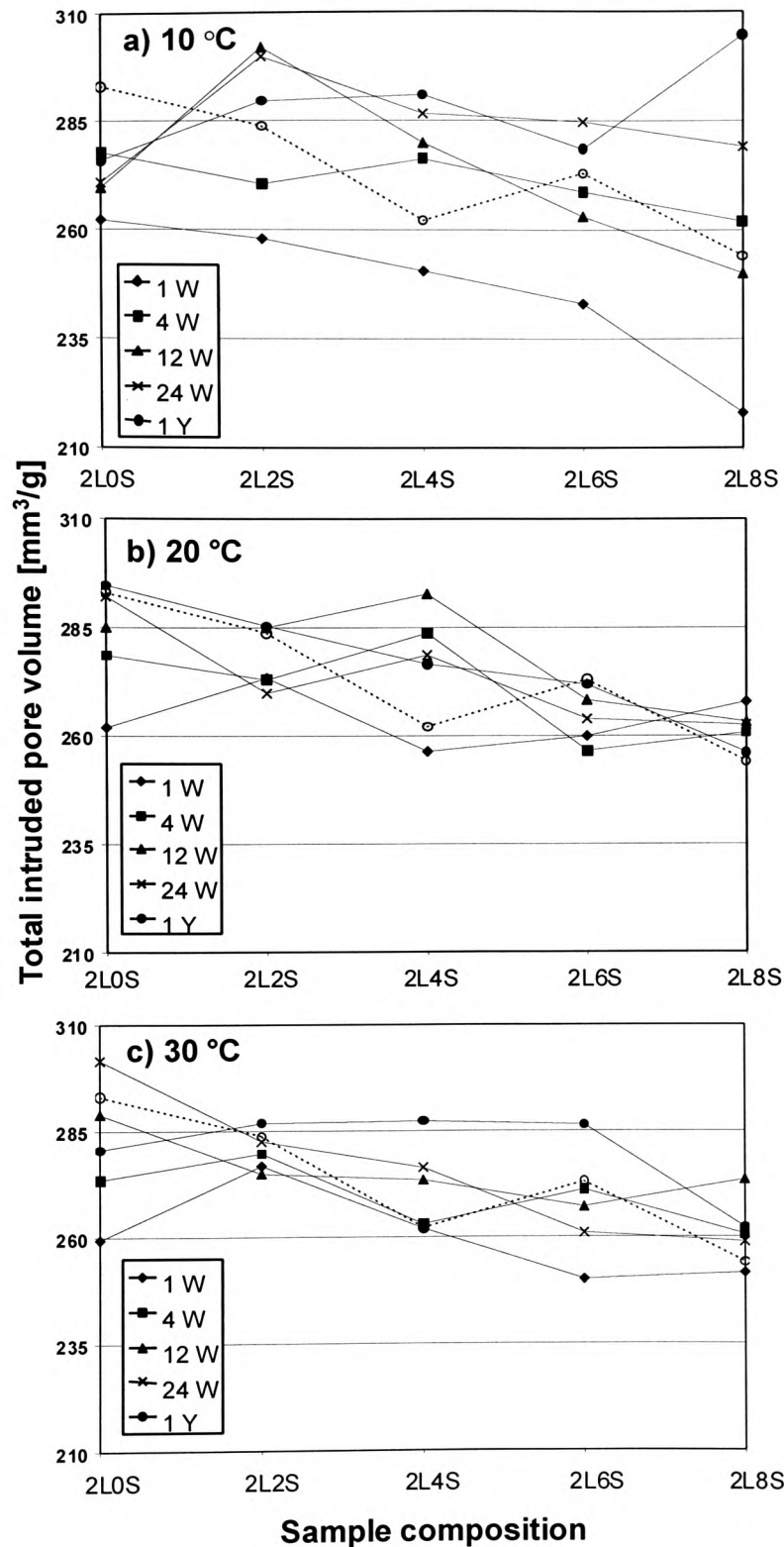
Figure 7.14 *Total intruded pore volume [mm³/g] of kaolinite stabilised with various slag/lime ratios after curing for 1, 4, 12, 24 and 52 weeks (dotted lines indicate results of specimens tested immediately after compaction) at a) 10 °C, b) 20 °C and c) 30 °C in the presence of 6% gypsum*
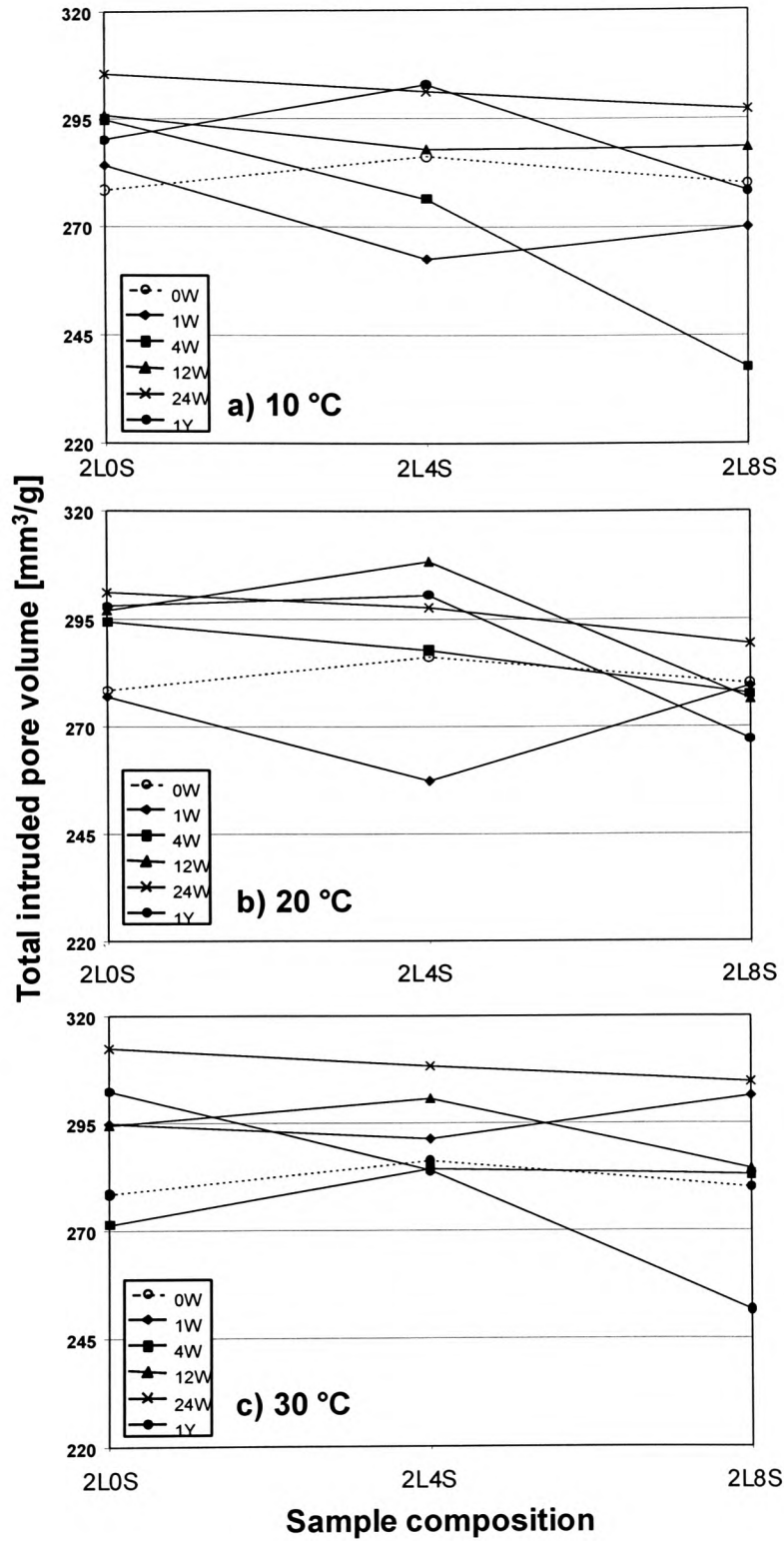
Figure 7.15 *Total intruded pore volume [mm³/g] of kaolinite stabilised with various slag/lime ratios after curing for 1, 4, 12, 24 and 52 weeks (dotted line indicates results of specimens tested immediately after compaction) at a) 10 °C, b) 20 °C and c) 30 °C without gypsum addition*

7.1.2.3 Pore size distribution within lime-ggbs-stabilised kaolinite

The percentage of the pore volume occupied by pores with radii $\leq 0.1\mu m$, $\leq 0.05\mu m$ and $\leq 0.02\mu m$ in stabilised kaolinite specimens containing 6% gypsum, is outlined in Figure 7.16. Dotted lines indicate values for immediately tested specimens and show an initial reduction ($\overline{AA'}$ to $\overline{BB'}$) in the proportion of pores with a radius $0.1 \geq r > 0.05\mu m$ by approximately 20%, when the slag addition is increased form 0 to 8%. The percentage of smaller pores ($r \leq 0.05\mu m$) appears not to be affected by slag addition.

For uncured samples, coarse porosity ($> 0.1\mu m$) increases with increasing slag content whereas for cured samples coarse porosity decreases. Thus for cured samples with high slag content (2L8S) coarse porosity (21%) is substantially less than for uncured samples (39%). Conversely fine porosity ($< 0.02\mu m$) gradually increases with slag content for cured samples whereas it shows little systematic change for uncured samples. The most significant effect is shown by the proportion of pores with radii $\leq 0.05\mu m$. For the uncured samples the proportion of the pore volume consisting of pores with radii $> 0.05\mu m$ remains constant at about 80% and those $< 0.05\mu m$ at about 20%. However, because for the uncured samples the fine porosity increases with increase in slag content and the coarse porosity decreases, there is a 77% ($> 0.05\mu m$):23% ($< 0.05\mu m$) distribution for the 2L0S cured samples (similar to the uncured samples) but a 48% ($> 0.05\mu m$):52% ($< 0.05\mu m$) distribution or the 2L8S cured samples. Curing of gypsum containing samples therefore produces pore refinement and that pore refinement clearly increases with increase in slag content. This is reflected in the strength development profiles in Figures 7.7 (compressive strength) and 7.9 (indirect tensile strength). Figure 7.17 shows the manner in which the process of pore refinement is influenced by both curing time and curing temperature. It is clear from this Figure that the principal pore refinement occurs within the first seven days of curing and that curing temperature has a relatively minor influence on this process. However, for the ultrafine porosity ($< 0.02\mu m$), there is a discernible change with increase in curing temperature. At 10 °C there is little change in the proportion of ultra fine pores with increase in curing time, at 20 °C there is a small but discernible increase and at 30 °C this increase is more pronounced, although still very small.
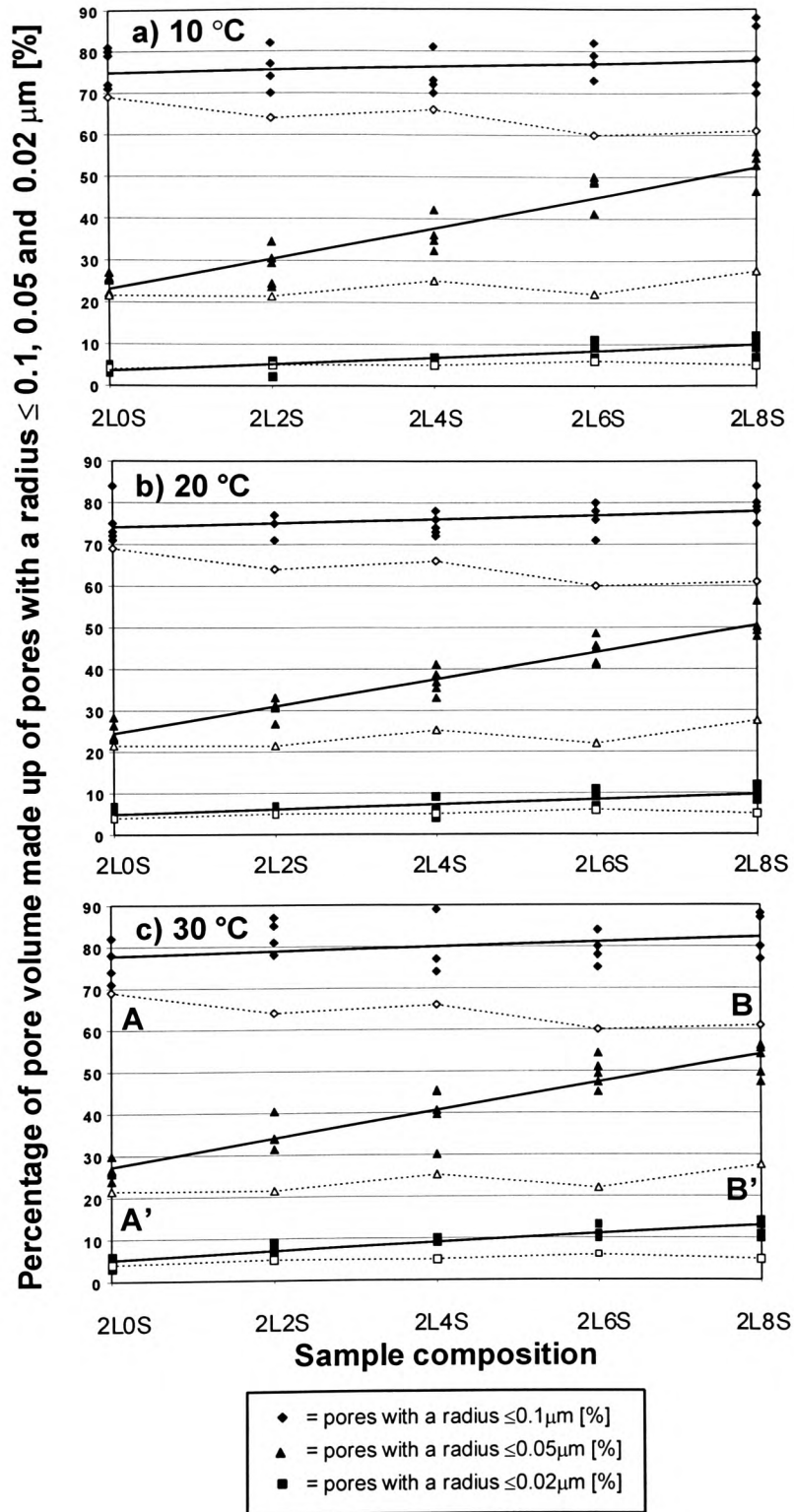
Figure 7.16 *Influence of curing temperature and sample composition on pore size distribution (r≤0.1 μm, 0.05 μm and 0.02 μm) of kaolinite (+ 6% gypsum), stabilised with various slag/lime ratios after curing periods of 1, 4, 12, 24 and 52 weeks (dotted lines indicate results of specimens tested immediately after compaction)*
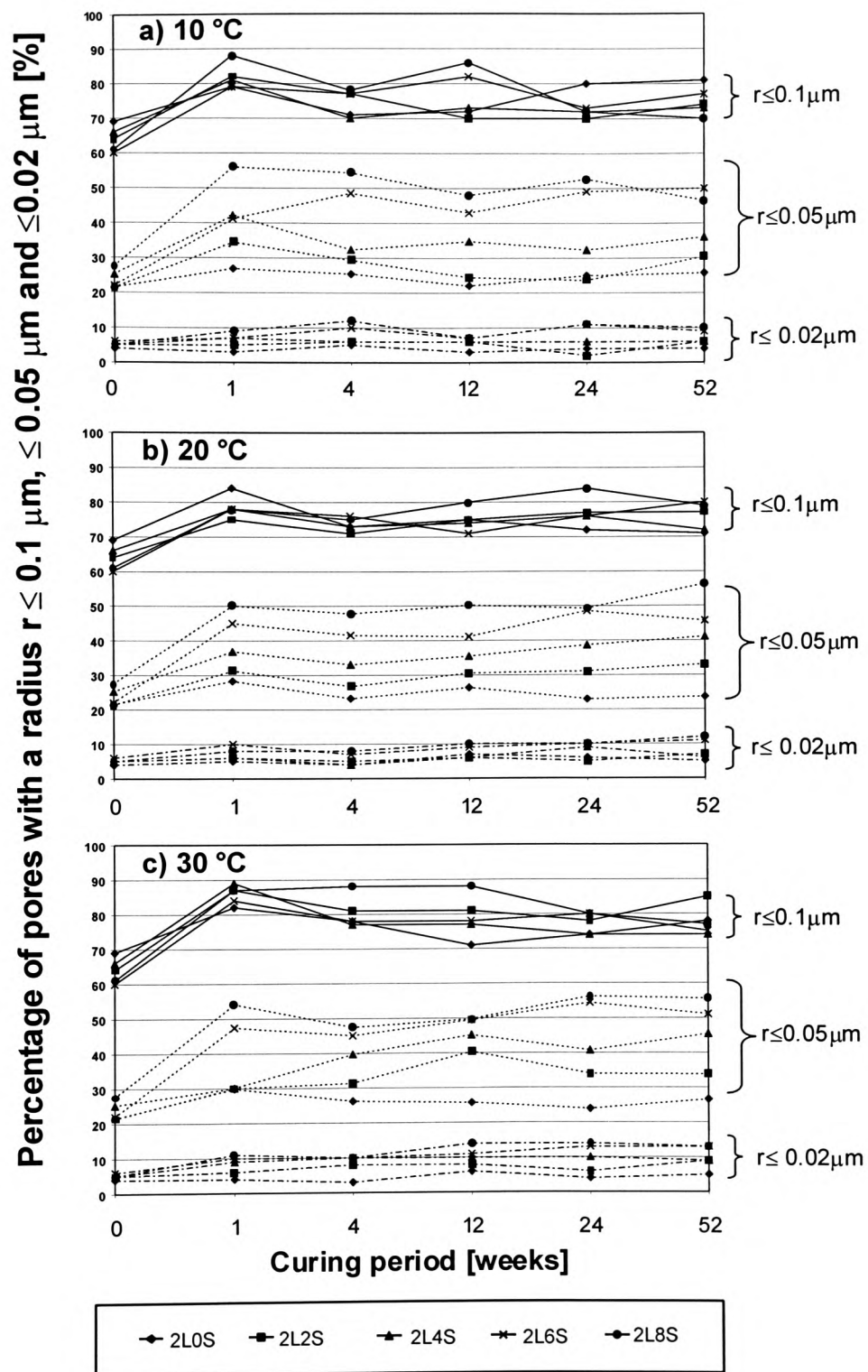
Figure 7.17 *Influence of curing period and curing temperature on the development of the percentage of pores with radius r≤0.1 µm, ≤0.05 µm and ≤0.02 µm in kaolinite specimens stabilised with 2% lime and various ggbs additions in the presence of 6% gypsum*

The development of pore volume occupied by pores with radii $\leq 0.1 \mu m$, $\leq 0.05 \mu m$ and $\leq 0.02 \mu m$ in stabilised kaolinite without gypsum is given in Figure 7.18. Reasonable trends could only be established for specimens cured at 10 °C (Figure 7.18a). This is mainly due to a high variability within the soil mix with curing age, particularly for specimens with high slag additions (Figure 7.19). However, Figure 7.18 indicates that slag addition does not significantly influence the pore size distribution of immediately tested specimens (dotted lines) and that little pore redistribution occurs for specimens of all mix compositions when cured up to one year at 10 °C.

Figure 7.19 shows the pore size distribution changes with curing time for samples without gypsum addition cured at different temperatures. Although the general pattern of changes in pore size distribution is similar for these specimens as for the gypsum addition specimens, there are distinct differences. The reduction in coarse porosity (pores with a radius $\geq 0.1 \mu m$) occurs at a much slower rate at the lower curing temperatures (10 and 20 °C) and does not stabilise until 28 days (compared to 7 days for gypsum containing material). The development of a finer pore structure (pores with a radius $\leq 0.05 \mu m$) clearly occurs at a slower rate when gypsum is not present and still shows development beyond 28 days. In addition the change in pore size distribution is little influenced by slag content which is also reflected in the strength development profiles in Figure 7.7 (compressive strength) and 7.9 (indirect tensile strength). However, curing for a period between 24 weeks and 1 year results, particularly for slag-containing specimens in distinct pore refinement with a substantial increase in the pore volume occupied by pores with a radius $\leq 0.05 \mu m$. Lower slag additions and lower curing temperatures weaken this effect. The observed pore refinement is also reflected in the substantial shear strength increase as illustrated in Figure 7.5. It should also be noted that specimens of the mix composition 2L0S0G (lime as the only stabiliser) show a significant reduction in the percentage of pore volume occupied by pores with a radius $\leq 0.1 \mu m$ if curing is at 10 °C for a period of beyond 24 weeks, and a reduction in the presence of pores with a radius range $0.1 \mu m < r \leq 0.02 \mu m$ if the curing is beyond 24 weeks at 20 °C. Curing at 30 °C appears not to affect these pore fractions. This reduction is not reflected by the shear strength development (Figure 7.5), thus it is possible that it is mainly induced by the drying process prior to mercury intrusion.
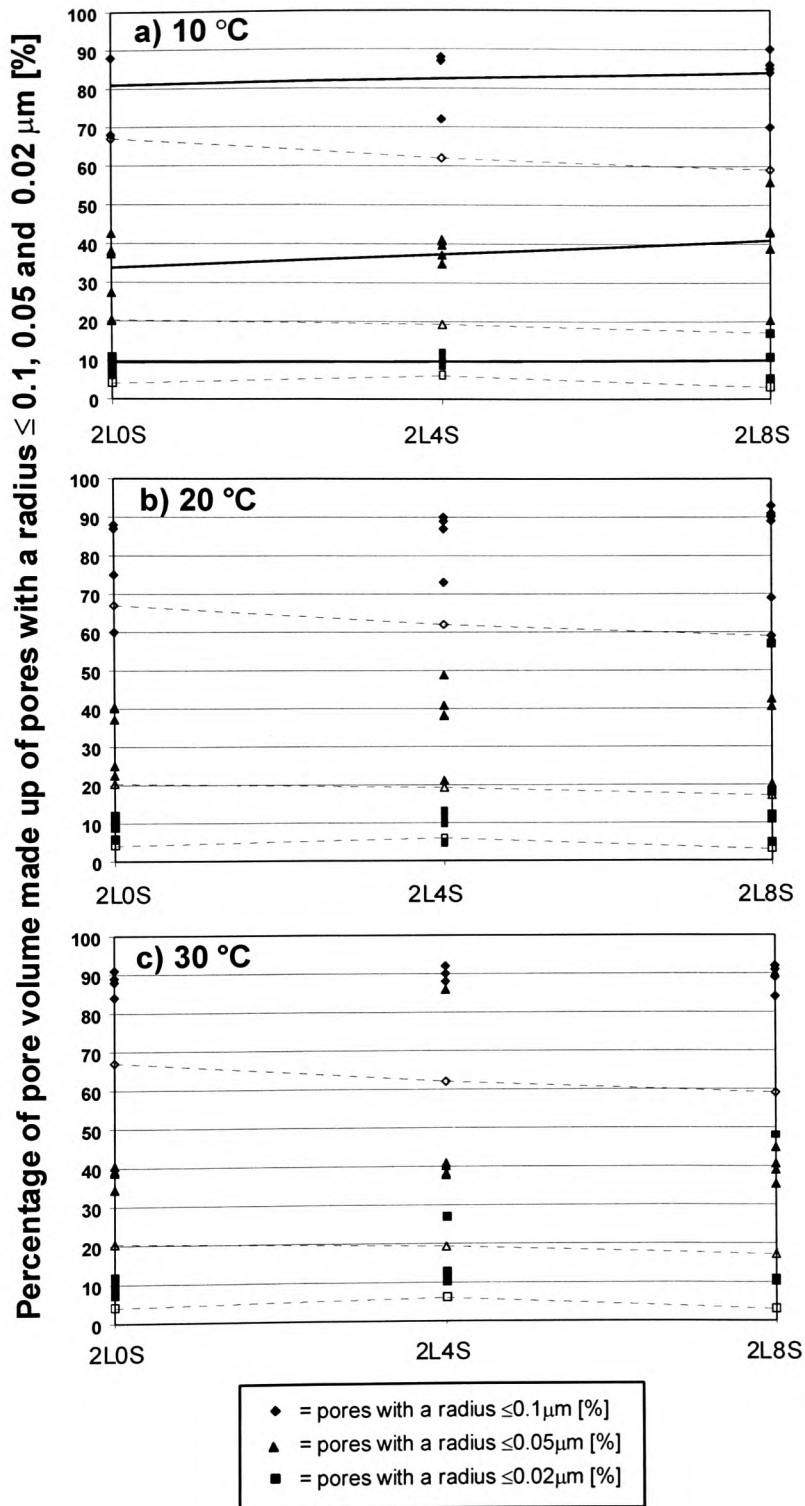
Figure 7.18 *Influence of curing temperature and sample composition on pore size distribution (r≤0.1 μm, 0.05 μm and 0.02 μm) of kaolinite, stabilised with various slag/lime ratios after curing periods of 1, 4, 12, 24 and 52 weeks (dotted lines indicate results of specimens tested immediately after compaction)*
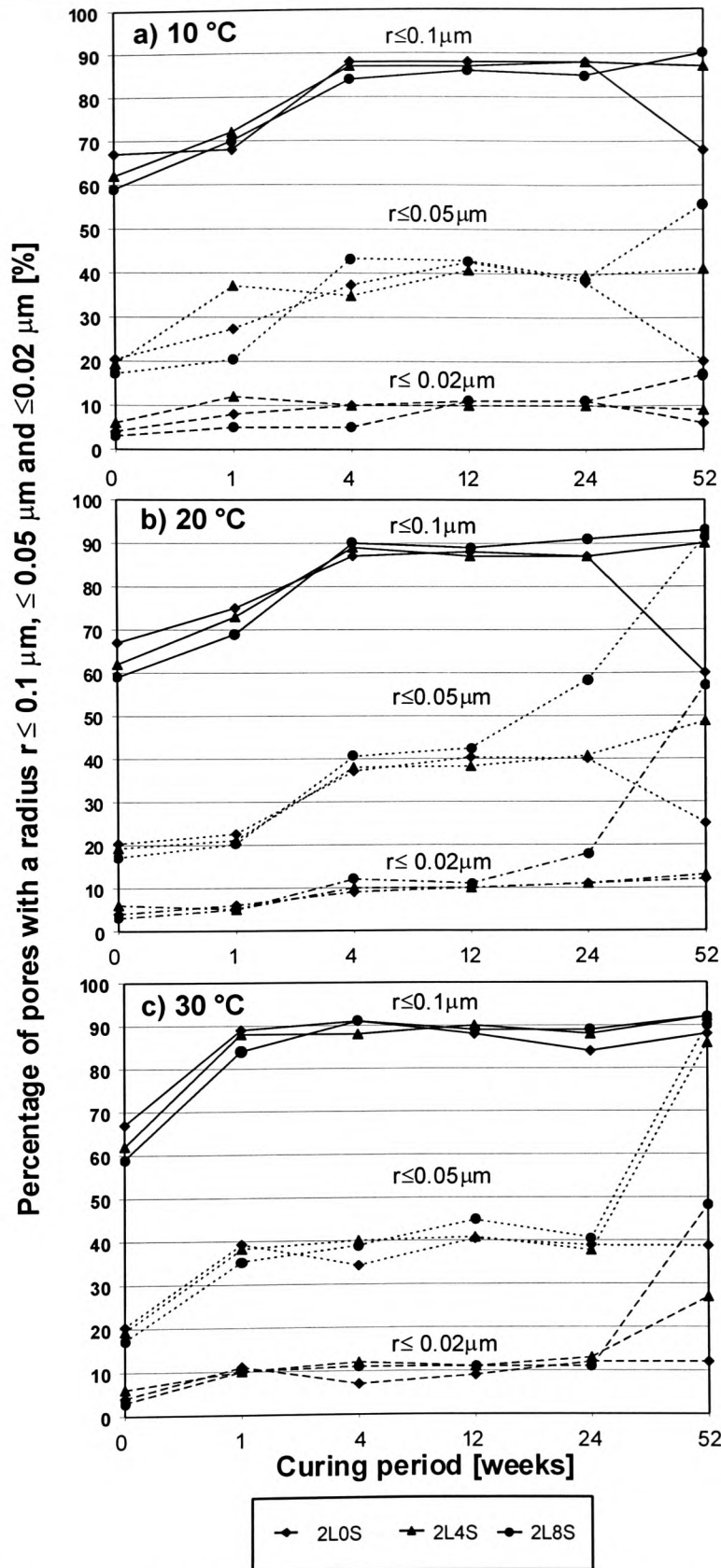
Figure 7.19 *Influence of curing temperature, curing period and sample composition on the development of the percentage of pores with radius $r \leq 0.1$ µm, ≤ 0.05 µm and ≤ 0.02 µm in kaolinite specimens stabilised with various slag/lime ratios in the absence of gypsum*

The presented data also confirm published data on strength development of lime-slag stabilised kaolinite with and without gypsum by Wild et al. [1998]. They showed that at high slag contents with sulphate present, most of the strength gain occurs in the first seven days, whereas without sulphate present, strength develops more slowly.

As already outlined in section 7.1.3.1 (preliminary considerations), the gypsum content appears to significantly affect the pore fraction with a radius $0.08\mu m \leq r < 1.0\mu m$ (see Figure 7.13). Figure 7.20 gives an overview over the development of the percentage of pores in this pore size range and also the pore fraction $r \leq 0.05$ μm for kaolinite specimens which were stabilised with 2% lime and increasing slag additions with additions of 2, 4 and 6% gypsum. Curing was at 30 °C for 1, 4 and 12 weeks for all specimens. The percentage of the pore volume comprising the small pores range ($r \leq 0.05$ μm) increases significantly for the gypsum addition specimens as the slag content increases and, as expected, the percentage of the pore volume comprising the coarse pores (0.08-$1.0\mu m$) simultaneously decreases. After 1 week of curing, there are no major changes in this pattern of behaviour and the degree of pore refinement is essentially similar after both 1 and 12 weeks. In addition the pattern of pore refinement does not appear to show any systematic trends in relation to the level of gypsum content and the degree of pore refinement actually decreases with increase in gypsum addition for the four week cured samples.

Figure 7.21 shows the threshold radius measurements for stabilised kaolinite in the presence (a) and absence (b) of 6% gypsum after various curing periods over the whole temperature range. Dotted lines indicate results for specimens for which curing was omitted. A systematic reduction in threshold radius with increase in slag content can be observed in the kaolinite-lime-ggbs-gypsum system, which is indicative of pore refinement associated with the development of a high percentage of well-connected pore channels characterised by a maximum radius below the values measured for the threshold radius. The critical pore radius is in fact reduced by almost 50% from a value of $r \approx 0.12\mu m$ to $\approx 0.06\mu m$ when 8% ggbs is added to kaolinite stabilised with 2% lime. A similar trend has been reported by Khatib and Wild [1996] for Portland cement pastes with increasing levels of metakaolin, which again was indicative of pore refinement.
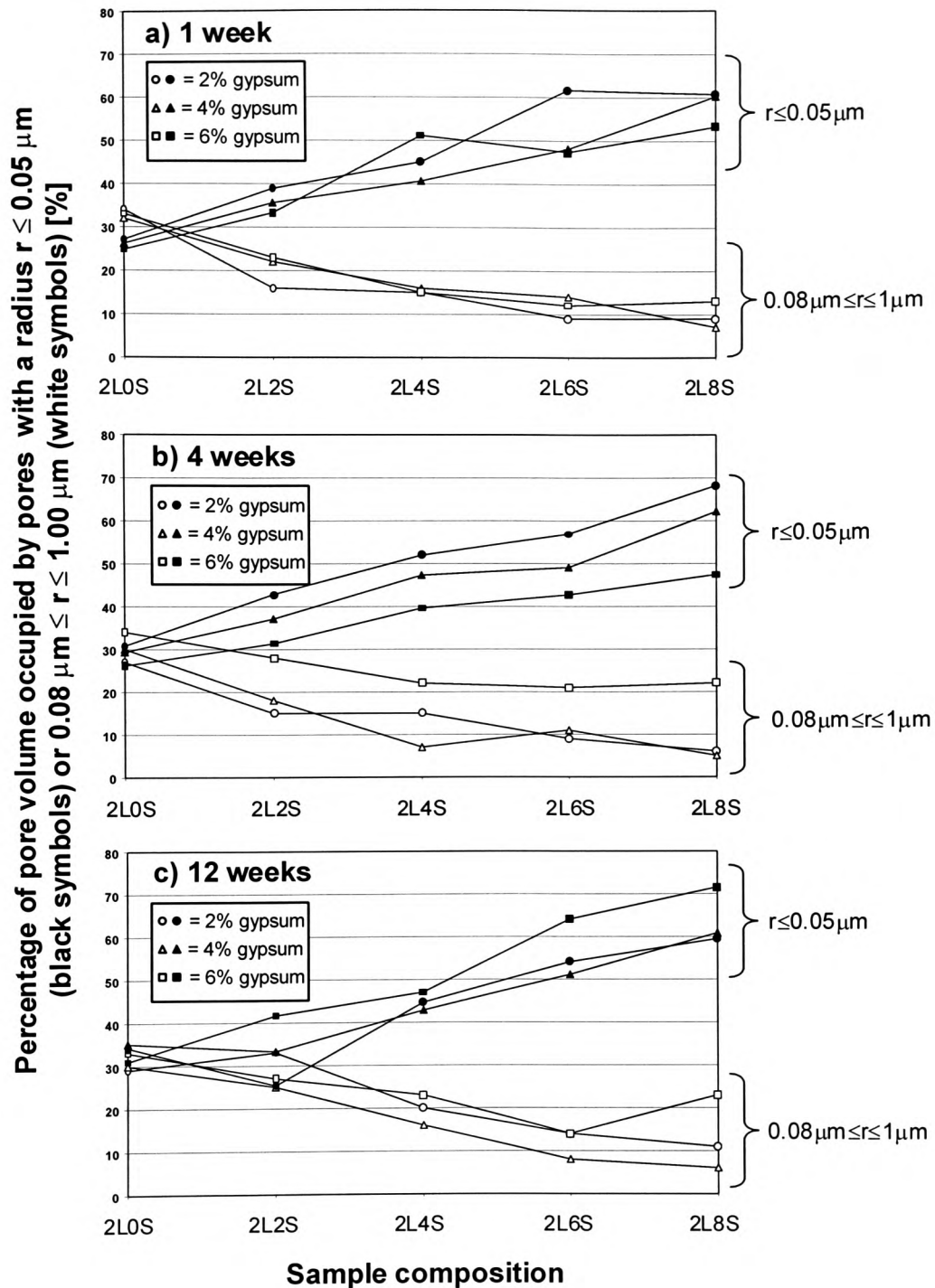
Figure 7.20 *Influence of curing period and sample composition (slag/lime ratio) on the development of the percentage of pore volume occupied by pores with radius $r \leq 0.05$ μm and 0.08 $\mu m \leq r \leq 1.0$ μm for kaolinite specimens in the presence of 2, 4 and 6% gypsum (curing temperature = 30 °C)*

The absence of gypsum results in a different threshold radii development. No systematic change in the critical pore radius could be identified with change in sample composition. However, the highest values for the threshold radius were exhibited by specimens cured for only 1 week independent of sample composition. Whereas curing
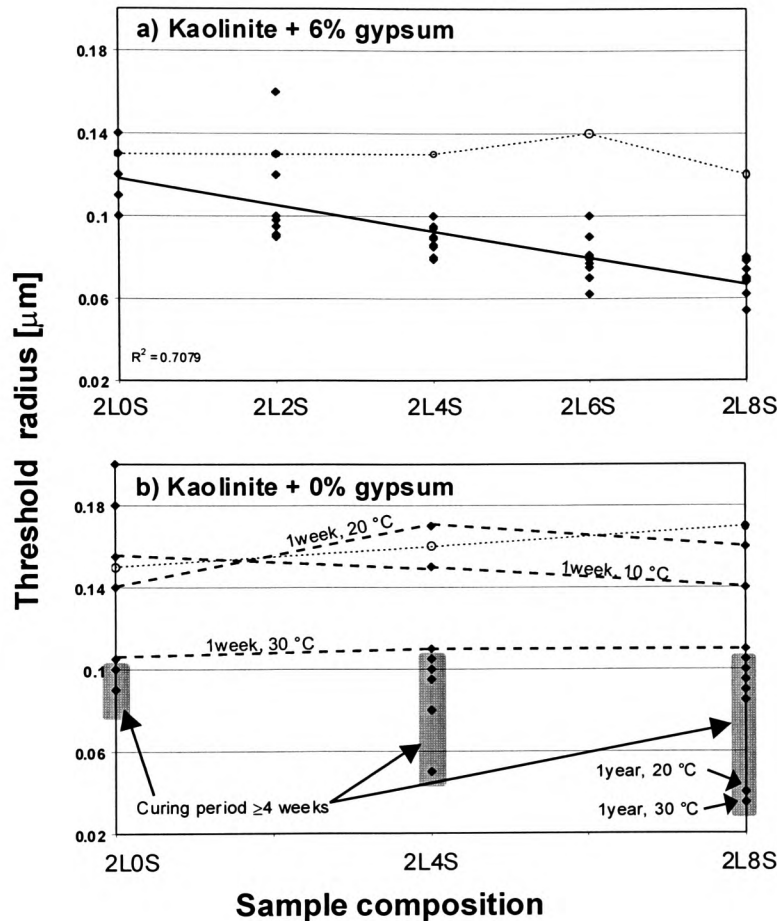
Figure 7.21 *Threshold radius versus sample composition for kaolinite specimens cured for up to one year at 10, 20 and 30 ℃ in the presence (a) and absence (b) of 6% gypsum (dotted lines indicate results for specimens which have been tested without curing)*

at 10 and 20 °C for 1 week results in threshold radii comparable to those obtained from specimens which were not cured at all, curing at 30 °C leads to significantly reduced threshold radii comparable to values obtained from specimens cured for 4 weeks and beyond. This is indicative of limited pore refinement due to limited cementation. However, measured threshold radii of gypsum free specimens cured for up to 24 weeks are overall larger than those obtained from specimens prepared in the presence of

gypsum. Curing for 1 year at elevated temperatures results, for specimens stabilised with 8% ggbs in the absence of gypsum, in lower threshold radii and thus a higher degree of pore refinement than in the presence of gypsum (two labelled points in the bottom right corner of Figure 7.21b). This higher degree of pore refinement is also apparent from the substantial percentage of pore volume occupied by small pores ($r<0.05\mu m$) for these specimens as illustrated in Figure 7.19c.

7.1.3 Effect of porosity and pore size distribution on the strength development of kaolinite stabilised with lime-activated ggbs

There is general agreement amongst researchers that the microstructure of a specimen determines to a large degree the performance of the sample with regard to various engineering properties, some of which, for example permeability or frost resistance, are often considered as a measure of specimen durability. This section is an attempt to correlate observed changes in strength to changes in the sample structure, expressed by porosity and pore size distribution.

When analysing the results of the triaxial tests it is apparent from comparison of the changes in shear strength τ_u (based on normal stress $\sigma_n = 1000$ kN/m^2) with curing time and curing temperature with respect to the MIP data that there is a relationship between exhibited shear strength, threshold radius and pore size distribution. The relationships are shown in Figure 7.22, where shear strength τ_u, calculated based on a normal stress of $\sigma_n = 1000$ kN/m^2, is plotted against the threshold radius (a), the proportion of pores with radius $r \leq 0.05$ µm (b) and the total intruded pore volume (c). It is interesting to see that strength increases with reduction of the threshold radius and increases with an increase in the percentage of pores with a pore radius $r \leq 0.05$ µm (Figure 7.22a and b respectively). The total porosity (Figure 7.22c) appears to have little influence on the exhibited shear strength.

In Figure 7.23 the same relationships are plotted for stabilised kaolinite in the absence of gypsum. Similar trends are apparent for both shear strength versus threshold radius and shear strength versus fine porosity although the numbers of data with high shear strength values are much lower because only specimens cured for 1 year developed substantial strength. The total intruded pore volume showed a slightly wider range of values (relative to Figure 7.22c), but again, no correlation with shear strength was apparent (Figure 7.23c).

The influence of various gypsum additions on the pore size distribution and its correlation with observed indirect tensile strength is shown in Figure 7.24, where the values for R_{it} are plotted against the percentage pore volume comprising pores with a radius ≤ 0.05 µm after curing periods of 1, 4 and 12 weeks. It is clear that the presence of gypsum affects the percentage of small pores created during slag hydration. If no gypsum is added at all, only around 40% of pores with the relevant pore size are created. However, the introduction of even small amounts of gypsum (2%) leads to an

increase in the percentage of small pores up to around 70%. The suggested trendline as a result of the linear function between R_{it} and percentage of pores with a radius $r \leq 0.05 \mu m$ also becomes steeper with increase in gypsum addition. This is indicative of microstructural changes initiated by the presence of sulphates, resulting in higher indirect tensile strength coupled with an increase in fine porosity, although the range of fine porosity developed does not vary significantly with change in sulphate content.

The percentage change in the amount of small pore ($r \leq 0.05 \mu m$) also affects the unconfined compressive strength of specimens cured up to 12 weeks at 30 °C in a similar way (Figure 7.25). Generally, good correlation between an increase in the fraction of pores with this specified pore radius and an increase in the measured UCS-values could be identified. However, in the absence of gypsum (Figure 7.25a), possibly also due to a smaller statistical sample size (only mixes 2L0S, 2L4S and 2L8S were considered), no correlation was apparent.
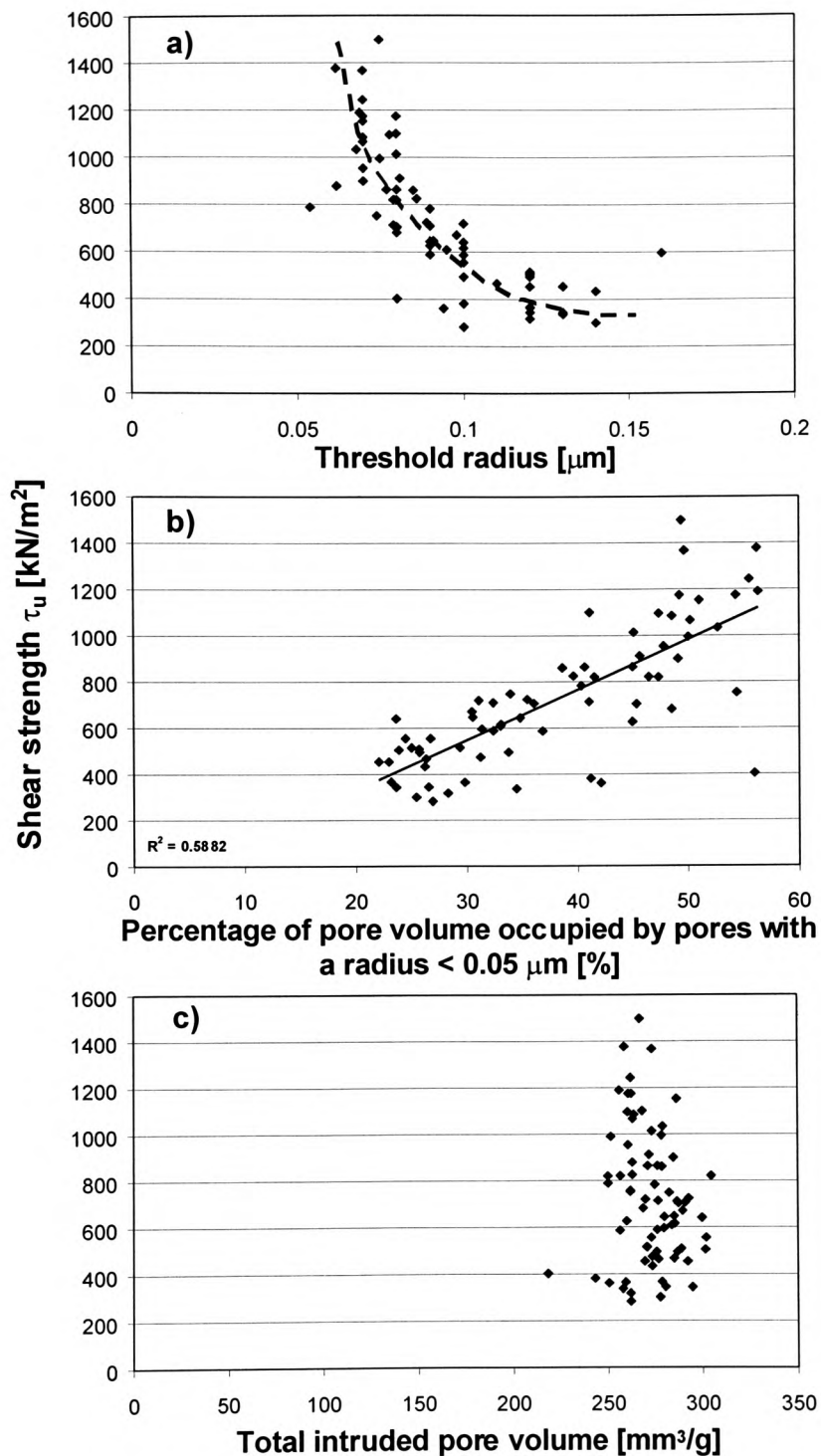
Figure 7.22 *Relationship between shear strength τ_u (σ_n=1000 kN/m²) and a) threshold radius, b) percentage of pore volume occupied by pores with a radius <0.05 μm and c) total intruded pore volume of kaolinite-lime-ggbs mixes (in the presence of 6% gypsum) cured for up to 1 year at 10, 20 and 30 °C*
(N.B.: Curve in Figure 7.22a) is not a mathematical fit)
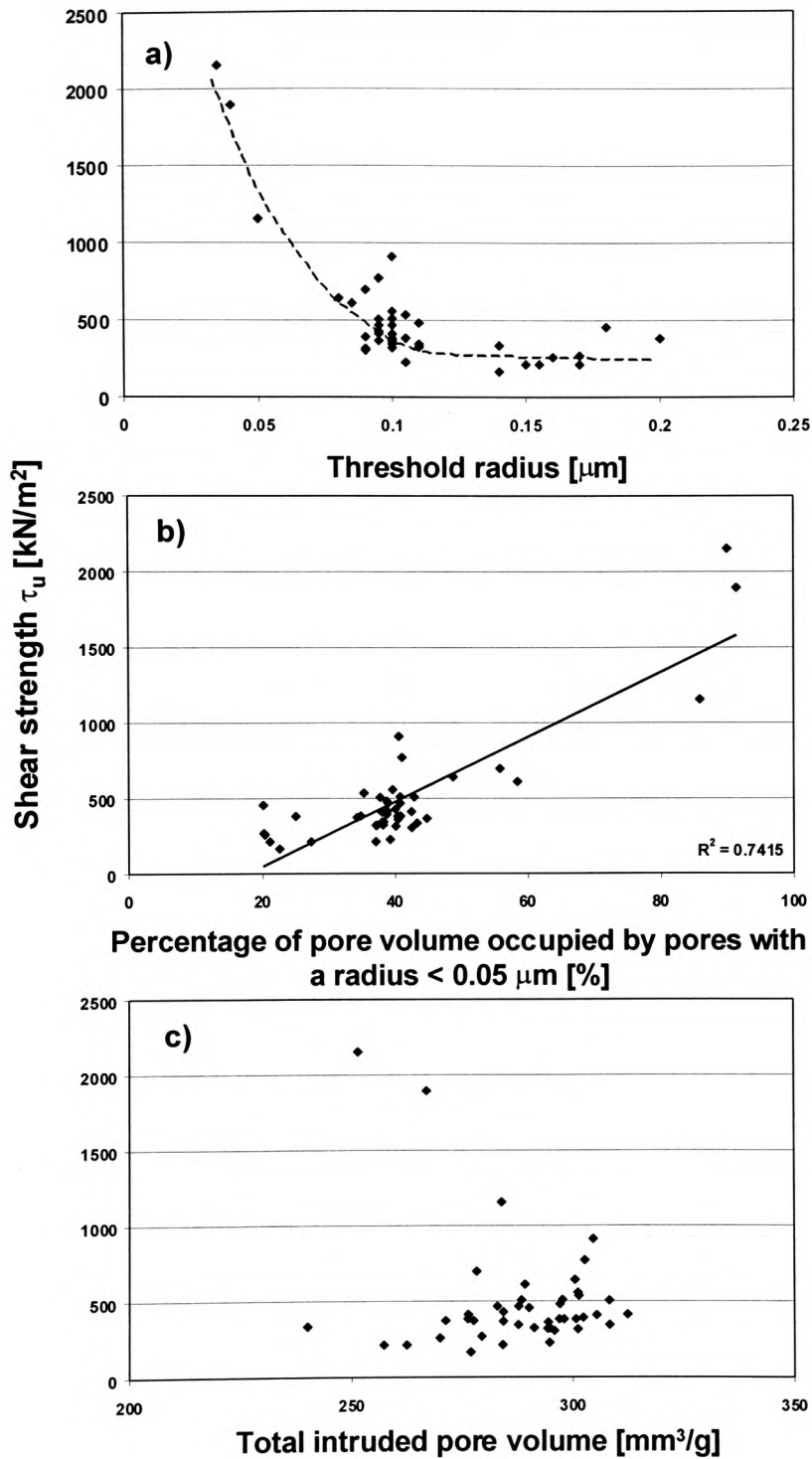
Figure 7.23 *Relationship between shear strength τ_u (σ_n=1000 kN/m²) and a) threshold radius, b) percentage of pore volume occupied by pores with a radius <0.05μm and c) total intruded pore volume of kaolinite-lime-ggbs mixes cured for up to 1 year at 10, 20 and 30 °C*
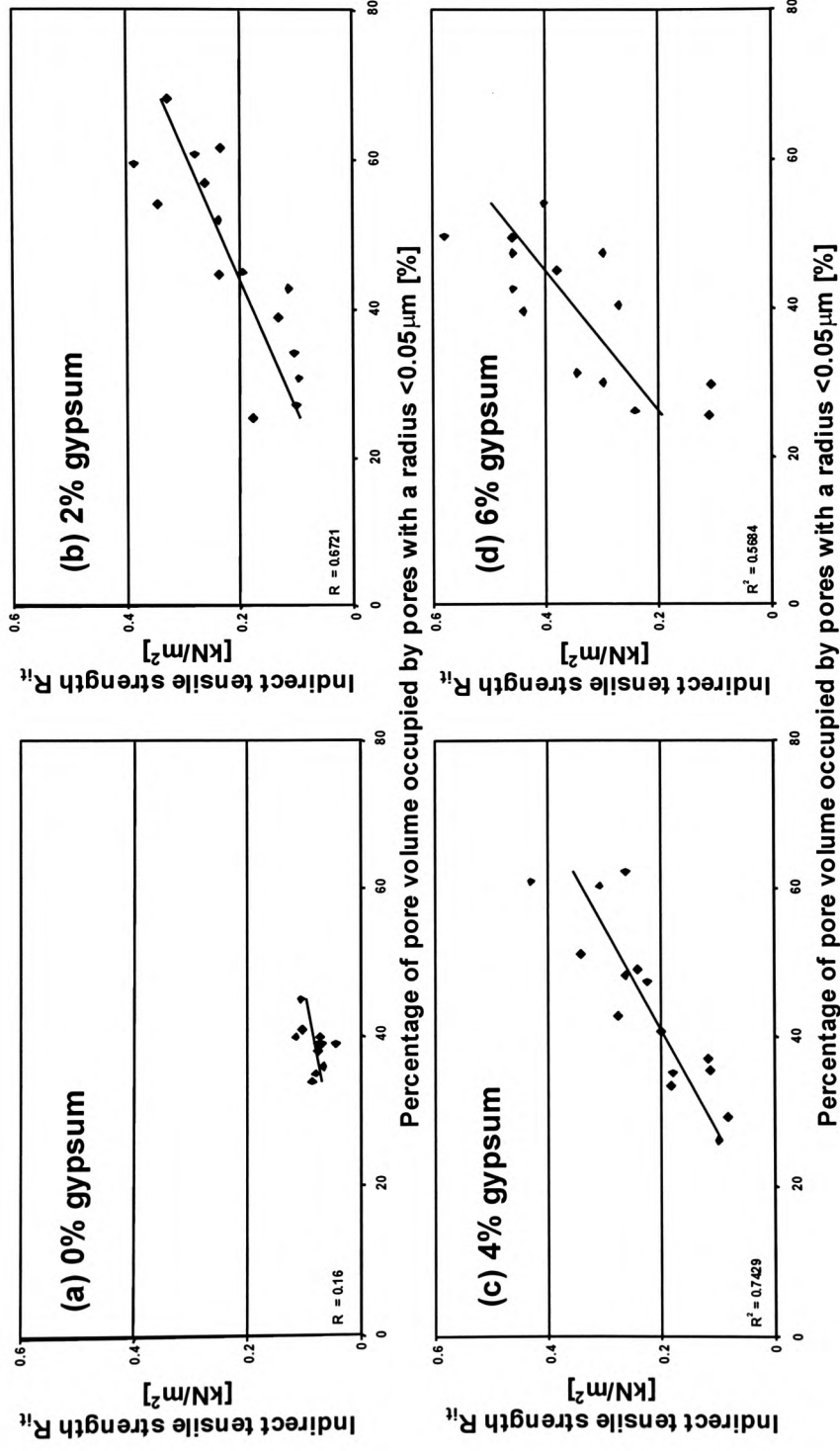
Figure 7.24 *Indirect tensile strength [kN/m²] versus percentage of pore volume occupied by pores with a radius ≤0.05 μm for kaolinite stabilised with various slag/lime ratios after curing for 1, 4 and 12 weeks at 30 °C in the presence of 0% (a), 2% (b), 4% (c) and 6% (d) gypsum*

Gabriele Veith
University of Glamorgan
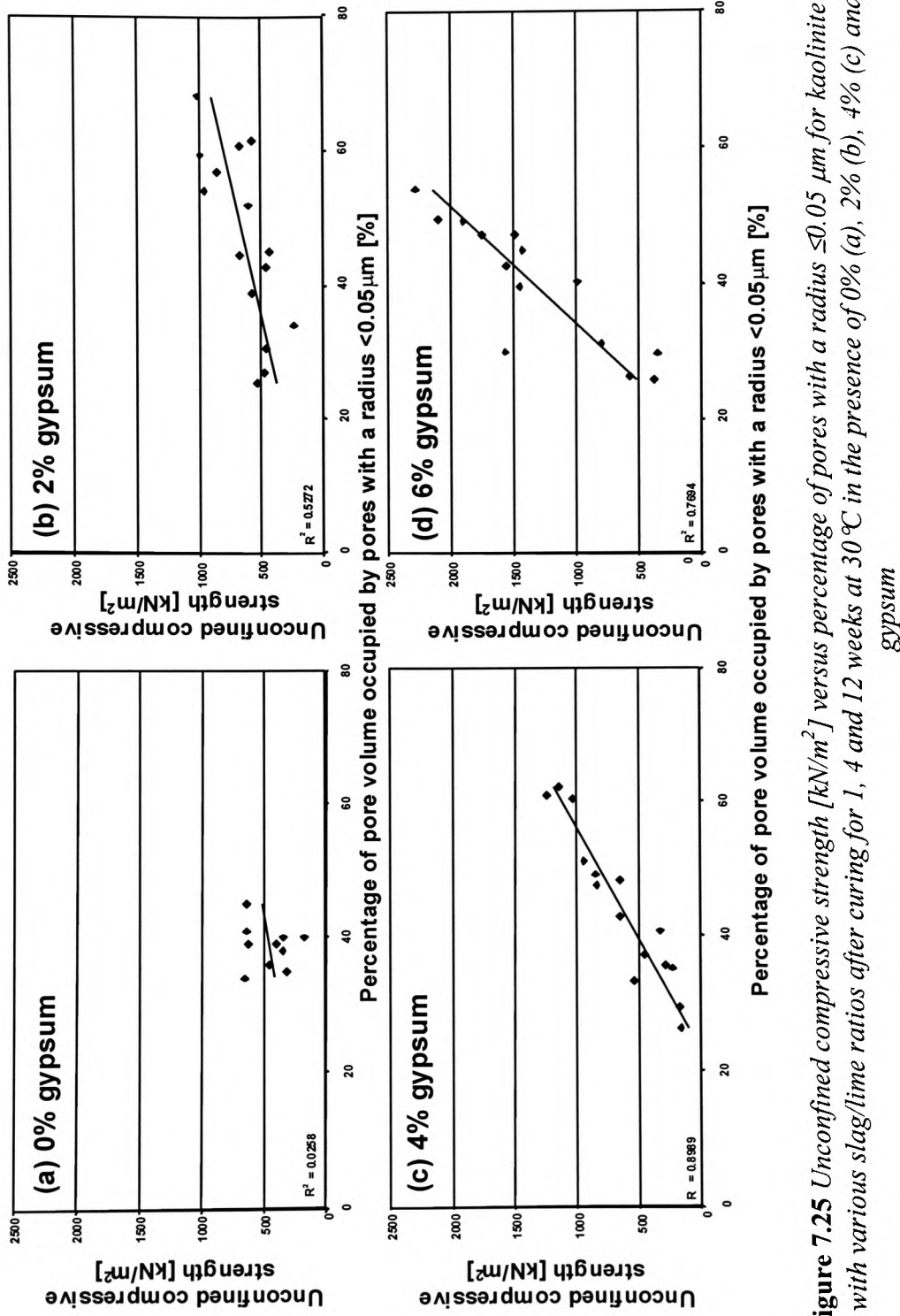
Figure 7.25 *Unconfined compressive strength [kN/m²] versus percentage of pores with a radius ≤0.05 µm for kaolinite stabilised with various slag/lime ratios after curing for 1, 4 and 12 weeks at 30 °C in the presence of 0% (a), 2% (b), 4% (c) and 6% (d) gypsum*

Gabriele Veith
University of Glamorgan

7.1.4 Permeability of kaolinite stabilised with lime-activated ggbs

Generally, a higher degree of variability in measured coefficients of permeability was observed for soils with high fineness and narrower grain size distribution, i.e. kaolinite showed a higher degree of variability than Lower Oxford Clay or Kimmeridge Clay (results of investigations carried out on lime-slag stabilised Kimmeridge Clay are given in Appendix 5, publications on Kimmeridge Clay).

A typical development of permeability for lime-slag stabilised kaolinite specimens (in the presence of 6% gypsum) cured at 10, 20 and 30 °C for up to one year is shown in Figure 7.26. The results cover a range of k-values from approximately 4×10^{-5} m/h (exhibited by the mix 2L6S cured for 1 week at 30 °C) down to 3×10^{-8} m/h, which is achieved by mixes cured for longer periods independent of curing temperature. If curing is only for 1 week the addition of slag appears to result in an increase in the observed k-values and this increase is more pronounced at elevated temperatures (20 and 30 °C) and high slag contents. Marginally reduced (relative to k-values of specimens tested immediately after compaction) coefficients of permeability are observed however, after curing for 1 week at 10 °C. As might be expected the values for specimens tested immediately show very little change with increase in slag/lime ratio. The effect of slightly higher density of specimens with higher slag additions, which derives from marginally reduced pore volume due to less flocculation on the measured k-values, seems to be negligible.

Curing temperature affects the coefficient of permeability to a large degree. In particular specimens which were stabilised with only 2% lime (2L0S) appear to be very sensitive to the temperature of the curing environment. Curing at 30 °C results in similar coefficients of permeability for specimens of all compositions after a curing period of 4 weeks and beyond. The mutual k-value is approximately $7.0\text{-}8.0 \times 10^{-8}$ m/h.

The absence of gypsum results in a somewhat different permeability pattern when kaolinite is stabilised with 2% lime and various ggbs additions as illustrated in Figure 7.27a-c. Unlike the gypsum containing samples, the gypsum free samples show very little reduction in permeability other than those cured at 30 °C.
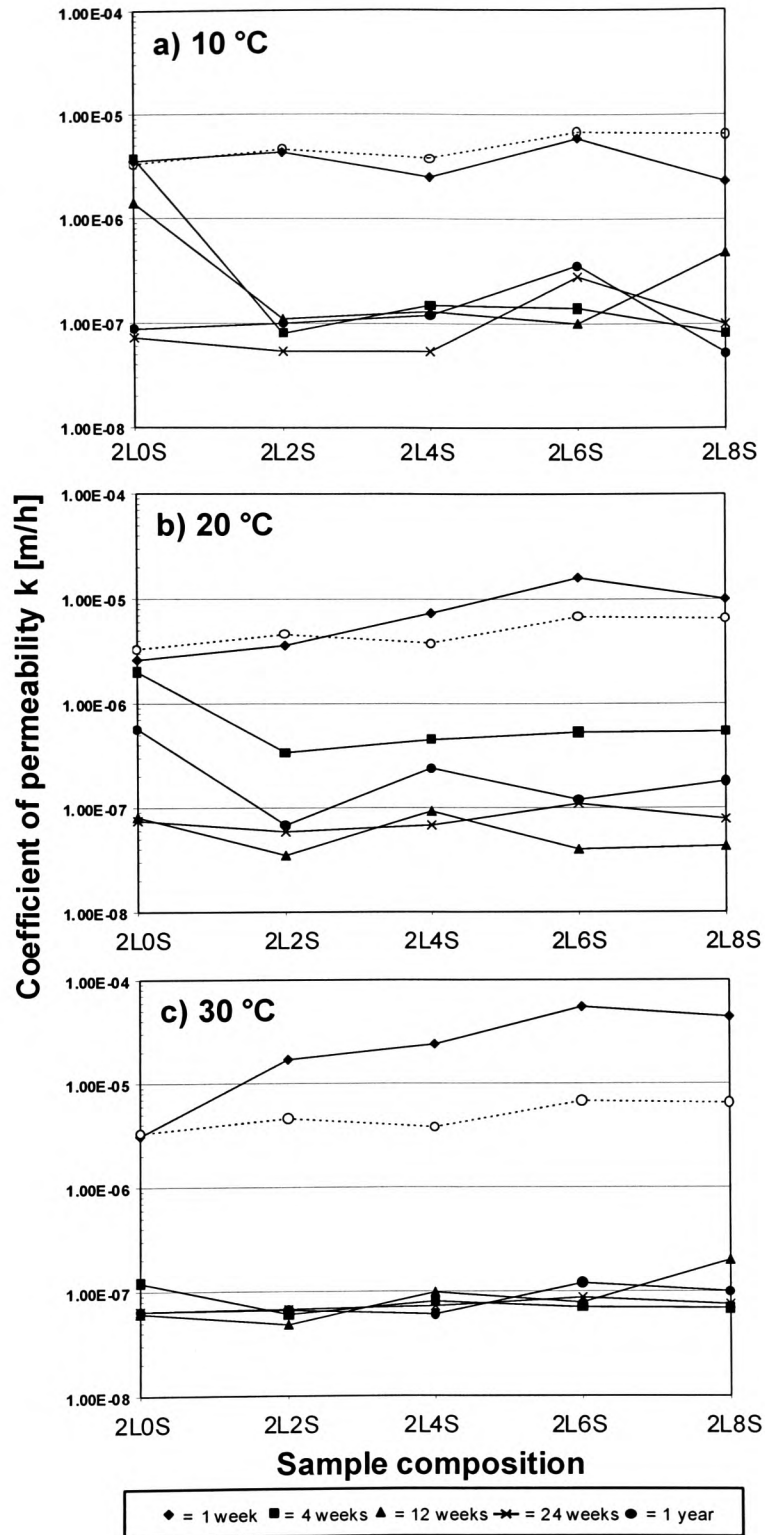
Figure 7.26 *Influence of curing temperature (10 (a), 20 (b) and 30 (c) °C), curing period and sample composition on the coefficient of permeability k [m/h] for stabilised kaolinite in the presence of 6% gypsum (dotted lines indicate test results of specimens for which curing was omitted)*

In common with specimens containing gypsum there is very little change in the coefficient of permeability k for specimens which have been tested immediately but, unlike specimens containing gypsum, there is also little change in k after a curing period of 1 week at 10, 20 or 30 °C. If curing is for 4 weeks the influence of the slag addition becomes very significant (Figure 7.28). Whereas the mix with lime only (2L0S0G) exhibits reduced permeability even if curing is at only 10 °C, the addition of slag results in no changes to k-values at 10 °C relative to immediately tested specimens (dotted lines). At 20 °C curing there is a significant reduction in permeability after 4 weeks for all samples including those with slag, but at longer curing periods k again increases. For example, if curing is further prolonged (12 and 24 weeks), it results in specimens exhibiting k-values close to those of uncured specimens, independent of slag addition (Figure 7.27b). If curing is at 30 °C (i.e. at 30 °C (Figure 7.27c) an increase in curing period leads to substantially reduced coefficients of permeability for specimens with a high ggbs content. The k-values of these lime-slag-stabilised specimens show negligible change in a cold curing environment (10 °C) after extended curing periods. This behaviour is reflected in the changes in undrained shear strength of these specimens shown in Figure 7.5. With gypsum present slag hydration is more rapid particularly at elevated temperatures and leads to a significant and permanent reduction in permeability after extended curing periods (6 to 12 months). Without gypsum, specimens only show a significant and permanent reduction in permeability at elevated temperatures and high slag contents.
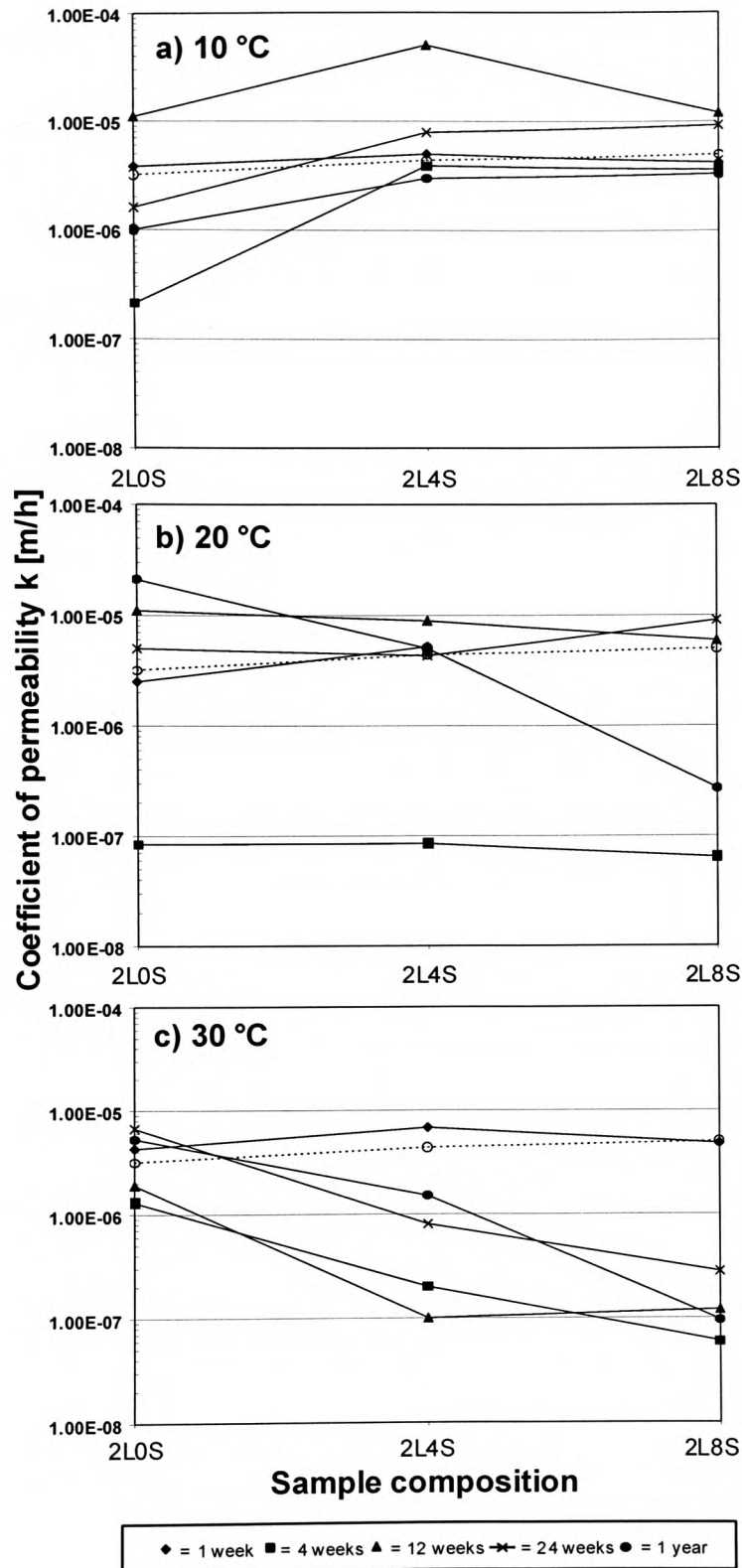
Figure 7.27 *Influence of curing temperature (10 (a), 20 (b) and 30 (c) °C), curing period and sample composition on the coefficient of permeability k [m/h] for stabilised kaolinite (dotted lines indicate test results of specimens for which curing was omitted)*
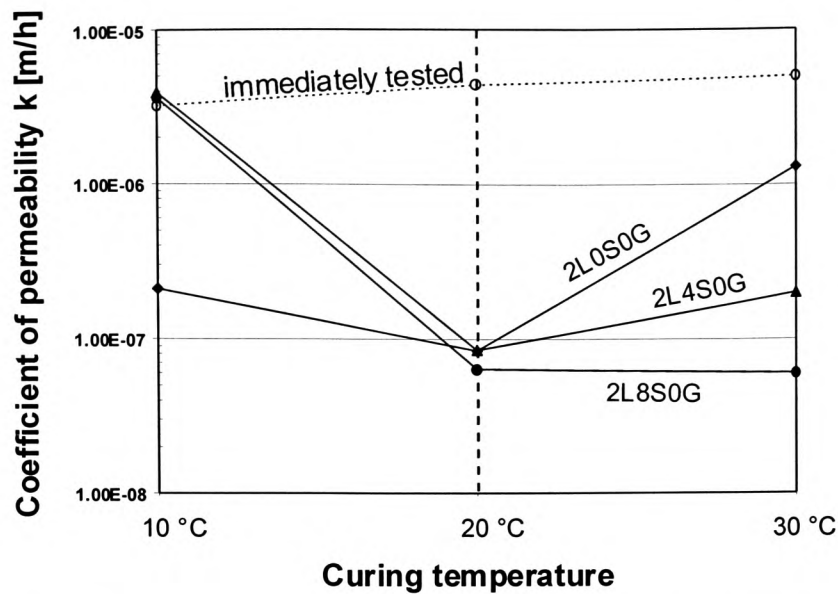
Figure 7.28 *Coefficient of permeability of kaolinite stabilised with 2% lime and 0, 4 and 8% ggbs after a curing period of 4 weeks at 10, 20 and 30 °C*

7.1.5 Frost resistance of kaolinite stabilised with lime-activated ggbs

In order to assess the influence of the initial moist curing period on the specimens' frost resistance, samples were cured for 1, 4, 12 and 24 weeks at 30 °C prior to being subjected to 12 freeze-thaw cycles. Figure 7.29 illustrates typical sample behaviour in terms of the change in height and weight of lime-ggbs stabilised kaolinite in the presence (a+b) and absence (c+d) of 6% gypsum after a curing period of 90 days prior to frost action. In the presence of gypsum, there is little effect of stabiliser content on the weight or height change during freeze-thaw cycling. Generally, slightly lower linear expansion and reduced weight gain with increase in ggbs content can be recorded. The comparably low weight gain due to water absorption of the sample 2L0S6G is due to the fact that the specimen's structure had lost nearly all its strength after the fifth freeze-thaw cycle and was thus no longer able to encapsulate the absorbed water within its soil skeleton. Subsequently, no further weight gain could be recorded.

The absence of gypsum results in a wider variation of the ultimate height and weight magnitudes relative to mix composition. In particular the ultimate change in height is
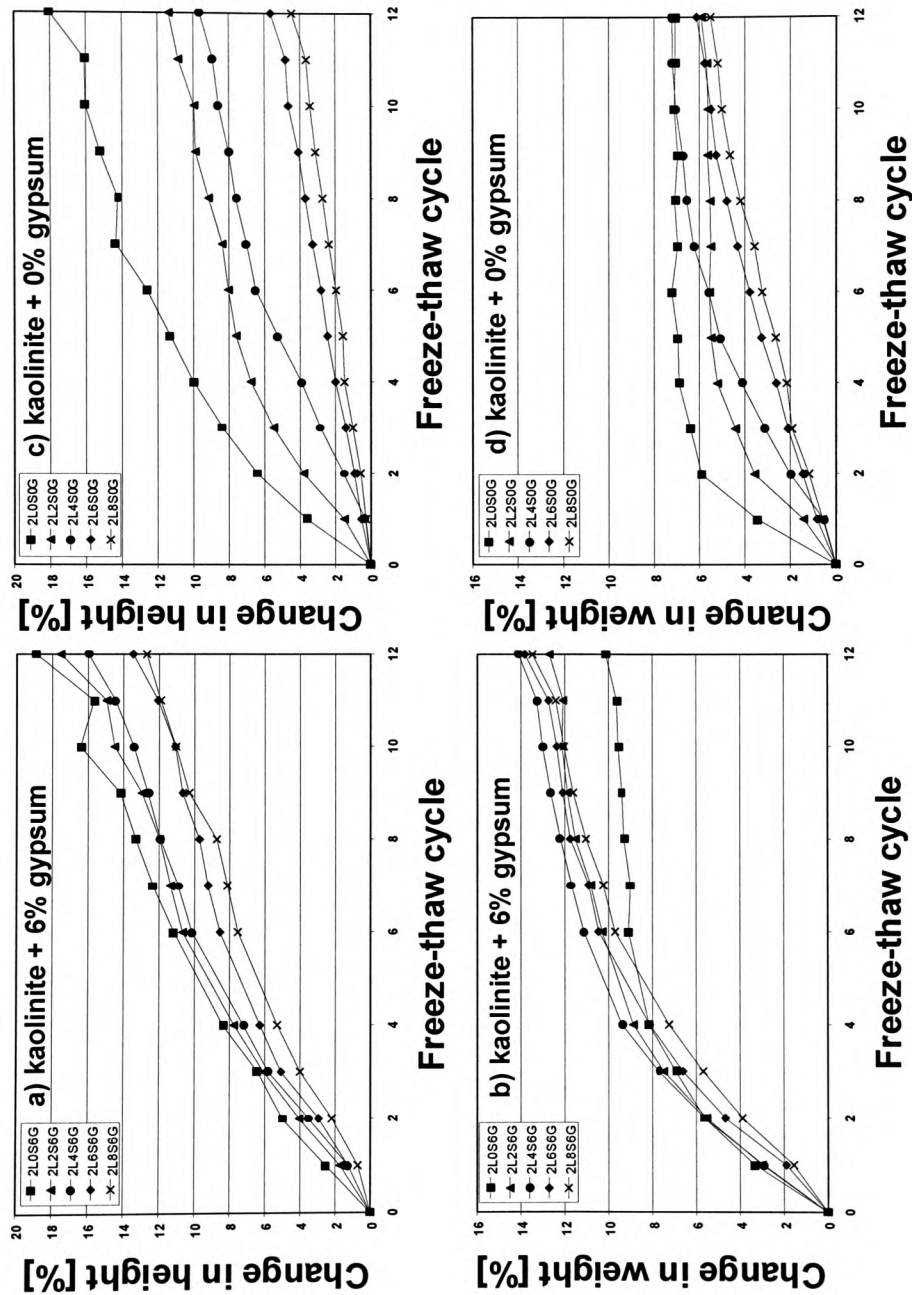
Figure 7.29 *Change in height and weight [%] of slag/lime stabilised kaolinite (moist cured for 90 days at 30 °C prior to frost action), in the presence (a+b) and absence (c+d) of 6% gypsum, during freeze-thaw cycling*

Gabriele Veith
University of Glamorgan

reduced substantially from 18% to 4.5% when 8% ggbs is added to the specimens stabilised with 2% lime (Figure 7.29c). Whereas the weight increase (Figure 7.29d) is more gradual with increase in the number of freeze-thaw cycles for specimens with higher ggbs additions, samples to which only lime had been added (2L0S0G) show weight increase only up to the third freeze-thaw cycle. Beyond this point, only marginal increases in weight were recorded.

Figure 7.30 summarises the ultimate height, weight and volume changes after 12 freeze-thaw cycles for specimens made of kaolinite, stabilised with 2 % lime and 0, 2, 4, 6 and 8 wt.% ggbs in the presence of 6 % gypsum and in the absence of gypsum after 7, 28, 90 and 180 days of moist curing at 30 °C prior to frost action.

For samples without gypsum and without slag the substantial height increase recorded (~17%) shows very little variation with increase in initial curing period. This is attributed to negligible cementation even for long initial curing periods. However as the amount of slag in these specimens is increased from 0-8%, increases in initial curing period lead to a substantial reduction in linear expansion as a result of frost attack. Typically, for the 2L8S samples linear expansion is 18% for specimens which have been initially cured for 7 days and only 4% for specimens which have been initially cured for 180 days.

The volume changes illustrated in Figure 7.30c were calculated based on the measurements of height and diameter change. The change in volume with change in composition and initial curing time observed for specimens without gypsum are similar to the trends observed for changes in height (Figure 7.30a). However, although as expected specimens containing gypsum show significantly greater volume changes than those without gypsum, gypsum containing specimens which have been cured for a short curing period show an increase in total volume with increase in slag content, not a decrease in contrast to the height changes. This difference in the results is because, for specimens with low slag content, the volume expansion arises predominantly from increase in specimen height whereas for specimens with high slag content the volume expansion is significantly influenced by increase in specimen diameter. This is illustrated in Figure 7.31, which shows a photograph of the changes in dimensions after12 freeze-thaw cycles of cylinders for the mixes 2L0S6G and 2L8S6G. Whereas samples with high slag additions (right) adopt an overall larger shape with particular emphasis on increase in diameter, a slimmer, longer shape is exhibited by specimens
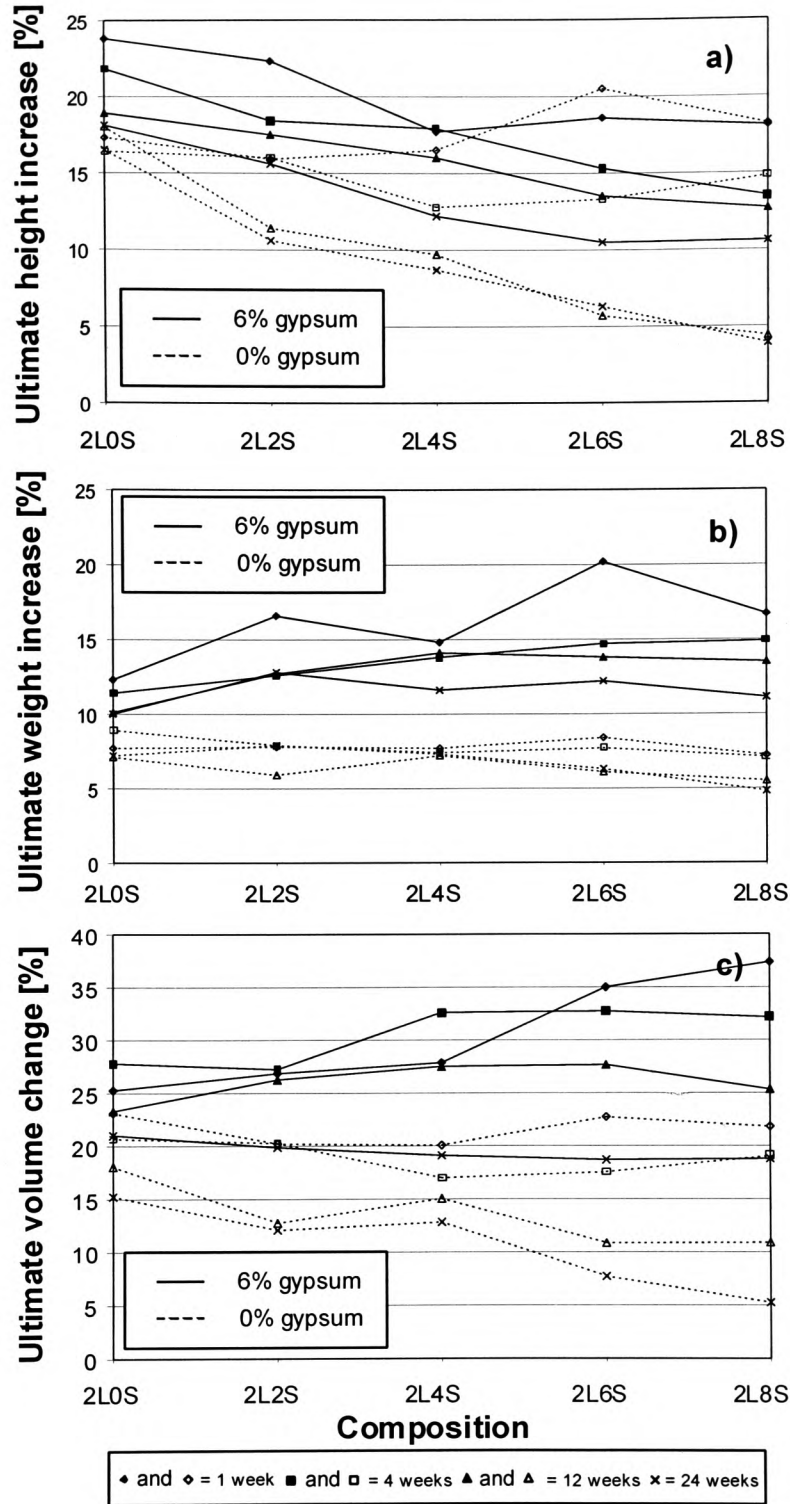
Figure 7.30 *Ultimate height (a), weight (b) and volume (c) increase of kaolinite in the presence of 6% gypsum (full lines) and absence of gypsum (dotted lines), stabilised with 2% lime and various ggbs additions after 1, 4, 12 and 24 weeks of moist curing prior to 12 freeze-thaw cycles*

which contain only lime as a stabiliser. The large increase in length with little associated increase in diameter for the slag free sample is attributed to the constraining influence of the rubber membrane on a sample which is poorly cemented and still in a highly plastic state. The suggested mechanism is illustrated in more detail in chapter 9.
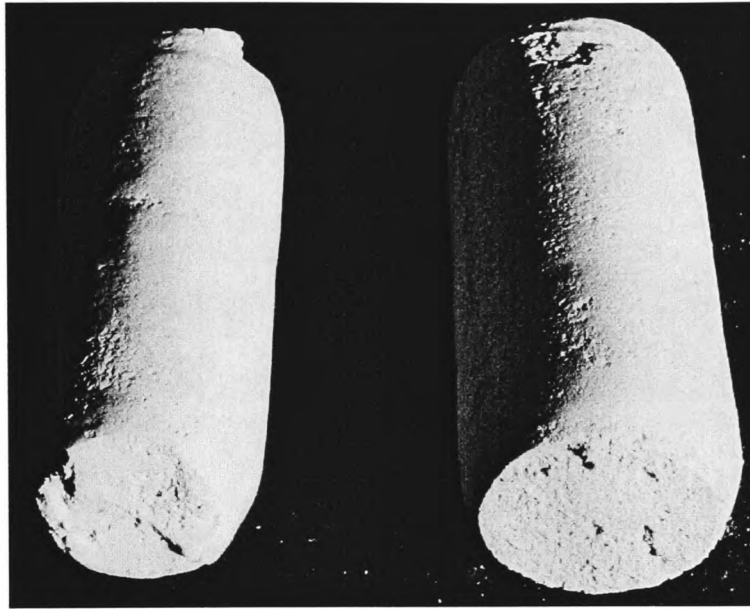
Figure 7.31 *Dimensions of specimens 2L0S6G (left) and 2L8S6G (right) cured for 7 days prior to frost action after 12 freeze-thaw cycles*

It can be misleading if an attempt is made to base the performance of specimens during freeze-thaw cycling solely on changes in dimension. A large weight increase, for example, which is due to the absorption of water (available in abundance in an open system), is not necessarily an indication for poor performance if the respective changes in volume are within tolerable limits. Thus Figure 7.32 gives an indication of how sensitive the stabilised specimens are to the water uptake they exhibit during freeze-thaw cycling by an assessment of the ultimate weight change/volume change (w/v) ratio. Although Figure 7.30 might give the impression that specimens stabilised in the absence of gypsum show a somewhat better degree of resistance to frost action, particularly after long curing periods, Figure 7.32b reveals that in fact the sensitivity of these specimens with regard to their volume stability after water uptake is, up to a curing period of 12 weeks prior to frost action, very similar to specimens with gypsum.
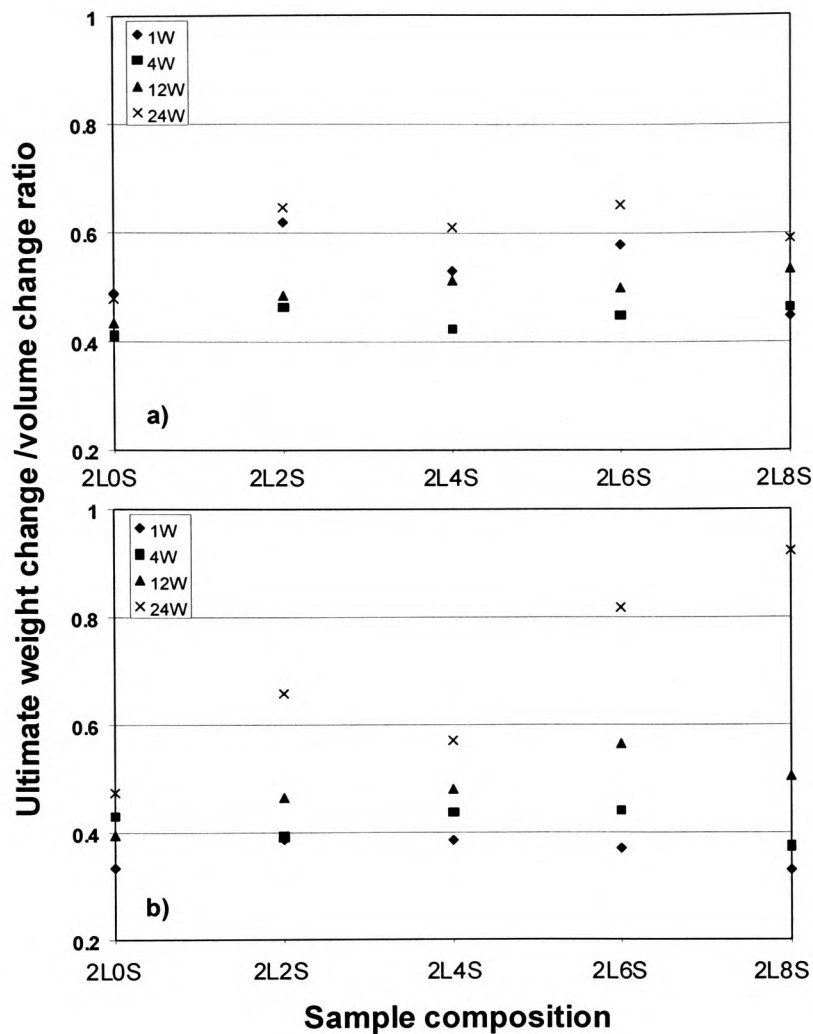
Figure 7.32 *Influence of initial curing period on the ultimate weight change/volume change ratio of stabilised kaolinite specimens after 12 freeze-thaw cycles in the presence (a) and absence (b) of 6% gypsum*

Based on the proposed relationship, a higher w/v ratio is an indication of a stronger specimens structure, which results in less difficulties in resisting the hydraulic pressure deriving from the absorbed water during freezing. As an overall trend, the increase in shear strength was reflected in an increase of the w/v ratio of gypsum-free specimens. However, this correlation was largely dependent on few high shear strength values obtained from specimens cured for 24 weeks. If these results were omitted, no significant relationship could be established. Specimens prepared in the presence of 6% gypsum did not show any correlation between strength and weight/volume change ratio. Interestingly, there was also no systematic trend between the changes in exhibited w/v

ratio and the indirect tensile strength values exhibited by specimens (in both the presence or absence of gypsum).

It is appreciated that a wide range of factors, which are discussed in detail in chapter 9, influence the sample structure and thus the ultimate weight/volume change ratio during frost action. These factors result in modified engineering properties and are affected by the chemical reactions occurring in the specimens during mixing and curing. Water, which is introduced in abundance during freeze-thaw cycling, will further modify the behaviour of specimens and subsequently result in additional difficulties in interpreting the observed changes with regard to specimen structure.

It should be noted that the observed weight change/volume change ratios and the subsequent interpretations are only tested on the scope of materials used for the current investigations.

7.1.6 Effect of porosity and pore size distribution on permeability and frost resistance of kaolinite stabilised with lime-activated ggbs

For both systems, kaolinite-ggbs-lime in the presence and absence of gypsum, attempts were made to identify relationships between permeability and pore structure (i.e. total porosity, pore size distribution and threshold radius), but no correlations were found and no systematic trends were apparent. When the coefficient of permeability was plotted against the percentage of pore space occupied by pores with a certain radius, the percentage of pore space occupied by pores with a certain diameter could not be related to the observed k-values. However, the observed variation in percentage of the different pore fractions in the case of pores with a radius r≤0.1μm was around 20% (over the whole range of curing temperature and duration). For the pores with a radius ≤0.02μm it was only 12% when the specimens were compacted in the presence of gypsum. From these comparably small changes one would expect little influence on observed coefficients of permeability. The percentage of pores with a radius ≤0.05μm changes by up to 40%, which one would expect to affect the k-values of the specimens to some degree. However, based on findings by Manmohan and Mehta [1981] who investigated the influence of slag on the pore size distribution and permeability of hardened cement paste and Goto and Roy [1981] who assessed the effect of w/c ratio and curing temperature on the permeability of cement paste, the k-values appear to be largely related to the presence of pores with radii greater than 0.05 and 0.075 μm, respectively.

Due to the fact that no systematic trends based on the presence of larger pores could be identified, there is some likelihood that other factors, for example shrinkage during drying prior to mercury intrusion, will have an effect on the pore structure and subsequently influence any relationships between pore size distribution and the measured k-values. This is discussed in more detail in Chapter 9.

If the total intruded pore volume is plotted against the observed k-values, there is also little evidence for good correlation between the two sample characteristics. Although the total intruded pore volume varies only by about 40 mm³/g between mainly 260 and 300 mm³/g, the k-values are scattered unsystematically between approximately 1.0×10^{-4} m/h and 6.0×10^{-8} m/h. This further emphasises the importance of detailed analysis of the actual pore size distribution within the specimen and how it is affected by factors such as the drying regime. However, independent of the pore volume or the way in which the pores are distributed, the k-values appear to asymptotically approach a

minimum coefficient of around 6.0×10^{-8} m/h. For the scope of the current work no lower values could be observed.

It has been established that the durability of stabilised and thus partially cemented soil specimens with regard to resistance to frost action is mainly determined by the ease with which water can migrate during frost action. Thus it might be expected that some correlation exists between frost damage, permeability and, indirectly, porosity and pore size distribution. Figure 7.33a shows the relationship between ultimate volume change and total intruded pore volume. However, the trend is the reverse of what might be expected in that as total intruded pore volume increases, the ultimate volume change decreases. One possible reason for this somewhat unexpected result is that specimens which contain gypsum are susceptible to substantial water absorption (Figure 7.29b) and swelling (Figures 7.35 and 7.36, see also Wild et al. [1999]), particularly if they have low slag and high gypsum contents. The porosity and pore size distribution measurements are made on cured specimens which have been dried at ambient temperature. Specimens containing gypsum will on drying therefore shrink much more than the gypsum free specimens which, depending on the degree of restraint, will produce a smaller total intruded pore volume. Conversely, the volume change on exposure to freeze-thaw is performed on saturated specimens, where one would expect (as observed) the ultimate volume change due to frost action to increase with increase in absorbed water (weight increase).

The reason for a lower ultimate volume change at the end of the freeze-thaw cycles exhibited by specimens which were prepared in the absence of gypsum is apparent from Figure 7.33a. Due to a higher initial pore volume their volume changes by up to 23% after frost action, whereas the presence of gypsum results in up to almost 40% ultimate volume change for the second set of specimens.

It may be suggested that although a higher pore volume allows easier water access during the thawing periods, there is also more pore space available to accommodate either growing ice crystals (when the pore area in question is close to the freezing front) or expelled water (as part of the hydraulic pressure if the pore space is ahead of the freezing front). Particularly well-cemented specimens with a strong soil skeleton could thus profit by a higher pore volume. However, as the specimens are in an almost fully saturated state there is not likely to be empty void space available to relieve the increase in hydraulic pressure during freezing.

No influence of the percentage of pore volume occupied by small pores (r≤0.05μm) on the frost resistance of stabilised specimens could be identified. However, there is a tendency for higher weight change to be observed with increase in the percentage of small pores from just over 20% to almost 60% if gypsum is present in the specimens.
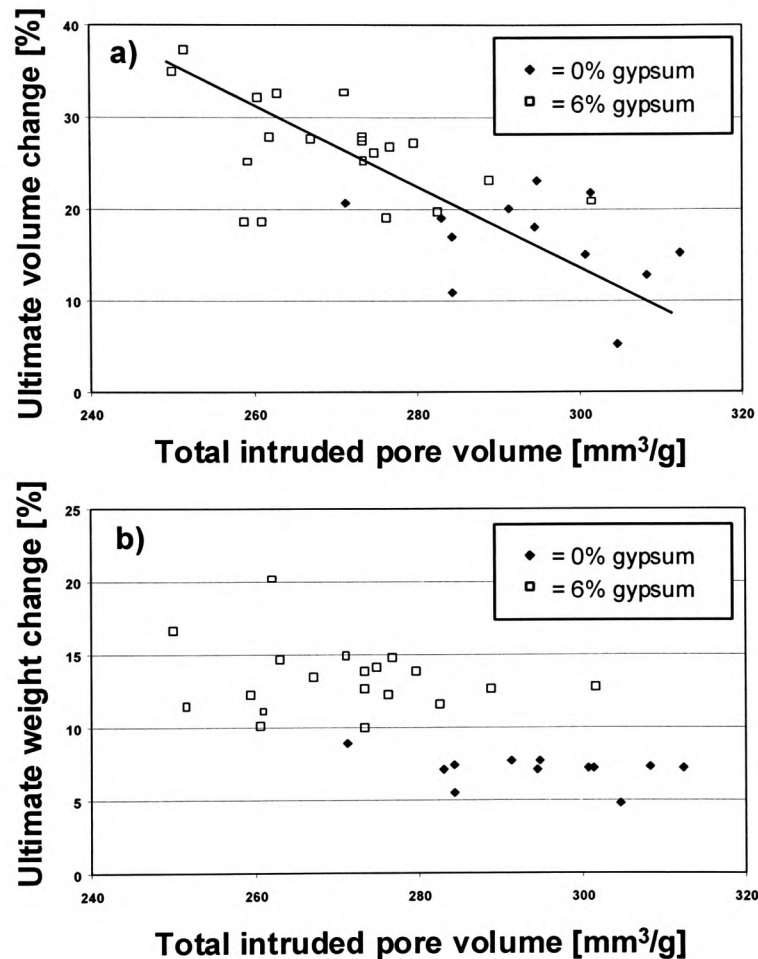
Figure 7.33 *Influence of the total intruded pore volume on ultimate volume change (a) and ultimate weight change (b) after 12 freeze-thaw cycles of kaolinite stabilised with various slag/lime ratios in the presence and absence of 6% gypsum*

The effect of permeability on the behaviour during frost action is illustrated in Figure 7.34. There appears to be a tendency for gypsum free specimens to exhibit lower ultimate volume change when the k-values are lower (Figure 7.34a). However, some of the gypsum containing specimens were found to have some of the lowest permeability coefficients, which could be due to the internally generated expansive products closing off capillary pores.

The weight change of kaolinite specimens with 6% gypsum seems to be reduced by lower k-values (Figure 7.34b). If the addition of gypsum is omitted, however, reduced permeability initiates only negligible weight changes. Independent of observed k-values these specimens exhibit comparably small weight gain of only between 5 and 10% at the end of freeze-thaw cycling.
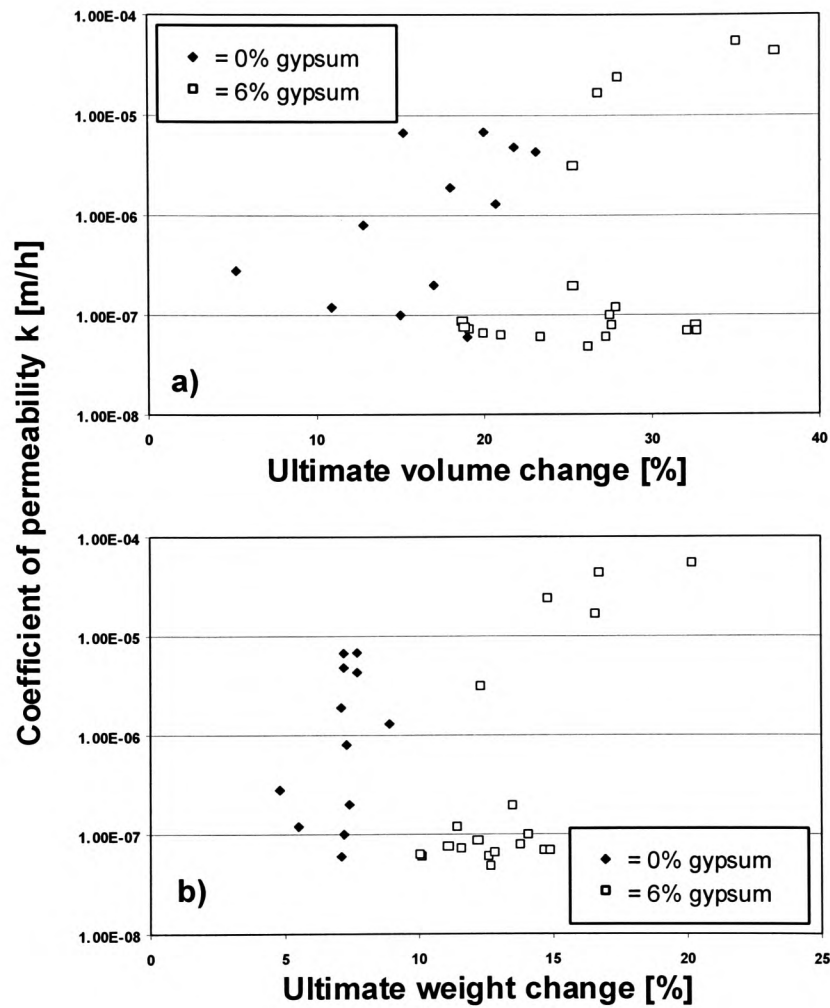
Figure 7.34 *Influence of coefficient of permeability k on the ultimate volume (a) and weight change (b) after 12 freeze-thaw cycles of kaolinite stabilised with various slag/lime ratios in the presence and absence of 6% gypsum*

7.2 Swelling and strength development of kaolinite with added gypsum stabilised with high slag/lime ratios

7.2.1 Linear expansion of sulphate-bearing kaolinite stabilised with high slag/lime ratios

In practice slag requires an activator to provide cementation. However, the expansion behaviour of sulphate-bearing kaolinite with slag as sole stabiliser and thus in the absence (or with insufficient levels) of lime as activator was considered to provide some insight into the slag hydration process and was thus investigated in more detail. It was soon discovered, however, that the original experimental set-up for linear expansion measurement, as introduced by Kinuthia [1997], had to be modified. The initial expansion magnitudes were found to be comparably small and thus even small effects, such as minimal loss of sample material at the exposed base after immersion in water, had to be counteracted. This was successfully achieved by non-confining 'encapsulation' of the sample base by a porous disc from underneath and a by a perspex ring with holes from the side, which allowed water to gain access but ensured that no material loss would occur. Figure 7.35 shows the comparison between expansion magnitudes obtained for kaolinite, stabilised with 0.5% lime and 5.5% ggbs before (a) and after (b) the introduction of modifications to the experimental set-up. In particular specimens to which larger percentages of gypsum had been added and which were thus more vulnerable to material loss due to increased flocculation, showed higher expansion magnitudes because material loss was completely avoided.

Generally a reduction in expansion upon soaking with increasing gypsum content could be observed. The highest swelling rates were observed within the first 30 days after soaking with approximately 80% of the ultimate swelling magnitudes reached after this period. The final expansion exhibited by the mix to which 2% gypsum had been added was 2.4% and it was 2.15%, 2.05% and 1.9% for the mixes with gypsum additions of 4, 6 and 8% respectively. The system stabilised after approximately 200 days, resulting in permanent expansion magnitudes. Although observations were continued up to 400 days, no delayed anomalous behaviour was recorded.

Changes in the slag/lime ratio from 11 (5.5% slag and 0.5% lime) to 5 (5% slag and 1% lime) result in modified expansion after soaking (Figure 7.36). In this case the highest expansion magnitude recorded after a total observation period of 540 days was exhibited by the mix 1L5S4G (2.6%), whereas the mix to which 8% gypsum had been added, showed the lowest swelling potential (1.3%). Similar to the mixes with a

slag/lime ratio of 11, expansion rates were the highest within the first month after soaking and dimensional stability was achieved after approximately one year.
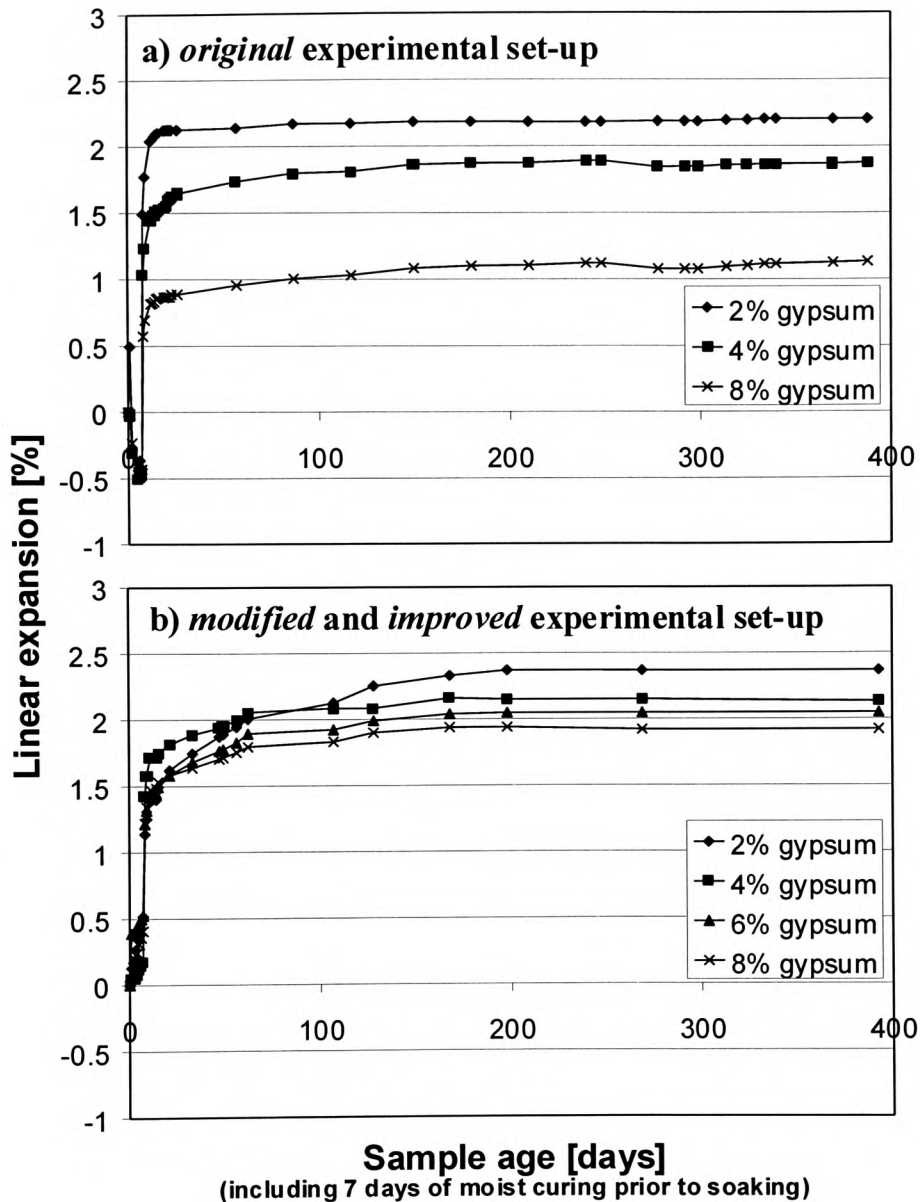
Figure 7.35 *Linear expansion of kaolinite samples stabilised with 0.5% lime and 5.5% ggbs in the presence of various gypsum additions after 7 days of moist curing at 30 °C and subsequent soaking.*
a) swelling magnitudes observed with original experimental set-up
b) swelling magnitudes observed with modified and improved experimental set-up
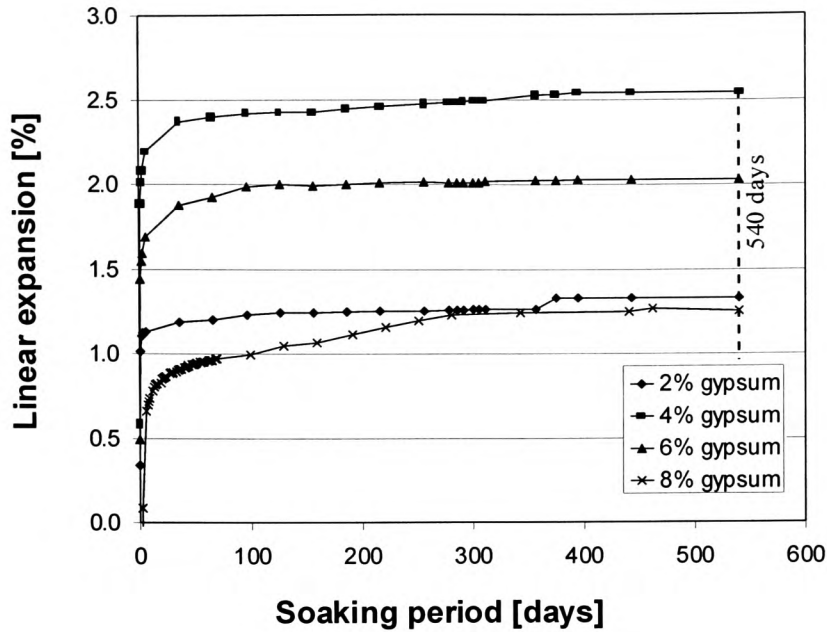
Figure 7.36 *Linear expansion upon soaking of kaolinite samples stabilised with 1% lime and 5% ggbs in the presence of various gypsum additions*

There is some indication that the magnitude of the ultimate expansion of specimens, when soaked after the initial 7-day moist curing period in the presence of high slag additions (5 and 5.5%), is mainly determined by the gypsum:lime ratio. Table 7.4 combines ultimate expansion magnitudes of specimens stabilised in the presence of 4% [Wild et al., 1999], 5% and 5.5% ggbs at various gypsum/lime (G:L) ratios.

Table 7.4 *Relationship between the gypsum:lime ratio (G:L) and the ultimate expansion [%] of lime-ggbs stabilised kaolinite after an initial 7-day moist curing period and subsequent soaking*

MIX 2L4S [after Wild et al., 1999]		MIX 1L5S		MIX 0.5L5.5S	
G:L ratio	Linear expansion [%]	G:L ratio	Linear expansion [%]	G:L ratio	Linear expansion [%]
1	0.5	2	1.3	4	2.4
2	2.1	4	2.6	8	2.2
3	2.5	6	1.9	12	2.05
4	5.0	8	1.25	16	1.9

Irrespective of specimen composition the highest expansion is recorded for specimens stabilised at a gypsum:lime ratio of 4. Higher or lower ratios result in lower percentage expansions.

7.2.2 Strength development of sulphate-bearing kaolinite stabilised with high slag-lime ratios

Figures 7.37a and c give an overview of the development of unconfined compressive strength of sulphate-bearing kaolinite specimens stabilised with slag/lime ratios of 11 and 5 after curing periods of 7, 28, 90 and 180 days at 30 °C. To identify the influence at the various curing ages of water saturation, an identical set of specimens was, at the end of the prescribed curing periods, soaked for 7 days at 30 °C and subsequently subjected to compressive strength testing. Figures 7.37b and d show the results obtained. An overall reduction in the exhibited strength values, for both slag/lime ratios and for all gypsum additions can be observed, when samples are immersed in water for 7 days prior to testing. This is particularly pronounced for shorter curing periods, i.e. 7 and 28 days. The variation in gypsum addition results in rather non-systematic strength variation over the various curing periods for both soaked and unsoaked specimens. However, highest strength values are exhibited by specimens with 6% gypsum for the 'soaked' system', whereas specimens with only 2% gypsum show the most superior strength development when soaking prior to testing is omitted. Little changes in compressive strength were obtained for curing periods beyond 90 days.
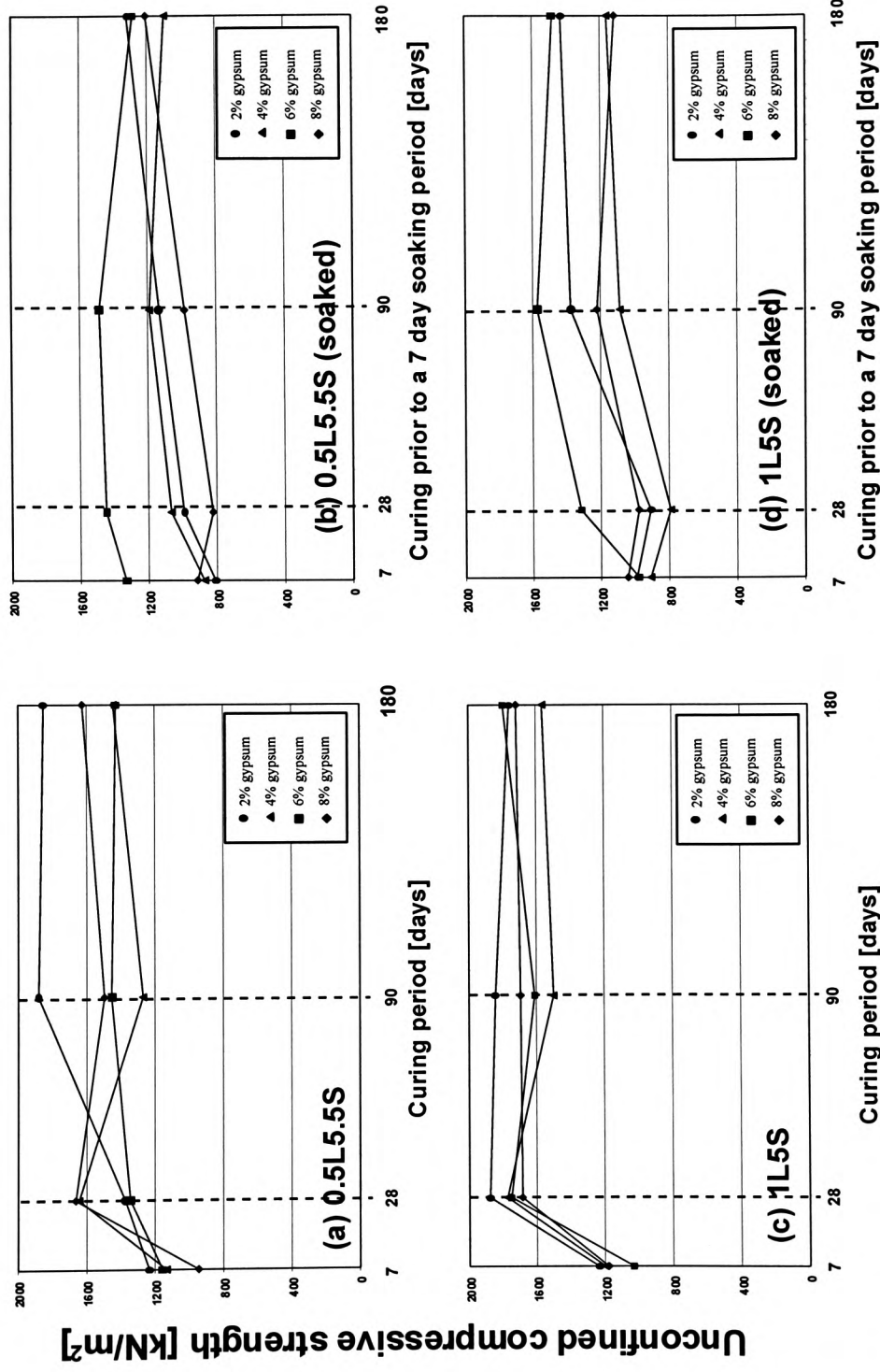
Figure 7.37 *Unconfined compressive strength of kaolinite stabilised with 0.5% lime and 1% lime and 5% ggbs (c+d) after moist curing (a+c) and moist curing followed by a 7 day soaking period (b+d) in the presence of 2, 4, 6 and 8% gypsum*

Gabriele Veith
University of Glamorgan

7.3 Slag-stabilised specimens in the presence of sulphates

Kinuthia [1997] observed that specimens stabilised with slag and gypsum alone (without lime), suddenly start to expand after several weeks of soaking. In order to investigate the influence of the gypsum content on this delayed expansion, samples with a slag content of 6%, containing 2, 4, 6 and 8 wt.% gypsum, were observed over several months.

On soaking, the specimens showed more or less instantaneous expansion ranging from 0.1 % for the 4 % gypsum sample to 7.3 % for the 6 % gypsum sample (Figure 7.38). The expansion values on soaking are the percentage expansions of the samples from the time at which their bases were immersed in water. All samples then exhibited delayed (=secondary) swelling. The sample with the highest sulphate content started its secondary swelling after 32 days (excluding the moist curing period of seven days). Up to that point the recorded expansion during soaking was only 2.1%. The ultimate expansion reached was 14.2 % at 142 days. The sample with only 6 % gypsum showed delayed secondary swelling after 51 days and reached a final swelling value of 18.1 %. The sample containing 4 wt.% gypsum did not start its delayed swelling until 111 days and its length increased eventually by 9.6 %. Finally, after 123 days, the sample containing only 2 % gypsum started its delayed expansion and exhibited an ultimate expansion of 10.5%. It should be noted that the gradients of the delayed expansion curves (①, ②, ③ and ④ in Figure 7.38) increase with increase in gypsum content, which is indicative of the rate of the chemical reaction occurring.

The pH of the soaking water for the sample 0L6S4G was monitored over 270 days. It commences at about 6, which might derive from traces of gypsum soluble in the water after soaking. After 41 days the pH rapidly rose to 9.0, increased even further and finally reached its peak after 70 days at 9.3. It then fell to a value of 8.2, which is the pH at which the sample started to expand after 111 days. No further significant change in pH occurred after the sample had stopped swelling. The change in pH does indicate that chemical changes are occurring with time. However, it is appreciated that the pH of the pore solution may be very different from that of the soaking water.

Prior to thermogravimetric testing, in order to determine the reaction products, the system was calibrated with a dry powder mixture of kaolinite, gypsum and ggbs of composition 0L6S6G. In comparison a test was run with the powder from the sample which had been dismantled just after swelling had commenced. The results of these
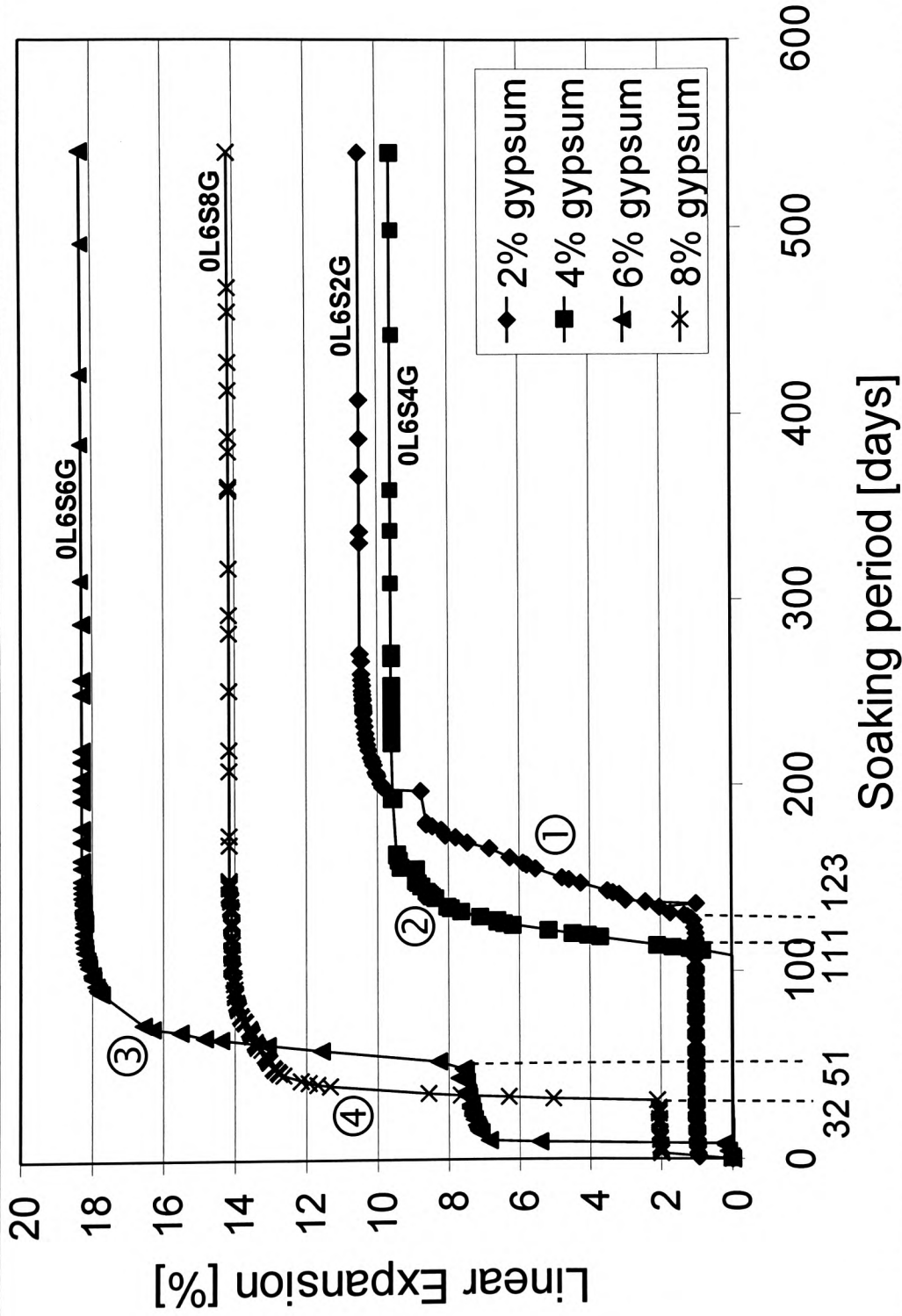
Figure 7.38 *Linear expansion of kaolinite stabilised with 6% ggbs and various amounts of gypsum after an initial 7-day moist curing period upon soaking*

Gabriele Veith
University of Glamorgan

tests are shown in Figure 7.39a+b. The results of the analysis of the powder (Figure 7.39a) show the characteristic double peak for gypsum at approximately 131 °C and 147 °C and the dehydroxylation of kaolinite at approximately 560 °C. Due to encapsulation of the sample in a sealed pan with a 75 μm pinhole in the aluminium lid, the dehydroxilation stages of gypsum can be resolved (see section 6.4.2). The improved resolution is the result of a retarded onset of the second dehydration phase (loss of 0.5 H_2O) which moves the peak to a higher temperature. The water vapour generated by the first water loss phase (1.5 H_2O) enriches the atmosphere and triggers the retardation [Dunn et al, 1987].

The observed weight losses of the powder mixture are in good agreement with those calculated based upon the known compositions of gypsum and kaolinite (Table 7.5). In comparison the weight loss trace for the reacted material (Figure 7.39b) shows significant new peaks at ~ 88 (①) and 118 °C (②), indicating ettringite decomposition (88 °C) and C-S-H gel dehydration (118 °C) [Wild et al., 1993]. The double peak at ~140/149 °C (③,④) is from the unreacted gypsum which was not completely consumed in the ettringite formation process.

Table 7.5 *Theoretical and observed weight losses for unreacted powder (0L6S6G) during TG analysis*

Mineral	observed weight loss [%]	calculated weight loss [%]
gypsum	1.16	1.12
kaolinite	10.45*	10.34

* observed during TG analysis of the mix beyond 600 °C

These analytical results were confirmed by SEM on specimens of composition 0L6S6G. Whereas the microstructure of the material did not show any unusual development after 1 day or at the end of the 7-day moist curing period (prior to soaking), the sample exhibited a significant amount of crystal growth after swelling had started (Figure 7.40). A similar crystal habit could be identified at the end of the soaking period (Figure 7.41). It is suggested that the crystals formed are well crystallised ettringite which correspond with the thermogravimetric observations. The rod-like needles appeared to radiate from localised regions, which were randomly distributed throughout the sample indicating a
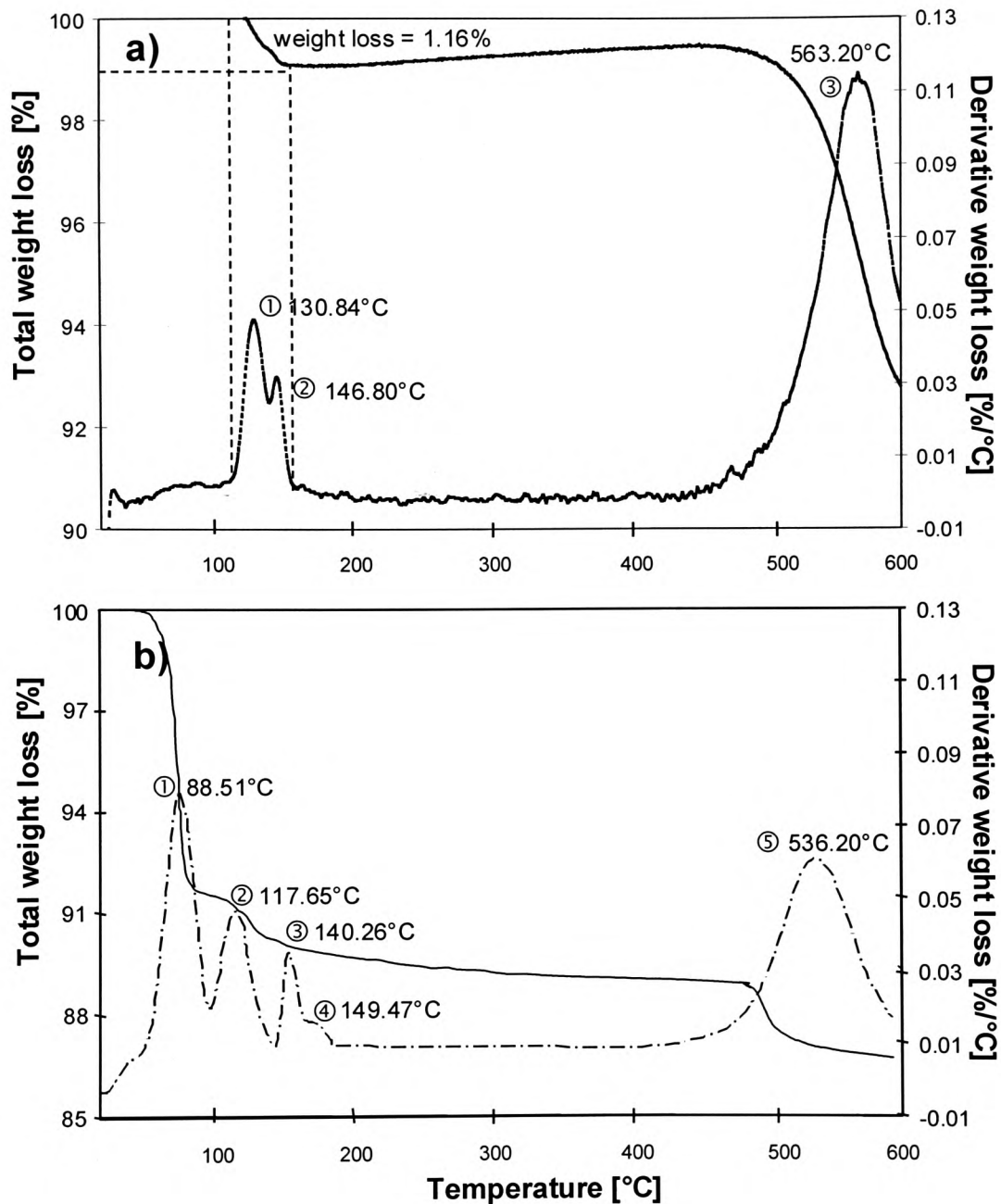
Figure 7.39 *TG analysis for a kaolinite specimen of mix composition 0L6S6G*

a) TG analysis of the dry powder mixture prior to water addition

b) TG analysis after delayed expansion had just started (51 days after soaking)

very focused source of the necessary components for crystal formation. The effects of slag as the sole stabilising agent with regard to strength was determined for the moist cured kaolinite specimens composed of composition 0L6S6G. They were subjected to unconfined compressive strength testing after curing periods of 7, 28, 90 and 180 days (Figure 7.42). The initially rather slow strength development (7 and 28 days) exhibited by the specimens during moist curing is followed by substantial strength gain at longer curing periods of 90 and 180 days. Reactions, which produce this enhanced rate of strength development appear to begin between 28 and 90 days. This is the period within which this specimen exhibits sudden secondary expansion during soaking (51 days). In order to gain further information with regard to the specific sample components, which contribute to crystal growth and strength development, a specimen consisting of 50% ggbs and 50% gypsum was prepared and soaked after a moist curing period of 7 days at 30 °C. After 20 weeks of soaking it exhibited only negligible expansion (0.88%). Subsequently the unconfined compressive strength of the sample was determined and found to be 7005 kN/m². Figure 7.43 shows an SEM micrograph taken from the dried and freshly broken surfaces of the specimen. As in the presence of clay, the 'flower bunch'-like ettringite habit could be clearly identified, confirming that the crystal formations are associated with the gypsum-slag combination and are independent of the presence of kaolnite. In order to further confirm the presence of the needle-shaped ettringite crystals, thermogravimetric analysis was carried out (unfortunately the TG analysis for this specimen was carried out before necessary recalibration of the TG analyser (see section 6.4.2) and the temperature values are enhanced by approximately 20 °C). The result can be seen in Figure 7.44. In addition to the gypsum peaks (③and ④), there is a substantial peak around 120 °C (①), which is characteristic of ettringite and a 'shoulder'(②, approximately 140 °C) which is identified as cementitious gel, probably C-S-H gel. Particularly the latter would account for the substantial strength, which was exhibited by the specimen.
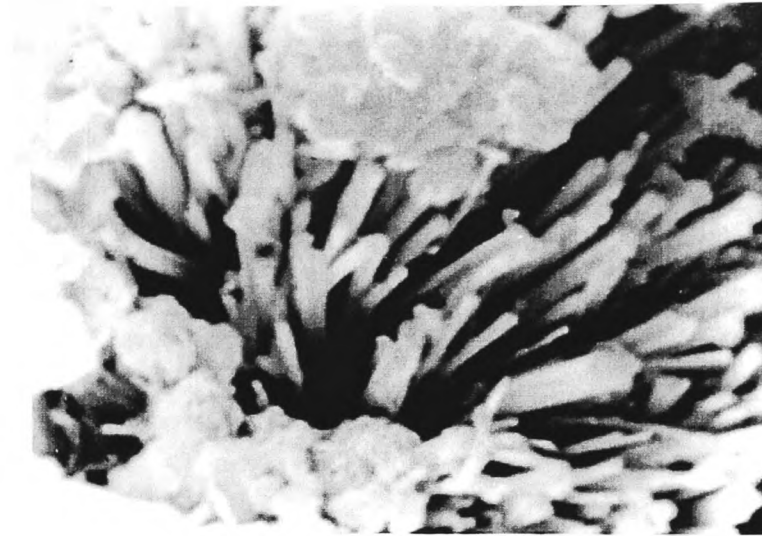
Figure 7.40 *Expansive crystals on a sample 0L6S6G after swelling had just started (x3400)*
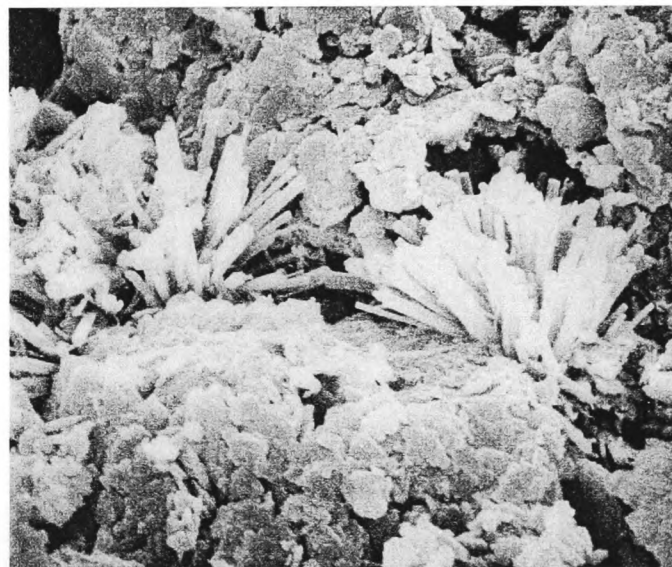
Figure 7.41 *Expansive crystals on a sample 0L6S6G at the end of the soaking period (x3000)*
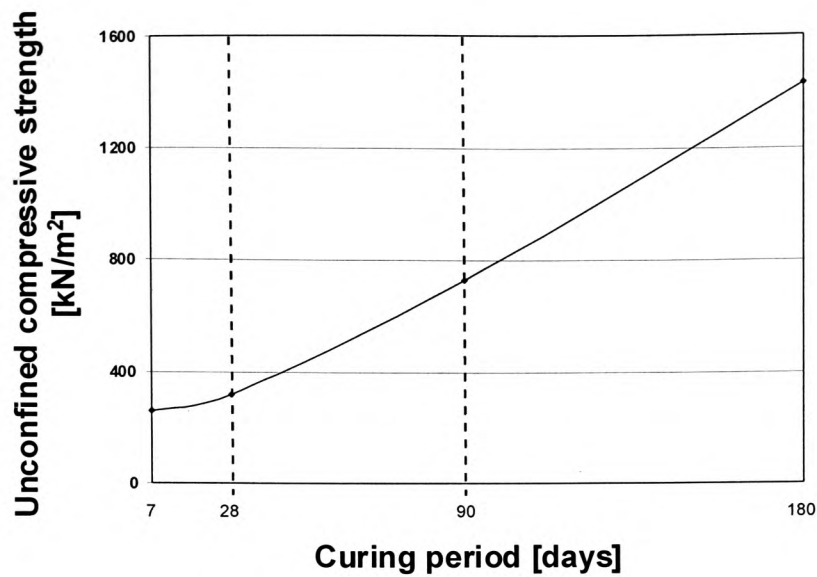
Figure 7.42 *Unconfined compressive strength of kaolinite stabilised with 6% ggbs in the presence of 6% gypsum (0L6S6G) after moist curing periods of 7, 28, 90 and 180 days*

Figure 7.43 *Expansive crystals on a sample consisting of 50% ggbs and 50% gypsum after 7 days of moist curing at 30 °C and subsequent soaking for 20 weeks (x2000)*
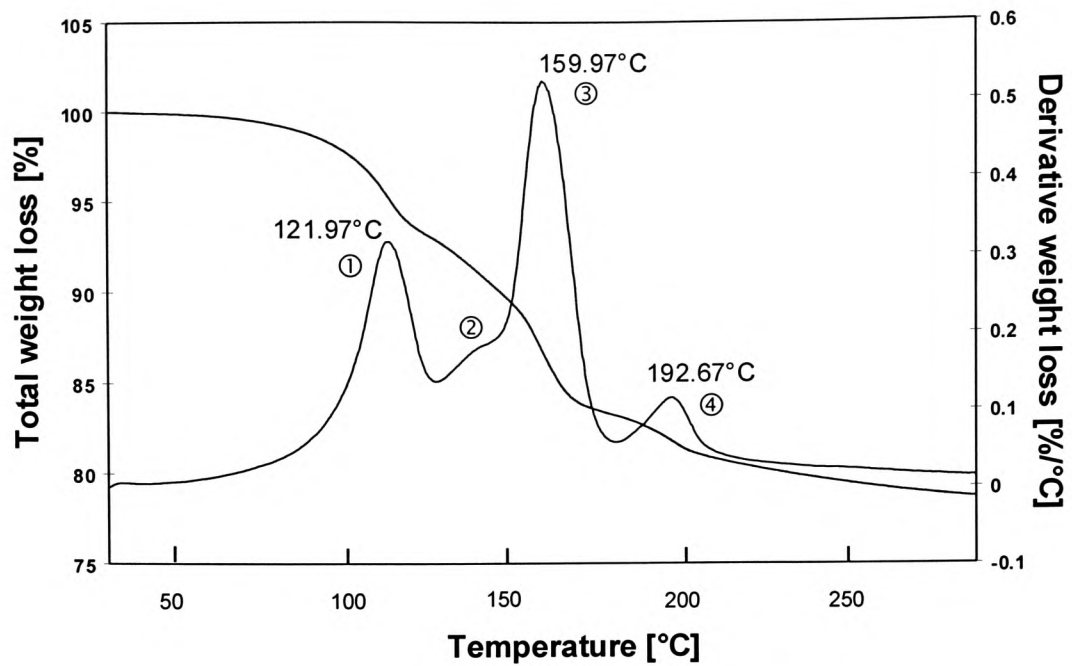
Figure 7.44 *Thermogravimetric analysis of specimens made of 50%ggbs and 50%gypsum after 7 days of moist curing at 30 ℃ and subsequent soaking for 20 weeks*

7.4 Lower Oxford Clay

Investigations into this natural clay with its high pyrite content (sulphide) were of interest because it is not well understood, how the addition of lime-activated ggbs will affect the sulphide oxidation, which in turn will have an effect on the engineering properties of the stabilised clay. It should be noted that the grain size range of Lower Oxford Clay is much wider than that of kaolinite. However, with regard to application of findings, in practice Lower Oxford Clay represents a typical in-situ natural material for soil stabilisation.

Although precautions were taken to ensure that the Lower Oxford Clay was homogenised, expansion tests (Figure 7.45) revealed that some specimens behaved non typically when subjected to water after a 7 day moist curing period. For example, the slow but gradual expansion of the specimen stabilised with 2% lime and
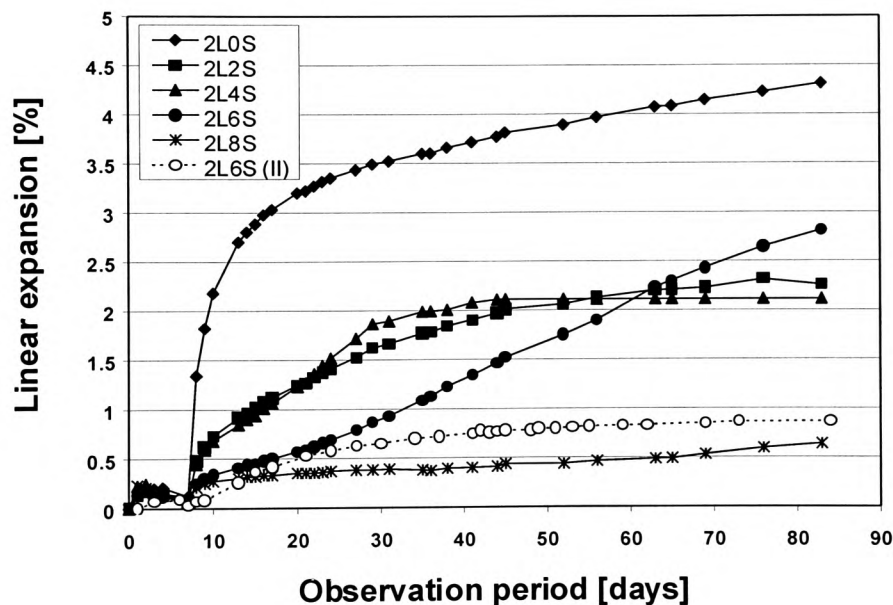
Figure 7.45 *Linear expansion of Lower Oxford Clay stabilised with various slag/lime ratios versus initial 7 days of moist curing and subsequent soaking*

6% ggbs (2L6S) was attributed to a higher concentration of sulphides in this particular sample, resulting in an ongoing sulphate source as oxidation continued. This in turn led to the observed expansion gradient which is illustrated in Figure 7.45. To confirm this hypothesis another specimen of the same mix composition was prepared (dotted

line, 2L6S(II)) which exhibited an expected typical expansion profile, confirming the overall finding that an increase in the slag/lime ratio results in a reduction in the linear expansion magnitude after soaking.

However, this example shows that results from specimens made of natural clay have to be assessed with far more caution than the findings obtained from ideal laboratory clays such as kaolinite. This localised variability deriving from the Lower Oxford Clay's natural origin was subsequently taken into account when assessing and interpreting the results presented on the following pages.

7.4.1 Strength development

7.4.1.1 Shear strength development

Figure 7.46 shows the shear strength development τ_u of specimens made of Lower Oxford Clay stabilised with 2% lime and 0, 2, 4, 6 and 8% ggbs after curing periods of 1, 4, 12, 24 and 52 weeks at 10, 20 and 30 °C. The values were calculated from the measured undrained, unconsolidated shear strength parameters (Table 7.6) based on a normal stress $\sigma_n = 1000$ kN/m^2.

There is an overall increase in shear strength with increase in ggbs addition and curing period, similar to that observed for the kaolnite-lime-slag specimens with 6% gypsum (Figure 7.2). Clay to which only 2% lime as stabiliser has been added, shows only marginal shear strength improvement with increase in curing temperature for all curing periods. This is particularly the case if curing is at 10 °C, where prolonged curing time has a negligible effect on the shear strength of the mix 2L0S. However, when slag is added, temperature has a significant influence on the strength development. The effect of temperature is far more pronounced for shorter curing periods. After curing for 1 week, specimens of composition 2L8S cured at 20 and 30 °C exhibit approximately 90% higher strength relative to the same specimen cured at 10 °C. If the strength values for a curing period of 1 year are compared, the effect of temperature is reflected by a mere 8% difference in strength development, with in fact the specimens cured at 20 °C exhibiting strength values exceeding those of samples cured at 10 or 30 °C. This is also reflected in the development of the shear strength ratio (based on σ_n=1000 kN/m^2) for curing at 30 °C (τ_{30}) in comparison to a curing
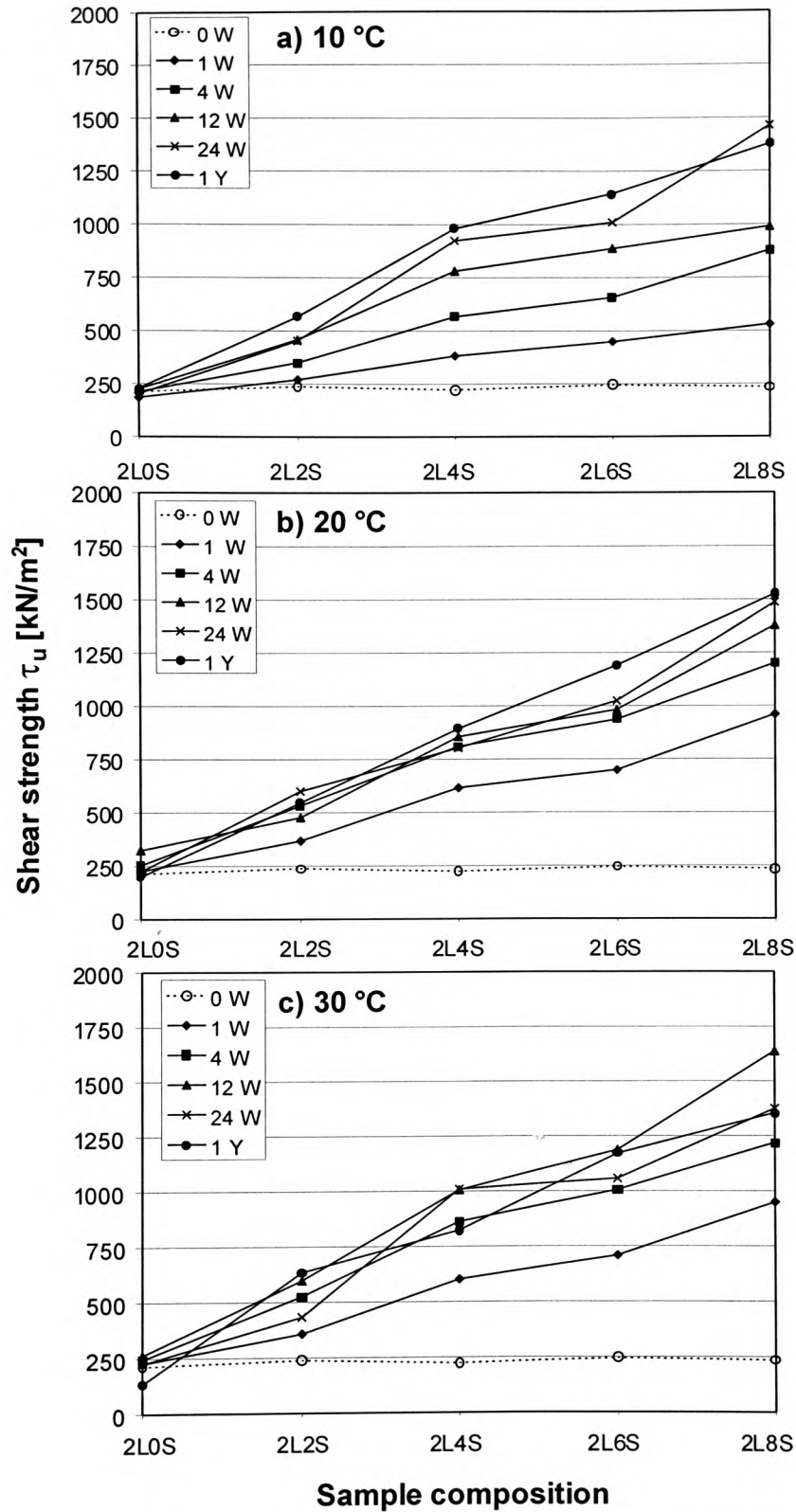
Figure 7.46 *Shear strength τ_u development (normal stress σ_n=1000 kN/m²) of Lower Oxford Clay stabilised with 2% lime and 0, 2, 4 6 and 8% ggbs after curing periods of 1, 4, 12, 24 weeks and 1 year at a) 10 °C, b) 20 °C and c) 30 °C*

temperature of 10 °C (τ_{10}) (Figure 7.47). A ratio of close to 1 ($\tau_{30}=\tau_{10}$) is obtained for specimens to which ggbs has been added after curing for 24 weeks or 1 year, whereas specimens of the same mix composition exhibit the highest ratios when cured for short periods. If lime is added as the sole stabiliser (2L0S), the shear strength ratio τ_{30}/τ_{10} is only reduced marginally if curing is prolonged (other than the result for 1 year which appears anomalous). This reflects the very low level of cementation in these specimens such that curing temperature is of little relevance. Thus the overall strength development as illustrated in Figure 7.46 has to be considered to allow an overall assessment of the stabiliser performance.
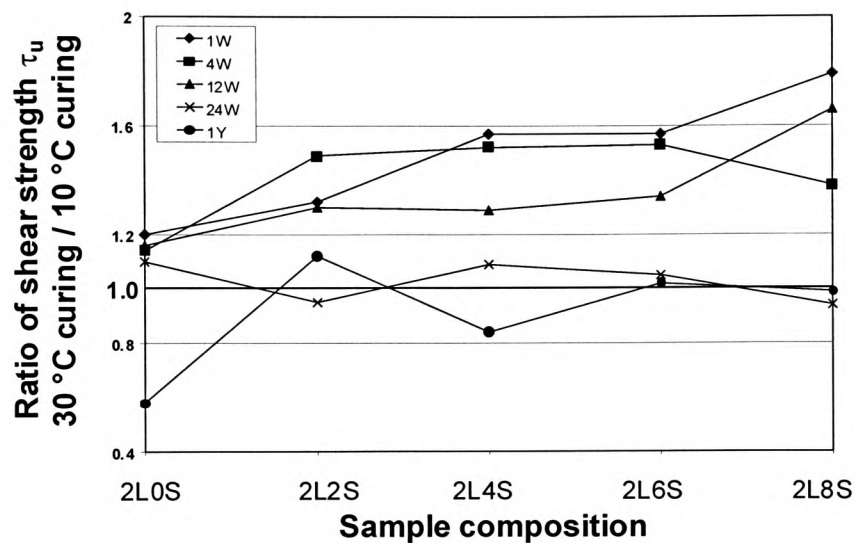
Figure 7.47 *Ratio of shear strength τ_u (based on $\sigma_n=1000$ kN/m^2) of Lower Oxford Clay (stabilised with 2% lime and 0, 2, 4, 6 and 8% ggbs after various curing periods) for curing temperatures 30 °C / 10 °C*

The increased rate of cementation with increase in curing temperature and slag content, which is apparent both for the kaolinite-gypsum samples (Figure 7.2) and the Lower Oxford Clay samples (Figure 7.46) but not for the gypsum free kaolinite specimens (Figure 7.5) indicates that sulphate plays a major role in activation of slag hydration and that this is strongly influenced by temperature.

In comparison to τ_u-values obtained for kaolinite-gypsum, Lower Oxford Clay yields an overall higher strength when stabilised with the same amount of lime and slag and cured for the same period in an identical curing environment. Lower Oxford Clay also

appears to stimulate more rapid cementation (and hence slag hydration) in comparison to kaolinite-gypsum. For longer curing periods the shear strength values obtained from stabilised Lower Oxford Clay cured at the lower curing temperatures are similar to those obtained from stabilised kaolinite specimens which had been cured at the more elevated temperatures.

Table 7.6 *Apparent shear strength parameters cohesion c_u [kN/m²] and angle of internal friction ϕ_u [°] of Lower Oxford Clay stabilised with 2% lime and 0, 2, 4 6 and 8% after curing periods of 1, 4, 12, 24 weeks and 1 year at 10, 20 and 30 °C*

Curing time	Sample composition	Curing temperature 10 °C		Curing temperature 20 °C		Curing temperature 30 °C	
		c_u [kN/m²]	ϕ_u [°]	c_u [kN/m²]	ϕ_u [°]	c_u [kN/m²]	ϕ_u [°]
1 week	2L0S	150	2.0	190	2.0	190	2.0
	2L2S	235	2.0	261	6.0	251	6.0
	2L4S	330	3.0	437	10.2	422	10.2
	2L6S	361	5.0	481	12.3	510	11.2
	2L8S	442	5.0	702	14.4	692	14.4
4 weeks	2L0S	195	1.0	200	3.0	190	3.0
	2L2S	315	2.0	481	3.0	437	5.0
	2L4S	443	7.1	612	11.2	518	19.0
	2L6S	496	9.1	637	16.7	727	15.5
	2L8S	557	17.8	856	19.0	852	20.1
12 weeks	2L0S	190	2.0	270	3.0	101	9.1
	2L2S	352	6.0	353	7.1	360	13.3
	2L4S	503	15.5	599	14.4	788	12.3
	2L6S	630	14.4	662	17.8	718	25.1
	2L8S	645	19.0	626	36.9	1139	26.4
24 weeks	2L0S	150	3.0	170	3.0	101	7.1
	2L2S	401	3.0	234	20.1	215	12.3
	2L4S	706	12.3	437	20.1	710	16.7
	2L6S	568	23.8	633	21.3	735	17.8
	2L8S	994	25.1	928	29.2	848	27.8
1 year	2L0S	141	5.0	110	5.0	80	3.0
	2L2S	386	10.2	404	8.1	266	20.1
	2L4S	723	14.4	550	19.0	353	25.1
	2L6S	648	26.4	846	19.0	505	33.7
	2L8S	626	36.9	1027	26.4	726	32.1

The higher shear strength values for Lower Oxford Clay relative to stabilised kaolinite (Figure 7.2) derive mainly from the higher values of apparent, undrained cohesion which specimens exhibit if cured at elevated temperatures (20 and 30 °C) and stabilised with larger slag/lime ratios (Table 7.6). However, curing at 10 °C results in larger c_u values for kaolinitic samples in the presence of 6% gypsum (see Table 7.3). It is quite likely that the conversion from sulphides to sulphates, which could co-activate the added ggbs, is promoted at higher temperatures and thus a substantial activation contribution cannot be made if Lower Oxford Clay is only cured for a short period at low temperatures prior to shear strength testing. Longer curing periods at elevated temperatures, however, allow substantial amounts of sulphides to be converted and thus larger amounts of sulphates are available to co-activate the slag additions. The values of the apparent angle of internal friction are overall lower for stabilised Lower Oxford Clay (Table 7.6) than for kaolinite (Table 7.1). Particularly if lime is added as the sole stabiliser the values tend to be very low (between 2 and 5 °).

In common with stabilised kaolinite-gypsum samples (Figure 7.3) cumulative strain values at failure for stabilised Lower Oxford Clay (Figure 7.48) decrease both with increase in curing temperature and increase in slag content. However, the changes for Lower Oxford Clay are much more systematic and show much less variability than for kaolinite which possibly reflects the much lower clay content of the former.

Overall (relative to kaolinite, Figure 7.3) a higher degree of brittleness is apparent in Lower Oxford Clay specimens to which lime-activated ggbs has been added, evident from the large percentage of specimens which fail at strain values of around 10% and less (even if curing is only at 10 °C). If curing is at 30 °C no further reduction in strain at failure is obtained beyond a slag addition of 4% (2L4S). Only a few specimens to which lime as the sole stabiliser had been added and which had been cured for short periods at 10 °C, exhibited failure due to barrelling and deformation. Thus the predominant failure mode was by exhibiting the classic shear failure plane. Figure 7.49 shows a selection of failed specimens, which had been cured for 1 year at 30 °C prior to shear testing. As can be seen, no signs of deformation prior to failure are visible, due to the high brittleness of the well-cemented specimens.
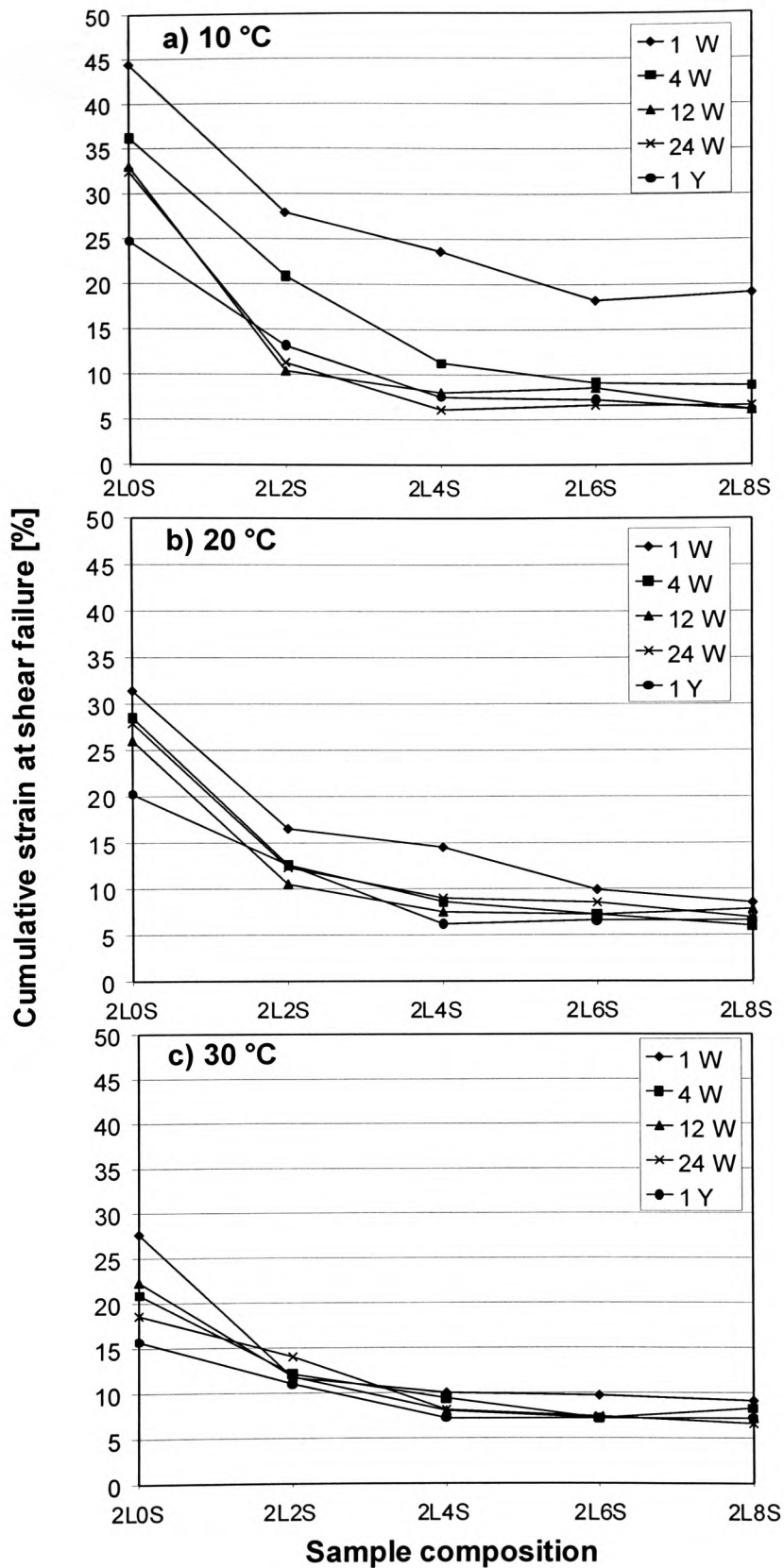
Figure 7.48 *Cumulative strain at shear failure of Lower Oxford Clay stabilised with 2% lime and 0, 2, 4 6 and 8% ggbs after curing periods of 1, 4, 12, 24 weeks and 1 year at a) 10 °C, b) 20 °C and c) 30 °C*

Figure 7.49 *Failed specimens exhibiting shear failure plane after a curing period of 1 year at 30 °C*

7.4.1.2 Unconfined compressive strength

Figure 7.50 illustrates the development of unconfined compressive strength of stabilised Lower Oxford Clay cured for 1, 4, 12 and 24 weeks at 30 °C prior to testing. Similar to results obtained from triaxial testing, the specimens stabilised with lime only (2L0S) show little strength improvement with increase in curing period. However, when slag is added the gain in strength is substantial, particularly for high slag contents, and the major part of the strength gain has in fact taken place within the first seven days. The effect of enhanced curing periods is more pronounced for specimens with ggbs additions of 4% and beyond. Particularly if curing is for 24 weeks the exhibited strength increases substantially with increasing ggbs addition. The additional curing time required to activate this additional strength potential could be indicative of further chemical transformations (oxidation of pyrites) which result in a higher sulphate level. Slag, which is available in abundance can then be more effectively activated and the observed strength development is the logical consequence. This dormant strength potential as a result of insufficiently activated ggsb results in an overall strength increase of 500% in comparison to stabilisation with lime alone (2L0S) after 24 weeks of curing. It could possibly be utilised at an earlier stage by ensuring that sulphide conversion is initiated prior to slag addition.
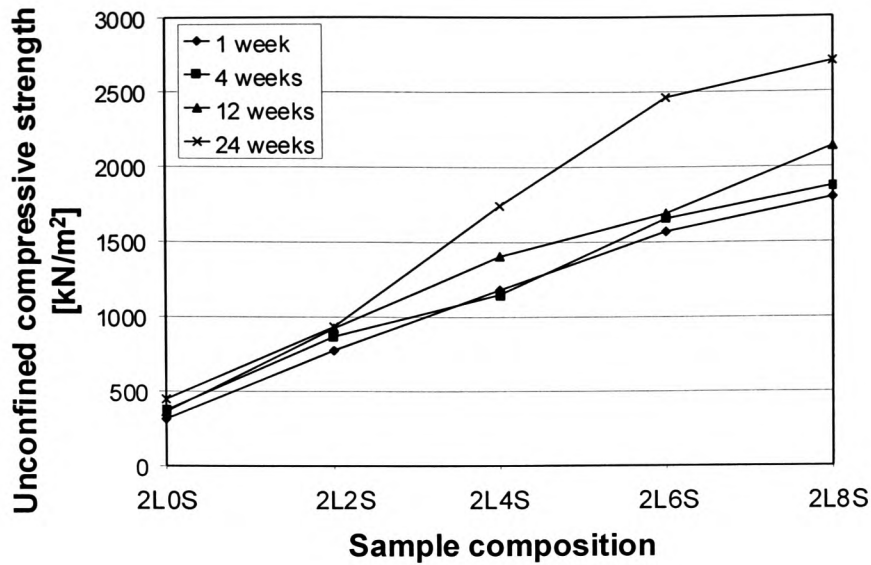
Figure 7.50 *Unconfined compressive strength of lime-slag-stabilised Lower Oxford Clay cured for 1, 4, 12 and 24 weeks at 30 ℃*

The influence of sulphates is very clearly illustrated in Figure 7.7 and 7.9 for stabilised kaolinite. The gradients of the compressive and indirect tensile strength versus slag content curves increase systematically with increase in gypsum content. There are clear similarities between Figure 7.7d (up to 12 weeks only) and Figure 7.50. It must, however, be emphasised that in the former all the sulphate is available at the onset of stabilisation, whereas in the latter the amount of available sulphate increases with time [Wild et al., 1999b]. Whether this process occurs in a saturated or in a moist environment may however be critical with regard to volume stability.

7.4.1.3 Indirect tensile strength

To assess the influence of sulphate on the indirect tensile strength of stabilised Lower Oxford Clay, the results are compared with the results obtained for kaolinite with 6% gypsum addition (Figure 7.51). The strength of sulphate-bearing kaolinite increases more rapidly than that of Lower Oxford Clay, particularly in the early stages of curing. Thus it requires larger ggbs additions (around 3%) to increase tensile strength in comparison to lime stabilisation alone. Even at higher percentages of slag addition,

the gradient is not as steep as in the case of kaolinite in the presence of 6% gypsum. However, longer curing periods result in higher values for R_{it} and it appears that, similar to the trend observed for UCS results, longer curing periods allow the activation of larger percentages of ggbs.
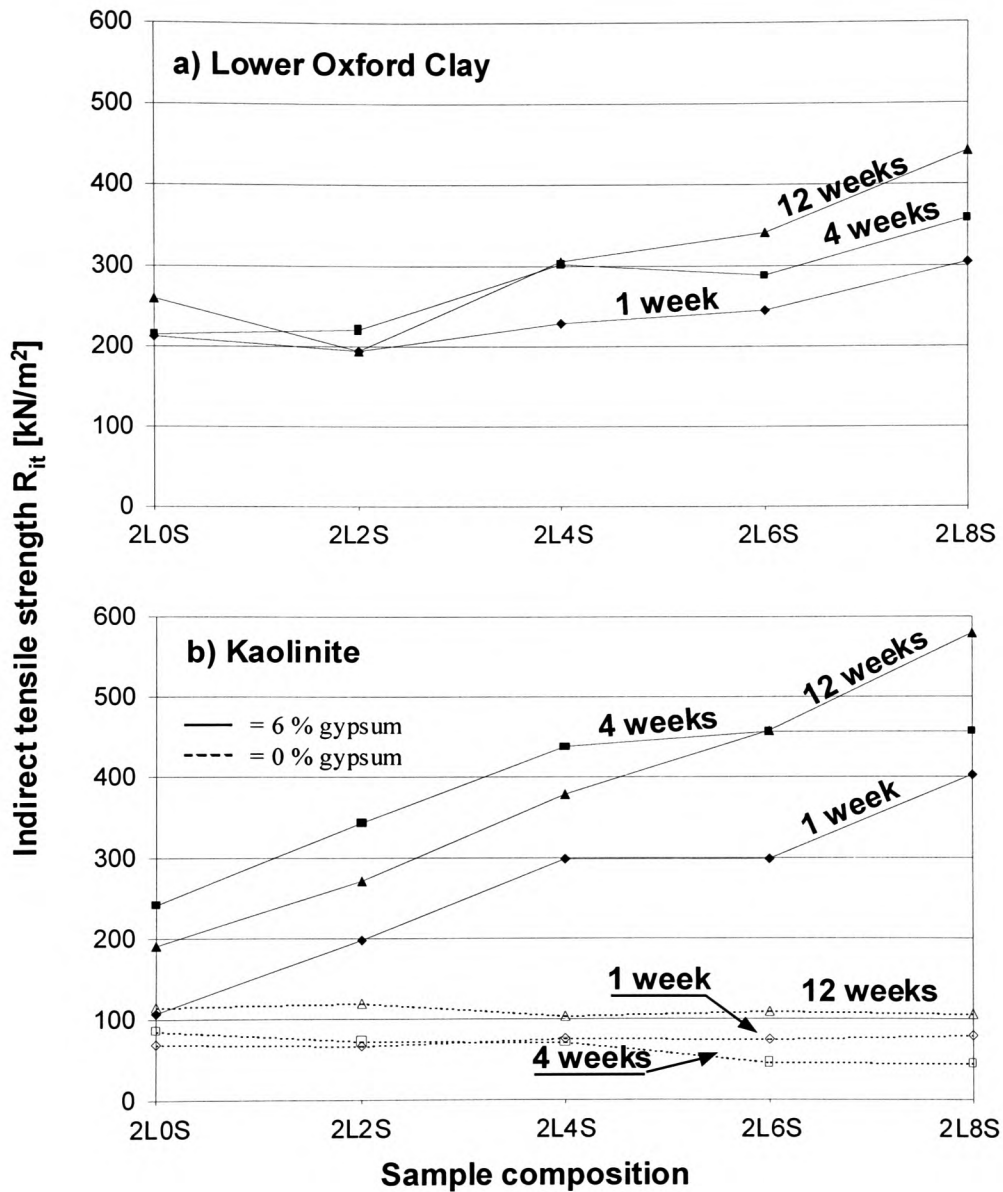
Figure 7.51 *Indirect tensile strength of lime-ggbs-stabilised Lower Oxford Clay and kaolinite (with and without 6% gypsum addition) after curing periods of 1, 4 and 12 weeks at 30 °C*

7.4.2 Porosity and pore size distribution of stabilised Lower Oxford Clay

The results of MIP show, with regard to the total intruded pore volume (Figure 7.52), a very different picture in comparison to trends obtained from investigations into stabilised kaolinite (Figures 7.14 and 7.15). For Lower Oxford Clay the introduction of ggbs in addition to 2% lime results in a marked increase in the intruded pore volume, with the increase being slightly more pronounced if curing is at elevated temperatures. It should be noted that even specimens which had been tested immediately after compaction (dotted lines) exhibit this trend, which suggests that the trend derives from the physical characteristics of the components. However, curing does tend to reinforce this development. The sole addition of lime results in a marginal increase in pore volume which is slightly enhanced for specimens cured at 30 °C. An influence of curing temperature is hard to identify which is probably because the effect is mainly due to the wide grain size distribution of the natural clay.

The observed increase on total pore volume is accompanied by relatively small differences in the percentage of larger pores ($r > 0.1$ μm) with respect to uncured material and an increase in smaller pore fractions (Figure 7.53). Most affected by the addition of ggbs is the pore fraction with a diameter of ≤ 0.05 μm with an increase of between 8 and 10% when 8% of slag is added to a specimen initially modified with 2% lime. More pronounced pore refinement is achieved at higher curing temperatures. Also the smallest pore fraction ($r \leq 0.02$ μm) increases by about 5% with little indication that temperature has a large influence.

In comparison to values obtained for stabilised kaolinite-6% gypsum (Figure 7.14) it is somewhat surprising to see that the generally 'coarser' Lower Oxford Clay exhibits overall a much higher percentage of the smaller pores (approximately 20-25% of pores with a radius ≤ 0.02 μm whereas values for kaolinite are around 5-10%). The percentage of pores of radius ≤ 0.05 μm (typical gel-size) is also significantly higher for Lower Oxford Clay, particularly for compositions with low slag content. However, a slag addition of 8% to kaolinite specimens results in similar percentage values with regard to this pore fraction ($r \leq 0.05$ μm) as exhibited by specimens made of Lower Oxford Clay. This may be a function of a lower clay content reducing the influence of flocculation combined with a wider grain size distribution and more effective packing.
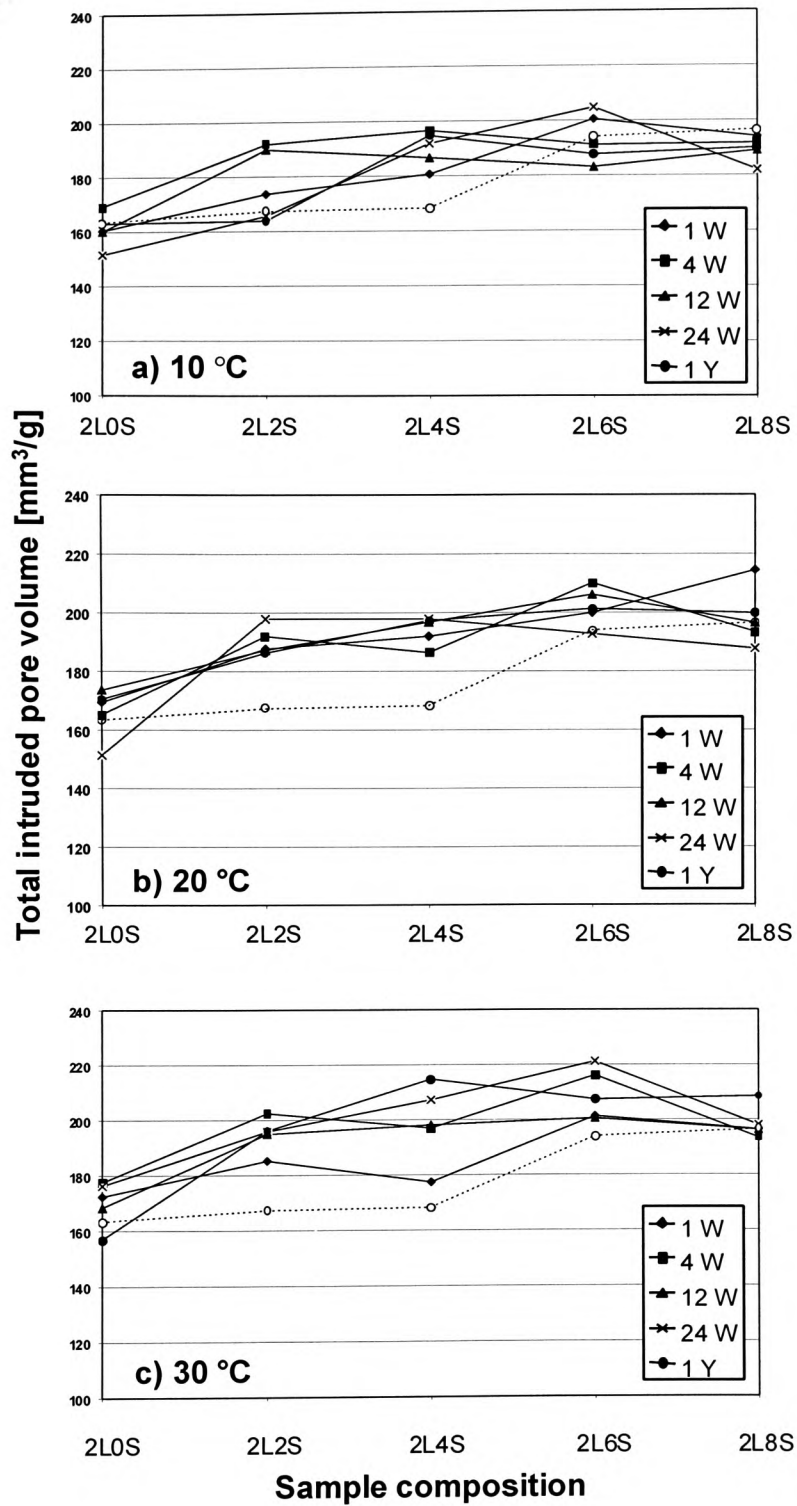
Figure 7.52 *Total intruded pore volume [mm^3/g] of Lower Oxford Clay stabilised with various slag/lime ratios after curing for 1, 4, 12, 24 and 52 weeks (dotted line indicates results of specimens tested immediately after compaction) at a) 10 °C, b) 20 °C and c) 30 °C*
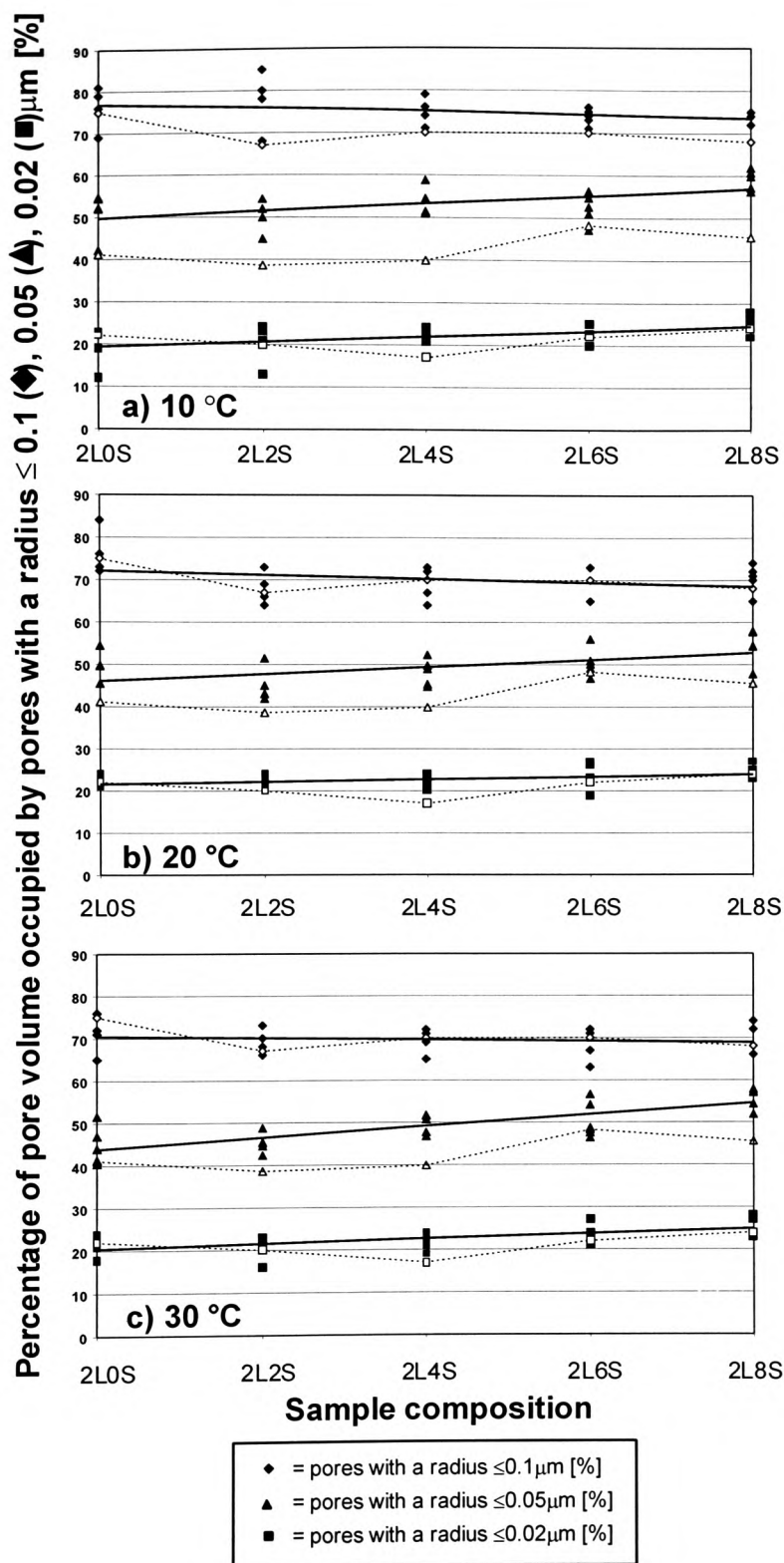
Figure 7.53 *Influence of curing temperature and sample composition on pore size distribution (r ≤0.1 μm, 0.05 μm and 0.02 μm) of Lower Oxford Clay stabilised with various slag/lime ratios after curing periods of 1, 4, 12, 24 and 52 weeks (dotted line indicates results of specimens tested immediately after compaction)*

7.4.3 Pore structure and its influence on strength of stabilised Lower Oxford Clay

It is appreciated that care must be taken when engineering properties are related to the results of mercury intrusion porosimetry. However, there is general agreement that the compressive strength of cementitious materials is related to porosity and pore size distribution [Marsh and Day, 1985, Kendall et al., 1983] in such a way that lower porosity and a higher degree of pore refinement results in better strength development.

With regard to possible relationships between strength development and pore structure, the data were processed in a similar manner to those for stabilised kaolinite (see Figures 7.22 and 7.23) and subsequently Figure 7.54 was compiled. As indicated previously, the threshold radius (see Figure 6.12) is a form of measurement of the pore connectivity but can also be utilised to get some indication of the pore refinement within a sample. Figure 7.54a shows that when the measured shear strength results (based on a normal stress of σ_n=1000kN/m^2) are analysed with regard to the change in threshold radius, specimens exhibiting the highest strength were those exhibiting a low threshold radius (r$\approx$0.1µm) and no specimens showing a high threshold radius exhibited high strength. It should be noted that Wild et al. [1987] identified this to be the upper value for the radius of cementitious gels, which has a pore size range of between 1 and 100 nm (=0.001-0.1 µm). Figure 7.54b gives the relationship between shear strength and the percentage of pores with a radius r$\leq$0.05 µm. Specimens with the highest strength all show pore refinement and no specimens with the coarser pore structure show enhanced strength. As with kaolinite (Figures 7.22c and 7.23c) there does not appear to be any significant relationship between shear strength and total porosity.

It is appreciated that there is a very wide scatter of data, however, the investigations were carried out on a heterogeneous, natural clay with a comparably wide grain size distribution, whereas the kaolinite samples are generally much more homogeneous and contain no coarse particles. It is suggested that it is the presence of these coarse particles which causes some of the stabilised Lower Oxford Clay specimens with a high percentage of fine porosity to fail at relatively low shear strength values.
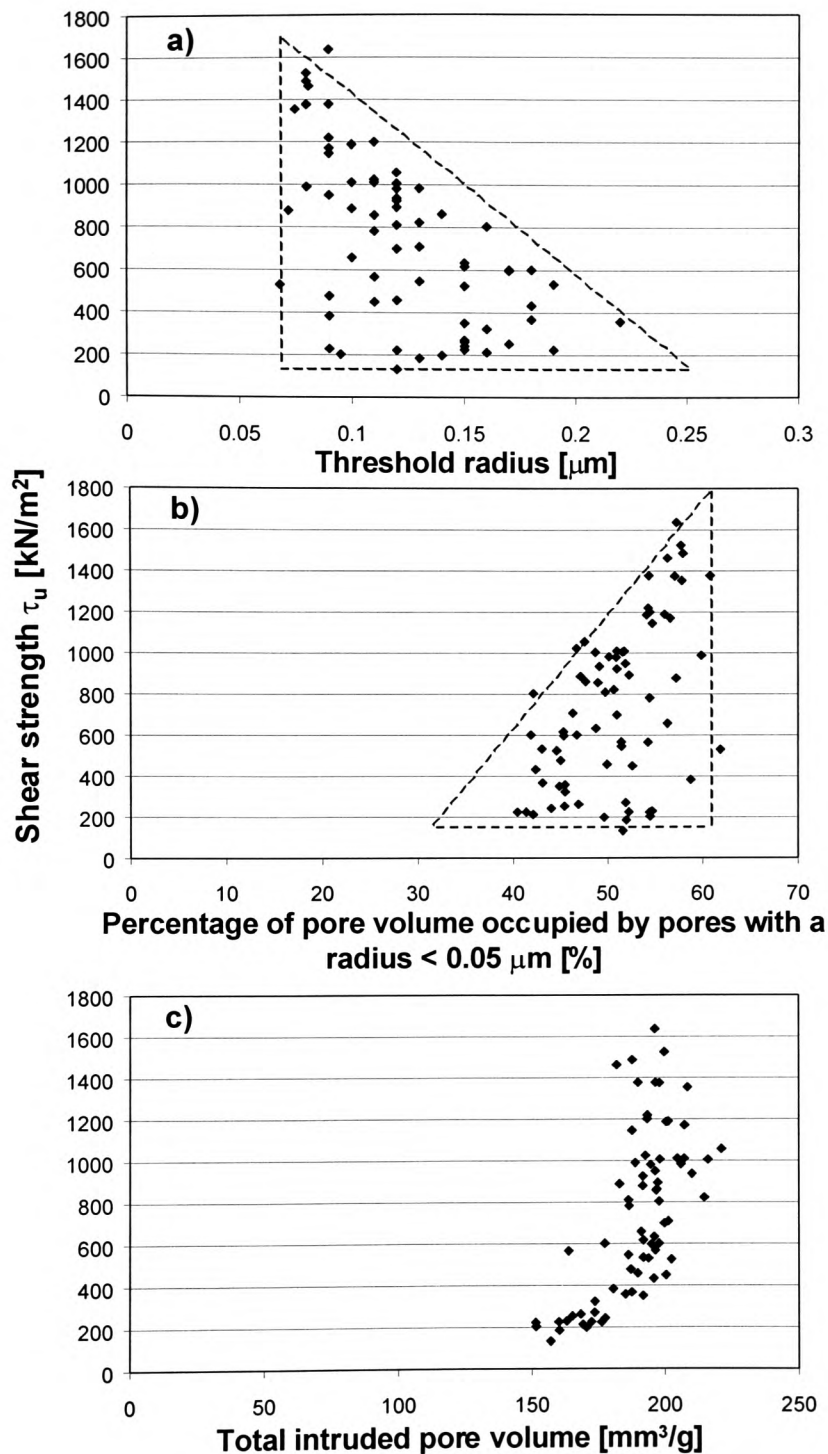
Figure 7.54 *Relationship between shear strength τ_u (σ_n=1000 kN/m^2) and a) threshold radius, b) percentage of pore volume occupied by pores with a radius <0.05 μm and c) total intruded pore volume of Lower Oxford Clay-lime-ggbs mixes cured for up to 1 year at 10, 20 and 30 °C*

Comparison of the relationship between indirect tensile strength (and unconfined compressive strength development) and the percentage of fine pores, for stabilised Lower Oxford Clay (Figure 7.55) and for stabilised kaolinite (Figures 7.24 and 7.25) reveal similar correlations. However, UCS and IT data are only available for curing at 30 °C. The R^2-value for compressive strength is 0.65 and for indirect tensile strength 0.87.
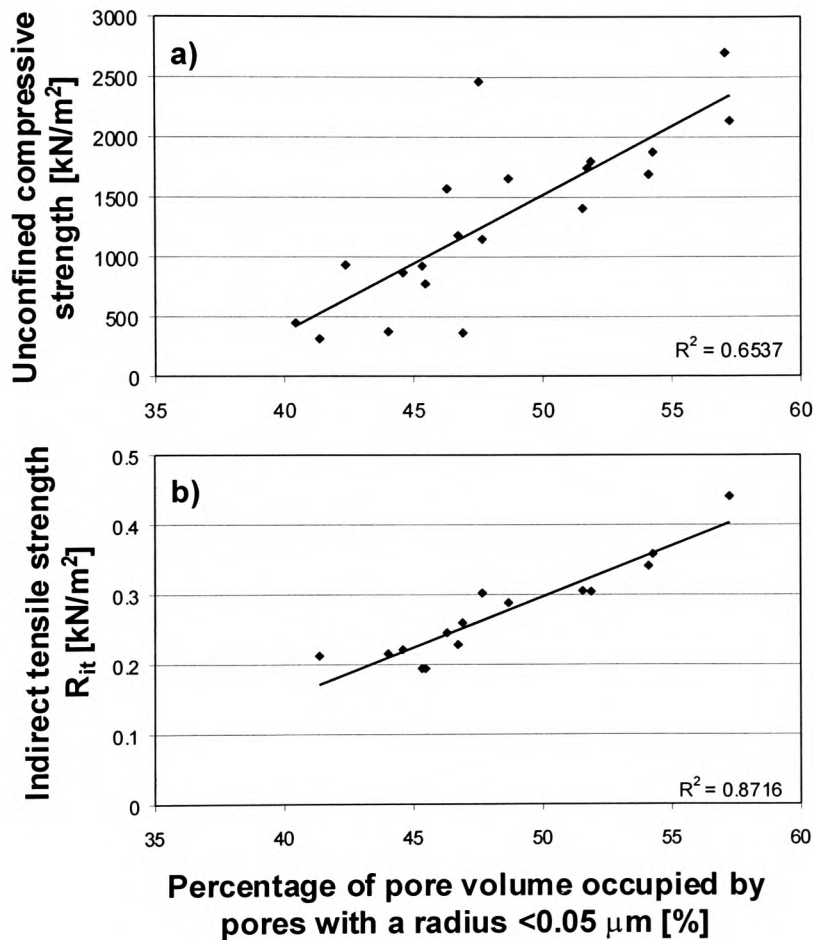
Figure 7.55 *Development of unconfined compressive strength (a) and indirect tensile strength (b) against percentage of pore volume occupied by pores with a radius <0.05 μm [%]*

7.4.4 Permeability

Figure 7.56 shows the development of the coefficient of permeability for lime-slag stabilised Lower Oxford Clay cured up to 1 year at 10, 20 and 30 °C. The permeability of uncured specimens measured immediately after compaction is indicated by the dotted line. The range of k-values stretches from the highest value of approximately 1.1×10^{-6} m/h down to a minimum of approximately 3.0×10^{-8} m/h over two ranges of magnitude. Lowest permeability coefficients are exhibited by specimens which have been cured for 24 weeks and 1 year, independent of sample composition. Overall the specimens exhibited reduced permeability with an increase in slag/lime ratio and curing period. These effects were more pronounced at higher curing temperatures. So all k-values for samples cured at 30 °C with slag additions of $\geq 4\%$ (independent of the duration of the curing period prior to testing) lie in the very narrow permeability range of between 8.0×10^{-8} and 1.0×10^{-7} m/h. For the mix 2L8S the range of k-values is narrowed down even further with only negligible difference in the permeability coefficients for the various samples after curing periods from 1 to 52 weeks.

If curing is at lower temperatures, the k-value development is somewhat less systematic. In a curing environment of 10 °C it is interesting to see that sample composition (i.e. the slag addition) has only negligible influence on the exhibited permeability particularly if curing is for up to 4 weeks. Curing durations of 12 weeks and beyond do result in reduced k-values for the whole mix range as observed at elevated curing temperatures. At a medium curing temperature (20 °C) the measured k-values are small at all compositions after curing for 24 weeks and beyond, whereas for shorter curing periods (1-12 weeks) k-values decrease with increasing slag content. Thus a slag/lime ratio of 8/2 results in similarly low k-values exhibited for all specimens independent of curing duration. At 30 °C curing, the fall in k-values for specimens with low slag/lime ratios is more rapid.

Although one would expect all measured coefficients of permeability to be lower than the ones exhibited by specimens which were tested directly after compaction, some exceptions could be observed during the course of the current project. All k-values for the mix 2L0S after curing was for only 1 week (independent of curing temperature) were found to be higher than the corresponding results obtained from samples tested
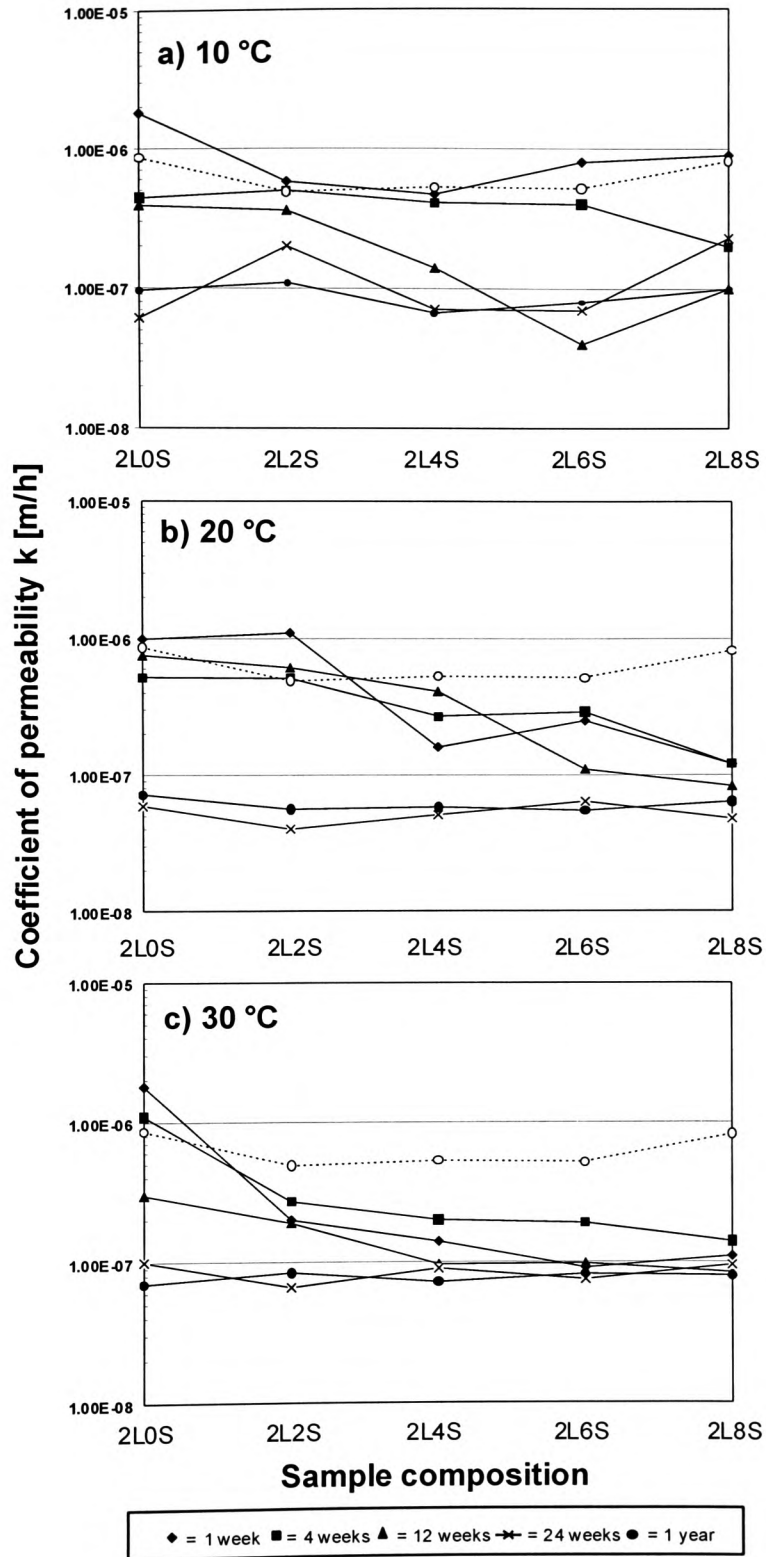
Figure 7.56 *Development of the coefficient of permeability k [m/h] of lime/slag stabilised Lower Oxford Clay after curing periods of 1, 4, 12, 24 and 52 weeks at 10, 20 and 30 °C*

immediately after compaction (this effect was also observed for kaolinite-slag-lime samples, Figure 7.26a), but at higher curing temperatures k-values dropped progressively below the control values as slag content increased due to increasing levels of slag hydration. This increase in permeability is thought to be due to enhanced flocculation during the early stages of curing. Also all 1-week cured stabilised Lower Oxford Clay specimens cured at 10 °C gave k-coefficients higher than or approaching those of immediately tested specimens.

7.4.5 Resistance to freeze-thaw cycling

The ultimate height, length and volume changes of frost-cycled lime-slag stabilised Lower Oxford specimens cured for various periods at 30 °C prior to frost action can be seen in Figure 7.57.

An increase in slag addition significantly reduces the length and ultimate weight change of the specimens (7.57a+b). However, when the ultimate volume changes (c) are considered, the effect is less marked. In fact only specimens cured for comparably long periods prior to being subjected to frost action show reduced volume increase with increasing slag content. However, even the lower values of volume change (around 11%) are still comparably high and the material would hardly be suitable in practice under severe freeze-thaw conditions.

The change in weight reflects the absorption potential of specimens during the thaw phases. Higher slag additions and longer curing, however, reduce the weight change only by up to 2%. It was not expected that such minor change would result in significantly improved volume stability.

The specimens prepared from stabilised Lower Oxford Clay show an overall reduction in ultimate weight change/volume change ratio with increase in curing period (Figure 7.58). Generally higher strength gain is associated with longer curing periods (Figure 7.50) and subsequently more volume stability (and thus higher weight change/volume change ratios) as exhibited by stabilised kaolinite (Figure 7.32). An increase in stabiliser content, however, weakens this effect and results in little change of weight change/volume change ratio for the specimens of the mix composition 2L8S with regard to curing period. To understand this anomalous behaviour, it has to be taken into consideration that an increase in curing period can be expected to result in an increase in the sulphate levels of the Lower Oxford Clay due to a higher degree of
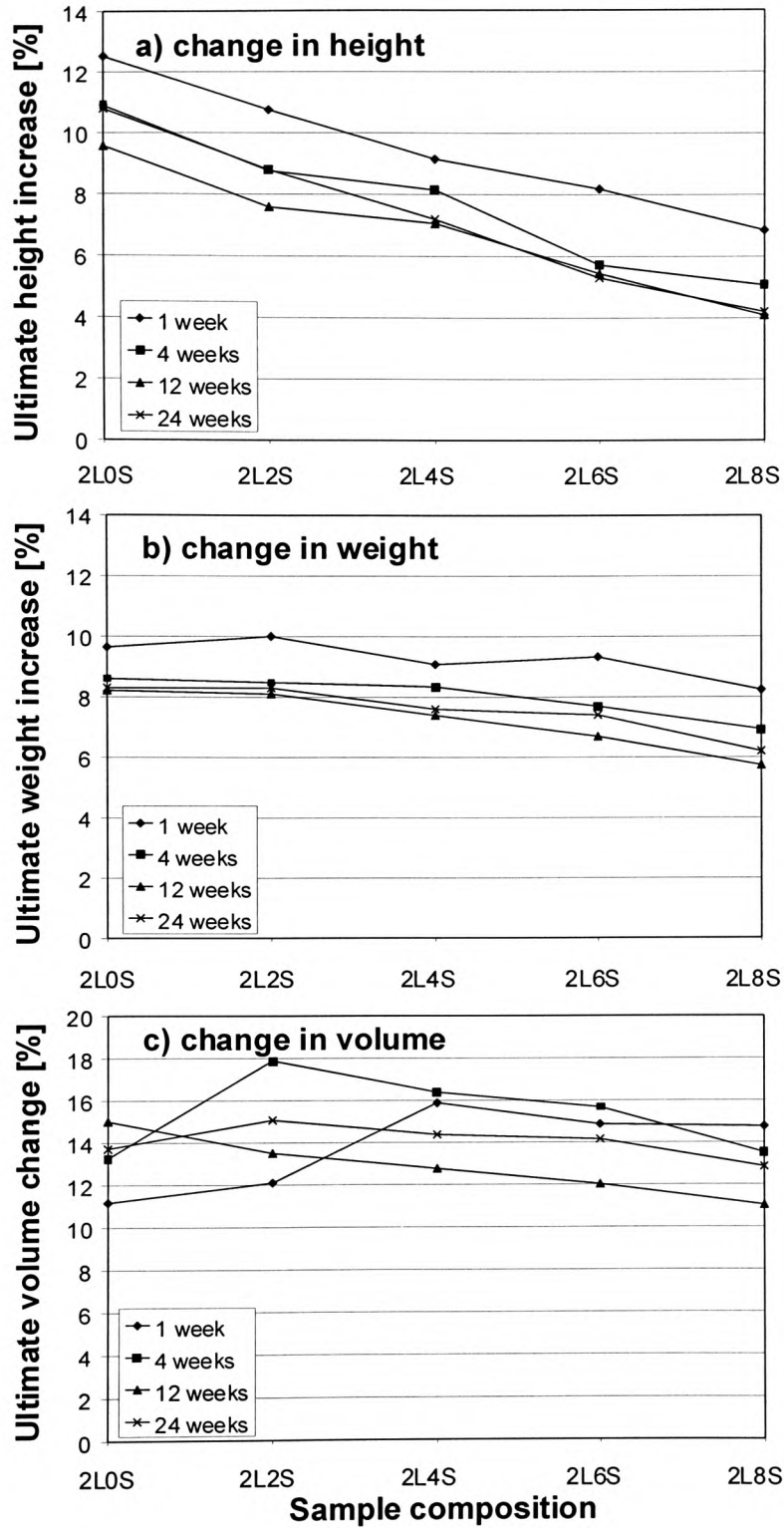
Figure 7.57 *Ultimate height (a), weight (b) and volume (c) increase of Lower Oxford Clay, stabilised with 2% lime and various ggbs additions after 1, 4, 12 and 24 weeks of moist curing prior to 12 freeze-thaw cycles*
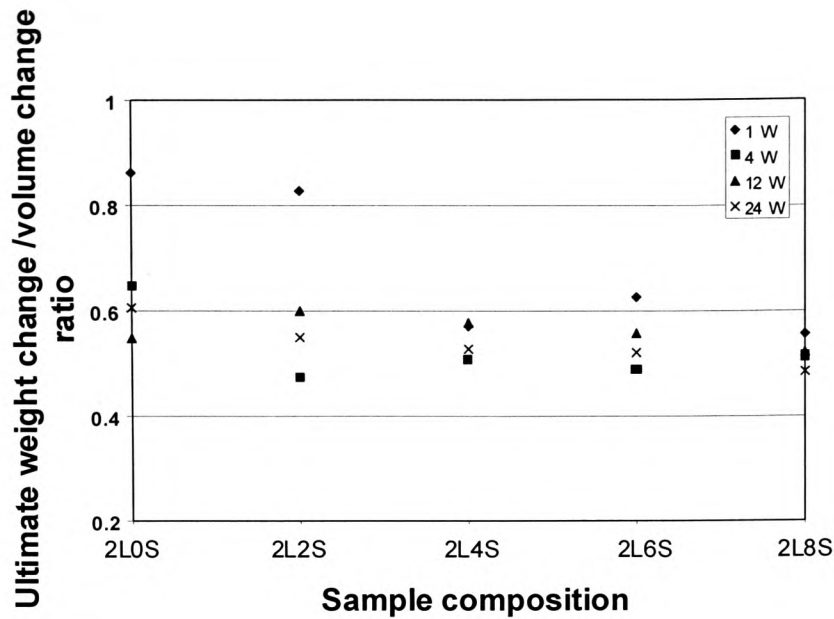
Figure 7.58 *Influence of initial curing period on the ultimate weight change/volume change ratio of stabilised Lower Oxford Clay specimens after 12 freeze-thaw cycles*

oxidation of pyrites present. The overproportional change in volume (i.e. lower w/v ratios) during freeze-thaw cycling after longer initial moist curing periods in the absence of high additions of ggbs could thus be the result of a large availability of sulphates which could be utilised to form expansive products. These products have a large affinity to absorb water provided during freeze-thaw cycling and will increase their volume. Higher slag additions, however, counteract this effect by creating a stronger sample structure during hydration, which will be able to withstand the expansion pressure exerted by the expansive products. Thus at high slag additions, lower w/v ratios were observed.

7.4.6 Effect of pore structure on permeability and frost resistance of stabilised Lower Oxford Clay

It has been shown that porosity and pore size distribution of stabilised soil specimens are generally related to the strength developed. To establish any relationships between permeability and MIP results, however, has been generally unsuccessful (see section 4.5.2.1). Marsh and Day [1985], for example, state that there is little likelihood of obtaining good agreement between porosity measurements via mercury intrusion and measured coefficients of permeability of blended cement specimens. They found,

however, that the determination of porosity via helium pycnometry results in values which show good correlation to permeability measurements due to the fact that the technique provides a good measure of the accessible inter-connected pore space.

With regard to the results obtained from investigations into stabilised Lower Oxford Clay, little evidence of systematic change of k-values with change in total pore volume (Figure 7.59) could be identified (similar to observations for the kaolinite system). Similarly no systematic changes could be observed between k-values and the degree of pore refinement (Figure 7.60).
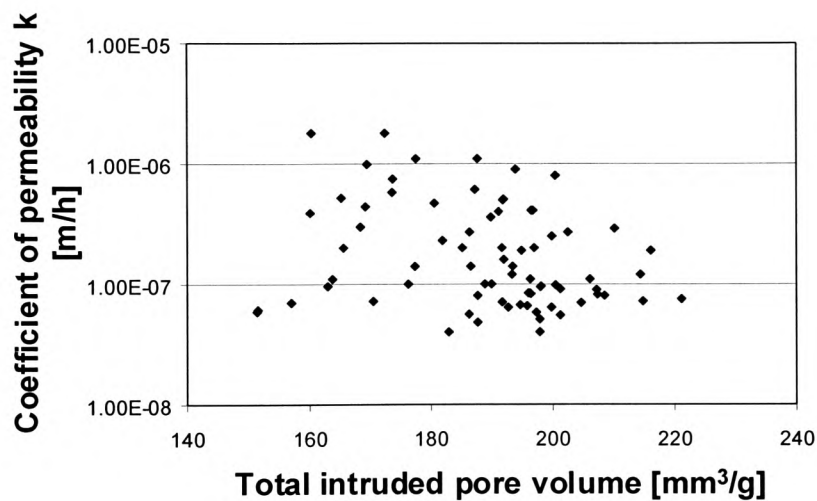
Figure 7.59 *Effect of total intruded pore volume on the coefficient of permeability of lime-ggbs stabilised Lower Oxford Clay*
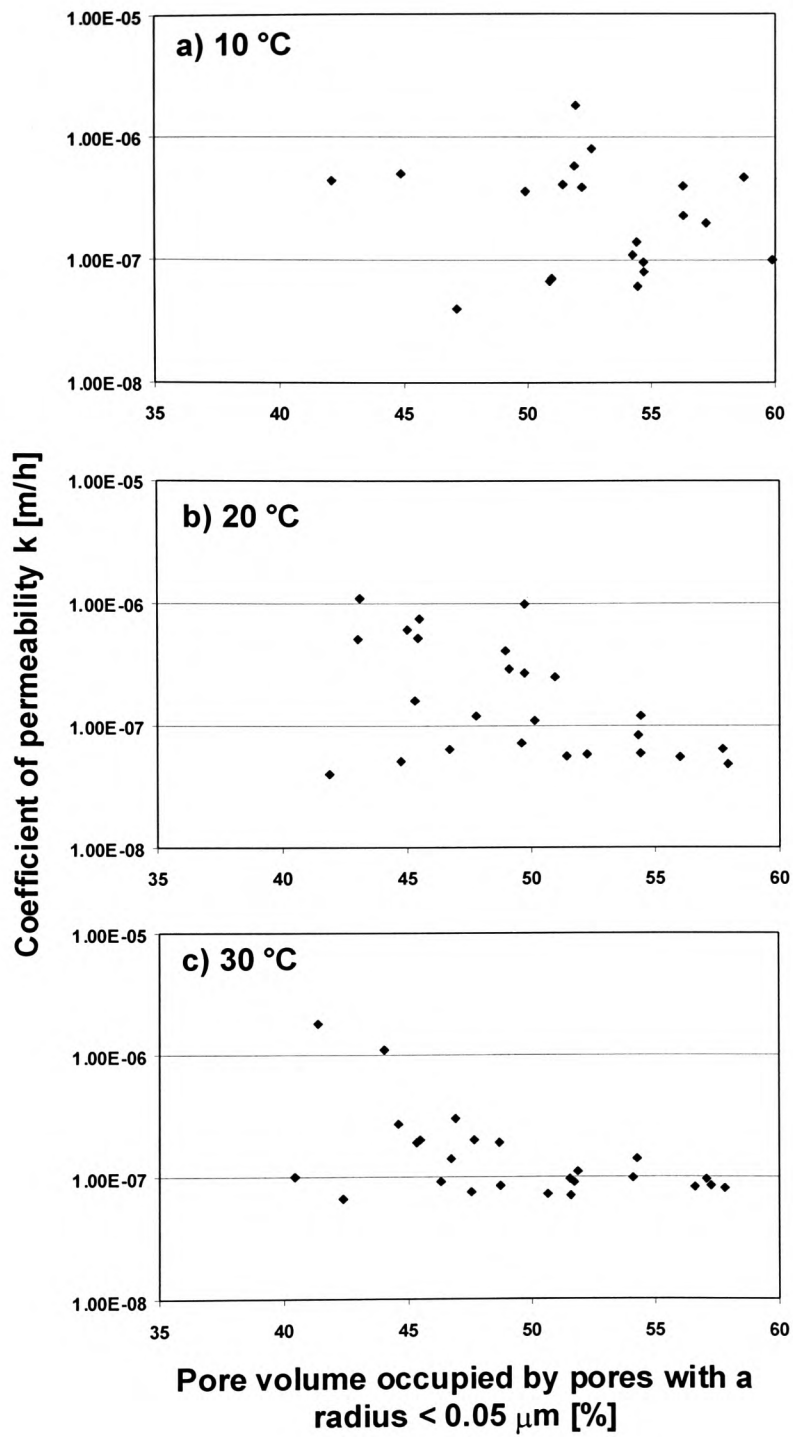
Figure 7.60 *Coefficient of permeability of specimens of stabilised Lower Oxford Clay versus pore volume occupied by pores with a radius <0.05 μm*

No systematic relationship between strength development and ultimate weight change/volume change could be identified and there appears also to be little correlation between the ultimate weight change after frost action and the exhibited porosity of the specimens (Figure 7.61b). However, whereas stabilised kaolinite exhibited a reduction in volume change with increase in total porosity (Figure 7.33a), there is no indication that changes in the pore volume of stabilised Lower Oxford Clay affect the ultimate volume change during frost action (Figure 7.61a).
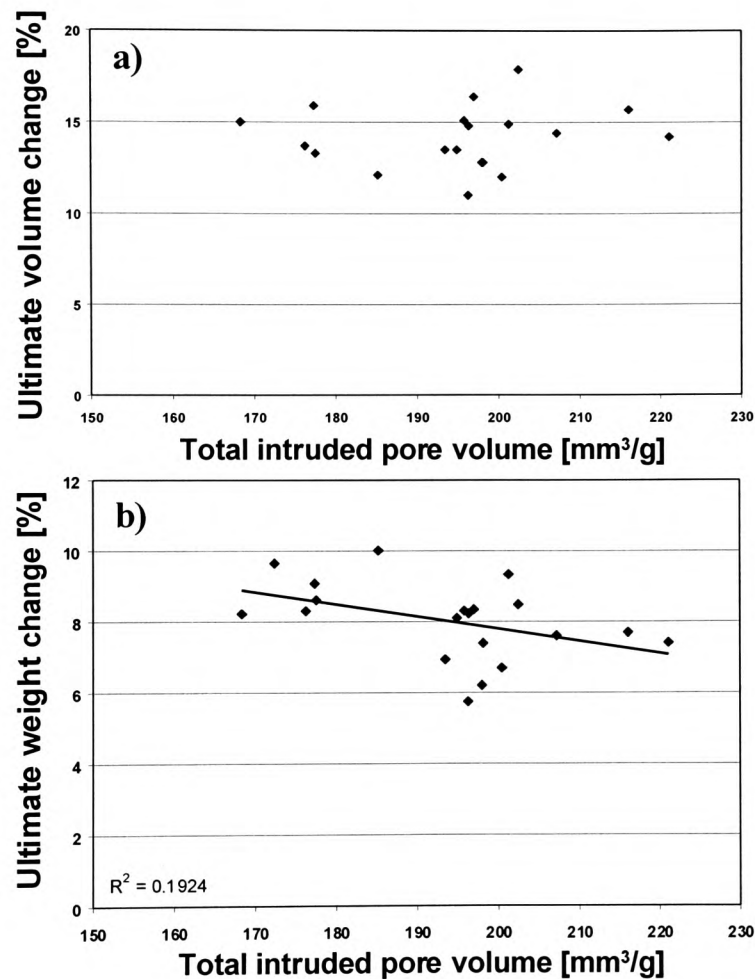
Figure 7.61 *Ultimate volume (a) and weight change (b) of stabilised Lower Oxford Clay specimens after 12 freeze-thaw cycles (moist curing periods of 1, 4, 12 and 24 weeks prior to frost action) versus total intruded pore volume*

Chapter 8 – Case studies

To outline the practicability of the proposed method and its possible application in practice, two case studies were carried out. The first case from Germany identifies the sulphate-lime-clay reaction, as introduced in chapter 3, as the cause of substantial heave of a lime-stabilised highway. Microstructural investigations (SEM and XRD) were carried out to confirm the suggested mechanisms. The second case outlines how soil stabilisation with lime-activated ggbs was successfully employed as a construction technique for a temporary diversion during the construction of a by-pass near Tingewick/Buckinghamshire. Financial implications of the lime-ggbs stabilisation method are outlined in a cost comparison.

8.1 Case study 1: Failed lime-stabilised sub-base of a rural carriageway near Böblingen/Germany

8.1.1 Case background

Through the Ministry of Environment and Transport Baden-Württemberg in Stuttgart/Germany, an opportunity arose to carry out microstructural investigations on lime-stabilised Mercia mudstone (formerly known as 'Keuper marl'), taken from the formation level of a heaved highway near Böblingen in the Southern part of Germany. The heave of parts of the K1077 (rural carriageway near Böblingen) occurred in Spring 1996 after completion of the construction work in Autumn 1995. The heave reached a height of up to 20 cm and was most significant at the location of a traffic island. Initiated by the Ministry of Environment and Transport, a trial pit was excavated in order to establish cause and circumstances under which the heave had occurred. The road had been built on an embankment, consisting of material which was stored there during the construction of a tunnel nearby in 1976. The tunnel went through a mountain consisting of Keuper marl with significant gypsum content. This was visible in the form of large white inclusions in the re-located material. The road construction material was initially protected by a layer of silty soil, which was dug out from the fields nearby. It was initially planned to stabilise the subbase with 2-3 % lime (CaO), however, due to heavy rainfall during construction the amount of additive was increased in order to render the material more workable (addition of up to 5% according to the resident engineer).

The author was supplied with material originating from layers ① and ② from the trial pit (Figure 8.1). The natural moisture content of each layer was determined and delivered values of 56% and 13% respectively.

bituminous surface
lime-stabilised sub-base, layer ①
unstabilised sub-grade, layer ②
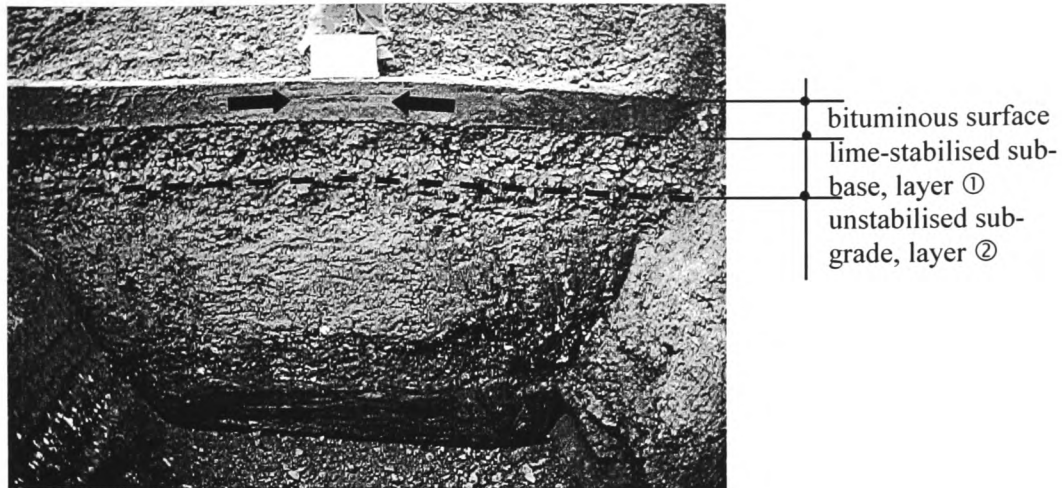
Figure 8.1 *Section through failed area (trial pit)*

8.1.2 Case results and discussion

The results of the SEM investigations carried out on freshly broken surfaces of dried specimens deriving from layer ① and ② are shown in Figure 8.2. The classic ettringite/thaumasite habit on the micrograph of the stabilised sub-base (left) gave a first indication of the cause of the observed heave.

Figure 8.2 *SE micrographs of the lime-stabilised layer ① (left) and the unstabilised layer ② (right)*

In comparison to the undisturbed clay plates of the unstabilised layer (right), the stabilised sub-base shows significant amounts of expansive crystals being formed, which result in expansion during the formation stage, when sufficient water can gain access. As heavy rainfall resulting in comparably wet material was reported by the site manager during the construction prior to stabilisation, the presence of sufficient gypsum in the lime-stabilised ground would allow the formation of harmful reaction products. In

order to confirm these suggestions, X-ray powder diffraction was employed. The traces of the XRD analysis carried out at Sheffield University on samples from layer ① and ② are shown in Figure 8.3 (a+b).
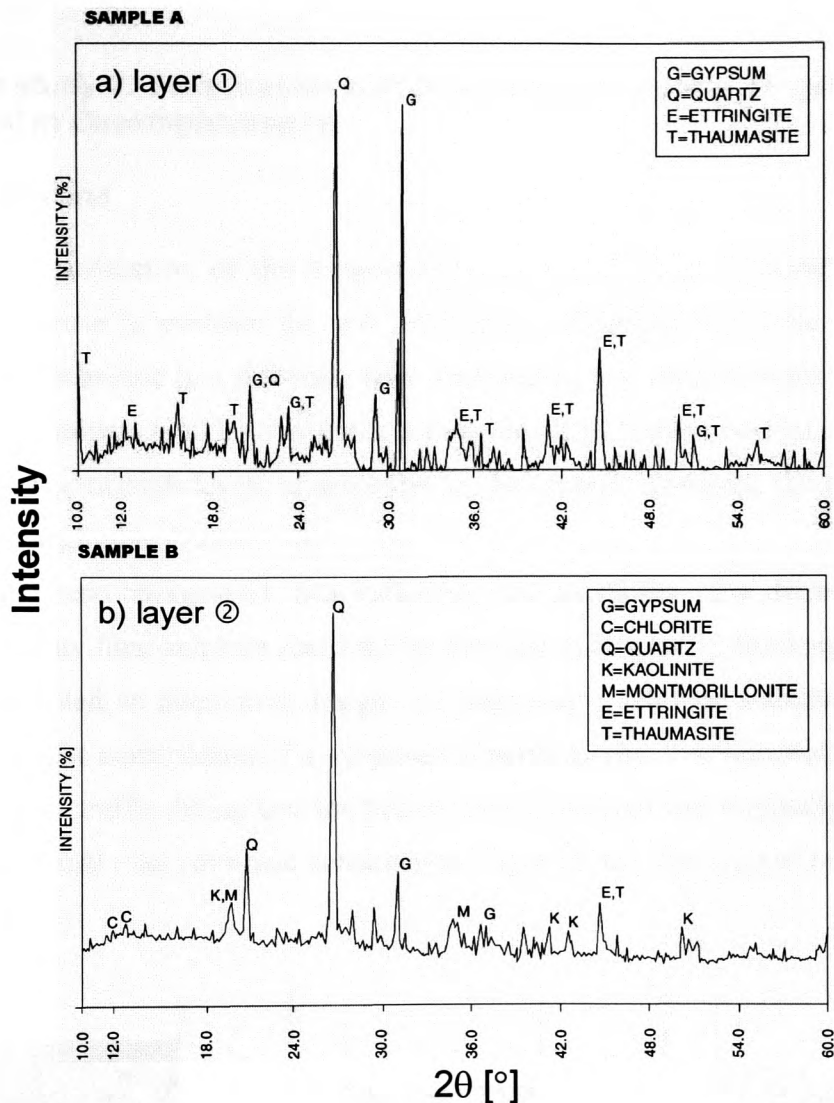
Figure 8.3 XRD-analysis of specimens from the trial pit

Sample A derives from layer ① and sample B from layer ②

The XRD trace of the first layer revealed quartz, gypsum, ettringite and thaumasite to be the most abundant minerals in the specimen. The gypsum is probably a remnant of the gypsum present in the soil before soil stabilisation was undertaken. Only small amounts of the original soil minerals (mainly quartz) were detected.

The crystalline minerals observed in layer ② are mainly quartz, kaolinite, chlorite, montmorillonite and gypsum. It is not clear if the gypsum found in this layer is

secondary or primary since no data on the original mineralogy of this soil was available. In addition negligible amounts of ettringite and thaumasite could be identified. These would, most probably form due to excess lime being leached out from the top layer.

8.2 Case study 2: Stabilisation with lime-activated ggbs – Tingewick full-scale trial in Buckinghamshire

8.2.1 Background

During the construction of the Tingewick by-pass (A421) in Buckinghamshire, an opportunity arose to evaluate the soil stabilisation technique with lime and ggbs by utilising the technique in a full-scale trial. Preliminary soil investigations had revealed that the predominant boulder clay had a comparably high sulphur content, probably due to the presence of high levels of sulphides in the ground. However, the total sulphate levels were negligible (Table 5.10).

Because of these background data indicating the possibility of a detrimental effect initiated by clay-lime-sulphate reactions (as outlined in chapter 3), Buckingham County Council accepted an alternative design, incorporating a sub-base stabilised with lime and ggbs for the construction of a temporary diversion. The diversion was necessary to carry the A421 traffic during construction of the by-pass and was originally specified to be of a traditional road pavement construction (Figure 8.4a). The suggestion to utilise a

a) original design
350 mm granular sub-base
190 mm bituminous surfacing

b) possible design according to French regulations
350mm stabilised sub-base
100 mm bituminous surfacing

c) chosen design
350 mm stabilised sub-base
130 mm bituminous surface
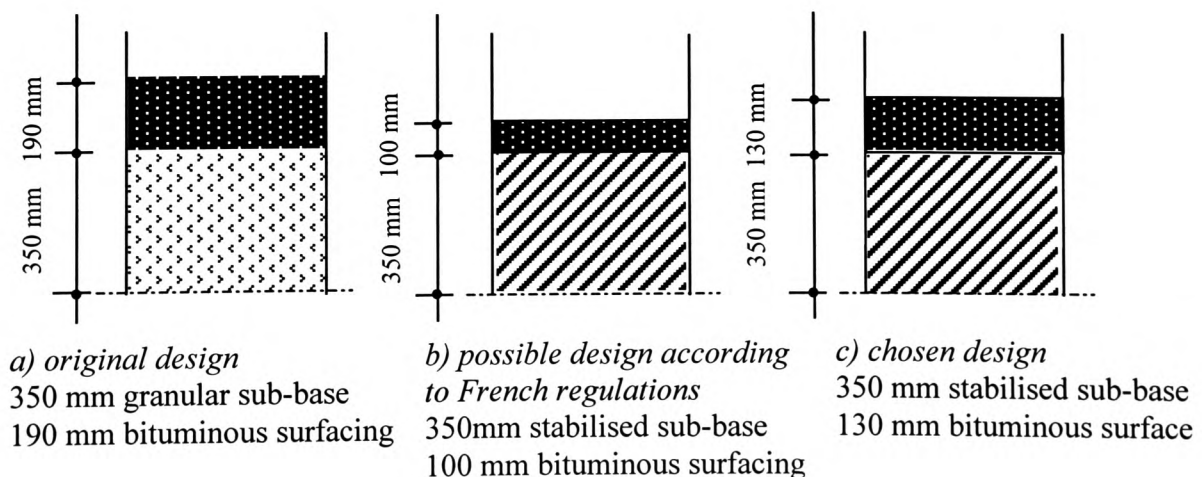
Figure 8.4   *Design options*

stabilised sub-base instead of granular fill, however, forced the authorities to re-consider the road design (Figure 8.4c). It should be noted that in the absence of British regulations for the design of road foundations on stabilised clays, French design recommendations had to be adopted (Figure 8.4b). The pilot trial area was sub-divided into 5 sections, for which 3 different combinations of stabilisation additives had been proposed. Figure 8.5 shows the allocated sections between chainage +160.00 and +400.00. A stabilisation depth of 350 mm was adopted for all mixes.
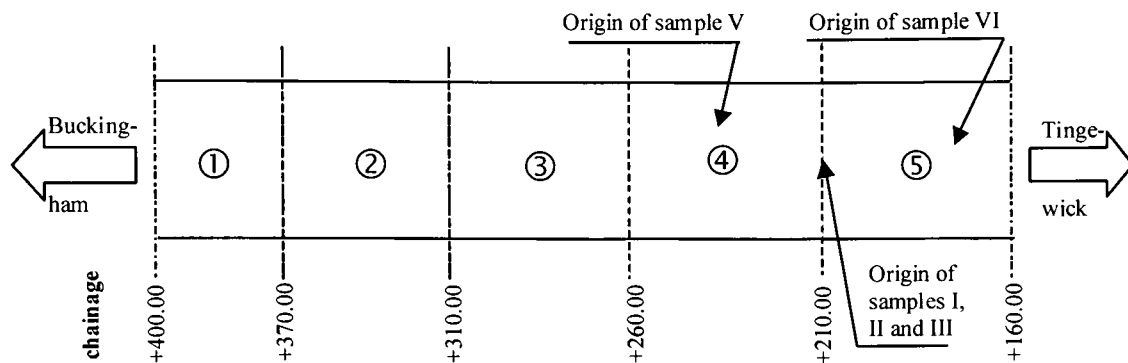
where

①	1.5 % CaO + 8.5 % cement	④	1.5 % CaO + 6.5 % ggbs
②	1.5 % CaO + 6.5 % ggbs	⑤	1.5 % CaO + 8.5 % ggbs
③	1.5 % CaO + 6.5 % ggbs		

Figure 8.5 *Layout of the full-scale trial area*

Prior to the addition of the main stabilising agents PC and ggbs, 1.5% quicklime (CaO) was uniformly spread over the whole trial area, rotorvated in and the material left to mellow for 72 hours. Subsequently the main stabiliser was mixed in for each section and the layer was then compacted. Finally, after a curing period of three days, a bitumen emulsion cure coat was applied. The unsurfaced trial area was used by site traffic for nearly two months until the blacktop was placed on the surface prior to the temporary by-pass being opened to traffic.

8.2.2 Assessment of performance

Due to delays during construction of the by-pass, the temporary diversion had been under traffic for 14 months prior to demolition. The overall performance of the lime-slag stabilised sub-base was satisfactory except for a prominant hump at chainage +210.00, which coincided exactly with the junction between the trial areas 4 (1.5% lime and 6.5% ggbs) and 5 (1.5% lime and 8.5% ggbs). After the bituminous surfacing had been removed, samples for CBR testing were taken by the author from the failure area (samples I, II and III) (section border) and from the middle of the sections 4 (sample V) and 5 (sample IV). The experiments were carried out according to BS 1924:part 2 [1990] and the results can be seen in Figure 8.6.
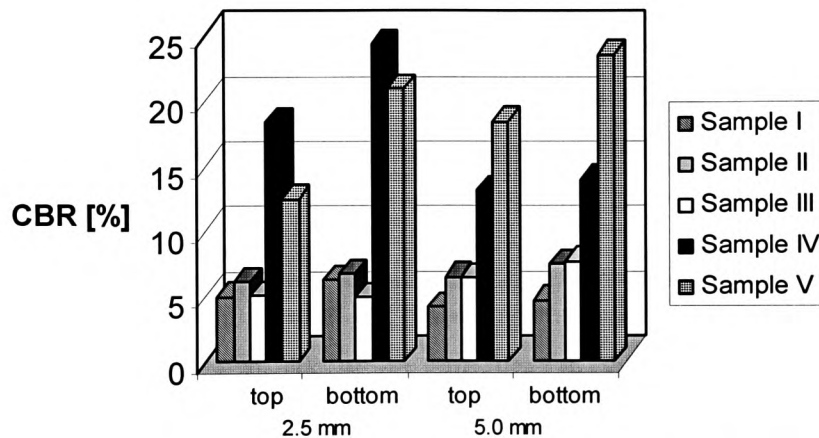
Figure 8.6 *CBR results of stabilised Tingewick Boulder* Clay

Based on the force required to penetrate the specimen surface (top and bottom of the sample) up to a depth of 2.5 and 5 mm, the CBR-values were calculated as a percentage of the standard force as given in BS 1924: part2. [1990].

Samples from the section border exhibit very low strength, indicating that the formation of cementitious products was somewhat inhibited or significantly retarded. Chemical analysis carried out by London&Scandinavian Metallurgical Co Ltd, Rotherham, on the same samples revealed a reduced level of CaO for the samples taken from the failed area, which was interpreted as indicative of lack of ggbs and thus reduced cementation. In order to check these CaO levels against those expected, chemical analysis was carried out on lime-treated soil which had no ggbs addition.

Based on a CaO content for the ggbs of 42% (see Table 5.14), a target CaO additive content of 2.6% (42% CaO of 6.5% ggbs = 2.6% CaO) would be expected from the slag

addition. This, combined with 15.8% CaO from the lime-treated clay (see Table 8.1) gives a total expected CaO content of 18.4%.

Samples taken from the centre of section 4, where performance had been excellent, exhibited a CaO content of 17.9%, which shows good agreement with the expected value of 18.4%. However, samples from the failed section areas at the section junction were found to have CaO contents of only 14.8% similar to the values for lime-treated soil with no ggbs and hence indicative of a serious deficiency of ggbs (Table 8.1).

Table 8.1 *Chemical analysis of specimens from the stabilised sub-base of the Tingewick full-scale trial*

	lime-treated material, no ggbs addition*	specimen from section ④ (chainage +225.00)	specimen from section border (failed section)
CaO content [%]	15.8	17.9	14.8
SO_3 [%]	0.98	3.24	2.98

[LSM Analytical Services, Rotherham, UK]
*sample(s) taken from lime-stabilised road embankment to which no slag was added.

It appears that during construction of the temporary diversion at the interface between sections 4 and 5 too much effort was put into avoiding overlap of the 6.5% and 8.5% ggbs sections, unfortunately resulting in the omission of treatment for a small strip. This untreated area exhibited a 'hump' at a later stage. Figure 8.7 shows schematically the rotorvator action during stabilisation and the resulting lack of homogenisation of the soil wedge at the section corner. The lack of CaO is not very likely to derive from a lack of lime due to the fact that all the sections were stabilised simultaneously with lime in one complete pass. Section borders were only introduced when the second additive was added.

Testing for sulphate (SO_3) carried out by LSM, Rotherham, on samples taken by the author after the demolition of the temporary diversion revealed that the sulphate levels had increased significantly producing values as high as 3.8% SO_3. This was almost certainly due to oxidation of pyrites. However, no damage due to sulphate attack of the lime-ggbs stabilised sub-base could be identified.
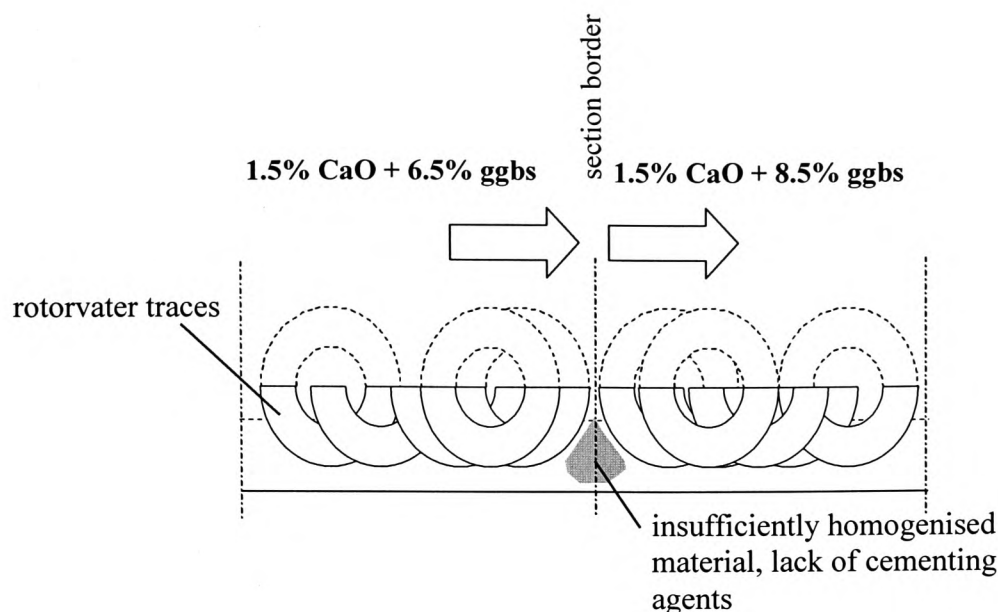
Figure 8.7 *Section border during stabilisation process*

Swelling tests on cylindrical specimens prepared from material sampled from sections ④ (1.5% lime and 6.5% ggbs) and ⑤ (1.5% lime and 8.5% ggbs) revealed ultimate swelling magnitudes (after soaking for 400 days = approximate duration of diversion under traffic) of 3.1% and 1.8%, respectively. These values are well within the limits given by the Department of Transport (4% average allowable limit) and further emphasise the potential for lime-ggbs stabilisation particularly for sulphate or sulphide bearing soils.

8.2.3. Costing

The use of a stabilised sub-base affects the construction costs three-fold: Firstly, the upper and lower roadbase, the sub-base and the capping layer can be completely replaced by a stabilised roadbase (Figure 8.8). In addition, the actual stabiliser utilised for the process can result in economic advantages and environmental advantages can also be identified. However, for the current project emphasis was put on the economic implications deriving from replacement of the classic stabiliser combination (lime and cement) with lime and ggbs.
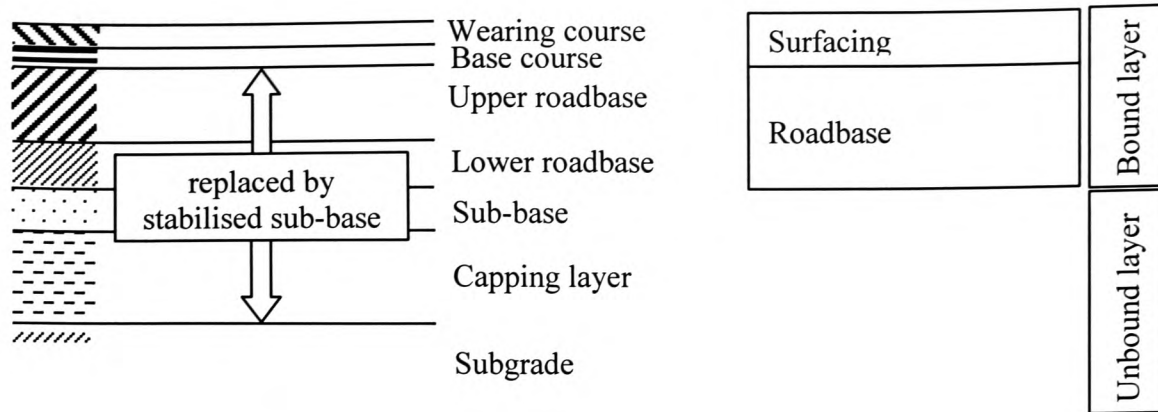
Figure 8.8 *Section through a flexible pavement [after Watson, 1994]*

8.2.3.1 Assumptions

The financial analysis is based on a series of assumptions, which relate to circumstances found in practice. These are

i) significant sulphate/sulphide content of the soil

Stabilisation with lime-activated ggbs is of particular interest, where sulphates or sulphides in the soil can be the cause of disruption and heave

ii) stabilisation depth

The calculations are based on a stabilisation depth of 350 mm

iii) transportation distance of imported materials

It is assumed that the construction site is not more than 50 miles away from the registered office of the company dealing with the stabilisation work

iv) water addition

The cost estimation does not take into account any costs for the addition of water during the stabilisation process. It is assumed that the natural moisture content of the clay is suitable for immediate stabilisation.

v) contract size

The participating contractors supplying information, raised the concern that the quantities outlined in the bill of quantities were comparably small and thus the cost estimation would not properly reflect market prices. In order to obtain useful and practice-related data, it was decided to obtain a quotation based on quantities which would relate to large scale soil stabilisation projects.

vi) Mix comparison

The prices compared are those of stabilisation with either 1.5% CaO and 8.5% PC or 1.5% CaO and 6.5% ggbs. Based on performance data and compressive strength test results obtained by the Transport Research Laboratory [Higgins and Kennedy, 1999] (the strength development of the 6.5%ggbs mix outperformed the 8.5%PC mix after a curing period of 28 days and beyond), it was considered that comparison of these two mix compositions could be justified.

8.2.3.2 Material prices

Initial investigations showed that the relative costs for the stabilisation methods available would be determined primarily by the cost of the materials utilised. Price enquiries suggested that the bulk price for cement (PC) lies in the region of £ 55/t and lime and ggbs are both about £ 50/t (all prices include haulage within a radius of 50 miles). It should be noted that the material prices are based on quotes from the producers/suppliers and not the building contractors, who would probably include the material delivery within their quote in practice, plus a working profit.

8.2.3.3 Data source

The price data were obtained by a survey carried out amongst a number of soil stabilisation contractors from England. Based on the assumptions outlined in the previous section, a bill of quantities (BOQ) for the stabilisation of a road subbase, comparable to that of the Tingewick full-scale trial was compiled (Figure 8.9). The contractors, a list of which was obtained through the kind help of the British Cement Association (BCA), were asked to prepare a quote for the work described in the BOQ.

The original BOQ was based on the classic technique, utilising a rotorvator, to mix in the stabilising agents, and subsequent compaction and grading processes. A number of quotes, however, suggested alternatives such as the utilisation of an "on board hopper", allowing spreading and mixing in one process avoiding the development of significant dust clouds. This piece of equipment, used by a soil stabilisation contractor from London, is mainly used when stabilisation work has to be carried out in highly populated areas, where dust development is not tolerable. However, the discharge from

Item	Description	Quantity	£ per unit	Total £
1	Deposit and roughly compact 350 mm thickness of Boulder Clay onto prepared sub-formation to form stabilised sub-base	600.00 m^3	N.A.	N.A.
2 *2.1*	*Stabilisation process* Method A – Lime and cement			
2.1.1	Stabilisation of clay (d=350 mm) to form sub-base using 1.5 % lime (approx. 35 kg/m^3)			
2.1.1.1	Material delivery	21.00 t	50.00	
2.1.1.2	Spreading of the material	21.00 t		
2.1.1.2	Rotovating	600.00 m^3		
2.1.1.3	Compacting	600.00 m^3		
2.1.2	Addititonal stabilisation with 8.5 % cement (PC) (approx. 200 kg/m^3)			
2.1.2.1	Material delivery	120.00 t	55.00	
2.1.2.2	Spreading of the material	120.00 t		
2.1.2.2	Rotovating	600.00 m^3		
2.1.2.3	Compacting	600.00 m^3		
2.1.2.4	Grading	600.00 m^3		
2.2	Method B – Lime and ground granulated blast furnace slag (ggbs)			
2.2.1	Stabilisation of clay (d=350 mm) to form sub-base using 1.5 % lime (approx. 35 kg/m^3)			
2.2.1.1	Material delivery	21.00 t	50.00	
2.2.1.2	Spreading of the material	21.00 t		
2.2.1.2	Rotovating	600.00 m^3		
2.2.1.3	Compacting	600.00 m^3		
2.2.2	Additional stabilisation with 6.5 % ggbs (approx. 150 kg/m^3)			
2.2.2.1	Material delivery	90.00 t	50.00	
2.2.2.2	Spreading of the material	90.00 t		
2.2.2.2	Rotovating	600.00 m^3		
2.2.2.3	Compacting	600.00 m^3		
2.2.2.4	Grading	600.00 m^3		
3	*Optional*			
3.1	Addition of water	150.00 m^3	N.A.	N.A.

Figure 8.9 *Bill of quantities for the survey*

the hopper is only about 500 kg per minute, which makes it comparably slow and expensive.

Another technique, in-plant-mixing, was also suggested. With the availability of mobile plants, mixing can take place at site, minimising transport to and from the mixing facility and resulting in substantial price advantages. This is further emphasised by the high mixing capacities (approximately 1000t/day).

The costs for the actual mixing processes are in the main independent of the stabilising agent(s) utilised, so that only price differences in the materials and in the particular mixing and stabilisation techniques employed lead to variation in costs.

8.2.3.4 Results

Due to the different stabilisation techniques suggested, the quotation sums varied considerably (Figure 8.10). For obvious reasons actual quotation prices cannot be disclosed here and thus comparison is achieved by assessing the cost of a quotation relative to the percentage by which that quotation exceeds the total sum quoted by the cheapest competitor.

The lowest quotes were, interestingly, obtained from contractors suggesting stabilisation with mobile in-plant mixers. Their quotations can be justified due to extremely high capacities and short 'feeding' distances. The state-of-the-art stabilisation with a rotorvator was about 30% more expensive, whereas the incorporation of the dust-minimising 'on-board-hopper' resulted in a significant price increase of an additional 150%.

Although in this case highly price competitive, it should be noted that in-plant mixing has a number of disadvantages, which – if quantified – might result in opting for a different mixing/stabilisation method. Firstly, the lime-stabilised material is, during the mellowing period, not available to form an interim surface for site traffic roads. It would be highly uneconomic to re-deposit, roughly compact and finally return it to the plant for the main stabiliser to be added once the mellowing period was complete. Thus the material has to be stockpiled, resulting in the fact that additional space has to be allocated which is a second disadvantage, particularly at sites where little storage space is available. In addition further heavy site traffic is created in order to ensure continuous feeding of the plant.
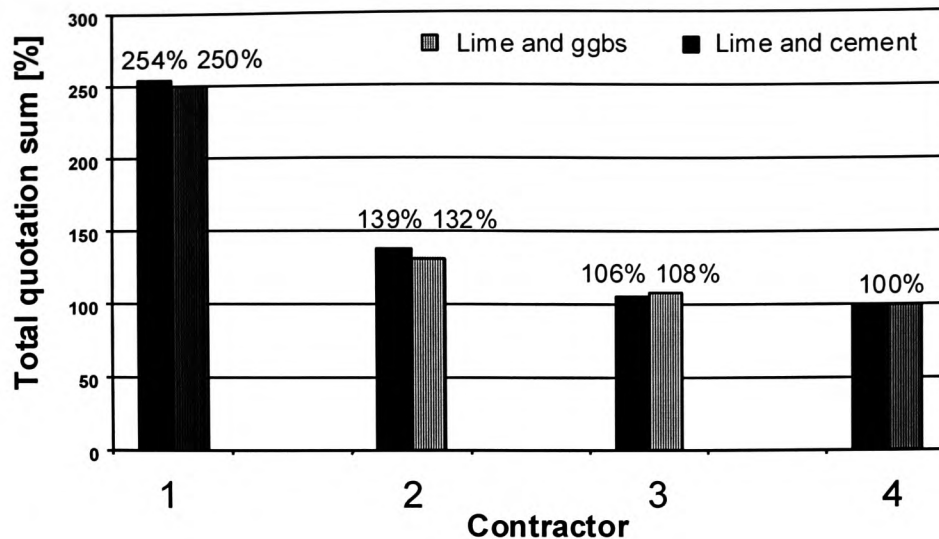
Figure 8.10 *Total quotation sum comparison [%] from the returned BOQ*

Due to a material price advantage of around 10% of ggbs over cement, the combined stabilisation method with ggbs and lime is overall cheaper than the method combining cement and lime (Figure 8.11). Depending on the type of stabilisation technique suggested the cost advantage varies between 2.6 and 24.4%. However, the average of the quotation sums of contractors 1, 2 and 3 result in a price advantage of ggbs stabilisation over stabilisation with cement of around 21.5%.

It is appreciated that variation in the suggested costs, for example based on the geographical location of the stabilisation site, can occur. However, the basic economic and environmental advantage of the utilisation of ggbs is clearly apparent.

It should be noted that the cost comparison based on the 'Tingewick trial' implied a mellowing period of 72 hours of the lime-stabilised material prior to the addition of ggbs. This refers to common practice in lime stabilisation of soils in accordance with the Specification for Highway Works, clause 615 [Department of Transport, 1986]. It is generally assumed that this mellowing period of 24 to 72 hours aids in the breakdown of large clay clods and contributes to a better homogenity of the soils in order to achieve the intended improvements in strength and consistency. However, there is evidence that neither the consistency limits [Wild et al., 1998] nor other relevant long-term engineering properties such as strength development or swelling are strongly affected when both components are added at the same time and mellowing (up to 3 days) is omitted. In fact, investigations by the author into the compressive strength development of lime-stabilised kaolinite specimens, to which ggbs was added with a delay of 0, 1, 3

and 7 days, revealed that a delay should possibly be avoided (see Appendix 4). Strength development is more rapid in the absence of a delay because sulphate from the soil is available to accelerate the lime-activated slag hydration. By delaying prior to adding the slag, lime-sulphate-clay reactions proceed, depleting the system of both lime and
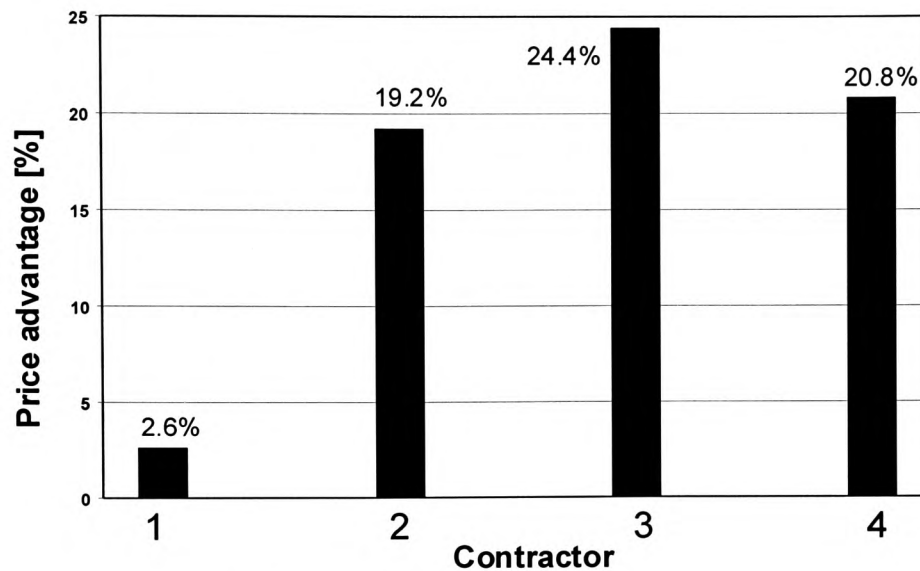
Figure 8.11 *Total price advantage [%] of stabilisation method with ggbs over stabilisation with cement based on returned quotations form 4 contractors*

sulphate and thus activation of the slag is less effective. However, a delay was found to be advantageous with regard to reducing even further the linear expansion on soaking, i.e. the reduction in swelling potential initiated by ggbs addition was improved to an even higher degree when mellowing was introduced. This is because some of the deleterious expansion products are able to from prior to compaction. Detailed results can be found in Appendix 4. However, with regard to the financial situation this means that the actual cost for the stabilisation process could be reduced substantially due to the fact that spreading and mixing of both binders could be carried out simultaneously.

8.2.4 Environmental aspects

The benefits of using stabilised foundations are both economic and environmental, the latter being sometimes hard to quantify [Chaddock and Atkinson, 1997]. In comparison to ordinary, unbound granular Type 1 sub-bases, a stabilised sub-base can be constructed much thinner but exhibit the same structural performance, resulting in an economic advantage. Alternatively by maintaining, with regard to its thickness, an overdesigned stabilised sub-base with thus a higher stiffness than required, the overlying road base could be thinned. Chaddock and Atkinson [1997] identify the environmental benefits to be mainly in reduced traffic congestion around and on the construction site and reduced quantities of extracted material. Secondary benefits result from reduced environmental damage due to reduced transport activities to and from the site. In addition, reduced quarrying and landfill operations provide a substantial environmental benefit, which is hard to quantify. Sherwood [1995] emphasises that environmental factors almost invariably favour stabilised sub-bases. He has, however, to admit that to-date no recognised method of assessing these benefits is available. During cement production large amounts of energy are required. This demand comprises mainly energy needed to crush, grind and blend the raw materials (usually chalk or limestone and clay/shale) and energy to heat the kiln in order to obtain calcination of the mixes. In addition vast quantities of CO_2 are produced during cement production and released into the atmosphere. As a rule of thumb, 1 tonne of CO_2 is released into the atmosphere for every tonne of cement produced. With the utilisation of ggbs, a by-product is re-introduced into the production cycle. It is appreciated, however, that grinding is necessary to enhance the latent-hydraulic properties of the slag. However, in comparison to cement production the energy requirements and emissions produced are negligible.

Chapter 9 – Summary of results and discussion

Experimental results described in chapter 7 and observations made during the case studies illustrated in chapter 8 will be discussed in detail in this section of the thesis. Observations and experimental results are interpreted and suggestions for possible mechanisms with respect to the research findings are made. Because of the fact that the different availability of sulphates is of some significance with regard to the engineering properties displayed by the two main soils of the project, kaolinite and Lower Oxford Clay, the discussion is divided into two main sections the first of which deals with the laboratory-prepared kaolinite soil mix (with and without gypsum) and the second analyses the observations made for the stabilised natural clay, Lower Oxford Clay.

9.1 General

In the current project an attempt was undertaken to assess the overall durability of sulphate-bearing clay soils, stabilised with lime and ggbs, with regard to key engineering properties such as strength, permeability, porosity, pore size distribution and resistance to frost action. A sufficiently wide range of stabiliser combinations was employed to allow a better understanding of modifications to the slag hydration process in the presence of artificially added or naturally present sulphates and to assess how the presence of these sulphates affects the performance of the stabilised soil.

Prior to detailed discussion of the results, the reader should be reminded that ggbs on its own is classified as a latent-hydraulic binder, i.e. for it to hydrate and thus subsequently result in cementation, it requires a suitable activator. The aim of the added activator is to disturb the outer, pseudomorphic layer of the slag grain, which develops as soon as the slag is in contact with water [Feng et al., 1989, Mehta, 1989]. Damage to this layer, which in fact protects the slag grain from significant hydration, is influenced by environmental conditions, including temperature, humidity/water availability and pH of the pore solution. In addition the effect of accelerating agents has also to be taken into account.

Slag hydration, however, is not the only process which affects the engineering properties of slag-lime stabilised clay. As a basic mechanism, the pozzolanic lime-clay reaction provides some strength enhancement initiated by lime which was not utilised in the initial stages of soil modification as a result of cation exchange. If sulphates are present, the formation of expansive phases is yet another process which affects performance, particularly if water is available in abundance. All these reactions occur to some degree in parallel in lime-slag sulphate-bearing clay and 'compete' for the limited

availability of calcium, an element which plays an important role in the formation of both cementitious products and expansive phases. If the composition of the system is modified, for example by omission of gypsum or clay, or by a change in the binder ratio, single reactions might be enhanced, retarded or not occur at all. The reader should therefore take into account the complex system when in the following sections the changes in observed engineering properties of stabilised soils are described and interpreted. This is particularly the case when mechanisms are suggested (which occur within the sample structure on a microscale) to explain how these changes relate to sample performance.

9.2 Stabilised kaolinite

In the current project the strength development of soil specimens stabilised with lime and ggbs was assessed based on unconsolidated, undrained triaxial tests, unconfined compression tests, indirect direct tensile and penetration (CBR, utilised during analysis of the observations made during the Tingewick full-scale trial) test methods. Increasing additions of ggbs to kaolinite specimens containing 6% gypsum, which have been stabilised with 2% $Ca(OH)_2$, result in substantial shear strength increases (Figure 7.2) accompanied by a reduction in the cumulative strain at failure (Figure 7.3). The latter is due to developed brittleness as a result of increasing cementation within the specimens. If the addition of gypsum is increased, the compressive strength and also indirect tensile strength undergo significant improvement with increase in the addition of ggbs (Figures 7.7 and 7.9). However, specimens to which no gypsum has been added show an overall inferior strength development after curing periods of up to 24 weeks (Figure 7.5).

The mechanism behind the strength gain in lime-stabilised samples (2L0SXG) is well researched and found to be the pozzolanic reaction which results mainly in the formation of poorly crystalline calcium-silicate-hydrate (C-S-H) gel as cementing agent [Abdi, 1992, Wild et al., 1987]. However, the addition of only 2% lime has no practical relevance with regard to improvement of the bearing capacity and delivers strength developments which are of no significance in comparison to higher lime additions found in practice [Arabi and Wild, 1989]. Soil modification, due to cation exchange involving Ca^{2+} ions and cations on the clay mineral surfaces resulting in soil flocculation, is initiated satisfactorily by even small lime additions [Kinuthia. 1997].

However, the amount of lime available for the pozzolanic reaction is expected to be negligible if only 2% lime is added. In addition, the presence of sulphates will lead to the formation of ettringite, although the amount of ettringite formed initially is expected to be comparably small. Immediately after mixing most of the calcium necessary for its formation will be consumed during the initial and comparably rapid cation exchange. Thus the ettringite formed will neither contribute significantly to an increase in strength nor result in expansion due to the limited availability of water [Mehta and Hu, 1978].

The very significant strength development observed in the presence of ggbs (Figures 7.2, 7.7 and 7.9) is the result of slag hydration, during which cementitious products, such as C-S-H and C-A-H gels are formed on the surface of the slag grains [Glasser, 1991, Richardson and Groves, 1992]. Slag is associated with the provision of additional freely available alumina and silica to the system in the presence of lime, the latter increasing the pH within the pore solution of the system and thus the solubility of these components [Yuan et al., 1988]. The removal of these critical constituents to form strength enhancing gels drives the slag hydration reaction forwards. The intensity of the reaction also depends on the amount of sulphate present in the sample, which is reflected, for example, in the increased compressive and indirect tensile strength development with various gypsum additions (Figure 7.7 and 7.9). In the absence of gypsum (Figure 7.5, 7.7a and 7.9a) only comparably small strength gains are obtained up to a curing period of 24 weeks, even when the ggbs addition is increased. A strongly reduced slag hydration rate results in less pore volume occupied by a fine pore fraction, the pore radius of which is usually associated with the presence of cementitious gels ($r \leq 0.05 \mu m$) (Figure 7.19) [Wild et al., 1987]. Only if curing is beyond 24 weeks and at elevated temperatures, is there evidence for intensive slag hydration in the absence of accelerating sulphates, manifested in substantially increased shear strength (Figure 7.5) and a significantly higher percentage of pore volume occupied by pores with a radius $r \leq 0.05 \mu m$ (Figure 7.19). In the presence of sulphates, hydration is initiated quickly and effectively with higher ggbs additions resulting in higher strength (Figure 7.2) and reduced porosity (Figure 7.14).

Findings from research into the microstructure of cement blends suggest that higher slag additions result in substantial pore refinement due to the production of cementitious gels as observed for slag cements [Uchikawa, 1980, Roy and Idorn, 1985]. The overall pore

volume decreases as a consequence of gel formation and subsequent pore volume redistribution (Figure 7.20) and the specimens exhibit a higher percentage of pores with a radius r≤0.05μm, a pore fraction which is by some authors considered too small to contribute significantly to the flow of water through the system [Goto and Roy, 1981, Wild et al., 1987]. Also, as shown by O'Farrell [1999] for mortars, to which ground brick had been added as partial cement replacement and further illustrated in the current research (Figure 7.23b), there is a relationship between an increase in strength and an increase in the percentage of the pore volume occupied by these smaller pores (r≤0.05μm). This is generally believed to be the result of densification of the soil's microstructure which is then able to distribute stresses deriving from compressive, shear or tensile forces more evenly and thus resist them to a higher degree.

The pore refinement results from the replacement of larger pores (initially just air or water-filled pores) with cementitious precipitates of lower porosity and thus an overall denser microstructure develops, which imparts higher strength [Kendall et al., 1983]. The degree of precipitation of cementitious gels and thus the change in pore structure as a result of the slag hydration process is also reflected in the development of the shear strength parameters represented in Figure 7.4. Generally, the sole presence of pore blocking gels will affect the cohesion due to a reduction in pore space (Figure 7.4b) and thus an increase in the attraction between adjacent particles. This was confirmed by findings of Thompson [1966], who investigated the increase in c_u-values deriving from undrained, unconsolidated triaxial tests of lime-stabilised Bryce clay and found that it was well reflected in an increase in the compressive strength of the specimens. He could not identify any correlation between ϕ_u and the exhibited strength of the stabilised specimens. However, it should be noted that he only assessed the results obtained from samples, which had been cured for up to 7 days, a time span in which very little cementitious gel development will have occurred. Extended interparticle bonding within the sample structure is only achieved after longer curing periods, when the developed gels create new links between themselves and adjacent soil particles. This finally results in a strong, well-developed interlocking particle network, comprising a matrix which contains much finer pores [Scherer, 1999] (Figure 7.4a). In parallel the threshold radius, which is usually associated with being a measure for pore refinement and connectivity, undergoes significant reduction (Figure 7.21a) due to high slag hydration activity and the marked increase in the amount of precipitated cementitious products. Lower

hydration rates, as obtained in the absence of gypsum, however, result in substantial threshold radii reduction (Figure 7.21b) only after much longer curing periods.

It should be noted that in lime-slag stabilised clays, in addition to C-S-H and C-A-H phases, other aluminate hydrates such as AFt and AFm phase are expected to form. Richardson and Groves [1992] observed AFm and AFt in PC-ggbs blends and found them to be identical in morphology to those in pure PC pastes. However, in the current project, where sulphate is widely available, there is little likelihood of AFm phase being formed. This is confirmed by findings of investigations carried out by Glasser [1991], who assessed reaction products from slag hydration initiated by different activators. The combination of portlandite and gypsum with slag is thus likely to result in the formation of C-S-H gel, C_4AH_{13} and AFt. It is suggested that ettringite, the tricalcium aluminate form of the AFt phase, contributes to some extent to the observed strength gain in the stabilised soil specimens in the presence of gypsum. As in supersulphated cement, the ettringite manifests itself in long, lath-like crystals, a habit which typically forms when the pH of the pore solution is between 10 and 12 [Chartschenko et al., 1993] and provides some interlocking effect resulting in strength gain. However, Smolczyk [1961] claimed that AFt phase contributes only marginally to the strength development in supersulphated cement. According to Smolczyk, the strength development superceeds the formation of ettringite, which is still forming at a stage when the cement has already developed very high strength. In the current work on the kaolinite-lime-slag system without gypsum, negligible slag hydration and the complete absence of ettringite results, in low strength at short (up to 12 week) curing periods (Figure 7.5). Other authors [Wild et al., 1993, Stark et al., 1998] claim that ettringite forms rather rapidly when its main chemical constituents, i.e. sulphate, calcium and alumina, are available. The main sulphate source in the case of gypsum-containing kaolinite, stabilised with lime-activated ggbs, is obviously the gypsum, whereas the alumina in the early stages is supplied by the clay. The formation of ettringite, however, will depend on the supply of Ca ions. These will, in the initial stages of the formation process, derive from the added lime (although most of it will be utilised for cation exchange) and from the thin outer layer of cementitious products, which coats the slag grain like a protective shield and thus normally inhibits the slag hydration [Feng et al., 1989]. By utilisation of calcium from the slag surface in ettringite formation, damage is inflicted to the protective layer and unreacted slag grain surface is exposed to the pore solution. The prevailing pH-

value of the pore solution is still high enough to subsequently result in dissolution of alumina and silica from the exposed slag surface which can subsequently be combined with calcium to form cementitious gels. However, the fact that ettringite is initially the predominant reactant with respect to slag hydration and calcium consumption, and thus has actually reduced the size of the 'calcium pool' available in the soil mix for the formation of cementitious precipitates, has a significant effect on the long term strength development of the soil specimens. This is reflected by the fact that, in contrast to the short-term strength, the long term strength (1 year) of specimens prepared in the presence of sulphates is inferior to specimens to which no sulphates have been added (Figures 7.2 and 7.5).

If no gypsum is added to the system, the strength development is substantially retarded due to a lack of a slag activation trigger. The added lime has principally been consumed by the soil modification process and a thin coating of cementitous gels has formed around the slag grain. Based on results obtained from the observation of the pH-value of the soaking solution of a kaolinite specimen compacted only with slag and gypsum (0L6S6G, section 7.3) and on observations by Motz and Geiseler [1987], it can be assumed that ggbs releases calcium after a dormant period during which it behaves relatively inertly. Feng et al. [1989], who investigated the degree of ion migration from the inner slag hydration product through the barrier layer, suggest that after the initial encapsulation reaction, Ca, Al and Si are major elements to migrate through the barrier coating into the pore solution. Thus the porosity of the initially rather dense inner slag hydrate increases and further migration is facilitated. This ion release is mainly time dependent, however, the current work suggests that its rate can be influenced by the curing environment, i.e. mainly temperature and humidity. The calcium release results in an immediate increase in the pH-value of the pore solution and has thus a further damaging effect on the outer layer of the slag grain. The higher pH of the pore solution contributes to an increase in the solubility of alumina and silica from the slag and the slag hydration is further accelerated. As already pointed out earlier, it is probably due to the fact that no calcium is consumed in the formation of ettringite (with little strength enhancing effect) that the ultimate strength of specimens without gypsum addition (Figure 7.5) is higher in comparison to specimens in which the slag hydration has been accelerated by the addition of gypsum. However, this high ultimate strength is achieved at the cost of accelerated early strength development, a phenomenon which will be reviewed subsequently with regard to applications in practice.

It has been established that in the presence of gypsum, disruption of the protective slag grain coating due to the formation of calcium sulpho-aluminate product, which in fact forms not only on the slag grains but also in a more colloidal form on the clay particles [Abdi, 1992], enhances slag hydration in the short term. The disruption of the pseudomorphic layer is, as pointed out earlier, partially due to the utilisation of elements (mainly calcium) from the outer protective slag coating, but is also promoted by the fact that calcium sulpho-aluminate product formation removes Ca^{2+} from the pore solution. The 'external' ettringite formation process on the clay particles precedes the formation of ettringite on the slag grain and provides a 'sink' for Ca^{2+}. Thus the calcium ion concentration gradient across the protective pseudomorphic layer on the slag grains is strongly increased, which favours its disruption based on an osmotic mechanism in order to obtain concentration equilibrium between the pore solution and inner slag product (Figure 9.1a). If no gypsum is present in the system, it takes a much longer time for the smaller Ca^{2+} concentration difference between the pore solution and the protective membrane to reach a level which can be considered large enough to contribute to the disruption of the outer slag grain coating by ion migration (Figure 9.1b). Subsequently slag hydration is substantially delayed.

Considerations of calcium ions released by the slag throw new light on the behaviour of specimens stabilised with only gypsum and ggbs (section 7.3). Although the kaolinite system stabilised only with ggbs and gypsum would generally be considered as 'stable' (associated with relative volume stability during soaking and little strength development), substantial secondary swelling was observed, the onset of which occurred earlier as the amount of added gypsum increased (Figure 7.38). An attempt at an explanation of this secondary swelling must also take account of the observations of the behaviour of the kaolinite free 50% ggbs/50% gypsum system during soaking, which exhibited only negligible expansion but developed substantial strength. This system also produced ettringite crystals with the same peculiar flower-bunch like habit (Figure 7.43) that was observed in the kaolinite-gypsum-ggbs system (Figures 7.40 and 7.41).

The difference between the kaolinite-ggbs-gypsum system and the ggbs-gypsum system is clearly the amount of stabiliser present (12% in the former and 100% in the latter) but also the presence of kaolinite as a substantial alumina (and silica) source.

Both systems are characterised by an initial dormant period at the beginning of which (i.e. during mixing) the outer coating forms around the slag grain [Feng et al., 1989]. In the kaolinite-ggbs-gypsum system, upon soaking, the pH of the soaking solution is
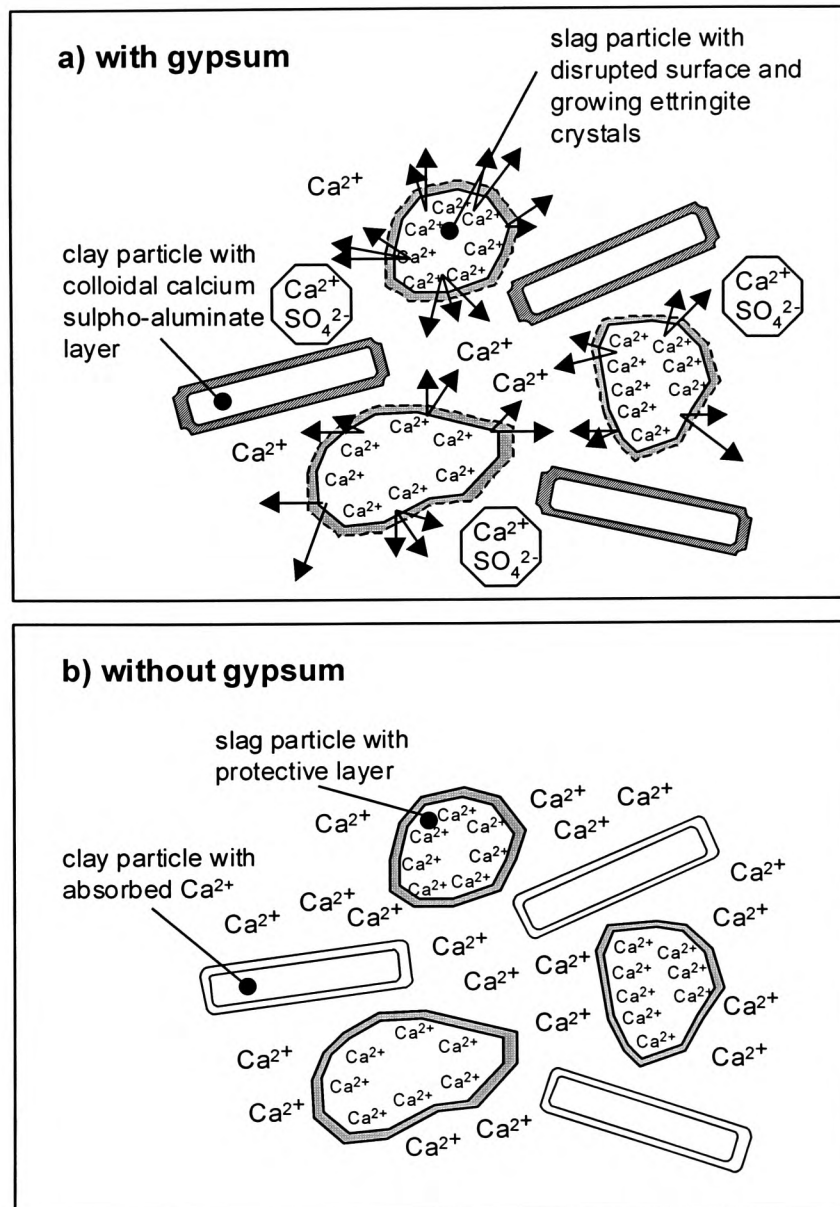
Figure 9.1 *Reactions in the kaolinite-lime-ggbs system in the presence (a) and absence (b) of gypsum*

around 6 (made slightly acidic by the added gypsum) and, although this might not be exactly identical to the pH-value of the pore solution, there is not sufficient alkalinity provided to promote an attack on the slag grain coating, with subsequent provision of

the components necessary for the formation of cementitious products during slag hydration. However, the tendency of ggbs to release calcium after an initial dormant period results in a subsequent and substantial increase in the pH-value of the pore solution (Figure 9.2).

It should be noted that investigations by the current author have demonstrated that the pH of saturated gypsum solution is increased from around 6.0 (saturated gypsum solution) to 11.6 by introducing lime at a gypsum:lime ratio of 9:1 (saturated lime solution has a pH of 12.4). If the ratio is reduced to 7:3, a pH of 12.1 can be obtained. Thus it appears that minor amounts of calcium (and OH^- groups) released by the slag
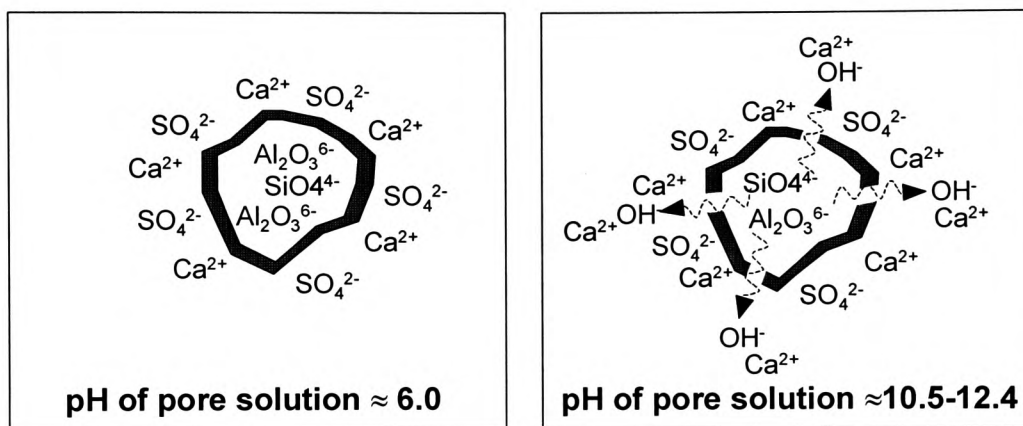
Figure 9.2 *Change on the pore solution due to calcium release from the ggbs grains*

can increase the pH of the pore solution sufficient to promote self-activation. The effect of the self activation process is reflected by good strength development of the moist cured mix 0L6S6G (less moisture availability = reduced and slightly delayed ion migration [Clark and Brown, 1999]) at extended curing times (between 28 and 90 days)) as illustrated in Figure 7.42. It is therefore not surprising that Kinuthia [1997] observed only negligible UCS-values for kaolinite specimens stabilised with 6% ggbs in the presence of 2 and 4% gypsum after a moist curing period of *only* 28 days.

However, in addition to a certain degree of self activation at a later stage (see strength development in Figure 7.42), secondary swelling is induced in the kaolinite-gypsum-ggbs system in the presence of an abundance of water provided during soaking. All previous work on lime-stabilised kaolinite in the presence of sulphates [Abdi, 1992, Kinuthia, 1997] has demonstrated that swelling occurs as a result of expansive calcium sulpho-aluminate product forming on the surface of the kaolinite particles. However, for

calcium sulpho-aluminate product to form on the kaolinite particles in this system, additional calcium is required and this can only come from the hydrating slag which will release Ca^{2+} into the pore solution. Together with the alumina from the kaolinite, there is at the end of the dormant period sufficient alumina and sulphate (from the gypsum) in the pore solution to form calcium sulpho-aluminate product, which is known to result in water absorption and subsequent swelling when formed in the presence of water. The shift in the onset of swelling in relation to different gypsum additions suggests that sulphate is the critical compound during the ettringite formation process. The sulphate added in the form of gypsum is the only sulphate source (Feng et al. [1989] showed that sulphate migration from the slag is negligible) and lower availability results in less ettringite formed at a lower reaction rate and thus a delay in the onset of expansion. The ettringite needles observed in these samples appear to have formed at localised points (resulting in the characteristic 'flower-bunch' like habit) from which the calcium source has derived [Motz and Geiseler, 1987]. This source is believed to be the disrupted slag grain surface (Figure 9.3).

The main reason for only negligible expansion (0.88% after soaking for 20 weeks) in the pure binder system (50%gypsum and 50%ggbs) has to be the absence of kaolinite, which also results in a much lower alumina concentration. The presence of some flower-bunch like ettringite crystals (Figure 7.45) and a peak in the TG analysis at around 120 °C (Figure 7.44) demonstrates that ettringite has formed along with C-S-H gel (peak at ~140 °C). However, the absence of kaolinite particles as potential formation sites of 'colloidal' ettringite inhibits the formation of potentially swelling calcium sulpho-aluminate product. It should be noted that the relatively high strength achieved in this system will also contribute to resisting any potential swelling pressure created by ettringite forming under saturated conditions.

In the clay system, released calcium is immediately utilised for the formation of colloidal calcium sulpho-aluminate product on the clay particles, which has been shown to be highly expansive if an abundance of water is present [Mehta, 1973b, Wild et al., 1993]. It is this colloidal product which is believed to be responsible for the initiation of expansion in the clay system. In addition, some ettringite rods, will form on the outer slag surface, during ion migration (Figures 7.40 and 7.41). However, based on findings by Mehta [1973b] there are indications that this lath-like ettringite habit is not responsible for swelling.
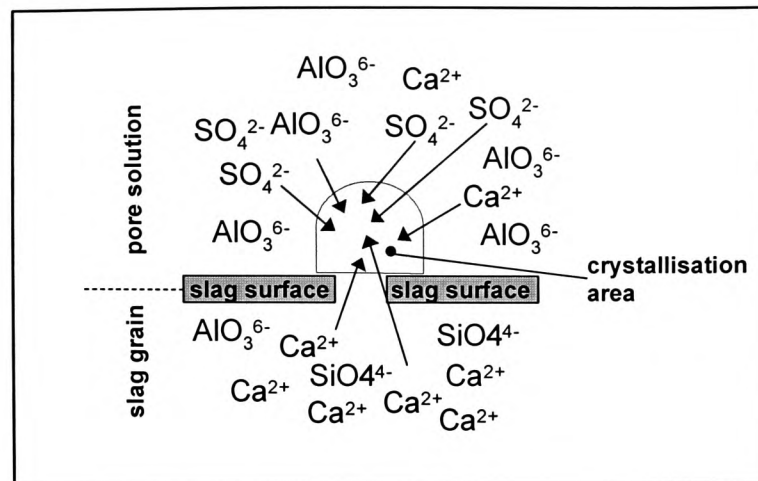
Figure 9.3 *Crystallisation area of ettringite on disrupted slag surface*

In the absence of clay, ggbs is the only possible alumina source in the binder system with an alumina content of 11.6% (Table 5.14) (consideration of the ASTM standard C989-1985 thus suggests a classification as a 'low-alumina' slag, whereas at least 18% Al_2O_3 is required for a 'high-alumina' slag). As already pointed out for the clay-lime-gypsum-ggbs system, ettringite formation during the early stages of Ca ion migration (initiated by the concentration gradient) appears to be the trigger in the binder system, which initiates the slag hydration due to interference with the outer slag grain surface layer.

Depending on the presence of clay and thus the rate of colloidal ettringite/cementitious phase production, it is either calcium sulpho-aluminate product (formed on the clay particles, Figure 9.4a) which will be produced to a higher degree and result in swelling (as observed for specimens with low binder ratio Figure 7.38) or the absence of nucleation sites for colloidal ettringite will lead to the fact that only negligible expansion can be recorded (Figure 9.4b). In addition cementitious gels will further contribute to an increase in inner bonding.

In addition to the availability of the critical ettringite constituents, the effect on the pH-value, particularly by the gypsum:lime ratio on observed expansion has to be considered (Table 7.4). As demonstrated by the author, an increase in G:L ratio will generally result in a decrease of the pH-value of the pore solution. Thus low G:L ratios (<4) will provide a comparably high pH which will result in rapid cementation due to effective slag hydration and thus resist expansion. Also initial rapid reaction allows expansive

products to form in the very early stages prior to saturation, and hence reduces its influence on swelling. As the G:L ratio increases to around 4, slag activation will be

a) kaolinite-ggbs-gypsum system

slag particle with disrupted surface and growing ettringite crystals

clay particle with colloidal calcium sulpho-aluminate layer

N.B.: Initially no freely available Ca^{2+} in the pore solution, i.e. high concentration gradient between encapsulated slag grain and pore solution

b) ggbs-gypsum system

N.B.: Initially no freely available Ca^{2+} in the pore solution, i.e. high concentration gradient between encapsulated slag grain and pore solution

Figure 9.4 *Gypsum-ggbs interaction and formation of potentially swelling calcium sulpho-aluminate product in the presence (a) and absence (b) of kaolinite*

increasingly retarded (pH-value of the pore solution drops) providing poorer cementation and hence less resistance and greater expansion. At even higher G:L ratios (>4), although there will be even less cementation, the pH will fall to a level at which ettringite is unstable [Chartschenko et al., 1993]. Its formation will be retarded and expansion will decline.

It is well established that the pozzolanic reaction initiated by the addition of lime in soils is very sensitive to temperature [Arabi and Wild, 1989, Bell and Coulthard, 1990]. Reduced environmental temperatures slow the process down substantially and can even result in a dormant period during which no further reaction occurs until the temperature rises again [Bell and Tyrer, 1987]. Takemoto and Uchikawa [1980] assessed the amount of reacted portlandite in a system with Japanese pozzolana over a temperature range from 20 to 60 °C and found an increase in the amount of reacted $Ca(OH)_2$ with increase in curing temperature, which was particularly emphasised for shorter curing periods up to 28 days. With the results derived from the current investigations, an attempt to assess the temperature sensitivity of the slag hydration mechanism can be undertaken.

Figure 7.2 a-c compares the shear strength development of slag-lime stabilised specimens in the presence of 6% sulphates over a temperature range from 10 to 30 °C. The gradual increase in strength gain with increase in temperature suggests that the slag hydration process is sensitive to temperature. This is also reflected when the development of the coefficient of permeability (Figure 7.26) is considered. A higher reaction rate is here reflected by a significant reduction in k-value after curing periods of 28 days and beyond if curing is at 30 °C. The temperature-accelerated reaction results in formation of increased amounts of cementitious products which affects the specimen porosity even for curing periods of up to 28 days [Takemoto and Uchikawa, 1980] This is supported by findings of Johansson [1978] who assessed the effectiveness of slag cements in countries with harsh winters. He found that not only does slag cement hydrate initially much more slowly at temperatures lower than 20 °C in comparison to normal PC (which is to be expected, see Bijen [1996]) but it also achieves a reduced ultimate strength. This can partially be attributed to the fact that the solubility of most chemical compounds is reduced when the temperature of the pore liquid drops. However, the solubility of gypsum and lime actually increase (although only marginally) with reduced temperature. Thus the main reason for the observed retardation is the fact that temperature affects the reaction kinetics which influence the number of reactant molecules available to achieve the minimum kinetic energy needed to react. In stabilised soil, evidence for the fact that the slag hydration process is only slowed down and thus prolonged, without temperature affecting the ultimate strength that a mix can achieve, is apparent when the shear strength values after different curing periods in different curing environments are compared (Figure 7.2). The same shear

strength, say ~1000 kN/m², may be obtained if, for example, a specimen of mix composition 2L8S is either cured for 24 weeks at 10 °C, for 12 weeks at 20 °C or for 1 week at 30 °C. Observations like these support the utilisation of an 'equivalent age' concept, which is sometimes used to equate strength results for concrete deriving from curing at different temperatures. However, whereas a relationship can be established reasonably easily for pure Portland cement paste, as is achieved with the Nurse-Saul formula (equ. 9.1),

$$F = \frac{(T+10)}{30}$$ **(equ. 9.1)**

where F is the equivalent age factor and T is the actual curing temperature (reference temperature = 20°), the concept is somewhat harder to apply to slag blend cements [Glasser, 1991]. The difficulties become even more substantial when inhomogenities in stabilised soils and subsequently greater variability of the strength results have to be taken into account. Thus boundary conditions for an 'equivalent age' concept for stabilised soils would have to consider in addition to stabiliser combination and amount, the sulphate, sulphide and organic content and compaction density and moisture content of the specimen.

An apparent anomaly exists in that the reduced strength exhibited at lower curing temperatures (Figure 7.2) is not reflected by a modified pore size distribution, i.e. reduced percentage of pore volume occupied by fine pores (r≤0.05μm) (Figure 7.17). This could be taken as further indication that it is not solely the presence of the cementitious precipitates which affects the exhibited strength of a specimen, but mainly the degree of interlocking obtained between the precipitated gel and the soil particles. In the case of the shear strength parameters the presence of gel was introduced to explain the change in apparent cohesion and interparticle bonding was identified as the cause for increased friction. There are also two strength enhancing structural changes, i.e. the presence and the interconnectivity of cementitious precipitates, which appear to affect pore size distribution and exhibited strength, respectively.

The significance of permeability in determining the durability of concrete has been recognised for some time [Mehta, 1992, Diamond, 1999] and a similar influence would be expected for stabilised soils. The possibility of chemical attack due to sulphates in ground water or the role of permeability in the resistance to frost action in fact confirm

that this is also an issue for stabilised soils. Data from the current study indicate that the addition of ggbs as stabilising agent results in a more rapid reduction in the coefficient of permeability at all curing temperatures in comparison to stabilisation with 2% lime alone (in the presence of gypsum, Figure 7.26). The development of the observed k-values is somewhat less systematic in the absence of gypsum (Figure 7.27), however, all specimens which exhibited higher strength (Figure 7.5) were also found to have comparably low k-values. Thus, there is evidence that cementitious precipitates, which also contribute to the strength enhancement, form in the pores of the soil matrix and subsequently reduce the pore space, which itself contributes to the flow of water through the system [Scherer, 1999]. Whereas after short curing periods the sole presence of cementitious precipitates results in a significant reduction in the coefficient of permeability (i.e. after curing periods of only 4 weeks at 30 °C (Figure 7.26c)), they still lack interconnectivity and well-developed bonding interlinking the soil particles, which would subsequently be reflected in the development of higher strength (Figure 7.2c).

The development of permeability of lime-slag stabilised soil has to be appreciated as a two stage process. In an initial step, cation exchange and subsequent flocculation initiated by the added lime, result in increased permeability, based on reduction in the thickness of the water layer surrounding the clay particles [Arabi and Wild, 1989]. This is reflected by an overall increase in k-values for specimens cured for up to 1 week in comparison to specimens tested immediately after compaction (Figure 7.26). However, comparison with k-values obtained from the kaolinite-slag-lime system after 1 week (Figure 7.27), where flocculation results in only marginal changes to k-values obtained from immediately tested specimens (although the same amount of lime was added), suggests that cation exchange is only one component which affects the sample's capability to contribute to flow after short curing periods. The difference in the systems is the presence of gypsum, which was earlier identified as being an accelerator of the slag hydration process by interference with the protective layer surrounding the slag grain during the formation of ettringite. It appears logical that this ettringite formation process, resulting in needle-shaped crystals during the pre-hydration phase, affects the pore space (due to the nature of the ettringite habit) and thus the exhibited k-values. The needles will open up pores, which will not be completely filled with the sulpho-aluminate hydrates and thus allow additional water flow. Subsequently, however, this

space is utilised for the precipitation of cementitious products and the closing off of pore space and reduction in interconnectivity between pores which is particularly influenced by the curing temperature (Figure 7.26). Thus at high curing temperatures the k-values drop more rapidly.

It is well recognised that not only the overall porosity but also the manner in which pores are distributed within the specimens have an effect on the flow of water through porous media [Manmohan and Mehta, 1981, Wild et al., 1987, Goto and Roy, 1981]. However, care has to be taken when attempts are made to correlate observed k-values to measured porosity values from MIP investigations. This becomes evident when the reader is reminded that no systematic correlation between the development of the observed k-values and the measured total intruded pore volume could be established in the current project. The key difference between results obtained from permeability tests and quantitative pore characteristics deriving from mercury intrusion is the fact that the former measures k-values in-situ, i.e. on the saturated samples, whereas the latter technique requires the specimens to be dried thoroughly. Shrinkage as a result of water loss cannot be avoided, even if drying is carried out in a gentle manner as in the current project [Diamond, 1970, Wild et al., 1995, Scherer, 1999]. Although the presence of cementitious precipitates will (in the saturated condition) reduce pore space, they will also shrink on drying and, due to internal restraint, this will open up some new pore space during drying. Investigations into the structure and properties of inorganic gels affected by shrinkage has revealed that due to the scale of the porous matrix, capillary pressures of the order of 10 to 100 MPa develop, when liquid evaporates from the gel [Scherer, 1999]. Thus, it is suggested that specimens are more affected by shrinkage when their pore skeleton is not capable of withstanding the stresses deriving from water evaporation. Scherer [1999] based his investigations into the effects of drying shrinkage on cement pastes. He suggested that drying shrinkage of specimens made of cement paste can be reduced by ageing prior to drying. In contrast, the pore structure of stabilised soils is substantially weaker, i.e. the effects of unavoidable shrinkage are bound to be even more pronounced [Diamond, 1970]. Thus only the presence of formed cementitious products, particularly when they have achieved a higher degree of densification and are thus less affected by water loss, can counteract the collapse of the pore structure initiated by water evaporation. The skeleton of the cementitious products supports the pore structure and hence reduces the effects of shrinkage. Evidence for this is apparent in total porosity measurements illustrated in Figure 7.14 at various curing

periods. The general reduction in porosity with increase in ggbs content can mainly be attributed to the slightly denser packing when the amount of added ggbs is increased (accompanied by a relatively small reduction in lime addition, due to a higher binder content) and thus less flocculation. However, the presence of cementitious products formed during slag hydration, is confirmed by an increase in the percentage pore volume with radius <0.05μm with increase in ggbs addition (Figure 7.16). In contrast to specimens cured at 10 °C, samples with high slag additions cured at 30 °C (Figure 7.14) exhibit a less significant reduction in total pore volume with increase in ggbs addition after a curing period of 1 week. Also for curing times greater than 1 week the total intruded pore volume increases, an effect attributed to shrinkage in drying. Strength data (Figures 7.5a and c) confirm that comparably large amounts of cementitious gels are produced after only short curing periods if curing is at elevated temperatures in the presence of gypsum (also supported by measured k-values in Figure 7.26c), however, much lower shear strength is obtained after 1 week if curing is only at 10 °C. Thus the collapse of pore structures due to the absence of a rigid supportive network [Wild et al., 1987] deriving from the gels will result in a more pronounced reduction of total pore volume at lower curing temperatures. Due to a much slower overall production of gel in the case of high slag addition specimens cured at 10 °C, a much higher variation in the measured pore volume can be observed (Figure 7.14a).

The fact that less cementitious precipitates are available to occupy pore space in gypsum free stabilised kaolinite is reflected by an overall higher pore volume (Figure 7.15). Due to the fact that the slag is dormant for a much longer period, which is the result of a lack of the hydration 'trigger' from gypsum (Figure 7.5, 7.7a and 7.9a), a much less obvious reduction in porosity with increase in ggbs content can be observed. However, curing periods of 24 weeks and 1 year at elevated temperatures result in the precipitation of cementitious products, which lead to a higher degree of densification and as a result to a significant reduction in total pore volume and higher strength (Figure 7.6 and 7.23b).

All engineering properties discussed so far (all of them related to microstructural changes) will affect the resistance of stabilised ground to frost action. Changes on a microscale have to be considered when the behaviour of specimens during freeze-thaw cycling is assessed. However, the frost resistance of lime-slag stabilised and thus partially cemented soil has to be analysed with reference to freeze thaw mechanisms

characteristic for both pure soils and cement. Due to the comparably small stabiliser content within the soil mass (up to 10%), the formation of ice lenses are still likely to occur (in particular for specimens tested after short curing periods and consequently with less cemented structures) similar to those in pure soils. In contrast, resistance to freeze-thaw cycling of specimens which have exhibited substantial strength increase due to good cementation has to be analysed with reference to mechanisms usually attributed to frost damage in concrete, i.e. the 'closed container mechanism' and the 'hydraulic pressure hypothesis' (see also section 3.2.1.2.3). This means that the behaviour of stabilised soil specimens subjected to frost action is complex. Figure 9.5 gives an overview of the physically and chemically induced structural changes that can occur within a stabilised soil, which together with the major engineering properties influence the ability of the material to resist severe frost action.
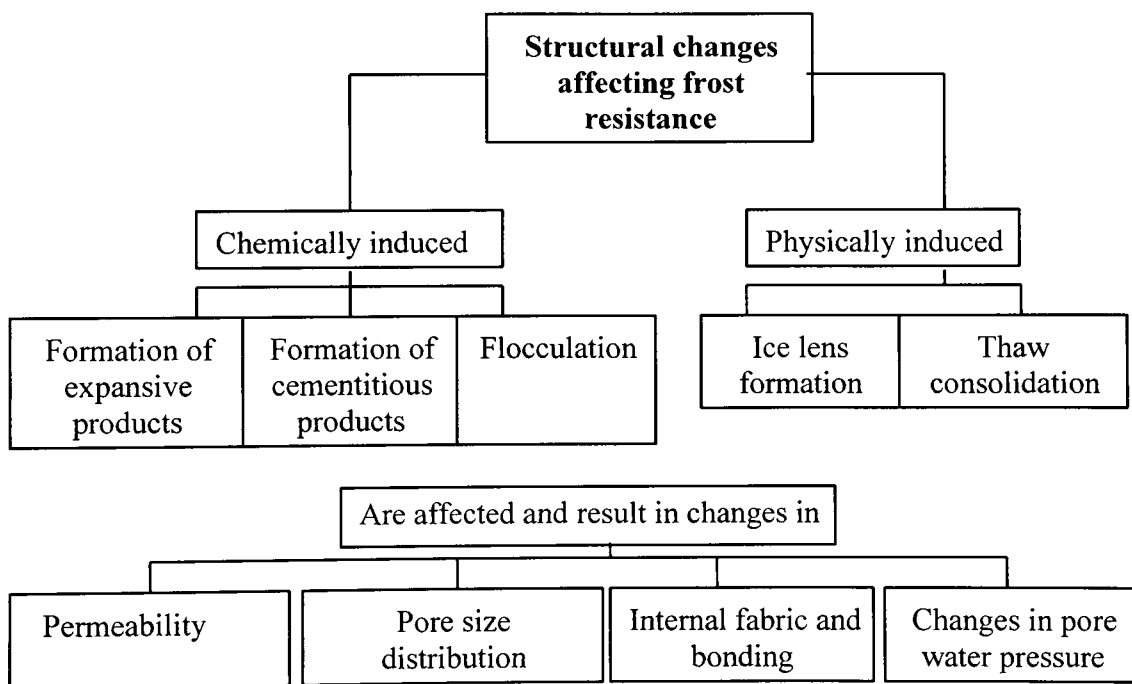
Figure 9.5 *Structural changes and engineering properties affecting the frost susceptibility of lime-slag stabilised clays*

The internal fabric and bonding, result from the formation of cementitious products within the specimen structure, and are generally considered to be of major significance with regard to the frost resistance of stabilised soils [Arabi and Wild, 1989]. However,

as a 'chemical' component the presence or absence of gypsum has a fundamental effect on the behaviour of lime-ggbs stabilised specimens during frost action (Figure 7.30). With gypsum being the key compound in the formation process of ettringite, its significance for the current study is manifested in the fact that specimens without gypsum addition exhibited little inner bonding during shear, compressive and indirect tensile testing (Figures 7.5 7.7a and 7.9a) but outperformed kaolinite specimens with sulphates (which had shown to have developed significant strength) with regard to their volume stability during frost action. It has been established that specimens prepared with gypsum show, up to an age of 24 weeks, much higher pore refinement in comparison to gypsum-free specimens, manifested in a higher percentage of pore volume occupied by pores with a radius <0.05µm (Figure 7.17), and strongly reduced k-values (Figure 7.26). However, together with the overall lower porosity of these specimens in comparison to specimens prepared in the absence of gypsum (Figures 7.14 and 7.15), findings by Stark et al. [1997] suggest that a higher degree of pore refinement and lower coefficients of permability, which are generally associated with being advantageous for sample durability, are in fact detrimental for frost resistance when gypsum is present in the specimens. Stark et al. [1997], who confirmed findings by Ouyang and Lane [1997], assessed secondary damage in concrete during frost action due to the presence of ettringite and pointed out that the damage mechanism is twofold. Firstly, the affinity of the calcium sulpho-aluminate hydrate for water increases the amount of moisture present in the microstructure during frost action, whereas, secondly, the presence of the phase itself restricts the room for expansion during the freeze-thaw attack. For the current study, the ettringite formation process (in specimens containing gypsum) will affect the frost resistance of specimens due to a higher degree of water uptake in the early stages of freeze-thaw cycling (Figure 7.29b in comparison to Figure 7.29d). Thus the modified, water-enriched specimen structure will have a tendency to expand to a higher degree during frost action to accommodate the larger amount of ice, although less pore space is available in dry specimens in comparison to gypsum free samples (Figure 7.33a). The inner bonding will thus be substantially weakened and further pore space will be created and filled with more, potentially detrimental moisture during the next thaw phase. Once water has gained access assisted by the high absorption potential of the ettringite, the initial lower porosity and the larger percentage

of smaller pores, which are advantageous for good strength development, are in fact detrimental with regard to volume stability during frost action.

Without gypsum, high slag additions and long curing periods lead to satisfactorily volume stability of stabilised kaolinite specimens during frost action. In comparison to gypsum containing specimens, particularly if they have low lime and high ggbs additions, gypsum free specimens have much less tendency to absorb water (Figure 7.33b). In addition the generally higher pore volume available provides less confinement to a smaller amount of moisture present, which leads to less volume change in comparison to gypsum containing specimens (Figure 7.33a).

The overall degree of specimen weakness during frost action is also reflected by the ultimate change in height after freeze-thaw cycling. In order to avoid substantial material loss during frost action (initial trials without material confinement resulted in specimens collapsing after a few cycles), a low restraint confinement method had to be found for specimens during freeze-thaw cycling. It was decided to utilise a rubber membrane. However, very weak specimens adopted a new, slimmer shape once their outer shell was sufficiently weakened by the formation of the freezing front (sample 2L0S6G in Figure 7.31). Only the dehydrated inner core which formed during freezing due to water migration to the freezing front in the outer shell of the specimens, retained some strength, whereas the outer areas were very weak, water-enriched and thus 'remoulded' by the rubber membrane. This was reflected in substantial height changes (Figure 9.6).
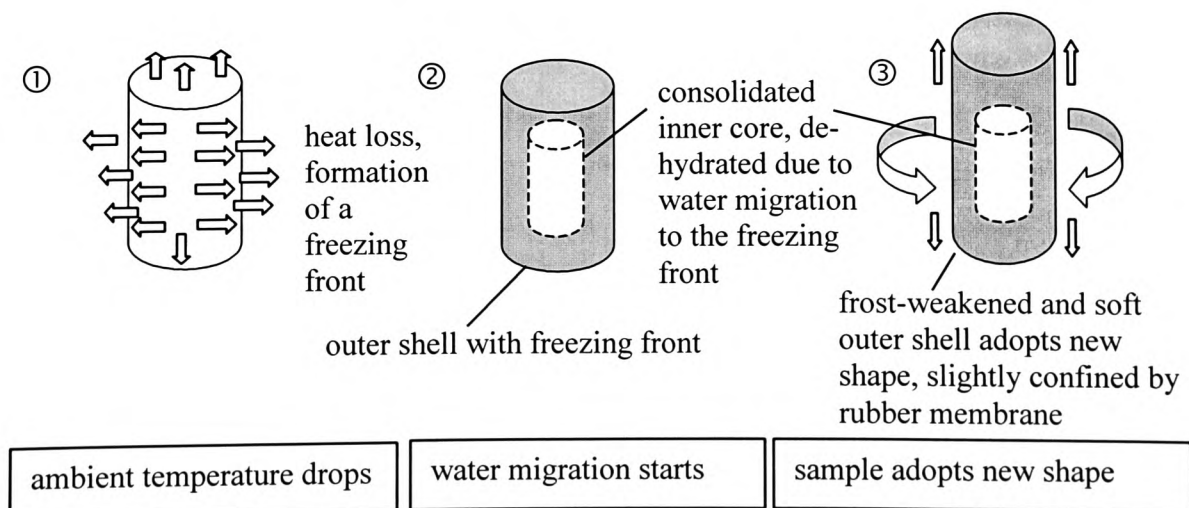
.**Figure 9.6** Frost induced height change of weaker soil specimens

At the end of freeze-thaw cycling, specimens to which only lime as a stabiliser had been added (2L0S), showed rather large height increases. However, they exhibited little variation in height, volume and weight change with respect to the various initial moist curing periods. The degree of variation in the measurements increased with increase in slag content (Figure 7.30). Without slag and with only a little lime there is limited if any formation of cementitious products, which has been shown to affect the resistance to frost action [Arabi and Wild, 1989, Brandl, 1981]. As suggested by Brandl [1981], there is some likelihood that the flocculation initiated by the lime results in additional pore space, which can be utilised to relieve hydraulic pressure during freezing. However, the sample structure is bound to be very weak and thus overall large changes in height and volume were recorded.

Although it is generally believed that the frost resistance of ground is influenced by its tensile strength, no correlation between these sample characteristics could be identified for the current project. Townsend [1965] also reports that studies into the suitability of the tensile splitting test as a measure of resistance to frost heaving of lime-stabilised soils, were discontinued because they showed lack of correlation. He suggested further investigations in order to understand the mechanisms by which stabilised soils resist deterioration during frost action.

9.3 Lower Oxford Clay

In contrast to results obtained from artificially prepared kaolinite mixes, observations with regard to the development of the engineering properties of stabilised Lower Oxford Clay have to be assessed with particular care (as emphasised by the apparently anomalous linear expansion of the mix 2L6S in Figure 7.45 due to soil inhomogenity). In addition the following points should also be taken into consideration:

i) Lower Oxford Clay is a natural clay with localised variability in composition

ii) The sulphates in this clay are mainly secondary in nature and are expected to increase by oxidation of the sulphides (mainly pyrites) present, particularly as a result of the increase in alkalinity when lime is added and exposure to the atmosphere during mixing.

iii) Lower Oxford Clay has a wider grain size distribution than kaolinite (Figure 3.2) with a larger percentage of coarse particles

iv) Lower Oxford Clay contains a number of compounds, for example organic components, which have not been identified in detail but will affect its performance in the current project. For example, when the swelling of the lime-stabilised specimen of mix composition 2L0S (Figure 7.45) is compared with that of a compacted specimen made of pure Lower Oxford Clay, the latter showed a linear expansion curve, which was basically identical to the one plotted for the mix 2L0S in Figure 7.45. This is indicative of the fact that swelling in Lower Oxford Clay specimens is not solely caused by lime-sulphate interaction but by reactions amongst other soil compounds within the Lower Oxford Clay. However, two different types of swelling have to be distinguished. Terzaghi and Peck [1967] showed that *all* remoulded clays have a tendency to swell. This is due to the further absorption of water molecules between the realigned clay particles and is usually reflected by quick, instantaneous expansion on soaking. In contrast, continuously increasing expansion with soaking time over an extended period (in this case over 3 months), as observed for both stabilised (Figure 7.45) and pure Lower Oxford Clay, is indicative of chemical reaction as the underlying cause.

The strength development observed for slag-lime stabilised kaolinite specimens due to the hydration of the added ggbs was identified to be a function of the amount of sulphates (as gypsum) present, which activates slag hydration (Figures 7.7 and 7.9). In

contrast the strength gain in stabilised Lower Oxford Clay appears to be determined predominantly by the rate by which sulphides oxidise to sulphates, which then accelerate the slag hydration. Although the initial sulphate content of Lower Oxford Clay, prior to stabiliser addition and mixing is small (Table 5.8), a pH and probably temperature dependent oxidation process will convert sulphides to sulphates [Jackson and Cripps, 1997]. The rate of this conversion process is bound to be high during water addition and mixing in the atmosphere and in the initial stages of curing. This has been confirmed by Wild et al. [1999b], who have shown that the sulphate content (wt.% SO_3) of the Lower Oxford Clay used in this study increased from 0.97% for the dry material to 1.92% after mixing with 2% lime and water and subsequently mellowing for 3 days prior to compaction followed by a seven day moist curing period. The sulphate content further increased to 3.76% if the moist curing period was followed by 14 days of soaking in aerated water. In addition to the formation of cementitious phases, however, a less uniform grain size distribution within the natural clay, which results in more resistance to shear failure, led to the fact that stabilised Lower Oxford Clay showed better shear strength development at higher ggbs additions than stabilised kaolinite (Figure 7.46). Also, a significant sulphate source from the oxidation of sulphide might be expected to result in better early strength development due to the accelerating effect described in section 9.2 (note that the potential sulphate content of Lower Oxford Clay, if all sulphide is oxidised to sulphate, is 6.24% SO_3 (see section 5.1.3)). If only lime is added as a stabiliser (2L0S, Figure 7.46), the presence of organic matter has to be considered to establish the cause of the generally lower strength in comparison to stabilised kaolinite (2L0S6G, Figure 7.2). Its presence has been shown to retard or even inhibit hydration due to its affinity for calcium ions [Bell and Coulthard, 1990]. Thus less calcium to initiate the pozzolanic lime-clay reaction is available and only marginal strength gain over long curing periods can be obtained for these specimens.

The accelerating effect of the oxidised sulphides on the formation of cementitious gels as proposed in section 9.2 for kaolinite, is very well illustrated when the UCS-development of stabilised Lower Oxford Clay (Figure 7.50) is considered. The compressive strength increases with increase in ggbs content and for higher ggbs contents there is a systematic increase in strength with increase in curing period. It is apparent from Wild et al.'s work [1999b] that the amount of sulphate increases with increase in curing time. Subsequently longer curing periods will provide additional sulphates, which are then available to contribute to the slag hydration process by

promoting further slag hydration. Thus longer curing periods will result in higher strength.

In addition to a higher degree of activation and thus a higher rate of slag hydration by oxidised sulphides, the overall coarser Lower Oxford Clay with a lower clay minerals content will require less cementitious gel for its particles to be bound together in a rigid network. Subsequently, less cementitious products would be expected to result in higher strength development in comparison to kaolinite. The kaolonite structure, determined by uniformly fine particles has a much larger total surface area per unit mass and thus requires at a given minimum thickness a larger amount of cementitious product to obtain the same cementing effect that can be achieved with less gel for the comparably coarse Lower Oxford Clay. Some of the large and possibly inert non-clay mineral particles within the Lower Oxford Clay, once bonded together in a well-cemented specimen structure, will contribute significantly to the exhibited strength, particularly by resisting shear. This is reflected in the lower strain at failure for stabilised Lower Oxford Clay (Figure 7.48), in comparison to stabilised kaolinite (Figure 7.3), even at shorter curing periods and over the whole temperature range

Whereas stabilised kaolinite exhibited a reduction in total porosity with increase in ggbs content (Figure 7.14), a slight increase in intruded pore volume for stabilised Lower Oxford Clay is observed (Figure 7.52). There is generally no doubt that cementitious precipitates, their presence being reflected by strength (Figures 7.46, 7.50 and 7.51) and pore size distribution development (Figure 7.53), will affect the porosity of Lower Oxford Clay. However, there is indication that the nature of the Lower Oxford Clay itself is influencing the microstructural development. Evidence can be gathered by consideration of Figure 7.53, where a relatively small increase in fine porosity ($r \leq 0.05 \mu m$ characteristic for cementitious gels) of only ~15% with increase in slag addition from 0 to 8% suggests a relatively small influence on cementitious gel formation. This is also reflected by the fact that after extended curing times only high slag additions provide a marked reduction in k-values for stabilised Lower Oxford Clay particularly if curing is at 30 °C (Figure 7.56c), whereas for stabilised kaolinite after curing periods of 1 week all compositions give low k-values. Observations for kaolinite indicate that the percentage of pore volume occupied by the pore fraction with $r \leq 0.05 \mu m$ has basically doubled (Figure 7.14) and the k-values drop to a minimum

within a curing period of only 4 weeks. Thus there is evidence that the development of cementitious gel in Lower Oxford Clay will result in only negligible porosity change. In addition, the somewhat unexpected increase in porosity of Lower Oxford Clay with increase in ggbs content can be explained with reference to observations of cement and cement-blend pastes investigated by Xi and Jenning [1997]. They showed that the pores of the outer product, surrounding a hydrating particle, are slightly larger in size than the pores found in the inner layer and established that shrinkage within the structure (in the current work initiated by the drying phase prior to MIP) is mostly initiated by shrinkage of the outer layer of gel within the hydration mass. However, due to non-shrinking inclusions in the porous network, the shrinking components (i.e. the gel and the clay) cannot pull the inclusions together and instead this opens up the pores. Due to the presence of a wide range of coarse, partially inert non clay mineral impurities in Lower Oxford Clay, in comparison to the 'pure' kaolinite, the above described mechanism is very likely to increase the amount of pores observed after drying with increase in the degree of slag hydration (Figure 9.7). Once internal shrinkage within the specimen occurs pores are opened further, or even newly created, to an increasing degree. The increase in total porosity with increase in ggbs content is more pronounced at higher curing temperatures than if curing is at 10 °C (Figure 7.52), due to higher initial rates of gel production which subsequently result in higher porosity after drying.

Overall micropore strength-correlation results are much better defined in the case of kaolinite because it is a much more homogenous soil, which when stabilised gives a more consistent and reproducible material. The more heterogeneous and variable Lower Oxford Clay is a less consistent material. This becomes evident when the strength-pore characteristic relationships in Figure 7.54 are considered. On a microscale the results for stabilised Lower Oxford Clay suggest very limited pore refinement (Figure 7.53). Within the bulk sample macro flaws will therefore be present, which will lead to reduced strength. Thus, as indicated in Figure 7.54b, specimens showing limited pore refinement exhibit low strength, whereas specimens showing good pore refinement do not always exhibit high strength. It is therefore suggested that the presence of coarser particles in Lower Oxford Clay is principally responsible for the different porosities and pore size distributions observed for this material in comparison to kaolinite.
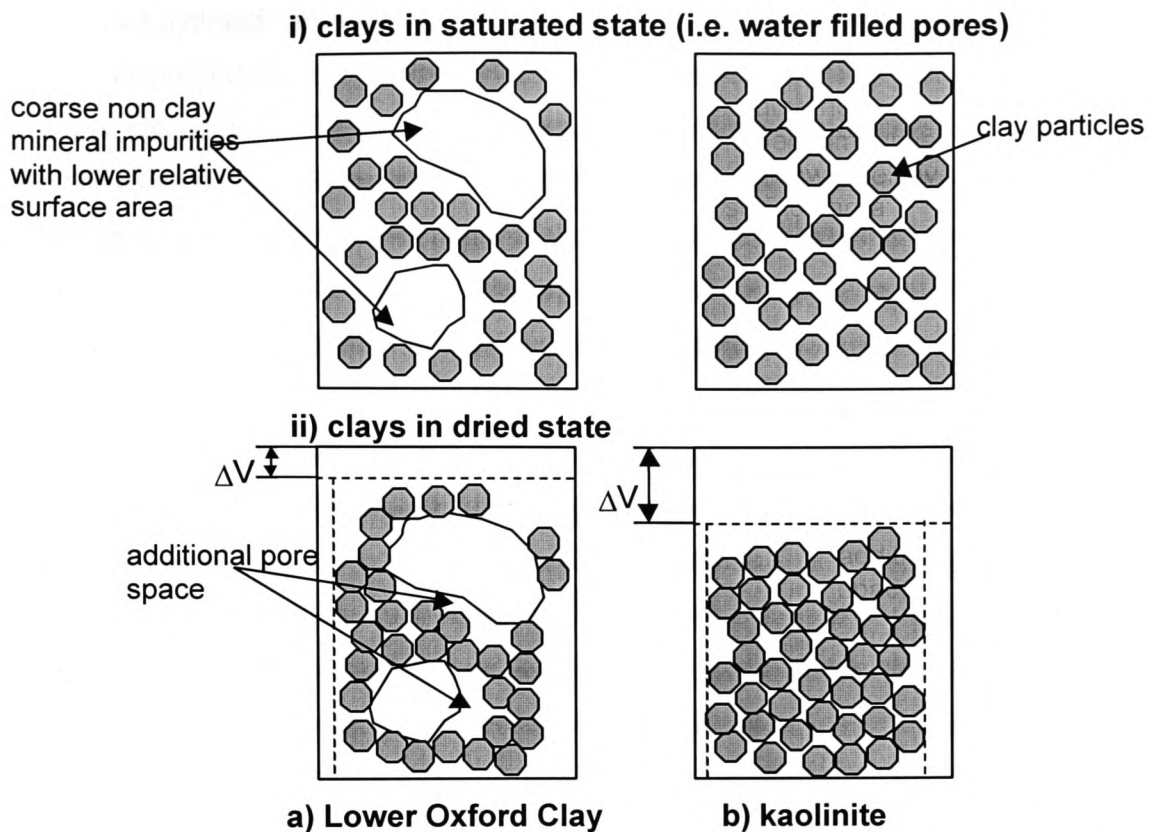
Figure 9.7 *Particles in a) Lower Oxford Clay and b) kaolinite in saturated (i) and dried (ii) condition*

Stabilised Lower Oxford Clay appears to be overall less sensitive to frost action than stabilised kaolinite, generally showing smaller height and volume changes (Figures 7.30 and 7.57). Stabilised Lower Oxford Clay also responds less to the confining pressure of the rubber membrane, which appears to be the main cause for the marked elongation of the kaolinite specimens (Figure 9.4). Due to a coarser soil structure and higher k-values (Figure 7.56) an overall higher flow rate (and thus less hydraulic pressure in the pores) during the water migration to the freezing front is possible, particularly if stabilisation was carried out with lime only or with low ggbs additions.

The effect of weight gain due to water absorption on the volume change (Figure 7.58) is contrary to the relation observed for kaolinite, where in the absence of gypsum an increase in ggbs content resulted in higher w/v ratios for longer curing periods (Figure 7.32b). This means that longer curing periods prior to frost action result in larger volume changes relative to water absorption than shorter curing periods. Although an increase in cementation with increase in curing period can be achieved, usually

associated with the provision of a stronger soil skeleton which should be able to counteract hydraulic pressure during freezing to some degree, the formation of sulpho-aluminate product might counteract this effect. As indicated for kaolinite, a reduction in the w/v change ratio (Figure 7.58) is indicative of a relative increase in the effect of weight gain (i.e. water absorption) on volume change. The effect is more pronounced when expansive products block some of the pore space and thus increase the hydraulic pressure developing during freezing [Stark et al., 1997, Ouyang and Lane, 1997]. The formation of these potentially detrimental products in sulphate-bearing kaolinite results in reduced volume stability after shorter curing periods, when the water absorption during the formation process leads to large volume changes (particularly when the pore space is, in addition, narrowed by precipitated cementitious products if high ggbs additions are present, even when only comparably little inner bonding has yet been achieved). In contrast, the duration of the curing period has only a small effect on the volume stability of stabilised Lower Oxford Clay (Figure 7.57c). The components for the formation of sulpho-aluminate product are readily available in the kaolinite-gypsum system but only negligible amounts of sulphates are immediately present after mixing in stabilised Lower Oxford Clay. Thus, little expansive product can form after short curing periods and good cementitious bonding can develop without too much calcium being consumed for ettringite formation. Alternatively, longer curing periods lead to a higher availability of sulphates, which will result in exertion of pressure within the stabilised soil skeleton and subsequently lead to reduced volume stability. However, no really significant change in volume will be noticed (Figure 7.57c) due to an already rather rigid specimen structure, which will mainly affect the height changes induced by the confining rubber membrane (Figure 7.57a).

Overall, longer curing periods prior to freeze-thaw cycling are advantageous for slag-stabilised ground (in the absence of effective activators) when sulphates are immediately available in the soil (kaolinite+gypsum), but they can be reduced when the sulphate source is secondary in nature (sulphides) and thus develops with time (Lower Oxford Clay).

Chapter 10 – Conclusions and recommendations for future work

The research was carried out to assess the potential utilisation of lime-activated ggbs in the stabilisation of sulphate-bearing clay soils. In particular the effect on engineering properties and underlying mechanisms has been addressed.
This final chapter summarises the conclusions which can be drawn based on the work carried out during the project and suggests further research avenues which might result in a useful contribution in understanding the role of ggbs as a soil stabilising agent.

10.1 Conclusions

The work presented in this thesis is the first comprehensive assessment of changes in the engineering properties of clay soils (in the presence and absence of sulphates) initiated by lime-activated ggbs. Laboratory studies and a full-scale field trial have been utilised to identify the influence of environmental conditions (temperature and moisture content), binder content and chemical composition of the soil on stabilisation. The investigated properties included strength development using unconfined and confined compressive and indirect tensile tests, durability assessment based on measurements of permeability, porosity and pore size distribution, and frost resistance. Additional experiments involved tests on the influence of gypsum on the swelling and strength development of slag-stabilised specimens.

The salient conclusions of the work are summarised below.

1. The utilisation of lime-activated ggbs as a soil stabilising agent results in substantial strength enhancement due to the formation of cementitious gels during the slag hydration process. However, it has been shown that the slag/lime ratio and the amount of sulphates present in the soil, have a large influence on the rate at which the hydration process occurs and subsequently on the engineering properties.

2. The presence of sulphates (gypsum) has been shown to affect particularly the early strength development of specimens (up to 24 weeks) but simultaneously results in a reduction of the ultimate strength obtained in comparison to gypsum-free specimens. It is suggested that the formation of ettringite consumes calcium, which would otherwise be available to contribute to the formation of cementitious gels and thus strength enhancement in the long term.

3. The influence of soil type on stabilised soil properties has been made apparent by comparison of a laboratory prepared soil mix (kaolinite in the presence and absence of gypsum) with a natural clay (Lower Oxford Clay with a high natural sulphide content). From the current study it can be concluded that the sulphate content and the particle size distribution (particularly in relation to larger, non clay mineral particles) are of particular significance when lime and ggbs are added as stabilising agents.

4. The addition of ggbs in sulphate-containing samples, results in overall rapid pore refinement and affects particularly the percentage of the pore volume occupied by pores with a radius $<0.05\mu m$. The increase in this pore fraction showed good overall agreement with the increase in observed strength. In the absence of accelerating sulphates, pore refinement due to delayed slag hydration was substantially reduced for curing periods of up to 24 weeks particularly at low curing temperatures. However, the ultimate strength values obtained after long curing periods, were higher than the values from specimens which had been activated in the presence of gypsum, the slag hydration accelerator.

5. It was established that shrinkage as a result of drying prior to mercury intrusion affects the stabilised soil specimens and thus influences the results of porosity and pore size distribution measurements. The effects of shrinkage (resulting in the collapse of weak soil skeletons in the absence of a supportive network of cementitious precipitates) are particularly pronounced and result in lower sample porosity for specimens in which little slag hydration, and thus only limited formation of cementitious products prior to drying, had occurred.

Comparably coarse, inert non clay impurities, as present in Lower Oxford Clay, result in overall reduced shrinkage and new pore space is opened when the drying clay particles, surrounding the impurities, shrink.

6. No firm conclusions can be made as to the influence of ggbs as a soil stabilising agent on the permeability of stabilised soil. Overall the formation of slag hydration products results in a reduction of the k-values. However, this reduction in permeability is more systematic only at high curing temperatures (30 °C) and after long curing periods at high ggbs additions.

7. The freeze-thaw resistance of ggbs-stabilised soil is significantly affected by both the sulphate content and the clay type. The greatest degree of volume stability after frost action was obtained for kaolinite specimens compacted with high slag/lime ratios in the absence of sulphates. There are strong indications that the formation of calcium sulpho-aluminate hydrates, which absorb large amounts of water during formation, affect the volume stability of specimens during freeze-thaw cycling, particularly when curing prior to frost action was only for short periods. If no sulphates are added, these compounds do not form and thus overall more pore space is available to accommodate hydraulic pressure deriving from water migration upon freezing.

8. Curing temperature affects the length of the dormant period prior to slag hydration and the speed at which the process occurs. Overall slag hydration showed similar temperature sensitivity as the lime-clay reaction, however, the effect of temperature retardation can be partially compensated for by an increase in the amount of ggbs added.

9. Investigations into the economic implications of the lime-slag stabilisation method, in comparison to the classic lime-cement method, have shown that it is price competitive. Although environmental factors have not been quantified in detail, there is, based on energy requirements and emissions during production, no doubt that lime-ggbs stabilisation outperforms techniques utilising lime and cement with regard to these aspects.

10. The onset of secondary swelling on soaking of sulphate containing specimens stabilised only with ggbs is substantially influenced by the amount of sulphate present. Initially, ggbs appears to undergo a dormant period, after which chemical interaction with the added sulphates results in the formation of potentially expansive products. The slag provides the source of Ca ions for the formation of ettringite if sulphates are present. Thus, the gypsum/lime ratio is significant in relation to the formation of calcium sulpho-aluminates and determines the swelling magnitudes when specimens are subjected to soaking.

10.2 Recommendations for future work

The current investigations have shown that there is significant potential for the utilisation of environmentally friendly ggbs in the stabilisation of land. However, depending on the clay type to be stabilised and thus the variety of different chemical compounds present, the stabilisation effectiveness will vary. In addition to sulphate content and particle size distribution, further factors such as the content of organic matter of a soil should be taken into consideration when stabilisation with lime-activated ggbs is undertaken.

Although the research project has addressed the key elements, which are relevant with regard to possible utilisation of ggbs-stabilised ground for practical work, it has largely been confined to an experimental study conducted on laboratory specimens. Comparison of obtained laboratory results with findings deriving from full-sale trials showed good agreement with regard to strength development. However, laboratory experiments carried out on the freeze-thaw resistance of stabilised specimens cannot replace experience obtained from utilisation of the method in practice. Thus a field test in an area with more severe cyclic variation in temperature would be helpful in modelling the field potential for the utilisation of lime-activated ggbs as a soil stabilising agent.

With regard to the mechanisms responsible for the resistance of stabilised specimens to frost action, more emphasis should be put on the microstructural changes initiated by the water migration processes during freezing. For this purpose quite a range of techniques, such as SEM and mercury intrusion could be employed. The current study also focused on the volume stability of these specimens when subjected to severe temperatures. However, the development of the bearing capacity of specimens which have undergone severe freezing action, relative to their strength before frost action would be a helpful factor in determining the effectiveness of the stabilisation technique for use in practice. In addition an area which needs to be developed is to identify the resistance of lime-ggbs stabilised ground to de-icing salts. If lime-ggbs stabilisation is going to be applied in practice, there is a definite requirement to identify if any damaging interaction between chlorides and the stabilised ground will take place.

Due to its widespread abundance in soils, gypsum was chosen for the current project as a typical artificial sulphate addition. However, previous work [Kinuthia, 1997] has shown that the type of sulphate added affects the strength and swelling properties of stabilised clay soils. Thus further work into durability would be helpful in identifying how different types of sulphates modify the permeability, porosity and freeze-thaw resistance of lime-ggbs stabilised ground.

Lower Oxford Clay was chosen for the research project because of its high content of potentially detrimental sulphides (pyrite). However, no detailed investigations have been carried out in this study to assess how much sulphide is converted (and under what circumstances) after stabilisation with lime and ggbs. Further work should focus on the determination of the sulphate content over time in typical stabilised environments to give an indication as to how the stabilisation method could be modified to ensure that no harmful chemical reactions occur.

Undrained, unconsolidated triaxial tests have been performed to assess the general development of the shear strength of the stabilised soil. Hence, only the apparent shear parameters were determined and basic interpretation of the findings with regard to the scope of the project was undertaken. However, determination of the effective shear strength parameters would allow a more comprehensive assessment of the influence of the degree of slag hydration and cementation on the shear strength parameters.

It has been shown that ggbs activated with comparably small amounts of lime impart significant strength development to clay soil. However, the strength gain occurs after a rather long dormant period. Suggestions for the mechanism behind these observations have been made. Further work could address this issue in more detail, and microstructural investigations utilising, for example, an environmental scanning electron microscope, could contribute to a full understanding of the phenomenon. As indicated in the thesis, an 'equivalent age concept' which could involve numerical modelling based on empirical data, would be helpful in producing a guideline document, summarising the conditions under which lime-ggbs stabilisation is appropriate. These guidelines should incorporate information with regard to the influence of chemical components, environmental conditions and stabilisation methods on the final performance of the stabilised soil. An additional project could compare the

highly temperature dependent reaction rate of the pozzolanic reaction (with lime as a stabiliser) to the rate of slag hydration.

It has been shown that low temperatures have a substantial effect on the strength development of lime-ggbs stabilised ground. Further work could study and identify the effects on the chemistry of specimens if low temperatures prevail. In particular investigations into the formation of thaumasite, a sulpho-silicate hydrate, which has been identified to be partially responsible for the detrimental damage to stabilised ground and buried concrete structures, could be of interest if curing is at very low temperatures.

Finally a more comprehensive study on the financial impact of the stabilisation method, particularly in relation to the delayed strength development in the absence of accelerating sulphates (in comparison to conventional stabilisation methods), could be undertaken. Although it is appreciated that quantification of the environmental implication of the proposed stabilisation method is not easy, an attempt to do so (for example by utilising a point score system based on a survey amongst contractors and their clients) could assist in emphasising the possible potential of stabilisation with lime and ggbs.

References

Abdi, M R (1992), "Effects of calcium sulphate on lime stabilised kaolinite", PhD thesis, Polytechnic of Wales, Pontypridd, UK

Al-Tabbaa, A (1998), "Geoenvironmental applications for soil-tyre mixtures", Ground Engineering, 31, November 1998, pp 24-25

American Society for Testing and Materials (1996), "Standard test methods for frost heave and thaw weakening susceptibility of soils", ASTM D5918-96, West Conshohocken, USA

Anderson, D M, Pusch, R and Penner, E (1978), "Physical and thermal properties of frozen ground", in: Geotechnical Engineering for cold regions", Andersland, O B and Anderson, D M (edts), Mc Graw-Hill Inc, New York, pp 37-102

Arabi, M (1987), "Fabric and strength of clays stabilised with lime", PhD thesis, Polytechnic of Wales, Pontypridd

Arabi, M and Wild, S (1986), "Microstructural development in cured soil-lime composites", Journal of Materials Science, 21, pp 497-503

Arabi, M and Wild, S (1989), "Property changes induced in clay soils when using lime stabilisation", Municipal Engineer, 6, April 1989, pp 85-99

Asim, M E (1992), "Die Verarbeitung von Hochofenschlacken zu Zumahlstoffzementen (Blast furnace slag processing to blended cements)", in German, Zement-Kalk-Gips, 45, no 10, pp 519-528

Auberg, R and Setzer, M J (1997), "Influence of water uptake during freezing and thawing", in :Frost resistance of concrete, Setzer, M J and Auberg, R (edt), E & FN Spon, London, pp 232-245

Bàgel, L and Zivica, V (1997), "Relationship between pore structure and permeability of hardened cement mortars: on the choice of the effective pore structure parameter", Cement and Concrete Research, 27, no 8, pp 1225-1235

Bagonza, S, Peete, J M, Newill, D and Freer-Hewish, R (1987), "Carbonation of stabilised soil-cement and soil-lime mixtures", Proceedings of the 15th Annual Summer Meeting, PTRC Europe Transport and Planning, University of Bath, 7-11th September 1987, P295, pp 2-48

Bailey, S W , Brindley, G W, Johns, W D, Martin, R D and Ross, M (1971), "Summary of national and international recommendations on the clay mineral nomenclatura and report of nomenclatura committee", Clays and Clay Minerals, 19, pp 129-133

Balduzzi, F (1973), "Frost – properties of cement stabilised bases and subbases", Proceedings of the Symposium on frost action on roads, Norwegian Road Research Laboratory, Oslo, pp 196-201

Barden, L (1971), " Examples of clay structure and its influence on engineering behaviour", Proceedings of the Roscoe Memorial Symposium, Cambridge, 29.-31. March 1971, pp 195-205

Bell, F G (1988), "Stabilisation and treatment of clay soils with lime: part 1 - basic principles", Ground Engineering, January, pp 10-15

Bell, F G and Coulthard, J M (1990), "Stabilisation of clay soils with lime", Municipal Engineer, 7, June 1990, pp 125-140

Bell, F G and Tyrer, M J (1987), "Lime stabilisation and clay mineralogy", Proceedings of the International Conference of Foundations and Tunnels, Forde, M C (edt), London, 2, pp 1-7

Bensted, J (1999), "Thaumasite – background and nature in deterioration of cements, mortars and concretes", Cement and Concrete Composites, 21, pp 117-121

Bensted, J (1988), "Thaumasite – a deterioration product of hardened cement structures", Il Cemento, 1, pp 3-10

Bensted, J and Varma, S P (1976), "A discussion of the paper "Thaumasite formation: a cause of deterioration of Portland cement and related substances in the presence of sulphates" by J H P van Aardt and S Visser", Cement and Concrete Research, 6, pp 321-322

Berra, M and Baronio, G (1989), "Thaumasite in deteriorated concretes in the presence of sulphates", Proceeings of the American Concrete Institute, SP 100, 2, SP 100-106, pp 2073-2089

Beskow, G (1935), "Soil freezing and frost heaving with special application to roads and railroads", The Swedish Geological Society, no 375, year book no 3, Technological Institute, Northwestern University, Evanston, Illinois

Bessey, G E and Lea, F M (1953), "The distribution of sulphates in clay soils and groundwater", Proceedings of the Institution of Civil Engineers, paper no 5883, 2, pp 159-181

Bickley, J A, Hemmings, R T, Hooton, R D and Balinski, J (1994), "Thaumasite related deterioration of concrete structures", Proceedings of the American Concrete Institute, part 144, SP 144-8, pp 159-175

Bier, T A, Kropp, J and Hilsdorf, H K (1989), "The formation of silica gel during carbonation of cementitious systems containing slag cements, 3rd CANMET/ACI International Conference on fly-ash, silica fume, slag and natural pozzolans in concrete, Malhotra, V M (edt), 2, SP114-69, pp 1413-1428

Bijen, J (1996), "Blast furnace slag cement", VNC Association of the Netherlands Cement Industry, s'-Hertogenbosch, Netherlands, CIP Royal Library Den Haag

Bishop, A W (1954), "The use of pore pressure coefficients in practice", Geotechnique, 4, no 4, pp 148-152

Bjerrum, L and Huder, J (1975), "Measurement of the permeability of compacted clay", Proceedings of the 4th International Conference of Soil Mechanics and Foundation Engineering, London, 1, pp 6-8

Black, D K and Lee, K L (1973), "Saturating laboratory samples by back pressure", Journal of the Soil Mechanics and Foundations Division, ASCE, 99, January 1973, pp 75-93

Bostock Hill and Rigby Ltd (1987), "Expansive slags", Building Technical File, no 17, April 1987, pp 29-32

Brandl, H (1981), "Alteration of soil parameters by stabilisation with lime", Proceedings of the 10th International Conference on Soil Mechanics, Stockholm, Sweden, 3, pp 587-594

Brindley, G W and MacEwan, D (1953), "Structural aspects of the mineralogy of clays and related silicates", Ceramics: A Symposium, British Ceramic Society, pp 15-19

British Standard Institution (1990), "Stabilised materials for civil engineering purposes", BS 1924:part 2, 1990, Methods of test for cement-stabilised and lime-stabilised materials, HMSO, London, UK

British Standard Institution (1990), "British standard methods for soils for civil engineering purposes", BS 1377: 1990, HMSO, London, UK

British Standards Institution (1983), "Methods for the chemical analysis for blast furnace slag", BS 1047 : 1983, HMSO, London, UK

Brown, G (1984), "Crystal structures of clay minerals and related phyllosilicates", Phil.Trans. of the Royal Society, London, A311, pp 221-240

Brown, P W, Shi, D and Skalny, J (1991), "Porosity/permeability relationships", in: Materials Science of Concrete II, Skalny, J P and Mindless, S (edts), American Concrete Society, Westerville, Ohio, pp 83-109

Building Research Establishment (1991), "Sulphate and acid resistance of concrete in the ground", BRE Digest 363, Watford, UK

Buoyoucos, G (1920), "Degree of temperature to which soils can be cooled without freezing", Journal of Agricultural Research, 20, no 4, pp 267-269

Burns, J (1977), "The effect of water table on the frost susceptibility of a roadmaking material", Transport and Road Research Laboratory, TRRL supplementary report no 305, Berkshire, UK

Buttle, J W , Daniels, D J and Beckett, P J (1981), "Chemistry: a unified approach", 4th edition, Butterworth & Co, London

Buxton Lime Industries (1990), "Lime stabilisation manual", 2nd edition, Buxton Lime Industries, Buxton, UK

Cao, H T, Bucea, L, Ray, A and Yozghatlian, S (1997), "The effect of cement composition and pH of environment on sulphate resistance of Portland cements and blended cements", Cement and Concrete Composites, 19, pp 161-171

Chaddock, B C J and Atkinson, V M (1997), "Stabilised sub-bases in road foundations: structural assessment and benefits", Transport Research Laboratory, TRL Report 248, Crowthorne, UK

Chamberlain, E J (1987), "A freeze-thaw test to determine the frost susceptibility of soils", CRREL SR-87-1, Cold Regions Research & Engineering Laboratory, Hanover, New Hampshire, USA

Chamberlain, E J (1989), "Physical changes in clays due to frost action and their effect on engineering structures", Proceedings of the International Conference on Frost in Geotechnical Engineering, Espoo, Finland, Technical Research Centre of Finland, pp 863-893

Chamberlain, E J and Gow, A J (1979), "Effect of freezing and thawing on the permeability and structure of soils", Engineering Geology, 13, pp 73-92

Chandler, R J, Crilly, M S and Montgomery-Smith, G (1992), "A low-cost method of assessing clay desiccation for low-rise buildings", Proceedings of the Institution of Civil Engineers, Civil Engineering, 92, no 2, pp 82-89

Chartschenko, J, Volke, K and Stark, J (1993), "Untersuchungen über den Einfluß des pH-Wertes auf die Ettringitbildung (Investigations into the influence of the pH-value on the formation of ettringite)", in German, Wissenschaftliche Zeitschrift der Hochschule für Architektur und Bauwesen Weimar, 3. Heft, Ausgabe A, 39, pp 171-176

Chattopadhyay, P K (1972), "Residual shear strength of some pure clay minerals", PhD thesis, University of Alberta, Edmonton, Canada

Childs, E C and Collis-George, N (1950), "The permeability of porous materials", Proceedings of the Royal Society, A201, pp 392-408

Chuvivlin, Y M and Yazynin, O M (1988), "Frozen soil macro- and microtexture formation", Proceedings of the 5th International Conference on Permafrost, Trondheim/Norway, pp 320-328

Clare, K E and Cruchley, A E (1957), "Laboratory experiments in the stabilisation of clays with hydrated lime", Geotechnique, 7, pp 97-111

Clark, B A and Brown, P W (1999), "The formation of calcium sulfoaluminate hydrate compounds – part I", Cement and Concrete Research, 29, pp 1943-1948

Coale, R D, "Wolhuter, C W, Jochens, P R and Howat, D D (1973), "Cementitious properties of metallurgical slags", Cement and Concrete Research, 3, pp 81-92

Cobbe, M I (1988), "Lime modification of kaolinite-illite clays", Civil Engineering Technology, February 1988, pp 9-15

Collepardi, M (1999), "Thaumasite formation and deterioration in historic buildings", Cement and Concrete Composites, 21, pp 147-154

Concrete Society (1992), "The use of ggbs and pfa in concrete", Technical Report no 40, The Concrete Society (publ), Wexham, Slough, UK

Cook, D J, Hinczak, I and Cao, H T (1988), "Hydration and morphological characteristics of cements containing blast furnace slag", Concrete 88 - International Workshop on the use of fly-ash, slag and other silicious materials, Concrete Institute of Australia, Sydney, pp 433-448

Craighill, A and Powell, J (1998), "UK landfill tax: its effects on civil engineering", Proceedings of the Institution of Civil Engineers, November 1998, 126, no 4, pp 187-189

Crammond, N J and Halliwell, M A (1995), "The thaumasite form of sulphate attack in concretes containing a source of carbonate ions – a microstrucutral overview", 2nd Symposium on Advances in Concrete Technology, ACISP 154, SP154-19, pp 135-380

Croney, D and Jacobs, J C (1967), "The frost susceptibility of soils and road materials", TRRL Report LR90, Road Research Laboratory, Ministry of Transport, UK

Czurda, K A and Schaeberle, R (1988), "Influence of freezing and thawing on the physical and chemical properties of swelling clays", 5th International Symposium on Ground Freezing, Nottingham, England, Jones and Holden (edt), A A Balkema, Rotterdam, pp 51-58

Daimon, M, (1980), "Mechanism and kinetics of slag cement hydration", 7th International Congress on the Chemistry of Cement, Paris, vol 1, Sub-theme III-2, pp III-2/1-III-2/9

Daugherty, K E, Saad, B, Weirich, C and Eberendu, A (1983), "The glass content of slag and hydraulic activity", Silicates Industriels, no 4-5. pp 107-110

Day, R, W (1992), "Effective cohesion for compacted clay", Journal of Geotechnical Engineering, 118, no 4, pp 611-619

De Silvia, P S and Glasser, F P (1992), "Pozzolanic activation of metakaolin", Advances in Cement Research, 4, no 16, pp 167-178

Deer, W A, Howie, R A and Zussman, J (1992), "An introduction to the rock-forming minerals", 2nd edition, Longman Scientific & Technical, Harlow, UK

Demoulian, E, Gourdin, P, Hawthorn, F and Vernet, C (1980), "Influence of slag chemical composition and texture on their hydraulicity", in French, 7th Congress on Cement Chemistry, Paris, vol 2, pp III-89-III-94

Dennen, W H and Moore, B R (1986), "Geology and engineering", W M C Brown Publishers, Dubuque, Iowa, USA

Department of the Environment, Transport and the Regions (1999), "The thaumasite form of sulphate attack: risks, diagnosis, remedial works and guidance on new construction", Report of the Thaumasite Expert Group, London, UK

Department of Transport (1993), "Manual of contract documents for highway works (MCHW): volume 1: Specification for highway works", HMSO, London, UK

Department of Transport (1996), "Specification for highway works", part2, series 600-earthworks, HMSO, August 1986, London, UK

Deutsches Institut für Normung (1996), "German proposal for a test method on freeze-thaw resistance of hydraulically bound bases", CEN/TC 227/WG 4 N187 E – hydraulically bound and unbound mixtures, DIN Deutsches Institut für Normung e.V., Berlin, Germany

Diamond, S (1970), "Pore size distribution in clays", Clays and clay minerals", 18, pp 7-23

Diamond, S (1999), "Aspects of concrete porosity revisited", Cement and Concrete Research, 29, pp 1181-1188

Doner, H E and Warren, C L (1977), "Carbonate, halide, sulfate and sulfide minerals" in: Minerals in soil environments, Dixon, J G and Weed, S B (edts), Soil Science Society of America, Madison, Wisconsin, pp 79-98

Dumbleton, M J (1962), "Investigations to assess the potentialities of lime for soil stabilisation in the United Kingdom", Road Research Technical Paper no 64, HMSO, London, UK

Dunn, J, Oliver, K, Nguyen, G and Sills, I (1987), "The quantitative determination of hydrated calcium sulphates in cement by DSC", Thermochimica Acta, 121, pp 181-191

Dutta, D K and Borthakur, P C (1990), "Activation of low lime high alumina granulated blast furnace slag by anhydrite", Cement and Concrete Research, 20, pp 711-722

Eades, J L and Grim, R E (1960), "Reaction of hydrated lime with pure clay minerals in soil stabilisation", Highway research Board, Bulletin 262, Washington DC, USA, pp 51-63

ECC International (1987), "China and ball clays for the ceramic industry", Company brochure, St Austell, Cornwall, UK

El-Rawi, N M and Awad, A A (1981), "Permeability of lime-stabilised soils", ASCE Transportation Engineering Journal, TE1, January 1981, pp 25-35

Fagerlund, G (1997), "Internal frost attack –state of the art", in :Frost resistance of concrete, Setzer, M J and Auberg, R (edt), E & FN Spon, London, pp 321-338

Fasiska, E J, Wagenblast, H and Dougherty, M T (1974), "The oxidation mechanism of sulfide minerals", Bulletin of the Association of Engineering Geologists, 11, no 1, pp 75-82

Feldman, R F (1984), "Pore structure damage in blended cements caused by mercury intrusion", Journal of the American Ceramic Society, 67, no 1, pp 30-33

Feng, Q L, Lachowski, E E and Glasser, F P (1989), "Densification and migration of ions in blast furnace slag-Portland cement pastes, Proceedings of the Materials Research Symposium, Materials Research Society, 136, pp 263-272

Fernandez-Jimenez, A, Puertas, F and Fernandez, L (1996), "Alkaline-sulphate activation process of a Spanish blast furnace slag", Materiales de Construccion, 46, no 241, pp 23-37

Ferris, G A, Eades, J L, Graves, R E and McClellan, G H (1991), "Improved characteristics in sulphate soils treated with barium compounds before lime stabilisation", Transportation Research Record 1295, pp 45-51

Foster, M D (1953), "Geochemical studies of clay minerals: II- relation between ionic substitution and swelling in montmorillonite", American Mineralogist, 30, pp 994-1006

Foster, M D (1955), "The relation between composition and swelling in clays", Clay and Clay Minerals, 3, 99 205-220

Fletcher, N H (1970), "The chemical physics of ice", Cambridge University Press, UK

Frearson, J P H (1986), "Sulphate resistance of combinations of Portland cement and ground granulated blast furnace slag", Proceedings of the 2nd International Conference on Fly-ash, Silica-fume, Slag and natural Pozzolans in Concrete, Madrid, Spain, vol 2, SP91-74, pp 1495-1524

Frearson, J P H and Uren, J M (1986), "Investigations of a ground granulated blast furnace slag containing merwinitic crystallisation", Proceedings of the 2nd International Conference on Fly-ash, Silica-fume, Slag and natural Pozzolans in Concrete, Madrid, Spain, vol 2, SP91-69, pp 1401-1421

Fredlund, D G and Rahardjo, H (1993), "Soil mechanics for unsaturated soils", John Wiley & Sons Inc, New York

Fukudome, K, Miyano, K, Taniguchi, H and Kita, T (1992), "Resistance to freezing and thawing and chloride diffusion of anti-washout underwater concrete containing blast furnace slag", Proceedings of the 4th International Conference on Fly ash, Silica

fume, Slag and natural Pozzolans in Concrete, Istanbul, Turkey, May 1992, Malhorta, V M (edt), vol II, SP132-84, pp 1565-1582

Gaze, M E (1997), "The effects of varying gypsum content on thaumasite formation in a cement:lime:sand mortar at 5 ₒC", Cement and Concrete Research, 27, no 2, pp 259-265

Geiseler, J (1992), "Verwertung von Hochofen- und Stahlwerksschlacken (Utilisation of blast furnace and steel slags)" (in German), in: "Eisenhüttenschlacken – Eigenschaften und Verwertung", Referate aus dem Zeitraum 1988-1991, Heft 1, Forschungsgemeinschaft Eisenhüttenschlacken, Duisburg, Germany, pp 1-32

Geiseler, J (1996), "Use of steelwork slag in Europe", Waste Management, 16, no 1-3, pp 59-63

Geiseler, J (1997), Forschungsgemeinschaft Eisenhüttenschlacken, Duisburg, Germany, private communication

Gillott, J E (1987), "Clay in engineering geology", Elsevier Science Publishers B V, Amsterdam, The Netherlands

Gillott, J E, Penner, E and Eden, W J (1974), "Microstructure of billings shale and biochemical alteration products, Ottawa, Canada", Canadian Geotechnical Journal, 11, 482-489

Gjorv, O E (1989), "Alkali activation of a Norwegian blast furnace slag", 3rd CANMET/ACI International Conference on fly-ash, silica fume, slag and natural pozzolans in concrete, Malhotra, V M (edt), vol 2, SP114-73, pp 1501-1517

Glasser, F P (1991), "Chemical, mineralogical and microstructural changes occurring in hydrated slag-cement blends", in: Materials Science of Concrete II, Skalny, J and Mindess, S (edts), The American Ceramic Society, 1991, pp. 41-81

Gore, A (1992), "Earth in the balance", Houghton Mifflin Company

Goto, S and Roy, D M (1981), "The effect of w/c ratio and curing temperature on the permeability of hardened cement paste", Cement and Concrete Research, 11, no 4, pp 575-579

Greaves, H (1999), personal communication

Grim, R E (1962), "Applied Clay Mineralogy", Mc Graw Hill Book Company

Gupta, S and Seehra, S S (1989), "Studies on lime-granulated blast furnace slag as an alternative binder to cement", Highway Research Bulletin, New Delhi, 38, pp 81-97

Gutierrez, R, Delvasto, S and Talero, R (1998), "Performance of ggbs cements", Journal of Solid Waste Technology and Management", 25, no 2, pp 112-115

Häkkinen, T (1993), "The influence of slag content on the microstructure, permeability and mechanical properties on concrete. Part 1: Microstructural studies and basic mechanical properties", Cement and Concrete Research, 23, pp 407-421

Hanafusa, M and Watanabe, T (1991), "The effectiveness of granulated blast furnace slag", in: "Waste materials in Construction", Proceedings of the International Conference on environmental Implications of Construction with Waste Materials, Maastricht, The Netherlands, 10-14th November 1991, pp 467-474

Harlan, R L and Nixon, J F (1978), "Ground thermal regime", in: Geotechnical Engineering for cold regions", Andersland, O B and Anderson, D M (edts), Mc Graw-Hill Inc, New York, pp 103-163

Hartshorn, S A, Sharp, J H and Swamy, R N (1999), "Thaumasite formation in Portland-limestone cement pastes", Cement and Concrete Research, 29, pp 1331-1340

Hasaba, S, Kawamura, M and Torii, K (1982), "Reaction products and strength characteristics in the stabilised oil using desulfurisation by-product and blast furnace slag", Transactions of the Japanese Society of Civil Engineers, Soil Mechanics and Foundation Engineering Division, 14, pp 251-253

Haynes, D J and Connell, M D (1996), "GGBS an environmental cement", in: Concrete for Environment Enhancement and Protection, Proceedings of the International Conference held at the University of Dundee, Scotland, 24-26 June, 1996, Dhir, R K and Dyer, T D (edts), E & FN Spon, London, UK

Head, K H (1986), "Manual of soil laboratory testing – volume 3: effective stress tests", Pentech Press, London

Hiersche, E U and Wörner, T (1990), "Alternative Baustoffe im Bauwesen (Alternative materials in the construction industry)", Berlin, Germany

Higgins, D D and Kennedy, J (1999), "Lime + ground granulated blast furnace slag stabilisation of boulder clay on the A421 Tingewick bypass", 3rd European Symposium on the performance and durability of bituminous materials and hydraulic stabilised composites, Leeds, 8-9th April 1999

Highways Agency (1995), "Design manual for roads and bridges", volume 4, section1: Earthworks, part 6, HA74/95, HMSO, London, UK

Hilt, G H and Davidson, G T (1960), "Lime fixation in clayey soils", Highway Research Board Bulletin 262, pp 20-32

Hogan, F J and Meusel, J W (1981), "Evaluation for durability and strength development of a ground granulated blast furnace slag", Cement, Concrete and Aggregates, CCAGDP, 3, no1, pp 40-52

Holtz, W G (1983), "The influence of vegetation on the swelling and shrinking of clays in the United States of America", Geotechnique, 33, no 2, pp 159-163

Hooton, R D (1986), "Permeability and pore structure of cement pastes containing fly-ash, slag and silica fume", Blended Cements, ASTM STP 897, Frohnsdorff, G (edt), American Society for Testing and Materials, Philadelphia, USA, pp 128-143

Hooton, R D and Wakeley, L D (1988), "Influence of the test conditions on water permeability of concrete in a triaxial cell", Materials Research Society Symposium Proceedings "Pore structure and permeability of cementitious materials", vol 137, Boston, Massachusetts, USA, pp 157-164

Hooton., R D (1989), "What is needed in a permeability test for evaluation of concrete quality?", Materials Research Society Symposium Proceedings "Pore structure and permeability of cementitious materials", 137, Boston, Massachusetts, USA, pp 141-149

Houghton, J (1997), "Global warming – the complete briefing", 2nd edition, Cambridge University Press, Cambridge, UK

Hughes, D C (1985), "Pore structure and permeability of hardened cement paste", Magazine of Concrete Research, 37, no 133, December 1985, pp 227-233

Hunter, D (1988), "Lime-induced heave in sulphate-bearing clay soils", ASCE Journal of Geotechnical Engineering, 114, no 2, pp 150-167

Ingles, O G and Metcalf, J B (1972), "Soil stabilisation: principles and practice", Butterworth & Co Publishers, London, UK

Jackson, D and Cripps, J C (1997), "Investigation on the effect of bacterial action on the chemistry and mineralogy of pyritic shale", Proceedings of the International Conference on the Implications of Ground Chemistry and Microbiology for Construction, University of Bristol 1992, A A Balkema, Rotterdam, 2-3, pp 89-100

Johansson, S E (1978), "Relation between strengths of slag cement and properties of slag", Silicates Industrielles, 43, no 7-8, pp 139-143

Kawamura, M and Diamond, S (1975), "Stabilisation of clay soils against erosion loss"" Clays and Clay Minerals, 23, pp 444-451

Kendall, K, Howard, A J and Birchall, J D (1983), "The relation between porosity, microstructure and strength and the approach to advanced cement-based materials", Philosophical Transactions of the Royal Society of London, A310, pp 139-154

Kennedy, J (1996), "Insitu stabilisation using ggbs", Highways & Transportation, October 1996, pp 26

Kertscher, H (1988), "Wasserdurchlässigkeit bindiger Böden bei Kalkstabilisierung (Permeability of cohesive lime-stabilised soils)", *in German*, Leichtweiss-Institut für Wasserbau der Technischen Universität Braunschweig, Mitteilungen Heft 101/1988, Braunschweig, Germany

Khatib, J M and Wild, S (1996), "Pore size distribution of metakaolin paste", Cement and Concrete Research, 26, no 10, pp 1545-1553

Khatri, R P and Sirivivatnanon, V (1997), "Role of permeability in sulphate attack", Cement and Concrete Research, 27, no 8, pp 1179-1189

Kinuthia, J M (1997), "Property changes and mechanisms in lime-stabilised kaolinite in the presence of metal sulphates", PhD thesis, University of Glamorgan, Pontypridd, UK

Kleber, W (1970), "An introduction to crystallography", Verlag Technik, Berlin, Germany, p 138

Knöfel, D and Wang, J (1993), "Die Carbonatisierung der Schnellzemente und die Bildung der drei $CaCO_3$-Modifikationen Calcit, Vaterit und Aragonit (The carbonation of fast-setting cements and the formation of the three $CaCO_3$ modifications calcite, vaterite and aragonite)", *in German*, Wissenschaftliche Zeitschrift der Hochschule für Architektur und Bauwesen Weimar, Ausgabe A, 39, no 3, pp 225-229

Konecny, L and Naqvi, S J (1993), "The effect of different drying techniques on the pore size distribution of blended cement mortars", Cement and Concrete Research, 23, pp 1223-1228

Konrad, J M and Morgenstern N R (1980), "A mechanistic theory if ice lens formation in fine-grained soils", Canadian Geotechnical Journal, 17, pp 473-486

Konrad, J M and Morgenstern, N R (1981), "The segregation potential of a freezing soil", Canadian Geotechnical Journal, 18, pp 482-491

Krohn, J P and Slosson, J E (1980), "Assessment of expansive soils in the United States", Proceedings of the 4th International Conference on Expansive Soils, Denver/Colorado, vol 1, American Society of Civil Engineers, pp 596-608

Ladd, C C (1959), "Mechanisms of swelling by compacted clay", Highway Research Board Bulletin no 245, National Academy of Science, pp 10- 26

Lade, P V and De Boer, R (1997), "The concept of effective stress for soil, concrete and rock", Geotechnique, vol 47, no 1, pp 61-78

Lambe, T W and Whitman, R V (1979), "Soil mechanics, SI version", John Wiley & Sons, New York, USA

Lawes, G (1987), "Scanning electron microscopy and X-ray microanalysis", Open Learning, ACOL, Thames Polytechnic, London, John Wiley & Sons, Chichester, UK

Li, C, Yoda, A and Yokomur, T (1998), "Pore structure, strength and carbonation of cement pastes containing ground granulated blast furnace slag", Proceedings of the

6th CANMET/ACI International Conference on fly-ash, silica fume, slag and pozzolans in concrete, SP 178-45, Bangkok, Thailand, 2, pp 875-892

Lindmark, S (1999), "Mechanism of salt frost scaling of Portland cement-bound materials – Studies and hypothesis", PhD thesis, Lund University, Division of Building Materials, Sweden

Locat, J, Tremblay, H and Leroueil, S (1996), "Mechanical and hydraulic behaviour of a soft inorganic clay treated with lime", Canadian Geotechnical Journal, 33, pp 654-669

Locher, F W (1998), "The sulphate resistance of cement and its testing", Zement-Kalk-Gips ZKG International, 51, no 7, pp 388-398

Lowe, J and Johnson, T C (1960), "Use of back pressure to increase degree of saturation of triaxial test specimens", Proceedings of the ASCE Research Conference on Shear Strength of cohesive Soils, Boulder, Colorado, USA, pp 819-836

Mageau, D W and Morgenstern, N R (1980), "Observations on moisture migration in frozen soils", Canadian Geotechnical Journal, 17, pp 54-60

Malhotra, V M (1989), "Mechanical properties and freezing and thawing durability of concrete incorporating a ground granulated blast furnace slag", Canadian Journal of Civil Engineering, 16, part 2, pp 140-156

Malhotra, V M and Mehta, P K (1996), "Pozzolanic and cementitious materials", Advances in Concrete Technology, 1, Gordon and Breach Publishers, Amsterdam, Netherlands

Manmohan, D and Mehta, P K (1981), "Influence of pozzolanic, slag and chemical admixtures on pore size distribution and permeability of hardened cement pastes", Cement, Concrete and Aggregates, CCAGDP, 3, no 1, pp 63-67

Marion, G M (1995), "Freeze-thaw processes and soil chemistry", US Army Corps of Engineers, Cold Regions Research & Engineering Laboratory, Special Report No 95-12, New Hampshire, March 1995

Marsh, B K (1984), "Relationships between engineering properties and microstructural characteristics of hardened cement paste containing pulverised-fuel-ash as a partial cement replacement", PhD thesis, Hatfield Polytechnic, UK

Marsh, B K and Day, R L (1985), "Some difficulties in the assessment of pore structure of high performance blended cement paste", Proceedings of a Materials Research Society Symposium, 42, pp 113-121

Marshall, C E (1964), "The physical chemistry and mineralogy of soils", 1, Soil Materials, John Wiley & Sons, New York, USA

Marshall, T J (1958), "A relation between permeability and size distribution of pores", Journal of Soil Science, 9, no 1, pp 1-8

Mateos, M (1964), "Soil-lime research at Iowa State University", Journal of Soil Mechanics, Foundations Division, American Society of Civil Engineers, SM2, pp 127-153

McAllister, L D and Petry, T M (1992), "Leach tests on lime-treated clays", Geotechnical Testing Journal, GTJODJ, 15, no 2, pp 106-114

McElroy, C H (1987), "Using hydrated lime to control erosion of dispersive clays", Lime for environmental uses, ASTM STP 931, Gutschick, K A (edt), American Society for Testing and Materials, Philadelphia, pp 100-114

Mehta, P K (1973a), "Effect of lime on hydration of pastes containing gypsum and calcium aluminates or calcium sulfoaluminate", Journal of the American Ceramic Society, 56, pp 315-319

Mehta, P K (1973b), "Mechanism of expansion associated with ettringite formation", Cement and Concrete Research, 3, pp 1-6

Mehta, P K (1983), "Mechanism of sulphate attack on Portland cement - another look", Cement and Concrete Research, 12, pp 401-406

Mehta, P K (1989), "Pozzolanic and cementitious by-products in concrete – another look", 3rd CANMET/ACI International Conference on fly-ash, silica fume, slag and natural pozzolans in concrete, Malhotra, V M (edt), vol 1, SP114-1, pp 1-43

Mehta, P K (1992), "Sulfate attack on concrete – a critical review", Materials Science of Concrete III, American Ceramic Society, Skalny, J (edt), pp 102-130

Mehta, P K and Hu, F (1978), "Further evidence for expansion of ettringite by water absorption", Journal of the American Ceramic Society, 61, no 3-4, pp 179-181

Mehta, P K, Pirtz, D and Polivka, M (1979), "Properties of alite cements", Cement and Concrete Research, 9, pp 439-450

Mehta, P K and Manmohan, D (1980), "Pore size distribution and permeability of hardened cement pastes", 7th International Conference on the Chemistry of Cement, Paris, 3, pp VII1-VII5

Meng, B (1994), "Resolution-dependent characterisation of interconnected pore systems: development and suitability of a new method", Materials and Structures, 27, 63-70

Menzies, B K (1988), "A computer controlled hydraulic triaxial testing system", Special Technical Publication 977 1988, American Society for Testing and Materials, pp 82 – 94

Michaelis, W (1892), "Der Zementbazillus" (the cement bug)", in German, Tonindustrie-Zeitung, 16, pp 105-106

Mielenz, R C and King, M E (1955), "Physical chemical properties and engineering performance of clays"" Calif. Div. Mines Bulletin, 169, pp 196-254

Miller, R D (1977), "Lens initiation in secondary heaving", Proceedings of the International Symposium on Frost Action in Soils, Lulea, Sweden, vol 2, pp 68-74

Miller, R D (1980), "Freezing phenomena in soils", in: Applications of soil physics, San Diego, Academic Press, pp 254-299

Mitchell, J K (1973), "Recent advances in the understanding of the influences of mineralogy and pore solution chemistry on the swelling and stability of clays", 3rd International Conference on Expansive Soils, 2, pp 11-25

Mitchell, J K (1982), "Soil improvement – its past, present and prospects for the future", Proceedings of the International Conference of Mexican Society of Soil Mechanics, Mexico City, 2-4 August 1982, pp 135-147

Mitchell, J K (1986), "Delayed failure of lime-stabilised pavement bases", Journal of Geotechnical Engineering, 112, pp 274-279

Mitchell, J K (1993), "Fundamentals of soil behaviour", 2nd edition, John Wiley & Sons, New York, USA

Mitchell, J K and Hooper, D R (1961), "Influence of time between mixing and compaction on properties of lime-stabilised expansive clay", Highway Research Board, Bulletin no 304, Washington D C, USA , pp 14-31

Moranville-Regourd, M (1998), "Cements made from Blast furnace slag", in: Lea's chemistry of cement and concrete, Hewlett, P C (edt), 4th edition, John Wiley & Sons Inc, New York, pp 633-674

Motz, H and Geiseler, J (1987), "Selbsthärtende Schichten aus Hochofenschlacken (Self-hardening capping layers with blast furnace slag)", in German, Straßen- und Tiefbau, 41, no 4, pp 24-33

Nakamoto, J and Togawa, K (1995), "A study of strength development and carbonation of concrete incorporating high volume blast furnace slag", 5th International Conference on Fly-ash, Silica Fume, Slag and Natural Pozzolans in Concrete, Milwaukee, Wisconsin, USA, Malhotra V M (edt), vol2, SP 153-59, pp 1121-1139

Neville, A M (1995), "Properties of concrete", 4th edition, Addison Wesley Longman Ltd, Harlow, UK

Ngala, V T and Page, C L (1997), "Effects of carbonation on pore structure and diffusional properties of hydrated cement pastes", Cement and Concrete Research, 27, no 7, pp 995-1007

Nyame, B K and Illston, J M (1980), "Capillary pore structure and permeability of hardened cement paste", ", 7th International Conference on the Chemistry of Cement, Paris, 3, pp VI181-VI185

Nyame, B K and Illston, J M (1981), "Relationships between permeability and pore structure of hardened cement paste", Magazine of Concrete Research, 33, no 116, September 1981, pp 139-146

Obika, B and Freer-Hewish, R J (1990), "Soluble salt damage to thin bituminous surfacings of roads and runways", Australian Road Research, 20, no 4, December 1990, pp 24-41

Odler, I and Jawed, I (1991), "Expansive reactions in concrete", in Materials Science of Concrete II, Skalny, J P and Mindless, S (edts), American Ceramic Society, pp 221-247

Olson, R E (1974), "Shearing strengths of kaolinite, illite and montmorillonite", ASCE Journal of the Geotechnical Engineering Division, 100, GT11, November 1974, pp 1215-1229

Osbaeck, B (1989), "Ground granulated blast furnace slags grinding methods, particle size distribution and properties", 3rd CANMET/ACI International Conference on fly-ash, silica fume, slag and natural pozzolans in concrete, Malhotra, V M (edt), vol 2, SP114-60, pp 1239-1263

Osborne, G J (1999), "Durability of Portland blast furnace slag cement concrete", Cement and Concrete Composites, 21, pp 11-21

Ouynag, C and Lane, J (1997), "Freeze-thaw durability of concretes with infilling of ettringite in voids", ACI Spring Convention, Seattle, USA, American Concrete Institute

Pèra, J, Ambroise, J and Chabannet, M (1999), "Properties of blast furnace slags containing high amounts of manganese", Cement and Concrete Research, 29, pp 171-177

Petry, T M and Armstrong, J C (1989), "Stabilisation of expansive clay soils", Transportation Research Record 1219, pp 103-112

Powers,T C (1954), "Void spacing as a basis for producing air-entrained concrete", Proceedings of the American Concrete Institute, Bulletin no 49, 50, May 1954, pp 741-760

Powers, T C (1945), "A working hypothesis for further studies of frost resistance of concrete", Proceedings of the American Concrete Institute, 41, no 4, pp 245-272

Powers, T C and Hellmuth, R A (1953), "Theory of volume changes in hardened Portland cement paste during freezing", Proceedings, Highway Research Board 32, PCA Bull 46

Rahmann, A A (1984), "Characterisation of the porosity of hydrated cement pastes", in: The chemistry and chemically related properties of cement, Glasser, F P (edt), British Ceramic Proceedings, no 35, pp 249-266

Rasheeduzzafar, F H, Dakhil, A S, Al-Gahtani, S S, Al-Saadoun and Bader, M A [1990], "Influence of cement composition on the corrosion of reinforcement and sulphate resistance of concrete", ACI Materials Journal, 87, pp 114-122

Reed, M A, Lovell, C W, Altschaeffl, A G and Wood, L E (1979), "Frost heaving rate predicted from pore size distribution", Canadian Geotechnical Journal, 16, pp 463-472

Regourd, M (1980), "Structure and behaviour of slag Portland cement hydrates", 7th International Congress on the Chemistry of Concrete, Paris, vol 1, Sub-theme III-2, pp III-2/10-III-2/26

Regourd, M (1986), "Slags and slag cements", in: Cement replacement materials, Swamy, R N (edt), 3, Concrete Technology and Design, Surrey University Press, London, UK

Richardson, I G (1999), "The nature of C-S-H in hardened cements", Cement and Concrete Research, 29, pp 1131-1147

Richardson, I G and Groves, G W (1992), "Microstructure and microanalysis of hardened cement pastes involving ground granulated blast furnace slag", Journal of Materials Science, 27, pp 6204-6212

Rieke, R D, Vinson, T S and Mageau, D W (1983), "The role of specific surface are and related index properties in the frost heave susceptibility of soils", Proceedings of the 4th International Conference on Permafrost, Fairbanks, Alaska, USA, pp 1066-1071

Rogers, C D F, Glendinning, S and Roff, T E J (1997), "Lime modification of clay soils for construction expediency", Proceedings of the Institution of Civil Engineers, Geotechnical Engineering, 125, October 1997, pp 242-249

Rossato, G, Ninis, N L amd Jardine, R J (1992), ""Properties of some kaolin-based model clay soils", Geotechnical Testing Journal, GTJODJ, 15, no 2, pp 166-179

Roy, D M and Idorn, G M (1985), "Relation between strength, pore structure and associated properties of slag-containing cementitious materials", Symposium "Very high strength cement-based materials", Materials Research Society Symposia Proceedings, 42, Young, J F (edt), Boston, Massachusetts, USA, pp 133-141

Roy, D M and Parker, K M (1983), "Microstructures and properties of granulated slag-Portland cement blends at normal and elevated temperatures", American Concrete Institute, 1, part SP79-21, pp 397-414

Sabry, M M and Parcher, J V (1979), "Engineering properties of soil-lime mixtures", ASCE Transportation Engineering Journal, TE1, January 1979, pp 59-70

Samuels, S G (1950), "The effect of base exchange on the engineering properties of soils", Building Research Station, Department of Science and Industrial Research, report no C176, pp 1-16

Scherer, G W (1999), "Structure and properties of gels", Cement and Concrete Research, 29, pp 1149-1157

Schulson, E M (1998), "Ice damage to concrete", US Army Corps of Engineers, Cold Regions Research & Engineering Laboratory, Special Report No 98-6, New Hampshire, April 1998

Sharma, K M and Ahluwalia, S C (1995), "Cement blends using steel slag", World Cement, 26, no 12, pp 74-77

Sheeran, D E and Yong, R N (1975), "Water and salt redistribution in freezing soils", Conference on Soil and Water Problems in cold Regions, Division of Hydrology, American Geophysical Union, Calgary, Alberta, Canada, 6th-7th May 1975, pp 58-69

Sherwood, P T (1962), "Effect of sulphates on cement- and lime-stabilised soils", Highway Research Board Bulletin 353, pp 98-107

Sherwood, P T (1992), "Stabilised capping layers using either lime or cement or lime and cement", Transport Research Laboratory-Department of Transport, Contractor Report 151, Crowthorne, UK

Sherwood, P T (1995), "Alternative materials in road construction", Thomas Telford Publications, London, UK

Shi, C and Day, R L (1995), "A calorimetric study of early hydration of alkali-slag cement", Cement and Concrete Research, 25, no 6, pp 1333-1346

Skempton, A W (1953), "The colloidal activity of clay", Proceedings of the 3rd International Conference on Soil Mechanics and Foundation Engineering, 1, pp 57-61

Skempton, A W (1954), "The pore pressure coefficients A and B", Geotechnique, vol 4, no 4, pp 143-147

Slavin, C (1999), "The development of soil stabilisation", Redmediation, recycling and piling with lime and other binders, British Lime Association Seminars, London and Manchester, pp 1-3

Sloan, R L (1965), "Early reaction in the kaolinite-hydrated lime-water system", Proceedings of the 6th International Conference on Soil Mechanics and Foundation Engineering, Montreal, 1, pp 121-125

Smolczyk, H G (1961), "Die Ettringitphasen im Hochofenzement (Types of ettringite in slag cements)", Zement-Kalk-Gips, in German, 14, no 7, pp 277-284

Smolczyk, H G (1980), "Slag structure and identification of slags", 7th International Congress on the Chemistry of Cement, Paris, vol 1, Sub-theme III-1, pp III-1/3-III-1/17

Snedker, E A and Temporal, J (1990), "M40 Banbury IV Contract – Lime stabilisation", Highway and Transportation, December 1990

Song, S and Jennings, H M (1999), "Pore solution chemistry of alkali-activated ground granulated blast furnace slag", Cement and Concrete Research, 29, pp 159-170

Sposito, G (1989), "The chemistry of soils", Oxford University Press, New York, USA

Stark, J and Ludwig, H M (1997), "Freeze-thaw and freeze-deicing salt resistance of concretes containing cement rich in granulated blast furnace slag", ACI Materials Journal, 94, no 1, pp 47-55

Stark, J and Ludwig, H M, (1995), "The influence of the type of cement on the freeze-thaw/freeze-deicing salt resistance of concrete", International Conference on Concrete under severe Conditions: Environment and loading, CONSEC, Sapporo, Japan, Sakai, K, Banthia, N and Gjorv, O E (edt), pp 245-254

Stark, J, Bollmann, K and Seyfarth, K (1998), "Ettringite – cause of damage, damage-intensifier or uninolved third party?", Zement-Kalk-Gips (ZKG) International, 51, no 5, pp 280-292

Taber, S (1929), "Frost heaving", Journal of Geology, 37, pp 428-461

Taber, S (1930), "The mechanics of frost heaving", Journal of Geology, 38, 303-317

Takemoto, K and Uchikawa, H (1980), "Hydration of pozzolanic cements", 7th International Congress on the Chemistry of Cement, Paris, vol 1, sub-theme IV-2, pp IV-2/1-IV-2/28

Talling, B and Brandstetr, J (1989), "Present state and future of alkali-activated slag concretes", 3rd CANMET/ACI International Conference on fly-ash, silica fume, slag and natural pozzolans in concrete, Malhotra, V M (edt), vol 2, SP114-74, pp 1519-1545

Tan, K and Pu, X (1998), "Strengthening effects of finely ground fly-ash, granulated blast furnace slag and their combination", Cement and Concrete Research, 28, no 12, pp 1819-1825

Taylor, H F W (1997), "Cement chemistry", 2nd edition, Thomas Telford Publishing, London, UK

Teoreanu, I (1991), "The interaction mechanism of blast furnace slags with water – the role of the activating agents", Il Cemento, 8, no 2, pp 91-97

Terzaghi, K and Peck, R B (1967), "Soil mechanics in engineering practice", 2nd edition, John Wiley and Sons, New York, USA

Tester, R E and Gaskin, P N (1996), "Effect on fines content on frost heave", Canadian Geotechnical Journal, 33, pp 678-680

Thomas, M D A, Kettle, R J and Morton, J A (1989), "The oxidation of pyrite in cement stabilised colliery shale", Quarterly Journal of Engineering Geology, 22, pp 207-218

Thompson, M R (1966), "Shear strength and elastic properties of soil-lime mixtures", Highway Research Record no 139, Washington, USA, pp 1-14

Thompson, M R and Harty, J R (1973), "Lime ractivity of ropial and subtropical soils", Highway Research Record 442, Highway Research Board, Washington DC, USA, pp105-112

Totani, Y, Saito, Y, Kageyama, M and Tanaka, H (1980), "The hydration of blast furnace slag cement", 7th Int. Congress on Cement Chemistry, Paris, pp III-95-III-98

Townsend, D L (1965), a discussion to "Split-tensile strength of lime-stabilised soils" by M R Thompson, Highway Research Record no 92, pp 81-82

Transport and Road Research Laboratory (1977), "The "LR90" frost heave test – interim specification for use with granular material", TRRl Supplementary Report 318. Department of the Environment and Department of Transport, Crowthorne, Berkshire

Transport Research Board (1976), "State of the art: lime stabilisation", Transport Research Circular, no 180, September 1976, Washington, USA

Tüfekci, M, Demirbas, A and Genc, H (1997), "Evaluation of steel furnace slags as cement additives", Cement and Concrete Research, 27, no 11, pp 1713-1717

Uchikawa, H (1986), "Effect of blending components on hydration and structure formation", Proceedings of the 8th International Congress on Chemistry of Cements, Rio de Janeiro, vol 1, sub-theme 3.3, pp 250-280

Uomoto, T and Kobayashi, K (1989), "Effect of curing temperature and humidity on strength of concrete containing blast furnace slag admixture", Proceedings of the 3rd International Conference "Fly-ash, silica fume, slag and natural pozzolans in concrete", Malhotra, V M (edt), Trondheim, Norway, 2, SP 114-65, pp 1345-1359

Van Aardt, J H P and Visser, S (1975), "Thaumasite formation: a cause of deterioration of Portland cement and related substances in the presence of sulphates", Cement and Concrete Research, 5, pp 225-232

Van Vliet-Lanoë, B (1985), "Frost effects on soils", in: Soils and quaternary landscape evolution, Boardman, J (edt), John Wiley & Sons Ltd, pp 117-158

Varma, S P and Bensted, J (1973), "Studies of thaumasite", Silicates Industriels, 38, pp 29-32

Veith, G, Tasong, W A, Wild, S and Robinson, R B (1999), "Delayed expansion of slag-stabilised kaolinite in the presence of sulphates", to be submitted to Cement and Concrete Research

Velde, B (1992), "Introduction to clay minerals", Chapman & Hall, London, UK

Vitton, S J and Harris, W W (1996), "The engineering significance of shrinkage and swelling soils in blast damage investigations", Proceedings of the 12th Annual Symposium on Explosives and Blasting Research, pp 65-75

Vosteen, B (1993), "Eignungsprüfung bei Bodenverbesserung und Bodenverfestigung mit Feinkalk und Kalkhydrat (Suitability check for soil stabilisation and modification with quicklime and hydrated lime)", *in German*, Erd- und Grundbautagung 1993, Vorträge der FGSV Tagung am 29. und 30. April in Goslar, Heft 6, Kirschbaum-Verlag, Bonn, Germany, pp 44-49

Wada, S and Igawa, (1966), "The influence of slag grain size distribution on the quality of Portland blast furnace slag cement", Cement Association Japan, Review of the 20th Annual Meeting, pp 91-93

Wang, S D and Scrivener, K L (1995), "Hydration products of alkali-activated slag cement", Cement and Concrete Research, 25, no 3, pp 561-571

Wang, S D, Pu, X, Scrivener, K L and Pratt, P L (1995), "Alkali-activated slag cement and concrete: a review of properties and problems", Advances in Cement Research, 7, no 27, pp 93-102

Washburn, E W (1921), "Note on a method of determining the distribution of pore sizes in porous materials", Proceedings of the International Academy of Science, 7, USA, pp 115-116

Watson, J (1994), "Highway construction and maintenance", Longman Scientific & Technical, 2nd edition, Burnt Hill, Harlow, UK

Whitbread, M, Marsey, A and Tunnell, C (1991), "Occurrence and the utilisation of mineral and construction wastes", Report for the Department of the Environment, HMSO, London

White, T L and Williams, P J (1994), "Cyrogenic alteration of frost susceptible soils", in: Ground Freezing, Proceedings of the 7th International Symposium on Ground Freezing, Fremdond (edt), Balkema, Rotterdam, pp 17-24

Whitlow, R. (1990), "Basic Soil Mechanics, 2nd edt., New York

Wild, S (1996b), "Observations on the use of ground waste brick as a cement replacement material", Building Research and Information, 24, no 1, pp 35-40

Wild, S, Abdi, M R and Leng-Ward, G (1993), "Sulphate expansion of lime-stabilised kaolinite: II. Reaction products and expansion", Clay Minerals, 28, pp 569-583

Wild, S, Arabi, M and Rowlands, G O (1987), "Relation between pore size distribution, permeability and cementitious gel formation in cured clay-lime systems", Material Science and Technology, 3, December 1987, pp 1005-1011

Wild, S, Hadi, M and Khatib, J (1995), "The influence of gypsum content on the porosity and pore size distribution of cured pfa-lime mixes", Advances in Cement Research, 7, no 26, pp 47-55

Wild, S, Hadi, M and Leng Ward, G (1990), "The influence of gypsum content on microstructural development, strength and expansion of cured lime-pfa mixes", Advances in Cement Research, 3, no 12, pp 153-166

Wild, S, Khatib, J and Addis, S D (1996a), "The potential of fired brick clay as a partial cement replacement material", International Congress − Concrete in the Service of Mankind, Concrete for Environment Enhancement and Protection, Theme 6: Waste Materials and Alternative Products, University of Dundee, Dhir, R K and Dyer, T D (edts), E & FN Spon, pp 685-696

Wild, S, Kinuthia, J M, Jones, G I and Higgins, D D (1998), "Effects of partial substitution of lime with ground granulated blast furnace slag (ggbs) on the strength properties of lime-stabilised sulphate-bearing clay soils", Engineering Geology, 51, pp 37-53

Wild, S, Kinuthia, J M, Jones, G I and Higgins, D D (1999), "Suppression of swelling associated with ettringite formation in lime stabilised sulphate bearing soils by partial substitution of lime with ground granulated blast furnace slag", Engineering Geology, 51, pp 257-277

Wild, S, Kinuthia, J M, Robinson, R B and Humphreys, I (1996), "Effects of ground granulated blast furnace slag (ggbs) on the strength and swelling properties of lime-stabilised kaolinite in the presence of sulphates", Clay Minerals, 31, pp 423-433

Wild, S, Tasong, W A and Veith, G (1997), "Utilisation of waste materials in the stabilisation of land", Report for the progress meeting of partners, University of Glamorgan, Building Materials Research Unit, UK

Wild, S, Tasong, W A and Veith, G (1998a), "Utilisation of waste materials in the stabilisation of land", Report for the progress meeting of partners, report no 2, University of Glamorgan, Building Materials Research Unit, UK

Wild, S, Tasong, W A, Veith, G and Thomas, B (1998b), "Utilisation of waste materials in the stabilisation of land", Report for the progress meeting of partners, report no 3, University of Glamorgan, Building Materials Research Unit, UK

Wild, S, Tasong, W A, Veith, G and Thomas, B (1999a), "Utilisation of waste materials in the stabilisation of land", Report for the progress meeting of partners, report no 4, University of Glamorgan, Building Materials Research Unit, UK

Wild, S, Tasong, W A, Veith, G and Thomas, B (1999b), "Utilisation of waste materials in the stabilisation of land", Report for the progress meeting of partners, report no 5, University of Glamorgan, Building Materials Research Unit, UK

Wilson, M J (1978), "Occurrence of thaumasite in weathered furnace slag, Merthyr Tydfil", Mineralogical Magazine, June 1978, 42, pp 290-291

Wimpenny, D E, Ellis, C, Reeves, C M and Higgins, D D (1989), "The development of strength and elastic properties in slag cement concretes under low temperature curing periods", Proceedings of the CANMET/ACI International Symposium 'Advance in Concrete Technology', SP 114-62, **2**, pp 1283-1306

Winslow, D (1989), "Some experimental possibilities with mercury intrusion porosimetry", Materials Research Society Symposium Proceedings "Pore structure and permeability of cementitious materials", **137**, Boston, Massachusetts, USA, pp 93-103

Winslow, D N and Diamond, S (1970), "A mercury porosimetry study of the evolution of porosity in Portland cement", Journal of Materials, JMLSA, **5**, no 3, pp 564-585

Winslow, D N and Lovell, C W (1981), "Measurements of pore size distributions in cements, aggregates and soils", Powder Technology, **29**, pp 151-165

Wu, X, Jiang, W and Roy, D M (1990), "Early activation and properties of slag cement", Cement and Concrete Research, **20**, pp 961-974

Xie, P and Beaudoin, J J (1992), "Mechanisms of sulphate expansion – I. Thermodynamic principle of crystallisation pressure", Cement and Concrete Research, **22**, pp 631-640

Xuequan, W, Sheng, Y, Xiaodong, S and Mingshu, T (1991), "Alkali-activated slag cement based radioactive waste forms", Cement and Concrete Research, **21**, pp 16-20

Yong, R N, Boonsinsuk, P and Yin, C W P (1985), "Alteration of soil behaviour after cyclic freezing and thawing", Fourth International Symp. on Ground Freezing, Sapporo, Japan, 5-7 August 1985, pp 187-195

Young, J F (1988), "A review of the pore structure of cement paste and concrete and its influence on permeability", ACI Convention on Permeability of Concrete, SP108-1, pp 1-18

Yuan, R, Gao, Q and Ouyang, S (1988), "Study on structure and latent hydraulic activity of slag and its activation mechanism", Silicates Industriels, no 3-4, pp 55-59

Zhou, H, Wu, X, Xu, Z and Tang, M (1993), "Kinetic study of hydration of alkali-activated slag", Cement and Concrete Research, **23**, pp 1253-1258

APPENDICES

Appendix 1 – Preliminary investigations

A1.1 Initial consumption of lime

It should be noted that pH measurements are generally difficult to perform accurately due to a high sensitivity of the equipment with regard to temperature and a short life span of the involved pH probes. Thus the pH meter was calibrated prior to each ICL test and the measurements were interpreted based on the pH value delivered for the lime solution. Sections A2.1.1, A2.1.2 and A2.1.3 show the results obtained from ICL tests on kaolnite, Kimmeridge Clay and Lower Oxford Clay respectively, which were carried according to BS 1924: part2: 1990.

A1.1.1 ICL test for Kaolinite

Sample no	Amount of kaolinite [g]	Amount of lime [%]	pH at 26 °C	Corrected pH to 25 °C *
1	20	0	6.27	6.30
2	20	2	12.60	12.63
3	20	3	12.70	12.73
4	20	4	12.74	12.77
5	20	5	12.78	12.81
6	20	6	12.82	12.85
7	0	100	12.83	12.86
78	20	7	12.84	12.87

* correction according to BS 1924: part 2: 1990 (section 5.4)

A1.1.2 ICL test for Kimmeridge Clay

Sample no	Amount of kaolinite [g]	Amount of lime [%]	pH at 26 °C	Corrected pH to 25 °C *
1	20	0	9.54	9.59
2	20	2	12.34	12.39
3	20	3	12.36	12.41
4	20	4	12.38	12.43
5	20	5	12.70	12.75
6	20	6	12.72	12.77
7	0	100	12.15	12.42

* correction according to BS 1924: part 2: 1990 (section 5.4)

A1.1.3 ICL test for Lower Oxford Clay

Sample no	Amount of kaolinite [g]	Amount of lime [%]	pH at 25 °C
1	20	0	7.48
2	20	0.5	10.83
3	20	1	11.13
4	20	1.5	11.23
5	20	2	11.27
6	*20*	*2.5*	*11.29*
7	20	3	11.38
8	20	4	11.40
9	20	5	11.41
10	20	6	11.42
11	20	7	11.46
12	*0*	*100*	*11.33*

A1.2 Atterberg limits

In order to allow an initial assessment of the modifications of the soil consistency brought about by the addition of lime and ggbs, the Atterberg limits of stabilised kaolinite and Lower Oxford Clay were determined according to BS 1377: part 2: 1990.

A1.2.1 Stabilised Kaolinite

Sample composition	Liquid Limit	Plastic limit	Plasticity index
2L0S	40	88	48
2L2S	38	81	43
2L4S	44	78	34
2L6S	41	82	41
2L8S	40	80	40

A1.2.2 Stabilised Lower Oxford Clay

Sample composition	Liquid Limit	Plastic limit	Plasticity index
pure Lower Oxford Clay	56	34	21
2L0S	78	49	29
2L2S	76	50	26
2L4S	75	48	27
2L6S	66	43	23
2L8S	58	44	14

Appendix 2 – Sample preparation

A2.1 Optimum moisture content (OMC) and maximum dry density (MDD)

The values for MDD and OMC for the various soil mix compositions had arrived from a series of standard Proctor compaction tests (2.5 kg rammer method) which were carried out in accordance with BS 1377: part4: 1990.

A2.1.1 MDD and OMC for stabilised Lower Oxford Clay

Mix	MDD [Mg/m^3]	OMC [%]
2L0S	1.360	28.2
2L2S	1.370	27.3
2L4S	1.370	26.5
2L6S	1.375	26.3
2L8S	13.80	26.2

A2.1.2 MDD and OMC for stabilised Kaolinite + 6% gypsum

Mix	MDD [Mg/m^3]	OMC [%]
2L0S6G	1.390	30.1
2L2S6G	1.400	28.2
2L4S6G	1.420	27.0
2L6S6G	1.430	26.8
2L8S6G	1.440	26.6

A2.1.3 MDD and OMC for stabilised Kaolinite + 0% gypsum

Mix	MDD [Mg/m^3]	OMC [%]
2L0S0G	1.442	31.0
2L2S0G	1.448	30.9
2L4S0G	1.450	30.1
2L6S0G	1.455	29.8
2L8S0G	1.480	29.6

A2.1.4 MDD and OMC for stabilised Kaolinite + 2% gypsum

Mix	MDD [Mg/m³]	OMC [%]
2L0S2G	1.440	31.2
2L2S2G	1.446	30.7
2L4S2G	1.452	30.2
2L6S2G	1.462	30.0
2L8S2G	1.472	29.7

A2.1.5 MDD and OMC for stabilised Kaolinite + 4% gypsum

Mix	MDD [Mg/m³]	OMC [%]
2L0S4G	1.412	31.5
2L2S4G	1.4250	31.2
2L4S4G	1.438	30.9
2L6S4G	1.457	29.6
2L8S4G	1.484	29.1

A2.2 Sample material computation

Example:
Mix 2L4S6G with a MDD (φ_d) of 1.420 Mg/m³ and an OMC (w) of 27.0%

Sample volume: V = 8.619273 E-05 m³ (sample size h= 76 mm and d=38 mm)

Determination of bulk density : $\varphi_b = \varphi_d \times (1+w) = 1.420 \times (1+0.27) = 1.8034$ Mg/m³

Mass = Density × volume , M = D×V

ergo: Determination of sample mass: M = $\varphi_b \times$ V
                                        M = 1.8034 Mg/m³ × 8.619273 E-05 m³
                                        M = 1.554 E-04 Mg = 155.40 g

Amount of kaolinite : 1.00K

2% lime =   0.02K (as a percentage of the clay)
4% ggbs =   0.04K
6% gypsum   0.06K
Total   1.12K (whole dry weight of soil + additives)

M = whole dry weight of soil + additives + (water content × dry weight of soil + additives)

$$= 1.12K + (0.27 \times 1.12K)$$
$$= 1.4224K$$

1.4224K = 155.40g   thus K = 109.25g

                         thus L =   2.19g (2%)

                         thus S =   4.37g (4%)

                         thusG = ___6.56g_(6%)

Total dry mass   122.37g

ergo determination of water addition: 27% × 122.37g = 33.04g

Check calculations: target sample weight = calculated sample weight

                                 155.40g = dry material + water

                                 155.40g = 122.37 + 33.04g

                                 155.40g ≈155.41g q.e.d.

Appendix 3 - Experimental data

A3.1 Shear strength development data

The GDS records stress paths up to the maximum values at failure and beyond that point until a pre-set percentage of strain is achieved. If the stress combinations at failure for different confining pressures are joined by a line, the modified failure envelope is created (Figure A3.1). To obtain the classic Mohr circle failure envelope, designated by the tangential points of the circles, a simple trigonometrical conversion is necessary.
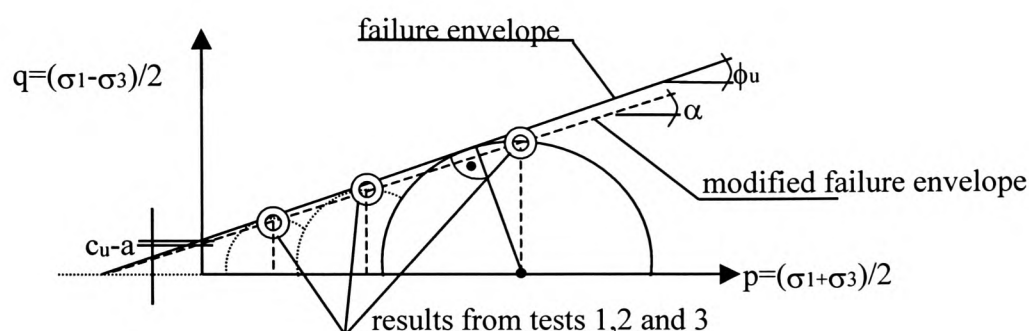
Figure A3.1 *Failure envelope and modified failure envelope*

A3.1.1 Kaolinite + 6% gypsum - angle of internal friction ϕ_u

Sample composition	Measured values (α)			Converted values $\tan^{\alpha} = \sin\phi_u$		
1 week	*10 ℃*	*20 ℃*	*30 ℃*	*10 ℃*	*20 ℃*	*30 ℃*
2L0S6G	9	6	8	9.1	6.0	8.1
2L2S6G	11	12	12	11.2	12.3	12.3
2L4S6G	11	16	18	11.2	16.7	19.0
2L6S6G	12	17	18	12.3	17.8	19.0
2L8S6G	12	17	18	12.3	17.8	19.0
4 weeks	*10 ℃*	*20 ℃*	*30 ℃*	*10 ℃*	*20 ℃*	*30 ℃*
2L0S6G	7	7	10	7.1	7.1	10.2
2L2S6G	13	12	12	13.3	12.3	12.3
2L4S6G	14	14	19	14.4	14.4	20.1
2L6S6G	14	20	20	14.4	21.3	21.3
2L8S6G	17	19	32	17.8	20.1	38.7
12 weeks	*10 ℃*	*20 ℃*	*30 ℃*	*10 ℃*	*20 ℃*	*30 ℃*
2L0S6G	5	7	16	5.0	7.1	16.7
2L2S6G	9	11	19	9.1	11.2	20.1
2L4S6G	16	18	20	16.7	19.0	21.3
2L6S6G	25	28	33	27.8	32.1	40.5

2L8S6G	26	28	33	29.2	32.1	40.5
24 weeks	*10 ᵒC*	*20 ᵒC*	*30 ᵒC*	*10 ᵒC*	*20 ᵒC*	*30 ᵒC*
2L0S6G	11	12	11	11.2	12.3	11.2
2L2S6G	18	21	16	19.0	22.6	16.7
2L4S6G	17	21	16	17.8	22.6	16.7
2L6S6G	17	18	21	17.8	19.0	22.6
2L8S6G	24	22	31	26.4	23.8	36.9
1 year	*10 ᵒC*	*20 ᵒC*	*30 ᵒC*	*10 ᵒC*	*20 ᵒC*	*30 ᵒC*
2L0S6G	5	9	8	5.0	9.1	8.1
2L2S6G	14	11	8	14.4	11.2	8.1
2L4S6G	16	20	18	16.7	21.3	19.0
2L6S6G	18	23	21	19.0	25.1	22.6
2L8S6G	20	26	27	21.3	29.2	30.6

A3.1.2 Kaolinite + 6% gypsum – cohesion c_u

Sample composition	Measured values (a)			Converted values $c_u = a/\cos\phi_u$		
1 week	*10 ᵒC*	*20 ᵒC*	*30 ᵒC*	*10 ᵒC*	*20 ᵒC*	*30 ᵒC*
2L0S6G	120	210	220	122	211	222
2L2S6G	135	250	240	138	256	246
2L4S6G	160	275	390	163	287	412
2L6S6G	160	290	450	164	305	476
2L8S6G	180	415	610	184	436	645
4 weeks	*10 ᵒC*	*20 ᵒC*	*30 ᵒC*	*10 ᵒC*	*20 ᵒC*	*30 ᵒC*
2L0S6G	175	240	250	176	242	254
2L2S6G	270	330	370	277	338	379
2L4S6G	320	340	430	330	351	458
2L6S6G	410	400	440	423	429	472
2L8S6G	410	550	230	431	586	295
12 weeks	*10 ᵒC*	*20 ᵒC*	*30 ᵒC*	*10 ᵒC*	*20 ᵒC*	*30 ᵒC*
2L0S6G	365	340	200	366	343	209
2L2S6G	390	440	390	395	449	415
2L4S6G	330	360	580	344	381	623
2L6S6G	310	400	490	350	472	644
2L8S6G	200	370	390	229	437	513
24 weeks	*10 ᵒC*	*20 ᵒC*	*30 ᵒC*	*10 ᵒC*	*20 ᵒC*	*30 ᵒC*
2L0S6G	310	230	300	316	235	306
2L2S6G	280	280	430	296	303	449
2L4S6G	370	410	540	389	444	564
2L6S6G	550	700	700	578	740	758
2L8S6G	480	670	500	536	732	626
1 year	*10 ᵒC*	*20 ᵒC*	*30 ᵒC*	*10 ᵒC*	*20 ᵒC*	*30 ᵒC*
2L0S6G	405	180	200	407	182	202
2L2S6G	400	410	350	413	418	354
2L4S6G	390	300	340	407	322	360
2L6S6G	615	400	680	650	442	736
2L8S6G	400	550	560	429	630	651

A3.1.3 Kaolinite without gypsum addition – angle of internal friction ϕ^u

Sample composition	Measured values (α)			Converted values $\tan\alpha = \sin\phi_u$		
1 week	*10 °C*	*20 °C*	*30 °C*	*10 °C*	*20 °C*	*30 °C*
2L0S0G	3	2	6	3.0	2.0	6.0
2L4S0G	3	3	8	3.0	3.0	8.1
2L8S0G	5	5	12	5.0	5.0	12.3
4 weeks	*10 °C*	*20 °C*	*30 °C*	*10 °C*	*20 °C*	*30 °C*
2L0S0G	6	12	16	6.0	12.3	16.7
2L4S0G	10	8	18	10.2	8.1	19.0
2L8S0G	14	11	20	14.4	11.2	21.3
12 weeks	*10 °C*	*20 °C*	*30 °C*	*10 °C*	*20 °C*	*30 °C*
2L0S0G	12	13	13	12.3	13.3	13.3
2L4S0G	16	8	11	16.7	8.1	11.2
2L8S0G	18	12	10	19.0	12.3	10.2
24 weeks	*10 °C*	*20 °C*	*30 °C*	*10 °C*	*20 °C*	*30 °C*
2L0S0G	10	11	14	10.2	11.2	14.4
2L4S0G	14	17	14	14.4	17.8	14.4
2L8S0G	15	21	28	15.5	22.6	32.1
1 year	*10 °C*	*20 °C*	*30 °C*	*10 °C*	*20 °C*	*30 °C*
2L0S0G	8	12	15	8.1	12.3	15.5
2L4S0G	19	17	26	20.1	17.8	29.2
2L8S0G	25	23	31	27.8	25.1	36.9

A3.1.4 Kaolinite without gypsum addition – cohesion c_u

Sample composition	Measured values (a)			Converted values $c_u = a/\cos\phi_u$		
1 week	*10 °C*	*20 °C*	*30 °C*	*10 °C*	*20 °C*	*30 °C*
2L0S0G	160	130	120	160	130	121
2L4S0G	160	160	180	160	160	182
2L8S0G	170	180	310	171	181	317
4 weeks	*10 °C*	*20 °C*	*30 °C*	*10 °C*	*20 °C*	*30 °C*
2L0S0G	215	100	70	216	102	73
2L4S0G	200	200	80	203	202	85
2L8S0G	75	170	70	77	173	75
12 weeks	*10 °C*	*20 °C*	*30 °C*	*10 °C*	*20 °C*	*30 °C*
2L0S0G	85	140	120	87	144	123
2L4S0G	160	200	180	167	202	184
2L8S0G	155	190	185	164	194	188
24 weeks	*10 °C*	*20 °C*	*30 °C*	*10 °C*	*20 °C*	*30 °C*
2L0S0G	225	115	150	229	117	155
2L4S0G	290	180	240	299	189	248
2L8S0G	195	180	240	202	195	283
1 year	*10 °C*	*20 °C*	*30 °C*	*10 °C*	*20 °C*	*30 °C*
2L0S0G	310	160	110	313	164	114
2L4S0G	380	305	520	405	320	596
2L8S0G	150	1290	1120	170	1425	1401

A3.1.5 Lower Oxford Clay – angle of internal friction ϕ^u

Sample composition	Measured values (α)			Converted values tanα= sinφ$_u$		
1 week	*10 °C*	*20 °C*	*30 °C*	*10 °C*	*20 °C*	*30 °C*
2L0S	2	2	2	2.0	2.0	2.0
2L2S	2	6	6	2.0	6.0	6.0
2L4S	3	10	10	3.0	10.2	10.2
2L6S	5	12	11	5.0	12.3	11.2
2L8S	5	14	14	5.0	14.4	14.4
4 weeks	*10 °C*	*20 °C*	*30 °C*	*10 °C*	*20 °C*	*30 °C*
2L0S	1	3	3	1.0	3.0	3.0
2L2S	2	3	5	2.0	3.0	5.0
2L4S	7	11	18	7.1	11.2	19.0
2L6S	9	16	15	9.1	16.7	15.5
2L8S	17	18	19	17.8	19.0	20.1
12 weeks	*10 °C*	*20 °C*	*30 °C*	*10 °C*	*20 °C*	*30 °C*
2L0S	2	3	9	2.0	3.0	9.1
2L2S	6	7	13	6.0	7.1	13.3
2L4S	15	14	12	15.5	14.4	12.3
2L6S	14	17	23	14.4	17.8	25.1
2L8S	18	31	24	19.0	36.9	26.4
24 weeks	*10 °C*	*20 °C*	*30 °C*	*10 °C*	*20 °C*	*30 °C*
2L0S	3	3	7	3.0	3.0	7.1
2L2S	3	19	12	3.0	20.1	12.3
2L4S	12	19	16	12.3	20.1	16.7
2L6S	22	20	17	23.8	21.3	17.8
2L8S	23	26	25	25.1	29.2	27.8
1 year	*10 °C*	*20 °C*	*30 °C*	*10 °C*	*20 °C*	*30 °C*
2L0S	5	5	3	5.0	5.0	3.0
2L2S	10	8	19	10.2	8.1	20.1
2L4S	14	18	23	14.4	19.0	25.1
2L6S	24	18	29	26.4	19.0	33.7
2L8S	31	24	28	36.9	26.4	32.1

A3.1.6 Lower Oxford Clay – cohesion c_u

Sample composition	Measured values (a)			Converted values $c_u = a/\cos\phi_u$		
1 week	*10 $\circ C$*	*20 $\circ C$*	*30 $\circ C$*	*10 $\circ C$*	*20 $\circ C$*	*30 $\circ C$*
2L0S	150	190	190	150	190	190
2L2S	235	260	250	235	261	251
2L4S	330	430	415	330	437	422
2L6S	360	470	500	361	481	510
2L8S	440	680	670	442	702	692
4 weeks	*10 $\circ C$*	*20 $\circ C$*	*30 $\circ C$*	*10 $\circ C$*	*20 $\circ C$*	*30 $\circ C$*
2L0S	195	200	190	195	200	190
2L2S	315	480	435	315	481	437
2L4S	440	600	490	443	612	518
2L6S	490	610	700	496	637	727
2L8S	530	810	800	557	856	852
12 weeks	*10 $\circ C$*	*20 $\circ C$*	*30 $\circ C$*	*10 $\circ C$*	*20 $\circ C$*	*30 $\circ C$*
2L0S	190	270	100	190	270	101
2L2S	350	350	350	352	353	360
2L4S	485	580	770	503	599	788
2L6S	610	630	650	630	662	718
2L8S	610	500	1020	645	626	1139
24 weeks	*10 $\circ C$*	*20 $\circ C$*	*30 $\circ C$*	*10 $\circ C$*	*20 $\circ C$*	*30 $\circ C$*
2L0S	150	170	100	150	170	101
2L2S	400	220	210	401	234	215
2L4S	690	410	680	706	437	710
2L6S	520	590	700	568	633	735
2L8S	900	810	750	994	928	848
1 year	*10 $\circ C$*	*20 $\circ C$*	*30 $\circ C$*	*10 $\circ C$*	*20 $\circ C$*	*30 $\circ C$*
2L0S	140	110	80	141	110	80
2L2S	380	400	250	386	404	266
2L4S	700	520	320	723	550	353
2L6S	580	800	420	648	846	505
2L8S	500	920	615	626	1027	726

A3.2 Unconfined compressive strength

Curing was for all specimens at 30 °C. The shown value is the average value from test results obtained from at least three specimens.

A3.2.1 Kaolinite with various gypsum additions

Curing period	Sample composition	0% gypsum	2% gypsum	4% gypsum	6% gypsum
0 weeks	2L0S	105.7	-	-	330.9
	2L2S	125.3	-	-	308.4
	2L4S	190.9	-	-	340.2
	2L6S	104.8	-	-	325.5
	2L8S	91.1	-	-	283.9
1 week	2L0S	627.6	478.3	166.4	342.7
	2L2S	451.8	572.7	281.0	664.3
	2L4S	350.5	436.7	327.5	1564.0
	2L6S	398.0	577.1	653.0	1486.7
	2L8S	312.8	675.0	1035.3	2283.1
4 weeks	2L0S	655.5	458.2	175.7	564.4
	2L2S	441.5	463.6	449.9	798.9
	2L4S	344.1	602.1	838.1	1451.9
	2L6S	352.5	854.7	851.3	1551.8
	2L8S	401.4	1014.3	1140.6	1752.0
12 weeks	2L0S	174.8	241.8	229.1	369.1
	2L2S	542.9	527.2	538.5	988.3
	2L4S	644.7	677.5	651.1	1425.5
	2L6S	664.3	960.4	939.4	1897.4
	2L8S	643.2	988.8	1242.9	2097.6

A3.2.2 The effect of soaking on the UCS of kaolinite stabilised with high slag/lime ratios

Kaolinite with 1% lime and 5% ggbs moist cured

Curing period	1L5S2G	1L5S4G	1L5S6G	1L5S8G
1 week	1236.0	1199.3	1032.9	1179.7
4 weeks	1876.8	1774.0	1750.0	1685.4
12 weeks	1842.1	1499.4	1611.0	1693.2
24 weeks	1757.4	1562.1	1794.1	1716.3

Kaolinite with 1% lime and 5% ggbs moist cured and subsequently soaked for 7 days prior to testing

Curing period	1L5S2G	1L5S4G	1L5S6G	1L5S8G
1 week	991.8	910.5	978.5	1043.7
4 weeks	908.5	792.0	1317.3	978.5
12 weeks	1377.0	1088.2	1573.3	1222.3
24 weeks	1433.3	1163.1	1481.8	1118.1

Kaolinite with 0.5% lime and 5.5% ggbs moist cured

Curing period	0.5L5.5S2G	0.5L5.5S4G	0.5L5.5S6G	0.5L5.5S8G
1 week	1233.6	1133.7	1155.8	944.8
4 weeks	1374.1	1645.8	1346.2	1664.4
12 weeks	1882.2	1271.3	1455.3	1496.9
24 weeks	1852.8	1444.1	1428.9	1626.2

Kaolinite with 0.5% lime and 5.5% ggbs moist cured and subsequently soaked for 7 days prior to testing

Curing period	0.5L5.5S2G	0.5L5.5S4G	0.5L5.5S6G	0.5L5.5S8G
1 week	811.1	874.8	1333.0	916.4
4 weeks	991.3	1067.6	1449.0	823.4
12 weeks	1133.7	1191.0	1485.7	985.4
24 weeks	1318.3	1099.5	1283.5	1207.2

A3.2.3 Lower Oxford Clay

Curing period	Sample composition	UCS $[kN/m^2]$
1 week	2L0S	313.8
	2L2S	774.4
	2L4S	1180.2
	2L6S	1569.4
	2L8S	1797.0
4 weeks	2L0S	374.5
	2L2S	867.4
	2L4S	1148.4
	2L6S	1655.1
	2L8S	1874.4
12 weeks	2L0S	363.7
	2L2S	923.2
	2L4S	1405.4
	2L6S	1689.3
	2L8S	2136.8
24 weeks	2L0S	447.9
	2L2S	933.0
	2L4S	1742.0
	2L6S	2462.3
	2L8S	2703.2

A3.3 Indirect tensile strength

A3.3.1 Kaolinite

Curing period	Sample composition	0% gypsum	2% gypsum	4% gypsum	6% gypsum
0 weeks	2L0S	0.058	-	-	0.051
	2L2S	0.044	-	-	0.058
	2L4S	0.051	-	-	0.044
	2L6S	0.056	-	-	0.046
	2L8S	0.052	-	-	0.048
1 week	2L0S	0.068	0.101	0.098	0.107
	2L2S	0.067	0.132	0.114	0.198
	2L4S	0.076	0.194	0.200	0.298
	2L6S	0.075	0.233	0.264	0.298
	2L8S	0.080	0.278	0.308	0.402
4 weeks	2L0S	0.085	0.096	0.082	0.241
	2L2S	0.073	0.113	0.118	0.343
	2L4S	0.072	0.238	0.224	0.439
	2L6S	0.046	0.261	0.241	0.457
	2L8S	0.045	0.325	0.263	0.457
12 weeks	2L0S	0.115	0.104	0.178	0.190
	2L2S	0.119	0.177	0.182	0.270
	2L4S	0.103	0.236	0.276	0.378
	2L6S	0.109	0.344	0.342	0.458
	2L8S	0.105	0.384	0.430	0.579

A3.3.2 Lower Oxford Clay

Curing period	Sample composition	R_{it} [kN/m^2]
1 week	2L0S	0.212
	2L2S	0.194
	2L4S	0.228
	2L6S	0.245
	2L8S	0.304
4 weeks	2L0S	0.215
	2L2S	0.221
	2L4S	0.302
	2L6S	0.288
	2L8S	0.358
12 weeks	2L0S	0.25935
	2L2S	0.193907
	2L4S	0.305
	2L6S	0.341
	2L8S	0.441

A3.4 Permeability data

A3.4.1 Kaolinite + 6% gypsum

Sample composition	Measured k-values [m/h]		
1 week	*10 °C*	*20 °C*	*30 °C*
2L0S6G	3.50E-06	2.60E-06	3.10E-06
2L2S6G	4.30E-06	3.60E-06	1.70E-05
2L4S6G	2.50E-06	7.30E-06	2.40E-05
2L6S6G	5.90E-06	1.60E-05	5.50E-05
2L8S6G	2.30E-06	1.00E-05	4.40E-05
4 weeks	*10 °C*	*20 °C*	*30 °C*
2L0S6G	3.80E-06	2.00E-06	1.20E-07
2L2S6G	8.00E-08	3.40E-07	6.00E-08
2L4S6G	1.50E-07	4.50E-07	8.00E-08
2L6S6G	1.40E-07	5.30E-07	7.00E-08
2L8S6G	8.10E-08	5.40E-07	6.90E-08
12 weeks	*10 °C*	*20 °C*	*30 °C*
2L0S6G	1.40E-06	8.10E-08	6.10E-08
2L2S6G	1.10E-07	3.50E-08	4.80E-08
2L4S6G	1.30E-07	9.30E-08	9.80E-08
2L6S6G	1.00E-07	4.00E-08	7.80E-08
2L8S6G	4.80E-07	4.30E-08	2.00E-07
24 weeks	*10 °C*	*20 °C*	*30 °C*
2L0S6G	7.20E-08	7.50E-08	6.40E-08
2L2S6G	5.40E-08	5.90E-08	6.70E-08
2L4S6G	5.40E-08	6.80E-08	7.20E-08
2L6S6G	2.80E-07	1.10E-07	8.70E-08
2L8S6G	1.00E-07	7.80E-08	7.50E-08
1 year	*10 °C*	*20 °C*	*30 °C*
2L0S6G	8.70E-08	5.70E-07	6.40E-08
2L2S6G	1.00E-07	6.80E-08	6.60E-08
2L4S6G	1.20E-07	2.40E-07	6.00E-08
2L6S6G	3.60E-07	1.20E-07	1.20E-07
2L8S6G	5.30E-08	1.80E-07	1.00E-07

A3.4.2 Kaolinite without gypsum addition

Sample composition	Measured k-values [m/h]		
1 week	10 °C	20 °C	30 °C
2L0S0G	3.80E-06	4.00E-06	4.30E-06
2L4S0G	5.00E-06	2.50E-06	6.80E-06
2L8S0G	4.20E-06	5.20E-06	4.80E-06
4 weeks	10 °C	20 °C	30 °C
2L0S0G	2.10E-07	8.40E-08	1.30E-06
2L4S0G	3.90E-06	8.50E-08	2.00E-07
2L8S0G	3.60E-06	6.40E-08	6.00E-08
12 weeks	10 °C	20 °C	30 °C
2L0S0G	1.10E-05	1.10E-05	1.90E-06
2L4S0G	5.00E-05	8.90E-06	1.00E-07
2L8S0G	1.20E-05	5.90E-06	1.20E-07
24 weeks	10 °C	20 °C	30 °C
2L0S0G	1.60E-06	5.00E-06	6.70E-06
2L4S0G	7.90E-06	4.30E-06	8.00E-07
2L8S0G	9.20E-06	9.00E-06	2.80E-07
1 year	10 °C	20 °C	30 °C
2L0S0G	1.00E-06	2.10E-05	5.30E-06
2L4S0G	3.00E-06	5.00E-06	1.50E-06
2L8S0G	3.30E-06	2.70E-07	9.60E-08

A3.4.3 Lower Oxford Clay

Sample composition	Measured k-values [m/h]		
1 week	*10 °C*	*20 °C*	*30 °C*
2L0S	1.80E-06	9.90E-07	1.80E-06
2L2S	5.80E-07	1.10E-06	2.00E-07
2L4S	4.70E-07	1.60E-07	1.40E-07
2L6S	8.00E-07	2.50E-07	9.10E-08
2L8S	9.00E-07	1.20E-07	1.10E-07
4 weeks	*10 °C*	*20 °C*	*30 °C*
2L0S	4.40E-07	5.20E-07	1.10E-06
2L2S	5.00E-07	5.10E-07	2.70E-07
2L4S	4.10E-07	2.70E-07	2.00E-07
2L6S	4.00E-07	2.90E-07	1.90E-07
2L8S	2.00E-07	1.20E-07	1.40E-07
12 weeks	*10 °C*	*20 °C*	*30 °C*
2L0S	3.90E-07	7.50E-07	3.00E-07
2L2S	3.60E-07	6.10E-07	1.90E-07
2L4S	1.40E-07	4.10E-07	9.60E-08
2L6S	4.00E-08	1.10E-07	9.80E-08
2L8S	1.00E-07	8.30E-08	8.40E-08
24 weeks	*10 °C*	*20 °C*	*30 °C*
2L0S	6.10E-08	5.90E-08	1.00E-07
2L2S	2.00E-07	4.00E-08	6.60E-08
2L4S	7.10E-08	5.10E-08	9.00E-08
2L6S	7.00E-08	6.40E-08	7.50E-08
2L8S	2.30E-07	4.80E-08	9.50E-08
1 year	*10 °C*	*20 °C*	*30 °C*
2L0S	9.60E-08	7.20E-08	7.00E-08
2L2S	1.10E-07	5.60E-08	8.40E-08
2L4S	6.70E-08	5.80E-08	7.20E-08
2L6S	8.00E-08	5.50E-08	8.20E-08
2L8S	1.00E-07	6.40E-08	8.00E-08

A3.5 Mercury intrusion data

A3.5.1 Kaolinite + 6% gypsum

Percentage of pore volume occupied by pores with a radius < 0.05 μm [%]

Sample composition	1 week			4 weeks			12 weeks			24 weeks			1 year		
	10°C	20°C	30°C	10°C	20°C	30°C	10°C	20°C	30°C	10°C	20°C	30°C	10°C	20°C	30°C
2L0S6G	26.9	28.3	29.8	25.5	23.2	26.2	22.1	26.3	25.7	25.0	23.0	23.9	25.7	23.6	26.6
2L2S6G	34.5	31.2	29.9	29.4	26.7	31.3	24.5	30.5	40.4	23.6	31.1	33.9	30.5	33.1	33.8
2L4S6G	42.1	36.8	30.1	32.4	33.0	39.6	34.8	35.4	45.1	32.4	38.6	40.6	36.1	41.1	45.4
2L6S6G	41.2	45.0	47.4	48.6	41.5	45.0	42.7	41.1	49.4	49.1	48.6	54.3	50.1	45.7	51.0
2L8S6G	56.0	50.1	54.1	54.4	47.8	47.4	48.1	50.2	49.7	52.7	49.3	56.2	46.5	56.3	55.5

Total intruded pore volume [mm³/g]

Sample composition	1 week			4 weeks			12 weeks			24 weeks			1 year		
	10°C	20°C	30°C	10°C	20°C	30°C	10°C	20°C	30°C	10°C	20°C	30°C	10°C	20°C	30°C
2L0S6G	262.1	262.0	259.3	277.7	278.6	273.4	269.5	285.0	288.8	270.7	292.1	301.5	275.8	294.7	280.5
2L2S6G	257.9	273.4	276.7	270.4	272.9	279.6	301.9	285.0	274.8	299.8	269.8	282.5	289.5	285.3	286.8
2L4S6G	250.5	256.4	262.0	276.2	283.7	263.0	279.9	292.7	273.3	286.6	278.7	276.3	290.9	276.6	287.3
2L6S6G	243.1	260.0	250.0	268.7	256.6	271.1	263.0	268.3	267.0	284.7	263.9	260.9	278.5	271.9	286.4
2L8S6G	218.1	267.9	251.5	261.9	260.7	260.5	250.1	263.2	273.4	279.1	262.5	258.8	304.6	256.1	262.2

Gabriele Veith
University of Glamorgan

A3.5.2 Kaolinite without gypsum addition

Percentage of pore volume occupied by pores with a radius < 0.05 μm [%]

Sample composition	1 week			4 weeks			12 weeks			24 weeks			1 year		
	10°C	20°C	30°C	10°C	20°C	30°C	10°C	20°C	30°C	10°C	20°C	30°C	10°C	20°C	30°C
2L0S0G	27.3	22.6	39.3	37.3	37.1	34.3	42.5	40.4	40.5	38.0	40.1	38.9	41.0	40.4	42.1
2L4S0G	37.1	21.1	38.2	34.8	38.1	40.0	40.8	38.3	40.8	39.6	40.8	37.7	43.1	48.8	85.9
2L8S0G	20.4	20.2	35.3	22.5	40.6	38.9	42.9	42.5	44.8	38.7	58.5	40.6	55.8	91.4	90.0

Total intruded pore volume [mm³/g]

Sample composition	1 week			4 weeks			12 weeks			24 weeks			1 year		
	10°C	20°C	30°C	10°C	20°C	30°C	10°C	20°C	30°C	10°C	20°C	30°C	10°C	20°C	30°C
2L0S0G	284.2	276.9	294.7	294.8	294.3	271.3	295.8	297.0	294.5	305.4	301.1	312.4	282.1	298.0	297.3
2L4S0G	262.5	257.3	291.3	276.3	287.7	284.3	287.8	308.3	300.7	301.1	297.7	308.3	285.2	300.5	283.9
2L8S0G	270.0	279.4	301.4	237.6	277.6	283.0	288.4	276.4	284.3	297.1	289.3	304.6	278.3	267.0	251.5

A3.5.3 Kaolinite + 2% gypsum

Percentage of pore volume occupied by pores with a radius < 0.05 μm [%]

Sample composition	1 week	4 weeks	12 weeks
2L0S2G	27.1	30.8	34.2
2L2S2G	38.9	42.8	25.3
2L4S2G	45.1	52.0	44.7
2L6S2G	61.7	56.9	54.1
2L8S2G	60.8	68.2	59.5

Total intruded pore volume [mm³/g]

Sample composition	1 week	4 weeks	12 weeks
2L0S2G	276.2	266.2	255.4
2L2S2G	276.7	273.2	178.0
2L4S2G	261.9	258.4	226.9
2L6S2G	256.8	259.2	253.5
2L8S2G	251.5	249.0	230.0

A3.5.4 Kaolinite + 4% gypsum

Percentage of pore volume occupied by pores with a radius < 0.05 μm [%]

Sample composition	1 week	4 weeks	12 weeks
2L0S4G	26.2	29.3	35.1
2L2S4G	35.6	37.1	33.3
2L4S4G	40.6	47.3	42.8
2L6S4G	48.1	49.1	51.1
2L8S4G	60.3	62.2	60.8

Total intruded pore volume [mm³/g]

Sample composition	1 week	4 weeks	12 weeks
2L0S4G	279.7	273.8	251.3
2L2S4G	261.1	263.7	271.4
2L4S4G	262.6	259.0	244.9
2L6S4G	258.2	254.0	253.7
2L8S4G	251.3	253.4	

A3.5.5 *Lower Oxford Clay*

Percentage of pore volume occupied by pores with a radius < 0.05 μm [%]

Sample composition	1 week			4 weeks			12 weeks			24 weeks			1 year		
	10°C	20°C	30°C	10°C	20°C	30°C	10°C	20°C	30°C	10°C	20°C	30°C	10°C	20°C	30°C
2L0S	51.96	49.74	41.4	42.1	45.42	44.0	52.2	45.48	46.9	54.4	54.42	40.4	54.6	49.61	51.6
2L2S	51.9	43.09	45.5	44.8	43.02	44.6	49.9	45	45.3	52.1	41.87	42.4	54.2	51.44	48.7
2L4S	58.73	45.3	46.7	51.4	49.73	47.7	54.4	48.96	51.6	50.9	44.73	51.7	50.8	52.26	50.7
2L6S	52.6	50.97	46.3	56.2	49.11	48.7	47.1	50.14	54.1	50.9	46.69	47.5	54.7	56	56.6
2L8S	61.84	47.77	51.9	57.2	54.43	54.3	59.8	54.33	57.3	56.3	57.92	57.1	60.7	57.71	57.8

Total intruded pore volume [mm³/g]

Sample composition	1 week			4 weeks			12 weeks			24 weeks			1 year		
	10°C	20°C	30°C	10°C	20°C	30°C	10°C	20°C	30°C	10°C	20°C	30°C	10°C	20°C	30°C
2L0S	160.3	169.5	172.4	169.2	165.2	177.5	160.1	173.7	168.4	151.5	151.4	176.3	163.0	170.5	157.0
2L2S	173.6	187.7	185.2	191.8	192.0	202.5	189.9	187.2	194.9	165.6	197.9	195.8	163.8	186.3	196.0
2L4S	180.6	192.0	177.4	196.5	186.3	197.0	186.5	196.8	198.1	191.8	197.9	207.2	194.7	197.3	214.8
2L6S	200.4	199.9	201.3	191.1	210.1	216.1	183.0	206.1	200.5	204.7	192.7	221.1	187.7	201.3	207.4
2L8S	193.9	214.4	196.4	191.7	193.3	193.5	188.9	196.4	196.3	181.9	187.7	198.0	190.0	199.8	208.5

Gabriele Veith
University of Glamorgan

A3.6 Freeze-thaw resistance

A3.6.1 Kaolinite with 6% gypsum

Curing period prior to frost action: 7 days

	2L0S6G		2L2S6G		2L4S6G		2L6S6G		2L8S6G	
	weight		weight		weight		weight		weight	
	total	%	total	%	total	%	total	%	total	%
0	426.7	0.0	432.6	0.0	438.8	0.0	439.2	0.0	440.6	0.0
1	459.4	7.7	457.5	5.8	463.3	5.6	459.7	4.7	462.2	4.9
2	466.8	9.4	475.1	9.8	479.6	9.3	476.1	8.4	475.1	7.8
3	471.3	10.5	484.1	11.9	479.8	9.3	485.1	10.5	482.8	9.6
4	474.0	11.1	489.8	13.2	482.3	9.9	489.5	11.5	490.4	11.3
5	476.5	11.7	495.2	14.5	487.1	11.0	495.2	12.8	498.0	13.0
6	477.3	11.9	500.8	15.8	491.0	11.9	499.7	13.8	503.8	14.4
7	478.7	12.2	500.6	15.7	494.5	12.7	512.2	16.6	509.7	15.7
8	480.4	12.6	499.6	15.5	497.1	13.3	512.6	16.7	506.2	14.9
9	478.8	12.2	501.6	16.0	502.8	14.6	514.6	17.2	513.7	16.6
11	478.9	12.2	501.2	15.9	502.0	14.4	519.0	18.2	512.4	16.3
12	479.4	12.3	504.5	16.6	503.7	14.8	528.0	20.2	514.3	16.7

	2L0S6G		2L2S6G		2L4S6G		2L6S6G		2L8S6G	
	height		height		height		height		height	
	total	%	total	%	total	%	total	%	total	%
0	1778	0	1885	0	1752	0	2300	0	2302	0
1	9402	7.4	6560	4.5	6208	4.3	5560	3.2	5741	3.3
2	11650	9.6	10595	8.5	9810	7.8	8980	6.5	8861	6.4
3	13260	11.1	13100	10.9	11680	9.6	11780	9.2	11870	9.3
4	16650	14.4	15950	13.7	11682	9.6	12090	9.5	11920	9.3
5	19300	17.0	16860	14.5	13850	11.7	13150	10.5	14870	12.2
6	20420	18.1	19420	17.0	14750	12.6	17100	14.4	16700	14.0
7	21950	19.6	20100	17.7	15700	13.5	17520	14.8	16900	14.2
8	25500	23.0	20700	18.3	16300	14.1	19300	16.5	18350	15.6
9	25000	22.5	21400	18.9	16900	14.7	18700	15.9	19400	16.6
11	25670	23.2	23340	20.8	17420	15.2	20750	17.9	20010	17.2
12	26250	23.8	24900	22.3	19940	17.7	21500	18.6	20860	18.0

Curing period prior to frost action: 28 days

	2L0S6G		2L2S6G		2L4S6G		2L6S6G		2L8S6G	
	weight		weight		weight		weight		weight	
	total	%	total	%	total	%	total	%	total	%
0	429.9	0.0	433.6	0.0	438.3	0.0	445.0	0.0	439.9	0.0
1	448.8	4.4	449.4	3.6	452.1	3.2	452.6	1.7	448.7	2.0
2	463.8	7.9	465.3	7.3	467.9	6.8	469.9	5.6	462.9	5.2
3	469.9	9.3	476.1	9.8	479.4	9.4	479.8	7.8	473.0	7.5
4	474.0	10.2	480.5	10.8	485.2	10.7	485.8	9.2	479.8	9.1
5	475.1	10.5	484.6	11.8	489.7	11.7	491.7	10.5	486.6	10.6
6	478.6	11.3	486.9	12.3	492.6	12.4	496.1	11.5	491.5	11.7
7	479.8	11.6	485.2	11.9	495.7	13.1	499.9	12.4	495.9	12.7
8	482.3	12.2	488.1	12.6	497.3	13.5	503.0	13.1	498.5	13.3
9	478.9	11.4	488.1	12.6	496.6	13.3	507.1	14.0	501.9	14.1
11	479.0	11.4	489.5	12.9	499.5	14.0	508.2	14.2	503.6	14.5
12	479.2	11.4	488.1	12.6	499.0	13.8	510.5	14.7	505.4	14.9

	2L0S6G		2L2S6G		2L4S6G		2L6S6G		2L8S6G	
	height		height		height		height		height	
	total	%	total	%	total	%	total	%	total	%
0	1718	0	1891	0	2175	0	4212	0	2300	0
1	5960	4.1	5131	3.1	4640	2.4	5529	1.3	3570	1.2
2	8950	7.0	8100	6.0	7742	5.4	8369	4.0	5941	3.5
3	12080	10.1	10549	8.4	10750	8.3	10430	6.0	8223	5.8
4	14580	12.5	12050	9.9	12340	9.9	11780	7.3	10000	7.5
5	16200	14.1	14600	12.3	14530	12.0	12960	8.5	11610	9.0
6	17870	15.7	15900	13.6	15460	12.9	15610	11.1	12810	10.2
7	20162	17.9	16420	14.1	16870	14.3	16112	11.6	13910	11.3
8	22100	19.8	18200	15.8	17800	15.2	17050	12.5	13950	11.3
9	22600	20.3	18840	16.5	18700	16.0	17920	13.3	14750	12.1
11	23300	21.0	20750	18.3	19600	16.9	19290	14.6	15320	12.6
12	24200	21.8	20900	18.5	20600	17.9	20010	15.3	16250	13.5

Curing period prior to frost action: 90 days

	2L0S6G		2L2S6G		2L4S6G		2L6S6G		2L8S6G	
	weight		weight		weight		weight		weight	
	total	%	total	%	total	%	total	%	total	%
0	428.8	0.0	434.6	0.0	447.5	0.0	440.1	0.0	439.3	0.0
1	443.1	3.3	447.6	3.0	460.6	2.9	448.5	1.9	446.1	1.6
2	453.0	5.6	458.6	5.5	472.8	5.6	460.7	4.7	456.4	3.9
3	458.6	6.9	467.1	7.5	482.0	7.7	469.2	6.6	464.2	5.7
4	463.8	8.2	473.2	8.9	489.6	9.4	475.9	8.1	471.1	7.2
6	467.8	9.1	479.4	10.3	497.4	11.1	486.2	10.5	481.9	9.7
7	467.5	9.0	481.6	10.8	499.9	11.7	488.2	10.9	484.3	10.2
8	468.7	9.3	484.7	11.5	502.2	12.2	491.9	11.8	487.8	11.0
9	469.1	9.4	486.3	11.9	504.2	12.7	493.4	12.1	490.4	11.6
10	469.8	9.6	487.3	12.1	505.8	13.0	494.6	12.4	492.2	12.0
11	470.1	9.6	487.1	12.1	506.9	13.3	496.2	12.7	493.8	12.4
12	472.3	10.1	489.8	12.7	510.7	14.1	501.0	13.8	498.5	13.5

Gabriele Veith
University of Glamorgan

	2L0S6G		2L2S6G		2L4S6G		2L6S6G		2L8S6G	
	height		height		height		height		height	
	total	%	total	%	total	%	total	%	total	%
0	2900	0	3350	0	5860	0	3230	0	3126	0
1	5510	2.5	5130	1.7	7150	1.3	4530	1.3	3860	0.7
2	8064	5.0	7518	4.0	9480	3.5	6253	2.9	5384	2.2
3	9520	6.4	9600	6.1	11840	5.8	8470	5.1	7251	4.0
4	11550	8.4	11350	7.8	13320	7.2	9720	6.3	8590	5.3
6	14400	11.2	14350	10.7	16300	10.1	12050	8.6	10900	7.5
7	15620	12.3	15050	11.4	17120	10.9	12750	9.2	11510	8.1
8	16600	13.3	15680	12.0	18150	11.9	13250	9.7	12140	8.8
9	17520	14.2	16710	13.0	18870	12.6	14220	10.7	13740	10.3
10	19820	16.4	18300	14.5	19700	13.4	14660	11.1	14500	11.0
11	19050	15.7	18760	15.0	20750	14.5	15650	12.1	15400	11.9
12	22370	18.9	21420	17.5	22310	16.0	17110	13.5	16200	12.7

Curing period prior to frost action: 180 days

	2L0S6G		2L2S6G		2L4S6G		2L6S6G		2L8S6G	
	weight		weight		weight		weight		weight	
	total	%	total	%	total	%	total	%	total	%
0	425.6	0.0	429.6	0.0	437.2	0.0	437.8	0.0	443.1	0.0
1	440.5	3.5	443.9	3.3	447.2	2.3	445.8	1.8	448.5	1.2
2	450.2	5.8	454.1	5.7	455.2	4.1	455.0	3.9	454.3	2.5
4	459.8	8.0	468.8	9.1	469.4	7.4	470.5	7.5	467.8	5.6
5	462.2	8.6	472.5	10.0	474.7	8.6	476.8	8.9	474.8	7.2
7	466.6	9.7	477.6	11.2	480.2	9.8	482.6	10.2	483.2	9.1
8	466.6	9.6	477.8	11.2	482.2	10.3	484.6	10.7	485.2	9.5
9	467.1	9.8	480.5	11.8	483.8	10.7	486.4	11.1	487.6	10.0
10	467.3	9.8	482.6	12.3	485.0	10.9	488.6	11.6	489.8	10.6
11	468.5	10.1	483.7	12.6	486.5	11.3	489.7	11.9	490.9	10.8
12	468.3	10.0	484.5	12.8	488.0	11.6	491.2	12.2	492.5	11.1

	2L0S6G		2L2S6G		2L4S6G		2L6S6G		2L8S6G	
	height		height		height		height		height	
	total	%	total	%	total	%	total	%	total	%
0	15671	0	16160	0	16400	0	16720	0	16610	0
1	18690	2.9	18270	2.0	17360	0.9	17360	0.6	17030	0.4
2	20870	5.0	20550	4.3	18960	2.5	18920	2.1	18100	1.4
3	22420	6.6	22440	6.1	21010	4.5	20850	4.0	19930	3.2
4	23920	8.0	23840	7.5	22620	6.0	22120	5.2	21271	4.5
5	25550	9.6	25170	8.7	23890	7.3	23280	6.4	22850	6.1
7	27850	11.8	27850	11.3	25830	9.2	24720	7.8	24730	7.9
8	29020	13.0	28720	12.2	26800	10.1	25840	8.9	25530	8.7
9	30030	13.9	29580	13.0	27000	10.3	26180	9.2	25770	8.9
10	31410	15.3	30650	14.1	27860	11.1	26600	9.6	26760	9.9
11	32460	16.3	31500	14.9	27960	11.2	27000	10.0	26920	10.0
12	34320	18.1	32250	15.6	28950	12.2	27510	10.5	27500	10.6

Gabriele Veith
University of Glamorgan

A3.6.2 Kaolinite without gypsum

Curing period prior to frost action: 7 days

	2L0S0G		2L2S0G		2L4S0G		2L6S0G		2L8S0G	
	weight		weight		weight		weight		weight	
	total	%	total	%	total	%	total	%	total	%
0	425.6	0.0	423.4	0.0	426.6	0.0	430.0	0.0	441.3	0.0
1	439.1	3.2	436.7	3.1	440.6	3.3	443.1	3.1	452.9	2.6
2	447.3	5.1	445.5	5.2	448.7	5.2	453.7	5.5	461.7	4.6
3	450.2	5.8	448.5	5.9	452.5	6.1	457.2	6.3	465.5	5.5
4	451.9	6.2	450.3	6.3	454.1	6.4	458.2	6.6	467.0	5.8
5	453.1	6.4	452.2	6.8	455.4	6.7	458.4	6.6	468.2	6.1
6	453.9	6.6	453.1	7.0	456.3	6.9	460.5	7.1	469.3	6.3
7	455.2	6.9	453.7	7.2	456.7	7.0	460.8	7.2	470.8	6.7
8	455.6	7.0	454.2	7.3	457.8	7.3	462.0	7.5	471.5	6.8
9	456.5	7.3	455.0	7.5	457.4	7.2	462.1	7.5	470.7	6.6
10	457.3	7.4	454.9	7.4	458.1	7.4	462.7	7.6	472.1	7.0
12	458.4	7.7	456.5	7.8	459.6	7.7	465.9	8.4	472.9	7.2

	2L0S0G		2L2S0G		2L4S0G		2L6S0G		2L8S0G	
	height		height		height		height		height	
	total	%	total	%	total	%	total	%	total	%
0	945	0	1542	0	919	0	872	0	3061	0
1	4778	3.7	5221	3.6	4710	3.7	4700	3.7	6425	3.3
2	7060	5.9	6661	5.0	6960	5.9	7349	6.3	8150	4.9
3	9000	7.8	8270	6.5	8610	7.5	10940	9.8	10430	7.2
4	9380	8.2	9910	8.1	9550	8.4	12140	10.9	12000	8.7
5	11170	9.9	11310	9.5	11260	10.0	13500	12.3	13630	10.3
6	12380	11.1	12360	10.5	11780	10.5	14560	13.3	14460	11.1
7	14410	13.1	12620	10.8	12770	11.5	15860	14.6	16510	13.1
8	14500	13.2	14320	12.4	14500	13.2	17864	16.5	17480	14.0
9	16400	15.0	15630	13.7	15380	14.0	18460	17.1	19000	15.5
10	16860	15.5	16380	14.4	15660	14.3	19990	18.6	19320	15.8
12	18810	17.3	17970	15.9	17910	16.5	22000	20.5	21800	18.2

Curing period prior to frost action: 28 days

	2L0S0G weight		2L2S0G weight		2L4S0G weight		2L6S0G weight		2L8S0G weight	
	total	%	total	%	total	%	total	%	total	%
0	421.3	0.0	426.4	0.0	426.5	0.0	427.0	0.0	427.8	0.0
1	432.7	2.7	437.1	2.5	439.9	3.1	439.6	3.0	438.0	2.4
2	440.8	4.6	445.3	4.4	446.5	4.7	447.4	4.8	444.9	4.0
3	445.9	5.8	450.0	5.5	449.9	5.5	451.8	5.8	450.1	5.2
5	451.5	7.2	455.5	6.8	454.8	6.6	455.8	6.7	454.2	6.2
6	452.3	7.4	454.9	6.7	455.2	6.7	455.1	6.6	454.6	6.3
7	454.0	7.8	455.2	6.8	455.4	6.8	455.4	6.7	454.5	6.3
8	452.3	7.4	454.4	6.6	456.1	6.9	456.5	6.9	456.1	6.6
9	453.3	7.6	454.7	6.6	456.4	7.0	457.1	7.0	455.5	6.5
10	454.5	7.9	455.1	6.7	457.1	7.2	457.8	7.2	456.5	6.7
12	458.7	8.9	460.1	7.9	458.2	7.4	460.0	7.7	458.0	7.1

	2L0S0G height		2L2S0G height		2L4S0G height		2L6S0G height		2L8S0G height	
	total	%	total	%	total	%	total	%	total	%
0	1021	0	934	0	1195	0	1470	0	804	0
1	3860	2.8	4075	3.0	4665	3.4	4840	3.3	3680	2.8
2	5530	4.4	5841	4.8	6516	5.2	6480	4.9	5535	4.6
3	7460	6.3	7740	6.6	7800	6.4	8260	6.6	7470	6.5
5	10650	9.3	11050	9.8	9552	8.1	9570	7.9	9630	8.6
6	11310	10.0	11520	10.3	10510	9.0	11120	9.4	10850	9.8
7	12550	11.2	12210	10.9	11450	10.0	12090	10.3	11540	10.4
8	13350	12.0	12950	11.7	11880	10.4	13380	11.6	12520	11.4
9	14320	12.9	13600	12.3	12850	11.3	14700	12.8	13500	12.3
10	15320	13.9	14705	13.4	13460	11.9	15100	13.2	14020	12.8
12	17910	16.4	17420	16.0	14420	12.8	15230	13.4	16070	14.8

Curing period prior to frost action: 90 days

	2L0S0G weight		2L2S0G weight		2L4S0G weight		2L6S0G weight		2L8S0G weight	
	total	%	total	%	total	%	total	%	total	%
0	427.5	0.0	439.2	0.0	429.2	0.0	428.0	0.0	431.4	0.0
1	442.3	3.5	445.4	1.4	431.6	0.5	431.5	0.8	433.9	0.6
2	452.7	5.9	454.9	3.6	437.9	2.0	434.2	1.5	436.4	1.2
3	454.8	6.4	458.6	4.4	442.6	3.1	437.0	2.1	439.7	1.9
4	457.0	6.9	462.1	5.2	447.0	4.1	439.2	2.6	440.7	2.2
5	457.1	6.9	463.3	5.5	451.2	5.1	442.0	3.3	442.8	2.6
6	458.4	7.2	463.6	5.6	453.2	5.6	444.1	3.8	445.3	3.2
7	457.2	7.0	463.3	5.5	456.1	6.2	446.5	4.3	446.8	3.6
8	457.8	7.1	463.4	5.5	457.4	6.6	448.5	4.8	449.5	4.2
9	457.2	7.0	464.0	5.6	458.1	6.7	450.5	5.3	451.4	4.6
10	457.9	7.1	463.9	5.6	459.5	7.0	451.5	5.5	453.0	5.0
11	457.7	7.1	464.1	5.7	460.1	7.2	452.6	5.8	453.8	5.2
12	457.7	7.1	465.1	5.9	460.2	7.2	454.2	6.1	455.2	5.5

	2L0S0G		2L2S0G		2L4S0G		2L6S0G		2L8S0G	
	height		height		height		height		height	
	total	%	total	%	total	%	total	%	total	%
0	14781	0	16421	0	14520	0	14680	0	14596	0
1	18510	3.6	17965	1.5	14845	0.3	15231	0.5	14891	0.3
2	21400	6.4	20330	3.8	16110	1.5	15620	0.9	15185	0.6
3	23410	8.4	22080	5.5	17451	2.8	16140	1.4	15630	1.0
4	25100	10.0	23400	6.8	18560	3.9	16730	2.0	16130	1.5
5	26430	11.3	24260	7.6	19930	5.3	17190	2.4	16220	1.6
6	27790	12.6	24700	8.0	21210	6.5	17571	2.8	16610	2.0
7	29560	14.3	25060	8.4	21750	7.0	18060	3.3	17032	2.4
8	29440	14.2	25850	9.2	22380	7.6	18480	3.7	17390	2.7
9	30480	15.2	26600	9.9	22790	8.0	18890	4.1	17810	3.1
10	31300	16.0	26670	10.0	23360	8.6	19460	4.6	18120	3.4
11	31350	16.1	27600	10.9	23700	8.9	19630	4.8	18340	3.6
12	33360	18.0	28150	11.4	24460	9.7	20500	5.7	19180	4.5

Curing period prior to frost action: 180 days

	2L0S0G		2L2S0G		2L4S0G		2L6S0G		2L8S0G	
	weight		weight		weight		weight		weight	
	total	%	total	%	total	%	total	%	total	%
0	437.1	0.0	425.7	0.0	430.5	0.0	430.8	0.0	434.2	0.0
1	451.5	3.3	429.7	0.9	433.7	0.7	433.7	0.7	435.8	0.4
3	465.9	6.6	442.3	3.9	441.7	2.6	439.5	2.0	439.4	1.2
4	466.7	6.8	446.9	5.0	445.7	3.5	442.2	2.6	440.9	1.5
6	471.3	7.8	453.0	6.4	453.7	5.4	449.8	4.4	445.8	2.7
7	469.7	7.5	454.0	6.6	455.4	5.8	451.9	4.9	448.6	3.3
8	468.7	7.2	455.4	7.0	457.1	6.2	454.1	5.4	450.8	3.8
9	469.2	7.3	455.0	6.9	458.8	6.6	455.2	5.7	452.3	4.2
10	468.4	7.2	457.0	7.4	459.4	6.7	456.3	5.9	453.1	4.4
11	468.4	7.2	458.1	7.6	460.8	7.0	457.2	6.1	454.4	4.7
12	468.4	7.2	459.2	7.9	462.0	7.3	458.2	6.3	455.1	4.8

	2L0S0G		2L2S0G		2L4S0G		2L6S0G		2L8S0G	
	height		height		height		height		height	
	total	%	total	%	total	%	total	%	total	%
0	16450	0	14290	0	14190	0	14000	0	14530	0
1	20160	3.6	15130	0.8	14660	0.5	14271	0.3	14700	0.2
3	24360	7.7	18120	3.7	16410	2.2	15440	1.4	15479	0.9
4	25900	9.2	19750	5.3	17780	3.5	16180	2.1	16090	1.5
6	30500	13.6	22500	8.0	20400	6.0	18015	3.9	16641	2.0
7	31200	14.3	23430	8.9	20420	6.0	18305	4.2	17050	2.4
8	33320	16.4	23650	9.1	21220	6.8	19190	5.0	17720	3.1
9	33400	16.5	24150	9.6	21510	7.1	19340	5.2	17470	2.9
10	33400	16.5	24900	10.3	22090	7.7	19650	5.5	17790	3.2
11	33400	16.5	25200	10.6	22420	8.0	19800	5.6	17900	3.3
12	33400	16.5	25170	10.6	23120	8.7	20500	6.3	18560	3.9

A3.6.3 Lower Oxford Clay

Curing period prior to frost action: 7 days

	2L0S		2L2S		2L4S		2L6S		2L8S	
	weight		weight		weight		weight		weight	
	total	%	total	%	total	%	total	%	total	%
0	420.3	0.0	424.1	0.0	433.7	0.0	424.6	0.0	427.6	0.0
1	433.3	3.1	428.9	1.1	437.0	0.7	431.4	1.6	430.4	0.7
2	444.5	5.8	441.5	4.1	445.4	2.7	437.8	3.1	434.6	1.6
3	449.7	7.0	449.1	5.9	454.8	4.9	443.8	4.5	441.2	3.2
4	451.6	7.4	453.8	7.0	460.7	6.2	450.3	6.1	445.9	4.3
5	453.4	7.9	456.1	7.5	464.9	7.2	453.9	6.9	451.4	5.5
6	454.8	8.2	458.4	8.1	467.2	7.7	456.1	7.4	454.5	6.3
7	455.7	8.4	460.0	8.5	469.2	8.2	457.7	7.8	456.7	6.8
8	457.3	8.8	461.7	8.9	469.7	8.3	459.7	8.3	458.6	7.2
9	457.8	8.9	462.2	9.0	471.3	8.7	460.7	8.5	459.6	7.5
10	459.1	9.2	463.5	9.3	471.6	8.7	462.9	9.0	460.8	7.8
11	460.2	9.5	464.6	9.5	472.5	8.9	463.0	9.1	461.6	7.9
12	460.9	9.7	466.6	10.0	473.1	9.1	464.2	9.3	462.8	8.2

	2L0S		2L2S		2L4S		2L6S		2L8S	
	height		height		height		height		height	
	total	%	total	%	total	%	total	%	total	%
0	0	0	570	0	2100	0	160	0	480	0
1	3424	3.3	1725	1.1	2798	0.7	1580	1.4	1000	0.5
2	5500	5.3	3996	3.3	4430	2.3	3018	2.8	2069	1.5
3	7140	6.9	5670	5.0	6380	4.2	3940	3.7	2958	2.4
4	7720	7.5	6825	6.1	7875	5.6	5180	4.9	4141	3.6
5	8970	8.7	7650	6.9	8610	6.3	5860	5.5	4880	4.3
6	9460	9.2	8670	7.9	9250	6.9	6390	6.0	5500	4.9
7	10410	10.1	9100	8.3	9940	7.6	6838	6.5	6130	5.5
8	10990	10.7	10030	9.2	10280	7.9	7500	7.1	6490	5.8
9	11650	11.3	10901	10.0	10690	8.3	7920	7.5	7260	6.6
10	12250	11.9	11030	10.2	10700	8.3	8030	7.6	6880	6.2
11	12750	12.4	11500	10.6	11280	8.9	8470	8.1	7500	6.8
12	12900	12.5	11640	10.7	11530	9.2	8600	8.2	7530	6.8

Curing period prior to frost action: 28 days

	2L0S		2L2S		2L4S		2L6S		2L8S	
	weight		weight		weight		weight		weight	
	total	%	total	%	total	%	total	%	total	%
0	431.4	0.0	421.1	0.0	425.6	0.0	427.4	0.0	426.5	0.0
1	444.4	3.0	426.5	1.3	428.0	0.6	430.0	0.6	427.6	0.3
2	454.0	5.2	437.6	3.9	433.8	1.9	433.9	1.5	431.8	1.2
3	459.3	6.5	444.8	5.6	441.4	3.7	439.3	2.8	434.9	2.0
4	461.6	7.0	450.3	7.0	447.0	5.0	444.0	3.9	438.1	2.7
5	463.2	7.4	452.6	7.5	452.3	6.3	448.6	5.0	442.1	3.7
7	465.9	8.0	455.9	8.3	457.7	7.5	454.6	6.4	449.6	5.4
8	466.0	8.0	458.2	8.8	458.0	7.6	456.1	6.7	451.4	5.8
9	466.4	8.1	457.7	8.7	458.8	7.8	456.9	6.9	452.7	6.1
10	467.7	8.4	457.7	8.7	459.9	8.0	458.2	7.2	453.8	6.4
11	467.6	8.4	457.8	8.7	460.6	8.2	459.5	7.5	454.9	6.7
12	468.6	8.6	456.8	8.5	461.2	8.3	460.2	7.7	456.1	6.9

	2L0S		2L2S		2L4S		2L6S		2L8S	
	height		height		height		height		height	
	total	%	total	%	total	%	total	%	total	%
0	2310	0	380	0	320	0	515	0	170	0
1	5441	3.0	1450	1.0	800	0.5	965	0.4	370	0.2
2	6598	4.2	2564	2.1	1300	1.0	986	0.5	420	0.2
3	8120	5.6	5049	4.5	2874	2.5	2141	1.6	800	0.6
4	9250	6.7	5230	4.7	4341	3.9	3087	2.5	1819	1.6
5	10610	8.1	5960	5.4	5732	5.3	3885	3.3	2512	2.3
7	11400	8.8	7380	6.8	7200	6.7	5100	4.5	3680	3.4
8	11730	9.1	7480	6.9	7250	6.7	5430	4.8	4105	3.8
9	12340	9.7	8120	7.5	7790	7.3	5890	5.2	4520	4.2
10	12650	10.0	8500	7.9	8000	7.5	6030	5.4	4700	4.4
11	13205	10.6	9040	8.4	8710	8.1	6840	6.1	5170	4.9
12	13540	10.9	9410	8.8	8720	8.2	6410	5.7	5380	5.1

Gabriele Veith
University of Glamorgan

Curing period prior to frost action: 90 days

	2L0S		2L2S		2L4S		2L6S		2L8S	
	weight		weight		weight		weight		weight	
	total	%	total	%	total	%	total	%	total	%
0	419.7	0.0	421.1	0.0	426.9	0.0	429.4	0.0	429.1	0.0
3	448.6	6.9	441.0	4.7	437.6	2.5	436.8	1.7	436.0	1.6
5	451.8	7.6	448.6	6.5	447.1	4.7	443.5	3.3	439.9	2.5
7	452.7	7.9	452.0	7.3	451.8	5.8	450.8	5.0	445.1	3.7
8	453.1	8.0	451.9	7.3	453.2	6.2	452.8	5.5	447.6	4.3
9	452.9	7.9	452.8	7.5	454.5	6.5	454.4	5.8	449.5	4.8
10	452.7	7.9	453.2	7.6	455.5	6.7	455.2	6.0	451.3	5.2
11	452.6	7.8	453.6	7.7	456.6	7.0	456.4	6.3	452.2	5.4
12	454.1	8.2	455.2	8.1	458.4	7.4	458.1	6.7	453.8	5.7

	2L0S		2L2S		2L4S		2L6S		2L8S	
	height		height		height		height		height	
	total	%	total	%	total	%	total	%	total	%
0	14640	0	14590	0	15025	0	14620	0	14400	0
3	21120	6.3	18250	3.6	17310	2.2	15920	1.3	15380	1.0
5	22320	7.5	20130	5.4	19010	3.9	17140	2.4	16160	1.7
7	23250	8.4	20930	6.2	20140	5.0	18400	3.7	16990	2.5
8	23380	8.5	21250	6.5	20400	5.2	18920	4.2	17540	3.0
9	23730	8.8	21700	6.9	20910	5.7	19410	4.7	17780	3.3
10	23500	8.6	21300	6.5	21000	5.8	19480	4.7	18100	3.6
11	23850	8.9	21750	7.0	21720	6.5	20000	5.2	18360	3.8
12	24500	9.6	22400	7.6	22300	7.1	20220	5.4	18600	4.1

Curing period prior to frost action: 180 days

	2L0S		2L2S		2L4S		2L6S		2L8S	
	weight		weight		weight		weight		weight	
	total	%	total	%	total	%	total	%	total	%
0	420.6	0.0	422.6	0.0	425.8	0.0	424.9	0.0	427.2	0.0
1	433.5	3.1	426.4	0.9	428.9	0.7	426.5	0.4	428.4	0.3
2	444.6	5.7	437.4	3.5	432.0	1.4	429.9	1.2	431.3	0.9
5	452.7	7.6	451.7	6.9	447.4	5.1	442.4	4.1	437.3	2.4
7	455.1	8.2	455.5	7.8	453.1	6.4	450.0	5.9	443.7	3.8
9	456.0	8.4	457.0	8.1	456.1	7.1	453.6	6.8	449.5	5.2
10	455.6	8.3	456.7	8.1	455.9	7.0	453.9	6.8	450.6	5.5
11	455.5	8.3	457.2	8.2	456.7	7.2	455.2	7.1	452.3	5.9
12	455.6	8.3	457.6	8.3	458.3	7.6	456.4	7.4	453.7	6.2

	2L0S		2L2S		2L4S		2L6S		2L8S	
	height		height		height		height		height	
	total	%	total	%	total	%	total	%	total	%
0	15120	0	14430	0	14460	0	14830	0	14870	0
1	18200	3.0	15720	1.3	14880	0.4	14750	-0.1	15000	0.1
2	20690	5.4	17710	3.2	15750	1.3	15060	0.2	14940	0.1
5	24050	8.7	21300	6.7	19280	4.7	17650	2.7	16180	1.3
7	25400	10.0	22500	7.8	20450	5.8	18860	3.9	17270	2.3
9	26400	11.0	23150	8.5	21460	6.8	19800	4.8	18380	3.4
10	26400	11.0	23080	8.4	21200	6.5	19660	4.7	18630	3.7
11	26480	11.0	23450	8.8	21700	7.0	20280	5.3	19020	4.0
12	26250	10.8	23450	8.8	21850	7.2	20250	5.3	19190	4.2

Appendix 4 - Effects of the delayed addition of slag

4.1 Introduction

The utilisation of lime-activated ground granulated blast furnace slag (ggbs) in the stabilisation of sulphate bearing clay soils is a relatively new technique. It has been tested recently in a pilot trial during the construction of a temporary diversion of the A421 Tingewick by-pass in Buckinghamshire, England, where a heavy boulder clay was transformed into a combined foundation and roadbase for bituminous surfacing (see Chapter 8). In this trial – referring to common practice in lime stabilisation of soils in accordance with the Specifications for Highway Works (Department of Transport, 1991/94), clause 615 - the lime was uniformly spread on and mixed with the material in situ and then left for a mellowing period of 72 hours prior to any further treatment. It is generally assumed that this mellowing period of 24 to 72 hours (compulsory under paragraph 11 of clause 615, Specification for Highway Works, Department of Transport, 1991/94) aids in the breakdown of large clay clods and contributes to a better homogeneity of the soil in order to achieve the intended improvements in strength and consistency. Since there is, during practical work, a possibility of delay in the addition of ggbs due to late delivery or bad weather conditions, a number of tests were set up to investigate the influence of a delay on the strength and swelling properties of the stabilised material.

4.2 Experimental procedure

Kaolinite with additions of 0, 2, 4 and 6 % gypsum was stabilised using a total binder content of 6% (slag + lime) in order to investigate the influence of the delayed addition of slag to lime-activated slag stabilised soil. The slag/lime binder ratios were chosen as 0.2 (5%L(ime)1%S(lag)), 0.5 (4L2S), 1 (3L3S), 2 (2L4S) and 5 (1L5S).

The unconfined compressive strength after 28 days was determined using cylindrical samples with a diameter of 50 mm and a height of 100 mm, which had been compacted to a target maximum dry density of 1.41 Mg/m^3 at a moisture content of 30.55 %. These values derived from a series of standard compaction tests (2.5 kg rammer method) on the kaolinite with various slag/lime ratios in accordance with BS 1377: Part 4: 1990. In order to achieve the target density, sufficient material to fill a cylindrical split mould

was, prior to hand mixing with palette knives, homogeneously mixed in a variable speed Kenwood Chef Excell mixer for 2 minutes before slowly adding the water. A pre-fabricated split mould, with a collar in order to accommodate all the material necessary for one sample, ensured that the material was not overcompressed when compacted in a steel frame with a hydraulic jack. The cylinders were extruded using a steel plunger. They were then trimmed, cleaned of releasing oil, weighed and wrapped in several layers of cling film in order to avoid any moisture loss during curing. The curing period was 28 days at 30 °C and 100 % relative humidity. For the samples with the delayed addition of slag, the mixed material without the slag was (prior to compaction) cured in sealed plastic bags for 1, 3 and 7 days by storing in an oven at 30 °C and 100 % relative humidity. After this period, the prescribed amount of slag and the appropriate amount of water were added and the soil was re-mixed and compacted as described above.

To observe the swelling behaviour the samples were placed on a platform in a perspex container which was covered with a lid fitted with dial gauges. The perspex containers were kept in an environmental chamber capable of maintaining a temperature of 30 °C (± 2 °C) and 100 % relative humidity. After 7 days of moist curing the samples were soaked by raising the level of de-ionised water up to 15 mm above their base. Linear axial swelling was monitored until no further expansion occurred.

At the end of the moist curing period the samples were unwrapped and weighed in order to determine the moisture loss during curing. Testing for unconfined compressive strength was carried out utilising a JJ30 MK compression testing machine, applying load at a rate of 1 mm/min. Prior to aligning the samples centrally between the upper and the lower platten, a self-levelling device was placed between the tops of the samples and the upper platten in order to achieve uniaxial stress. Load was applied until failure was recorded. To establish consistency, two samples were prepared for each mix and if the results of these differed by more than 20 %, a third specimen was prepared and tested in order to determine the true trend. In order to identify the involved mechanisms more accurately, scanning electron microscopy was carried out on a selection of the samples.

4.3 Results

Unconfined compressive strength (UCS)

The results of all UCS tests are given in Figure A4.1. As already reported by Wild et al. [1996] increase in strength with increase in slag/lime ratio is confirmed for samples with slag added immediately at all gypsum levels. When no delay was employed (Figure A4.1a) there was a general tendency for strength to increase as the slag/lime ratio increased, particularly for specimens without gypsum. When delay occurred specimens with high slag/lime ratios showed significantly reduced strengths (Figures A4.1b-d). In all cases specimens containing 4 % gypsum consistently produced the highest strengths, with the greatest gains apparent for specimens with low/slag lime ratios (Figures A4.1b-d). For specimens with gypsum contents either above or below 4%, 7 days delay produced particularly low strengths. Also, when gypsum was present, variation in delay time produced much greater variation in strength for specimens with low slag/lime ratios than it did for specimens with high slag/lime ratios.

Linear expansion

Mixes with 6 % gypsum addition which had been prepared with and without a delay of seven days in the addition of slag, were subjected to an initial 7 days moist curing period and subsequent soaking in deionised water. The 6 % gypsum content specimens were chosen because this was the highest sulphate level used in previous work [Wild et al., 1996], which had shown that these would be most susceptible to sulphate expansion on soaking. During the initial moist curing period all samples exhibited a small level of expansion (up to 1.26 %) and no shrinkage at all was recorded The expansion results are shown in Figure A4.2. Generally, increase in slag/lime ratio produced a decrease in expansion. However, the samples to which the slag was added with a delay of seven days showed much smaller expansion values than those with no delay in slag addition. The magnitude and (percentage) of reduction in swelling was 11.2% (32.5 %) for the mix 5L1S, 7.8% (35.6%) for 4L2S, 4.8% (37.7%) for 3L3S, 2.0% (47.9%) for 2L4S and 1.8% (25 %) for the mix 1L5S. Thus the percentage reduction in expansion produced by a delay of 7 days does not vary systematically with change in composition and is similar for all compositions. However, because the amount of expansion decreases sharply with increasing slag/lime ratio, delay produces much smaller decreases in expansion for those compositions with high slag/lime ratios.
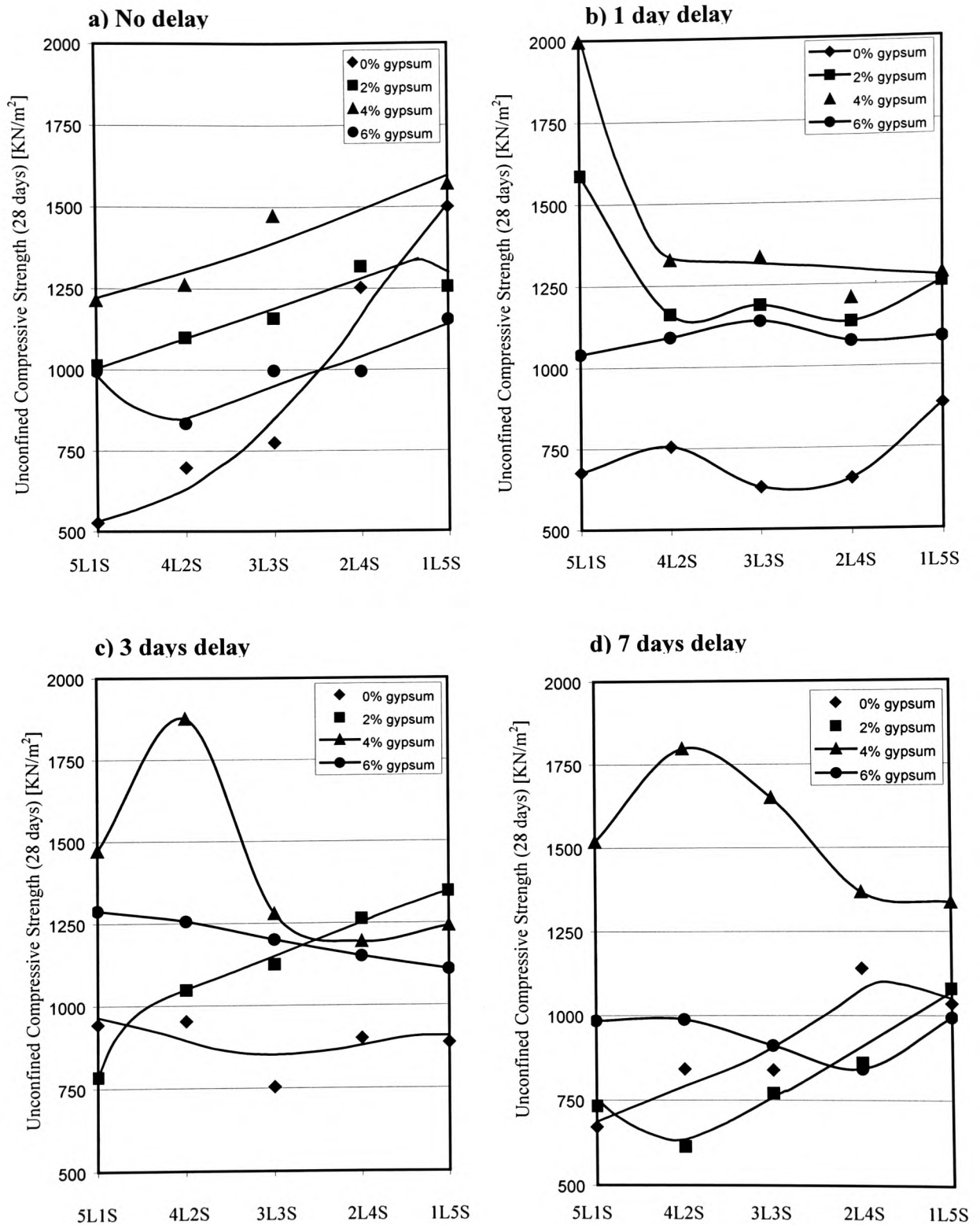
a) No delay

b) 1 day delay

c) 3 days delay

d) 7 days delay

Figure A4.1   **The effect of composition and delay time prior to slag addition on the compressive strength of 28 day moist cured kaolinite-ggbs-lime-gypsum cylinders**
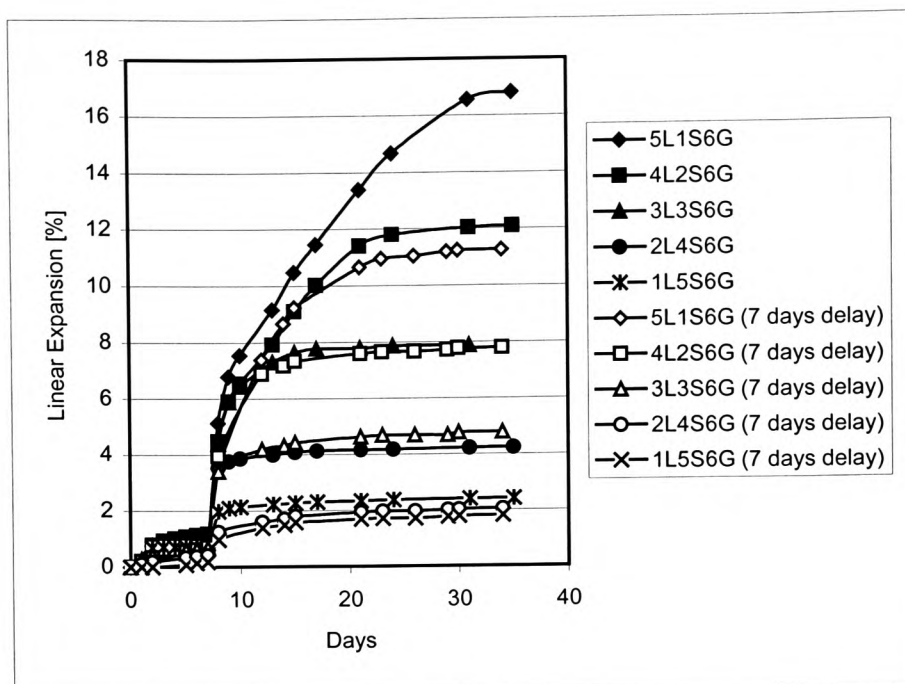
Figure A4.2   **Linear expansion of samples with various slag/lime contents and the addition of 6 % gypsum – comparison between swelling behaviour when the ggbs is added immediately and with a delay of 7 days**

4.4 Discussion

The observed behaviour is generally the result of three reactions, which occur in soil stabilised with slag and lime in the presence of sulphates:

①   The "normal" lime-clay reaction

In addition to the cation exchange process, which starts immediately after the lime is added and results in flocculation and changes in consistency, the clay-lime reaction will begin. The lime and the alumino silicates provided by the clay go into solution and subsequently precipitate as cementitious products consisting of C-S-A-H gel and crystalline calcium alumino–silicate hydrates [Arabi and Wild, 1989]. In the long term this leads to an increase in strength and an improved volume stability of the material.

②   The slag hydration

The activation of ggbs can occur only in an alkaline environment, which in this case is provided by the lime. The hydrated slag grains provide, in comparison to the above

mentioned clay lime reaction, much more rapid formation of cementitious products and more rapid strength gain.

③   The formation of ettringite

When lime and sulphates are available, ettringite can form in the presence of aluminium, deriving from the clay. Although ettringite also contributes to the strength development of a sample, its influence can prove to be deleterious when it forms where there is an abundant supply of water. Ettringite formation also consumes the lime which provides the alkaline environment for the activation of the slag.

All three of the above reactions require lime. When the slag is added with a delay, the clay-lime reaction and, in the presence of sulphates, the chemical reaction which leads to the formation of ettringite, have an initial advantage. Depending on the delay period, the amount of lime initially provided and the amount of slag added, the slag hydration may be either retarded because of a lack of lime or not even be initiated at all. This insufficient activation of ggbs with lime at high sulphate levels seems to be the reason for the generally lower strengths of samples containing sulphate with low lime contents and delayed slag addition. In the absence of sulphate the clay-lime reaction occurs very slowly. The formation of ettringite when sulphate is present seems to be the main cause for the retardation of slag activation and the deficiency of lime. For mixes with a high lime content, i.e. 5L1S, in the case of delayed addition of slag, there is an abundance of available lime and when sulphate is present the lime will rapidly be used for the formation of ettringite (the longer the delay, the more ettringite will be formed and the less lime is left to activate the anyway very small amount of slag). This results in quite a significant increase in strength. When there are no sulphates present at all (0% gypsum) the strength development of samples is not influenced by lime consumption due to the formation of ettringite. Lime is just consumed by the slow lime-clay reaction and enough is generally – even after a delay of seven days – left to activate the slag. As the slag hydration reaction is much more rapid than the lime-clay reaction the 28 day strength increases quite significantly with increase in slag/lime ratio.

To confirm the above explanation, scanning electron microscopy was carried out on the fracture surfaces of specimens of compositions 5L1S6G and 1L5S6G to which the slag had been added with a delay of 1, 3 and 7 days. The fracture surface of a specimen, to

which the slag had been added immediately, was also investigated. On Plate A4.1 the formation of ettringite crystals can easily be seen in the mix with a low slag/lime ratio (5L1S) to which the slag was added with a delay of 7 days. The initial abundance of available lime and a high sulphate content led to the formation of very well structured needle-shaped ettringite crystals. The longer the delay the more ettringite could be found. The same delay period resulted in hardly any ettringite formation (Plate A4.2) for the sample with the highest slag/lime ratio of 5 (1L5S). In the case of high slag/lime ratios, the amount of ettringite formed is very small, since the amount of lime provided for the formation of the crystals is very limited indeed. This leaves quite a substantial amount of the available sulphates "unused", which can be advantageous since Kinuthia [1997] reports that the slag hydration is accelerated by sulphates. However, sulphates available in abundance (i.e. > 4 %) appear to lead to a retardation in slag hydration. Hence the highest UCS values at all delay periods were achieved at a gypsum content of 4 %.
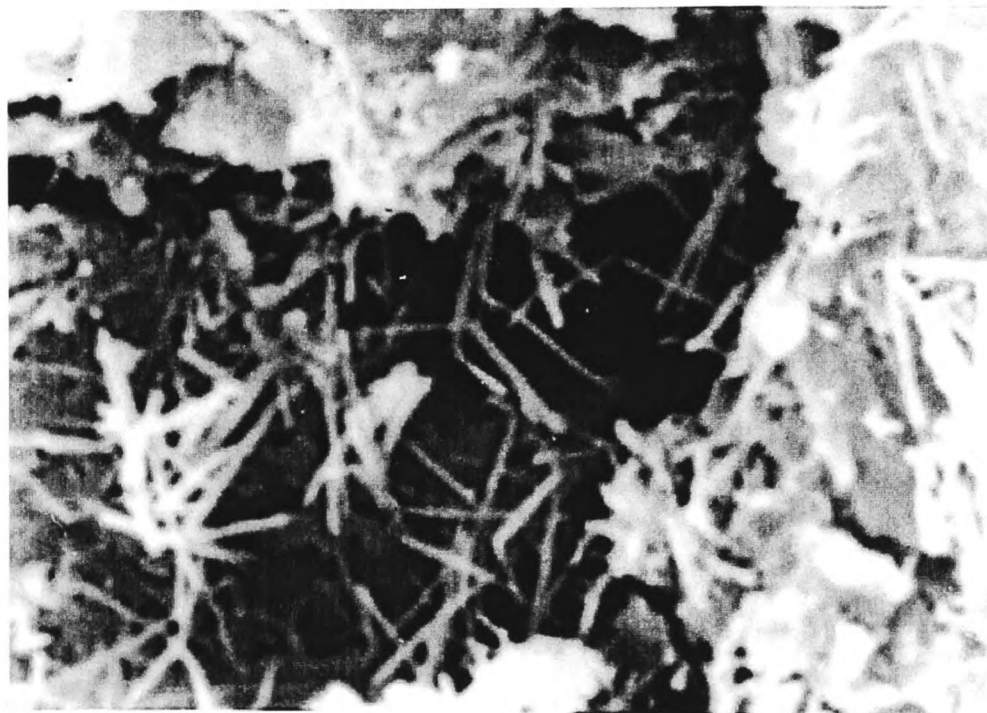

Plate A4.1   Kaolinite with 5 % lime and 1 % ggbs at a gypsum content of 6 % (5L1S6G) after the slag was added with a delay of 7 days and the sample was then cured for 28 days at 30 °C and 100 % relative humidity (x 2000).

Plate A4.2   Kaolinite with 1 % lime and 5 % ggbs at a gypsum content of 6 %. The slag was added with a delay of 7 days and the sample was then cured for 28 days at 30 °C and 100 % relative humidity (x 2000).

The reduction in swelling of the compacted and cured specimens as a result of delay seems to be mainly due to the fact that, especially with larger amounts of lime, much of the ettringite was able to form during the seven days delay period prior to compaction. Earlier work [Wild et al., 1998] has confirmed that the formation of ettringite leads to expansion only in the presence of excess water. During moist curing the amount of water available is limited and the expansion was expected to be less with the introduction of a delay in the addition of slag (which at the same time is also a delay in the provision of water). The formation of ettringite during the seven day curing period could, especially for the samples with a high lime content, continue very effectively. After the addition of slag prior to compaction and soaking, some of the lime is consumed in slag activation. The results indicate that a substantial amount of lime had already been used up by ettringite formation, hence the linear expansion would be reduced because a smaller number of additional crystals were able to form during soaking. Depending on the moisture content with which the samples are prepared prior

to slag addition and compaction, it is suggested that the amount of linear expansion could be reduced to an even lower value. The availability of water during the ettringite formation process will increase the amount of "harmless" ettringite produced during the delay period and therefore exhaust the source of reactants available for ettringite formation which would be detrimental after compaction.

The implications for practical work are:

i)   A delay in the addition of slag should be avoided if maximum strength enhancement is required, particularly for binders with high slag/lime ratios and soils with negligible sulphate content.

ii)   If the delay cannot be avoided and is for example caused by bad weather conditions, i.e. rain, then if sulphates are present in the soil, every precaution should be taken to protect the already lime modified material from access to water since this will definitely result in substantial heave, particularly when binders of low slag/lime ratios are used.

iii) When sulphates are present in the soil then delay before ggbs addition and compaction can produce significant reductions in expansion, particularly at low slag/lime ratios although long delays (i.e. 7 days) should be avoided as this generally results in reduced strength.

References

Arabi, M and Wild, S (1989), "Property changes induced in clay soils when using lime stabilisation", Municipal Engineer, **6**, pp85-99.

Kinuthia, J M (1997), "Property changes and mechanisms in lime-stabilised kaolinite in the presence of metal sulphates", PhD thesis, University of Glamorgan, Pontypridd, UK

Wild, S, Kinuthia, J M, Robinson, RB and Humphreys, I (1996), "Effects of ground granulated blast furnace slag (ggbs) on the strength and swelling properties of lime-stabilised kaolinite in the presence of sulphates", Clay Minerals, **31**, pp423-433

Wild, S, Kinuthia, J M, Jones, G I and Higgins, D D (1998), "Effects of partial substitution of lime with ground granulated blast furnace slag (ggbs) on the strength properties of lime-stabilised sulphate bearing clay soils", Engineering Geology, 51, pp37-53

Appendix 5 – Publications

Veith, G, Wild, S and Robinson, R B (1999), "Shear strength, permeability and porosity of Kimmeridge Clay, stabilised with lime and ground granulated blast furnace slag (ggbs)", 9th BCA Annual Conference on Higher Education and the Concrete Industry, Cardiff, 8-9 July 1999, pp 41-51

Veith, G (2000), "Green, ground and great: soil stabilisation with slag", Building Research and Information, **28**, no 1, pp 70-72

Veith, G, Wild S and Robinson, R B (1999), "Opportunities for the treatment of sulphate-bearing ground", British Lime Association Seminars 1999, "Recycling, remediation and piling", Manchester and London, p 1-12

Wild, S, Robinson, R B and Veith, G (1999), "Shear strength and permeability relationships for Kimmeridge Clay stabilised with lime-ground granulated blast furnace slag blends", 6th International Conference "Modern Building Materials, Structures and Techniques", Vilnius, Lithuania, **vol 1**, pp 92-98

Veith, G (1999), "Die Verwendung von Hüttensand bei der Bodenstabilisierung (the utilisation of ggbs in soil stabilisation)", *in German*, presentation at the Geotechnical Seminar Series jointly organised by the Technical University Stuttgart and the University of Applied Sciences Stuttgart, Germany

Reports for the meetings of industrial partners:

Wild, S, Tasong, W A and Veith, G (1997), "Utilisation of waste materials in the stabilisation of land", Report for the progress meeting of partners, University of Glamorgan, Building Materials Research Unit, UK

Wild, S, Tasong, W A and Veith, G (1998a), "Utilisation of waste materials in the stabilisation of land", Report for the progress meeting of partners, report no 2, University of Glamorgan, Building Materials Research Unit, UK

Wild, S, Tasong, W A, Veith, G and Thomas, B (1998b), "Utilisation of waste materials in the stabilisation of land", Report for the progress meeting of partners, report no 3, University of Glamorgan, Building Materials Research Unit, UK

Wild, S, Tasong, W A, Veith, G and Thomas, B (1999a), "Utilisation of waste materials in the stabilisation of land", Report for the progress meeting of partners, report no 4, University of Glamorgan, Building Materials Research Unit, UK

Wild, S, Tasong, W A, Veith, G and Thomas, B (1999b), "Utilisation of waste materials in the stabilisation of land", Report for the progress meeting of partners, report no 5, University of Glamorgan, Building Materials Research Unit, UK

Shear strength, permeability and porosity of Kimmeridge Clay, stabilised with lime and ground granulated blast furnace slag (ggbs)

G Veith, S Wild and R B Robinson
School of the Built Environment, University of Glamorgan

ABSTRACT

Kimmeridge Clay, obtained from Blackbird Leys near Oxford, England, UK, was stabilised with a total binder content of 8 % at various slag/lime ratios. The samples were cured for 12 weeks, 24 weeks and 1 year at 10, 20 and 30 °C. The shear strength development was assessed in a series of undrained, unconsolidated triaxial tests, during which the pore water pressure was measured. The permeability of the saturated soil-lime-ggbs mixes was measured in a computer controlled triaxial cell. The samples were then examined for their porosity and pore size distribution in order to assess the involved mechanisms.

The results indicate that, in general, the shear strength increases with increasing slag/lime ratio, particularly when the soil is cured at elevated temperatures. Also permeability drops significantly with increasing slag/lime ratio and increasing curing period, whereas curing temperature has only a minor influence on permeability. The pore refinement is maximised at replacement ratios of between 4% slag/4% lime and 6% slag/2% lime, denoted by the highest percentages of pores with a radius of <0.05 µm.

INTRODUCTION

In addition to economic aspects in foundation engineering and road-sub-base construction, environmental issues, such as the re-use of industrial by-products, have come more to the fore in recent years. One example is ground granulated blast furnace slag (ggbs), which is a by-product of the iron-making industry and has proven to be beneficial as an addition in concrete, particularly where high sulphate resistance is required. The use of ggbs as an additive for soil stabilisation is, however, a relatively new technique. In particular when sulphates are present in a soil, the classic soil stabilisation methods, which involve additions of lime and/or cement to the weak clay material, can result in the generation of substantial heave. This occurs as a result of the formation of expansive products and has been reported by various authors [1,2]. Wild et al. [3] and Higgins et al. [4] have shown that the incorporation of ggbs in a clay-lime mix reduces the swelling magnitude substantially and has no deleterious effect on the strength development. The soil stabilisation technique with lime-activated ggbs was also recently adopted for a successful full-scale site trial, where a highly-plastic boulder clay was stabilised to provide a combined foundation and roadbase (350 mm) for bituminous surfacing (130 mm) for a temporary diversion during the construction of a by-pass at Tingewick in Buckinghamshire. Samples, which were taken after the demolition of the

temporary diversion (under traffic for 15 months), confirmed that satisfactory compression strength was achieved [5]. However, little work has been carried out on the effects of a combined ggbs-lime addition on the shear strength parameters, the coefficient of permeability and the porosity and pore size distribution of a natural clay. This paper reports results which have been obtained as part of a large research project, currently being carried out at the University of Glamorgan, on the structure and engineering properties of clays stabilised with lime-activated ggbs. In the current work a natural clay, Kimmeridge Clay, was stabilised with various proportions of lime and ggbs and cured for 12, 24 and 52 weeks at 10 °C, 20 °C and 30 °C prior to being tested. Knowledge of the shear strength of soils is of significance for construction purposes, with the correct assessment of the stress distribution and deformation being of importance for the solution of bearing capacity problems. Extensive work has already been published on the permeability of lime-stabilised soils [6-8] but very little work has been carried out on the permeability development of soil stabilised with lime-activated ggbs. Numerous authors, however, have reported the results of work on the influence of ggbs on the permeability of concrete [9-11], establishing that the addition of ggbs reduces the mean pore size, which leads to a reduction in permeability and thus reduces the susceptibility to chemical attack. Pore size distribution and porosity as structural parameters influence both permeability and strength development and have therefore also been investigated.

EXPERIMENTAL DETAILS

Materials

The Kimmeridge Clay originated from Blackbird Leys, Oxford, UK. It was dried, crushed and ground to a greyish powder. Some basic engineering properties were determined according to BS 1377 (1990) and are summarised in Table 1.
Hydrated lime with the chemical formula $Ca(OH)_2$, commercially available under the trade name "Limbux", was supplied by Buxton Lime Industries Ltd., Buxton, Derbyshire. Ground granulated blast furnace slag was supplied by Civil and Marine Slag Cement Ltd., Llanwern, Newport, UK. These materials are further described in [3].

Table 1: Engineering properties of Kimmeridge Clay

Liquid Limit	65 %
Plastic Limit	33 %
Plasticity Index	32 %
Initial consumption of lime	3.5 %
Total sulphate	0.13 %*
water soluble sulphate	0.04 g/l*

* data supplied by Appleby Group Ltd.

Specimen preparation

Kimmeridge Clay was stabilised using a total binder content of 8 wt.%. The lime/slag binder ratios were chosen as 8/0 (8%L(ime)0%S(lag)), 6/2 (6L2S), 4/4 (4L4S), 2/6 (2L6S) and 0/8(0L8S).

The undrained unconsolidated shear strength parameters and the coefficient of permeability after 12, 24 and 52 weeks were determined using cylindrical samples with a diameter of 38 mm and a height of 76 mm, which had been compacted to a target maximum dry density of 1.489 Mg/m^3 at a moisture content of 24 %. In order to achieve the target density, enough material to fill a cylindrical split mould was, prior to hand mixing with palette knives, homogeneously mixed in a variable speed Kenwood Chef Excell mixer for 2 minutes before slowly adding the water. A pre-fabricated split mould, with a collar in order to accommodate all the material necessary for one sample, ensured that the material was not overcompressed when compacted in a steel frame with a hydraulic jack. The cylinders were extruded with a steel plunger, cleaned of releasing oil, weighed and wrapped in several layers of cling film in order to avoid any moisture loss during curing. Curing was for 12, 24 and 52 weeks at 10 °C, 20 °C and 30 °C and 100 % relative humidity.

Testing

Shear strength development To determine the undrained shear strength parameters of the samples, a computer controlled hydraulic triaxial testing system was used. Prior to testing the system was flushed with de-ionised water and de-aired. A sample was mounted onto a porous disc covering the base pedestal of the lower chamber in order to measure the pore pressure during testing. Then the sample was covered with a rubber membrane to prevent the access of water from the surrounding perspex cell. Confining cell pressures of 200, 350 or 700 kPa were applied via a hydraulic controller to the range of prepared samples. The strain rate was chosen as 90 mm/min. It should be noted that for some of the tested samples, especially those with a high content of ggbs cured at higher temperatures, the system was not capable of failing them at a cell pressure of 700 kPa. In such cases the test was repeated with a spare sample and a lower confining pressure was chosen in order to achieve shear failure.

Permeability The samples were initially saturated by the application of a back pressure accessing the sample via the bottom pedestal of the triaxial equipment. Saturation was achieved by an increase in the pressure in the pore fluid, forcing air in the pores to go into solution [12]. A laminar and constant flow was then initiated from the bottom to the top of the sample by a uniform increase of pore pressure through the bottom filter plate. To determine the coefficient of permeability and therefore achieve a constant flow, recordings over a period of 24 to 48 hours proved satisfactory. From the results obtained, the coefficient of permeability, k, was calculated using Darcy's law.

Porosity The porosimeter used was a Fisons Macropore Unit and a Fisons Porosimeter 2000W (pressure generation up to 2000 kPa), allowing the determination of pore volumes for pore sizes down to a diameter of 0.0037 μm. The samples were chosen to be around 1.5 g in weight after drying to constant weight and the pore radii corresponding to the mercury pressures were calculated using Washburn's equation [13].

To avoid damage to the sample structure, a gentle drying process in a desiccator over silica gel and carbosorb at room temperature was adopted.

RESULTS AND DISCUSSION

The variation in the undrained shear strength for samples cured for 12 and 24 weeks and 1 year at 10, 20 and 30 °C based on a chosen normal stress of 1000 kN/m^2 is shown in Figure 1. Generally the shear strength τ increases with increasing curing temperature and slag content up to a lime/slag ratio of between 4/4 and 2/6. Samples, for which lime
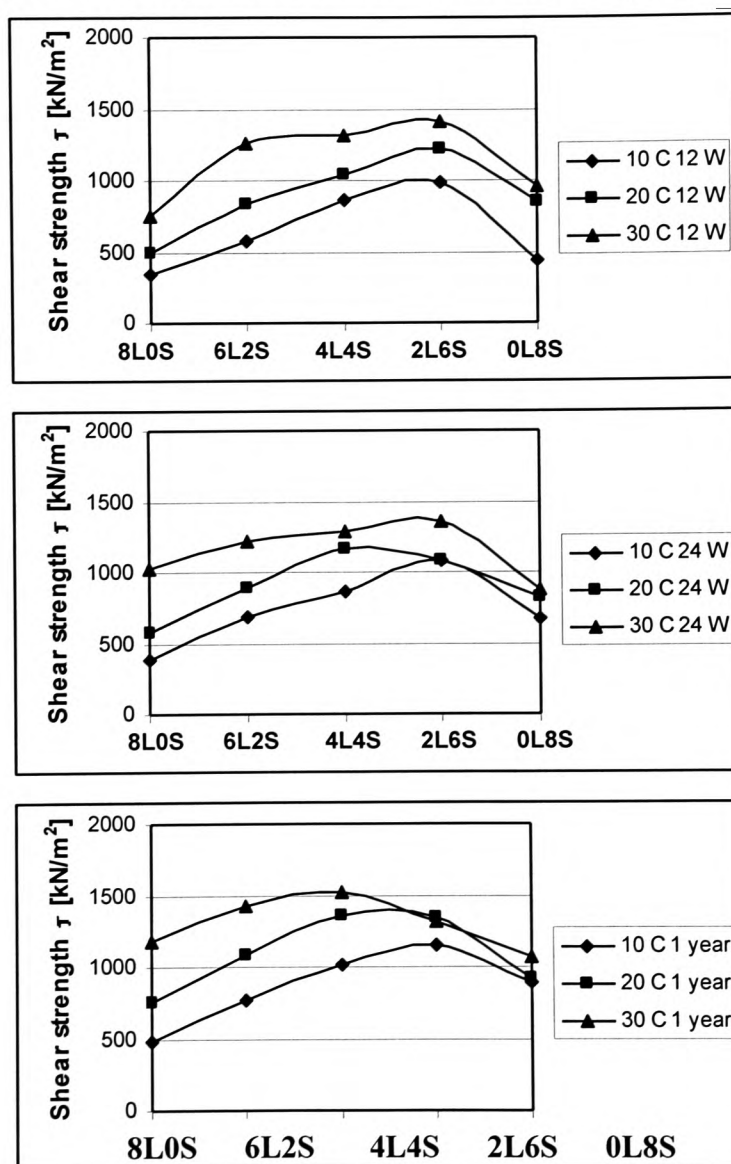
Figure 1: Unconsolidated, undrained shear strength (chosen normal stress = 1000 kN/m^2) for Kimmeridge Clay stabilised with various lime/ggbs ratios, cured for 12 and 24 weeks and 1 year at different temperatures.

is the predominant stabiliser (mixes 8L0S and 6L2S), exhibit generally a wide range of shear strength values over the curing temperature range investigated, particularly for

longer curing periods. If, however, ggbs is the main stabiliser (mix 2L6S), the shear strength results fall within a more narrow band. The sample to which only slag was added (0L8S) shows similar shear strength results for curing periods of 12 and 24 weeks. The overall strength development of this mix, however, does indicate that even without added lime the slag is activated. After 12 weeks, the strength is higher than the values obtained from the lime only mix but with increase in curing temperature and time the strength of the lime only mix progressively exceeds that of the slag only mix. It has been suggested by Wild et al. [15] from similar observations of the compressive
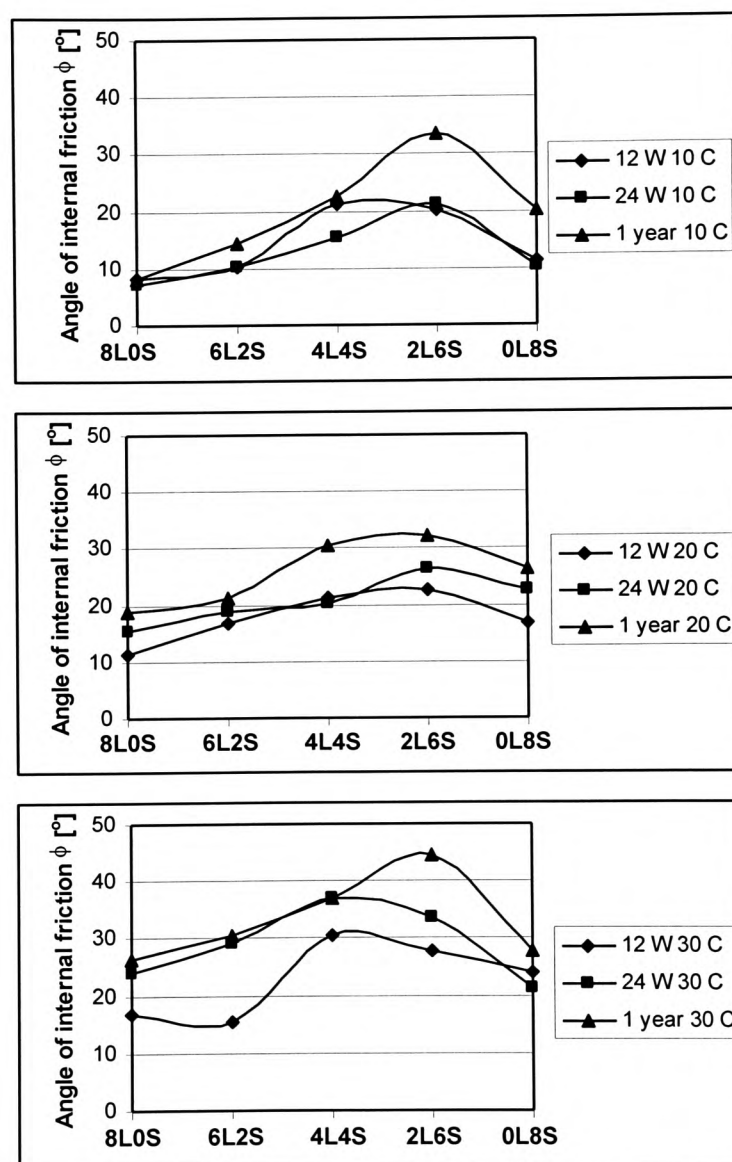
Figure 2: Apparent angle of internal friction φ of Kimmeridge Clay stabilised with various ggbs-lime ratios after a curing period of 12 and 24 weeks and 1 year at different temperatures

strength of lime/slag stabilised Kimmeridge Clay that particular minerals in the clay provide sufficient alkalinity to activate the slag. The replacement of lime with slag also results in a higher value of the apparent angle of shearing resistance φ (Figure 2). This

trend is independent of temperature and is particularly pronounced after a curing period of 1 year. The mix 0L8S exhibits after a curing period of beyond 24 weeks higher values for ϕ than the sample, to which only lime was added. The activation via an alkaline phase in the clay seems therefore to be dormant for some time but finally results in a comparatively strong sample, in particular when curing is at lower temperatures.

Another interesting trend, which indicates how much cementation occurs as a result of slag hydration, is illustrated in Figure 3. The strain at failure obtained from the triaxial tests gives some indication of the reduction in plasticity of the tested sample.
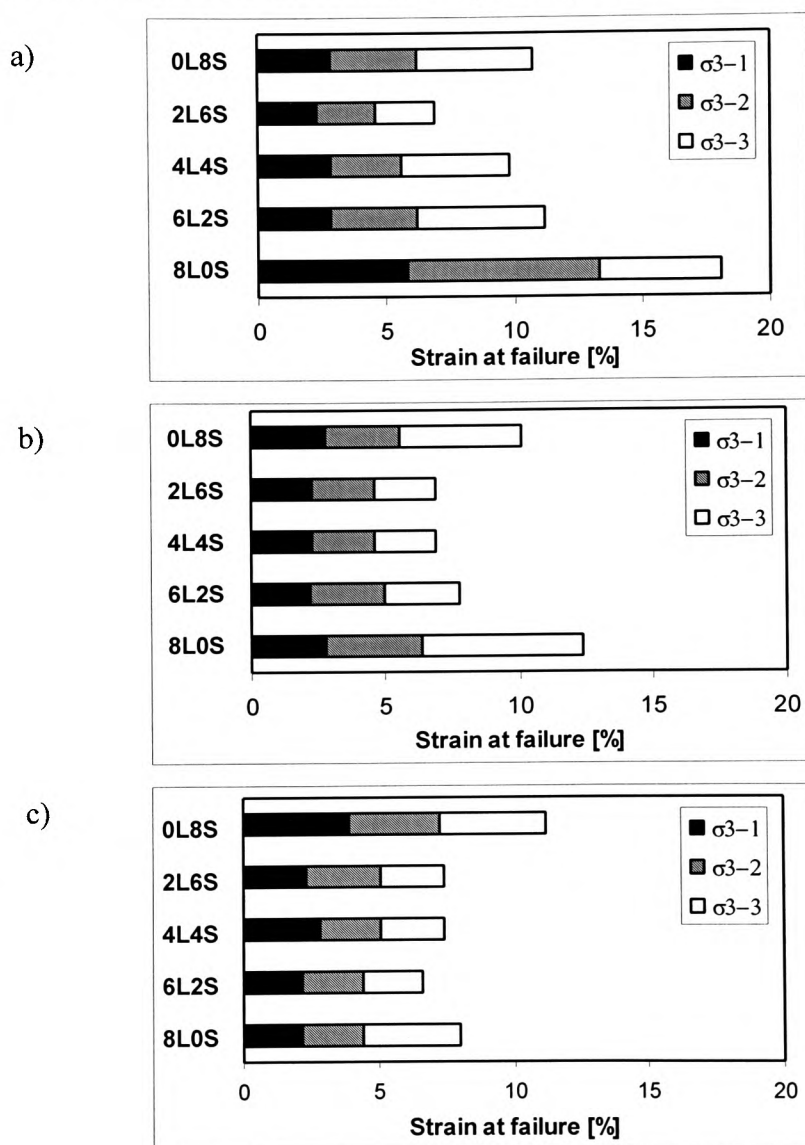
Figure 3: Strain at failure obtained from an undrained triaxial test (σ_{3-1} to σ_{3-3}) for Kimmeridge Clay stabilised with various slag/lime ratios and cured for one year at a) 10 °C b) 20 °C and c) 30 °C

For a well-cemented, brittle sample, the strain at failure tends to be much smaller than for a poorly cemented, plastic and deformable sample, which has undergone hardly any strength-enhancing changes due to very limited formation of cementitious products. It is well accepted that the strength-enhancing pozzolanic reaction, resulting in the formation

of cementitious products in clay-lime mixes, is very sensitive to temperature [6,14]. Considering the different curing environments, the samples prepared with the composition 2L6S show no change in the strain at failure with curing temperature after a curing period of 1 year. This is because after 1 year, cementation due to the slag
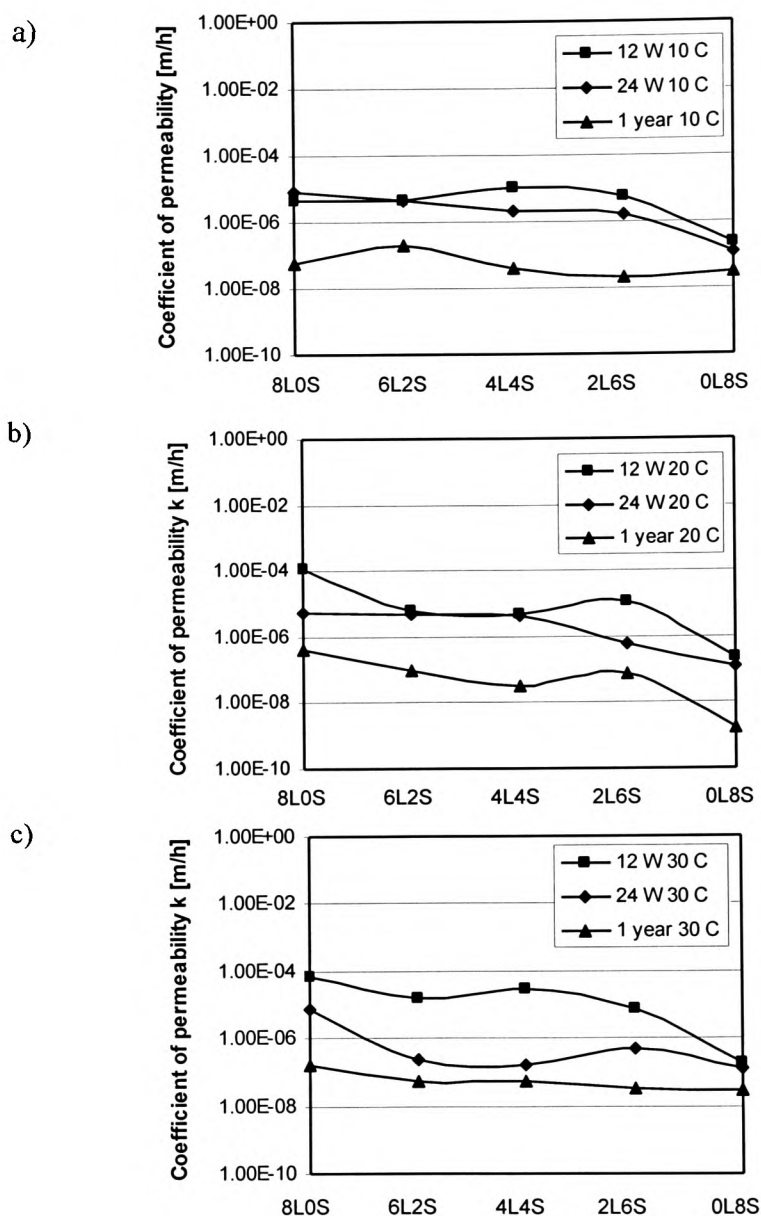
a)

b)

c)

Figure 4: Coefficient of permeability k for Kimmeridge Clay stabilised with various slag/lime ratios and cured for 12 and 24 weeks and 1 year at a) 10 °C, b) 20 °C and c) 30 °C

hydration process is fully completed even for specimens cured at the lowest temperatures. In contrast the mixes with high lime additions confirm the temperature sensitivity of the pozzolanic reaction, which forms the base for their strength enhancement. Percentages of strain at failure comparable to mixes with high slag

additions, are reached only if curing for 1 year is at 30 °C. At lower temperatures little cementing action occurs, resulting in relatively weaker and more plastic samples.

Figure 4 shows the development of the coefficient of permeability of Kimmeridge clay stabilised using slag/lime ratios 8:0, 6:2, 4:4; 2:6 and 0:8 after curing periods of 12 and 24 weeks and one year at various curing temperatures. Overall, the permeability at all curing temperatures is reduced when both curing time and slag content are increased. Comparison of Figures 4a)-c) indicate that temperature has little effect on permeability over the temperature range investigated.

The general reduction in permeability with reduction in lime content and increase in slag content can in part be attributed to the reduced level of flocculation of the clay as the lime content decreases and in part to the greater and more rapid cementitious gel formation due to slag hydration relative to the slow lime-clay pozzolanic reaction[6,7].

The effect of less initial flocculation at higher lime-replacement levels results in less available pore space, which can be quickly blocked by the slag hydration products. Curing time seems to have very little influence at all on the development of the permeability of samples which have been stabilised with slag only (0L8S). Evidence from the shear strength data suggests that even after one year there is limited slag activation and therefore very little variation in permeability with increased curing time would be expected.
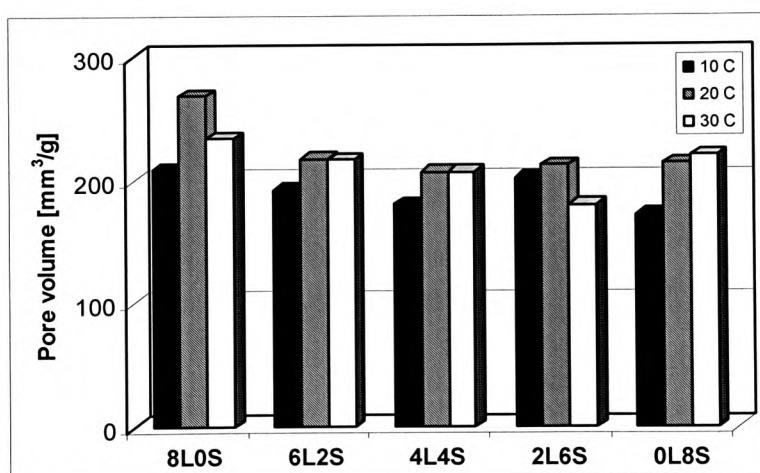

Figure 5: Pore volume of Kimmeridge Clay-lime-ggbs mixes, cured for 1year at 10, 20 and 30 °C

Figure 5 shows the pore volume for Kimmeridge Clay stabilised with various slag/lime ratios after a curing period of 1 year at different curing temperatures. The material stabilised with lime only (8L0S) exhibits the highest porosity, independent of the curing temperature. There is an overall trend towards a reduced pore volume with increasing slag content up to a lime/slag ratio of 2/6. The decrease in pore volume with increasing slag content is thought to be the result of the formation of increasing amounts of cementitious gel, brought about by the slag hydration, coupled with reduced levels of initial flocculation due to the lower lime contents. The tendency for a marked increase in pore volume for the 0L8S composition is due to much reduced slag hydration and hence gel formation, when no lime is added to initiate the process as an activator.

Figure 6 shows that after one year at curing temperatures of 10 °C and 20 °C, maximum pore refinement occurs for slag/lime compositions between 4L4S and 2L6S.
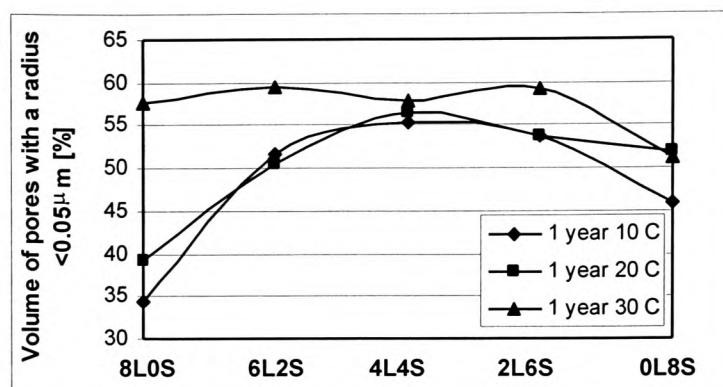
Figure 6: Percentage of pore volume occupied by pores with a radius < 0.05 μm for Kimmeridge Clay stabilised with various slag/lime ratios and cured for one year at 10, 20 and 30 °C

However, after one year at a curing temperature of 30 °C, the degree of pore refinement is similar for all compositions except 0L8S which is again significantly lower. It is suggested that at 30 °C there has, after one year of curing, been extensive pozzolanic reaction in the high lime/low slag compositions specimens. Thus the pore blocking gel, which has been formed is sufficient to produce a level of pore refinement which is equivalent to that produced by the hydrated slag in the low lime/high slag composition specimens.

CONCLUSIONS

In terms of the properties which are developed (i.e. shear strength, permeability and porosity/pore size distribution) soil stabilisation (particularly of sulphate-bearing clays) with lime-activated ggbs has distinct advantages in comparison to stabilisation with lime alone. In particular in countries of the Northern hemisphere, where temperatures rarely rise to such a degree that benefit could be gained from the pozzolanic reaction being substantially accelerated, the less temperature dependent stabilisation method with a lime-ggbs combination is preferable.

Ggbs generally increases the shear strength of clay, when activated by comparably small amounts of added lime or other alkaline phases present in the clay. The permeability of samples of Kimmeridge Clay is reduced with increasing lime replacement level, diminishing the likelihood of distress brought about by water access and the subsequent possibility of chemical attack or frost attack. This reduction in permeability appears to be initiated by the slag hydration, resulting in the formation of pores with a diameter too small to contribute to water permeability. Parallel to a reduction in overall porosity with increasing slag content, the percentage of pores with a diameter of <0.05 μm increases, possibly improving the shear strength development.

This effect could possibly be even further enhanced by replacing a percentage of lime by cement and thus utilise it - together with the lime - as an additional activator for the ggbs. The incorporation of cement might improve the sulphate resistance of soils stabilised with slag in a similar manner, to that by which slag-rich cements produce

concrete with a higher resistance to sulphate attack. It is, however, not advisable to add cement on its own as an additive since the workability of the treated clay soils depends heavily on the flocculation induced by lime additions.

Finally, ggbs is less expensive than lime and/or cement and is an advantageous environmentally friendly by-product, which should be fed back into the industrial society from whence it originated.

ACKNOWLEDGEMENTS

REFERENCES

1. Snedker, E.A. (1996), "M40 – Lime stabilisation experiences", in : Lime stabilisation, Proceedings of a seminar, Civil and Building Engineering Department, Loughborough University, pp. 142-153

2. Hunter, D. (1988), "Lime-induced heave in sulphate bearing clay soils, ASCE Journal of Geotechnical Engineering, 114, no 2, pp. 150-167

3. Wild, S., Kinuthia, J.M., Robinson, R.B. and Humphreys, I. (1996), "Effects of ground granulated blast furnace slag (ggbs) on the strength and swelling properties of lime stabilised kaolinite in the presence of sulphates", Clay Minerals, 31, pp. 423-433

4. Higgins, D.D, Kinuthia, J.M. and Wild. S. (1998), "Soils stabilisation using lime-activated ggbs", 6th Int. Conf. on fly ash, silica fume, slag and natural pozzolans in concrete, 1998, 2, pp. 1057-1074

5. Higgins, D D (1998), "What's new with ggbs?", Concrete Magazine, 32, 5, pp. 16-18

6. Bell, F.G. and Coulthard, J.M., 1990, "Stabilisation of clay soils with lime", Municipal Engineer, 7, pp. 125-140

7. Wild, S., Arabi, M and Rowlands, G O. (1987), "Relation between pore size distribution, permeability and cementitious gel formation in cured clay-lime systems", Materials Science and Technology, 3, pp. 1005-1011

8. Brandl, H (1981), "Alteration of soil parameters by stabilisation with lime", Proceedings of the 10th International Conference on Soil Mechanics, Stockholm, 1981, 3, pp. 587-594

9. Hooton, R.D. (1986), "Permeability and pore structure of cement paste containing fly-ash, slag and silica fume", Blended Cements, STP897, ASTM, Philadelphia, pp. 128-143

10. Kharti, R.P, Sirivivatnanon, V. and Yu, L.K. (1997), "Effect of curing on water permeability of concretes prepared with normal Portland cement and with slag and silica fume", Magazine of Concrete Research, 49, no. 180, pp. 167-172

11. Yamanouchi, T., Monna, I. and Hirose, T. (1982), "Seepage-cut soil stabilisation with a newly developed slag cement", Symposium on recent developments in ground improvement techniques, Bangkok, 1982, pp. 507-511

12. Lowe, J. and Johnson, T.C. (1960), "Use of back pressure to increase the degree of saturation of triaxial test specimens", Proceedings of the ASCE Research Conference on Shear Strength of cohesive Soils, Boulder, Colorado, USA, pp. 819-836

13. Washburn, E. (1921), "Note on a method of determining the distribution of pore sizes in a porous material", Proc. Int. Acad. Sci., 7, USA, pp. 115-116

14. Arabi, M and Wild, S. (1989), "Property changes induced in clay soils when using lime stabilisation", Municipal Engineer, 6, pp. 85-99

15. Wild, S., Kinuthia, J.M., Jones, G. I. and Higgins, D.D. (1999), "Suppression of swelling associated with ettringite formation in lime stabilised sulphate bearing clay soils by partial substitution of lime with ground granulated blast furnace slag (ggbs)", Engineering Geology, 51, pp. 257-277

Essay competition

Green, ground and great: soil stabilization with slag

G. Veith

School of Technology, Division of Built Environment, University of Glamorgan, Pontypridd CF37 1DL, UK

E-mail: gveith@glam.ac.uk

The reuse of materials, which would in the past have been considered as waste to be dumped at some landfill site, possibly in the middle of attractive countryside, has now become a very desirable option. It is a popular way for companies to demonstrate and advertise environmentally friendly behaviour and has in some cases proved to have considerable economic advantages. Within the context of increasing landfill taxes and possible health hazards often associated with stockpiling of the waste, no material can afford to be stigmatized as a 'waste product' any more. Labelled as 'by-products' or 'recycled goods', the 'waste' material is now fed into the industry from whence it originated to be reprocessed for a wide range of other applications. Thus old tyres, brick waste or even empty soda and lager cans are finding new and innovative uses and many yet undreamt of applications wait to be tried. A less visible but nonetheless useful 'waste' material has already found reapplication in the construction industry: ground granulated blast furnace slag (GGBS) has been known for some time to improve the sulphate resistance of concrete, when incorporated into cement. Its application for geotechnical purposes, however, has been rather limited in the past.

During geo-environmental investigations carried out in my current research programme, emphasis has been on the possible utilization of GGBS as a binder in the stabilization of clay soils. 'Classic' soil stabilization methods for roads involve the addition of lime in order to change the consistency of the usually heavy clay and to increase the generally very low bearing capacity. In the past, this has led to some expensive failures in which the treated areas have exhibited dramatic heave. Subsequent remediation entailed costly excavation, disposal of the affected soil and the import of quarried material to fill the gap. For example, this phenomenon occurred during the construction of the lime-stabilized sub-base of the M40 motorway near Banbury in 1990 and more recently on an urban carriageway in Böblingen near Stuttgart, Germany, which was investigated by the author. The reasons for the heave are now well known and result from chemical reactions between the added lime, sulphates and aluminates which derive from the clay itself. Needle-shaped crystals develop which cause heave when subjected to water during their formation process. The final product of the reaction has a larger volume and therefore claims more space than the combined volume of the individual components. Consequently, the whole road construction is pushed upwards and shows the characteristic heave. The remedy to stem the growth of these crystal forests is to use ordinary ground granulated blast furnace slag, widely available and – in comparison to lime – very cost-competitive.

Soil, stabilized with lime-activated slag has shown significant strength enhancement relative to lime-stabilized soil and also very good volume stability when subjected to water in the presence of the aggressive sulphates. The latter is impressively demonstrated in Fig. 1.
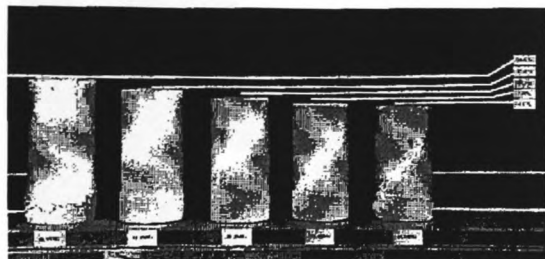
Fig. 1. Swelling magnitudes of clay samples with increasing slag content.

The slag content of the clay samples increases from left to right and reduces the swelling magnitudes of the material from more than 28% (which would, even with the restraint of the overlying material of a road, have formed quite a prominent hump) down to a mere 4%, which is within the limits given by the Department of Transport.

The reduction in swelling potential is mainly due to the formation of cementitious products which are created when the slag, activated by small lime additions, hydrates. These cementitious gels stick the soil particles together and enable them to resist the considerable swelling pressure, which can be generated when the needle-shaped ettringite crystals form in the presence of water. The typical crystal habit can be easily detected with a scanning electron microscope. Fig. 2 gives an example of the microstructural changes brought about by the incorporation of slag in a lime-stabilized clay (kaolinite).

For the GGBS to contribute to the increase in strength it needs to hydrate and form cementi-

tious gels and to do this it must be activated. Potential activators can either be alkaline (for example hydrated lime ($Ca(OH)_2$)) or acidic (for example gypsum ($CaSO_4 \cdot 2H_2O$)) in nature. The incorporation of GGBS leads not only to a more swelling resistant structure by forming the 'glue-like' pore-blocking cementitious gels but also reduces the amount of lime available for the formation of damaging ettringite crystals by utilizing it for the products of its own hydration. It is the pore blocking effect of the hydration products, however, which is responsible for the reduction in permeability of GGBS stabilized material. Laboratory tests, utilizing a triaxial cell in which water was forced through a soil sample by a computer-controlled hydraulic pressure generator at a pre-calculated flow rate, revealed that the flow was significantly reduced with increasing GGBS addition. These observations suggest that GGBS treated soils are generally less susceptible to chemical attack from aggressive ions carried by the water, because the transport of the harmful 'ingredients' between blocked pores is restricted. The influence of the pore blocking gels in restricting the movement of water is also apparent in the performance of clay, stabilized with lime-activated GGBS, when subjected to alternating freeze-thaw cycles. Fig. 3 shows the condition of samples stabilized with various GGBS additions after they have been subjected to 12 24-hour freeze-thaw cycles, undergoing temperature changes from $+20°C$ to $-17.5°C$.

In comparison to the original sample shape (top row) the sample with the highest slag content (far right) maintained its shape and exhibited little

Fig. 2. Kaolinite sample stabilized with 5% lime and only 1% GGBS (left), leading to the formation of a significant amount of ettringite. On the right, however, after the addition of only 1% lime and 5% GGBS, no apparent signs of ettringite at all could be observed.

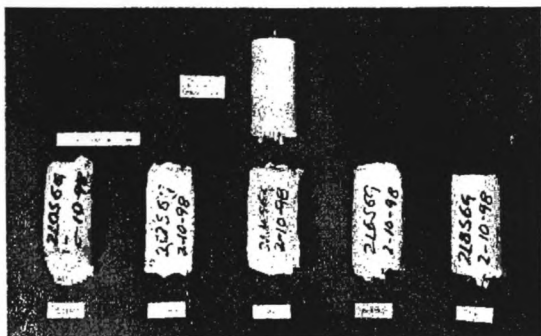Gabriele Veith
University of Glamorgan

A-57

Fig. 3. Kaolinite samples with 2% lime and various GGBS additions after 12 freeze-thaw cycles.

frost heave. The sample to which only lime had been added (far left), however, collapsed. With increasing slag content (from left to right) the volume stability increased due to the increase in internal strength, originating from increased production of cementitious products.

The substitution for conventional stabilization methods with this innovative sub-base improvement technique utilizing GGBS has numerous benefits. Firstly, the clay's engineering properties, including strength development, swelling resis-

tance, permeability and frost resistance are greatly improved when additions of GGBS, activated by relatively small amounts of lime, are incorporated in the soil. Secondly, within the context of a growing environmental awareness by both industry and its clients, GGBS has to be the preferred choice when competing with conventional additives such as lime or cement. Being basically a waste product of the iron making industry, it has environmental advantages over its main 'competitors' lime and cement, as their production is very energy intensive and produces large quantities of the greenhouse gas carbon dioxide (production of 1 ton of cement releases 1 ton of CO_2). The case for wider utilization of GGBS is even stronger when economic considerations are taken into account. In comparison to conventional stabilization materials (lime and/or cement), GGBS is very price competitive and should thus be given serious consideration when soil stabilizing techniques are specified for highways and foundations.

Reference

Snedker, E.A. and Temporal, J. (1990) M40 Motorway Banbury IV Contract – Lime stabilisation. *Highways and Transportation*, December, pp. 7–8

Gabriele Veith
University of Glamorgan

Opportunities for the treatment of sulphate-bearing ground

by

G Veith, S Wild and R B Robinson
University of Glamorgan, School of Technology, Division of the Built Environment,
Pontypridd, CF37 1DL, UK

Synopsis

Lime is being used to modify and stabilise soils for a wide range of construction purposes. However, lime stabilisation is occasionally avoided due to the occurrence of sulphates or sulphides in the ground. These have a tendency to react with cementitious agents produced during the pozzolanic lime-clay reaction and can result in swelling and subsequent strength and durability loss.

By the introduction of a second supportive stabiliser, ground granulated blast furnace slag (ggbs), this can be avoided. This paper clarifies the reactions initiated in lime-stabilised clay soils in the presence of sulphates, and outlines the advantages of the introduction of ggbs. Blast furnace slag, a by-product of the steel making industry, is activated by the alkaline environment provided by the lime in the stabilised ground. Its hydration products are essentially similar to those of Portland cement and lead partially to the blockage of capillary pores. Thus the strength of the stabilised soil increases and its permeability is reduced. Laboratory tests on naturally sulphate-bearing soils and artificially prepared soil mixes to which sulphates in the form of gypsum were added, have shown that the hydration of lime-activated ggbs occurs faster and is less temperature sensitive than the clay-lime pozzolanic reaction alone. A combination of the stabilisers lime and ggbs, with the lime initiating the soil modification and activating the slag grains and the slag contributing predominantly to strength development, can be utilised to stabilise potentially heave-endangered soils with success.

1. Introduction

Lime is being used to modify and stabilise soils for a wide range of construction purposes. The addition of lime, particularly when heavy clay soils are treated, results in enhanced engineering properties (increased permeability, higher strength and increased volume stability) and transforms the clay into a friable material with good workability [Arabi et al., 1989]. These changes are the result of two major reactions, namely *cation exchange* and the *soil-lime pozzolanic reaction*. The former, which starts immediately when lime is added to soil material, results in flocculation and thus in changes in the consistency and appearance of the treated soil. The latter, which is highly temperature and time dependent, is influenced primarily by natural soil properties. Silica and alumina from the clay mineral lattices are dissolved at an elevated pH-value and precipitate with Ca^{2+} ions from the lime to form cementitious gels, affecting strength, permeability and durability of the stabilised layer. However, lime treatment is occasionally unsuitable due to the mineralogical composition of the soil, organic matter or sulphates present in the ground. Emphasis in this paper will lie on a discussion of the reactions initiated in lime-stabilised clay soils in the presence of sulphates. It will clarify the origin of sulphates and offer an economic and environmentally-friendly stabilisation method based on the introduction of a second supportive stabiliser, ground granulated blast furnace slag (ggbs).

2. The occurrence of sulphates in clay soils

Sulphate salts are basically found in a wide range of clay formations and are most commonly encountered as calcium sulphate (occurring as gypsum or selenite), sodium sulphate, potassium sulphate or magnesium sulphate [BRE, 1991]. They are usually absent in the surface layers of ground and the deposits can be found at a higher depth where they have been redeposited at the base of a weathered zone after leaching action. However, Na sulphates are usually transported upward in a layer through evaporation and thus found at the top of a soil profile [Sposito,1989]. The distribution of sulphates – even those of one kind - is highly non-uniform and thus continuous testing in the course of stabilisation work for large stabilisation projects is advisable [Sherwood, 1992].

Although sulphates can sometimes not be traced at all or are detected in negligible amounts in a soil sample, potential sulphates in the form of sulphides (for example iron sulphides (pyrites)) might be present. However, testing for total sulphur (for example according to BS1047:1983 – Methods for the chemical analysis of blast furnace slag) and subsequent comparison with the determined sulphate content of the sample, will provide data on the amount of potentially dangerous sulphides in the soil. Pyrites ("fool's gold") can occur naturally or from industrial wastes and can be oxidised to sulphates. The likelihood of the occurrence of such a problem will depend upon the rate and degree of oxidation of the pyrite after its exposure to the atmosphere and within the stabilised layer. The rate of oxidation will depend upon the chemical environment to which the pyrites is exposed. There is in fact good evidence that the rate of oxidation is accelerated in a highly alkaline environment. If, however, the pyrite remains below the water table or sealed within the ground, little or no oxidation will take place due to oxygen starvation.

3. Limitations of lime stabilisation for sulphate-bearing soils

Sulphates have basically no effect on the changes in plasticity of the treated soils brought about by the addition of lime. However, in the presence of moisture sulphates may react with the cementitious products produced during the pozzolanic reaction. Calcium sulphoaluminate hydrates, initially discovered more than 100 years ago, can form [Michaelis, 1892]. Of the two hydrates, termed "monosulphate" and "ettringite", ettringite appeared to be the most damaging. Ettringite, or the corresponding silicate form, "thaumasite", have been reported to form as a result of the chemical reactions occurring in lime-stabilised subgrades. In the presence of excess water their formation results in heave. This is basically due to the fact that as the reaction products form,, water is consumed , swelling takes place and more water is drawn up into the soil. Although ettringite, which forms acicular crystals, also contributes to the strength development of a stabilised layer, the volume changes during its formation in the presence of an abundance of water, can result in considerable heave and cracking of pavement surfaces. Factors, influencing the rate of what is known as "sulphate attack", are, for example, percentage of clay fraction (particles with a diameter of 2 μm or less) in the soil, availability of water, type and amount of soil stabiliser used type and

concentration of the sulphates (Sherwood [1992] raised concern about the possibility of expansive reactions and subsequent durability loss with as little as 0.25 % sulphates (expressed as SO_3) in cohesive soils although the Department of Transport (Specification for Highway Works, part 2, clause 615/2) specifies 1% SO_3).

4. The use of lime-activated ground granulated blast furnace slag (ggbs) in soil stabilisation

With regard to the limitations for soil stabilisation with lime in the presence of sulphates, the introduction of a second supporting additive appears desirable and should increase the range of cohesive soils suitable for stabilisation. It should allow for continued use of lime even at high sulphate levels and further improve the performance of the stabilised layers. To date, laboratory test results and results obtained from large full-scale trials in the field suggest that ground granulated blast furnace slag (ggbs) is an ideal agent for a combined economically and environmentally-friendly 'slag-lime stabilisation method'.

4.1 History and background

Ground granulated blast furnace slag is a by-product of the iron-making industry and consists predominantly of combined silica, alumina and lime. The large range of possible applications stretches from civil engineering to agricultural engineering and metallurgy. As early as 350 BC the scientist and philosopher Aristotle stated that "if iron is purified by fire, there forms a stone, known as iron slag. It is wonderfully effective in drying out wounds and results in other benefits.." [Geiseler, 1996]. It is not clear if these "other benefits" included the re-use of slag in building materials. However, the earliest recorded use of ggbs in the construction industry dates back to 1774, when it was added to a mortar based on slaked lime. The hydraulic properties of water-cooled blast furnace slag were discovered in 1862 by Emil Langen from Troisdorf, Germany, "*...feuerflüssige Hochofenschlacke erhält nach dem Einleiten in Wasser wertvolle hydraulische Eigenschaften...*(if subjected to cold water treatment, liquid blast furnace slag is given valuable hydraulic properties...)" [Geiseler, 1992]. It was also in Germany where the first commercial use of slag-lime cements started in 1865. Over the decades a Portland clinker, slag, calcium sulphate cement was mainly

used for concrete exposed to harsh conditions, for example for a North Sea Canal lock near Ijmuiden in the Netherlands. Finally, in 1917 after investigations carried out by the Material Testing Institute (Materialprüfungsamt) in Berlin, slag cement, was allocated the same standing as Portland cement within the cement range in Germany [Bijen, 1996].

4.2 Effects of ggbs in soil stabilisation

If activated by an alkaline environment in the soil, for example provided by the added lime ("lime-activated ggbs"), ggbs will hydrate and produce cementitious gels similar to those produced during the hydration of Portland cement. At a pH-value of around 12.4 or beyond, the glass component in the slag grain will break down and the hydration products will form on the surface of the slag grain. This results in a reduction of pore water or solution filled pore space and thus add density to the stabilised material. It is largely this increase in density and the related change in porosity which is thought to be responsible for subsequently observed improvement in strength, reduction in permeability and improved resistance to sulphate attack.

4.2.1. Strength development

The changes in strength development when ggbs is introduced in a lime-stabilised clay, can be seen in Figure 1. Lower Oxford Clay, a natural clay with a high sulphide content, was stabilised with 2 % lime ($Ca(OH)_2$) and 0 (2L(ime)0S(lag)), 2 (2L2S), 4 (2L4S), 6 (2L6S)and 8 % (2L8S)slag.

With increasing slag addition the UCS-values of the stabilised material increases significantly. The strength obtained after curing periods of 7, 28 and 90 days varies very little. However, if curing is for 24 weeks, particularly for slag additions of 4, 6 and 8 %, further improvement in UCS can be observed.

In order to establish how lime-slag stabilisation would affect a clay with high sulphate content, an artificial, laboratory-prepared soil mix, consisting of industrial kaolinite and gypsum, was utilised. The kaolinite mix allowed exact adjustment of the sulphate content and thus control of
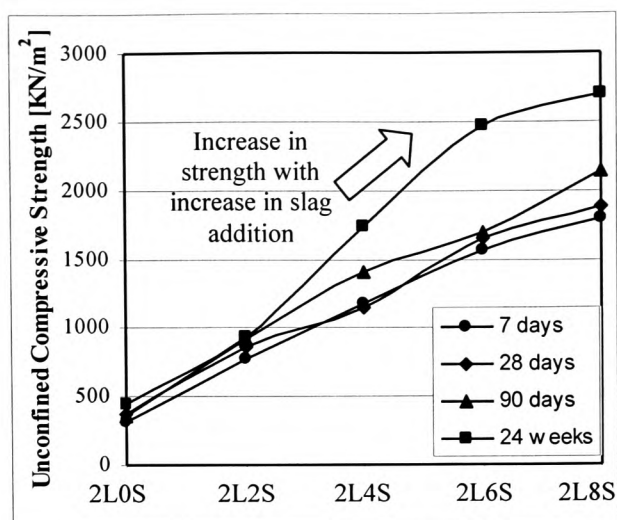
Figure 1 *Unconfined Compressive strength of Lower Oxford Clay stabilised with 2% lime and 0, 2, 4, 6 and 8% ggbs after various curing periods*

the level of the disruptive sulphate reaction. Figure 2 shows the strength development of kaolinite-lime-slag mixes in the presence of 0, 2, 4 and 6 % gypsum.
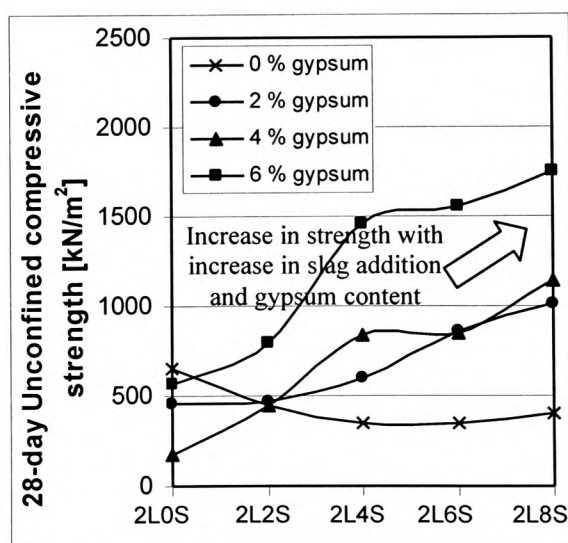
Figure 2 *Unconfined compressive strength after 28 days of kaolinite-lime-ggbs mixes in the presence of 0, 2, 4 and 6 % gypsum*

The presence of sulphates appears to be advantageous if lime and ggbs are combined as stabilisers and improves the compressive strength development significantly, particularly when larger percentages of slag are added. Sulphates have a tendency to accelerate the slag hydration process and can thus even be considered beneficial with regard to the strength development of lime-slag-stabilised ground.

2.2 Effects on swelling

Figure 3 demonstrates the effect of increasing slag additions on the swelling potential of lime-stabilised, sulphate-bearing kaolinite. As an artificial sulphate, 8% gypsum (=3.72% SO_3) had been added to the kaolinite. Prior to soaking in de-ionised water, the samples were cured for 7 days at 30 °C.

The percentage of added slag increases from left to right and results in a dramatic reduction of sulphate induced heave of the lime-stabilised kaolinite. In fact, the extreme expansion of 28.8% when 6% lime (and no slag) had been added as a stabiliser (far left) is reduced to less than 5.0% when 2%lime is combined with 4% ggbs (The regulations of the Department of Transport suggest that the average degree of swelling should be less than 5 mm (measured on the standard 127 mm high CBR mould) with no individual test specimen swelling more than 10 mm).
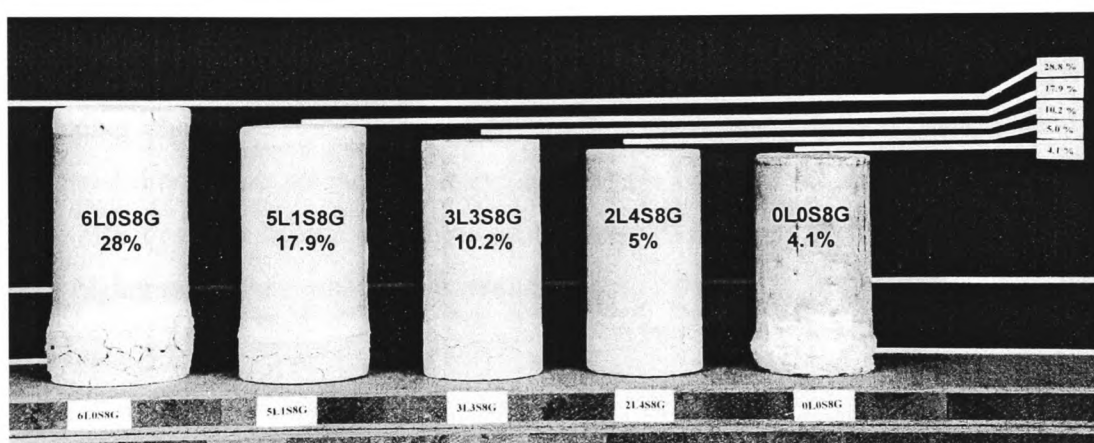

Figure 3 *Effect of slag-lime replacement on the swelling properties of kaolinite in the presence of 8 % gypsum*

4.2.3 Effects on permeability

It is highly likely that not only the cementing effect of the additives but also the pore blocking effect of the resulting cementitious products have a large influence on the performance of the stabilised layer in the presence of sulphates. Thus Figure 4 shows results of investigations into the development of the water permeability of lime and slag-stabilised Lower Oxford Clay after curing periods of up to one year.
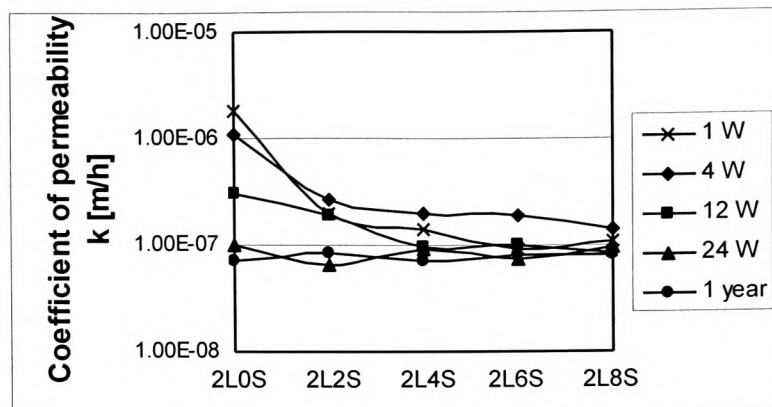
Figure 4 *Coefficient of permeability k for Lower Oxford Clay stabilised with 2% lime and 0, 2, 4, 6 and 8% ggbs after curing periods of 1, 4, 12, 24 weeks and 1 year*

This provides strong evidence that the quantity of cementitious products formed increases with increasing slag additions. These products result in a pore blocking effect reducing the water permeability of the stabilised samples and thus reduce the vulnerability of the soil to aggressive agents, for example sulphate containing water. The effect of pore blockage is more pronounced after longer curing periods and occurs at a higher rate, when more slag is added.

5. Summary

By combining the effect of lime and ggbs in soil treatment, a stabilisation method of superior engineering quality is created. The advantageous effects of both stabilisers are summarised in Figure 5.
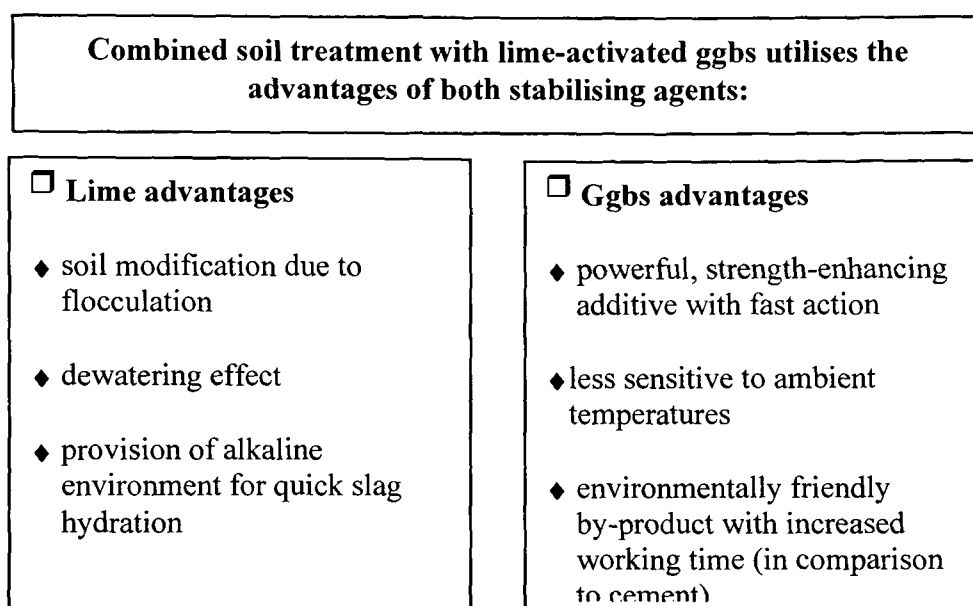
Combined soil treatment with lime-activated ggbs utilises the advantages of both stabilising agents:	
□ Lime advantages ♦ soil modification due to flocculation ♦ dewatering effect ♦ provision of alkaline environment for quick slag hydration	**□ Ggbs advantages** ♦ powerful, strength-enhancing additive with fast action ♦ less sensitive to ambient temperatures ♦ environmentally friendly by-product with increased working time (in comparison to cement)

Figure 5 *Advantages of lime and ggbs in soil stabilisation*

Stabilised ground with reduced permeability, improved and less temperature sensitive strength development, reduced swelling potential and good compaction properties is created. The range of applications for lime stabilisation is enlarged and environmental aspects are added by the introduction of a very price competitive by-product.

6.Acknowledgements

7. References

Arabi, M and Wild, S (1989), "Property changes induced in clay soils when using lime stabilisation", Municipal Engineer, **6**, April 1989, pp 85-99

Bijen, J (1996), "Blast furnace slag cement", VNC Association of the Netherlands Cement Industry, s'-Hertogenbosch, Netherlands, CIP Royal Library Den Haag

BRE (1991), "Sulphate and acid resistance of concrete in the ground", BRE Digest 363, July 1991, Watford, UK

Geiseler, J (1992), "Verwertung von Hochofen- und Stahlwerksschlacken (Utilisation of blast furnace and steel slags)" (in German), in: "Eisenhüttenschlacken – Eigenschaften und Verwertung", Referate aus dem Zeitraum 1988-1991, Heft 1, Forschungsgemeinschaft Eisenhüttenschlacken, Duisburg, Germany, pp 1-32

Geiseler, J (1996), "Use of steelwork slag in Europe", Waste Management, **16**, no 1-3, pp 59-63

Michaelis, W (1892), "Der Zementbazillus (The cement bug)", in German, Tonindustrie-Zeitung, **16**, pp 105-106

Sherwood, P T (1992), "Stabilised capping layers using either lime or cement, or lime and cement", Transport Research Laboratory, Contractor Report 151, Crowthorne, Berkshire, UK

Sposito, G (1989), "The chemistry of soils", Oxford University Press Inc, New York

S. Wild, R.B. Robinson and G. Veith

School of the Built Environment, University of Glamorgan, Pontypridd, CF37 1DL, UK.

Shear strength and permeability relationships for Kimmeridge Clay stabilised with lime-ground granulated blast furnace slag (ggbs) blends

Keywords: clay, permeability, porosity, lime, shear strength, slag

Abstract
Kimmeridge Clay, obtained from Blackbird Leys near Oxford, England, UK, was stabilised with a total binder content of 8 % at various slag/lime ratios. The samples were cured for 12 weeks, 24 weeks and 1 year at 10, 20 and 30 °C. The shear strength development was assessed in a series of undrained, unconsolidated triaxial tests, during which the pore water pressure was measured. The permeability of the saturated soil-lime-ggbs mixes was measured in a computer controlled triaxial cell.
The results indicate that, in general, the undrained shear strength increases with increasing slag/lime ratio, particularly when the soil is cured at elevated temperatures. Also permeability drops significantly with increasing slag/lime ratio and increasing curing period, whereas curing temperature has only a minor influence on permeability.

1. Introduction

When sulphates are present in a soil, the classic soil stabilisation using the common technique of mixing lime (either as quicklime (CaO) or slaked lime ($Ca(OH)_2$) with the soil can result in the generation of substantial heave. This occurs as a result of the formation of expansive reaction products and has been reported by various authors [1,2]. Wild et al. [3] and Higgins et al. [4] have shown that the incorporation of ggbs in a clay-lime mix reduces the swelling magnitude substantially and has no deleterious effect on the strength development. Little work, however, has been carried out on the shear strength development and permeability of clays to which lime-activated ggbs was added.

Knowledge of the undrained shear strength parameters c_u and ϕ_u of soils is of significance for construction purposes since the correct assessment of the stress distribution and deformation leads to a solution of the bearing capacity problem, resulting in an optimised design for foundations.

Extensive work has already been published on the permeability of lime-stabilised soils [5-7] but very little work has been carried out on the permeability development of clay soil stabilised with lime-activated blast furnace slag. Numerous authors, however, have reported the results of work on the influence of ggbs on the permeability of concrete [8-10], establishing that the addition of slag reduces the mean pore size, which leads to a reduction in permeability.

2. Experimental

2.1 Materials

The Kimmeridge Clay originated from Blackbird Leys, Oxford, UK. It was dried, crushed and ground to a greyish powder. Some basic engineering properties were determined according to BS 1377 (1990) and are summarised in Table 1.

Hydrated lime with the chemical formula $Ca(OH)_2$, commercially available under the trade name "Limbux", was supplied by Buxton Lime Industries Ltd., Buxton, Derbyshire. Ground granulated blast furnace slag was supplied by Civil and Marine Slag Cement Ltd., Llanwern, Newport, UK. These materials are further described in [3].

Table 1 Engineering properties of Kimmeridge Clay

Liquid Limit	65
Plastic Limit	33
Plasticity Index	35
Initial consumption of lime	3.5 %
Total sulphate	0.13 %*
water soluble sulphate	0.04 g/l*

*Appleby Group Ltd.

2.2 Specimen preparation

Kimmeridge Clay was stabilised using a total binder content of 8 wt.%. The lime/slag binder ratios were chosen as 8/0 (8%L(ime)0%S(lag)), 6/2 (6L2S), 4/4 (4L4S), 2/6 (2L6S) and 0/8(0L8S).

The undrained unconsolidated shear strength parameters and the coefficient of permeability after 12, 24 and 52 weeks were determined using cylindrical samples with a diameter of 38 mm and a height of 76 mm, which had been compacted to a target maximum dry density of 1.489 Mg/m^3 at a moisture content of 24.25%. In order to achieve the target density, enough material to fill a cylindrical split mould was, prior to hand mixing with palette knives, homogeneously mixed in a variable speed Kenwood Chef Excell mixer for 2 minutes before slowly adding the water. A pre-fabricated split mould, with a collar in order to accommodate all the material necessary for one sample, ensured that the material was not overcompressed when compacted in a steel frame with a hydraulic jack. The cylinders were extruded with a steel plunger, cleaned of releasing oil, weighed and wrapped in several layers of cling film in order to avoid any moisture loss during curing. Curing was for 12,24 and 52 weeks 10 °C, 20 °C and 30 °C and 100 % relative humidity.

2.3 Testing

Shear strength development

To determine the undrained shear strength parameters of the samples, a computer controlled hydraulic triaxial testing system was used. Prior to testing the system was flushed and de-aired. A sample was mounted onto a porous disc covering the base pedestal of the lower chamber in order to measure the pore pressure during testing. Then the sample was covered with a rubber membrane to prevent the access of water from the surrounding perspex cell. Confining cell pressures of 200, 350 or 700 kPa were

applied via a hydraulic controller to the range of prepared samples. The strain rate was chosen as 90 mm/hour. It should be noted that for some of the tested samples, especially those with a high content of ggbs cured at higher temperatures, the system was not capable of failing them at a cell pressure of 700 kPa. In such cases the test was repeated with a spare sample and a lower confining pressure was chosen in order to achieve shear failure.

Permeability

The samples were initially saturated by the application of a back pressure accessing the sample via the bottom pedestal of the triaxial equipment. Saturation was achieved by an increase in the pressure in the pore fluid, forcing air in the pores to go into solution [11]. A laminar and constant flow was then initiated from the bottom to the top of the sample by a uniform increase of pore pressure through the bottom filter plate. To determine the coefficient of permeability and therefore achieve a constant flow, recordings over a period of 24 to 48 hours proved satisfactory. From the results obtained, the coefficient of permeability, k, was calculated using Darcy's law.

3. Results and discussion

The variation in shear strength for samples cured at 10, 20 and 30 °C is shown in Figure 1 and the corresponding values of the undrained shear strength parameters can be seen in Figure 2. The trend in the development of shear strength of the samples generally increases with increasing slag content and curing temperature. The replacement of lime with slag also results in a higher angle of shearing resistance at all curing temperatures. Elevated curing temperatures lead to higher cohesion values when lime is the dominant stabiliser (8L0S and 6L2S). Beyond a replacement level of 50 %, however, the highest cohesion is observed for samples cured at medium temperature (20 °C). The sample stabilised with only ggbs exhibits the least variation in cohesion values (Figure 2). The strength development of this mix does indicate that even without added lime the slag is activated. At 10 °C the strength is higher than the lime only mix but with increase in curing temperature the strength of the lime only mix progressively exceeds that of the slag only mix. It has been suggested by Wild et al. [12] from similar observations of the compressive strength of lime/slag stabilised Kimmeridge Clay that particular minerals in the clay provide sufficient alkalinity to activate the slag.

Figure 3 shows the development of the coefficient of permeability of Kimmeridge clay stabilised using slag/lime ratios 8:0, 6:2, 4:4; 2:6 and 0:8 after curing periods of 12 and 24 weeks and one year at various curing temperatures. Overall, the permeability at all curing temperatures is reduced when both curing time and slag content are increased. Comparison of Figures 3a)-c) indicate that temperature has little effect on permeability over the temperature range investigated.

The general reduction in permeability with reduction in lime content and increase in slag content can in part be attributed to the reduced level of flocculation of the clay as the lime content decreases and in part to the greater and more rapid cementitious gel formation due to slag hydration relative to the slow lime-clay pozzolanic reaction [5,6].

The effect of less initial flocculation at higher lime-replacement levels results in less available pore space, which can be quickly blocked by the slag hydration products.

Curing time seems to have very little influence at all on the development of the permeability of samples which have been stabilised with slag only (0L8S). Evidence from the shear strength data suggests that even after one year there is limited slag activation and therefore very little variation in permeability with increased curing time would be expected.

a)

b)

c)
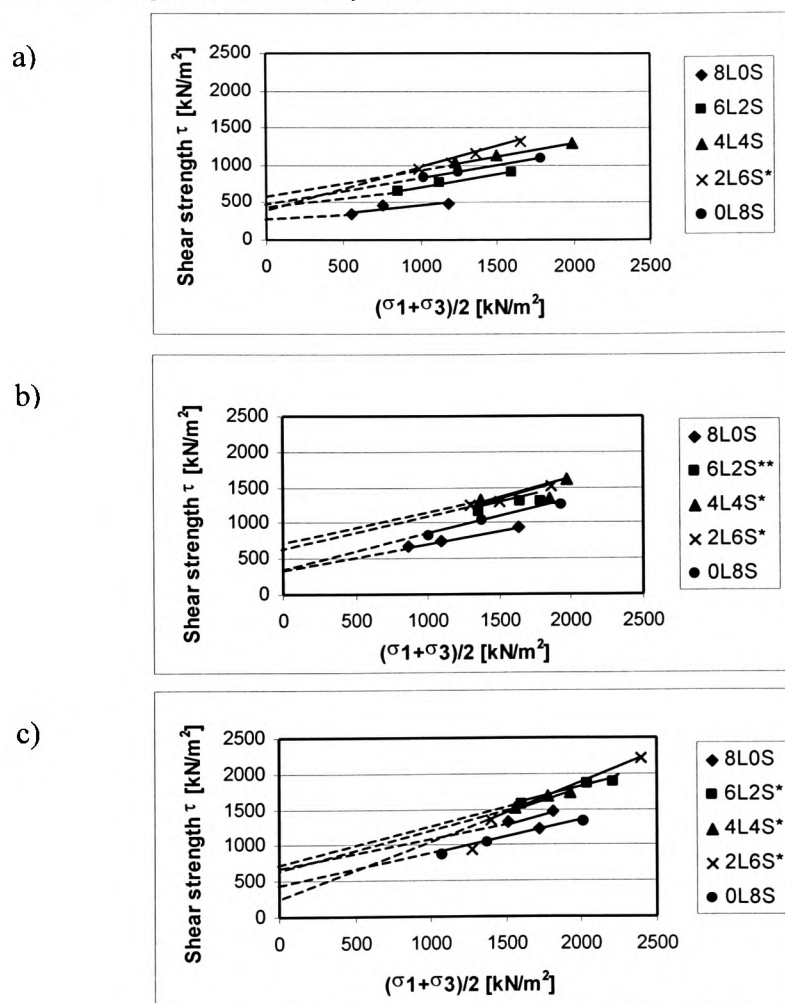
$*_{\sigma3}$=50, 200 and 350 kPa $**_{\sigma3}$=200, 350 and 500 kPa

Figure 1 Unconsolidated, undrained shear strength of Kimmeridge Clay cured for one year at a)10 °C, b) 20 °C and c) 30 °C
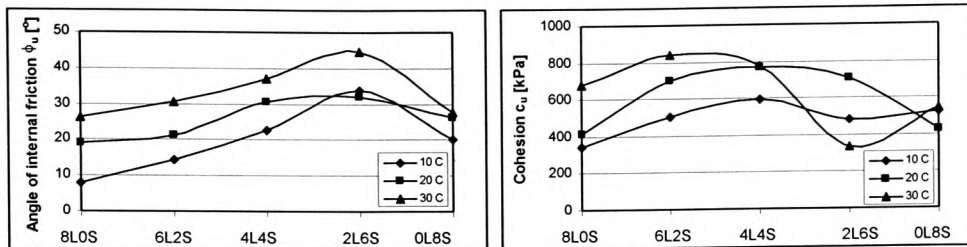
Figure 2   Undrained shear strength parameters for Kimmeridge Clay cured for 1 year at 10, 20 and 30 °C
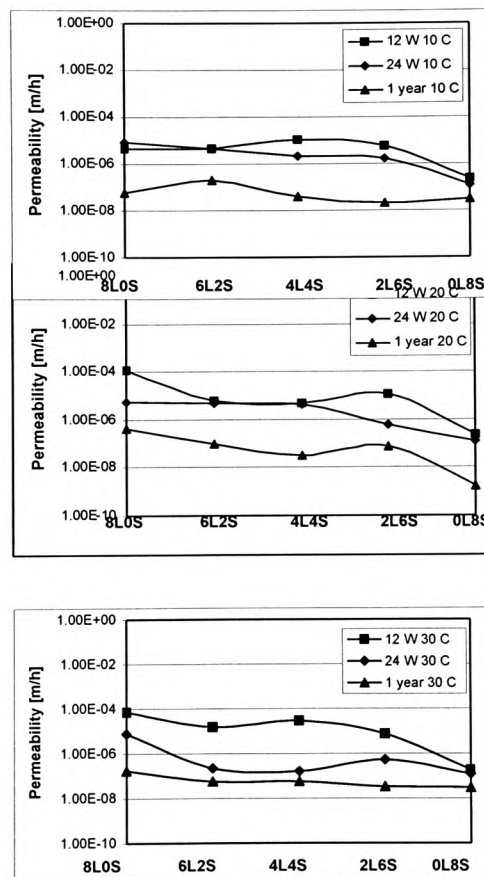

Figure 3 Permeability for Kimmeridge Clay stabilised with various slag/lime ratios and cured for 12 and 24 weeks and 1 year at a) 10, b) 20 and c) 30 °C

4. Conclusions

The partial replacement of lime with ggbs in stabilised Kimmeridge Clay has the following implications:

i)   Ggbs generally increases the shear strength of clay, when activated by comparably small amounts of added lime or other alkaline phases present in the clay.

ii)   The permeability of samples is reduced with increasing lime replacement level, diminishing the likelihood of distress brought about by water access and the subsequent possibility of sulphate attack.

5. Acknowledgements

6. References

1 Snedker, E.A. (1996), "M40 – Lime stabilisation experiences", in : Lime stabilisation, Proceedings of a seminar, Civil and Building Engineering Department, Loughborough University, pp. 142-153

2 Hunter, D. (1988), "Lime-induced heave in sulphate bearing clay soils, ASCE Journal of Geotechnical Engineering, vol. 114, no. 2, pp. 150-167

3 Wild, S., Kinuthia, J.M., Robinson, R.B. and Humphreys, I. (1996), "Effects of ground granulated blast furnace slag (ggbs) on the strength and swelling properties of lime stabilised kaolinite in the presence of sulphates", Clay Minerals, vol. 31, pp. 423-433

4 Higgins, D.D, Kinuthia, J.M. and Wild. S. (1998), "Soils stabilisation using lime-activated ggbs", 6th Int. Conf. on fly ash, silica fume, slag and natural pozzolans in concrete, 1998, vol. 2, pp. 1057-1074

5 Bell, F.G. and Coulthard, J.M., 1990, "Stabilisation of clay soils with lime", Mun. Engr., vol 7, pp. 125-140

6 Wild, S., Arabi, M and Rowlands, G O. (1987), "Relation between pore size distribution, permeability and cementitious gel formation in cured clay-lime systems", Materials Science and Technology, vol 3, pp. 1005-1011

7 Brandl, H (1981), "Alteration of soil parameters by stabilisation with lime", Proceedings of the 10th International Conference on Soil Mechanics, Stockholm, 1981, vol. 3, pp. 587-594

8 Hooton, R.D. (1986), "Permeability and pore structure of cement paste containing fly-ash, slag and silica fume", Blended Cements, STP897, ASTM, Philadelphia, pp. 128-143

9 Kharti, R.P, Sirivivatnanon, V. and Yu, L.K. (1997), "Effect of curing on water permeability of concretes prepared with normal Portland cement and with slag and silica fume", Magazine of Concrete Research, vol. 49, no. 180, pp. 167-172

10 Yamanouchi, T., Monna, I. and Hirose, T. (1982), "Seepage-cut soil stabilisation with a newly developed slag cement", Symposium on recent developments in ground improvement techniques, Bangkok, 1982, pp. 507-511

11 Lowe, J. and Johnson, T.C. (1960), "Use of back pressure to increase the degree of saturation of triaxial test specimens", Proceedings of the ASCE Research Conference on Shear Strength of cohesive Soils, Boulder, Colorado, USA, pp. 819-836

12 Wild, S., Kinuthia, J.M., Jones, G. I. and Higgins, D.D. (1999), "Suppression of swelling associated with ettringite formation in lime stabilised sulphate bearing clay soils by partical subsitution of lime with ground granulated blast furnace slag (ggbs)", Engineering Geology, vol. 51, pp. 257-277